

**NATURAL VENTILATION AND COOLING BY
EVAPORATION IN HOT-ARID CLIMATES**

By
MOHSEN M. ABOUL NAGA
BSc., MSc.
Architectural Engineering

Submitted in Accordance with the Requirements for
the *Degree of Doctor of Philosophy (Ph.D)*.
under the supervision of
Dr. D.FITZGERALD and Dr. W.HOUGHTON-EVANS

ARCHITECTURAL ENGINEERING RESEARCH SECTION
DEPARTMENT OF CIVIL ENGINEERING
THE UNIVERSITY OF LEEDS
February 1990

PAGE NUMBERING AS ORIGINAL

**VOLUME CONTAINS CLEAR OVERLAYS
OVERLAYS SCANNED SEPERATELY AND
OVER THE RELEVANT PAGE.**

ABSTRACT

In hot climates, outside air is too hot during the day. In hot arid climates, low humidity increases discomfort. For comfort, hot air should be cooled before flowing into dwellings and moisture in the moving air increased. For the poor, comfort must be sought cheaply. In places without electricity only 'natural' ventilation is feasible.

The air temperature difference between the sunny and the shaded side of a building can be exploited to promote ventilation. Ventilation cooling can be enhanced with an 'evaporative cooling cavity' attached to a dwelling on its shaded side. The cavity has a top external inlet and a bottom internal outlet, and incorporates one or two wet partitions. The air within the cavity, being moist, descends, drawing the outside warm and dry air into the cavity. Evaporation cools the air and raises its humidity. The cool incoming air will reduce inside air temperature and improve comfort.

The performance of a typical cavity to induce cooling ventilation by evaporation was investigated theoretically and experimentally with a full scale model. The temperature drop, velocity and relative humidity of the air were measured. The pattern of the air flow in the cavity was observed. The optimum dimensions of the cavity were established. Buoyancy air flow and fan-assisted air flow were analysed in the steady state.

Since a convective heat transfer coefficient for air flowing between two parallel vertical surfaces was not found in the literature, appropriate convective heat and surface mass transfer coefficients were derived from measurements. The results show the convective heat transfer coefficient to be independent of the separation of the wet surfaces, and that with separation greater than 30mm, each wet surface behaves as a 'free' surface.

The optimum separation between wet surfaces was assessed, and the water removed by evaporation was determined, and found to be small. The Admittance Method was used to assess comfort. Ventilation and evaporation effectiveness were evaluated. An outlet air velocity of 0.3m/s accompanied with a temperature drop of about 6K was achieved. Design proposals for hot arid climates are offered.

TO MY PARENTS and MY WIFE

ACKNOWLEDGEMENT

I acknowledge and appreciate any assistance and aid contributed towards my research. There are many who have contributed to its success but due to limited space I am unable to mention all of them. However, my special gratitude goes to:

Dr. D. Fitzgerald and Dr. W. Houghton-Evans, my supervisors, for their constant encouragement, useful discussions and unfailing advice.

Prof. R. A. Cusens, head of the department, for his support and encouragement during the research, and all members of staff for their friendship.

Mr. J. Higgins, R. Keene and B. Tomlinson of the department for their help during the experimental work.

Mr. G. Broadhead from Department of Electrical Engineering for his skill and help in the period of experimentation.

I would like to extend my special thanks to *my wife and my son* for their great patience and sacrifice during this study, and special thanks to my *father-in-law* for his encouragement during the period of work.

Finally, I would like to give my greatest appreciation to my *family* for their financial support, without it, this work could not be completed.

Nomenclature

This nomenclature is used throughout this thesis, unless locally indicated.

Symbol		Unit
A	area	m^2
BP	Buoyancy pressure	Pa
C_d	discharge coefficient	-
c_p	specific heat capacity of the air	J/kgK
D	cavity width	m
d	diameter	m
f	friction factor	-
g_v	acceleration due to gravity	m/s^2
Gr	Grashof number	-
G_s	vapour resistance of a material	Ns/kg
g	humidity ratio 'moisture content'	kg/kg
Δg	difference in the humidity ratio	kg/kg
h_r	radiation conductance	W/m^2K
h_c	convective heat transfer coefficient	W/m^2K
h_m	surface mass transfer coefficient	m/s
K	flow coefficient	m^2/s
L	length	m
L_e	latent heat of evaporation	J/kg
n	number of velocity heads, flow index	-
N	number of "air changes per hour"	h^{-1}
Nu	Nusselt number	-
m	air flow rate	kg/s
P	pressure	Pa
Pr	Prandtl number	-

P_a	partial pressure of water vapour in the air	Pa
P_s	partial pressure in the saturated boundary layer	Pa
R	gas constant	J/kg K
r	vapour resistivity	Ns/kgm
Q_c	rate of heat flow by convection	W
Q_{ev}	heat transfered by evaporation	W
Q_{cn}	heat flow by conduction	W
Q_r	heat flow by radiation	W
Q_s	sensible heat transfer	W
Q_v	rate of heat flow by ventilation	m ³ /s
Q_{vc}	rate of ventilation cooling	W
Ra	Raleigh number	-
Re	Reynolds number	-
SE	Saturation Efficiency	%
T	absolute temperature	°K
T_{ers}	dry resultant temperature	°C
T_{mr}	mean surface temperature	°C
t	time	s
ΔT	temperature difference	K
T_s	temperature of the surroundings	°C
V	ventilation	m ³ /s
w	water	litre
W	rate of evaporation	kg/m ² s
Y	length of cavity	m
Z	heightof the cavity	m

subscripts

ao	air outside
ai	air
cv	cavity
c	consumed
dep	depression

ev	evaporation
i	inside
in	inlet
mr	mean radiant
o	outside
out	outside, outlet
res	resultant
r	removed
s	surface
wa	water
w	wet

Greek

θ	temperature	$^{\circ}\text{C}$
δ	uncertainty	-
ρ	air density	kg/m^3
μ	dynamic viscosity	Pa s
β	volume coefficient of expansion of air	K^{-1}
λ	thermal conductivity	W/mK
η	ventilation efficiency	%
σ	Stefan-Boltzmann constant	$\text{W/m}^2\text{K}^4$
ε	emissivity of surface	-
$\alpha, \gamma, \omega, \psi, \phi, \varphi$	are constants used in the analysis	-

TABLE OF CONTENT

	Page
ABSTRACT	
ACKNOWLEDGEMENT	
NOMENCLATURE	
TABLE OF CONTENT	
CHAPTER ONE: INTRODUCTION	2
1.1. General	2
1.2. The climate	3
1.2.1. Climate classification with reference to passive design	3
1.2.1.1. The dry or 'arid' climate	4
1.2.2. The hot and arid climate of Egypt	4
1.2.3. Bioclimatic analysis of Cairo	8
1.3. Ventilation	15
1.3.1. Ventilation for health	15
1.3.2. Ventilation for cooling buildings	17
1.3.3. Ventilation for thermal comfort 'cooling the body'	18
1.4. Comfort in dwellings in hot arid climates	21
1.5. Architectural features providing comfort in Egypt	24
1.6. The present work	25
1.7. The purpose and scope of the study	30
1.8. Method of study	30
1.8.1. Historical	31
1.8.2. Experimental	31
1.8.3. Theoretical	32
CHAPTER TWO: EVAPORATIVE COOLING TECHNIQUES AND LITERATURE REVIEW	34
2.1. Introduction	34
2.2. Evaporative cooling systems	34
2.2.1. Direct evaporative cooling	34
2.2.2. Indirect evaporative cooling	35
2.3. Direct evaporative cooling in history	37
2.3.1. Courtyards	38

2.3.2.	Wind towers	40
2.3.3.	Water	40
2.3.4.	Windows	40
2.4.	Evaporative cooling in modern architecture	45
2.4.1.	Desert cooler	45
2.4.2.	Subterranean dwelling	45
2.4.3.	Solar dehumidification	49
2.4.4.	Radiative cooling	49
2.4.5.	Convective cooling	51

CHAPTER THREE: THEORY REVIEW AND ANALYSIS 54

3.1.	Introduction	54
3.2.	Ventilation theory	54
3.2.1.	Ventilation efficiency	59
3.3.	Evaporation	59
3.3.1.	Latent heat of evaporation	60
3.3.2.	Evaporation efficiency	60
3.3.3.	Evaporation at a plane vertical surface	61
3.3.3.1.	The rate of evaporation	62
3.3.3.2.	Vapour diffusion within materials	65
3.4.	Heat transfer in Buildings	66
3.4.1.	Conduction	66
3.4.2.	Radiation	67
3.4.3.	Convection	68
3.4.3.1.	Convective heat transfer coefficients	68
3.4.3.1.1.	Natural convective heat transfer coefficients	69
3.4.3.1.2.	Forced convective heat transfer coefficients	70
3.5.	Air flow and heat transfer in cavities	72
3.5.1.	Air flow in cavities	73
3.5.1.1.	Velocity heads	74
3.5.2.	Heat transfer in cavities	75
3.6.	Theoretical analysis	79
3.6.1.	Analysis of the buoyancy air flow analysis	79
3.6.2.	Analysis of the fan-assisted air flow model	85

CHAPTER FOUR: APPARATUS DESIGN AND MEASUREMENTS 93

4.1.	Introduction	93
4.2.	Design of the apparatus	94
4.2.1.	Apparatus heat flow	94
4.2.2.	Scale effect	95
4.3.	Physical description of the apparatus	96
4.3.1.	Forced flow apparatus	96
4.3.1.1.	The cavity	96
4.3.1.2.	The inlet and the outlet	96
4.3.1.3.	Air supply	100
4.3.1.4.	Air temperature simulation across the inlet	100
4.3.1.5.	Air velocity distribution across the inlet	101
4.3.2.	Buoyancy flow apparatus	101

4.3.2.1.	The cavity	101
4.3.2.2.	The inlet and the outlet	104
4.3.3.	The wet surface	104
4.3.3.1.	Positions of wet mats	104
4.3.3.2.	The wetting technique	104
4.4.	Equipment and control	107
4.4.1.	Air velocity	107
4.4.2.	Air relative humidity	108
4.4.3.	Temperature	109
4.4.4.	Temperature and speed control	110
4.4.6.	Flow visualisation	110
4.5.	Measurement procedures	114
4.6.	Apparatus limitation and range of application	116

CHAPTER FIVE: EVAPORATIVE COOLING BY BUOYANCY AIR FLOW: RESULTS 124

5.1.	Introduction	124
5.2.	The tests	124
5.3.	Tests of group one	126
5.4.	Results	128
5.4.1.	Initial flow visualisation	128
5.4.2.	Cooling	131
5.4.2.1.	Outlet air velocity	131
5.4.2.1.1.	The effect of the outlet height on air flow	135
5.4.2.1.2.	The effect of cavity width on outlet air velocity	136
5.4.2.2.	Outlet air relative humidity	138
5.4.2.3.	The effect of cavity width on air temperature drop	140
5.4.2.4.	The effect of cavity width on cooling by buoyancy air flow	140
5.4.3.	Difference in the humidity ratio (Δg)	143
5.4.3.1.	Water removed by evaporation	144
5.4.4.	The effect of wet mat separation on cooling	148
5.4.4.1.	The effect of wet mat separation on air velocity	149
5.4.4.2.	Nature of the flow	151
5.4.4.3.	The effect of wet mat separation on air relative humidity	153
5.4.4.4.	The effect of wet mat separation on the humidity ratio difference	156
5.4.4.5.	The effect of wet mat separation on the mass flow rate	161
5.4.4.5.1.	Air velocity distribution	161
5.4.4.5.2.	Flow visualisation of the 160 mm cavity	166
5.4.4.5.3.	Air relative humidity distribution	170
5.4.5.	Measured cooling as a function of time, or 'Cavity Life'	173
5.4.6.	The effect of inlet air temperature on cooling	174
5.5.	Tests of group two	177
5.6.	Results	180
5.6.1.	The effect of the temperature difference between the air in the room and that at the inlet on air temperature drop from evaporation	180
5.6.2.	The effect of the temperature difference between the air in room and that at the inlet on the outlet air velocity	180
5.6.3.	The effect of the temperature difference between the air in room and that at the inlet on the outlet air relative humidity	181

5.6.4.	The effect of the temperature difference between the air in the room and that at the inlet on cooling	181
5.6.5.	The effect of the temperature difference between the air in the room and that at the inlet on the ventilation rate	186
5.7.	Discussion and conclusion	187
5.7.1.	Tests of group one	187
5.7.2.	Tests of group two	191

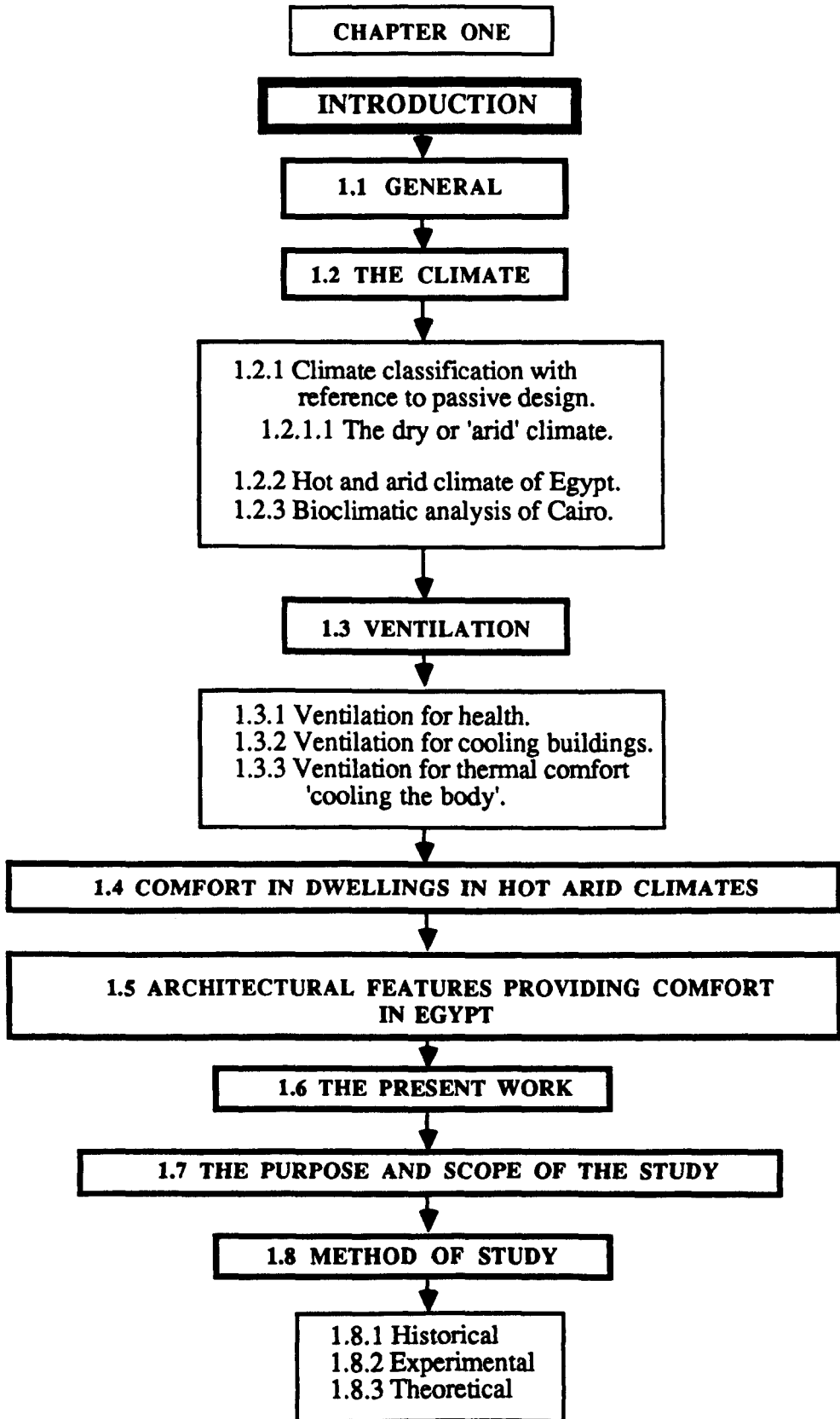
CHAPTER SIX: EVAPORATIVE COOLING BY FORCED AIR FLOW: RESULTS 194

6.1.	Introduction	194
6.2.	Preliminary observations	194
6.2.1.	Air velocity distribution at the inlet	194
6.2.2.	Air flow across the cavity	197
6.2.2.1.	The effect of cavity width on air flow pattern	197
6.3.	Evaporative cooling observations	204
6.4.	Results	204
6.4.1.	The effect of wet mat number and their separation	209
6.4.1.1.	Air temperature drop	209
6.4.1.2.	Air relative humidity at the outlet	209
6.4.1.3.	The cooling rate	210
6.4.2.	Outlet air velocity	212
6.4.2.1.	The effect of the outlet height on air flow	212
6.4.2.2.	The effect of the cavity width on air flow at the outlet	214
6.4.3.	Outlet air relative humidity	216
6.4.4.	Temperature drop	216
6.4.4.1.	The effect of the cavity width on air temperature drop between inlet and the outlet	216
6.4.4.2.	The effect of the outlet height on the air temperature drop between inlet and outlet	222
6.4.5.	Relative humidity	222
6.4.5.1.	The effect of the cavity width on air relative humidity at the outlet	222
6.4.5.2.	The effect of the outlet height on relative humidity	226
6.4.6.	Cooling	226
6.4.6.1.	The effect of the cavity width on cooling	226
6.4.6.2.	The effect of outlet height on cooling	227
6.4.7.	Further analysis	232
6.4.7.1.	The difference in the humidity ratio	232
6.4.7.2.	The effect of wet mat separation on the difference in the humidity ratio	233
6.4.7.3.	The convective heat transfer coefficient	237
6.8.	Discussion and conclusion	240

CHAPTER SEVEN: PREDICTED AND MEASURED CONVECTIVE HEAT TRANSFER COEFFICIENTS:GENERAL DISCUSSION 247

7.1.	Introduction	247
------	--------------	-----

7.2.	The uncertainties	247
7.3.	Results	253
7.3.1.	Buoyancy air flow	253
7.3.1.1.	Outlet air velocity	253
7.3.1.2.	Air temperature drop between inlet and outlet	257
7.3.1.3.	Cooling	259
7.4.	The surface mass transfer coefficient h_m	263
7.5.	Measured convective heat transfer coefficient h_c	263
7.5.1.	The convective heat transfer coefficient h_c for a 'free' surface	265
7.6.	Discussion and conclusion	
 CHAPTER EIGHT: DESIGN EVALUATION		270
8.1.	Introduction	271
8.2.	Evaluation of water consumption	271
8.2.1	Evaporatively cooled cavity with forced air flow	271
8.2.2	Evaporatively cooled cavity with buoyancy air flow	273
8.3	Evaluation of thermal comfort	278
8.4	Evaluation of ventilation rates	282
8.5	Design application	285
8.5.1	Ventilation effectiveness	290
8.5.1.1	Mixing and air movement	290
8.6	Discussion and conclusion	303
 CHAPTER NINE: CONCLUSIONS AND SUGGESTIONS FOR FURTHER WORK		304
9.1.	Conclusions	304
9.2.	Design application	308
9.3.	Suggestions for further work	312
 REFERENCES		313
Appendix A		323
Appendix B		324
Appendix C		325



CHAPTER ONE

INTRODUCTION

1.1 GENERAL

There is virtually no place on earth that is too hot for man to survive. In the long, slow course of evolution man's physiology has been tailored to his environment, meeting the challenges of mild and severe climate alike. For centuries, people in different parts of the world have lived in these inhospitable areas without mechanical cooling. They learnt to cope with and make use of the outside climate to create and provide a comfortable environment in their shelters. This was mainly accomplished by experience through generations and much trial and error.

One of the primary architectural functions of a building is to provide a healthy and comfortable environment. In cold climates such as that of Great Britain (Northern Europe), heat is needed in dwellings. In hot arid climates, cooling is a greater need.

Over the past three decades, it became possible with the advent of oil, gas and electricity to disregard completely the effect of climate in the design and construction of buildings. This was met by mechanical aids. Although these were successful in controlling the internal environment, they were dependent entirely on the use of large quantities of energy. Today, high energy costs impose restrictions on their application, and energy sources will not last indefinitely. The rapid increase of the world population, especially in the third world, a million new born infants every nine month in Egypt alone (United Nation statistics, 1988), reduces the amount of energy available per capita (United Nation statistics, 1970 to 1986, Table 1.1) which increases the importance of 'free energy' systems.

Table 1.1 Gross production and consumption of electricity in Egypt

Year	1970	73	75	78	79	80	81	82	83	84	85	1986
Consumption GJ per capita	17	19	25	34	34	35	37	37	38	38	38	38

Production = consumption in all years.

Source: United Nation energy statistics (1981 to 1986).

Because of the socioeconomic structure of Egypt's population, dependence on energy to provide a comfortable environment in buildings is especially questionable. Urbanisation, a result of rapid industrialisation in Egypt, was accompanied by much replacement of traditional housing with new high-rise blocks regardless of the surrounding microclimate. Moreover, modern large scale changes in buildings and housing layouts have changed the environment itself. Consumption of energy for lighting, cooling and electric appliances releases waste heat to the air. The United Nation energy statistics (1986) estimate the consumption of energy of 50kWh per month for a standard dwelling of 50m² (two rooms and a kitchen). Ultimately all of the energy consumed in dwellings or office blocks leaves as heat. As a result, a significant increase of the air temperature in cities takes place, commonly 6 to 10K (Abrams, 1985) and (Morris, 1980). In dwellings, an increase of 4K corresponds to an increase of 10% of the cooling requirements.

In hot climates, buildings have problems of cooling during the summer. In a temperate climate like that of Great Britain, cooling in summer can be achieved by cross-ventilation through open windows. In hot climates, the outside air is too hot during the day for cooling to be achieved in that way, especially when the air is above the body temperature.

In hot arid climates such as that of Egypt, air movement is not always cooling. It increases the feeling of heat by the convection current near the body, and it is therefore important that air should be cooled before flowing into dwellings.

It is important to study ways in which cooling ventilation could be improved by simple and cheap means. In hot arid climates, direct evaporative cooling may be desirable. Therefore, the purpose of this study is to examine the possibility of promoting cooling ventilation. Hot air may be cooled and moved by buoyancy resulting from evaporation before entering the dwelling. In this work attention is paid to the hot arid climate of Egypt.

1.2 THE CLIMATE

1.2.1 Climate classification with reference to passive design

Several attempts have been made to classify the climate, the first by the ancient Greeks, who classified the earth into three main divisions: torrid, temperate and frigid zones based on solar illumination, temperature difference but not precipitation (Miller,

1950). The classification of the climate specially in relation to passive design is mentioned by van Straatan (1967). In 1971, Barry and Chorley indicated the degree of aridity and warmth as significant criteria. The degree of aridity is determined by the "effective precipitation" which means precipitation minus evaporation. The Koppen classification recognises major regions of world climate (Trewartha, 1968):

- tropical rainy climates with no cool seasons
- dry climates
- middle latitude rainy climates with mild winters

These regions are subdivided into climates based on the seasonal distribution of rain or the degree of dryness or coldness. Our investigation was related to a hot dry or 'arid' climate which is described below.

1.2.1.1 The dry or 'arid' climate

Dry climates cover a considerable area of the world's land. Thornthwaites (1958) subdivided dry climate into two main types: arid or 'desert' and semi-arid or 'steppe'. The dominate feature of a dry climate is that the annual rainfall is very low. Koenigsberger and Ingersoll (1976) defined a dry climate as one where heat is the dominant problem. Rainfall and relative humidity are low, and potential of evaporation is high. Air usually contains some water vapour in a hot desert, but is far from saturation. Winds are inclined to be strong. There is a high degree of solar radiation and a high rate of radiation loss to the sky at night.

Meigs (1953) has defined the boundaries between 'arid' and 'semi-arid' zones by rainfall. In an arid zone, rainfall is not adequate for crop production, whereas in a 'semi-arid' zone it is sufficient for certain types of crops and grass. Within an 'arid zone', there are degrees of dryness. Meigs also divided the arid zone into two, 'arid' and 'extremely arid'. According to Koenigsberger and Ingersoll (1976), these zones occur in two belts: at latitudes between approximately 15° and 30°(North) and south of the Equator. Egypt is an example of these climates.

1.2.2 The hot and arid climate of Egypt

Egypt covers nearly one million square kilometres, between latitude 29° and 31°N. The population is about 55 millions (1989). Cairo is the largest city (the capital) with 15 million inhabitants. Although most of Egypt is desert, there are three exceptions

to this (Simiaika, 1953):

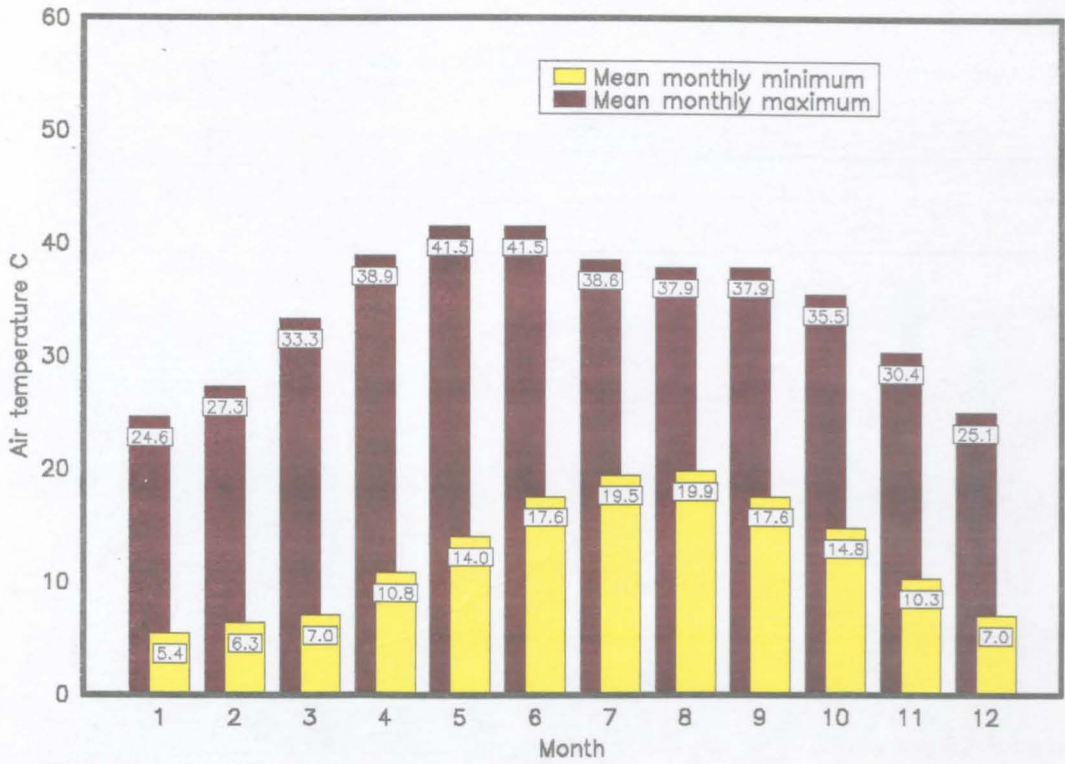
- the area along the river Nile
- the Mediterranean littoral
- the great oases.

The climate of Egypt can be divided into two main seasons: a long hot and dry summer and a short, mild and dry winter. The summer starts in June and continues until October. During summer, the air temperature reaches its peak in June and July. The mean air temperatures are 30, 32 and 30°C in June, July and August respectively. In winter, they are 16, 15 and 16°C in December, January and February respectively (Figure 1.1 b). The maximum monthly temperature is 41.5°C in May and June which are the hottest months (Figure 1.1 a).

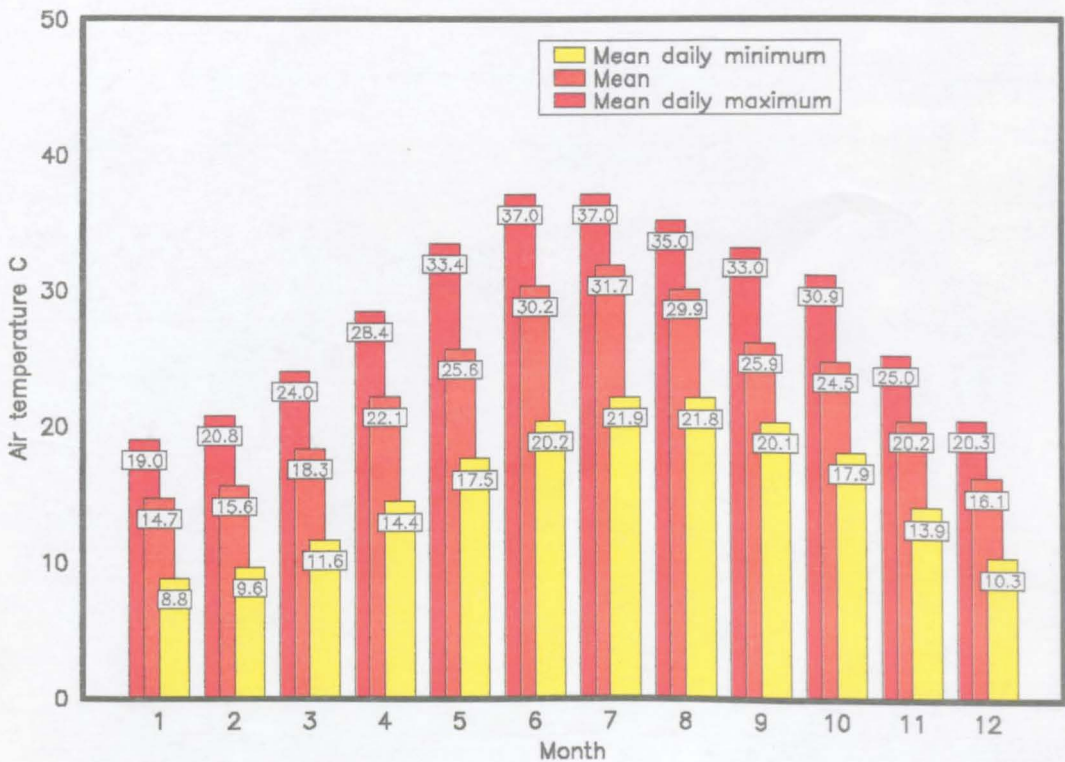
During summer the humidity is low (38%), but it is moderate in winter (60%), (Figure 1.2). In cities such as Aswan and Cairo, the humidity can be very low as shown in Table 1.2. At 0800 hours the annual mean is 39% and 63% respectively in the two cities, falling to 21% and 29% respectively at 1400 hours, clearly showing the potential of evaporative cooling. In Cairo, the average relative humidity in June, July and August at 0800 hours is 57%, falling to 21% at 1400 hours underlining the potential for cooling when it is very much needed.

Table 1.2 Mean relative humidity in major cities (Aswan and Cairo).

City	Hours	Relative humidity %											
		Jan	Feb	Mar	Apr	May	Jun	Jul	Aug	Sep	Oct	Nov	Dec
Aswan	0800	52	48	36	29	29	26	31	24	37	40	46	50
	1400	29	22	17	15	15	16	16	18	19	21	26	31
Cairo	0800	69	64	63	55	50	55	65	68	67	67	68	69
	1400	40	33	27	21	18	20	24	28	31	31	38	41



a- Monthly mean air temperature.



b- Daily air temperature

Figure 1.1 Monthly mean and daily air temperature in Cairo

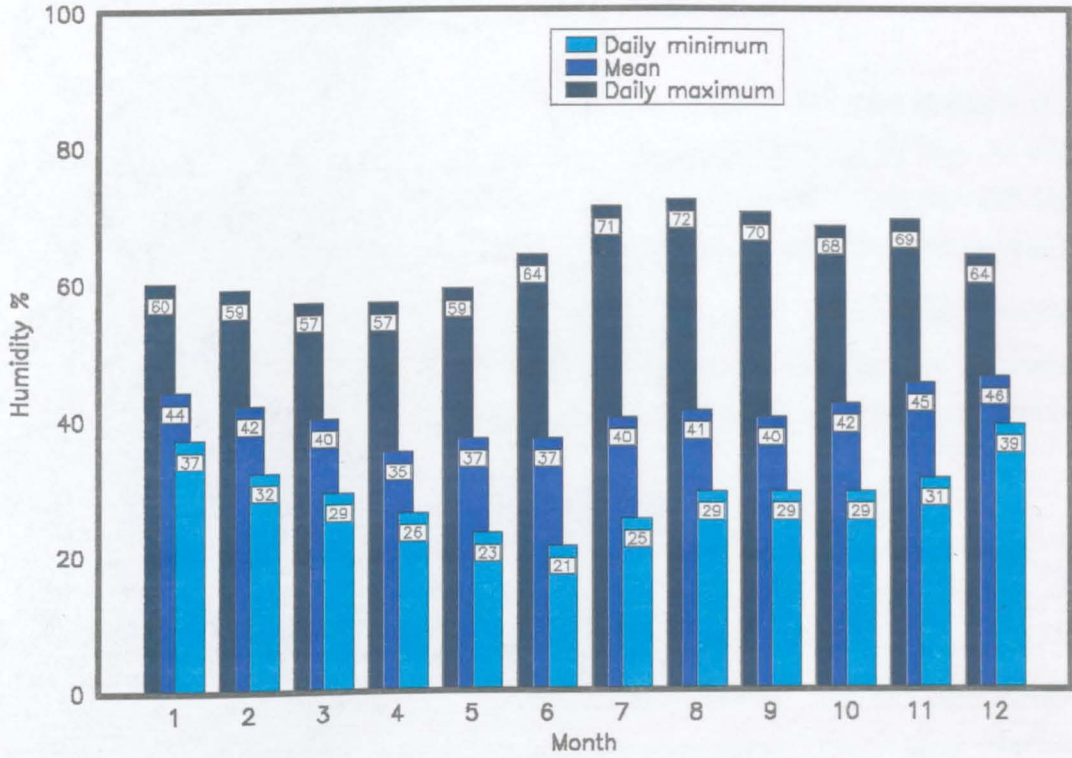


Figure 1.2 Monthly relative humidity in Cairo

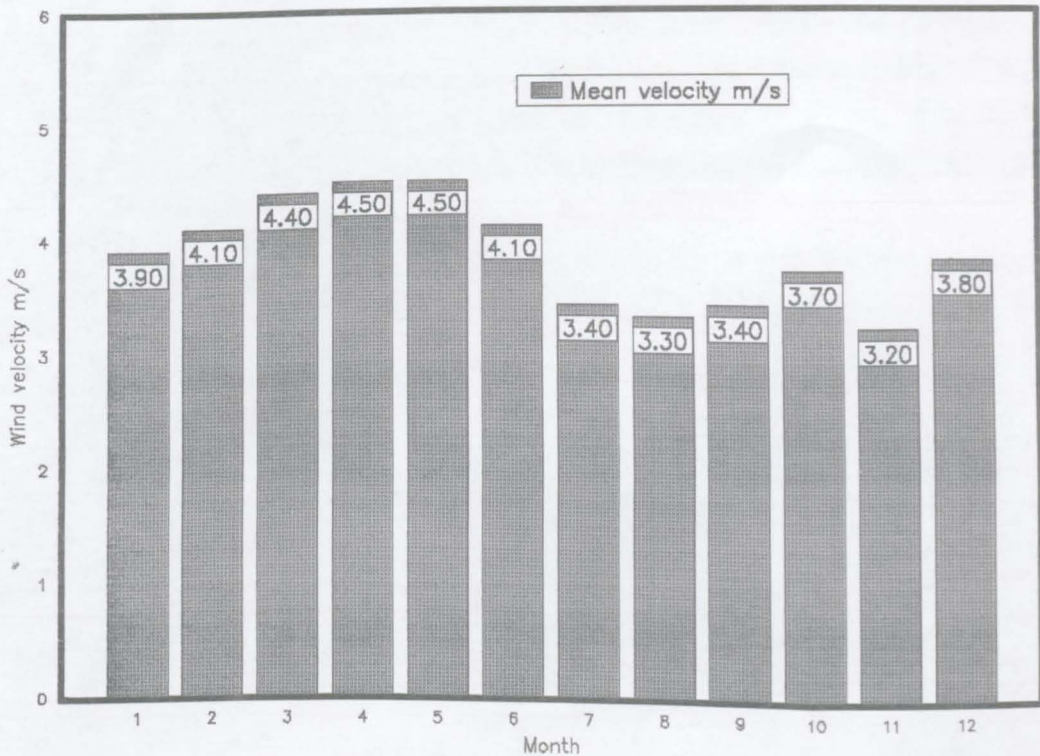


Figure 1.3 Monthly mean wind velocity in Cairo.

In general, wind is inclined to be strong. In summer, the mean wind speed in Cairo is about 3.5m/s (Figure 1.3), prevailing from north-west.

There is a little cloud with high insolation. The presence of a clear sky, low cloud cover and low humidity assist a quick rise in air temperature during the day. At night, energy is lost quickly and air temperatures fall. The variation between day and night becomes as much as 15K in some summer months. Most solar radiation goes to heat the ground. The surface temperature of the sand often exceeds 65°C near Cairo (Kendrew, 1942). The climatic data for Cairo (Appendix 1) shows that the hot summer is characterised by very low relative humidity (afternoon), high outside air temperature and low wind speed.

1.2.3 Bioclimatic analysis of Cairo

A Bioclimatic analysis requires some comfort indices to assess discomfort in Cairo. Carl Mahoney (1980) proposed a set of "comfort indices" which relate directly to air temperature and relative humidity. The limits of comfort vary with the "humidity group" of Table 1.3. The index makes an important distinction between comfort limits for the day and those for the night (Table 1.4). Evans (1980) proposed a set of "comfort indices" similar to those by Mahoney. The "comfort index" varies with humidity, the time of the day, air movement and the level of clothing. The index is divided into A, B and C. A is for light summer clothing and air movement of 1.0m/s. B is for light summer clothing and negligible air motion. C is for warm indoor clothing (Table 1.5).

Olgyay (1967) developed a 'Bioclimatic chart' which takes into consideration all main factors influencing thermal comfort (air temperature, humidity and movement, mean radiant temperature, solar radiation). The chart has been revised by Arens et al.(1984) to incorporate recent results and has become a 'Psychrometric format' or bioclimatic chart. An area in which an individual would feel comfortable is called a 'comfort zone'. The climatic data of Cairo (outside air temperature and relative humidity) were used in Evans's index, Olgyay's Bioclimatic chart, and Arens et al. charts to assess the severity of the climate. Results are shown in Figure 1.4 to Figure 1.6.

Table 1.3 Variations of "comfort indices" according to humidity.

Average relative humidity %	Humidity group
below 30	1
30 to 50	2
50 to 70	3
above 70	4

Table 1.4 Comfort indices (°C) according to Mahoney (1980).

Humidity group of Table 1.3	Annual average air temperatures					
	Over 20°C		15 - 20°C		Below 15°C	
	Day	Night	Day	Night	Day	Night
1	25-34	17-25	23-32	14-23	21-30	12-21
2	25-31	17-24	22-30	14-22	20-27	12-20
3	23-29	17-23	21-28	14-21	19-26	12-19
4	22-27	17-21	20-25	14-20	18-24	12-18

Table 1.5 Comfort indices (°C) according to Evans (1980).

Humidity group of Table 1.3	Comfort Indices					
	A		B		C	
	Day	Night	Day	Night	Day	Night
1	32.5-29.5	29.5-27.5	30-22.5	27.5-20	22.5-18	20-16
2	30.5-28.5	29-26.5	28.5-22.5	26.5-20	22.5-18	20-16
3	29.5-27.5	28.5-26	27.5-22.5	26-20	22.5-18	20-16
4	29-26	28-25.5	27-22.5	22.5-20	22.5-18	20-16

A for upper range of comfort with 1.0m/s air movement.

B for range of comfort with light clothing.

C for low range of comfort with normal or warm clothing.

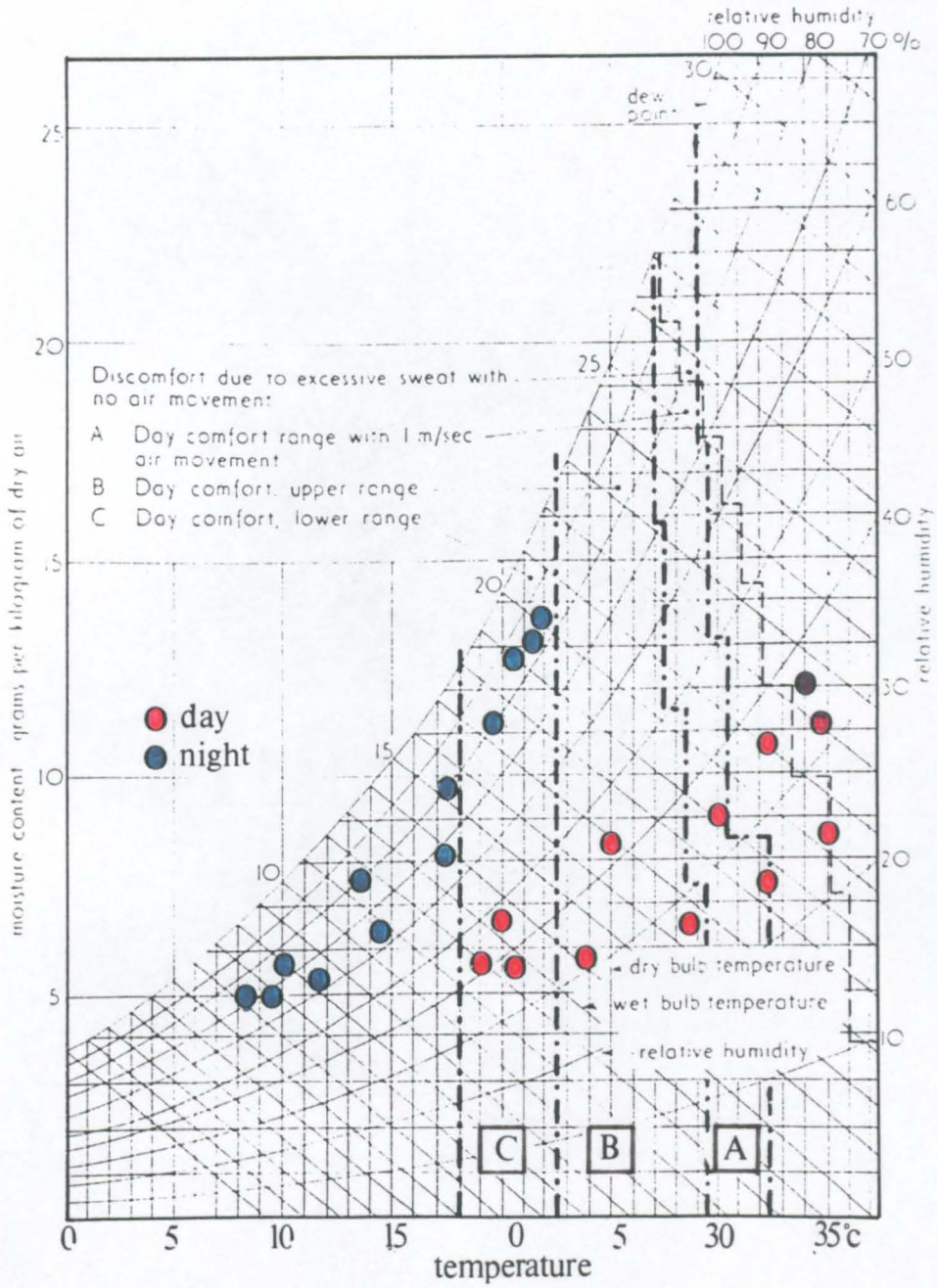
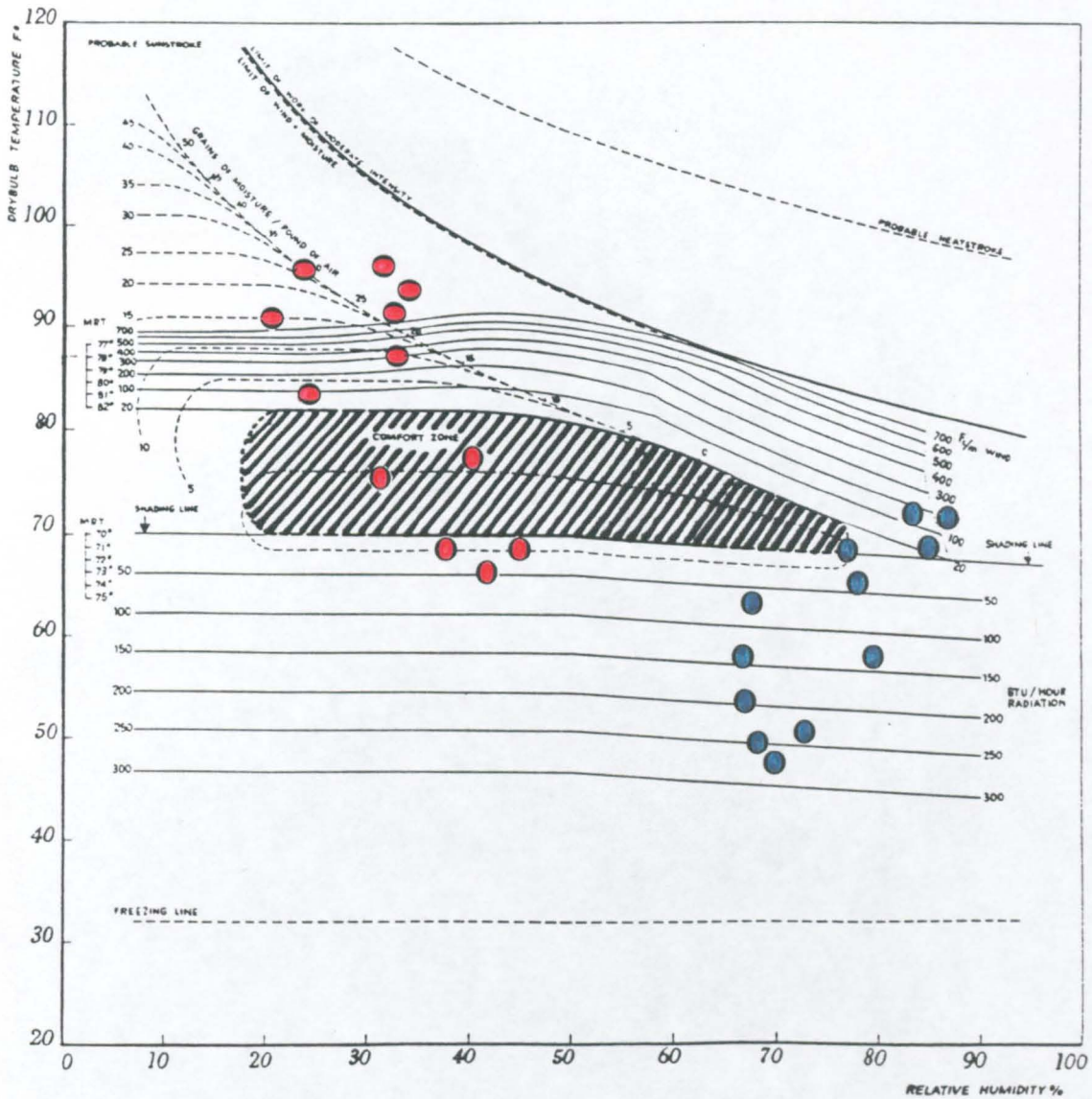
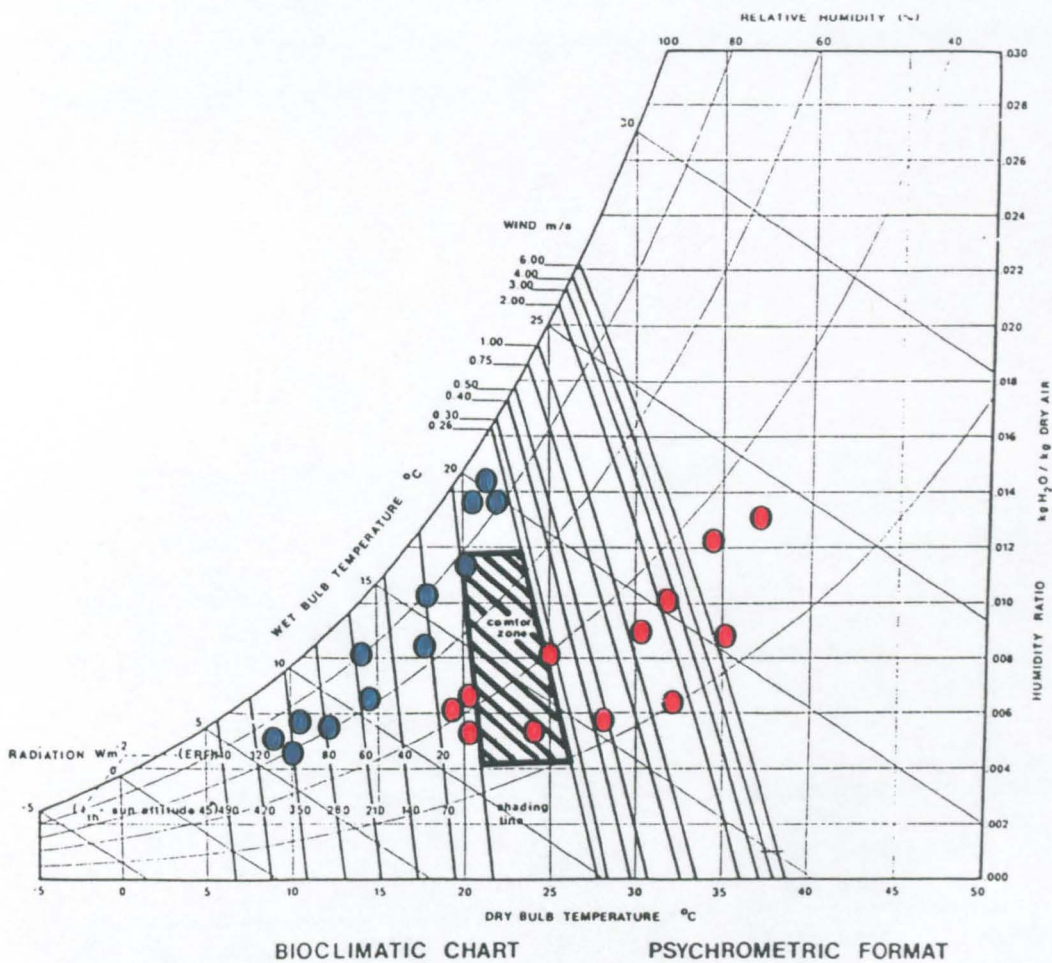


Figure 1.4 Air temperature and humidity of Cairo on Evans "comfort index".



● day
● night

Figure 1.5 Air temperature and humidity of Cairo on Olgyay's Bioclimatic chart.



- day
- night

Figure 1.6 Air temperature and humidity of Cairo on Arens et al. Bioclimatic chart or 'Psychrometric format'.

Figures 1.5 and 1.6 demonstrate that seven months of the year during the day are far above the upper boundary of the 'comfort zone' and three months are below it. Only two months are reasonably comfortable. Most nights are scattered outside the 'comfort zone'. Figures 1.5 and 1.6 also show that for a mean air temperature during the day above 30°C and about 30% R.H., air movement and moisture are required to reduce discomfort. In June, July and August (Figure 1.6) promoting air movement only is insufficient. Analysis was carried out to identify the period when moisture increase is needed so that discomfort is reduced. The months outside the 'comfort zone' were divided into four zones (Figure 1.7). Diagnosis and proposed prescription of each zone for day and night are given in Table 1.6.

Table 1.6 The bioclimatic diagnosis and prescription for Cairo.

Zone	Month		Diagnosis		Proposed prescription	
	Day	Night	Day air temp., R.H.	Night	Day	Night
1	Jan	Jan	Slightly cool	Cold	Mild exposure	Indirect solar
2	Feb	Feb	19 to 21°C		to direct solar	heat
		Mar			heat	190 to 360W/m
		Apr	Moderate low	Semi-humid		
		Dec	humidity			
2	Apr	May	Hot	Cool	Evaporative	Indirect solar
	May	Jul	28 to 32°C		cooling	heat
		Nov	Arid	Semi-humid	moisture needed	50 to 140 W/m
			25% R.H.		5 to 8 g/kg	
3	Jun	Aug	Very hot	Temperate	Evaporative	Air flow
	Sep	Sep	32 to 35°C		cooling	< 0.25 m/s
	Oct	Oct	Semi-arid to arid	Semi-humid	moisture needed	
			20 to 30%	to humid	8 to 12 g/kg	
4	Jul	—	Very hot	Slightly warm	Evaporative	—
	Aug		35 to 37°C		cooling	
			Semi- arid	humid	moisture needed	
			30 to 35%		12 to 14 g/kg	

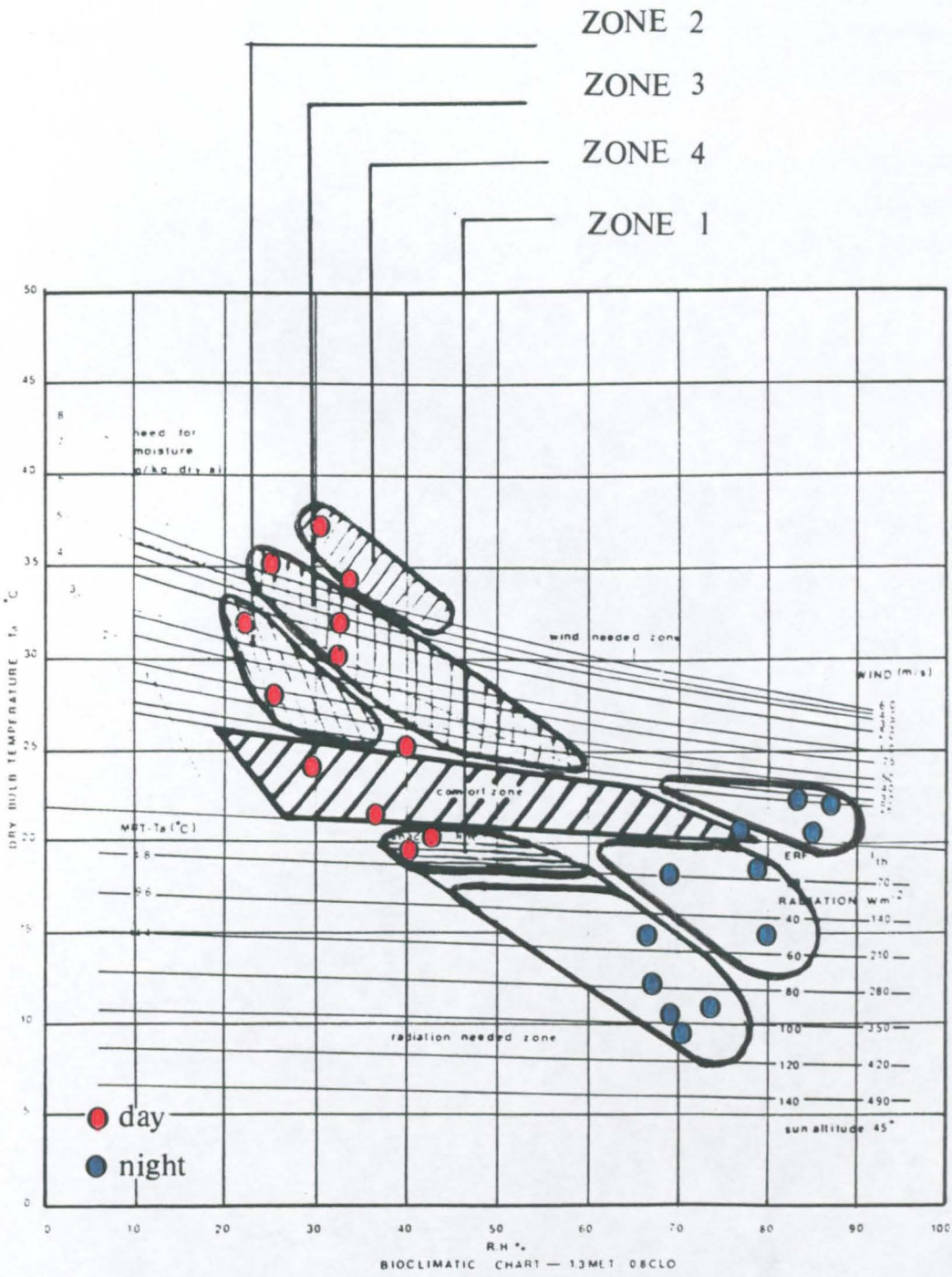


Figure 1.7 Summer and winter discomfort evaluation according to Arens Bioclimatic chart.

In order to reduce discomfort, a moisture increase of the air is needed from April to October (Table 1.6). Some days are slightly below the lower limit of comfort, however, the Mahoney scale considered them within the lower range of comfort (Index C). Although discomfort occurs in five months (Figure 1.4), air movement of above 1.0m/s is needed, and with high air temperature this could be insignificant.

In conclusion, the analysis suggests that comfort can be achieved during the summer if the moisture in the air is increased, and accompanied with air movement. These increases of moisture in the air which flow through dwellings during the day could be as follows (Table 1.6):

- in April to May, about 0.005 to $0.008 \text{kg}_{w,v}/\text{kg}_{air}$ (zone 2).
- in June, September and October, about 0.008 to $0.012 \text{kg}_{w,v}/\text{kg}_{air}$ (zone3).
- in July and August, about $0.014 \text{kg}_{w,v}/\text{kg}_{air}$ (zone 4).

This indicates that the moisture in the air should be increased from $0.005 \text{kg}_{w,v}/\text{kg}_{air}$ to $0.014 \text{kg}_{w,v}/\text{kg}_{air}$ during summer so that comfort in dwellings can be achieved.

1.3 VENTILATION

Ventilation provides cooling by using moving air to carry away heat. Air movement may be natural resulting from wind or convection, or by a fan. In either case, ventilation for cooling may involve either the building or the human body. In this study our concern is with natural ventilation in dwellings to maintain a healthy internal environment, to cool the surrounding surfaces of the dwelling (structural cooling), and to provide thermal comfort.



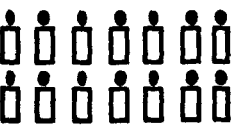
1.3.1 Ventilation for health

Ventilation is required to remove odours, products of combustion, pollutants generally, and to prevent condensation in dwellings. Ventilation is also essential to reduce the concentration of radon which comes out of the ground and from all building materials which have been in the ground. In recent years, attention was drawn to radon as a health hazard. Research carried out by the British Medical Association (BMA) relates lung cancer to radon coming from the ground beneath dwellings (BMA, 1989).

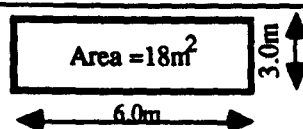
Ventilation required for health is little compared with that needed for cooling. Research suggests various ventilation standards for dwellings. Evans (1980) suggests one "air change per hour" as the minimum rate of ventilation for odour removal. Yaglou and Whitheridge (1937) suggest a minimum ventilation rate of 1L/s per person whatever the number of occupants (Table 1.7). Nevertheless, indoor pollution is far more now than we had then.

Klauss et al. (1970) summarised work done by Tredgold (1836) who reported that to remove carbon dioxide and moisture, and to provide oxygen to candles and lamps, the minimum air supply is 1.7L/s/person: double those of Table 1.7. ASHRAE (1986) recommended 2.3L/s/person as the minimum rate of ventilation (over twice that given by Yaglou and Whitheridge). Van Straatan (1967) has established a relation between the recommended ventilation rate and the 'air space' per person (Figure 1.8). For an 'air space' 40m³ occupied by three adults, the recommended rate of ventilation is 4.4L/s/person (Figure 1.8) which is higher than those above. However, Klauss et al.(1970) stated that the carbon dioxide concentration was not a very good indicator for ventilation requirements.

Table 1.7 Recommended ventilation rate for health by Yaglou and Witheridge (1937).

Ventilation rate L/s	Number of occupants Adults	Ventilation rate per person L/s
3		1
8		1
12		1

For an air space about 40m³
Height of the dwelling 2.25m



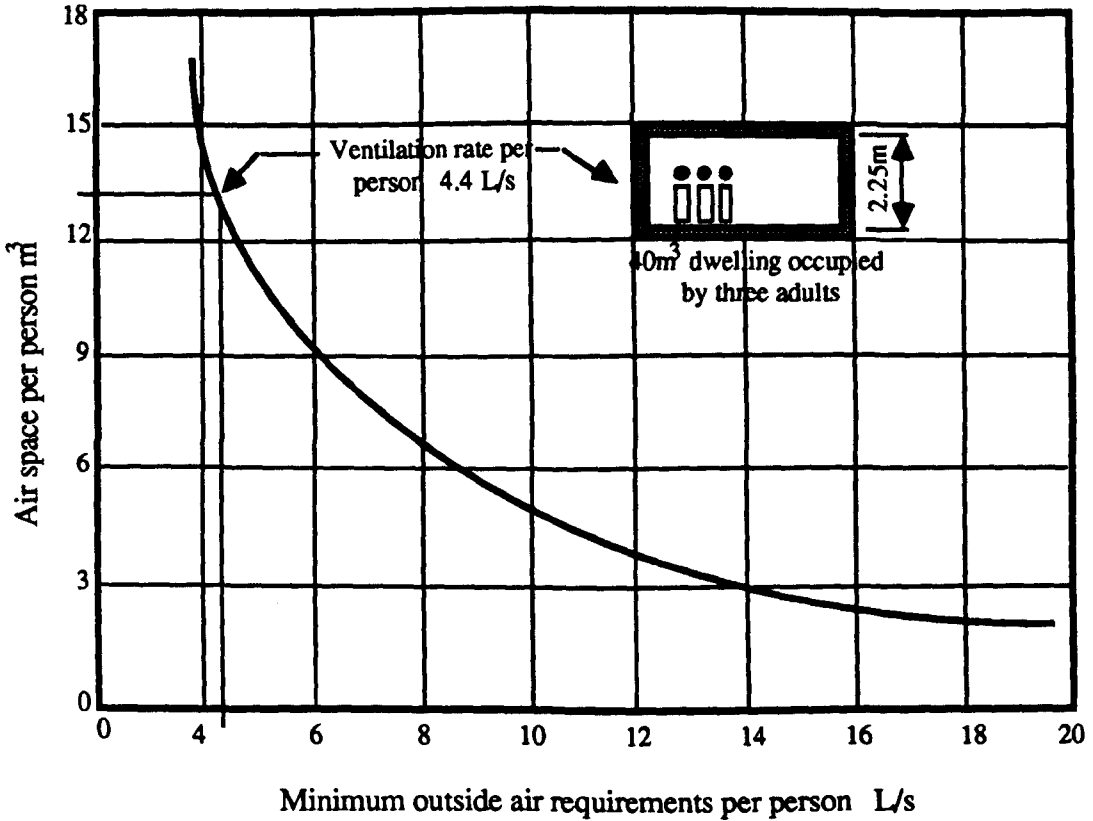


Figure 1.8 Minimum desirable ventilation requirements for unconditioned dwelling according to van Straatan (1967).

1.3.2 Ventilation for cooling buildings

Ventilation is useful in cooling buildings (structural cooling) when the interior air temperature is above the outside air temperature. Heavy buildings may require higher ventilation (especially in the afternoon, 1700 h) so that radiation of stored heat is reduced.

When a dwelling at air temperature T_{ai} is ventilated by outside air at temperature T_{ao} , the heat removed by ventilation Q_v is:

$$Q_v = m c (T_{ai} - T_{ao}) \quad \text{W} \quad [1.1]$$

where

m = air flow rate kg/s

c = specific heat capacity of air, 1000 J/kgK

As the air temperature in the dwelling falls, heat is transferred from the surrounding structure to the air by convection. Cooling by convection Q_c is expressed by:

$$Q_c = A h_c (T_s - T_{a0}) \quad \text{W} \quad [1.2]$$

where

A = area of heat transfer m^2
 h_c = convective heat transfer coefficient $\text{W/m}^2 \text{K}$
 T_s = temperature of the surroundings $^{\circ}\text{C}$

A study by Evans (1980) suggests that a ventilation rate of 10 "air changes per hour" is enough for building cooling. Using a wind tower to cool buildings via a basement, Yagoubi and Golneshan (1986) carried out theoretical work on the effect of ventilation at night and during the day on basement temperature. With ventilation from 2300 to 0600 hours, basement temperature remained constant using one "air change per hour". As ventilation increased to 12 "air changes per hour", air temperature fell by 2K. Increasing ventilation up to 30 "air changes per hour" was insignificant. They concluded that in hot arid climates day ventilation should be avoided while night ventilation should be promoted.

1.3.3 Ventilation for thermal comfort 'cooling the body'

Ventilation is extremely effective for cooling people directly. Air motion reduces the insulating effect of the layer of still air at the skin surface and produces the "wind-chill" effect. Air flow over the skin also increases the rate of evaporation from the skin. With sufficient ventilation, some people may feel comfortable even when the air temperature is above the normal limit of comfort.

In order to maintain the body temperature nearly constant at 37°C , the body must balance its rate of heat dissipation against its heat gain from metabolism plus any heat gained from the environment. Heat exchange between the body and the environment takes place through radiation, convection, conduction and heat loss from the body by evaporation as shown in Figure 1.9. Van Straatan (1967) shows at normal condition: air

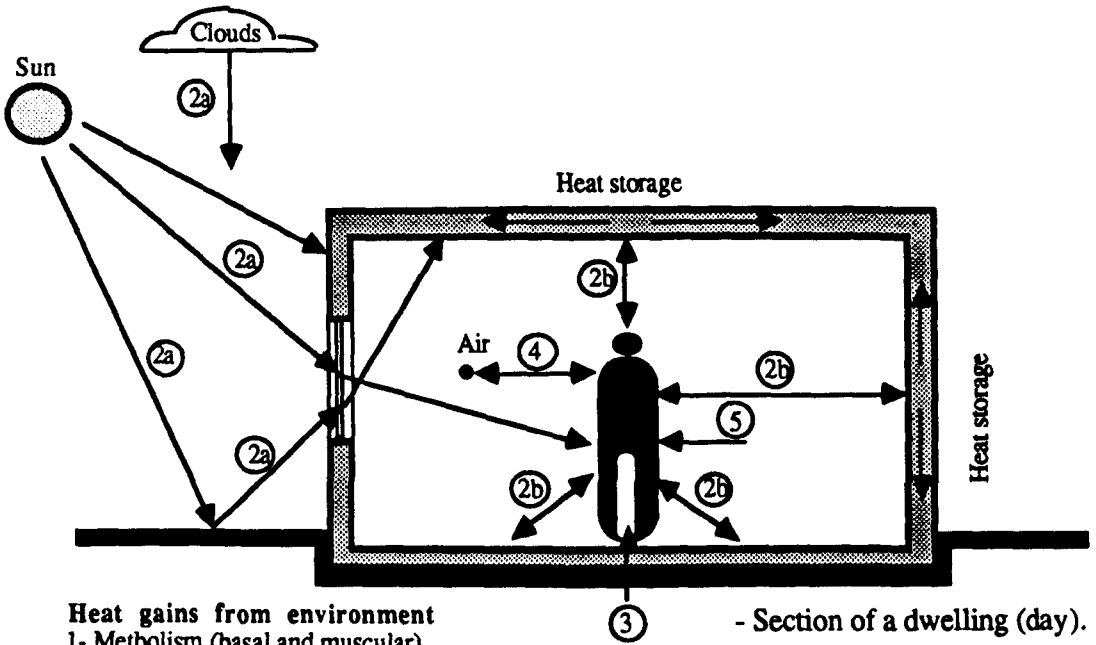
temperature 18°C, relative humidity of 40% to 60%, air velocity less than 0.25m/s and the person is sitting, heat will dissipated as described in Figure 1.10 a. The values given in Figure 1.10 b by the BRE (British Research Establishment, 1973) show little change.

Adolph (1947) and Givoni (1976) indicate that when the air temperature is higher than the temperature of the skin, the increase in convective heat exchange warms the body, but at the same time increased air velocity will increase the evaporation of moisture and consequently the cooling. The cooling effect in terms of air flow over the body according to Arens (1981) is given in Table 1.8. It is assumed that a typical individual is comfortable in light clothing with air temperature of 25°C and standing in "still air" (12K below skin temperature, sufficient to increase convection losses from the body). Table 1.8 shows that the increase in the comfort air temperature made possible by air motion. However, the dependence on air movement, especially dry air, as stated by Arens (1981) may be difficult when the temperature of the air is approaching that of the body.

Table 1.8 Cooling effect of air motion at 60% relative humidity.

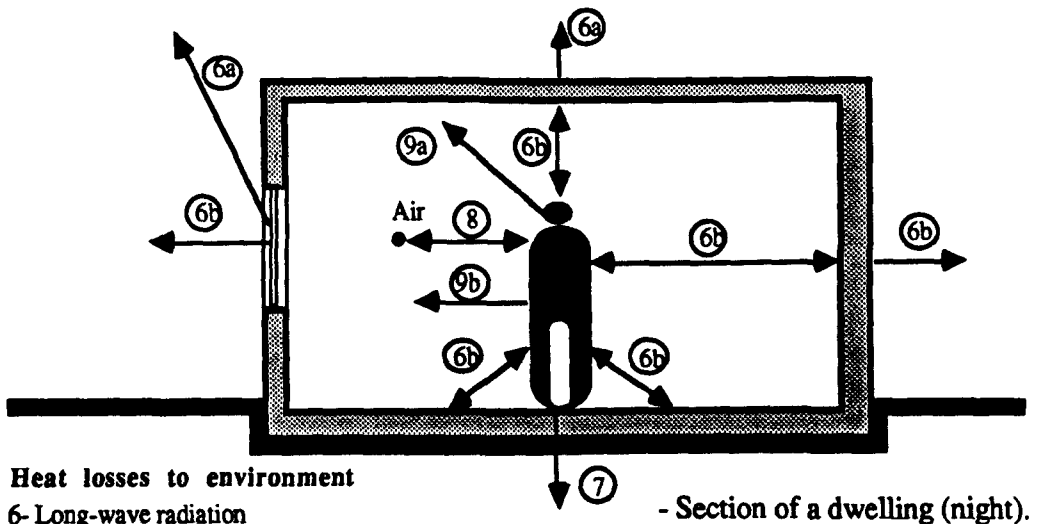
Air speed m/s	Air temperature °C	Air temperature difference* K
Below 0.1m/s ("Still air")	25	--
0.55	26	1
1.0	28	3
2.0	30	5
4.0	31	6

*Temperature difference is that between the comfort air temperature (25 C) ° and that of the air when increased.



Heat gains from environment

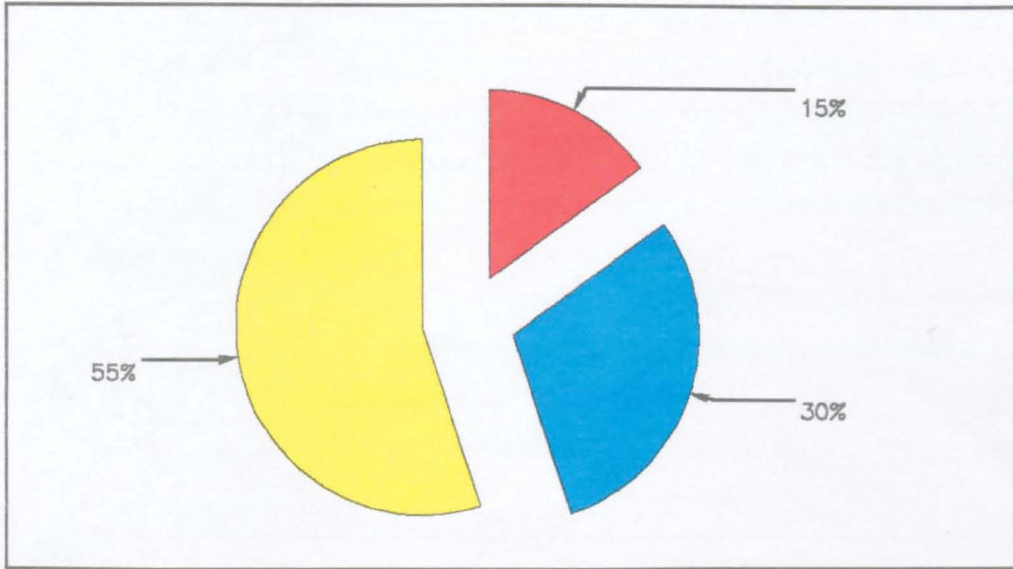
- 1- Metabolism (basal and muscular)
- 2- Absorption of radiation
 - a- short-wave radiation from sun, sky and surrounding
 - b- long-wave radiation exchange from warm surfaces
- 3- Heat conduction (by contacting hot surfaces, floor)
- 4- Convection from air (above skin temperature)
- 5- Condensation of air moisture (when clothes are dry)



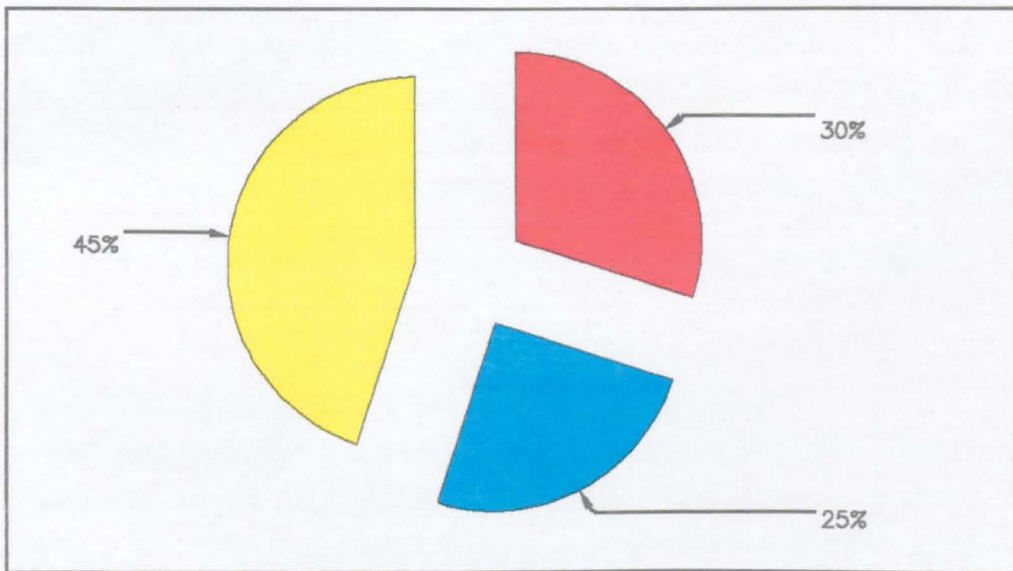
Heat losses to environment

- 6- Long-wave radiation
 - a- to the sky
 - b- to colder surfaces
- 7- Heat conduction (by contacting colder surfaces, floor)
- 8- Convection to air (below skin temperature)
- 9- Evaporation
 - a- by respiration
 - b- from skin

Figure 1.9 Heat exchange between man and surroundings.



a- Heat transfer from the body according to Straatan (1967).



b- Heat transfer from the body according to the BRE (1983).

■ Convection
 ■ Evaporation
 ■ Radiation

Convection loss to air depends on air movement and temperature differential.
 Evaporation loss to air—gradual increase above 16 C & its substantial above 20
 Radiation decreases as radiant temp. increases to a minimum at skin temperature

Figure 1.10 Heat transfer from the body to environment.

Fanger (1970) has shown that an increase of air velocity from 0.1m/s to 1.4m/s can result in discomfort, an effect which can be counteracted by increasing the temperature drop from 3.5K to 6K (depending on air relative humidity, type of clothes and the level of activity). At low air velocity, he shows that an increase from 0.1m/s to 0.3m/s can be met by an air temperature drop of 1.5K. However, the relationship between air speed and comfort is not exact and different researchers have arrived at various descriptions of the effect.

Winslow et al. (1939) investigated the influence upon heat losses from a dressed human; the convective heat transfer h_c was:

$$h_c = 12 v^{0.5} \quad [1.3]$$

where

v = air velocity m/s

For $v < 2.6$ m/s

The cooling effect of air at 0.5m/s is about double that of air at 0.1m/s. With higher air velocity (2.0m/s), the cooling effect could be greater. Nevertheless, it is agreed that the use of air flow to provide comfort at high air temperature is worth while. Abraham (1980) reported a rule-of-thumb in which an air speed of about 0.15m/s will allow comfortable conditions to be maintained if the air temperature increased by 1K.

1.4 COMFORT IN DWELLINGS IN HOT ARID CLIMATES

For an individual, thermal comfort in a dwelling depends upon various factors: environmental (air temperature, relative humidity, mean radiant temperature and air movement); physical (level of activity, clothing, age, body shape, diet and skin colour) and psychological (decor, colour and personal expectation). Most people (about 80%) would feel comfortable within a range of conditions known as the "comfort zone" (Koenigsberger and Ingersoll, 1974).

Several indices have been developed by Mahoney (1975), Evans (1980) and ASHRAE (1985) to assess thermal stress experienced by occupants in buildings. Boguslawa et al.(1988) developed a multi-index analysis of the thermal stress 'COLDHOT' for tropical climates, but no values were given for hot arid climates.

Olgay (1967) provides an index known as the 'Bioclimatic chart' which takes into account five major comfort factors assuming that the subject is in shade and still air. The two most significant factors are air temperature and relative humidity. The lower and the upper comfort limits are 21°C and 28°C (Figure 1.5) and have relative humidity between 20% to 50% respectively. To provide comfort with a relative humidity of 75%, the air temperature should be limited to 23°C. Although the chart was originally designed for cold climates, it could be used in the early stage of design for assessing and visualising the degree of discomfort with reference to warm climates. The chart has been revised by Arens et al. (1984). The subject is assumed at a sitting at medium level of activity and wearing light clothing. It indicates that comfort can be achieved at 80% relative humidity if air temperature be limited to about 20°C. In places where the air temperature is above 30°C air movement is insignificant in lowering the temperature of the air to a comfortable level.

Fanger (1963) gives a general equation for comfort where he includes environmental factors and type and level of activity. He develops comfort lines based on the mean radiant temperature in relation to air velocity with variable levels of activity. For an individual wearing light clothing and working, the comfort line ranges from 25°C to 28°C with air velocity up to 1.4m/s. When the air velocity is more than 0.6m/s, discomfort may be possible because of draughts.

The 'resultant temperature' (Missenard, 1933) is used as an 'index' to define comfort in cold climates, but is also suitable for hot climates (CIBSE Guide, 1986). It is usually recorded in the centre of a room by a blackened thermometer, 100mm in diameter. The 'resultant temperature' T_{res} is given by:

$$T_{res} = [T_{mr} + T_{ai} (10v)^{0.5}] / [1 + (10v)^{0.5}] \quad ^\circ\text{C} \quad [1.4]$$

where

T_{mr} = mean radiant temperature °C

T_{ai} = air temperature °C

When the indoor air velocity is at about 0.1m/s ("still air"), the resultant temperature simplifies to:

$$T_{res} = (T_{mr} + T_{ai}) / 2 \quad ^\circ\text{C} \quad [1.5]$$

For high air velocity (assumed 0.3m/s), the resultant temperature becomes:

$$T_{res} = 0.37 T_{mr} + 0.63 T_{ai} \quad ^\circ\text{C} \quad [1.6]$$

and if v be 0.4m/s, $T_{res} = (T_{mr} + 2T_{ai}) / 3 \quad ^\circ\text{C} \quad [1.7]$

This indicates that air movement lowers the effect on comfort of the 'mean radiant temperature' (MRT), but increases that of the air temperature. Since comfort is influenced to a greater extent by radiant temperature, an air velocity increase is useful in promoting comfort.

In hot arid climates, air movement may not be enough to combat discomfort (Figure 1.6). Building elements such as thick walls radiate stored heat into the interior. With no cooling, discomfort will increase since the body is not protected from the high resultant temperature during the day.

Webb (1964) studied comfort in hot arid climates, and found that a sitting acclimatised person, wearing normal clothing and working normally, was more comfortable in a hot dry than in a hot humid climate. The CIBSE Guide (1986) states that a comfortable resultant temperature with low air movement for the U.K is 20°C to 22°C, but could be as high as 28°C for hot climates. Nicol (1975) shows that for comfort in hot arid climates, the air temperature could be from 28°C to 36°C with an air velocity up to 0.25m/s.

Givoni (1984) suggested an air velocity up to 1.0m/s to provide comfort in dwellings in hot arid climates. For an air velocity of 0.7m/s, the resultant temperature becomes:

$$T_{res} = 0.27 T_{mr} + 0.73 T_{ai} \quad ^\circ\text{C} \quad [1.8]$$

Although the influence of the mean radiant temperature is progressively reduced as the velocity increases, the air temperature is increased. If the air temperature is below or near 30°C, this may improve comfort in dwellings. When the air temperature is about 37°C air movement is of no benefit.

1.5 ARCHITECTURAL FEATURES PROVIDING COMFORT IN EGYPT

Nowadays, comfort in dwellings can be provided by active systems (air conditioning) for people of high income. For the poor and in places without electricity, comfort must be sought in other ways.

Traditionally, different ways were used in the past by people to provide comfort indoors, and will be reviewed in detail in chapter two. These are:

- water pond or 'fountain' in courtyards or rooms.
- forms of roof (domes).
- underground buildings.
- vegetation.
- traditional windows.
- ventilation via a courtyard.

The rapid movement of modern architecture has changed the appearance of dwellings. Traditional ways of providing comfort have been neglected, and the traditional dwellings were maintained as symbols of historical architecture for tourism.

Modern dwellings are no longer comfortable, especially those in tall blocks built from steel and their facades covered by aluminium sheets and large windows. This leaves the building freely exposed to solar radiation, which increases the resultant temperature inside these dwellings.

1.6 THE PRESENT WORK

In hot arid climates such as that of Egypt, it is the high air temperature which causes discomfort since humidity remains low, and air movement through dwellings during the day is of no benefit. Windows are usually kept closed during the day and open for ventilation during the night. Dwellings with high thermal capacity absorb heat during the day (in the process protecting the dwelling) and radiate stored heat inwards at night. This brings about inevitable increases in the air and surface temperatures beyond the limits of comfort.

Insulation is useful. For this to work effectively, the average temperature (over day and night) must be comfortable. Good insulation requires few or no openings. The average temperature (over day and night) in Egypt is not comfortable (Figure 1.1 b) and large openings are required at night for ventilation. Therefore, insulation alone is not sufficient to cool dwellings.

In hot climates, people start work early in the morning when the air outside is cooler than that inside. When activities restart in the afternoon (1300h), the effective temperature inside rises above the upper limit of comfort. Sufficient heat transfer by conduction, radiation and convection becomes impossible. Heat transfer is still possible if the environment is able to accept water vapour so that the heat may be dissipated by evaporation. In a hot and humid environment, the limit could be established by the ultimate capacity of the air to absorb moisture from the skin. In a hot arid environment, the limit is more likely to be determined by the capacity of the body to perspire (Bazett, 1949).

When the air temperature is lower than the skin temperature, an increase in air movement will result in heat loss by convection. If the air temperature is higher than that of the skin, the increase in convective heat exchange warms up the body, but increased air velocity will increase evaporation and consequently provide cooling. Low humidity may cause unpleasantness due to excessive dryness of the lips and mucous-membrane in the upper respiratory tract (Givoni, 1976).

When evaporative cooling is required, humidity becomes important in determining the rate of sweat secretion and evaporation as well as contributing to the feeling of thermal comfort. If the outside air temperature approaches or exceeds that of the body's skin, humidity becomes the most important of all the environment factors (Yaglou, 1949).

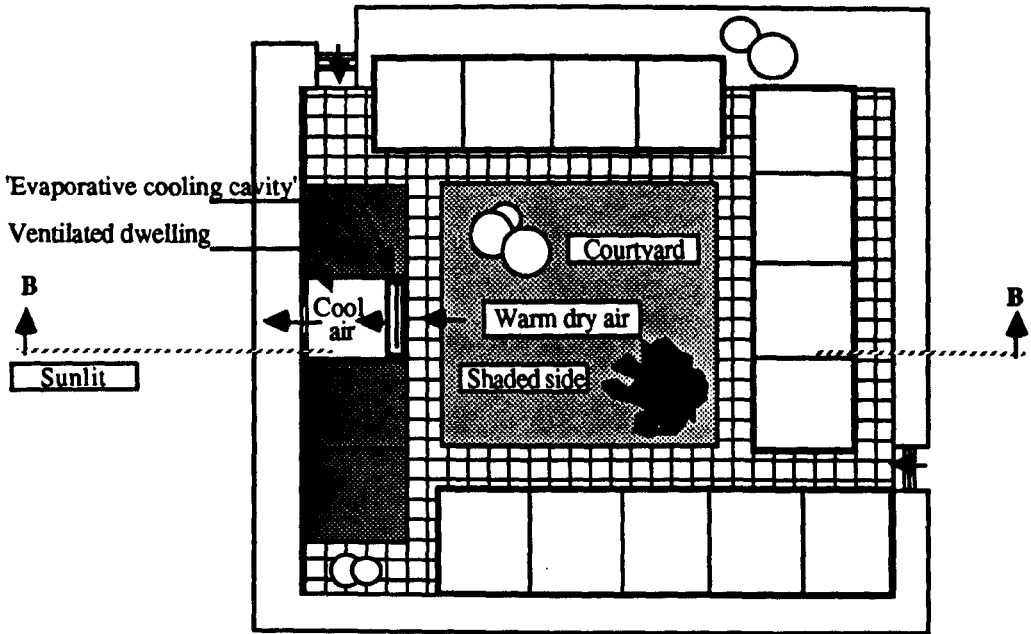
Ways of improving comfort inside dwellings during the day and night are important so that occupants can extend their activity and feel comfortable. This work investigates cooling by ventilation, exploiting the temperature difference between the sunny and the shaded sides of a building, and cooling incoming air by evaporation. Younes (1983) shows that in the shade of a courtyard outside air temperature may be up to 6K lower (Table 1.9).

Table 1.9 Field measurements of outside air temperature and those in shade of courtyards in hot arid climates (Younes, 1983).

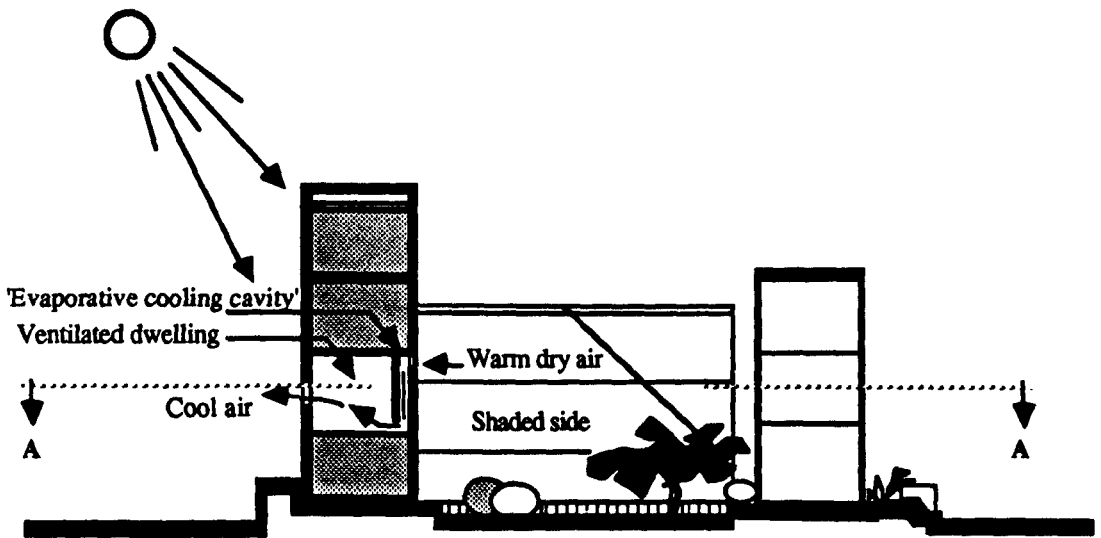
Dwelling	Month	Air temperature °C	
		Outside	in the courtyard
	June	37	32
	July	38	34
El-Din court		36	32
El-Seheamy court		36	30

Time of measurements 1400h, Cairo.

Figure 1.11 shows diagrammatically a possible design which exploits this, and incorporates an 'Evaporative cooling cavity', which may be formed in various ways, using normal building materials. It can be also added to existing dwellings. The proposed cavity has length Y, width D and a height Z (Figure 1.12). It will have an inlet and an outlet (initially closed) and incorporate one or two wet partitions (mats) so that it is passively cooled (Figure 1.13). When the dampers at the inlet and outlet, and the window of the dwelling are opened (Figure 1.12) the air within the cavity falls downwards by buoyancy, drawing outside warm and dry air through the inlet into the cavity. Evaporation taking place in the cavity will take heat out of the air. Hence its temperature falls and the latent heat of evaporation will increase the humidity of the air. As a result, the downward flow is prolonged. This will cool the air and the cavity, especially on the inside.



a- Layout A-A of a group of dwellings around a courtyard

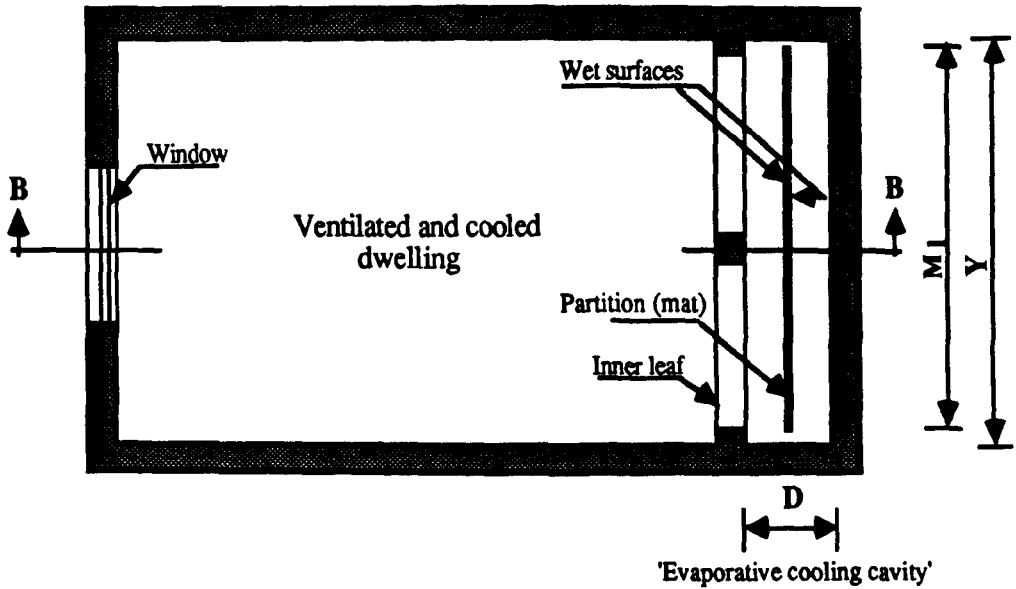


b- Section B-B through layout of group of dwellings around a courtyard

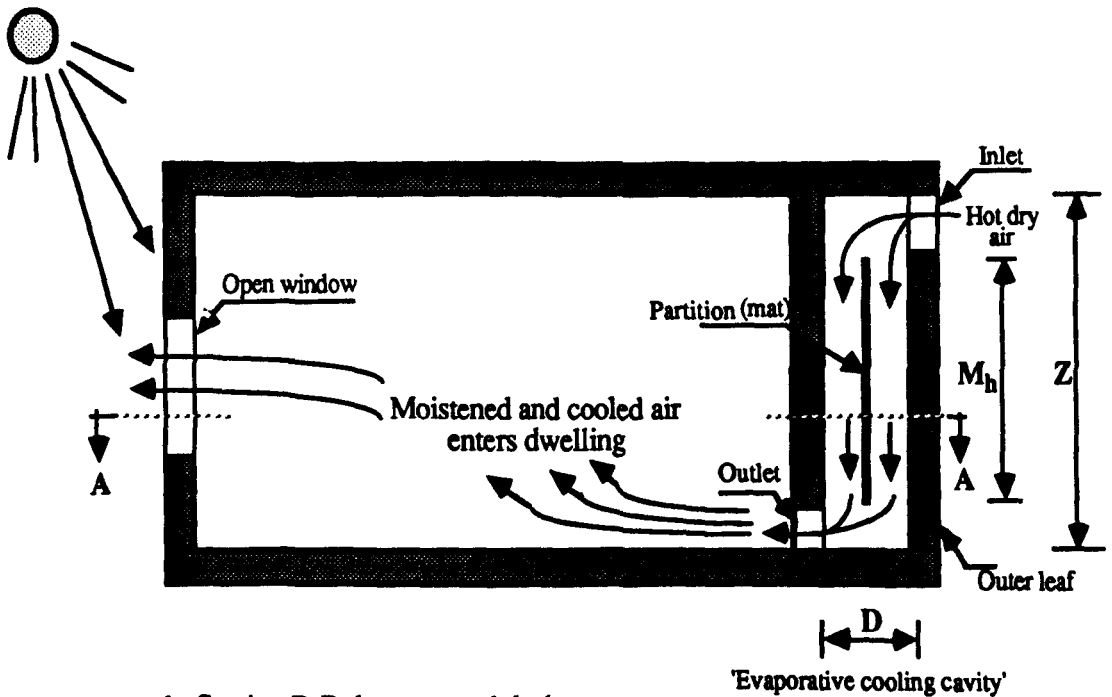
Figure 1.11 Layout of group of proposed dwellings around a courtyard.

sun side

Shaded side



a - Plan A-A of the proposed design



b- Section B-B the proposed design

Number of wet mats will be one or two (Figure 1.13)

Figure 1.12 The proposed design for buoyancy air flow.

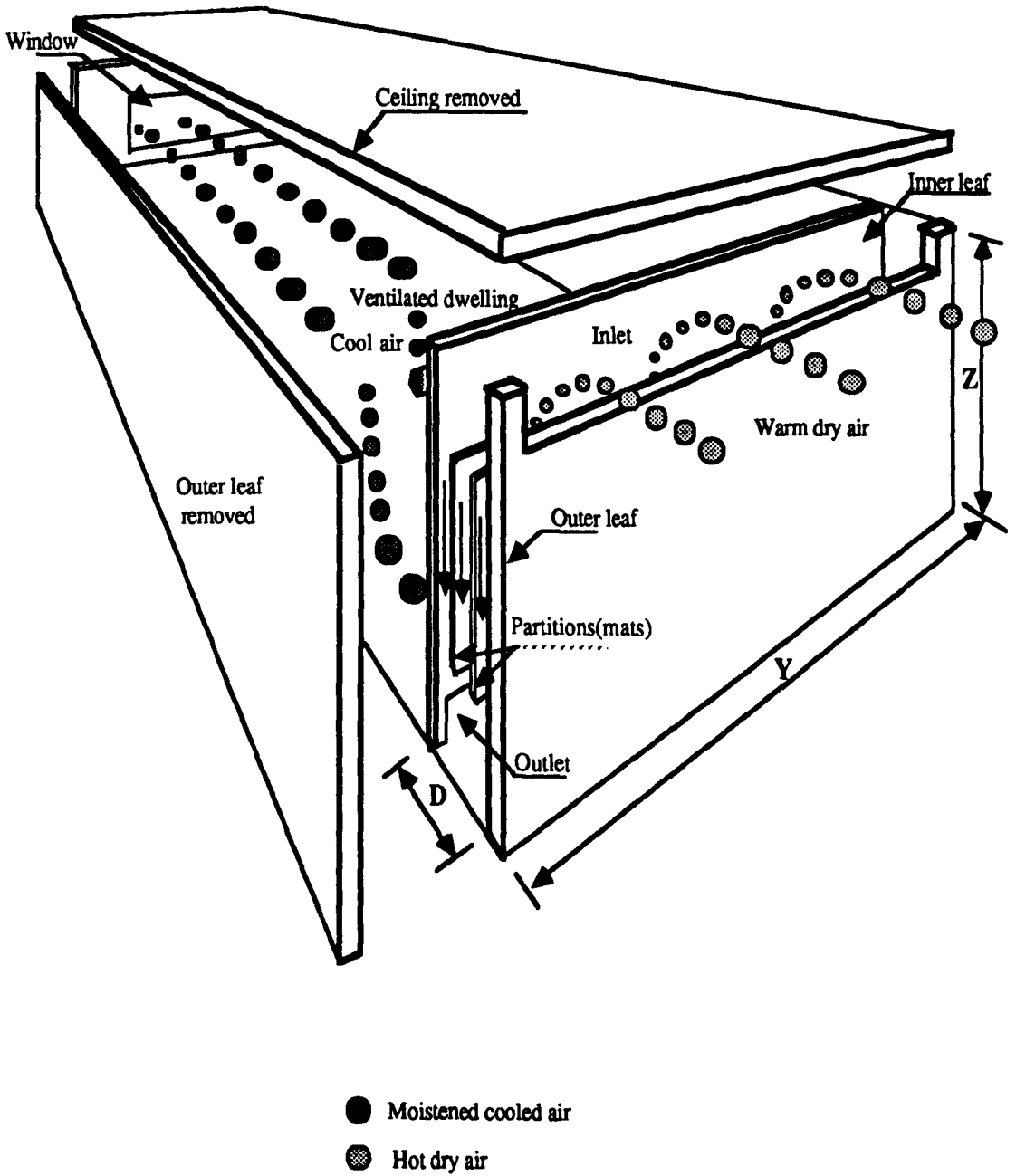


Figure 1.13 General view of a dwelling ventilated by an 'Evaporative cooling cavity'.

The design should be such that cooling ventilation will continue as long as is needed. Where electricity is available and cheap, a fan may be incorporated, but is not essential.

As the incoming air is cool and moving, it will lower the temperature of the air in the dwelling and consequently reduce the mean radiant temperature of the surroundings, cooling the dwelling's structure. The resultant temperature in the dwelling will be lowered as a direct impact of the air movement (eqn. 1.6). Moving air also increases heat losses from the body by increasing the rate of evaporation from the skin.

1.7 THE PURPOSE AND SCOPE OF THE STUDY

This study was carried out to investigate the proposal described above, aiming at an air speed of 0.25m/s as suggested by Nicol (1975), and increasing the humidity to the levels suggested by the bioclimatic analysis of Cairo (Table 1.6). Cool air with an air speed of up to 1.0m/s as recommended by Givoni (1984) was accepted as a target with fan-assisted 'forced flow'.

Air movement in a ventilated cavity or 'Evaporative cooling cavity' was tested in the laboratory, to examine cooling ventilation by 'buoyancy' air flow and cooling ventilation by 'forced' air flow. The temperature of the air and relative humidity with 'buoyancy' air flow were those in the laboratory (Leeds), and those with the 'forced' air flow were like those experienced in hot arid climates. The air flow and its pattern were examined. The effect of cavity width, outlet height and the separation between the wet surfaces on the performance of the cavity to promote evaporation and air flow were assessed. The cooling and ventilation generated by evaporation were determined. The optimum design of the 'Evaporative cooling cavity' was established. The heat transfer by evaporation was examined and the rate of evaporation was determined.

1.8 METHOD OF STUDY

The study was divided into three parts:

- Historical
- Experimental
- Theoretical

1.8.1 Historical

Evaporative cooling techniques in hot climates are reviewed (chapter two). These include direct and indirect evaporative cooling and methods to promote ventilation, using:

- courtyards
- wind towers
- water for evaporation
- windows.

Indirect evaporative cooling techniques in modern architecture are reviewed which include:

- desert coolers
- subterranean dwellings
- solar humidification
- radiative cooling (roof pond)
- water for evaporation.

Principles of ventilation, evaporation, air flow, and heat transfer in buildings and cavities are considered in chapter three.

1.8.2 Experimental

The experimental work was divided into two parts:

- observation of air flow by buoyancy.
- observation of forced air flow.

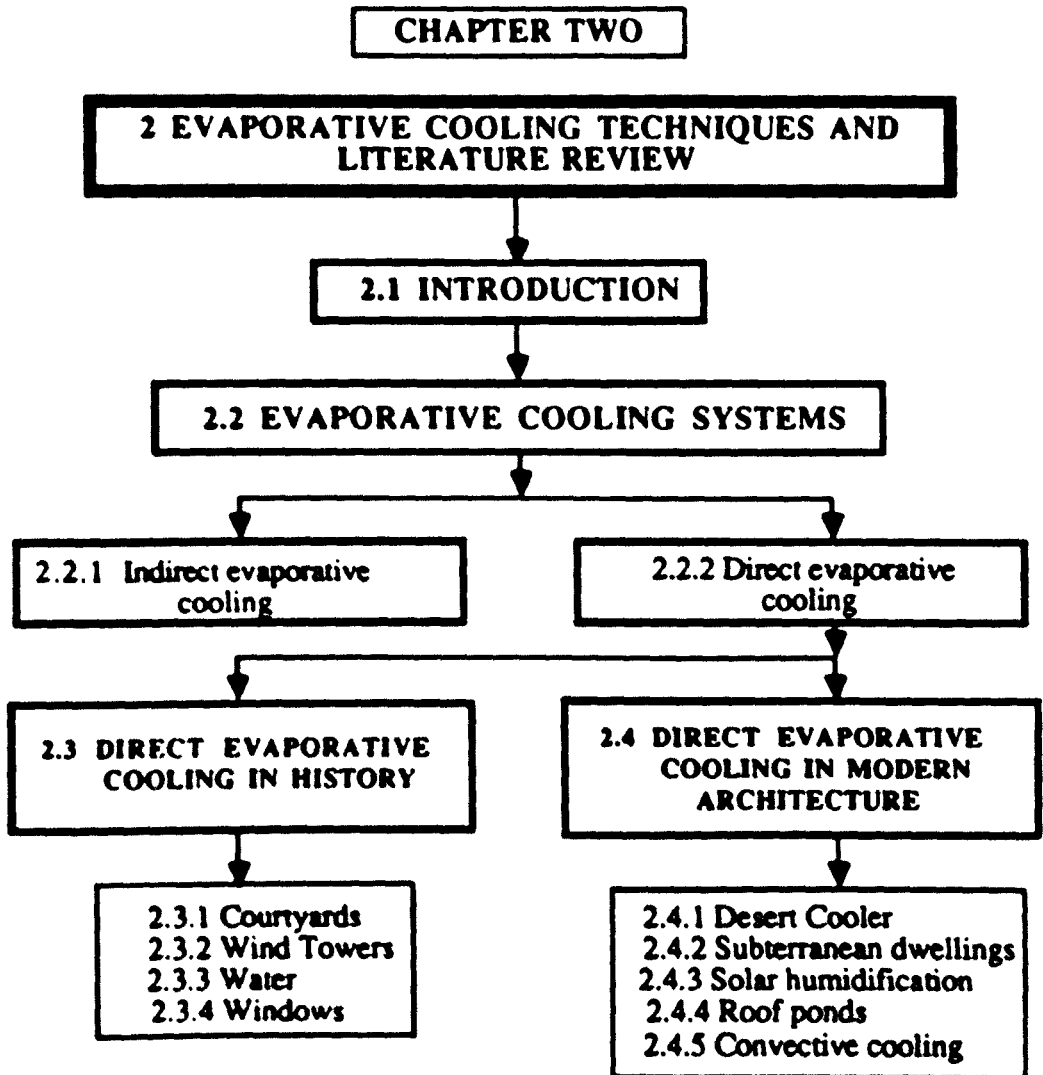
Laboratory observation was carried out to test the proposed design (Figure 1.12) and to determine the optimum design. Measurements of air velocity, air temperature, surface temperature and relative humidity of the air were made using a hot-wire anemometer, thermocouples and an electronic hygrometer. Smoke was used to observe the air flow and examine its pattern, of which a full description is given in chapter four.

The results of observations and the analysis of the measurements of the 'Evaporative cooling cavity' by buoyancy air flow are reported in chapter five, and that of the 'forced' air flow are in chapter six.

1.8.3 Theoretical

Buoyancy air flow and forced air flow were analysed in the steady state. The heat and surface mass transfer coefficients of evaporation were established based on measurements and observations (chapter seven). Design evaluation of water consumption, comfort and ventilation effectiveness were considered. The amount of water required to promote evaporation and cooling ('cavity life') were determined. The Admittance Method was used to determine the resultant temperature (hourly). Thermal comfort was assessed under various climatic conditions of Cairo (chapter eight).

Finally, design proposals for buildings in hot climates are offered. The conclusions and recommendations for further work are given in chapter nine.



CHAPTER TWO

EVAPORATIVE COOLING TECHNIQUES AND LITERATURE REVIEW

2.1 INTRODUCTION

Water has been used throughout history for cooling in various ways, especially in hot arid climates. The classic example of evaporative cooling is the cooling felt when a moistened hand is waved in the air. Evaporation removes sensible heat and replaces it with latent heat. The increase in the air moisture is accompanied by a drop in air temperature. Evaporative cooling of buildings is an effective method of controlling the internal environment in hot summers, unlike other passive methods which restrict the entry of heat into the enclosure. Evaporative cooling throughout history is reviewed briefly below.

2.2 EVAPORATIVE COOLING SYSTEMS

Evaporative cooling is either direct or indirect. In direct cooling, water is evaporated directly into the air that flows to the space. In indirect cooling, evaporation is separated from the air which is delivered to the space. Pools and fountains are examples of direct evaporative cooling in buildings. Indirect cooling includes roof ponds, a water film or spray over external walls. Cooling by evaporation may also be either single or multi-stage. A multi-stage system uses at least two evaporation processes, of which the first supplies cooled air to those later. Descriptions of such systems can be found in (Abrams 1985, and Sodha et al. 1986).

2.2.1 Direct evaporative cooling

In direct evaporative cooling, the air to be cooled is passed over water and cooled by evaporation and the latent heat is taken from the air (sensible heat reduced and latent heat increased) and then supplied to the building interior. This cool and more humid air absorbs sensible heat from the enclosure. Direct evaporative cooling systems humidify the air supplied to the building, so that the relative humidity indoors will always be higher than outdoors. Successful direct evaporative cooling depends on outdoor

humidity being well below that required for comfort, as is commonly found in hot arid regions. Figure 2.1 shows an example of direct evaporative cooling.

Direct evaporative cooling may be passive, active or hybrid. Active direct evaporative cooling systems include (Sodha et al., 1986):

- the drip evaporative or desert cooler
- the spray evaporative cooler
- the rotary-pad evaporative cooler.

Hybrid systems can combine any of the above systems with a passive one.

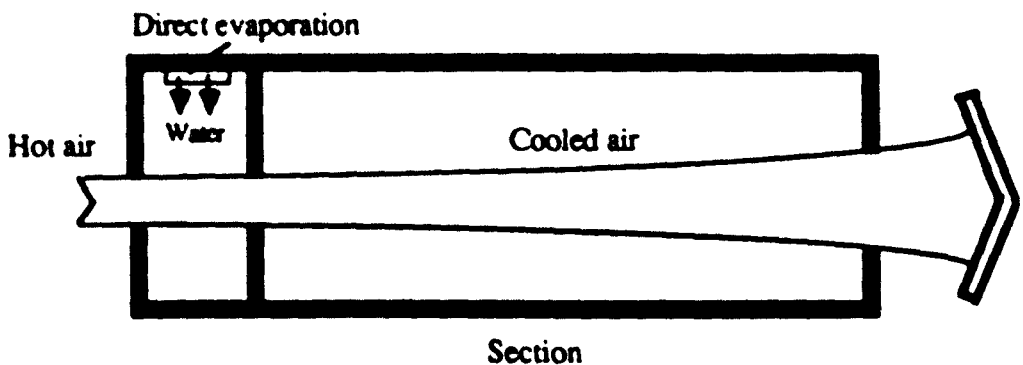


Figure 2.1 A direct evaporative cooling system.

2.2.2 Indirect evaporative cooling

Indirect evaporative cooling systems employ evaporation without increasing the amount of moisture in the air supplied to the building. Passive indirect evaporative cooling could be achieved either by having a water pond or by maintaining a moving water film over the roof of a building. A heat exchanger as shown in Figure 2.2 is used

to separate the direct evaporation from the air delivered to the interior. Direct evaporation first cools the air that flows across one side of the exchanger, removing heat and then exhausting it. The air to be supplied to the building flows across the other side of the heat exchanger and is cooled without directly receiving extra moisture. Indirect evaporative cooling can be passive or active as well as hybrid. Active indirect evaporative cooling may also employ:

- simple dry-surface cooling
- regenerative dry-surface cooling
- plate-type heat exchange cooling
- the Pennington heat-storage wheel system.

These are described in (Abrams 1985, Dunkle 1962 and Sodha et al. 1986).

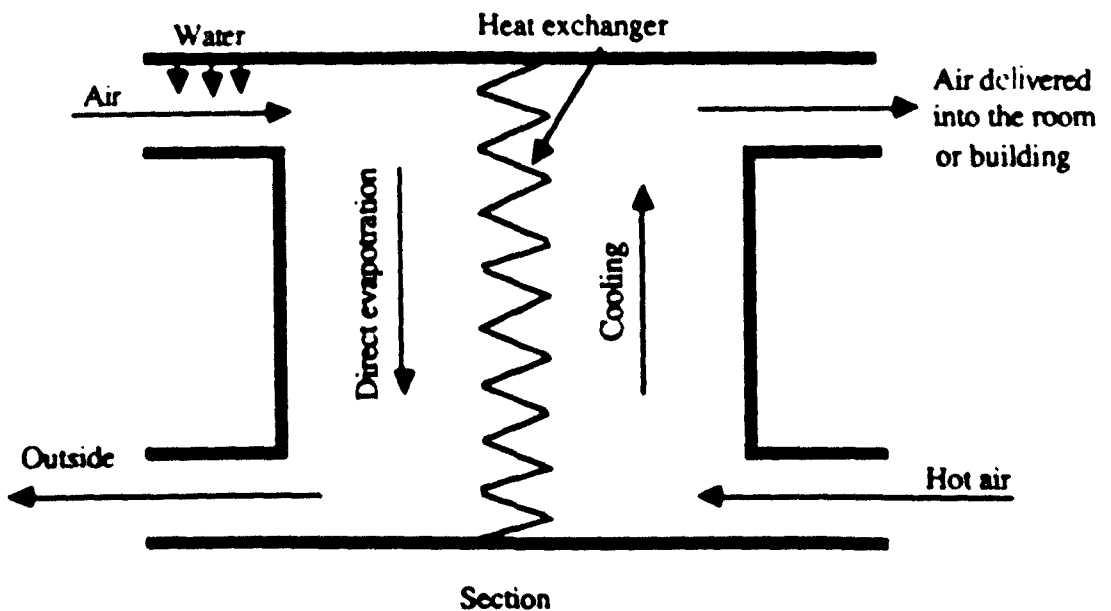
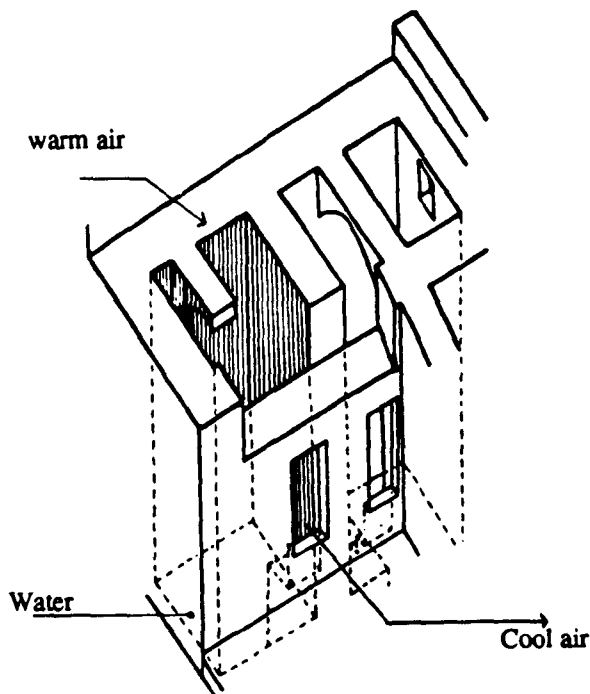


Figure 2.2 An indirect evaporative cooling system.

2.3 DIRECT EVAPORATIVE COOLING IN HISTORY

Ancient architecture, all over the world, had many characteristics which emphasise passive cooling in general and evaporative cooling especially. About 2500 B.C., ancient Egyptian painters showed slaves forming porous clay jars to provide cooling. Evaporative cooling was used some 4000 years ago in Memphis (Building I), (Figure 2.3). Persians and pre-columbian Americans used to cool their tents with damp felt or grass mats. In the simplest form of living, man used to wet the floor of his house. Konya (1980) describes a traditional way of evaporative or adiabatic cooling which uses thick straw matting in a wooden frame. Against this, water is thrown from time to time so that evaporation cools the surrounding air. Leonardo da Vinci (Abrams 1985) built an evaporative cooler for his wife's bed. In old houses, courtyards, wind towers, water and windows were exploited to promote evaporative cooling.



Perspective of part of the building I

Figure 2.3 Evaporative cooling in building I at Memphis, ancient Egypt.

2.3.1 Courtyards

Courtyards act as thermal regulators (Dunham 1960). During the night (after 0200 hours), they accumulate cool air until late in the day (Fathy 1986 and Mohsen 1979). They provide shade on vertical surfaces and paving. A pond, or fountain with plants was often used within the courtyards to provide cooling by evaporation, especially in dry areas.

In the Indus valley, the Harappans built their houses with a central court. The typical ancient Egyptian house (of 4000 years ago) was built in the form of a court surrounded by high walls (Golany 1980). At Ur in south Mesopotamia (2000 B.C.), a two-storey house was built around a courtyard. In Greece (700-146 B.C.), single storey houses were usually grouped around a court (Danby 1982). The Roman private house was greatly influenced by that of the Greeks. Typical examples have an atrium (open court) as the public part of the house, (Figure 2.4 to Figure 2.6). A common feature of Iraqi, Moorish, Persian and Turkish houses was the court (covered or uncovered) in the centre (Konya 1980 and Fathy 1973). In India and China, some typical houses were surrounded by two patios (Olgay 1967 and Pathorn 1983). In Spain, the Alhambra palace in Granada (1309/54 A.D) is an outstanding example. An Islamic house built in Fostat in Egypt illustrates the use of vegetation and fountains to promote evaporative cooling (Ettouny 1974 and Fathy 1983), (Figure 2.7).

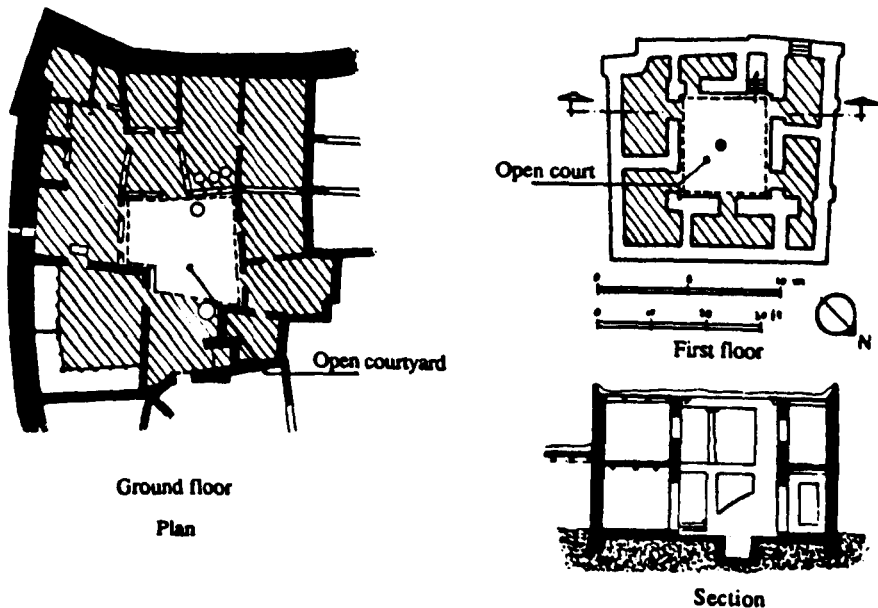
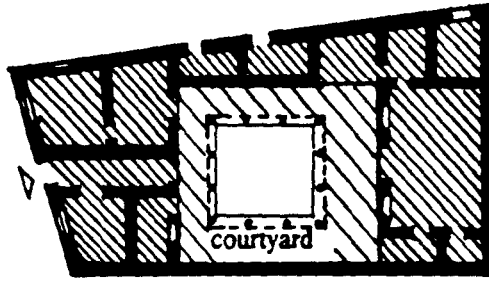
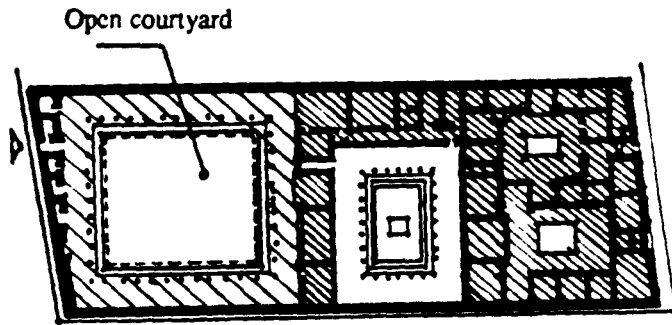


Figure 2.4 Typical house of the Sumerian period of Ur.



Ground floor
Plan

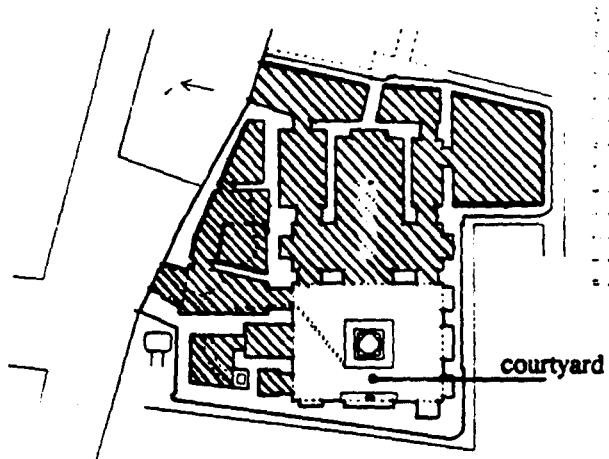
Figure 2.5 A Greek house with a courtyard (700-146 B.C.).



Plan

Ground floor

Figure 2.6 A Roman house, a colonnade surrounding a court.



Plan

Figure 2.7 Al-Fustat house, old Cairo.

2.3.2 Wind towers

A wind tower (alternatively 'catcher') uses convection and evaporation to promote cooling. In Egypt in 1300 B.C., wind towers were used as convective cooling systems (Fathy 1983 and Olgyay 1967). Oakley (1961) describes an evaporative cooler used in Egyptian villages, essentially a chimney in reverse. At roof level, a scoop oriented to capture prevailing wind, passes air down a shaft with a porous clay water jar at the bottom. The air is consequently cooled before it enters the room (Figure 2.8). Other examples are found in Iraq, Morocco, Iran and Turkey (Figure 2.9). In India, cities like Hyderabad and Sindh have developed a distinctive form of roof (Figure 2.10). In all these techniques, wind is used as the main force for operation.

2.3.3 Water

Creswell (1959 & 1965) describes old houses found in Egypt which show an early example of evaporation within rooms using a "Salsabil" (Figure 2.11). Another example of evaporative cooling in rooms is a "Mandarah" (Lane 1938 and Danby 1973) where a guest room is paved with stone and covered with a dampened mat in summer to give cooling (Figure 2.12).

The most commonly used device in Egypt is the fountain. It is placed in living rooms so that air movement will encourage evaporation (Figure 2.13). In still air evaporation will decrease due to the almost saturated air layer above the water. Figure 2.14 shows an opening in the ceiling to encourage air movement.

2.3.4 Windows

Apart from limiting the entry of undesirable aspects of the outdoor environment, the function of a window is to admit light, ventilation and provide view. These include excessive heat in hot arid areas. Lane (1938) describes a window or "Mashrabeyh" which reduces light and sun while permitting the entry of the air. Oakley (1961) describes windows in Egypt by which evaporative cooling can be achieved. Figure 2.15 shows how a window can project to allow more exposure to air currents. A porous water jar is placed behind the window so that air temperature will decrease as it is

moistened when it passes over the jar on its way indoors. Due to the scarcity of the skilled craftsmen and high cost, this method has vanished from today's architecture.

In parts of the Middle East, North Africa and India, a form of open woven matting or branches of lily roots were hung in front of windows and watered periodically to cool the air passing through. Air circulation is often difficult to obtain in compact, highly built-up urban areas.

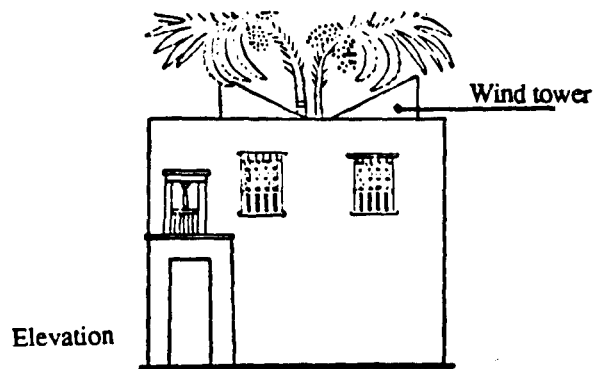


Figure 2.8 A typical house from Tel-el-Amarna, Egypt, 1350 B.C.

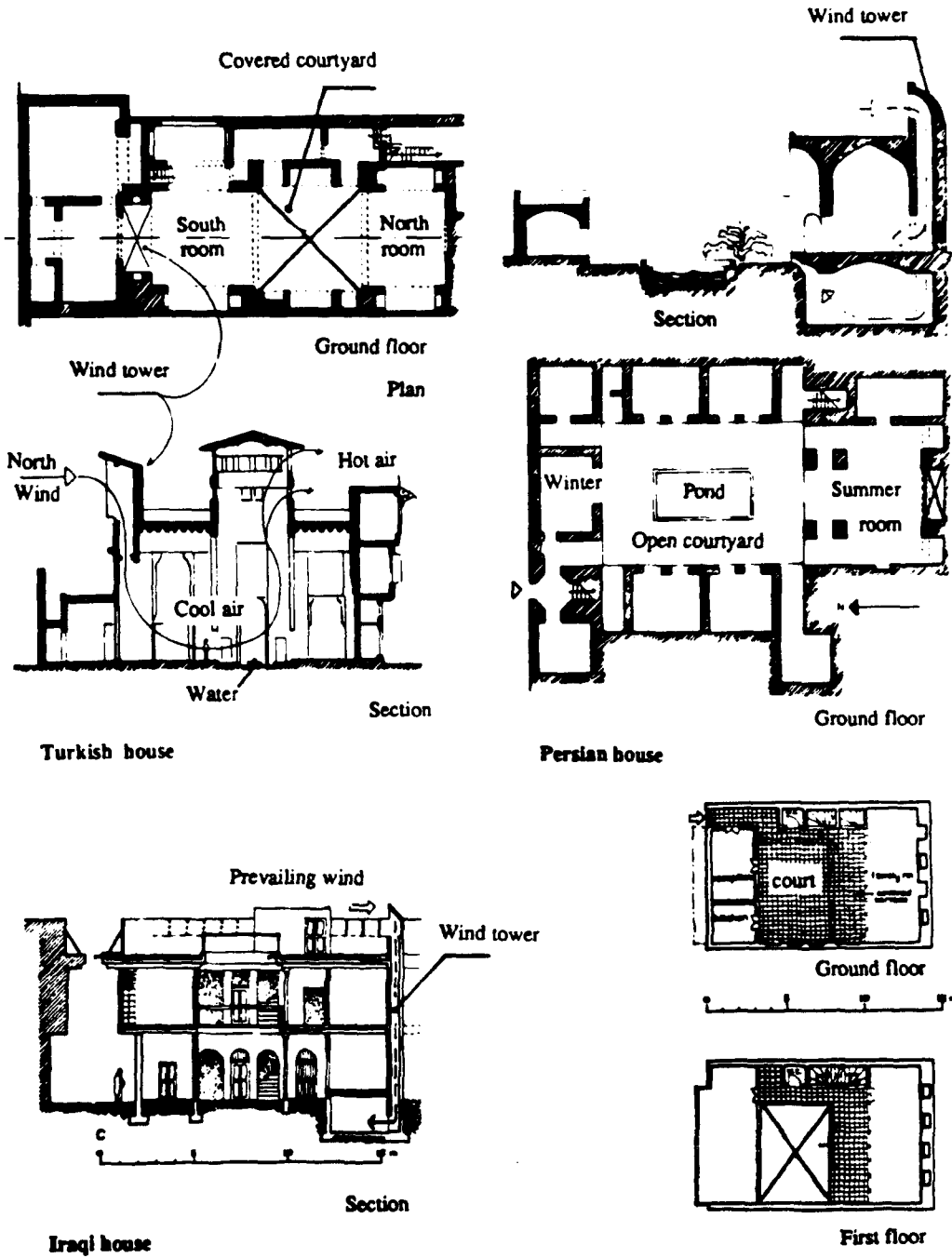


Figure 2.9 Iraqi, Persian and Turkish houses.



Figure 2.10 Wind towers house in Hyderabad, India.

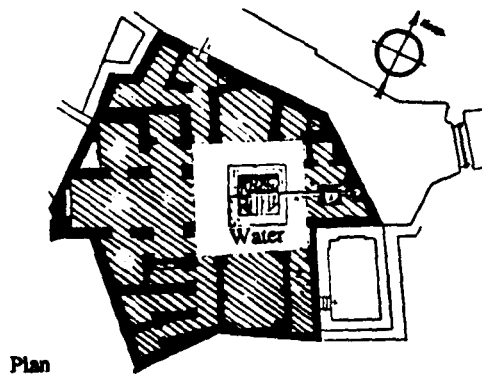


Figure 2.11 Fustat house with cooling system, according to Count (1959).

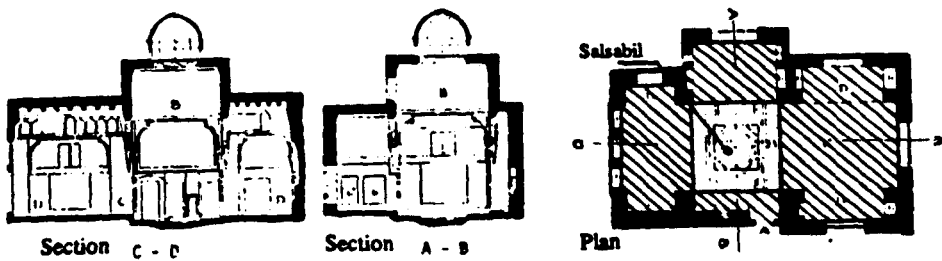


Figure 2.12 Cooling system: "Salsabil" in the summer room, according to Count (1890).

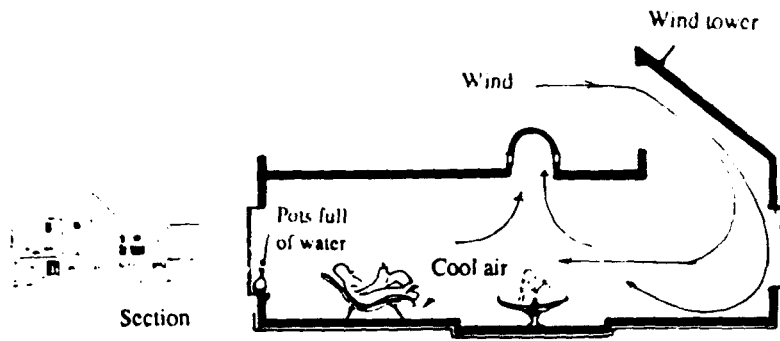


Figure 2.13 Summer room in an old Egyptian house, EL-Sinnari.

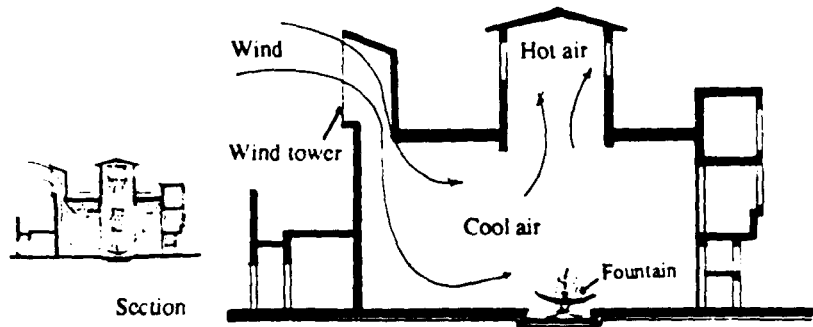


Figure 2.14 Another example of a summer room according to Alawa (1980).



View from outside

a



View from inside

b

Figure 2.15 a- The "Mashrabyah" from the outside. It is open in all directions and admits air which passes over a water jar, Lezine (1972);
 b- The "Mashrabyah" from inside. Note grille for air to pass over water jar, Revoult & Maury (1975).

2.4 EVAPORATIVE COOLING IN MODERN ARCHITECTURE

2.4.1 Desert cooler

Examples of evaporative cooling (direct or indirect) are found in modern architecture. To provide active evaporative cooling, the 'desert cooler' became popular in hot desert regions of the Southwest of America. It works well until the wet-bulb temperature approaches 21°C (Abrams 1985). From the physiological point of view, this approach is not always desirable since:

- cooled indoor air may be excessively humid.
- the high rate of air flow necessary for effective cooling causes draught.

Since 1900, evaporative coolers have been used in U.S. houses and by 1953, active evaporative cooling systems were common in places like Phoenix, Arizona.

Many innovative evaporative coolers have been developed by CSIRO in Australia during the past two decades. They typically include evaporative cooling followed by heat exchange. A full description of these systems can be found in (Dunkle 1962 and Sodha et al. 1986).

Aitchison (1962) observed a simple form of evaporative cooling used by farmers in the hot regions of South Africa, primarily for cool storage of perishable goods (Saini, 1980) (Figure 2.16). Aitchison suggests extending this to cool the whole house by installing coke-filled screens all around the sub-floor structure. A fan can be then used to generate an air current and guarantee the flow of cooled air throughout the room. The disadvantages of this method are:

- the need for a costly sub-floor structure.
- the application is limited to single storey buildings only because of the difficulties caused by wind in compact urban areas.

2.4.2 Subterranean dwellings

G.Golany (1980) describes innovative cooling for houses in hot-arid climates based on the integration of three ancient way of cooling: subterranean structure, ventilation and evaporation. The dominant system is cooling by evaporation. Ventilation

is difficult without wind, and is of little use if air is above body temperature. Evaporation is achieved by introducing a regulated amount of moisture into a shaft. Various methods were used: water was introduced through a filter, the walls of the shaft, or through misting as shown in Figure 2.17. The filter was of thorn bushes and fixed at the shaft inlet, where water dripped onto it. Such a filter will slow air movement and dry quickly.

Wall humidification (Figure 2.17A) was applied to improve the performance. Buried pipes with small holes facing the outer side of the wall introduced moisture to the inside by capillary action. Warm air moving through the shaft into the room will evaporate the moisture and cool the air. Although this method is simple, there are some disadvantages:

- dissolved minerals may damage the wall.
- unless the water supply is controlled, humidity within the wall may last into the night when cooling is not required.

Shaft humidification was introduced to overcome these drawbacks. Two ways were exploited: prefabricated blocks with tunnel and pipes (Figure 2.17B) and (more effectively), a shaft of ceramic material (Figure 2.17C). Humidification was also achieved through misting in which a pipe was inserted in the top of the ceramic shaft (Figure 2.17D).

Subterranean dwellings are usually more expensive to built, especially where the water table is high. They also create difficulties for people used to living above the ground. It is however significant that the soil temperature falls with depth and even in the hottest climates this offers obvious advantages (Figure 2.18).

Givoni (1979) defines techniques for cooling buildings naturally as:

- absorption operated by solar heat.
- solar humidification and evaporative cooling.
- long wave outgoing radiation at night.
- convection during the night.
- water evaporation.

A full description of the first system can be found in Givoni(1984).

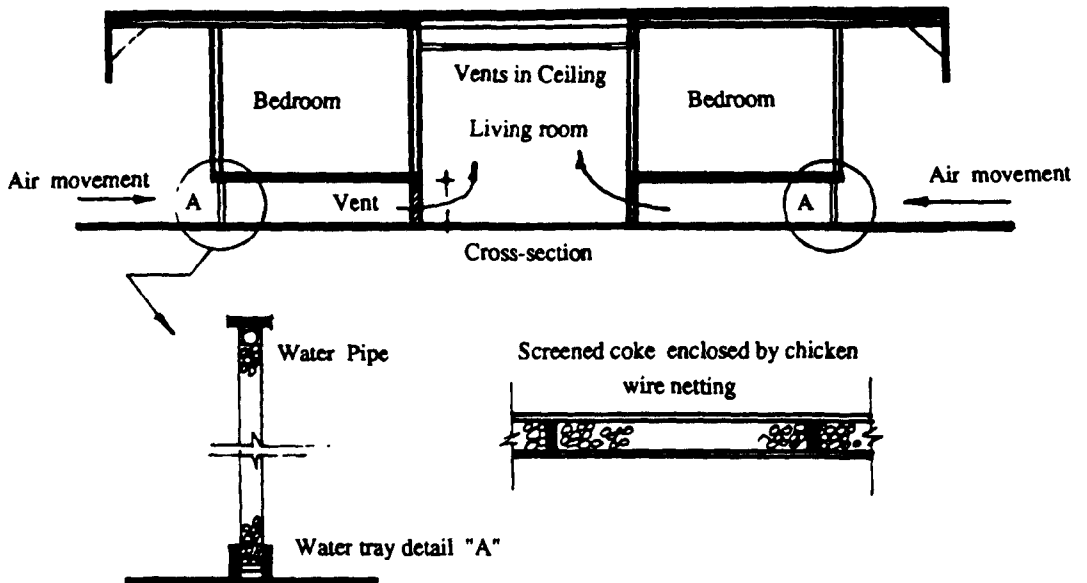


Figure 2.16 Cooling method used in South Africa.

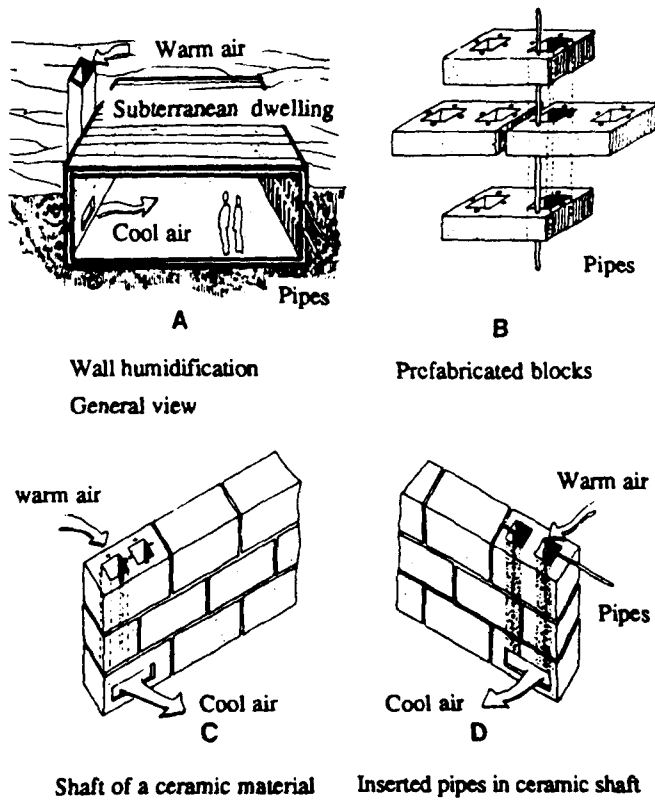


Figure 2.17 Cooling by evaporation in a subterranean dwelling in hot arid areas, according to Golany (1980).

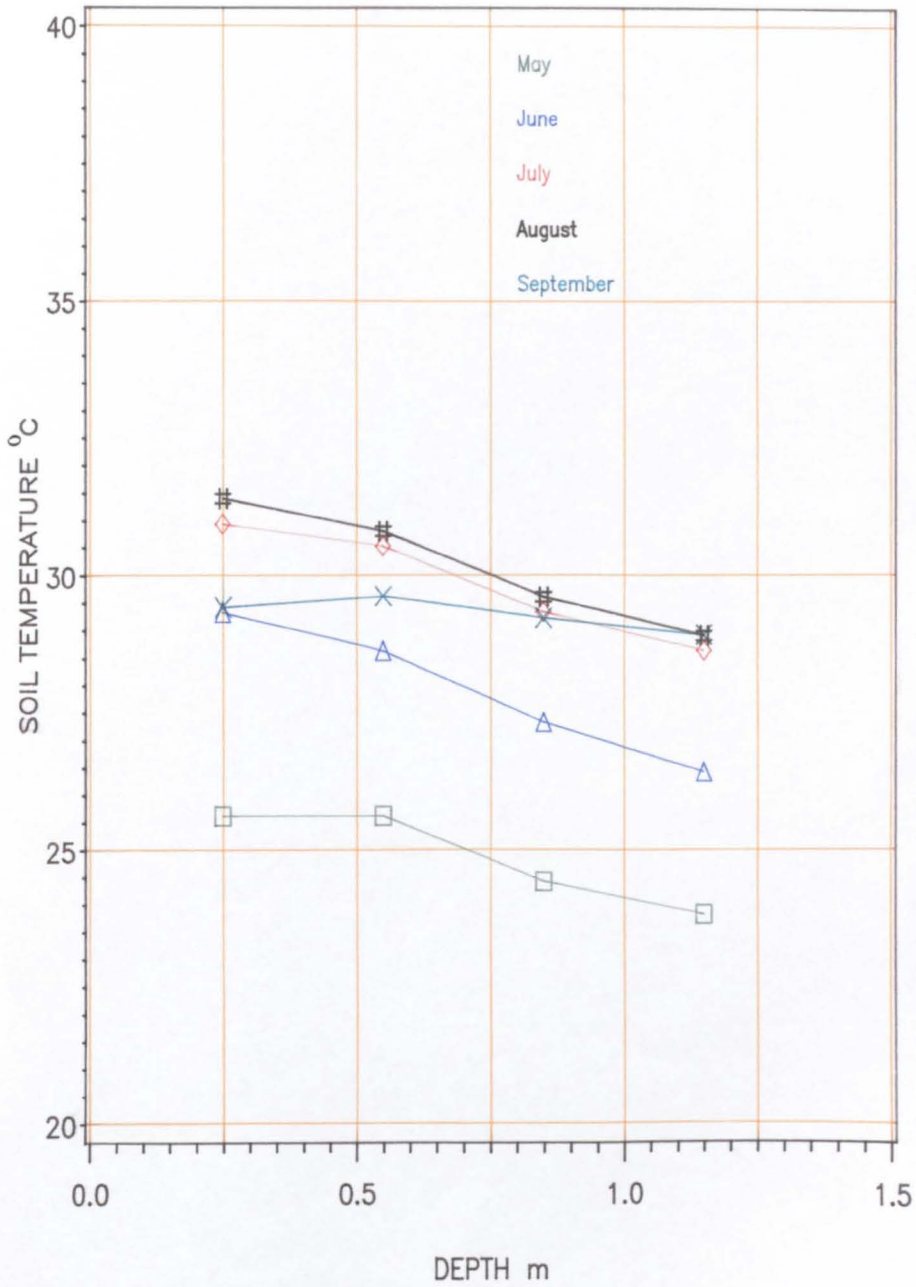


Figure 2.18 Soil Temperature, Cairo

2.4.3 Solar dehumidification

Denies (1959) proposes another system based on the use of solar energy for dehumidification and subsequent cooling of air (Givoni 1984). Tabor (1962) comments that such systems, in which water is added and removed from the air, involve heating air, absorbent material and water vapour. Consequently, the heat required is great. Such systems are most appropriate in very hot dry zones because of their low humidity.

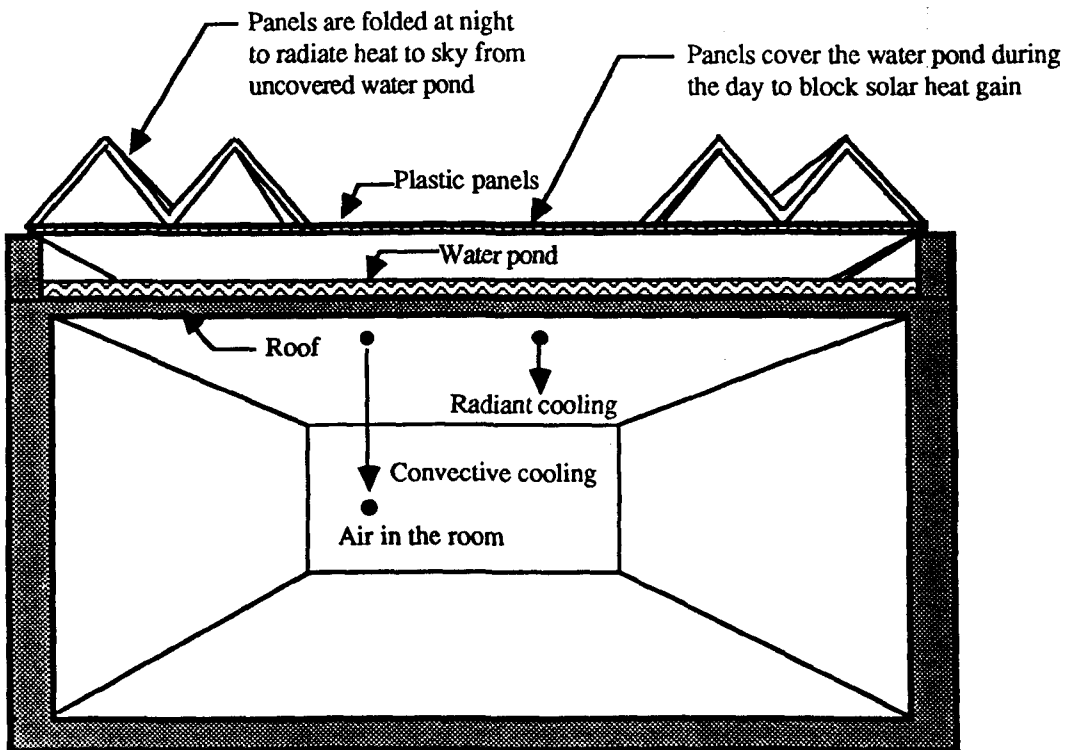
2.4.4 Radiative cooling

Another approach for cooling buildings by evaporation during the night is by long wave radiant cooling and convection. Hay and Yellott (1967-9) built a natural space cooling system into the Sky Therm house in Phoenix, Arizona. Hay (1975) built a solar house in Atascadero, California. These systems had flat roofs with water ponds. At night, cooling by evaporation and radiation takes place. During the day the water is covered with polyurethane sheet to cut off direct radiation so that water cools the space below. This approach is known as the 'Roof pond' (Figure 2.19).

Radiative cooling is effective mainly in regions with low vapour pressure and from a horizontal roof surface. Roof radiative cooling has two important effects in cooling of buildings. One is direct radiative cooling of the inhabitants by control of the radiant temperature of their immediate environment. The other is the discharge of heat from a radiative heat dissipator (such as a roof) to the cool sky. This approach was thoroughly tested by Houghton et al. (1940), Thoppen (1943), Holder (1957), Blount (1958), Sutton (1950), Yellott (1969), Jain and Rao (1974), Jain (1977) Jain and Kumar (1981) and Tiwari et al. (1982). Work covering various aspects of this approach has been carried out at Arizona State University, U.S.A., C.B.R.I, Roorkee; and I.I.T., Delhi. Sodha et al. (1981a) studied the roof pond (a pond implies a surface of water) in much detail. All these studies have been carried out on single storey buildings. Until 1986, radiative and evaporative cooling using roof water ponds was considered to be an adequate technique for cooling up to two-storeys.

Sodha et al. (1986) studied the thermal performance of an evaporatively cooled five-storey building. They concluded that for a typical summer day in Delhi (mean outdoor air temperature 38°C), evaporative cooling is adequate for the upper two storeys only.

Since in a country like Egypt, most dwellings are of three to five storeys, roof ponds are not applicable. However, it is appropriate in hot humid climates where relative humidity is high. Moreover, roof cooling has other problems: the extra load on the roof; leakage due to poor waterproofing and high cost.



Perspective section through a dwelling

Figure 2.19 Radiative cooling using a ' Roof pond'.

2.4.5 Convective cooling

Convective cooling can be effective where night air temperatures in the summer are below 19°C and wind speeds are about 1.5m/s (Givoni 1984). In Egypt, the daily minimum summer night air temperature in cities like Cairo and Aswan is always above 19°C (Table 2.1). According to Golneshan and Yagoubi (1984), a ventilation rate of 12 "air change per hour" will achieve comfort if a wind tower is used (convective cooling). However, air movement in the urban areas may be limited by the building layout. Wind tower is useful only if built high enough to capture the prevailing wind, and may be too expensive. In hot arid climates, the wind may be strong at night, and this may cause difficulty for ventilation.

Table 2.1 Summer night air temperature in Egypt.

City	Summer Months, °C				
	May	June	July	August	September
Aswan	23.3	25.5	26.1	26.1	23.8
Cairo	20.0	20.5	21.9	21.8	21.0

Data recorded between 1976 to 1985

Source: the Egyptian Meteorological office, Cairo.

Studies at the Environmental Research Laboratory in Tucson, Arizona, U.S.A. showed that better performance can be achieved when evaporative cooling is combined with natural convection (William et al. 1986). Moody et al.(1978) carried out work on a small down draught chimney. Experimental work on evaporative down draught chimneys was performed until 1984 (Mignon et al. 1985). In 1985, a theoretical study

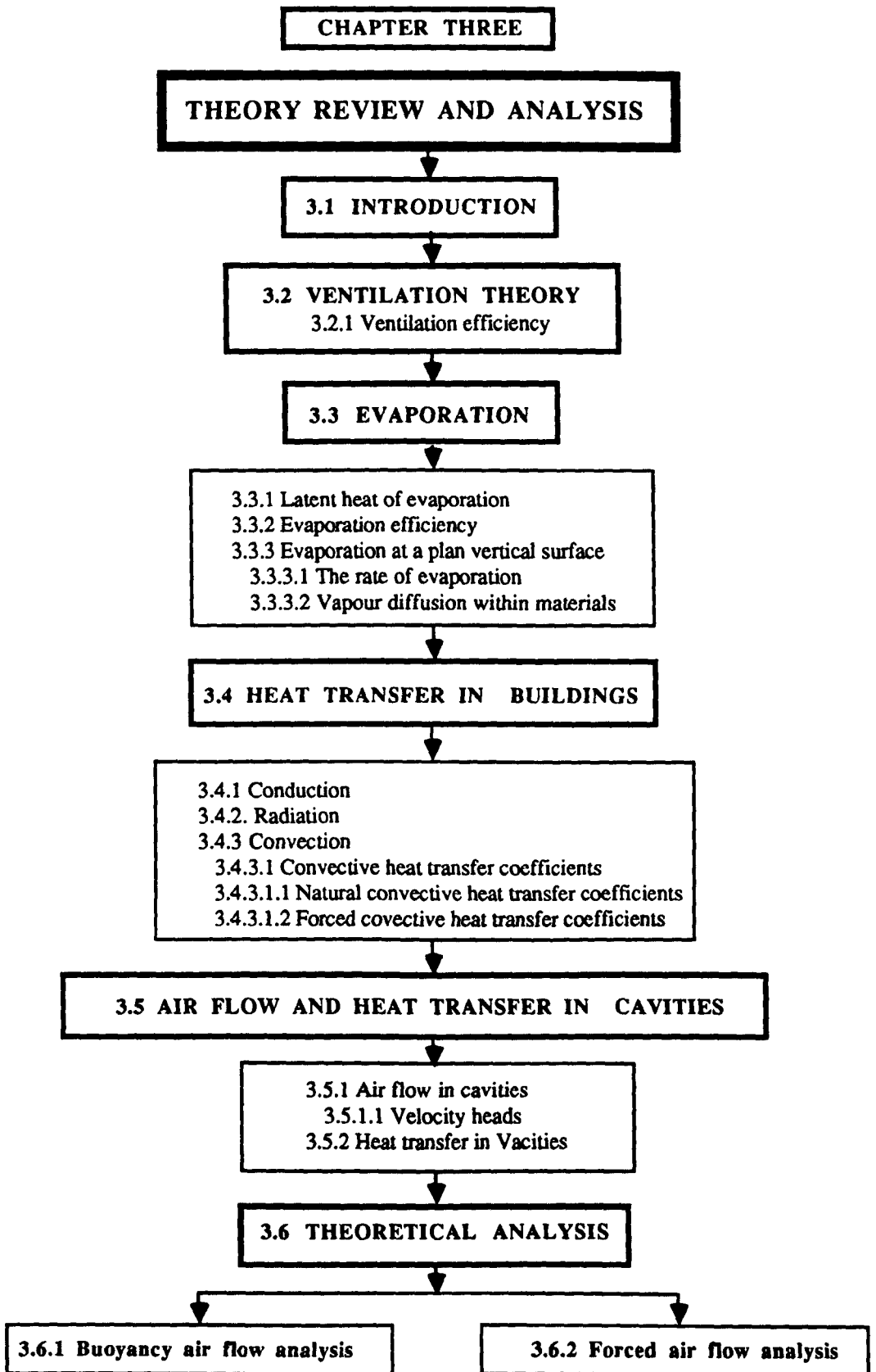
was carried out by Bohadori (1978, 1979, 1981 and 1985) to improve a wind tower with evaporative cooling using a traditional Iranian design, but no experimental results were reported.

Williams et al. (1986), at the University of Arizona, carried out a field study of passive cooling with natural draught evaporative cooling using a solar chimney. An evaporative cooling tower measuring 1.8m x 1.8m x 7.6m high was attached to one side of a well-insulated single storey house (93m²). The top of the tower was lined with vertical wetted cellulose pads 0.1m thick to cool the air. The other side of the house was connected to a solar chimney 1.2m x 1.2m x 3.4m high.

The evaporative cooling was good throughout the summer. With a wind speed from 1.5m/s to 2.5m/s and an outdoor peak air temperature of 34°C, the inside air temperature never exceeded 26°C. On a windless day, the tower was ineffective without the chimney (William et al. 1986). Wind was the significant factor. Since the size of the evaporative cooling tower is large in comparison with the house, the application to a three-storey or more building would require a bigger chimney which would be costly and difficult to construct.

Most studies of evaporative cooling have been concerned with the roof. Walls have been investigated mainly in terms of heating in colder climates (Sodha et al. 1986) etc., [Trombe (1972-4), Parry (1977), Maloney (1978), Fuchs and McClelland (1979) and Lee (1979)]. The performance of cavities in this respect is also well understood, [Parrts (1981) and Sodha et al. (1981 a.b)].

The purpose of this study is to investigate the potential of a cavity wall to promote natural ventilation by evaporative cooling in hot climates.



CHAPTER THREE

THEORY REVIEW AND ANALYSIS

3.1 INTRODUCTION

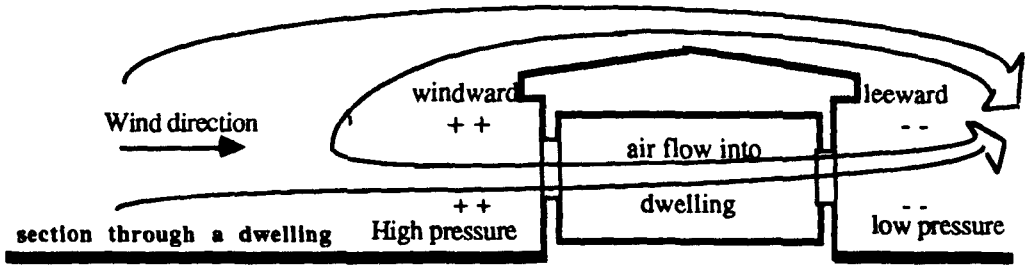
The theoretical background of ventilation, evaporation, heat transfer and air flow in buildings and cavities in particular were reviewed. Steady state theoretical analysis of an evaporative cooling cavity are included. In the first part, analysis concerns an evaporative cooling cavity with buoyancy air flow in which air moves downward and cools naturally by evaporation. The predictions of the average air velocity, the temperature drop and the associated cooling are presented. The second part is an analysis with forced air flow which incorporate one or more wet surfaces. The coefficients which relate the laboratory model of Leeds to conditions of Cairo are also presented.

3.2 VENTILATION THEORY

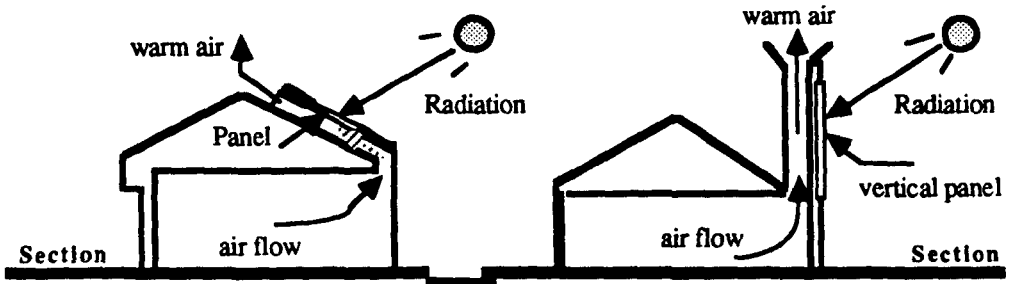
Ventilation may be either "natural" from the wind or "active" from a fan. Natural ventilation occurs as a result of a difference in the distribution of air pressure around buildings. Pressure difference causes the air to flow through dwellings in much the same way that air temperature differences cause the flow of heat through a wall or roof. A pressure differential may be caused by 'wind' or by a 'buoyancy force' that arises from the difference in density of the air at different temperatures. Ventilation may use air from either the inside or the outside of a dwelling.

Ventilation can result from:

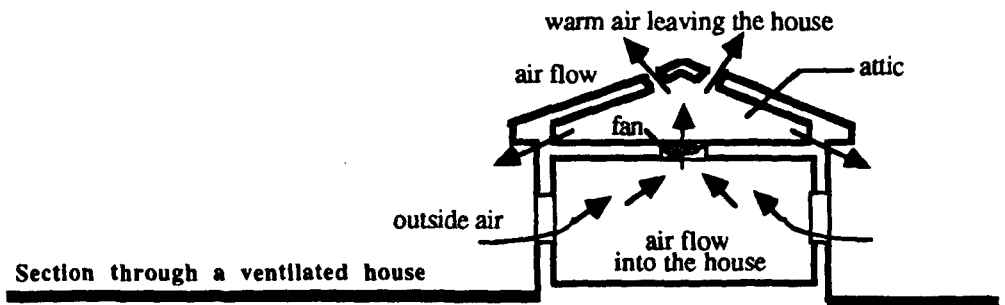
- the wind (Figure 3.1 a).
- a temperature difference or "stack-effect" (Figure 3.1 b).
- a solar chimney (Figure 3.1 b).
- whole-house fan (Figure 3.1 c).
- inside versus outside air movement 'cross-ventilation' (Figure 3.1d).



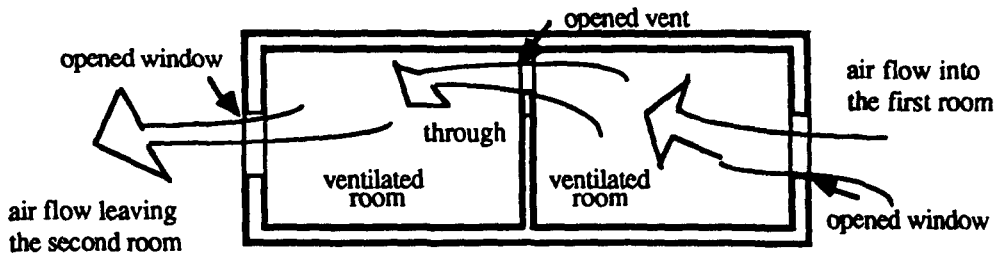
a- Wind-induced ventilation



b- Stack and panel type solar chimneys



c- Whole-house fan



Section through two rooms house

d- cross-ventilation through two rooms

Figure 3.1 diagrammatically shows different concepts of ventilation.

Air movement through an opening may be due to a pressure difference arising from density difference between air outside and inside. When the temperature of the air outside is higher than inside, air enters at a lower opening and leaves at an upper opening (Figure 3.2 a). When the two openings are opposite each other, air will flow from the lower to the upper opening (Figure 3.2 b).

The air flow V through an opening in a dwelling is given by:

$$V = K(\Delta P)^n \quad \text{m}^3/\text{s} \quad [3.1]$$

where

K = the flow coefficient m^3/s

ΔP = the pressure difference across opening Pa

n = the flow index

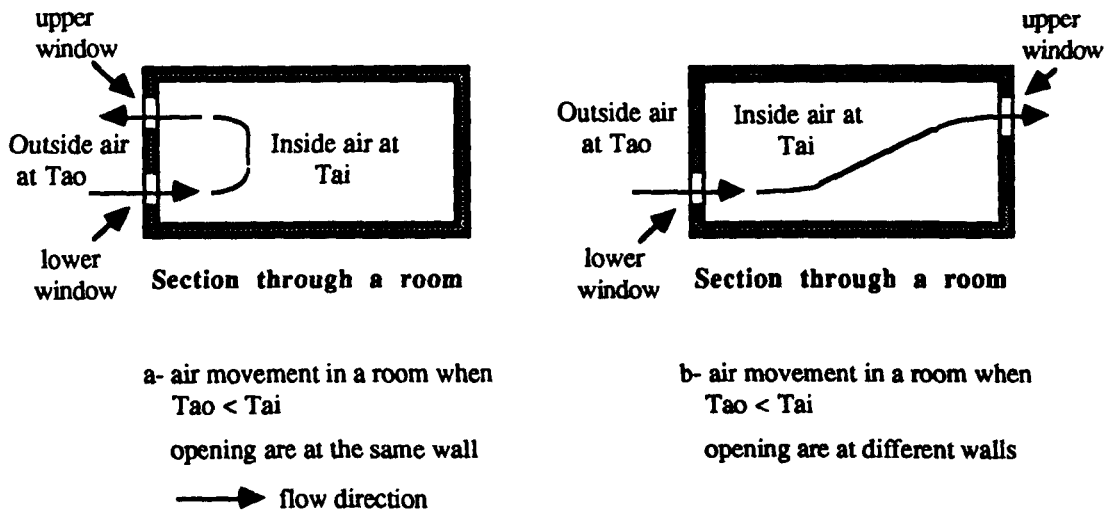


Figure 3.2 Air movement into a room caused by temperature difference or 'stack-effect'

In general, the pressure difference between two openings (Figure 3.2) due to temperature difference causing a density difference is given by:

$$\Delta p = gZ (\rho_{ai} - \rho_{ao}) \quad \text{Pa} \quad [3.2]$$

where

Z = height difference between the two openings m

ρ_{ai} and ρ_{ao} are air densities at the two openings kg/m³

For natural ventilation, the pressure difference across an opening is caused by wind, temperature difference between air inside and outside or both. In general, the pressure P_w due to the speed of the wind v_w is given by:

$$P_w = P_{co} (\rho (v_w)^2 / 2) \quad \text{Pa} \quad [3.4]$$

where

P_{co} = pressure coefficient --

ρ = air density kg/m³

wind speed v_w is obtained at a reference point 10m above the ground as recommended by the CIBSE Guide (1986).

The pressure caused by stack-effect P_s is given by:

$$P_s = \rho_o g 273 \{ (1/T_{ao}) - (1/T_{ai}) \} (h_2 - h_1) \quad \text{Pa} \quad [3.5]$$

where

ρ_o = air density at 273 °K (1.293 kg/m³ for dry air)

g = acceleration to gravity m/s²

T_{ao} and T_{ai} are outside and inside air absolute temperatures in °K respectively.

h_2 and h_1 are the heights of openings of a facade of a dwelling in m.

The above equation ignores the effect of water vapour 'moisture content' in the air.

If openings are at the same height, the air flow Q_v is given by:

$$Q_v = c_d (A/3) \{ (\Delta T d_h g) / (T + 273) \} \quad [3.6]$$

However, the air flow Q_v through an opening will depend on the shape of the opening. The CIBSE Guide (1986) expressed this by:

$$Q_v = C_d A \{ 2 (\Delta P / \rho) \}^{0.5} \quad \text{m}^3/\text{s} \quad [3.7]$$

where

C_d is the discharge coefficient (0.6), equal to that for a sharp-edged opening

A = area of the opening m^2

ΔP = pressure difference across opening Pa

For a typical dwelling with openings in various places, an effective area A_E is used to represent these openings. The effective area A_E of a number of openings A_1, A_2, \dots , and A_n in parallel across which the same pressure is applied, is expressed by the CIBSE Guide (1986) as:

$$A_E = A_1 + A_2 + \dots + A_n \quad \text{m}^2 \quad [3.8]$$

For a number of opening combined in series, the effective area may be obtained by :

$$1/A_E = 1/A_1 + 1/A_2 + \dots + 1/A_n \quad [3.9]$$

When the openings are equal, a maximum air flow is achieved. The amount of ventilation increases as the opening area is increased. When the area of two windows are not equal, the effective ventilation area A_E is given by:

$$A_E = (A_1 + A_2) / \{ (A_2)^2 + (A_1)^2 \}^{0.5} \quad [3.10]$$

3.2.1 Ventilation efficiency

Liddament (1987 a) reported work by Sandberg (1985) who introduced the concept of 'ventilation efficiency', initially to investigate contamination removal from buildings. Ventilation efficiency η_c is given by:

$$\eta_c = (C_e - C_s) / (C_i - C_s) \quad \% \quad [3.11]$$

where

C_e = concentration of substance in the air removed

C_s = concentration of substance in the air supplied

C_i = concentration of substance in the air in the building

Pitts (1986) indicates that the use of the word 'efficiency' might be seen as a misnomer since values in excess of 100% are both possible and desirable. In situations which involve heat supply or removal rather than contamination, Sandberg and Svensson (1986) modified his 'ventilation efficiency' to become 'temperature efficiency' η_t :

$$\eta_t = (T_e - T_s) / (T_i - T_s) \quad \% \quad [3.12]$$

where the suffixes are the same as those of eqn 3.11.

The above theory is for dry air, in some cases the effect of dry air might be negligible when the temperature is low. However, moisture becomes important when evaporation is intended. Evaporation induced ventilation is not studied. Theory of evaporation is reviewed below.

3.3 EVAPORATION

When hot air moves over a wet surface, it becomes cooler. This is described by Abrams (1985) as an 'adiabatic process' meaning that the total amount of heat in the system remains constant. As water evaporates, the 'sensible' heat content in the system falls, while the 'latent' heat content increases by an equal amount. The limit of temperature reduction of the air is to its 'wet-bulb temperature', when it is saturated with

water vapour (Abrams 1985). A simple measure of the potential for evaporative cooling at any given condition is the 'wet-bulb depression' W_{dep} , and is given by:

$$W_{dep} = T_{ai} - T_{wa} \quad [3.13]$$

where

W_{dep} = the wet bulb Depression K

T_{ai} = the inlet air temperature °C

T_{wa} = the inlet wet-bulb temperature °C

3.3.1 Latent heat of evaporation

Evaporative cooling results from a phase conversion, liquid water becoming water vapour. The amount of heat removed from the system as water changes from liquid to vapour is called the 'latent heat of evaporation' L_e of 2.26 MJ/kg water evaporated (CIBSE Guide, Sec. C, 1986).

3.3.2 Evaporation efficiency

Evaporative cooling has inherent inefficiencies and limitations that prevent it from operating effectively. In ideal evaporative cooling, all the air leaving is completely saturated with water vapour and thus leaves at 100% relative humidity. In an actual system, not all the air will be fully saturated. The capability of an evaporative cooling system to cool and humidify the outside air, and induce cool air inside buildings is termed the "Saturation Efficiency" SE, which is given by Abrams (1985) as:

$$SE = ((T_{ai} - T_{ao}) / W_{dep}) \times 100\% \quad [3.14]$$

where

T_{ai} = the air temperature at the inlet °C

T_{ao} = the air temperature at the outlet °C

W_{dep} = the difference between the temperature of the incoming air and its wet-bulb temperatures K

For cooling, Sodha et al.(1986) recommended that the SE should be 70% or more.

Pitts (1986) expressed the above terms (eqn.3.11 and 3.12) given by Sandberg (1984) differently from Abrams (1985) (eqn.3.14), he included the 'specific enthalpy' E for the air which is termed the 'thermal efficacy' ϵ_E (an indicator when water vapour in the air is increased), and therefore eqn. 3.11 and 3.12 becomes:

$$\epsilon_E = (E_e - E_s) / (E_i - E_s) \quad [3.15]$$

3.3.3 Evaporation at a plane vertical surface

When air flows past a wetted surface, heat is taken out of the air, its temperature falls, and the mass transfer by evaporation increases its humidity. If there is a difference in the temperature between the air and a wetted surface, heat will be transferred by convection. Evaporation of water at a wet surface occurs whenever unsaturated air comes in direct contact with that surface. The rate of 'sensible heat' transfer Q_s from the water surface to the air is:

$$Q_s = h_c A (T_s - T_{a0}) \quad W \quad [3.16]$$

where

h_c = convective heat transfer coefficient $W/m^2 K$

A = area of the wet surface m^2

T_s and T_{a0} are surface and incoming air temperatures respectively.

If there is a difference in the partial pressure of water vapour in the air and that at the wet surface, there will be a transfer of water vapour by evaporation. The rate of evaporation is proportional to the difference in the partial pressure of water vapour between the free air and that in the saturated 'boundary layer'. The 'boundary layer' is a very thin layer of air in contact with the wet surface which is considered to be saturated with water vapour. For water vapour, the surface mass transfer coefficient h_m is related to the convective heat transfer coefficient and is given by "Lewis relation" (CIBSE Guide 1986, Sec.C, A10-4) as:

$$h_m = h_c / \rho c_p \quad [3.17]$$

where

h_c = the convective heat transfer coefficient $W/m^2 K$

ρ = the density of the air kg/m^3

c_p = the specific heat capacity of the air J/kgK

It is easily shown that the dimensions of the surface mass transfer coefficient are:
 $(W/m^2K) / \{(kg/m^3) (J/kgK)\} = m/s$.

The density of the air depends on its temperature and humidity. The CIBSE Guide (1986) gives the value at 20°C to be 1.2kg/m³ and the specific heat capacity 1000J/kgK, then:

$$h_m = h_c / 1200 \quad m/s \quad [3.18]$$

3.3.3.1 The rate of evaporation

The rate of evaporation W at a $A m^2$ of a wet surface is given by (CIBSE Guide 1986, Sec.C, A10-4) as:

$$W = \{(h_m / RT) (P_s - P_a)\} \quad kg/m^2s \quad [3.19]$$

where

R = the gas constant $J/kg K$

T = the absolute temperature at the wet surface $^{\circ}K$

P_a = partial pressure of water vapour in the incoming air Pa

P_s = partial pressure of water vapour in the saturated boundary layer Pa

At 20°C, with $R = 461 J/kgK$ and $T = 293^{\circ}K$. $RT = 135 \times 10^3 J/kg$, eqn. [3.17] becomes:

$$W = (h_c / \rho c_p RT) (P_s - P_a) = \{h_c (P_s - P_a) / (1200 \times 135 \times 10^3)\} = 6.17 \times 10^{-9} h_c (P_s - P_a) \quad [3.20]$$

Thus the rate of evaporation can be related to the convective heat transfer coefficient and the humidity ratio or moisture content, as the partial pressure of water vapour is, very nearby, given by 160×10^3 g, where g is the humidity ratio or moisture content. This underlines the importance of the convective heat transfer coefficient in the evaporation process. However, in air cavities the heat transfer includes other mechanisms such as radiation and conduction. Radiation and conduction are insignificant, because temperatures, except that of the air, are all nearly the same. Heat transfer by convection between the air and the wet surface may be small compared with the latent heat needed for the evaporation water, but it is not negligible.

The heat transferred by evaporation Q_{ev} is given by:

$$Q_{ev} = W L_e = \{(h_c / \rho c_p RT) (P_s - P_a)\} L_e \quad \text{W/m}^2 \quad [3.21]$$

At 20°C, with $RT = 461 \text{ J/kgK} \times 293^\circ\text{K} = 135 \times 10^3 \text{ J/kg}$, Q_{ev} becomes:

$$Q_{ev} = \{6.17 \times 10^{-9} h_c (P_s - P_a)\} L_e \quad \text{W/m}^2 \quad [3.22]$$

The total heat transfer Q_T is termed the 'enthalpy potential' which is given by:

$$Q_T = Q_s - Q_{ev} \quad [3.23]$$

using eqns 3.16 and 3.22, eqn. 3.23 becomes:

$$Q_T = \{h_c A (T_s - (T_{ao} + T_{in})/2)\} - \{6.17 \times 10^{-9} h_c (P_s - P_a)\} L_e \quad \text{W/m}^2 \quad [3.24]$$

Stoecker (1982) indicates that the 'enthalpy potential' can provide a qualitative indication of the direction of the total heat flow Q_T . Three different cases are shown in Figure 3.3.

Case 1

Q_s, Q_{ev} and Q_T are from the air to the wet surface when:

$$\begin{aligned} T_{ao} &> T_{ws} \\ g_{air} &> g_{s.b. \text{ layer}} * \\ E_a &> E_{s.b. \text{ layer}} \end{aligned}$$

and since Q_s and Q_{ev} are from the air to the wet surface.

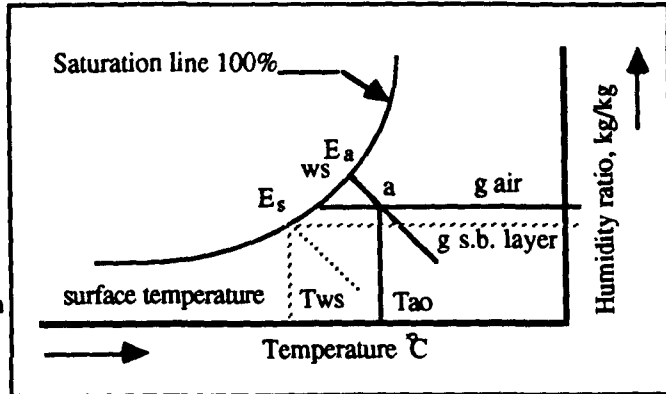


Figure 3.3 a Case 1, Q_T from air to wet surface

Case 2

Q_s and Q_T are from the air to the wet surface when:

$$\begin{aligned} T_{ao} &> T_{ws} \\ E_a &> E_{s.b. \text{ layer}} \end{aligned}$$

and Q_{ev} are from the wet surface to the air since:

$$g_{air} < g_{s.b. \text{ layer}}$$

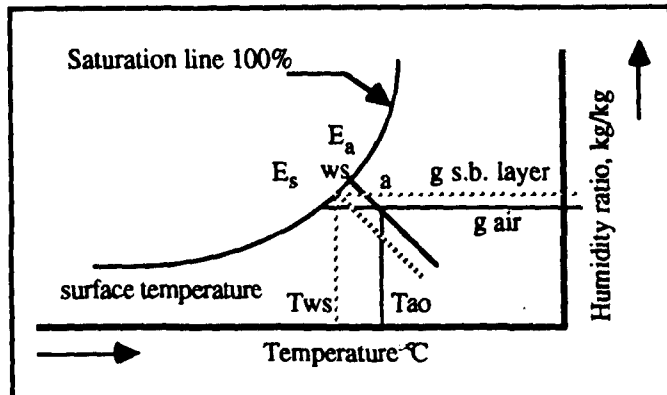


Figure 3.3 b Case 2, Q_T from air to wet surface

Case 3

Q_s is only from the air to the wet surface since

$$T_{ao} > T_{ws}$$

Q_{ev} and Q_T are from the wet surface to the air since:

$$\begin{aligned} g_{air} &< g_{s.b. \text{ layer}} \\ E_{air} &< E_{s.b. \text{ layer}} \end{aligned}$$

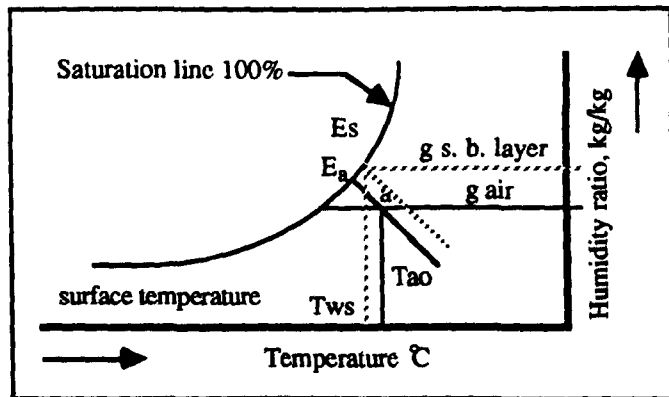


Figure 3.3 c Case 3, Q_T from wet surface to air

* saturated boundary layer

Figure 3.3 shows the directions of heat flow between the air and wetted surface according to the 'enthalpy potential'.

3.3.3.2 Vapour diffusion within materials

Another process which affects the rate of evaporation is vapour diffusion within the wet surface which depends on the vapour resistivity of the material of that surface, and the thickness through which the vapour diffuses. Most materials permit the diffusion of water vapour to some extent whenever there is a difference in the vapour pressure across the material. The rate of vapour transfer per unit area through an element of a given wet material is:

$$W = (P_s - P_a) / G_s \quad \text{kg/m}^2\text{s} \quad [3.26]$$

where G_s is the vapour resistance of the material Ns/kg .

The vapour resistance of an element thickness d_m of a given material is expressed by:

$$d_m = G_s / r \quad [3.27]$$

where r is the vapour resistivity of the material, in Ns/kgm .

The transfer of water vapour from a wet surface into air moving over it depends on the surface resistance, which may reduce the motion of the vapour into the air. The surface resistance may be defined as:

$$G_s = RT / h_m \quad \text{Ns/kg} \quad [3.28]$$

The rate of evaporation at a surface is also affected by the resistivity of the material of the surface. If the surface at which evaporation is taking place is no longer like that of a 'pool of water', a very crude approximation to reality, it may be supposed that the water vapour has to diffuse through a 'dry' layer between where the evaporation is taking place at a pool of water, and the air. The resistance to water vapour flow then is the sum of the surface resistance and that of the dry layer, $G_s + G_m$, given by:

$$G_s + G_m = RT / h_m + r d_m \quad \text{Ns/kg} \quad [3.29]$$

If the material through which evaporation takes place is not very different from 'strawboard', the vapour resistivity of which is 70 GNs/kgm, (CIBCE 1986 Table A10.4.), and if there is 1mm of 'dry' strawboard, we find:

$$G_s + G_m = (135 \times 10^3 / h_m) + 70 \times 10^9 \times 0.001 \quad \text{Ns/kg} \quad [3.30]$$

If $h_c \sim 3 \text{ W/m}^2\text{K}$, $h_m = 2.5 \times 10^{-3}$, eqn. 3.30 becomes:

$$G_s + G_m = \{ 54 \times 10^6 + 70 \times 10^6 \} \quad \text{Ns/kg} \quad [3.31]$$

so that the flow of water vapour is roughly halved accordingly.

Studies in the behaviour of concrete in the Department of Civil Engineering (J.Cabrera, 1989) show that the process considered here is very much more complicated than the crude approximation proposed.

The above review especially eqn.3.24, indicates that the convective heat transfer coefficient is an important parameter for both heat and mass transfer mechanisms 'sensible', and 'latent', and therefore a review of heat transfer in buildings, especially that of convection is included.

3.4 HEAT TRANSFER IN BUILDINGS

In a building, heat transfers by radiation, conduction, convection, and by evaporation, if a water 'fountain' is used.

3.4.1 Conduction

Heat transfers by conduction through the fabric of buildings. The rate in which heat flow depends on:

- the 'thermal conductivity' of the fabric.
- the area through which heat flows.
- the temperature gradient where the heat flows.
- the thickness of the material.

In general, the rate of heat flow by conduction Q_{cn} is given by:

$$Q_{cn}/A = -(\lambda dT)/dx \quad \text{W/m}^2\text{K} \quad [3.32]$$

where λ = thermal conductivity W/mK

3.4.2 Radiation

The heat transfer by radiation Q_r is given by:

$$Q_r = A \sigma \epsilon \{(T_2)^4 - (T_1)^4\} \quad \text{W} \quad [3.33]$$

where

A = the Area of the two surfaces m^2

σ = Stefan-Boltzmann constant (5.67×10^{-8}) $\text{W/m}^2 \text{ } ^\circ\text{K}^4$

ϵ = the emissivity of the surfaces --

$T_2 \& T_1$ = the absolute surface temperature $^\circ\text{K}$

It can be easily shown that Q_r is proportional to $T_2 - T_1$, if $T_2 - T_1$ be small enough.

If $T_2 - T_1 \ll 30$.

$$Q_r = A h_r (T_2 - T_1) \quad \text{W} \quad [3.34]$$

where

h_r = the radiative heat transfer coefficient $\text{W/m}^2\text{K}$

when radiation exchange between two surfaces with ϵ_1 and ϵ_2 , the term ϵ is replaced by configuration factor C_{12} which is given by:

$$C_{12} = 1 / \{(1/\epsilon_1) - 1 + (A_1/A_2) (1/\epsilon_2 - 1) + 1/F_{12}\} \quad [3.35]$$

where F_{12} = relative shape factor which depends on the configuration of the surfaces, relations of the shape factor is represented in detail in Wong (1977) and O'Callaghan (1980).

3.4.3 Convection

The motion of air is the result of buoyancy or an external force such as wind, or a combination of these. Convection whether natural or forced can be divided into: 'laminar' (when the air motion is highly ordered, and it is possible to identify the streamlines along which particles move), and 'turbulent' (when the air motion is irregular and has velocity fluctuations). The rate of heat transfer Q_c between a surface and the moving air may be calculated from:

$$Q_c/A = h_c (T_a - T_s) \quad \text{W/m}^2 \quad [3.36]$$

where

h_c = the convective heat transfer coefficient $\text{W/m}^2 \text{K}$

T_a = air temperature $^{\circ}\text{C}$

T_s = surface temperature $^{\circ}\text{C}$

3.4.3.1 Convective heat transfer coefficients

The convective heat transfer coefficient h_c depends on the geometry of the system, the velocity of the moving air and the temperature difference (average value between air and surface). It may be calculated from:

$$\text{Nu} = C (\text{Gr Pr})^n \quad [3.37]$$

where

Nu = Nusselt number

C = constant depends on orientation, geometry and the direction of the flow

Gr = Grashof number

Pr = Prandtl number

n = 1/3 for turbulent flow and 1/4 for laminar flow.

3.4.3.1.1 Natural convective heat transfer coefficients

Many natural convective heat transfer empirical relations found in the literature are based on two correlation: 'laminar' and 'turbulent'. McAdam (1958); O'Callaghan (1980); CIBSE Guide (1986); ASHRAE (1985); and Wong (1977). Almadri and Hammond (1983) developed a relation valid for laminar and turbulent flows. For a vertical surface where the heat flow is horizontal, the convective heat transfer coefficient may be found from:

$$h_c = [\{ 1.5(\Delta T/L)^{0.25} \}^6 + \{ 1.23(\Delta T)^{0.33} \}^6]^{1/6} \quad \text{W/m}^2\text{K} \quad [3.38]$$

where

ΔT = the temperature difference between the air and the surface K

L = a characteristic length m

For horizontal surfaces with upwards heat flow the convective heat transfer coefficient is given by:

$$h_c = [\{ 1.4(\Delta T/L)^{0.25} \}^6 + \{ 1.63(\Delta T)^{0.33} \}^6]^{1/6} \quad [3.39]$$

The length of the surface in eqn 3.38 is replaced by a relation between the two dimensions of the surface (Kreith 1973), and the CIBSE Guide (1986) suggested the mean between the two dimensions of the surface to be used as L . Incropera and De Witt (1981) used the area divided by the perimeter p (m). Almadri and Hammond (1983) proposed the hydraulic diameter d_h :




$$d_h = 4A/p \quad \text{m} \quad [3.40]$$

where

A = the area of the cross-section m^2

Equations 3.38 and 3.39 are valid only in the range of $10^4 < Gr Pr < 10^{12}$ which cover typical conditions in buildings. The convective heat transfer coefficients for surfaces of a naturally ventilated building for different heat flow direction suggested by CIBSE Guide (1986) are given in Table 3.1.

Table 3.1 The convective and surface mass transfer coefficient for different heat flow directions.

Heat flow direction	Convective heat transfer coefficient h_c $W/m^2 K$	Surface mass transfer coefficient h_m m/s
downwards 	1.5	1.25×10^{-3}
horizontal 	3.0	2.50×10^{-3}
upwards 	4.0	3.60×10^{-3}

Natural flows with air velocity less than 0.1 m/s

Air density of 1.2 kg/m^3 , specific heat capacity for air 1000 J/kgK .

3.4.3.1.2 Forced convective heat transfer coefficients

For forced flow, the convective heat transfer is based on the Reynolds and Prandtl Numbers. The CIBSE Guide (1986) gives the following equations for flow over vertical plates:

If $Re < 5 \times 10^5$, then flow is laminar

$$\text{and } Nu = 0.664 Re^{0.5} Pr^{0.33} \quad [3.41]$$

If $Re > 5 \times 10^5$, then the flow is turbulent

$$\text{and } Nu = 0.037 Re^{0.8} Pr^{0.33} \quad [3.42]$$

For air at 30°C , and laminar flow, eqn.3.41 becomes:

$$h_f = 3.96 (v / L)^{0.5} \quad [3.41.a]$$

where

h_f = the convective heat transfer coefficient $W/m^2 K$
 v = the velocity of the air m/s
 L = the characteristic length m

and for turbulent flow, eqn. 3.42 becomes:

$$h_f = 6.0 v^{0.8} L^{-0.2} \quad [3.42.a]$$

Van Straatan (1967) indicates that the convective heat transfer coefficient may be affected by other factors, such as air flow and the roughness of the plates. The above equations are valid only for flat plates. However, Nash et al. (1952) suggested that the convective heat transfer coefficient over a rough corrugated surface is of the order of 20% higher than those of the flat plates, because of the turbulent nature of the air flow over such a surface. The roughness of the surface also increases the effective area which consequently increases the heat transfer.

McAdam (1954) suggested a convective heat transfer coefficient for forced flow originally derived by Nusselt and Jurges (1922) as a function of wind speed which is given by :

$$h_f = 5.7 \{ a + b (v / 0.31)^n \} \quad [3.43]$$

where a, b and n are empirical constants

When wind speed is less than 4.8m/s, the constants a, b and n for a smooth surface are 0.99, 0.22 and 1.0. For a rough surface, they are 1.09, 0.23 and 1.0 respectively. Hence, eqn. 3.43 for a rough surface becomes:

$$h_f = 24.3 v \quad W/m^2 K \quad [3.43.a]$$

The above relation is valid for external surfaces exposed to the wind at a speed below 5m/s. However, forced and natural convection may occur simultaneously. McAdam (1954) recommended that both values be calculated and the greater used.

According to eqns 3.38 and 3.43.a, the h_c and h_f might change over a wide range. For example h_c is $0.6\text{W/m}^2\text{K}$ for natural convection when the temperature difference is 0.1K over a height 1.80m (eqn 3.38), and it could be as high as $24.3\text{W/m}^2\text{K}$ for forced flow at a speed 1.0m/s (eqn.3.43.a). However, it is believed that the convective heat transfer coefficient inside buildings is rather small compared with those near the outside surface of external walls due to the wind (Sharples 1983, and Ito et al. 1972).

3.5 AIR FLOW AND HEAT TRANSFER IN CAVITIES

In general, cavities are used in buildings to control moisture and act as thermal insulation. In hot climates, cavities, if applied, regulate heat flow into buildings, unlike in cold climates, they reduce heat losses from the warm inside into the outside 'heat conservation'. In wet climates such as that of Great Britain, cavities have been used to protect dwellings from wind-driven rain and ventilated and drained.

In air cavities, the thermal resistance depends upon the heat exchange between the two parallel surfaces and between the surfaces and the air. The main factors influencing the thermal resistance of enclosed cavities and heat flow significantly are:

- temperature difference between the two sides of the cavity
- the width of the cavity to its height
- the nature of the two surfaces facing each other
- the thermal conductivity of the walls
- whether the flow in the cavity is laminar or turbulent
- direction of the heat flow 'downward or upward'.
- external shading 'reduction of solar radiation received on external walls'

Cavities are closed or ventilated. When the cavity is ventilated, heat flow through the walls will be reduced as a direct effect of ventilation which indicates that night ventilation has an effect on the room air temperature compared with unventilated cavities. The rate of ventilation cooling Q_{vc} is given by:

$$Q_{vc} = V \rho c_p \Delta T \quad \text{W} \quad [3.44]$$

V = ventilation rate m^3/s

ΔT = temperature difference between the incoming air and that leaving K

3.5.1 Air flow in cavities

When air enters a cavity, passes through and out of the cavity, the flow is exposed to pressure losses due to this movement. The main losses are at the cavity inlet and outlet, and loss within the cavity is negligible compared with that. The traditional formula for the pressure loss due to friction of air flowing in a circular duct running uniformly is known as the D'Arcy equation,

$$\Delta P/L = 4f\{(\rho v^2 / 2) / d\} \quad \text{Pa/m} \quad [3.45]$$

where

f = the friction factor $-$
 L = length of the cavity m
 d = diameter m
 v = air speed m/s

For non-circular ducts of a constant cross-section, the diameter d may be taken as the 'hydraulic diameter' d_h given by eqn.3.40, and is equal to twice the spacing for a long slot. The coefficient of friction is a variable and depends on two factors:

a- the Reynolds number Re of the air moving in the cavity and is given by:

$$Re = v \rho d_h / \mu \quad -- \quad [3.46]$$

where

d_h = the hydraulic diameter m
 μ = dynamic viscosity $2 \times 10^{-5} \text{ Pa s}$ (for air temperature 30°C)

b- the roughness of the surface inside the cavity is expressed by a dimensionless ratio

k_s/d_t , where k_s is the absolute roughness and d_t is the thickness. The value of k_s is taken as 1.3 for 'fairface concrete' or brickwork (CIBSE Guide 1986, Table 4.2).

For air moving in a straight pipe the relation between the coefficient of friction and Re and the roughness of the surface depends on whether the flow is laminar or turbulent. If $Re < 2000$, the flow is laminar, and the friction factor is given by:

$$f = 16 / Re = (16\mu) / v \rho d_h \quad \text{--} \quad [3.47]$$

When eqn.3.46 used with eqn. 3.47, we find:

$$\Delta p / L = 32 \mu v / (d_h)^2 \quad \text{Pa/m} \quad [3.48]$$

In a cavity with length L_{cv} and laminar air flow, the pressure drop Δp in the cavity can be obtained by:

$$\Delta p = 32 \mu v L_{cv} / (d_h)^2 \quad \text{Pa} \quad [3.49]$$

If $Re > 4000$, the flow is turbulent, and the friction factor can be found from the CIBSE Guide (1985). However, the friction factor in the intermediate range 'transitional', $2000 < Re < 4000$ is not predictable.

3.5.1.1 Velocity heads

The velocity head is the kinetic energy per unit mass given by: $\rho v^2 / 2$ Pa. The pressure loss at the the exit of a pipe may be expressed as a number of velocity heads and the above equation may be expressed in terms of force as given by the CIBSE Guide (1986):

$$\text{'Head'} = n \rho v^2 / 2 \quad \text{Pa} \quad [3.50]$$

where n is the number of velocity heads --

The CIBSE Guide (1986) gives the number of velocity head for a clear opening as unity. For a cavity with a top external inlet and bottom internal outlet, the number n may be taken as 2 (inlet and outlet) and eqn 3.50 becomes: $2 (\rho v^2 / 2) \text{ Pa}$ [3.50.a].

The pressure drop at entry or exit is very much greater than the pressure drop in the cavity. For example: when air in a cavity (0.15m wide x 2m high) is moving at a velocity of the order of 0.1m/s, the pressure drop in the cavity according to eqn 3.49 is of the order of $1.42 \times 10^{-3} \text{ Pa}$. The pressure drop at the inlet or the outlet due to one or more velocity heads may range between about 6×10^{-2} to $11 \times 10^{-2} \text{ Pa}$, very much greater than that in the cavity.

3.5.2 Heat transfer in cavities

In general, cavities have been studied mainly with small surfaces for convective heat transfer. However, information on the design of wall cavities for ventilation in buildings is lacking, especially that exploiting evaporation to cool air flowing into a dwelling. Studies of cavities include: wall cavity, the Trombe wall, water cavity (Sodha et al. 1986).

Convection is thought to be the main cause of heat transfer in closed cavities. Free convection in air in an enclosure surrounded by vertical parallel walls as a result of the convective heat transfer between the surfaces and the air (Figure 3.4 a) has been investigated by Jakob (1946), Emery et al. (1965), Eckert (1961) and MacGregor et al. (1969).

Heat exchange by radiation and convection across the cavity may affect the convective air current in enclosed cavities. However, Sodha et al. (1986), indicated that 60% to 65% of the heat exchange takes place by radiation and the rest by convection.

Batchelor (1954) and van Straatan (1967) pointed out that heat transfer by conduction in air spaces wider than 20mm is almost negligible compared with both radiative and convective heat transfer.

Alawa (1980) studied the effect the thickness, position and type of insulation on a cavity wall. However, this study was to control heat gain into buildings. He concluded that up to 0.1m cavity width can be applied to buildings.

In general, heat transfer between a surface and the air in an enclosed cavity is given by:

$$Nu = C Gr^m (Z/D)^n \quad [3.51]$$

where

$C = 0.18$, $m = 1/4$ and $n = -1/9$ for laminar flow, and

$C = 0.065$, $m = 1/3$ and $n = -1/9$ for turbulent flow

Z and D are the height and width of the cavity respectively.

Heat transfer varies according to the type of the cavity. In a 'Trombe wall' (Balcomb 1978), the cavity is formed between external glazing (in some cases double glazing) and a massive wall, ventilated top and bottom (Figure 3.4 b). When the outer leaf of the wall is heated by radiation, the air near the wall becomes warmer. As convection takes place, air moves upwards by buoyancy, and enters the room (Figure 3.4 b).

Balcomb et al. (1977) studied convective heat transfer and air flow based on one dimensional thermal analysis using a forced convective heat transfer coefficient given by McAdams (1954). The flow rate obtained by equating the pressure caused by buoyancy with losses in the cavity (which considered to be negligible) compared with those of vents (inlet and outlet). The volume flow V was given as:

$$V = c_d A_{ven} \{2gZ\beta(T_{ac} - T_{ao})\}^{0.5} \quad m^3/s \quad [3.52]$$

where

c_d = coefficient of discharge between two openings 'vents', similar size in series = 0.6

A_{ven} = area of opening 'vents' m^2

T_{ac} = air temperature in the cavity $^{\circ}C$

β = volume coefficient of expansion of air K^{-1}

The 'Trombe wall' was also investigated by Akbarzadeh et al. (1982). The flow was observed to be turbulent, and they pointed out the geometry was beneficial in terms of cooling the air, especially when the width was 0.25m.

Heat transfer between small parallel plates with laminar air flow between them was studied by Elonbass (1948). The study indicates that since heat dissipation is dependent on height Z (for a very small separation) the formula to determine the convective heat transfer coefficient h_c given below can be used:

$$h_c = (\lambda_{\text{air}} / 24 Z) Ra \quad [3.53]$$

where λ_{air} is the thermal conductivity of the air w/mK and Ra is Raleigh number.

Eqn 3.53 is not applicable when the separation between the two plates is large, and the temperatures of both the air flow and the plates are equal. This indicates that with a temperature difference between the air and surfaces, eqn 3.53 cannot be used.

In England, Fitzgerald and Houghton-Evans (1987) reported work on a cavity wall to promote heating in dwellings (Figure 3.4.c). A conservatory built on the south-west side of a dwelling was used so that air in the conservatory is heated by radiation through inclined glazing. Warmed air is drawn into a secondary cavity through the ceiling of the dwelling, warming the fabric in the process, then the air passes through a vertical cavity (built on the other side of the dwelling), and then flows into the room (Figure 3.4 c). As a result, the interior is heated. Forced convective heat transfer coefficient was used.

The above review suggests that little work has been done related to two parallel plates with open ends.

What follows illustrates two theoretical analyses to predict the behaviour of an evaporative cooling cavity: first by buoyancy air flow; and the second by fan-assisted air flow.

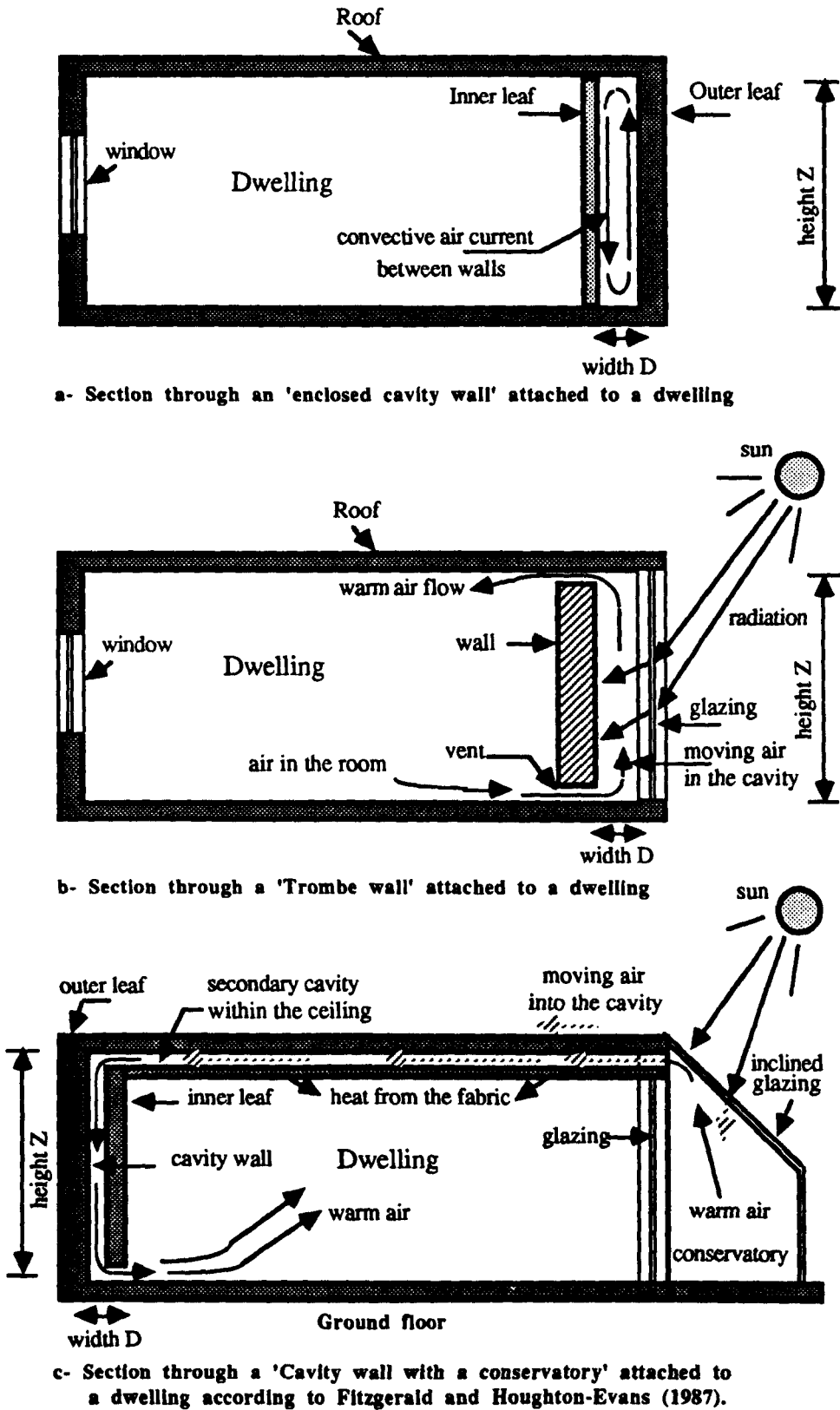


Figure 3.4 shows different types of air cavities.

3.6 THEORETICAL ANALYSIS

The first analysis is a buoyancy air flow model where air moves downward and cools naturally by virtue of evaporation. The second is a forced air flow model which predicts air temperature drop as a result of the evaporation process and the cooling. In the analysis which follows, the convective heat transfer coefficient for air between the walls is taken as recommended by the CIBSE Guide, Table 3.1 (1986). For the forced air flow model, it is taken according to eqns. 3.41.a and 3.42.a. Constants derived from the analysis for Leeds and Cairo are presented.

3.6.1 Analysis of the buoyancy air flow

For a cavity wall with height Z , breadth Y and has two wet surfaces at 100% saturation and temperature θ_{ws} , separated by D (Figure 3.5), the mass of a fluid 'air' in a cavity is $DYZ\rho_i$ (kg), the downwards force is $DYZ\rho_i g_v$ (N), and the downwards pressure is $Z\rho_i g_v$ (Pa).

a- Buoyancy pressure

Air in the cavity falls by buoyancy when it absorbs water vapour from the saturated boundary layer. The buoyancy pressure difference is caused by the density difference between the air in the cavity and that outside, and is given by:

$$BP = Z g_v (\rho_o - \rho_i) \quad \text{Pa} \quad [3.54]$$

where

BP = the buoyancy pressure	Pa
ρ_o = the density of the air outside	kg/m ³
ρ_i = the density of the air inside	kg/m ³
g_v = the acceleration of the gravity	m/s ²

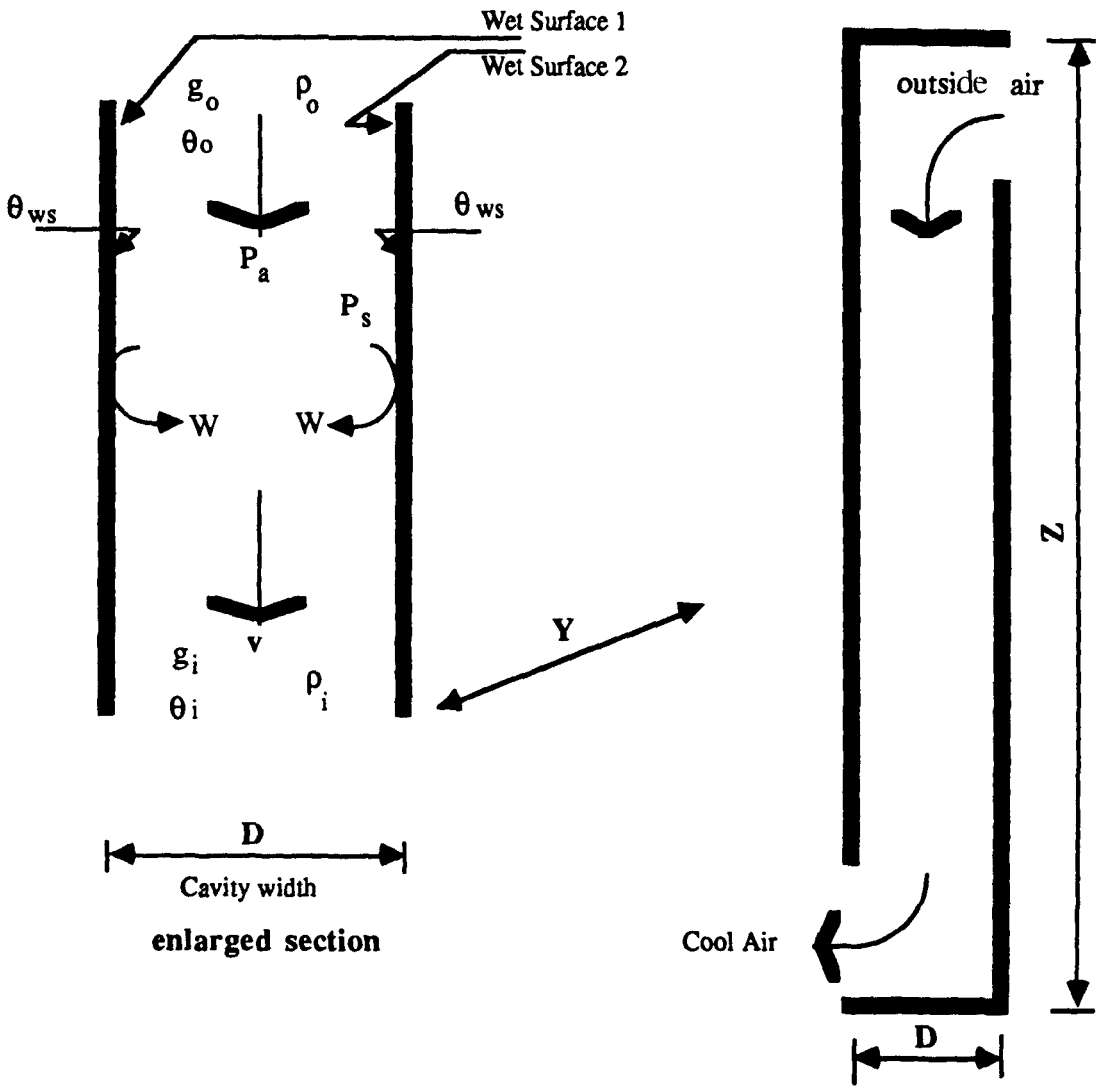


Figure 3.5 Section of the cavity used in the analysis of buoyancy air flow.

In general, for a gas 'air' $\rho_i = \rho_0 273 / (273 + \theta_i)$. The density of air at temperature θ is given by its temperature at a reference temperature usually 0°C , the CIBES Guide gives the value of $\rho_0 = 1 / 0.773 = 1.293 \text{ kg/m}^3$.

$$\rho_i = 353 / (273 + \theta_i) \quad \text{kg/m}^3 \quad [3.55]$$

So that eqn.3.54 becomes:

$$BP = g_v Z \{ [353 (\theta_i - \theta_0)] / \{ (273 + \theta_0) (273 + \theta_i) \} \} \text{ Pa} \quad [3.56]$$

A simplification is made in eqn 3.56 based on the assumption that change in the absolute air temperature $(273 + \theta)$ K is negligible. For example: in Leeds air enters the cavity at about 21°C (294°K), and the cooled air may be about 288°K . The change in the absolute temperature is about 2%. It is possible to assume that the absolute temperature of the outside air is equal to that inside. However, in hot arid climates air temperature could be as high as 35°C , thus the change in the absolute temperature $(273 + \theta)$ K of the air between the inlet and outlet is even smaller. However, this assumption is a good approximation when the difference between the inlet and outlet is small (about 8K). The buoyancy pressure BP is may be given by:

$$BP = \varphi Z (\theta_i - \theta_0) \quad \text{Pa} \quad [3.57]$$

where φ is a constant given by: $9.81 / 0.773 \{ 2(273 + \theta_0) (273 + \theta_i) \} = 138 \times 10^{-6}$, when θ_i and θ_0 are 30°C respectively. If the temperature difference is of the order of 6K to 8K, the pessure drop BP is 1.7×10^{-3} to 2.2×10^{-3} Pa

If θ_i and θ_0 are 21°C , the constant φ is given by: $3463 / \{ 2 (273 + \theta_0) (273 + \theta_i) \}$.

In temperate climates like that of Leeds, ϕ is 0.020, and in hot arid climates like that of Cairo, it is 0.018. The range of temperatures to determine the calculated constant ϕ of eqn.3.57 for Cairo represents a typical hot arid climate. The mean air temperature in hottest month in summer (June) 30°C, and the extreme about 42°C (Figure 1.1). The range of air temperatures in Leeds is restricted according to the condition in the laboratory. Table 3.2 shows that the variations in the constant ϕ of Cairo is 7% with temperature from 30°C to 42°C, and 4% with temperature from 17°C to 23°C for Leeds, and its negligible.

Table 3.2 The variations in the constant ϕ of Cairo and of Leeds as a function of the absolute air temperature.

Inlet air temp. °C	Absolute temp. °K	Coefficient of Cairo	Inlet air temp. °C	Absolute temp. °K	Coefficient of Leeds
28	301	0.01906	17	290	0.0205
30	303	0.01881			
32	305	0.01860	19	292	0.0203
34	307	0.01832			
36	309	0.01808	21	294	0.01998
38	311	0.01790			
40	313	0.01762	23	296	0.01971

b- Pressure changes

When air enters the cavity through the top inlet, passes downwards through the cavity and out, it is subject to pressure losses. However, this may be consumed at the cavity inlet and outlet. Assuming that the buoyancy pressure in eqn.3.56 is consumed by a number of velocity heads (inlet, outlet and the pressure drop within the walls). The buoyancy pressure can be expressed in terms of head losses:

$$npv^2/2 = nv^2 / (2 \times 2) [\{351 / (273 + \theta_i)\} + \{351 / (273 + \theta_o)\}] \quad [3.58]$$

where

n = number of velocity heads --

v = the velocity of the air m/s

For the same approximation as above, eqn 3.58 becomes:

$$npv^2/2 = \phi nv^2 \quad [3.59]$$

where ϕ is a constant (0.6 for Leeds and 0.57 for Cairo). The relation between the air temperature drop and the velocity of the moving air as a result of evaporation may be given by:

$$(\theta_i - \theta_o) / v^2 = (\epsilon n) / Z \quad [3.60]$$

where ϵ is a constant (30±5% for Leeds and 32±2% for Cairo).

For the incoming air at 21°C and relative humidity 60% (Leeds), moving over a wet surface at about 21°C, the evaporation rate W at entry obtained from equation 3. is 36.6×10^{-6} , based on the surface mass transfer coefficient recommended by the CIBSE Guide (1986). If the air at the outlet is saturated, the mean rate of evaporation may be given by:

$$W = [h_m / \{R(\theta_o + \theta_i)\}] \{P_s - (P_s + P_a) / 2\} \quad \text{kg/m}^2\text{s} \quad [3.61]$$

Eqn.3.61 yields an evaporation rate of 18.3×10^{-6} , if two wet partitions are used dividing the cavity into three gaps, moving air is in contact with four wet surfaces. Evaporation rates may thus be between 73.2×10^{-6} and 36.6×10^{-6} kg/m²s. In a cavity, the evaporation rate is somewhat the average of that of the top inlet and the bottom outlet. Thus, $73.2 \times 10^{-6} > W > 36.6 \times 10^{-6}$.

For air passing through a cavity of cross-sectional area DY , at a known speed v , the cooling rate from evaporation can be expressed as:

$$v DY \rho c_p (\theta_i - \theta_o) = L_e W (4 YZ) \quad W \quad [3.62]$$

where

D = the cavity width m

Y = the cavity length m

YZ = area of wet surface m²

from which:

$$v \{ (\theta_i - \theta_o) D \} / WZ = \gamma \quad [3.63]$$

where γ is constant = $(2.26 \times 10^6 \times 4) / 1.18 \times 1000 = 7661$ for Leeds and 8043 for Cairo. so that:

$$v^3 = \{ \gamma (W Z^2) / \{ \epsilon (nD) \} \} \quad [3.64]$$

The prediction of the velocity of air v from evaporation through a cavity 2m high can be obtained from:

$$v = \alpha [(4 W) / (n D)]^{1/3} \quad \text{m/s} \quad [3.65]$$

where $\alpha = \gamma / \epsilon = 6.35$

Using eqn 3.65 in eqn 3.63, the drop of air temperature $\Delta\theta$ may be obtained from:

$$\Delta\theta = \beta [(2W^2 n) / D^2]^{1/3} \quad \text{K} \quad [3.66]$$

where β is a constant = γ / α .

Using eqn 3.66 and eqn 3.65 in eqn 3.62, the cooling rate Q per metre length may be obtained from:

$$Q = \omega [2 (W Y)] \quad \text{W/m} \quad [3.67]$$

where $\omega = 1000 \times 1.18 \beta \alpha [DY \{ (WZ^2 / nD) (W^2ZD / D^2) \}]^{1/3}$

The constants α , β and ω of that of Leeds and Cairo are given in Table 3.3.

Table 3.3. The values of Leeds and Cairo coefficients

Coefficient	Leeds	Cairo
α	6.35	6.30
β	1207	1275
ω	$3.30 (10)^6$	$3.50 (10)^6$

Leeds: air temperature at 21°C & R.H. 60%

Cairo: air temperature at 35°C & R.H. 40%.

3.6.2 Analysis of the fan-assisted air flow model.

In a cavity of height Z , breadth Y , and incorporating two wet mats (four wet surfaces) at 100% saturation, and surface temperatures T_{ws} , separated by D , air enters the cavity through an inlet at temperature θ_0 and relative humidity g_0 (Figure 3.6), the air flow rate m can be found from:

$$m = v A \rho \quad \text{kg/s} \quad [3.68]$$

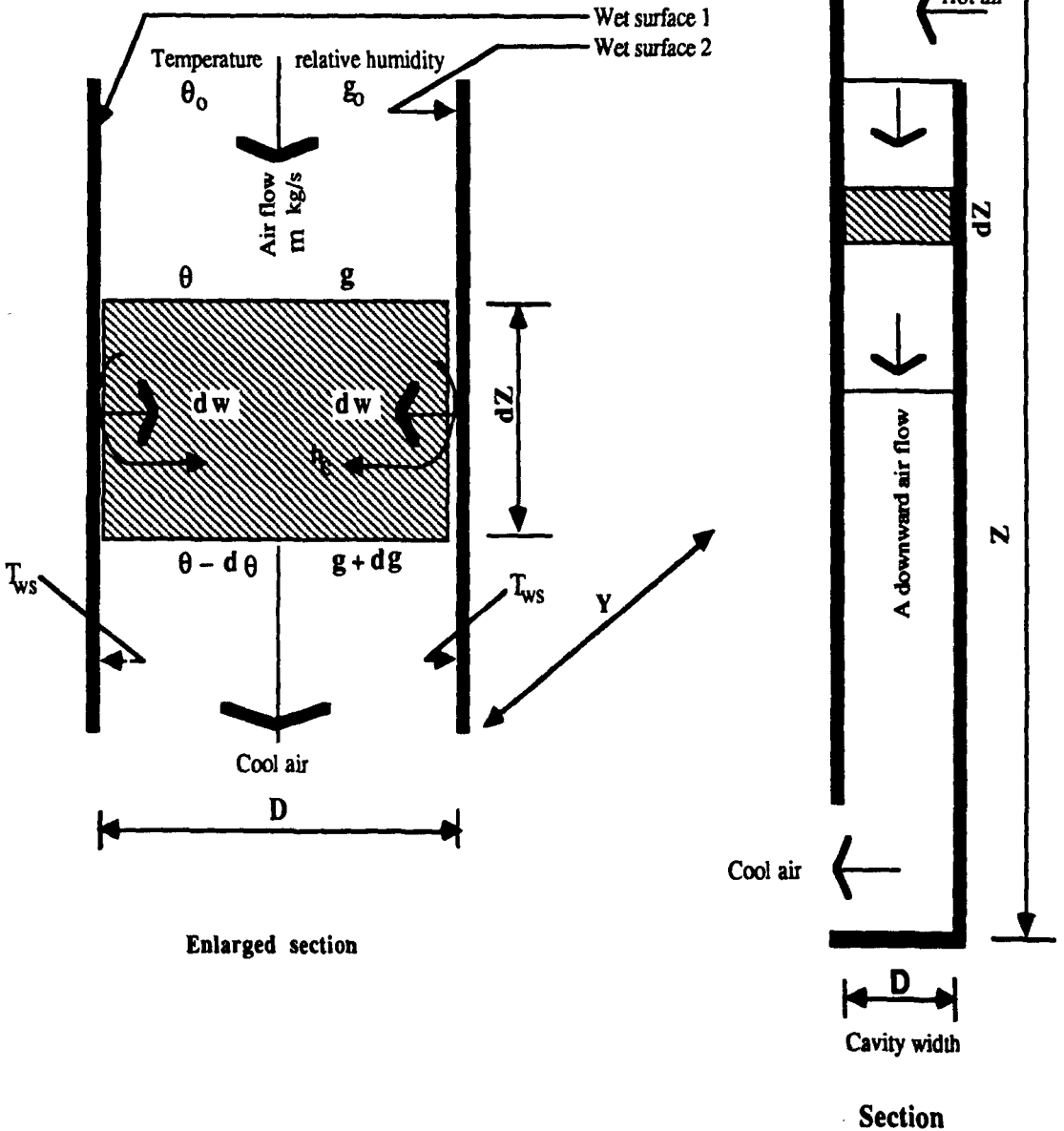


Figure 3.6 Section through the cavity used in the analysis of the forced air flow

The uncertainties of the air flow rate will depend on air velocity, area of air flow (the inlet, outlet or the cavity cross section), and the density of the air, and given by (Taylor, 1982) as:

$$(\partial m / m) = \{ (\partial v / v)^2 + (\partial A / A)^2 + (\partial \rho / \rho)^2 \}^{1/2} \quad [3.68.a]$$

If the error of air velocity is about $\pm 3\%$, air density $\pm 5\%$ and the area through which the air flows about 5% , the error of the air flow rate will be about 8% .

As dry air moves downwards adjacent to the saturated surfaces, it absorbs some water vapour. As a result, the temperature of the air starts to change and becomes θ and the humidity in the air increases g . When the air is moving along a height dZ , evaporation will take heat out of the air, and its temperature falls by $d\theta$. The relative humidity of the air increases by dg . The air temperature drop and the increase in relative humidity are expressed as $\theta - d\theta$ and $g + dg$ (Figure 3.6).

The density of air at temperature θ is given by its density at a reference temperature usually 0°C or 273°K , where dry air has a density of 1.293 kg/m^3 (CIBSE Guide, 1986). Thus, the density of air at temperature θ is given by:

$$\rho = ((1.293 \times 273) / (273 + \theta)) = ((353) / (273 + \theta)) \quad \text{kg/m}^3 \quad [3.69]$$

For air at temperature $\theta = 30^\circ\text{C}$, the density of the air $\rho = 353 / 303 = 1.16 \text{ kg/m}^3$

The rate of evaporation dW from two wet surfaces over a slice dZ of the height Z and of length Y may be given by :

$$dW = [h_c / \rho c R T] (P_s - P_a) Y dZ \quad \text{kg/s} \quad [3.70]$$

Based on eqns 3.41.a and 3.42.a, the convective heat transfer coefficient for flow at air speed about 1.2 m/s was found $4 \text{ W/m}^2\text{K}$ for a laminar flow, and $7 \text{ W/m}^2\text{K}$ when the flow

is turbulent. When the flow is laminar, eqn 3.70 becomes:

$$dW = 45.8 \times 10^{-9} (P_s - P_a) Y dZ \quad \text{kg/s} \quad [3.70.a]$$

and when the flow is turbulent, eqn 3.70 becomes:

$$dW = 80 \times 10^{-9} (P_s - P_a) Y dZ \quad \text{kg/s} \quad [3.70.b]$$

Considering the surface temperature as 20°C, the partial pressure in the saturated boundary layer g_s is 0.0148 kg_{w.v.}/kg_{dry air} (CIBSE Psychrometric Chart). This could be represented in terms of 160 x 10³g. Hence, it becomes 2368 Pa.

A linear approximation is made in the region between 15°C to 20°C and is given by:

$$10^3 g = 0.82\theta - 1.6 \quad \text{Pa} \quad [3.71]$$

Hence, the corresponding partial pressure $P(\theta)$ is given by:

$$160 \times 10^3 g = 131.2\theta - 256 \quad \text{Pa} \quad [3.72]$$

In temperate climate, if air enters a cavity at 7°C and 100% saturation (this value is considered for the average heating season in South England), the partial pressure is 992Pa. However, in hot climates, the partial pressure of air at 30°C and 40% saturation is 1744 Pa.

A mass balance at a slice height dZ may be given by:

$$m dg = dW = 10^{-3} \psi \{ (0.0148 - g) Y dZ \} \quad [3.73]$$

where ψ is a constant: 7.3 and 13 for turbulent and laminar flow respectively. However, these constants are 14.6 and 26 for a cavity having four wet surfaces. As air moves over

a height dZ , heat is removed from the air as a result of evaporation dW , and the change in air temperature is $d\theta$. The rate of heat removal dQ is given by:

$$dQ = dW L_e = - m c d\theta \quad [3.74]$$

Substituting the rate of evaporation dW from eqn.3.73 into eqn.3.74:

$$dQ = - m c d\theta = 10^{-3} \psi \{ (0.0148 - g) \} Y dZ L_e \quad [3.74.a]$$

Since

$$dg / d\theta = - c / L_e \quad [3.75]$$

The differential eqn 3.75 is solved, and the partial pressure g found by integration with respect to θ . The integration gives:

$$g = \text{constant} - c\theta / L_e \quad [3.75.a]$$

If $\theta = \theta_0$ (air entering the cavity) , $g = g_0$. The air relative humidity is:

$$g_0 = \text{constant} - c\theta_0 / L_e \quad [3.75.b]$$

Thus, $g - g_0 = (c / L_e) (\theta_0 - \theta)$ [3.76]

$$g = g_0 + (c / L_e) (\theta_0 - \theta) \quad [3.76.a]$$

Substituting g in eqn.3.74.a:

$$- m c d\theta = 10^{-3} \psi \{ 0.0148 - g_0 - (c / L_e) (\theta_0 - \theta) \} Y dZ L_e \quad [3.77]$$

from which:

$$d\theta / [(0.0148 - g_0) - (c / L_e) (\theta_0 - \theta)] = (- 10^{-3} \psi Y dZ L_e) / m c \quad [3.77.a]$$

$$d\theta / [(L_e / c) (0.0148 - g_0) - (\theta_0 - \theta)] = (- 10^{-3} \psi Y dZ) / m \quad [3.77.b]$$

The differential equation is solved, and the change in the temperature of the air found by

integrating with respect to Z. The integration gives:

$$\ln [(L_e/c) (0.0148 - g_o) - (\theta_o - \theta)] = \{- 10^{-3} \psi YZ/m\} + \text{constant} \quad [3.78]$$

If $Z = 0$, $\theta = \theta_o$, and the constant is:

$$\ln \{(L_e/c) (0.0148 - g_o)\} \quad [3.79]$$

thus eq3.78 becomes:

$$- 10^{-3} \psi YZ/m = \ln [1 - [(\theta_o - \theta) / \{(L_e/c) (0.0148 - g_o)\}]] \quad [3.80]$$

$$\exp - 10^{-3} \psi YZ/m = 1 - [(\theta_o - \theta) / \{(L_e/c) (0.0148 - g_o)\}] \quad [3.80.a]$$

$$[(\theta_o - \theta) / \{(L_e/c) (0.0148 - g_o)\}] = 1 - \exp - 10^{-3} \psi YZ/m \quad [3.81]$$

Whence the temperature fall, $(\theta_o - \theta)$

$$(\theta_o - \theta) = [(L_e/c) (0.0148 - g_o)] [1 - \exp - 10^{-3} \psi YZ/m] \quad [3.82]$$

$$(\theta_o - \theta) = [2.26 \times 10^3 (0.0148 - g_o)] [1 - \exp - 10^{-3} \psi YZ/m] \quad [3.83]$$

In a temperate climate like that of South England, the change in air temperature $\theta_o - \theta$ per unit length may be found from:

$$\theta_o - \theta = 19.44 \{(1 - \exp - 10^{-3} \psi Z / m)\} \quad \text{K} \quad [3.83.a]$$

In a hot arid climate, when air enters the cavity at 30°C and 40% saturation. The change in air temperature $\theta_o - \theta$ as a result of evaporation per unit length may be found from:

$$\theta_o - \theta = 8.81 \{(1 - \exp - 10^{-3} \psi Z / m)\} \quad \text{K} \quad [3.83.b]$$

If the air flow rate is of the order of 0.028kg/s, and turbulent, the drop in air temperature $\theta_0 - \theta$ over height of 2m is given by:

$$\theta_0 - \theta = 8.81 \{ (1 - \exp - 0.313 x2) \} = 4.0 \text{ K} \quad [3.83.c]$$

and for laminar flow:

$$\theta_0 - \theta = 8.81 \{ \{1 - \exp -0.557 x2\} \} = 5.9 \text{ K} \quad [3.83.d]$$

The humidity increase (g)

The humidity increase as a result of evaporation may be given by :

$$g = g_0 + 4.42 \times 10^{-4} (\theta_0 - \theta) \quad \% \quad [3.84]$$

For a height of 2m, the drop in the temperature of the air could be of the order of 6K, consequently, the increase in the air relative humidity as a result of evaporation when air enters at 30°C and 40% relative humidity could be of the order of about 63±2%. with an increase of 23±2%.

Cooling (Q)

The cooling rate per unit length of a cavity 2m high in temperate climates can be obtained from:

$$Q = m c \{ 19.44 (1 - \exp - \alpha Z) \} \quad \text{W/m} \quad [3.85]$$

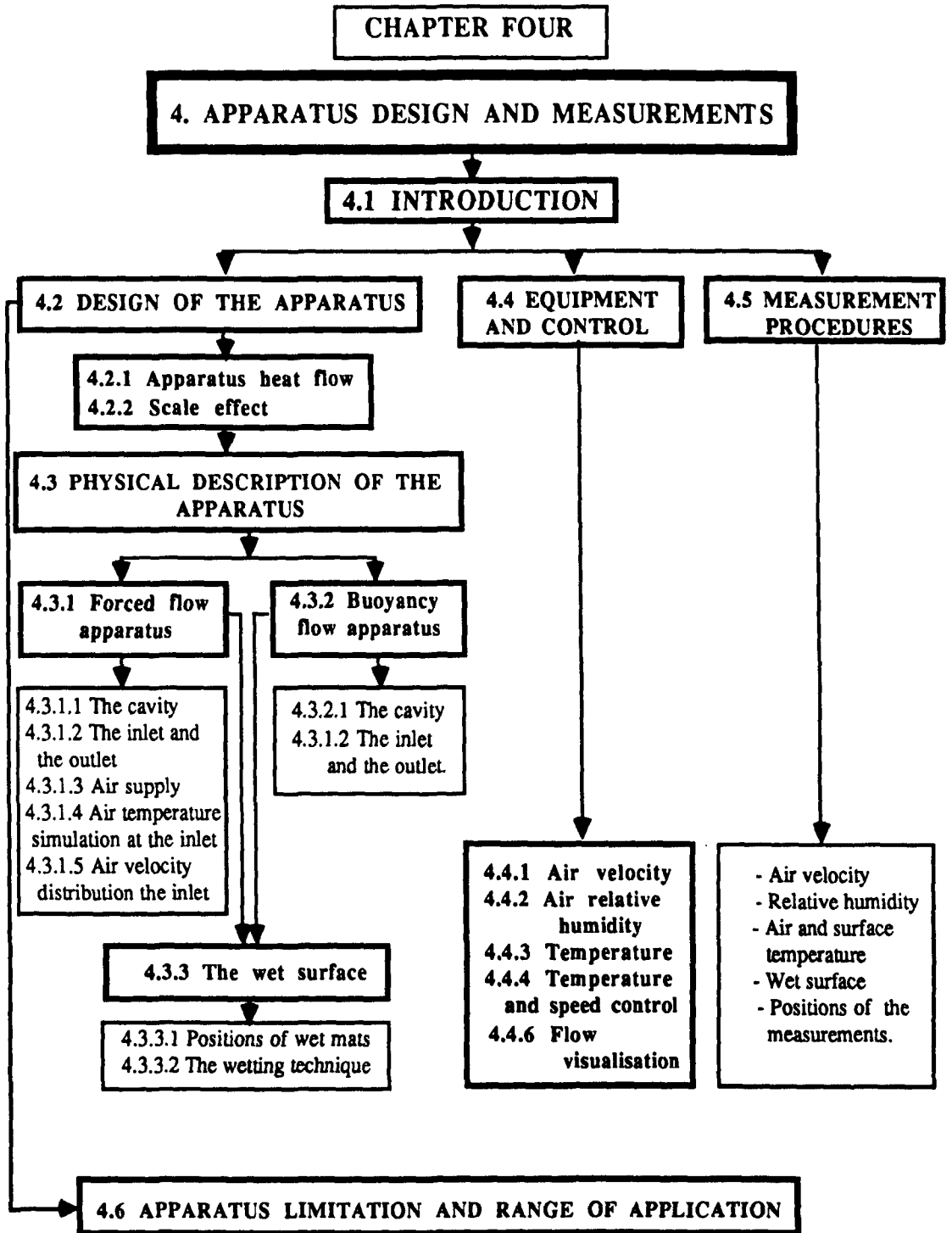
where α is the value of the constant 0.313 and 0.557 for turbulent and laminar air flow respectively moving between two wet surfaces with area of evaporation of the order of 3.6 m².

In hot arid climates the rate of cooling per unit length may be obtained from:

$$Q = m c \{ 8.81 (1 - \exp - \alpha Z) \} \quad \text{W/m} \quad [3.85.a]$$

when the air flow is of the order of 0.04 kg/s in a cavity 2m high, eqn.3.85.a becomes:

$$Q = 352 (1 - \exp - 2 \alpha) \quad \text{W/m} \quad [3.85.b]$$



CHAPTER FOUR

APPARATUS DESIGN AND MEASUREMENTS

4.1 INTRODUCTION

The aim of this chapter is to examine the application of cooling by evaporation in dwellings in a hot arid climate. Cooling could be obtained by exploiting one or more wet surfaces within a cavity wall built on the shaded side of a dwelling, where the air temperature is lower than that on the sunlit side (Figure 1.11 to Figure 1.13). The range of air temperatures is from 30°C to 35°C and that of the relative humidity is from 30% to 50%. These are typical of a hot arid climate like that of Egypt.

An apparatus was built to investigate:

- passive cooling of a room in which air moves and is cooled by buoyancy as a result of evaporation within the cavity;
- cooling of a room in which air is forced to move by a fan and is cooled by evaporation.

Practical circumstances limited the choice of the test cavity, but care was taken to avoid systematic errors. A full scale apparatus was used to minimise the influence of uncontrolled variables. Because of the limitations of time, cost and space, a single room only was simulated. A plan and a section of typical low-cost dwelling are shown in Figure 4.1.

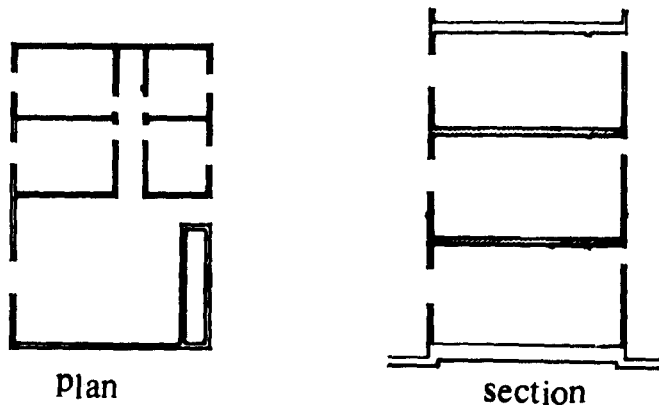


Figure 4.1 Plan and section of a typical low-cost dwelling in Egypt.

4.2 DESIGN OF THE APPARATUS

4.2.1 Apparatus heat flow

In a building of three storeys, energy flows in from two main directions: vertically through the roof, ground and intermediate floors; and horizontally through walls. The room was chosen to represent the middle storey where the effect of the roof and the ground on heat transmission is small. To simulate a real room in a dwelling with an evaporative cavity, the flow of energy, without a wet surface, should be taken into consideration. These flows are:

- heat introduced into the sunlit wall by solar radiation .
- diffused radiation and radiation reflected from the ground onto the shaded wall.
- heat gain of the room by conduction and convection through ventilation from outside air.
- energy introduced by occupants and appliances.

Since the purpose of the investigation was to examine air movement and cooling by evaporation, the following energy flows were not considered because of their negligible effects (see chapter three):

- heat gain due to radiation.
- heat input through the building envelope.
- heat produced by occupants and appliances.

When the wet surface is introduced, energy flows in the system are as follows:

- energy loss by ventilation mainly related to cooling by evaporation from the wet surfaces to the air (Figure 4.2).
- all other flows of energy in the system (without the wet surface).

Page (1964) stated that in order to conduct physical tests the following should be remembered:

- the condition of the testing should be such as to ensure physical dimensional similarity as far as possible.
- the relative importance of the different dimensional parameters should be carefully considered in relation to the problem under study
- in putting forward any experimental conclusion, the limits of the tested model must be stated.

- other factors such as cost, amount of the material, and the sizes of instruments should be taken into consideration.

The most important consideration in the design of the apparatus was to arrange the system so as to conform to the boundary conditions and flow of the physical problem. Since air flow over a vertical wet mat was taking place by buoyancy in the investigation, natural convection was involved, and the surface was made isothermal within a limited variation (about 1.5K). This was extremely important for measuring the air flow.

4.2.2 Scale effect

The use of a smaller than full size cavity can lead to a scale effect, which Wanneburg and van Straaten (1967) define as:

"a model may be said to be subject to scale effect if a change in the Reynolds number results in a change in the variation of non dimensional flow parameters". Ideally, the Reynolds number in the model test should be the same as that in the full size equivalent. To ensure this, a full scale apparatus is used for the investigation.

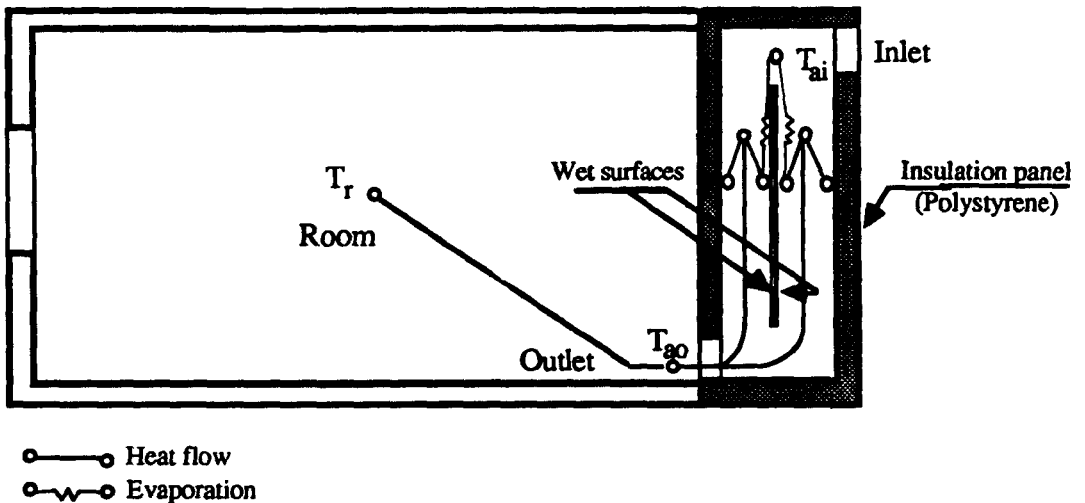


Figure 4.2 Heat and evaporation flow in the test cavity.

4.3 PHYSICAL DESCRIPTION OF THE APPARATUS

The apparatus was designed to study the effect of different parameters such as the cavity width and the size of the outlet on the air flow and cooling resulting from evaporation in the cavity. To simulate a real dwelling, a room (3000mm long, 3600mm wide and 2400mm high) with 50mm polystyrene foam insulation panels was built for the test. The panels were mounted on 25mm by 25mm steel frames, each 1200mm. They were made easy to remove so that the cavity could be adjusted (Plate 4.1).

4.3.1 Forced flow apparatus

4.3.1.1 The cavity

A cavity (1200mm long, 500mm wide and 2200mm high) was constructed from 50mm aluminium faced compressed polystyrene sheet (Figure 4.3). The walls had a thermal resistance of $2.2\text{m}^2 \text{K/W}$ so that heat transmission into or out from the cavity was mainly by ventilation. The cavity was designed of four walls (three fixed and one movable) so that the width of the cavity (in direction x, Figure 4.3) could be varied. The width was varied from 100mm to 125mm, 200mm, 300mm and 400mm. Extended area was provided to allow for the width to be varied (Figure 4.3). The movable wall was supported from the roof and was run on a 20mm wide channel marked at 100mm intervals so that the width of the cavity could be determined. It was strengthened with 30mm U-shaped aluminium channels to prevent damage (Figure 4.4). All gaps were filled with mastic to ensure that the cavity was air-tight.

A perspex panel (650mm long and 850mm high) was fixed on one side of the cavity to provide access for instruments and inspection. To avoid additional heat losses through the panel, it was covered with the same material as the walls. Two permanent perspex panels were also fixed into the side walls so that adjustments of the cavity width and smoke visualisation could be checked. Figure 4.3 shows the plan of the apparatus and Figure 4.4 shows a vertical section of the apparatus.

4.3.1.2 The inlet and the outlet

The top left side of the cavity was used for air entry. The inlet was 1140mm long and 250mm high. It was fixed at 250mm due to the limitation of the room height. The outlet into the room was 1200mm long and of a variable height of 100mm and 200mm.

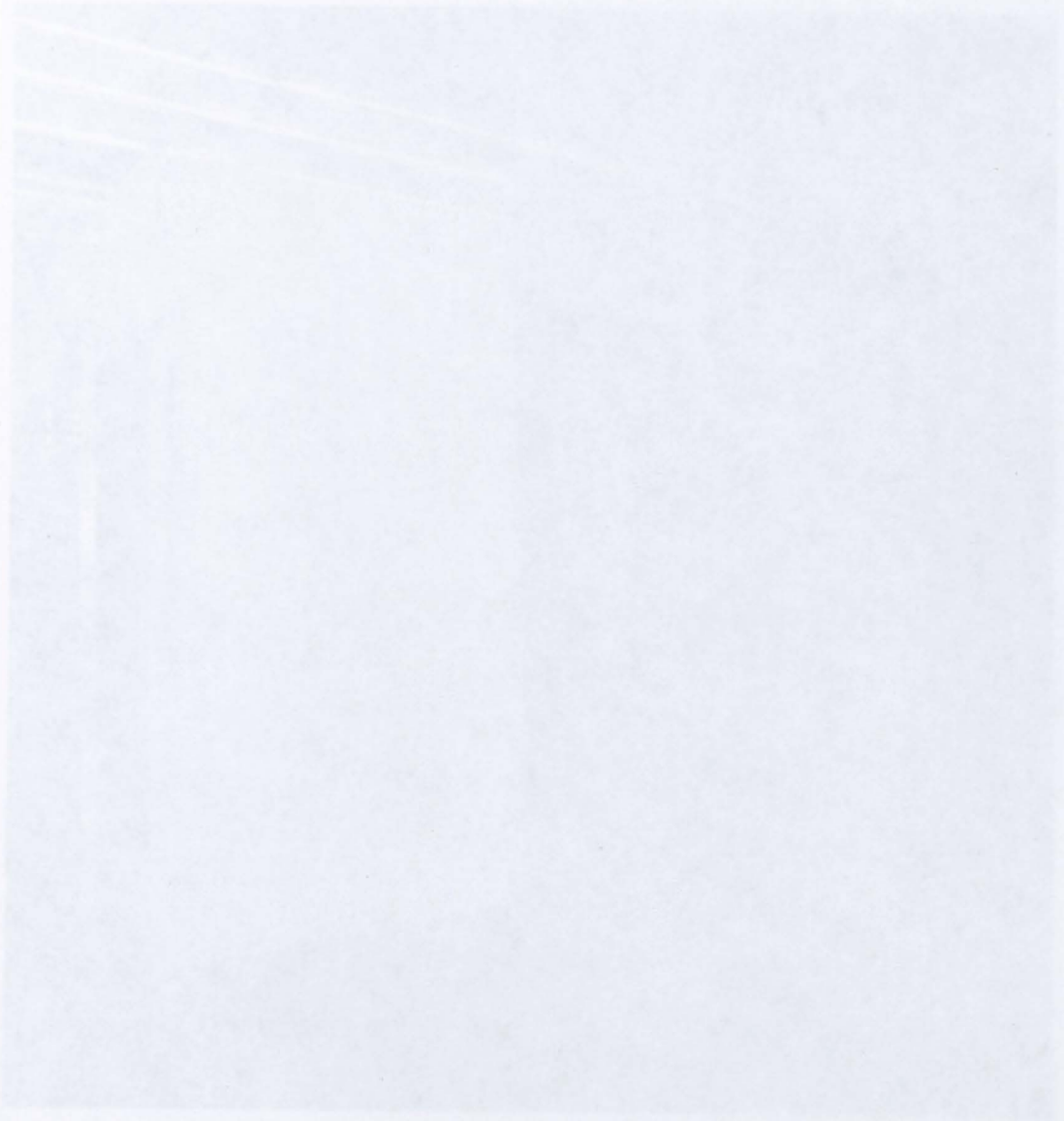


Plate 4.1 The room used for the test from a position indicated on Figure 4.3.



Plate 4.1 The room used for the test from a position indicated on **Figure 4.3**.



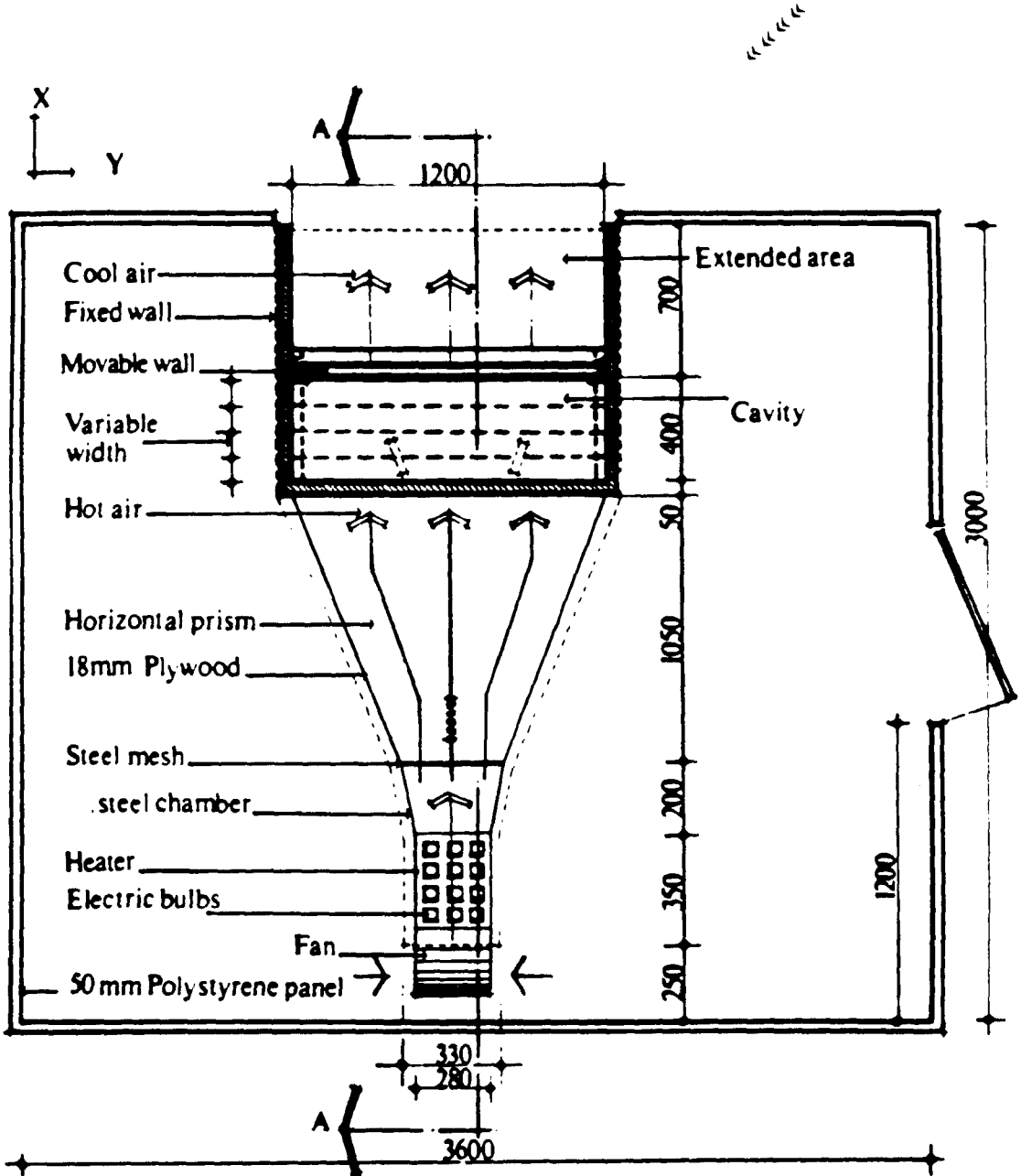
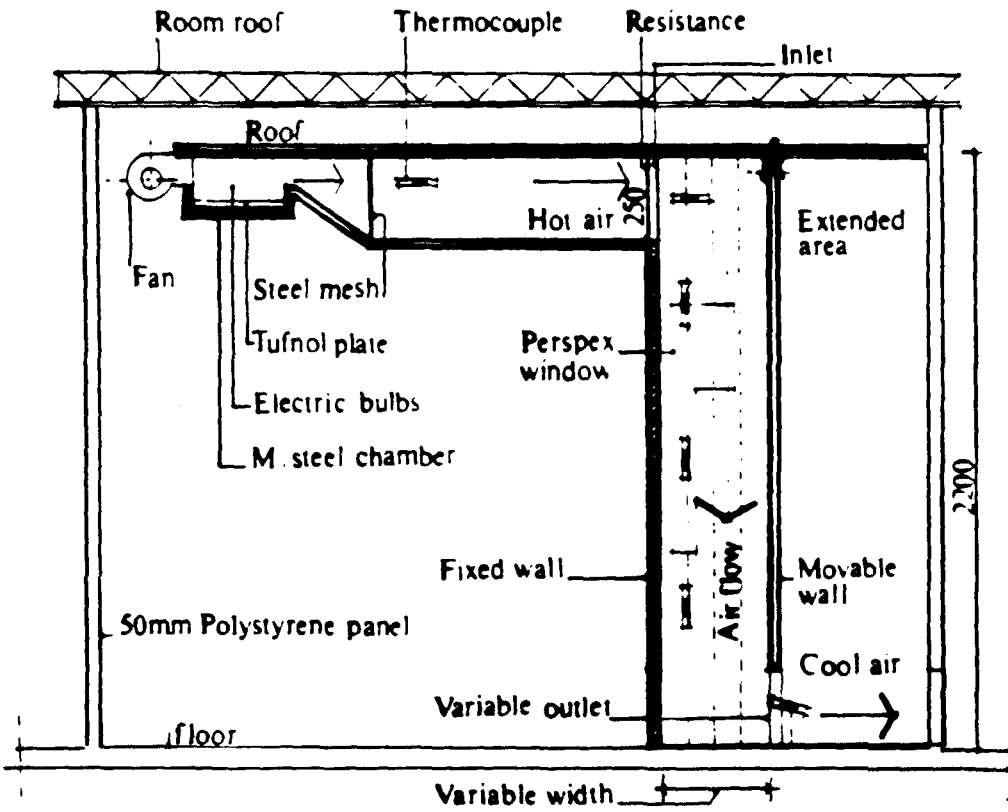


Figure 4.3 Plan of the apparatus (forced flow).



Section A-A

Figure 4.4 Section through the apparatus (forced flow).

4.3.1.3 Air supply

A fan was used to supply air horizontally from the laboratory where air temperature and relative humidity were stable. The ideal solution for supplying air would be to build a rectangular duct equal to the size of the inlet so that a uniform and homogeneous air distribution could be achieved. With a fan size 280mm x 100mm, it was necessary to make a horizontal prism of 18mm plywood sheets (insulated with 25mm polystyrene) between the inlet and the fan (Figure 4.3). The inner side was covered with aluminium foil which had the same emissivity as the cavity wall, and one side was made movable to gain access for installing air thermocouples and to inspect the heater.

To prevent fire, the smaller end of the plywood duct was joined to the fan via a 2mm mild-steel chamber containing the heater (Figure 4.4).

4.3.1.4 Air temperature simulation across the inlet

The apparatus was built to simulate the air temperature in a hot-arid climate (30°C to 35°C). The air temperature within the laboratory is usually from 18°C to 23°C. Air had therefore to be heated.

The air could have been heated by a convective fan heater. Most fan heaters have a fixed speed. These speeds were higher than the ranges required for observations (0.2m/s to 0.4m/s). This was being rejected because speed controlling was difficult. Electric light bulbs (100 Watts each) were used instead: twelve bulbs in four rows. They were fixed on a 15mm tufnol plate (350mm x 280mm). This, in turn, was fixed to the flat base of the steel chamber which was insulated with 25mm aluminium foil backed fibre glass. A steel mesh (380mm x 280mm) was used as an air distributor. It was placed away from the light bulbs so that a good air mixture and uniform temperature across the inlet could be achieved. The amount of heat (Q) needed was about 1.5kW:

$$Q = m c_p (T_r - T_l) \quad \text{W} \quad [4.1]$$

Where

m = mass flow rate of air through the fan kg/s

c_p = specific heat capacity of air 1000 J/kgK

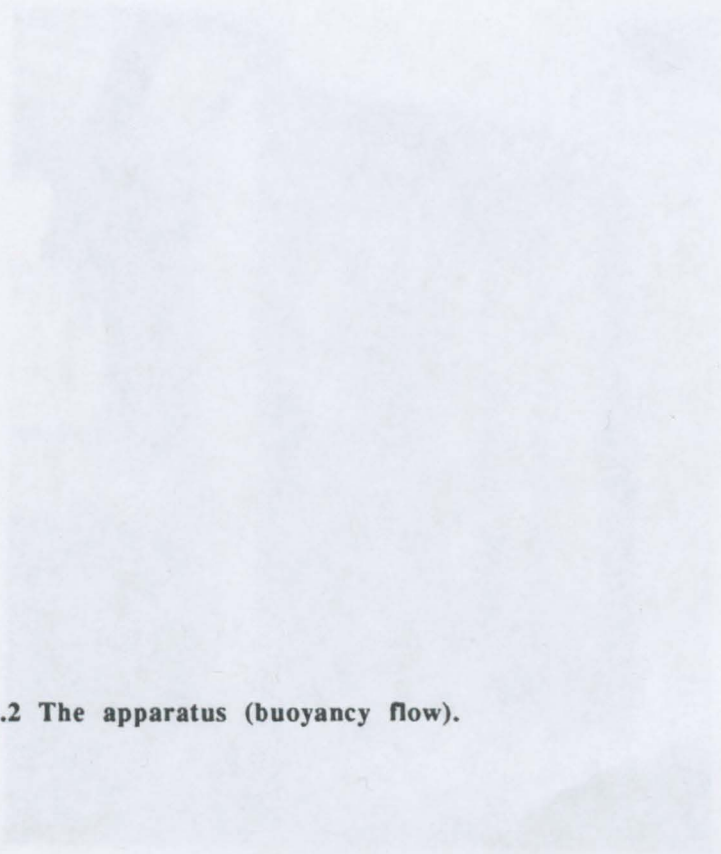
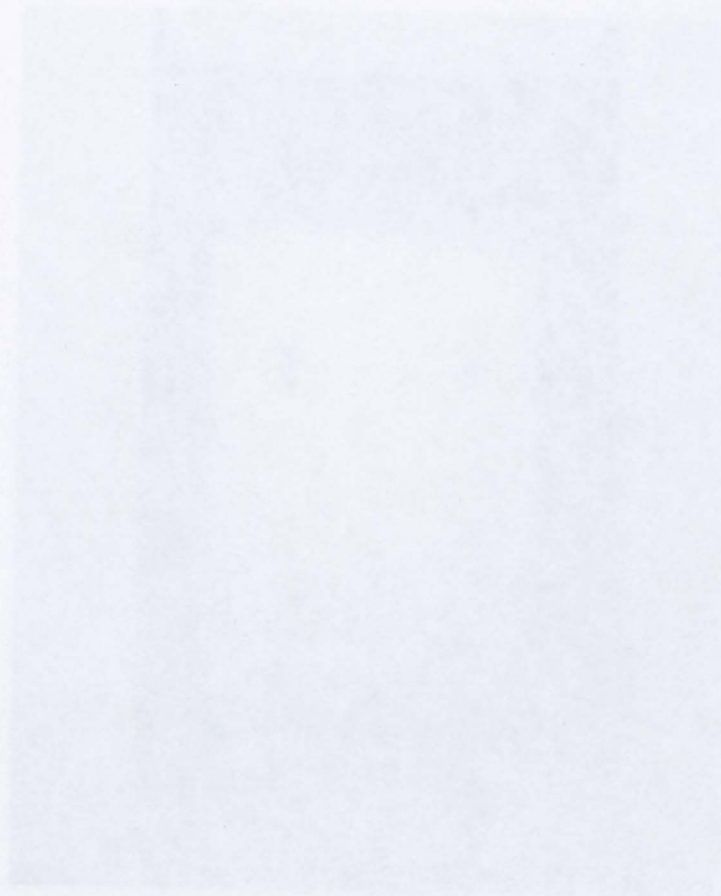


Plate 4.2 The apparatus (buoyancy flow).

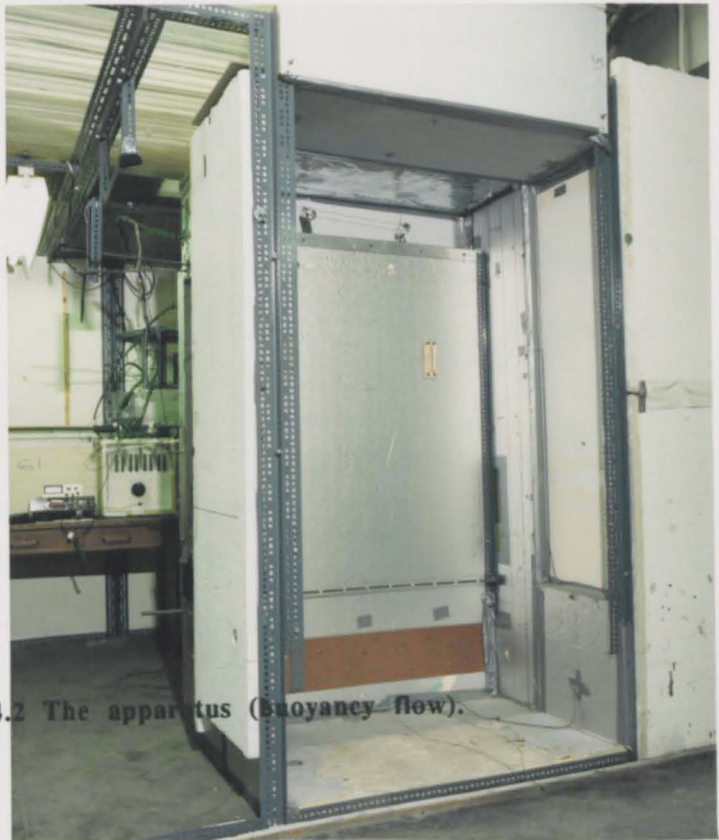
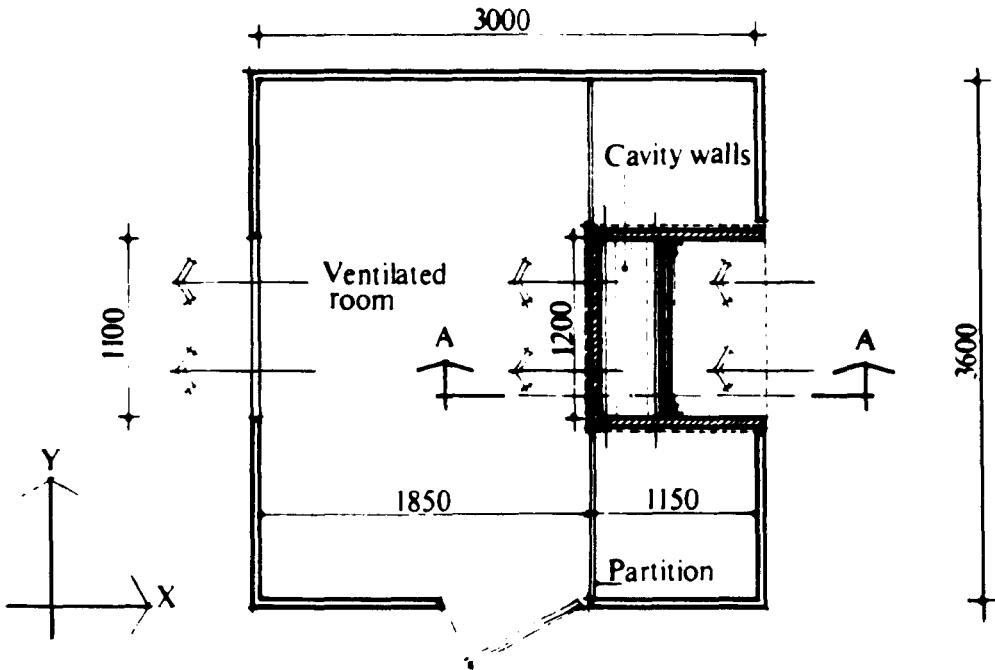
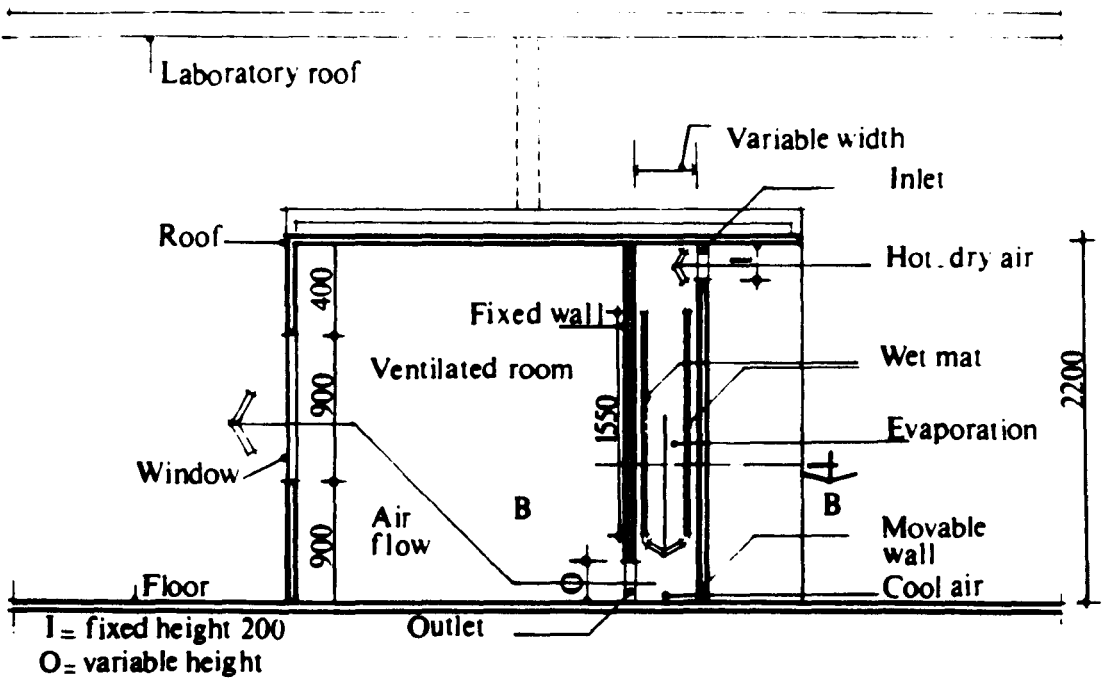


Plate 4.2 The apparatus (buoyancy flow).





B.B Plan of the apparatus (buoyancy)



A.A Section through the apparatus

Figure 4.5 Plan and section of the apparatus (buoyancy flow).

4.3.3 The wet surface

To demonstrate how air moves and cools as a result of evaporation, one or more vertical wet surfaces within the cavity wall were used. The material used had to:

- absorb much of the water;
- maintain water within its tissues;
- release water as required;
- be cheap and easily obtainable.

All man-made fabrics have low ability to absorb water. Natural materials such as linen or other cloth could be used; linen was rejected because of its cost, and other cloth was disregarded because of its low ability to absorb and maintain water. It was decided to use straw mats (2200mm long and 1800mm high) from Egypt. These were woven out of reeds, easily available and cheap. In the apparatus, these were 1150mm long and 1550mm high (Plate 4.3).

4.3.3.1 Position of the wet mats

The wet mats had different positions inside the cavity (Figure 4.6): first, "near the wall" (position [1]) where the area of evaporation was only one side of mat. Second, "in the middle of the cavity" (position [2]) where air flowed over both sides of the mat so that the area of evaporation was doubled. Third, "two mats were placed near the walls" (position [3]) so that the evaporation was double that of position [1]. Finally, "the two wet mats were placed between the walls" (position [4]) so that the area of evaporation was four times that of position [1]. In all positions, they were placed from 100mm below the inlet down to 1650mm.

4.3.3.2 The wetting technique

Two ways of wetting were considered: first water rising by capillarity using a 50mm x 50mm P.V.C trough. The mat was wetted first and immersed in the trough. Water rising through the mat was found to be about one-third its height (480mm). The second way was by rolling the mat and immersing it inside a P.V.C tube (100mm diameter and 1900mm long). The mat was left in water for 24 hours. It was placed outside the cavity to drain. 2mm polythene sheets were used to cover the mats so that little evaporation took place. After draining off excess water, mats were placed inside the cavity as required. The cavity was closed and sealed.



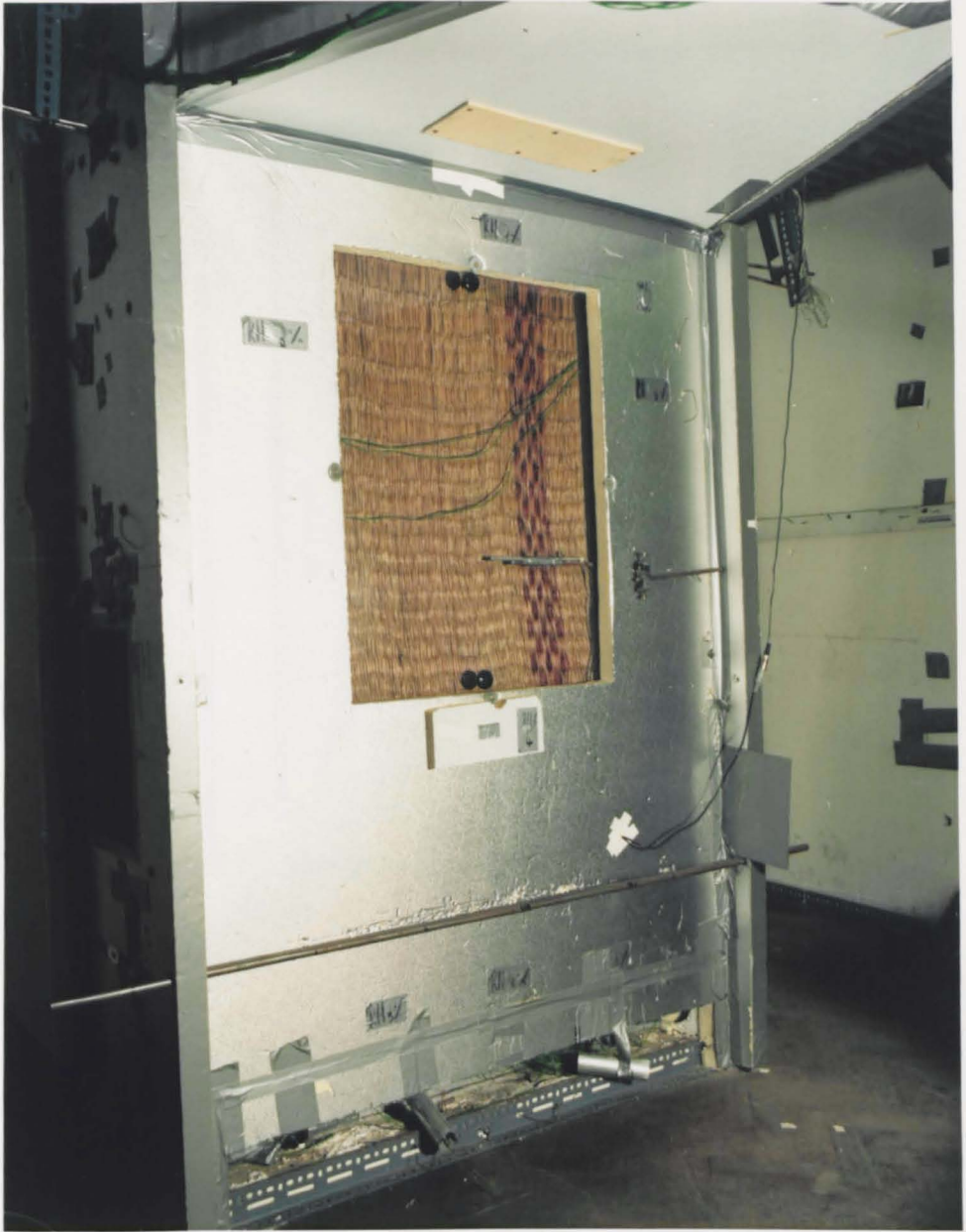
The mat

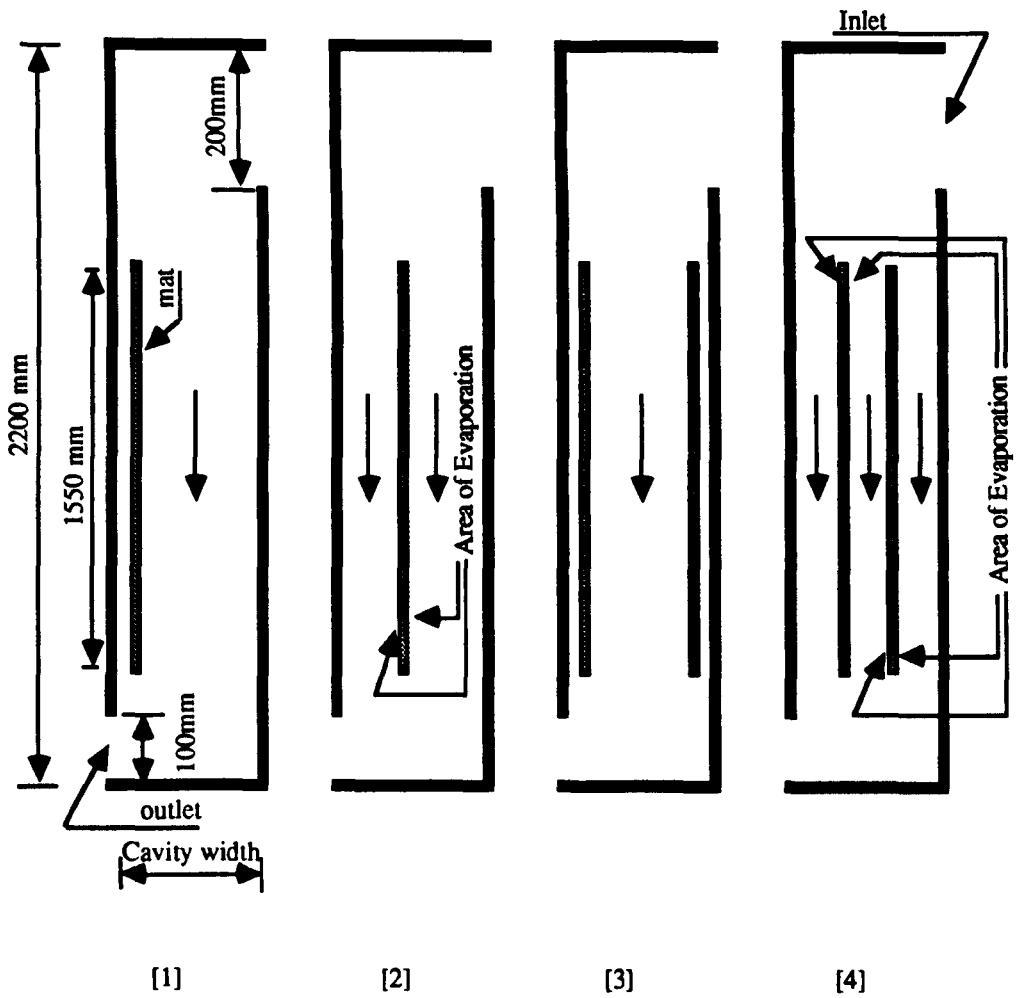
(one wet surface is seen from the window)

Plate 4.3 The mats in the apparatus.



Plate 4.3 The mats in the apparatus.





- [1] - one mat, evaporation one side.
- [2] - one mat, evaporation both sides.
- [3] - two mats, each evaporating from one side.
- [4] - two mats, each evaporating from both sides.

Figure 4.6 Section showing positions of the mats within the cavity.

4.4 EQUIPMENT AND CONTROL

To examine the cooling resulting from evaporation, and air flow generated by buoyancy as well as by a fan, apparatus was needed to measure air velocity, its temperature and relative humidity, and surface temperatures.

4.4.1 Air velocity

Air velocity was measured in both buoyancy flow and forced flow observations. The low air velocity created by buoyancy was difficult to measure accurately since it depends on its density, its pressure, temperature and direction. Continuous readings were required because the pressure gradients are small. Techniques based on pressure differential, such as the pitot tube, cannot be employed. Other instruments such as the deflection-vane anemometer are not well suited for measuring air velocity in cavities. The revolving-vane anemometer is only suited for greater flow. The heated thermistor anemometer is designed for measuring very low air velocity. A thermistor anemometer (model AV502 by Prosser) was available. It is capable of measuring air velocity up to 0.50m/s and the quoted accuracy is $\pm 5\%$ to $\pm 10\%$ of the reading above 0.050m/s. It was found that continuous measurements were not possible because the probe was too short and damage was inevitable, especially when the width of the cavity (100mm) was divided into three. The accuracy was unsatisfactory when air velocity was 0.1m/s to 0.4m/s and so it was rejected.

A hot-wire anemometer can measure very low velocities accurately, and responds to high frequency transients and turbulence. In this work, the hot-wire anemometer (Figure 4.7) used was model 1650 by T.S.I., U.S.A.. The probe can be extended to the desired length. It can measure air velocities up to 30m/s, the lower range being up to 1m/s with an accuracy $\pm 2\%$ of the reading.

The hot-wire anemometer was calibrated using a laser beam, and the accuracy of $\pm 2\%$ of the reading was confirmed. This was increased to $\pm 3\%$ of the full scale reading. Although the hot-wire anemometer is able to measure low air velocity, it cannot indicate the direction of the flow.

4.4.2 Air relative humidity

Air relative humidity, at the inlet, the outlet and in the cavity, was required to study the rate of evaporation and cooling. Air relative humidity is the amount of water vapour in the air as a fraction of the maximum water vapour the same air could carry at that temperature. A whirling hygrometer is designed to measure relative humidity. It was difficult to use because of the small height of the outlet.

Modern relative humidity measuring apparatus is electronic. In this work, model KM 8004 by Kane-May was used. It is capable of measuring relative humidity from 1% to 99%, with a resolution of 1%. The relative humidity sensor is a thin absorbent film within a hand held probe (Figure 4.7). The probe was 14mm diameter and 200mm long, small enough to ensure that obstruction to air flow was minimal. The probe also measures air temperature.

The probe was calibrated against the whirling hygrometer. The difference in air temperature between the room and the outlet air during calibration was small so that variations in the relative humidity could be reduced. The velocity of the air near the probe was also measured to ensure that it was stable. The obtained accuracy of relative humidity was $\pm 2\%$ of the reading. The values of the relative humidity measured and that given by the whirling hygrometer are compared in Table 4.1. They indicate that the difference was small.

Table 4.1 Measured outlet air relative humidity compared with that of the whirling hygrometer.

	Outlet air relative humidity %							
Measured	57	62	68	74	77	84	88	93
Whirling hygrometer	59	64	70	76	79	86	90	95
Differences	-2	-2	-2	-2	-2	-2	-2	-2

Although the KM 8004 is a reliable instrument for measuring air relative humidity, its application is limited, in that air relative humidity may vary by 0.5% due to an air temperature difference of 0.1K.

4.4.3 Temperatures

Air temperatures were measured at the inlet, the outlet, inside the cavity and in the laboratory to study the rate of evaporation and cooling. Temperature of the dry and wet surfaces within the cavity were also measured. The common temperature measuring techniques for natural flows are well understood, one of which is the thermocouple. It is widely used because of low cost. In this work, copper-constantan thermocouples were used. All thermocouples selected for air temperature measurements were wrapped in a bundle and marked at both ends with a coded two figure identifier. Air temperature sensors were located in their positions, protected from radiation (though it is negligible, chapter 3) by a polished aluminium cylinder (35mm diameter and 150mm long).

The thermocouples were glued directly to dry surfaces of the cavity. They were kept in contact along the surface for at least 150mm to avoid any false readings due to conduction along the wires. Wet surface sensors were difficult to fix to the mat. Each sensor was fixed to a reed within the matting and glued. Figure 4.8 shows the position of air and surfaces thermocouples inside the cavity.

Air and surface temperature thermocouples were connected to a 'Comark 5000' digital thermometer via 50 channel switch. To avoid temperature differences between switch inputs . 50mm polystyrene insulation sheets were used. The switch was covered by a perspex sheet to ensure good vision of channel numbers while readings were made. After checking each junction, all thermocouples were connected to the 50 channel switch (Figure 4.7).

Calibration of the thermocouples was made in a large vat of well stirred distilled water. The water temperature was varied from 0°C to 100°C, and measured with a 0.1K resolution mercury-in-glass precision thermometer. Readings were taken at 0.0, 20, 30 and 100°C. The maximum difference found between the thermocouples reading and those of the mercury-in-glass thermometer was about 0.1K. The accuracy is found to be $\pm 0.3K$.

4.4.4 Temperature and speed control

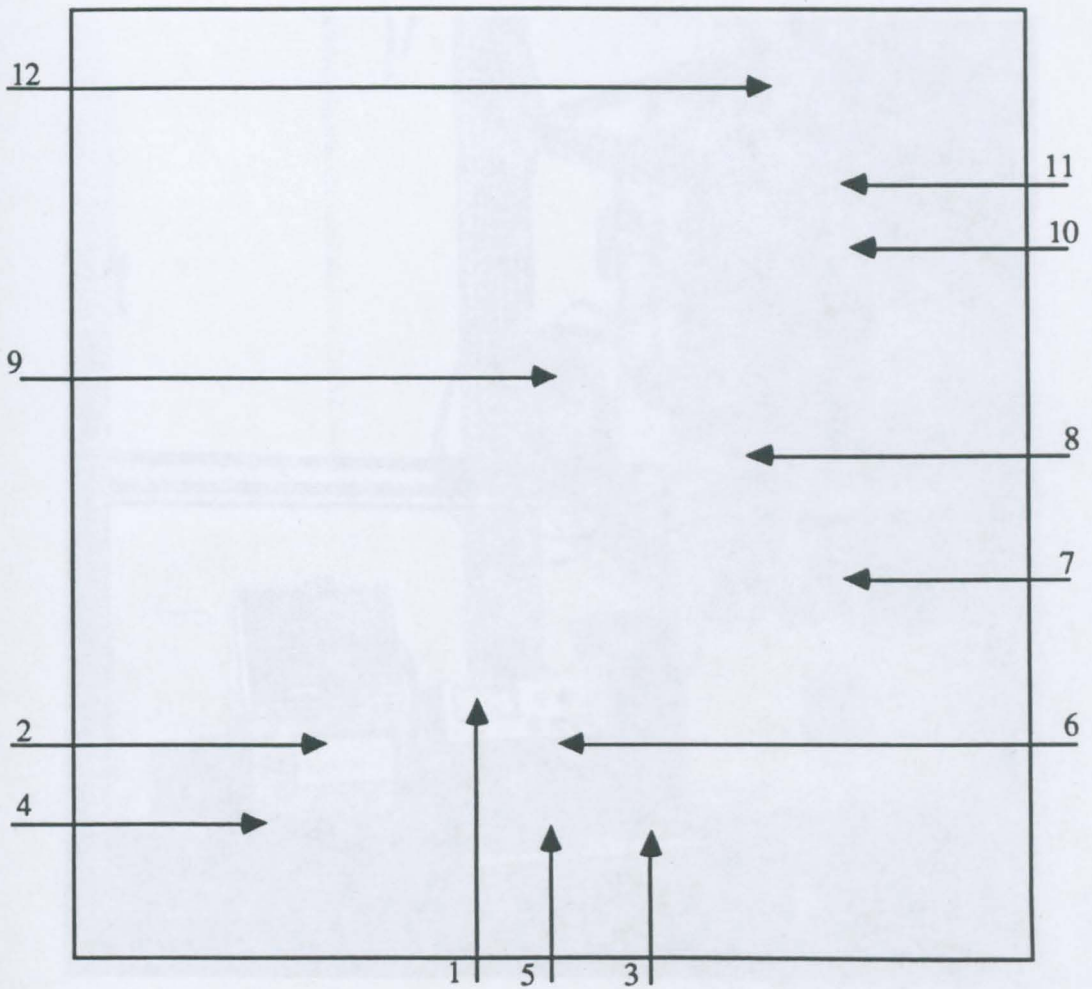
Two temperature controllers (Figure 4.7) were used: one for the fire regulation requirements for safety in the laboratory; and the second for controlling the temperature of the air at the inlet. A thermocouple on the second was placed in front of the steel mesh to ensure accurate reading of the air temperature within the horizontal prism where air flows (Figure 4.4). A speed controller was connected to the fan which draws air towards the inlet of the cavity. The controller was adjusted to give the air speeds of 0.18m/s and 0.37m/s, similar to those confirmed (Bouchair 1988, private communication) by a tested solar chimney attached to a room built in the Department of Civil Engineering of the University of Leeds.

4.4.5 Flow visualisation

Since the hot-wire anemometer was unable to detect the direction of the flow, visualisation of the air was important. Smoke was used to observe the direction of the flow in the cavity and to determine the pattern of the flow (laminar, intermediate or turbulent). Smoke pellets (P.H Smoke Product Ltd.) were used. One pellet was placed at the bottom of the cavity so that the pellet could be ignited without any interference with air flow at the outlet. One disadvantage was that the temperature of the air rose as the pellet was ignited.

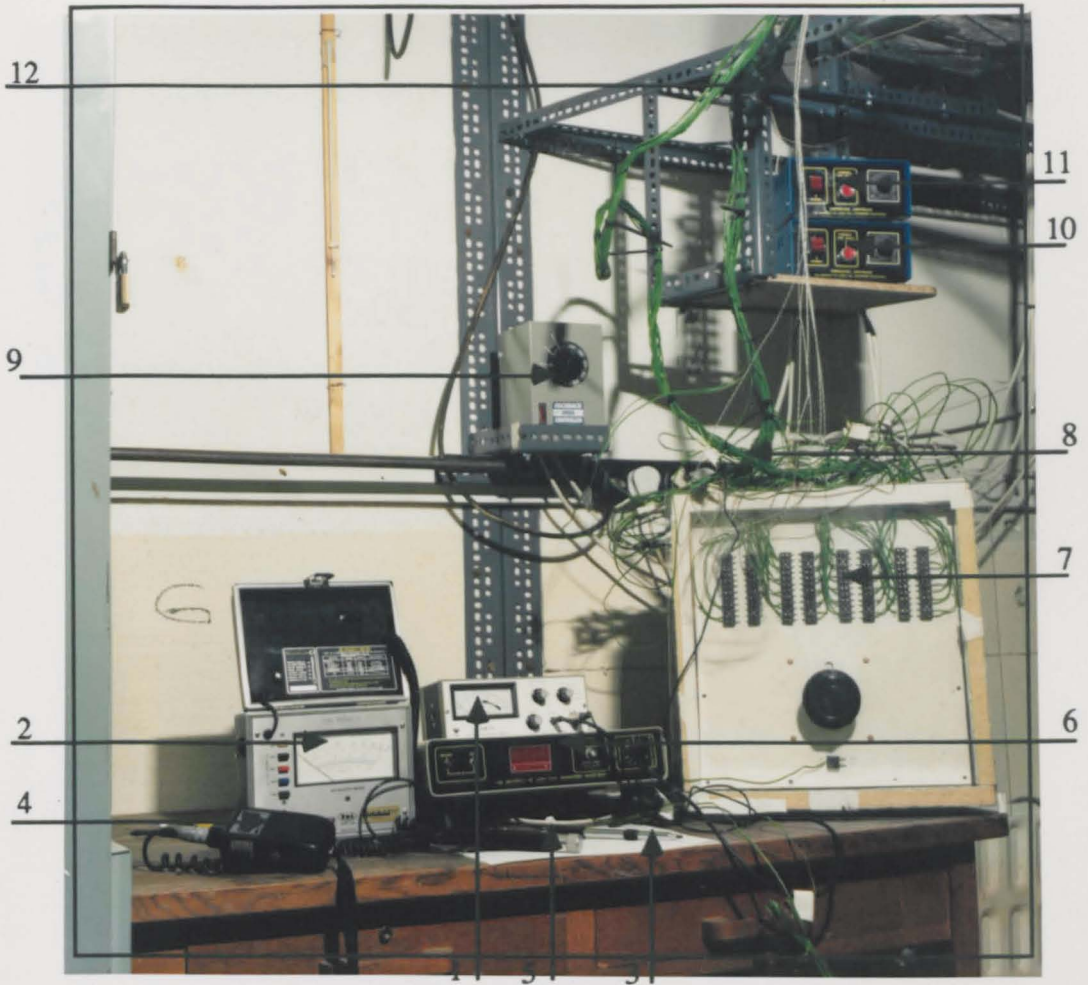
A smoke tube, type MSA (Britain Ltd.) was used for flow visualisation. Both ends of the tube were connected to a rubber one. One side was fixed to a copper tube having a very thin needle, while the other end was connected to an air supply generator. Thus, a single stream of white dense smoke of hydrochloric acid droplets was injected into the air. This kind of smoke was used because its temperature was equal to that of the air; one disadvantage was that the smoke was unpleasant to breath.

Two 12 volts flood light lamps (Hallogen 3-9) were used when photographs of the flow were taken. A video camera was used when prolonged recording was required.



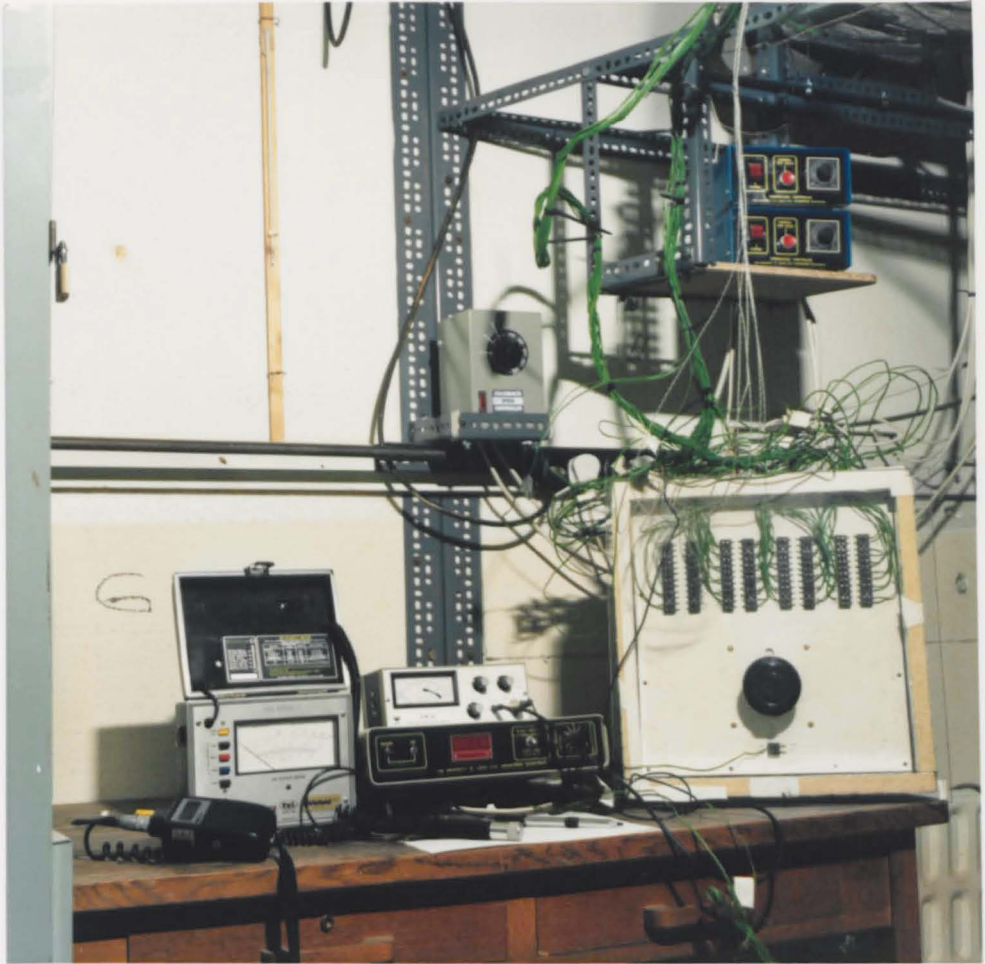
1. Heated thermistor anemometer, model AV502
2. Hot-wire anemometer, model 1650
3. The hot-wire sensor
4. Hygrometer, model KM 8004
5. The hygrometer sensor
6. Digital thermometer, Comark 5000
7. 50 channel switch
8. Thermocouples
9. Speed controller
10. Temperature controller
11. Safety controller
12. Fan

Figure 4.7 Equipment used for measurement.



1. Heated thermistor anemometer, model AV502
2. Hot-wire anemometer, model 1650
3. The hot-wire sensor
4. Hygrometer, model KM 8004
5. The hygrometer sensor
6. Digital thermometer, Comark 5000
7. 50 channel switch
8. Thermocouples
9. Speed controller
10. Temperature controller
11. Safety controller
12. Fan

Figure 4.7 Equipment used for measurement.



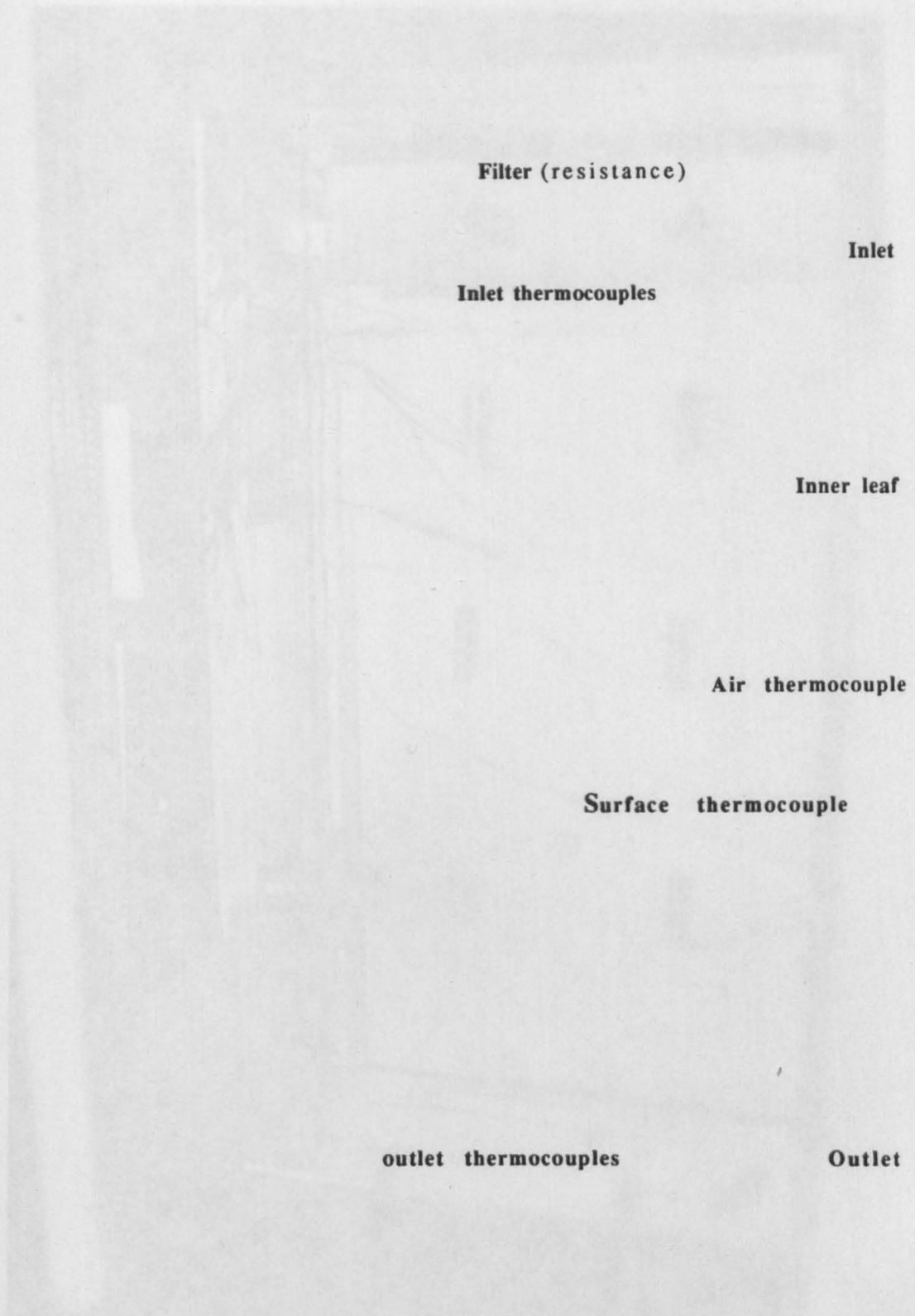


Plate 4.4 Air and surface thermocouples positions in the cavity (movable leaf removed).

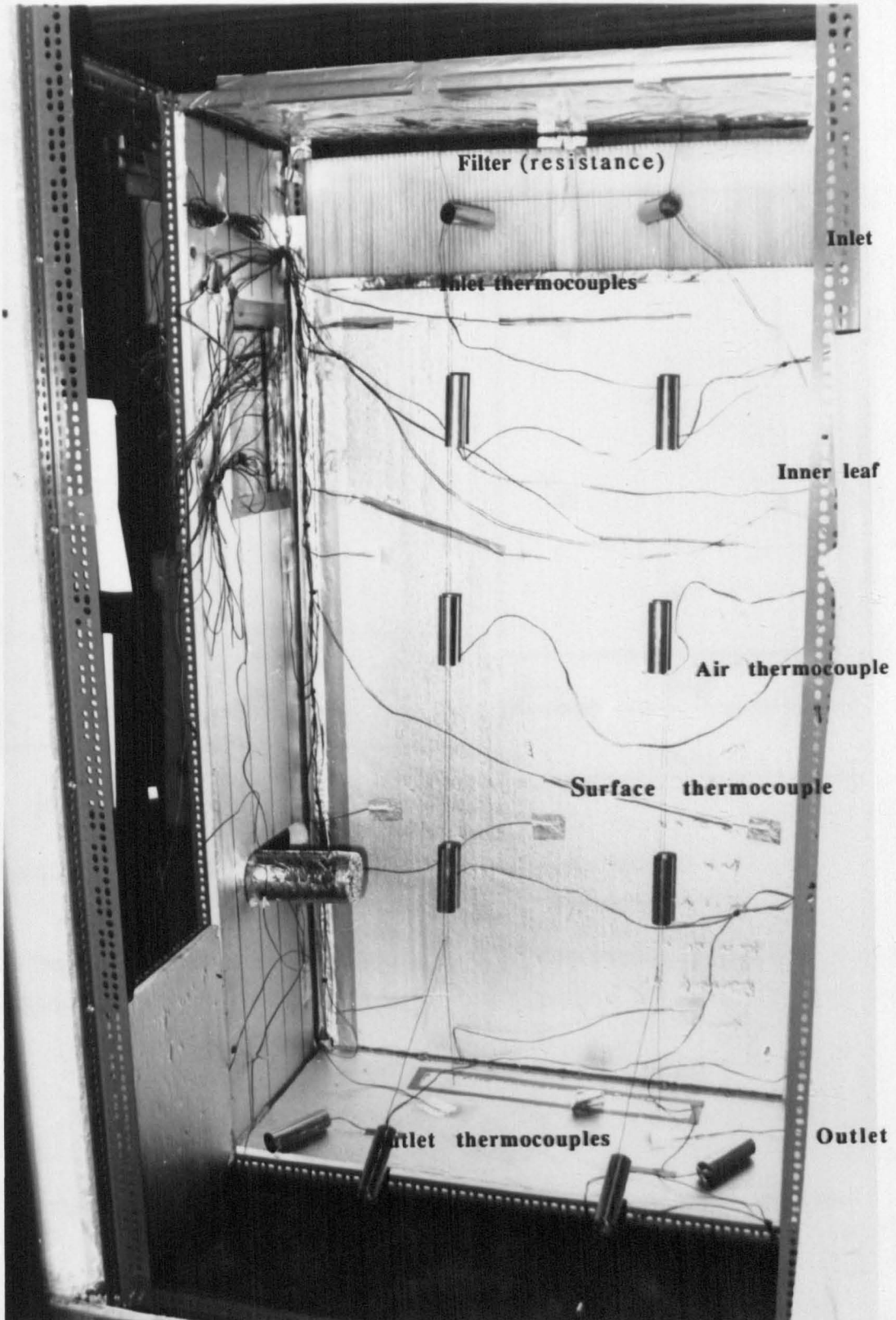
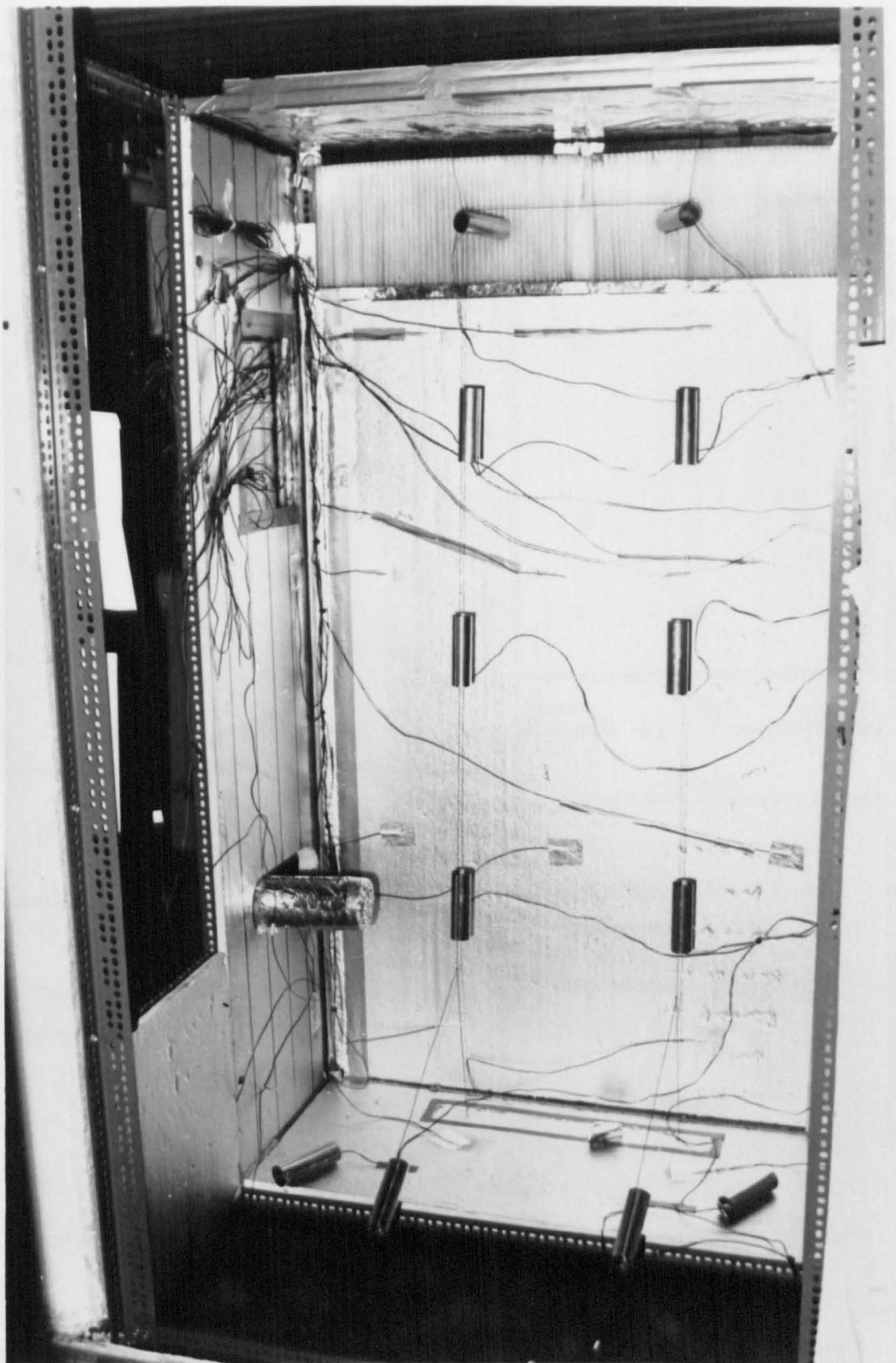


Plate 4.4 Air and surface thermocouples positions in the cavity (movable leaf removed).



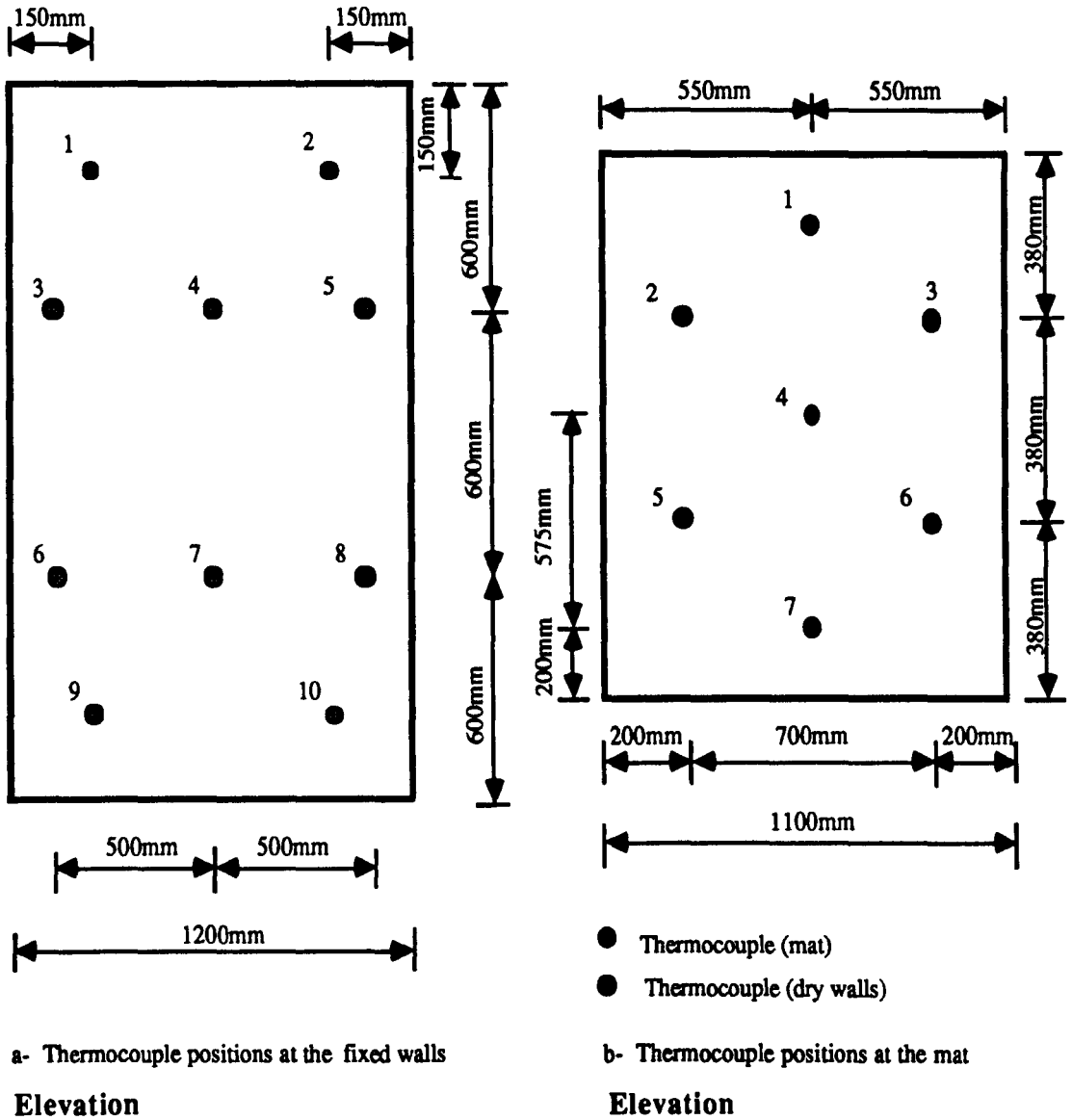


Figure 4.8 Thermocouples layout on the inner faces of the cavity and both sides of the mat.

4.5 MEASUREMENT PROCEDURES

The apparatus was constructed to measure air velocity, its relative humidity, its temperature at the inlet and outlet, and the temperature of the mat so that cooling and rate of evaporation could be determined. These were included in both the forced air flow and the buoyancy air flow measurements. The effects of various parameters on the cooling were examined in the buoyancy air flow apparatus by varying:

- the width of the cavity (walls separation).
- area of evaporation (number of mats).
- height of the outlet.
- air temperature at the inlet.
- air temperature in the room in relation to that at the inlet.

In the forced air flow apparatus, the cooling was examined by varying the first three parameters and the air velocity at the inlet. Air velocity used in the tests was controlled at about 0.2m/s and 0.4m/s.

The mat was wetted and placed in the cavity after the surplus water was drained. The cavity was left for at least 4 hours so that a stable environment was achieved. After the temperature of the mat and the air in the laboratory were stable, the probes of both the hot-wire anemometer and relative humidity (model MK 8004) were placed in their positions.

Air velocity measurements were made at the inlet, outlet and in the cavity. To ensure accurate measurements, the probe was positioned in the cavity and at the outlet so that air flowed directly through the window around the sensor. Deviation from these positions of more than about 5° in any direction could produce errors. A square wooden rod was inserted (horizontally) in the cavity so that the probe could be adjusted, and was then removed.

Air velocity, its relative humidity and temperature were read at the same time so that fluctuations were minimal. The velocity meter has no storage capacity, and is of the type which cannot be connected to a digital voltmeter, which stores readings. Mean values of air velocity and relative humidity were needed, and therefore a grid of measurements were taken across the outlet, the inlet and inside the cavity in both the buoyancy and forced air flow apparatus. In the buoyancy air flow apparatus, these were

made inside the cavity (Figure 4.9). Other measurements were made at the outlet (Figure 4.10 b).

In the forced air flow apparatus air velocity measurements were made at the inlet to ensure that the required air velocity (0.18m/s and 0.37m/s) were achieved (Figure 4.10 a). Measurements were made at the outlet (Figure 4.11). In the cavity, these were made to ensure that air was flowing over both walls of the cavity (before the mats were placed in the cavity) so that evaporation could take place effectively after the wet mats were introduced. These measurements were made at three levels (Figure 4.12): near the top (100mm below the inlet); the middle; and 500mm from the bottom. The first and the last were to avoid any changes in the velocity of the air due to the inlet and outlet effect. The mean value was taken to represent air velocity in the middle of each air space within the cavity.

In relative humidity measurements, the probe was located perpendicularly to the outlet to avoid any obstruction of the flow as well as the temperature difference which may exist across the room. Temperature measurements were made across the outlet using four thermocouples, and it was found that air temperature differences across the outlet were about 0.3K. As a result, the relative humidity may vary by 1.5%. The variation was unavoidable, but is acceptable. Eight points were chosen along the outlet and the inlet for air relative humidity measurements. Figure 4.13 a shows the grid at the inlet of the forced flow tests, and Figure 4.13 b shows the grid of measurements at the inlet and the outlet of the buoyancy flow apparatus. Holes were made in the cavity walls so that air relative humidity along the height of the cavity could be measured. Air temperature was measured at the inlet and outlet (Figure 4.14).

The tests were carried out in two stages: first by buoyancy air flow, where the cavity width was varied from 80mm to 100mm, 160mm, 200mm and 300mm, with outlet height of 200mm and 100mm; second by forced flow, where the cavity was varied from 100mm to 125mm, 200mm, 300mm and 400mm. In all tests, the following parameters were maintained:

- the length of the cavity (1200mm).
- the height of the cavity (2200mm).
- the length of the inlet (1140mm forced air flow, and 1200mm buoyancy air flow).
- the height of the mat (1550mm).

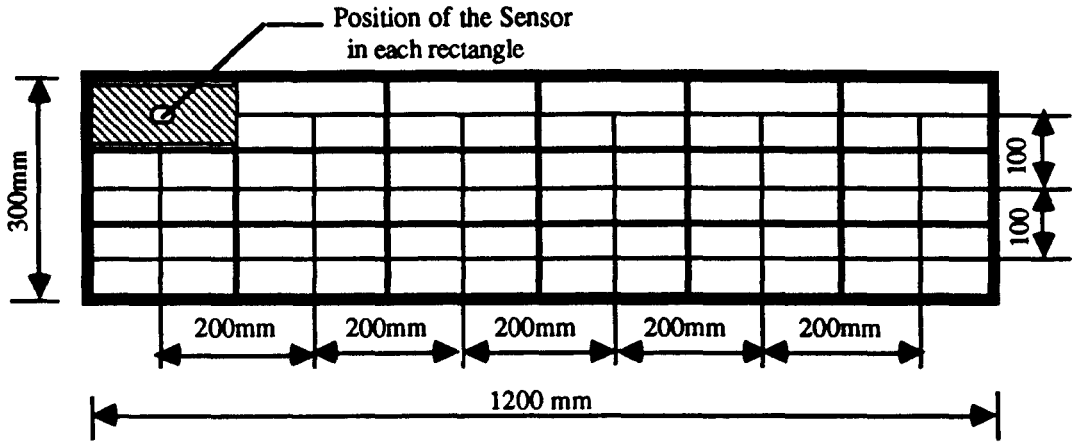
- the length of the mat (1150mm).
- inlet air temperature (buoyancy air flow, 18°C to 23°C being those in the laboratory) and (forced air flow, 30°C like that in the shade of a typical hot dry climate, Figure 1.1.a).
- inlet relative humidity (buoyancy air flow, 50% to 70% being those in the laboratory) and (forced air flow, 40% like that in hot dry climates, (Figure 1.2).
- air velocity at the inlet (forced air flow at 0.18m/s and 0.37m/s).
- inlet height (250mm, forced air flow) and (200mm, buoyancy air flow).

4.6 APPARATUS LIMITATION AND RANGE OF APPLICATION

Tests were carried out in the following circumstances, and the following limitations should be noted:

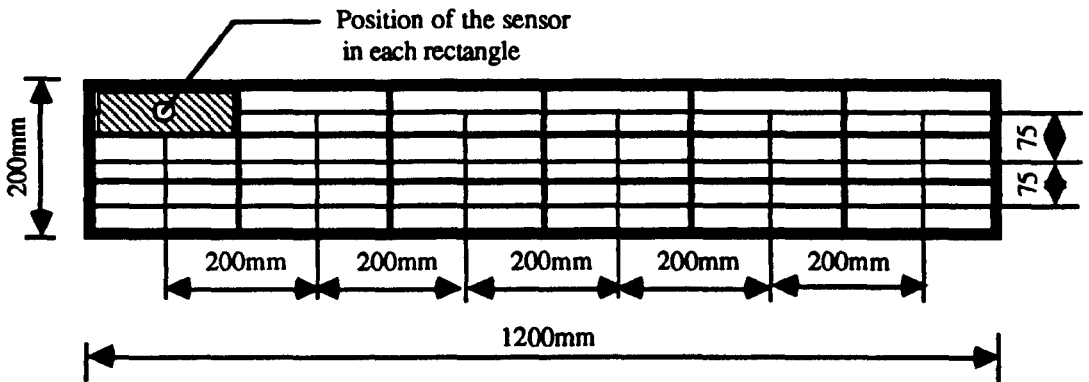
- there was no interference from wind, but readings had to be made on different days to offset fluctuations due to weather.
- the temperature of the mats was not constant and was influenced by water temperature
- water diffusion through the mats was not entirely uniform like that of a 'pool of water'.
- the hot-wire anemometer does not indicate the direction of the flow.
- there were sharp edges to both the inlet and outlet.
- handling the probe may have led to some inaccuracy in measurements of air velocity and relative humidity.

The results of the buoyancy air flow tests are presented and discussed in chapter five and those of the forced air flow are in chapter six.



Plan

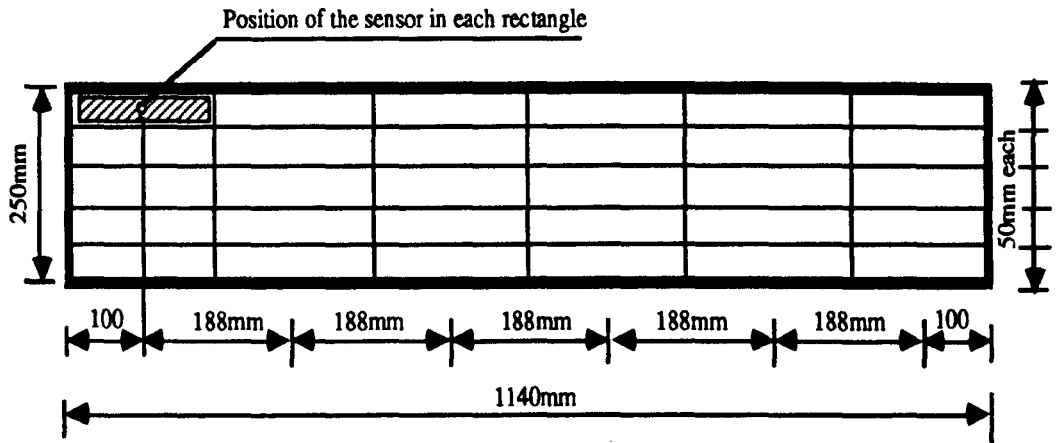
a- Positions of the hot-wire anemometer sensor in the 300mm cavity.



Plan

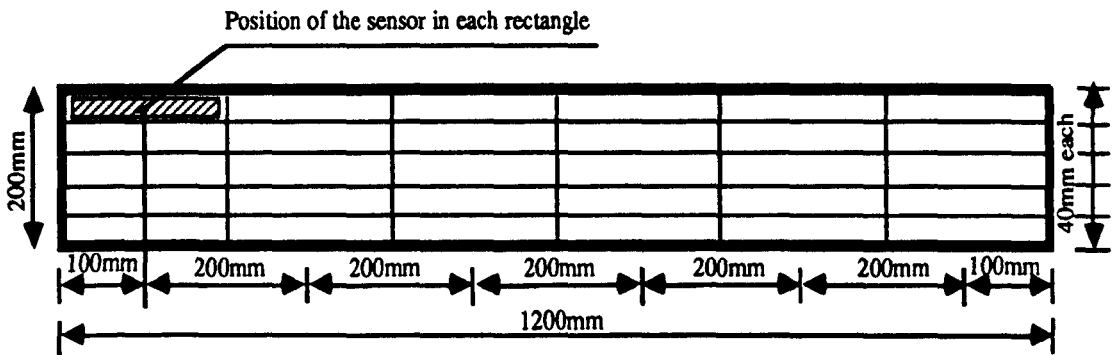
b- Positions of the hot-wire anemometer sensor in the 200mm cavity.

Figure 4.9 Layout of air velocity measurements in the cavity (buoyancy air flow).



Elevation

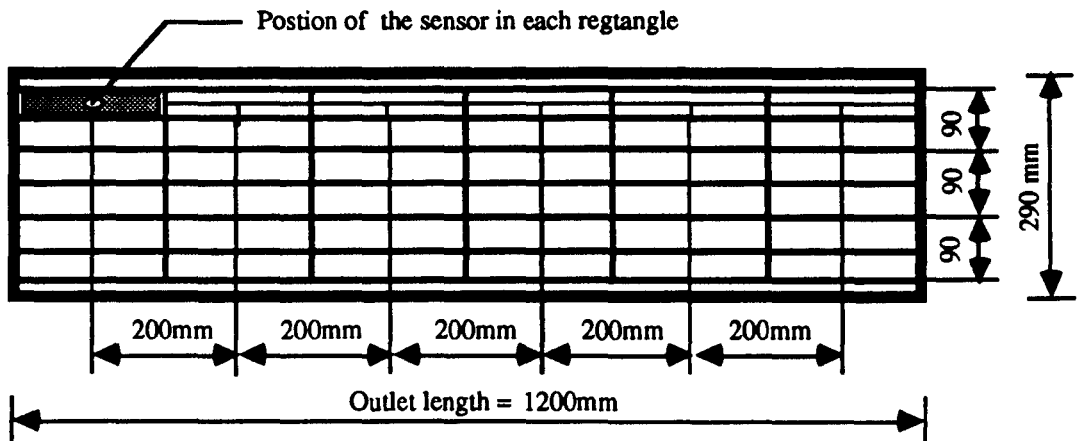
a- Positions of the hot-wire anemometer sensor at the inlet (forced flow)



Elevation

b- Positions of the hot-wire anemometer sensor at the inlet and outlet (buoyancy flow)

Figure 4.10 Layout of the air velocity measurements.



Elevation

a- Positions of the hot-wire anemometer sensor at the 290mm outlet (forced air flow)

Figure 4.11 Layout of air velocity measurements at the outlet of the cavity with forced air flow

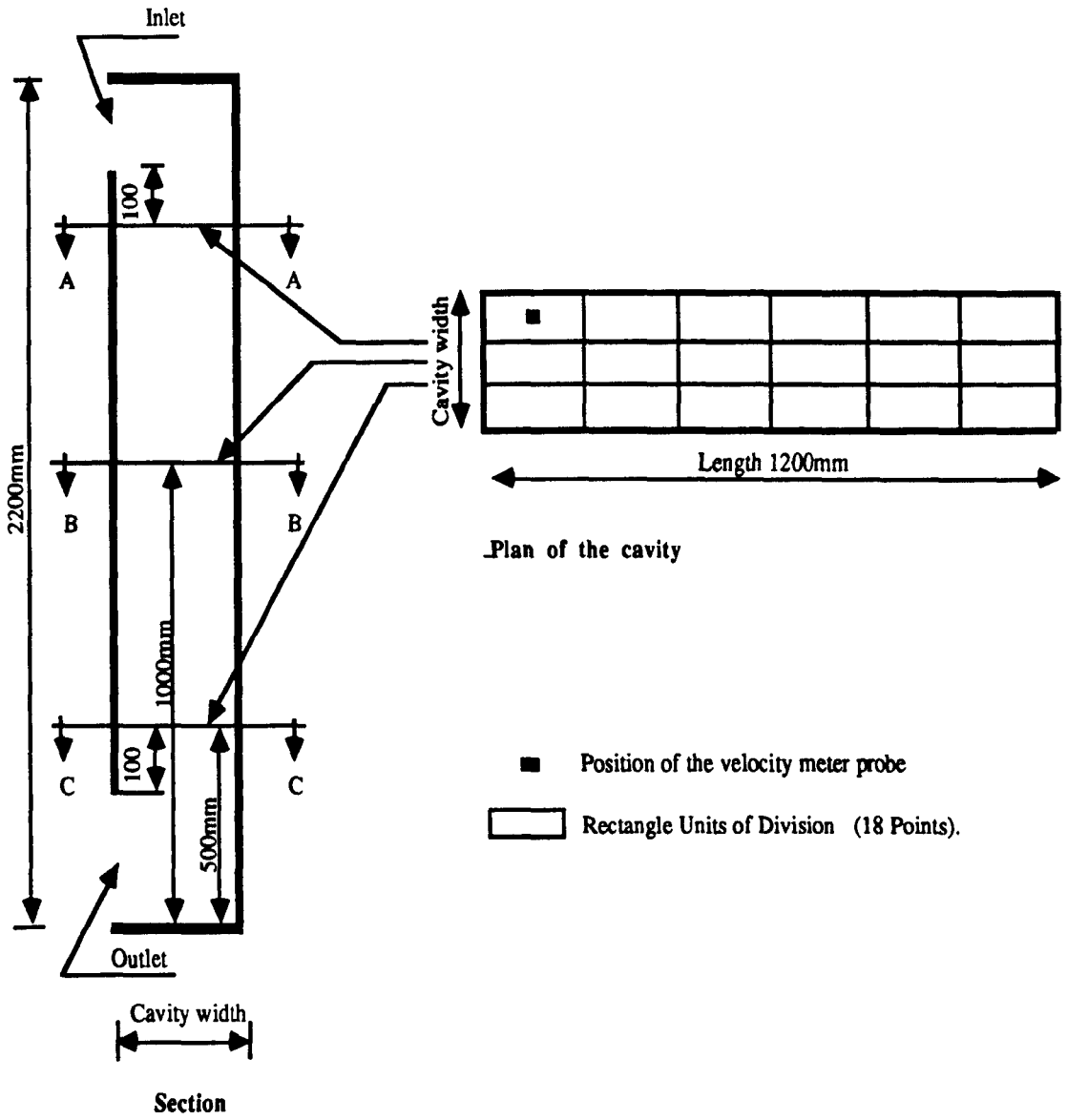
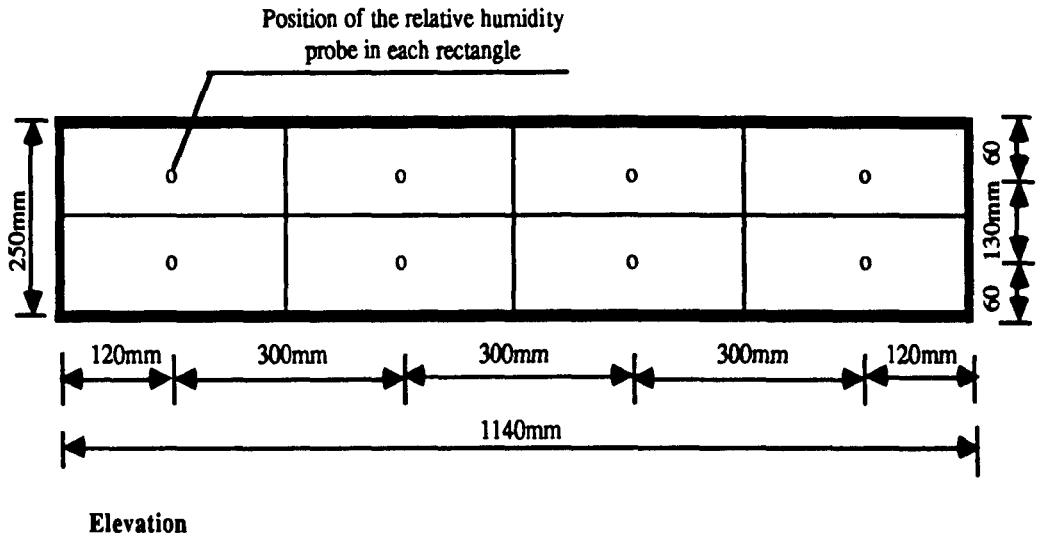
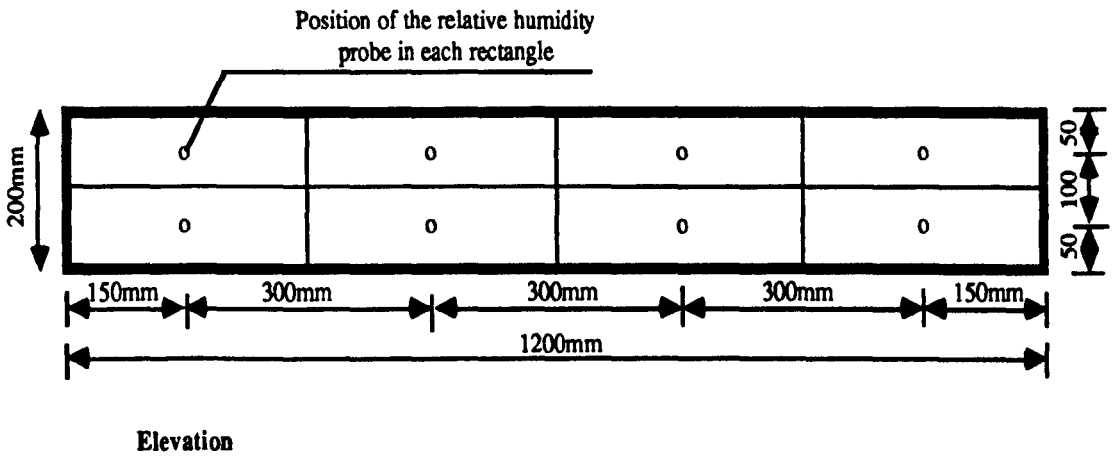


Figure 4.12 Levels of air velocity measurements along the cavity height.

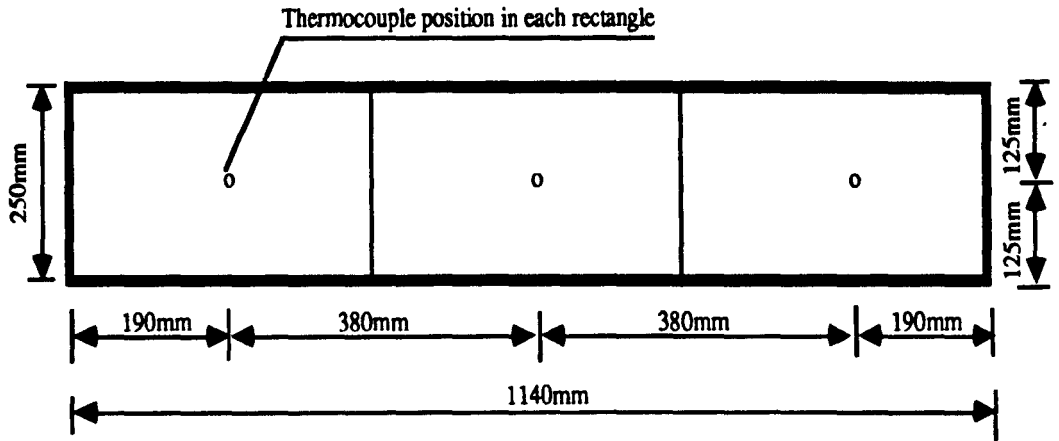


a- Positions of the relative humidity probe at the inlet (forced flow).



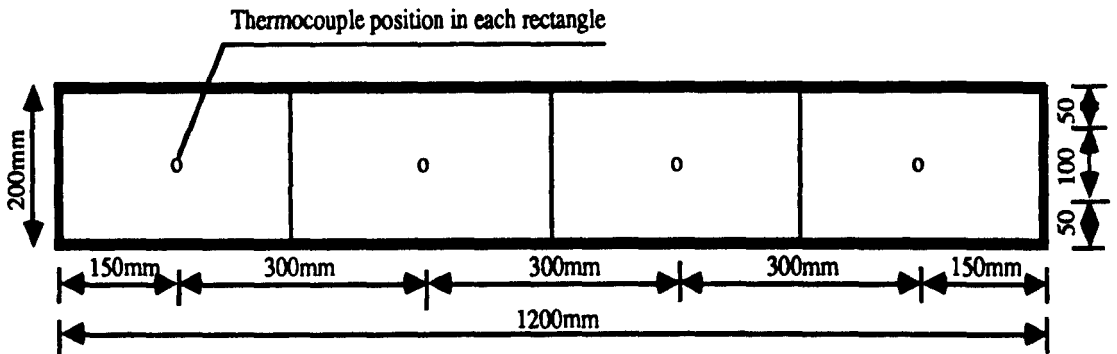
b- Positions of the relative humidity probe at the inlet and the outlet (buoyancy flow).

Figure 4.13 Layout of air relative humidity measurements.



Elevation

a- Positions of the thermocouples at the inlet (forced flow).



Elevation

b- Positions of thermocouples at the inlet and the outlet (buoyancy flow).

Figure 4.14 Layout of air temperature measurements

CHAPTER FIVE

EVAPORATIVE COOLING BY BUOYANCY FLOW: RESULTS

5.1 INTRODUCTION

5.2 TESTS

5.3 TESTS OF GROUP ONE

5.4 RESULTS

5.4.1 Initial flow visualisation

5.4.2 Cooling by buoyancy

5.4.2.1 Outlet air velocity

5.4.2.1.1 The effect of outlet height on air flow

5.4.2.1.2 The effect of cavity width on outlet air velocity

5.4.2.2 Outlet air relative humidity

5.4.2.3 The effect of cavity width on air temperature drop

5.4.2.4 The effect of cavity width on cooling

5.4.3 Humidity ratio difference

5.4.3.1 Water removed by evaporation

5.4.4 The effect of wet mat separation on cooling

5.4.4.1 The effect of wet mat separation on air velocity

5.4.4.2 Nature of air flow

5.4.4.3 The effect of wet mat separation on relative humidity

5.4.4.4 The effect of wet mat separation on the humidity ratio difference

5.4.4.5 The effect of wet mat separation on mass flow rate

5.4.4.5.1 Air velocity distribution

5.4.4.5.2 Flow visualisation

Verification of air velocity measurements

Air flow pattern

5.4.4.5.3 Air relative humidity distribution

5.4.5 Measured cooling with time 'Cavity Life'

5.4.6 The effect of inlet air temperature on cooling

5.5 TESTS OF GROUP TWO

5.6 RESULTS

The effect of temperature difference between air in the room and that at the inlet on the following:

5.6.1 Air temperature drop from evaporation

5.6.2 Outlet air velocity

5.6.3 Outlet relative humidity

5.6.4 Cooling

5.6.5 Ventilation rate

5.7 DISCUSSION AND CONCLUSION

5.7.1 group one

5.7.2 group two

CHAPTER FIVE

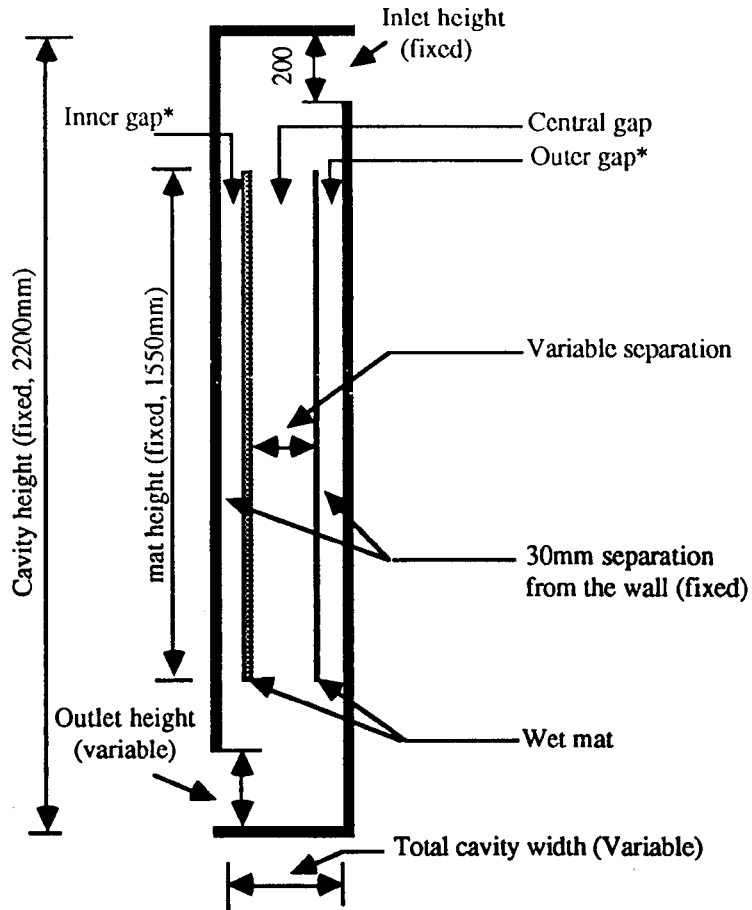
EVAPORATIVE COOLING BY BUOYANCY AIR FLOW: RESULTS

5.1 INTRODUCTION

The apparatus described in chapter four (buoyancy air flow) was used to observe the downward flow induced by buoyancy pressure difference caused by the density difference between the cooled air in the cavity by evaporation and that outside. Tests were carried out to study the effect of cavity width, outlet height and mats separation on cooling by evaporation. Results of these tests are presented. They are divided into two: in group one, cavities were tested in the steady state, with no air temperature difference between the cavity inlet and the room; and in group two, these temperatures were different. The discussion of the results and the conclusion for each group are also reported.

5.2 THE TESTS

Cooling, associated air velocity, the drop in air temperature between the inlet and the outlet and the increase in air relative humidity were measured using different cavity widths, inlet air temperatures, wet mat temperatures, air relative humidities and numbers of wet mats, as well as the separation between them. The input variables of the tests are listed in Table 5.1. Inlet air temperatures of 21°C and 19°C and relative humidities of 60% and 65% were used for most of the tests (being those of the laboratory). Two wet mats were employed for evaporation. The mats were placed 30mm from the cavity walls in the tests with 100mm, 200mm and 300mm cavity widths (Figure 5.1); they were 25mm from the walls in the 80mm width test. The temperatures of the mats were influenced by the temperature of the water in the laboratory (12°C to 15°C). The inlet and the outlet were initially of the same size (1200mm long x 200mm high). In this work the subdivision of the cavity is called: the 'outer gap', 'central gap' and 'inner gap' (Figure 5.1).



* The outer gap is adjacent to the external wall of the cavity in shade.

* The inner gap is adjacent to the internal wall of the cavity facing the room.

Figure 5.1 showing parameters varied in the tests.

Thirty three tests were carried out to investigate the air flow created by buoyancy and cooling by evaporation in cavities. In the tests of group one, the effects of the variables given in Table 5.1 on the following were investigated:

- initial air flow visualisation
- cooling
- air velocity at the outlet and in the cavity
- evaporation (air relative humidity changes in the cavity)
- air temperature drop between the inlet and outlet
- humidity ratio difference between the saturated boundary layer and incoming air (moisture content in the air flow, Δg)

- air flow pattern

Table 5.1 Parameters varied in tests of group one*

Cavity width mm	Separation between mats mm	Outlet height mm	Inlet air temperature °C	Inlet air relative humidity %	wet mats** temperature °C
300	230	200	17	55	12
200	130	100	19	60	13
160	50		21	65	14
100	30		23	70	15
80	20				

* Minimal temperature difference between air in the room and that at the inlet (0.1 to 0.4K).

** The temperature of the wet mat was influenced by that of the water in the laboratory.

The optimum size of the cavity established in group one tests was used for a further study in group two tests to assess its performance in conjunction with a room. The effect of the temperature difference between the air in the room and that at outside (at the inlet) on the following parameters was investigated:

- air temperature drop between the inlet and the outlet
- air velocity
- air relative humidity at the outlet
- cooling
- ventilation rate

5.3 TESTS OF GROUP ONE

In the first set of tests, the air temperature and its relative humidity at the inlet were fairly constant, those of the laboratory. Observations of air relative humidity distribution were made across the inlet (Figure 5.2) so that a satisfactory distribution across the inlet was achieved. The inlet and the outlet size were kept equal (1200mm long x 200mm high). The maximum variations of the inlet air temperature and its relative humidity in all tests were about 2K and 2%.

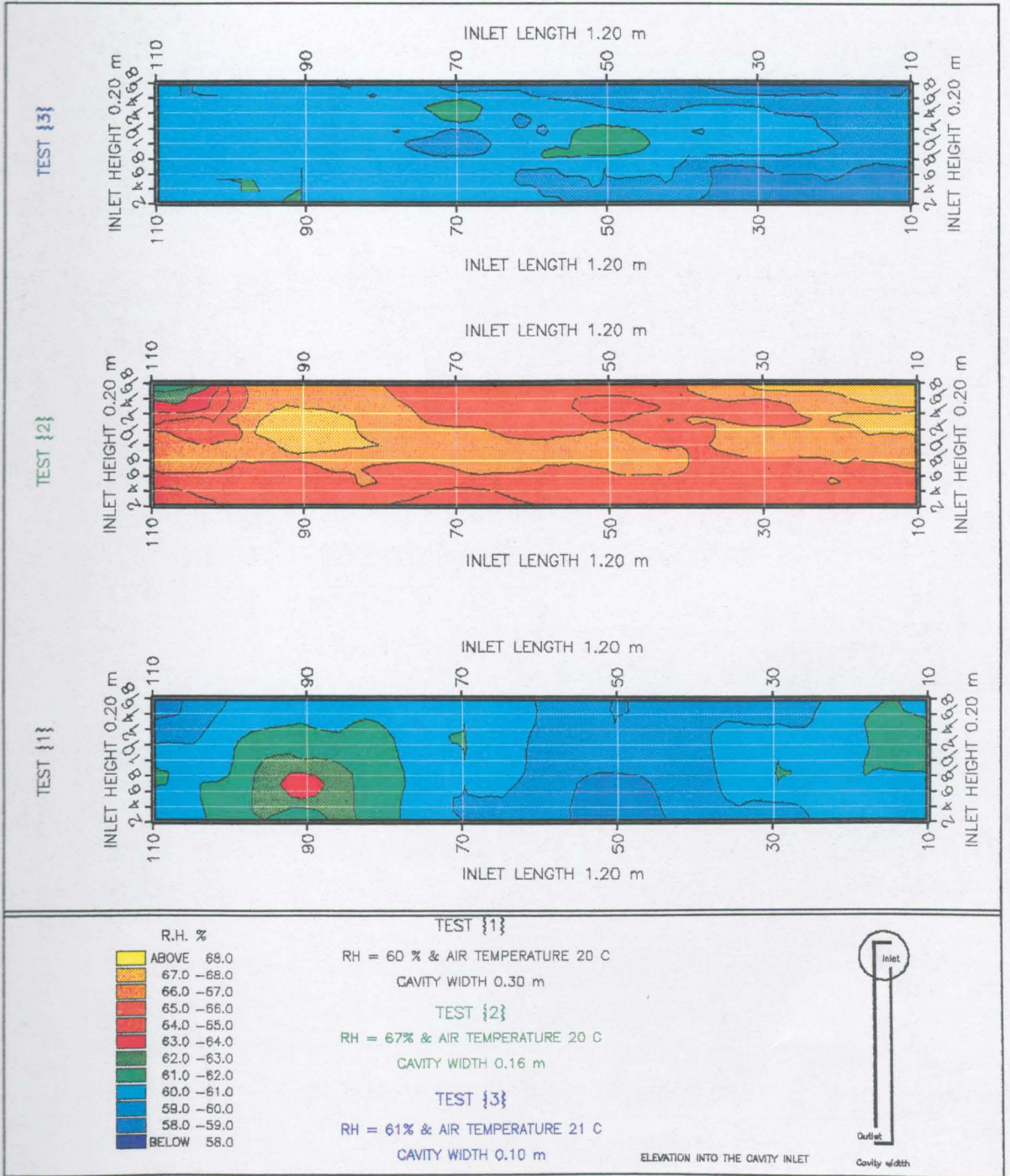


FIG 5.2 The Air Relative Humidity Distribution at the Cavity Inlet
 Inlet to Outlet Ratio = 2:1
 Inlet size 1.20 m x 0.20 m

5.4 RESULTS

5.4.1 Initial flow visualisation

It was important to observe the downward air flow caused by buoyancy pressure difference due to the density difference between the air in the cavity and that outside as a result of evaporation and hence cooling. Smoke was generated from pellets and photographs were taken every two seconds. The pellet was at the bottom of the 100mm cavity (two wet mats). The inlet air temperature and relative humidity were 21°C and 70%.

When the pellet was ignited, the smoke moved gradually upward and stopped at a height of 1160mm, then started to descend. The behaviour of air flow when the smoke was introduced is illustrated in Plate 5.1. The photograph represents the perspex window 950mm high (Figure 5.2). Section 1 (Plate 5.1) illustrates the illuminated cavity without the smoke. Sections 2 to 12 demonstrate the upward flow. The downward flow is shown in sections 13 to 20. Since the upward flow went only to about half the height of the cavity, a thermocouple was located above the smoke pellet in order to measure the smoke temperature so that the cause of the unexpected upward movement could be established.

The air temperature at the lower part of the cavity was originally 18°C. When the smoke was introduced, it went up to 60°C and started to decrease gradually (in two minutes) to 22°C. This indicates that the upward flow was caused by the sudden rise in air temperature which was initially greater than the density difference force caused by buoyancy.

Despite the upward flow, the smoke photographs indicate that a downward flow existed during the observation. Plate 5.1 shows that the nature of the flow (laminar or turbulent) was difficult to identify due to the lack of clarity of the smoke pattern. The rise in air temperature near the outlet may influence the evaporation process and the cooling, especially at 60°C. As a result, the use of smoke pellets was stopped. Smoke tubes (providing hydrochloride acid smoke without any rise in its temperature) were used to instead. Significant results are shown.

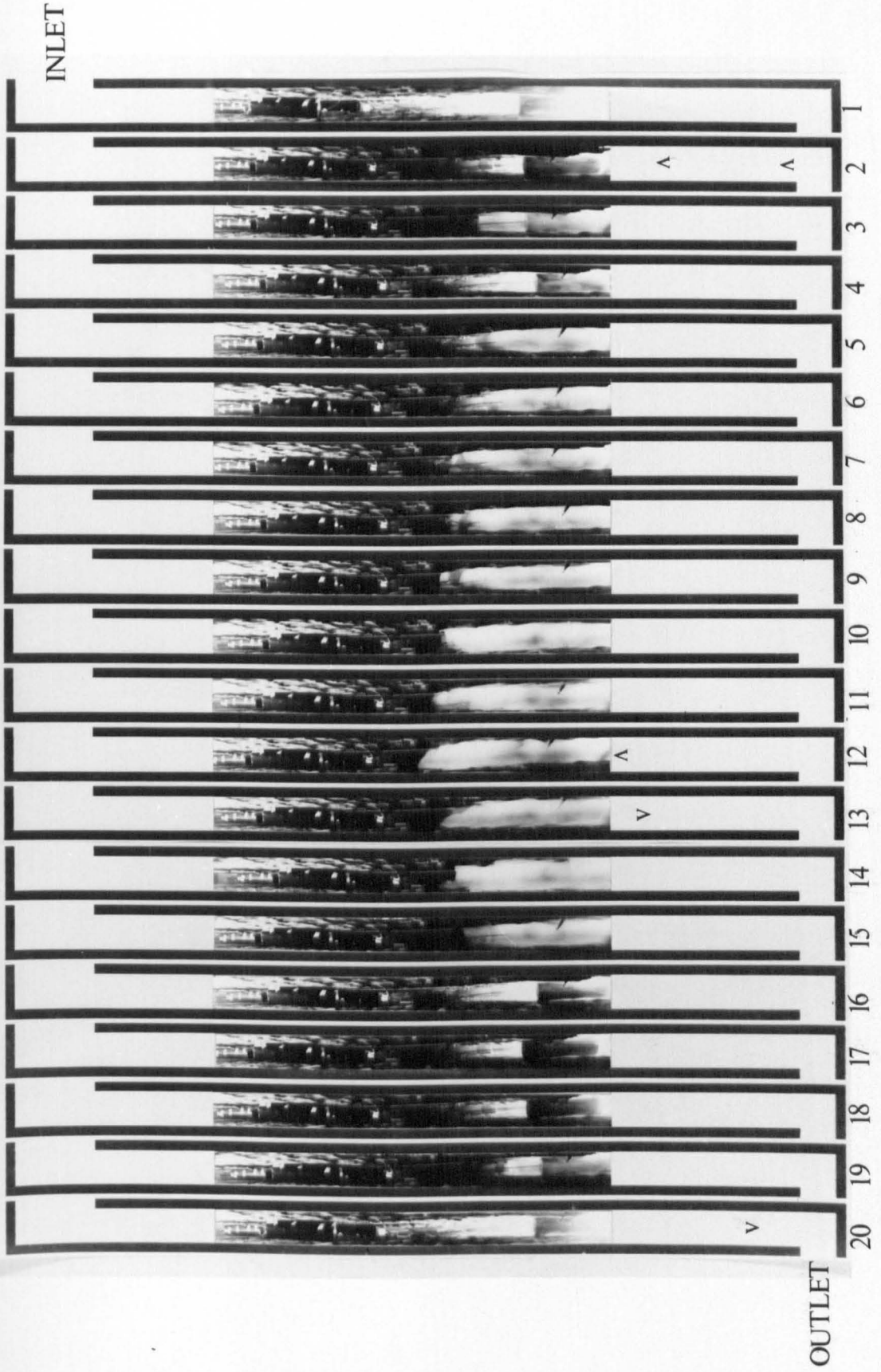
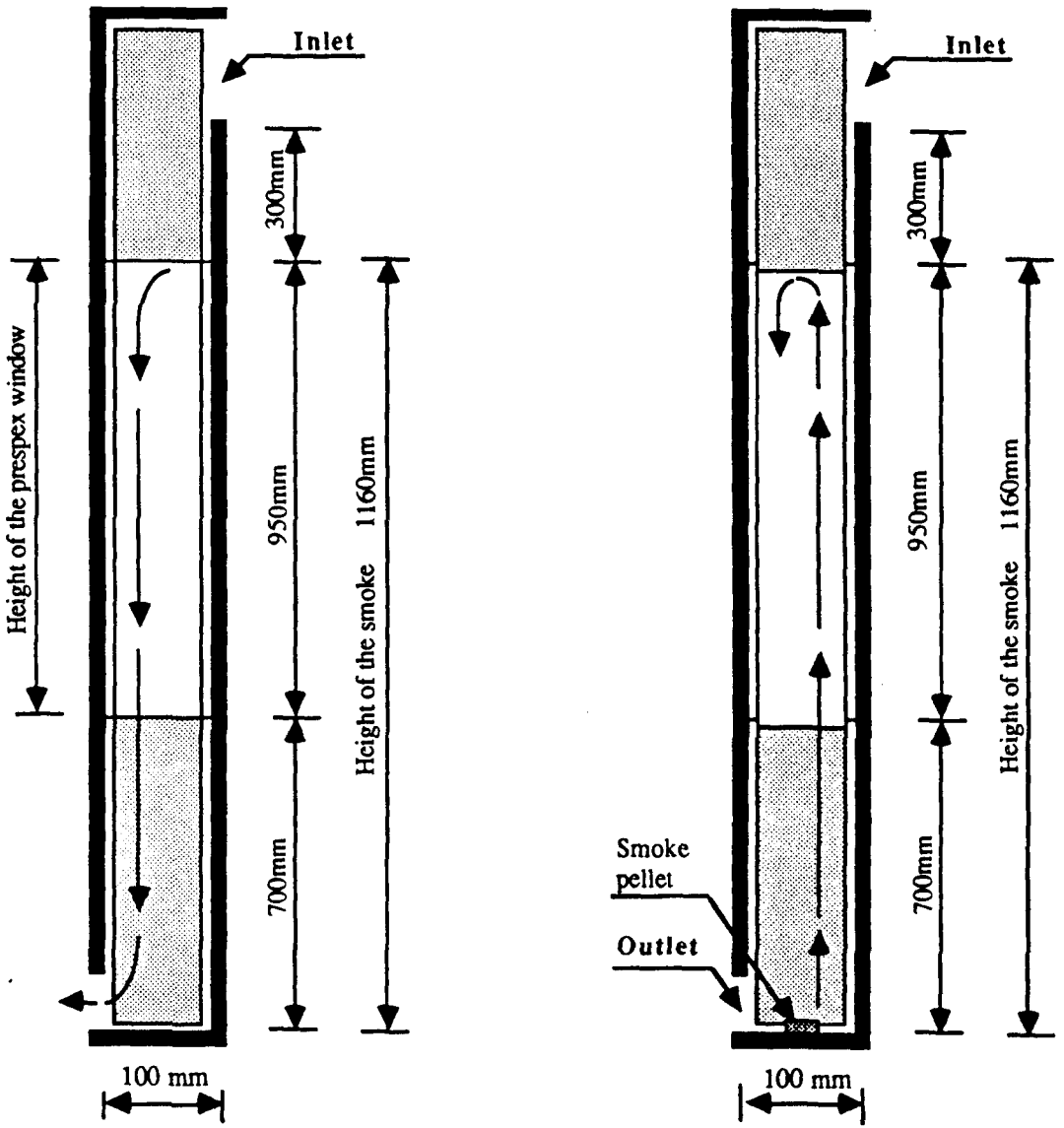


Plate 5.1 The behaviour of air flow



The downward smoke movement
(Sections 13 to 20)

The upward smoke movement
(Sections 2 to 12)

■ Top and bottom parts of the cavity section in plate 5.1

Figure 5.3 Detailed section of the smoke test shown in plate 5.1

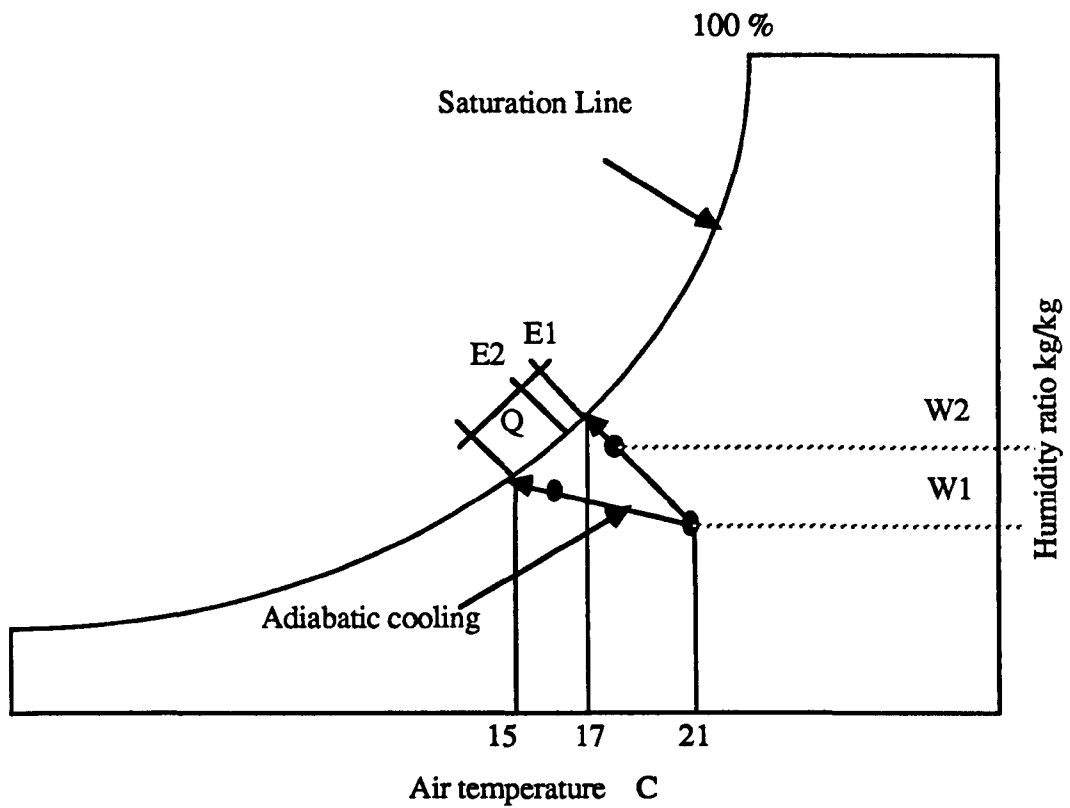
5.4.2 Cooling

Important cooling is the sensible cooling because the system attempts to approximate adiabatic saturation system, the cooling calculation from enthalpy will be much lower (Figure 5.3.a). The significance of cooling could be appraised using one of the following methods: first by the heat removal from the air as mentioned in chapter three, eqn.3.44, second by enthalpy differences between the inlet and the outlet using the CIBSE Psychrometric chart (1986) to determine the enthalpy at both the inlet and the outlet. Error analysis suggests that the use of the second method to assess the cooling would lead to a large error in the enthalpy difference (Table 5.2). The second method may be more appropriate for assessing the cooling because it includes the sensible state of the air at the inlet and outlet. However, these were included in the air density in the first method, so that the first method was used.

To establish the cooling resulting from evaporation, measurements of mass flow rate m (kg/s) and the difference between the inlet and outlet air temperature ΔT (K) were needed. The first of these depends on the average air velocity v (m/s), the density of the air ρ (kg/m³) and the area of air flow A (m²). The air velocity at the outlet and in the cavity and its relative humidity were required. The average air velocity at the cavity outlet and in the cavity was determined using micro-measurements as shown in Figure 4.9, Figure 4.10 and Figure 4.12 (Chapter Four) so that accurate values were achieved (see Chapter Four, part 4.6).

5.4.2.1 Outlet air velocity

Air velocity was measured at 42 points across the air flow path at the outlet (Figure 4.9). A 100mm cavity (with an outlet and inlet height of 200mm) was used. It was found that the air velocity along the outlet height was not distributed uniformly. Air velocity at the top was considerably less than that at the bottom. At some points there was no flow (Figure 5.4 a). This was due to the flow contraction and head losses. The distribution of air velocity in Figure 5.4 was plotted using a graphic package UNIRAS (Universal Raster System). The intersection of the white grids shows where each measurement was taken. In all tests of the 100mm width (with outlet height 200mm), the air flow was minimal in at least 90mm of that height and most of the flow was converging at the bottom. In one series of five vertical measurements on the outlet height (Figure 5.4 a), air velocity variations were as follows: at the bottom, 0.15m/s (orange



Q = Sensible cooling

E = Enthalpy

Figure 5.3.a The difference between the sensible cooling and cooling from enthalpy.

zone) and decreased as it went upwards from 0.12m/s to 0.1m/s, 0.08m/s and 0.02m/s (blue zone). Figure 5.4 a indicates that at least half the height of the outlet was ineffective in terms of air flow. These changes in the air flow at the outlet are related to the phenomenon which is closely connected with a flow from two different heights and passed through a sharp-edged orifice (Sobersky et al. 1971, and Rose 1982), (Figure 5.5). The stream lines converging from inside the cavity towards the orifice cannot suddenly turn into a horizontal direction but do so gradually, thus causing the flow to contract. As a result, the area of the streamlines is not equal to that of the outlet. This minimum section where the velocity was greater is called the "vena contracta". The area of the flow was 45% less than that of the outlet (Figure 5.4 a).

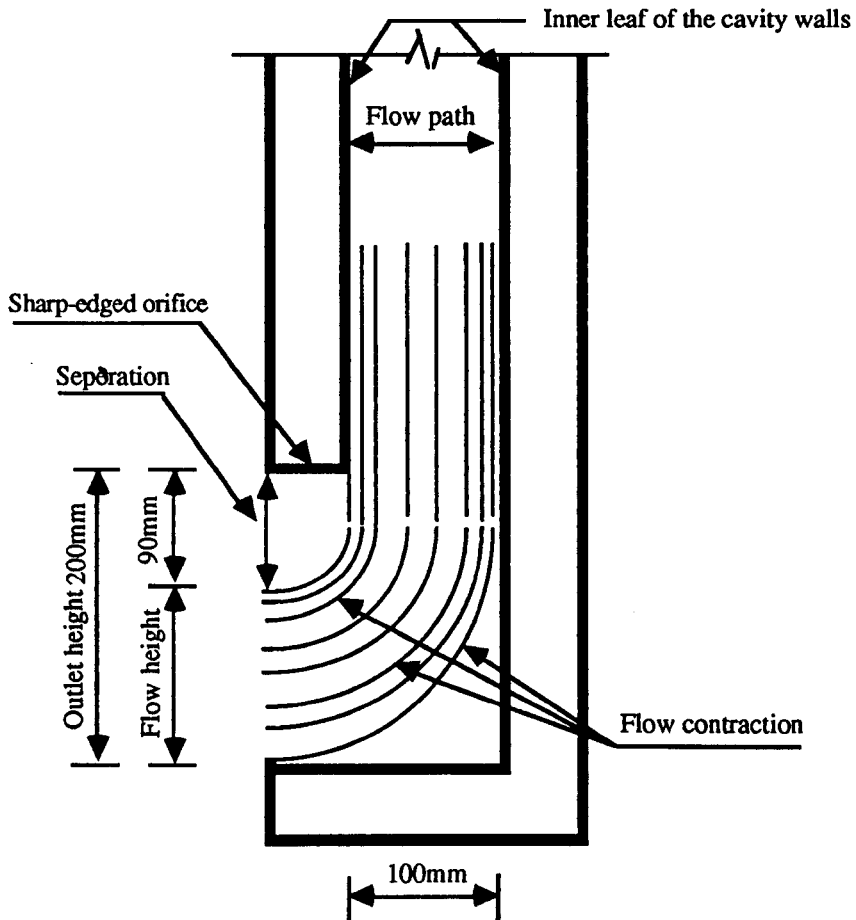


Figure 5.5 Section through the cavity showing the effect of the sharp-edged orifice on air flow at the outlet.

Table 5.2 Errors associated with cooling by evaporation using different methods.

	Temperature °C	R.H. %	Enthalpy E kJ/kg	ΔE kJ/kg	calculation for the outlet								
Inlet	21	60	44.85	3.85	Tout °C	R.H. %	E kJ/kg	ΔE kJ/kg	Mean E kJ/kg	% Error	Cooling Eqn (3.1) W/m	Cooling Enthalpy W/m	Diff. %
Outlet	16	86	41.00		16.30	88.00	42.80	+1.80	41.0	47.0	216.0	167.0	29.0
					16.30	84.00	41.90	+0.90					
					15.70	88.00	40.20	-0.80					
				15.70	84.00	39.20	-1.80						
Error	$\pm 0.3K$	$\pm 2\%$					± 1.80						

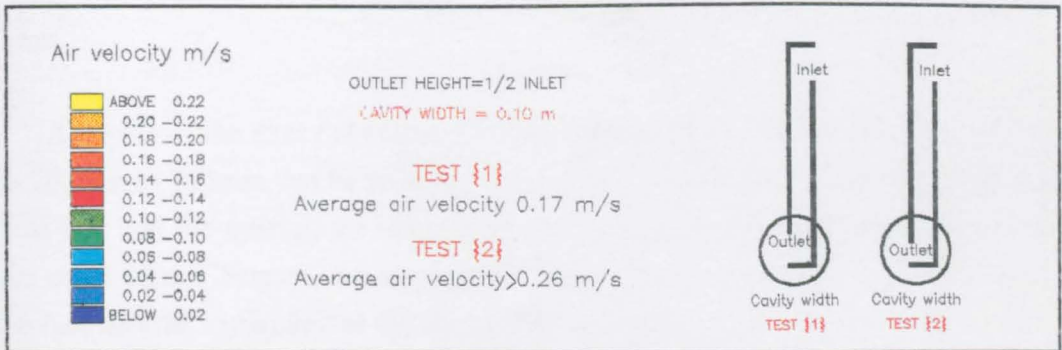
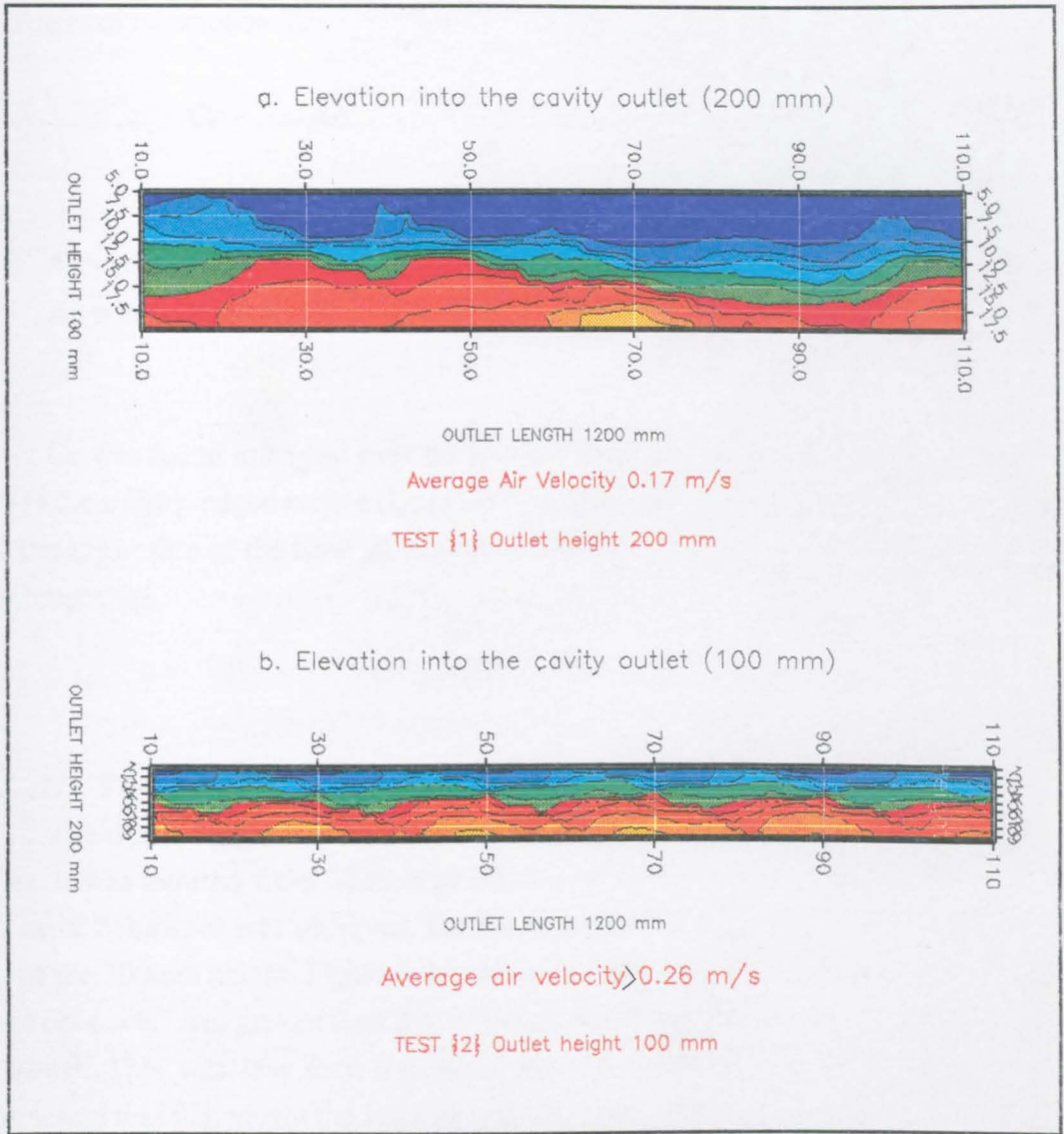


FIG 5.4 The Effect of the Outlet Height on Measured Air Velocity Distribution

Outlet Size: Height 0.10 & 0.20 m, Length 1.20 m

The average air velocity can be determined by introducing a correction factor; the coefficient of contraction C_c :

$$C_c = A_s / A_o \quad [5.1]$$

where

$$\begin{aligned} A_s &= \text{area of air stream} && \text{m}^2 \\ A_o &= \text{area of the outlet} && \text{m}^2 \end{aligned}$$

C_c was found to be just over the half the value recommended by Sobersky et al. (1971) for a sharp-edged orifice ($C_c=1.0$). The dark blue zone in Figure 5.4 a, indicates that the separation of the flow streamlines from the boundary was about 90mm below the abrupt edge.

5.4.2.1.1 The effect of the outlet height on air flow

The outlet height was varied in order to study its effect on the air flow at the outlet. It was reduced from 200mm to 100mm using the same cavity width (100mm). The same behaviour was observed, but the separation at the abrupt edge was less than that of the 200mm height. Figure 5.4.b shows that the dark blue zone vanished and the "vena contracta" was greater than that of the previous test. The area of the flow path was 0.108m^2 . This was less than the outlet area (0.12m^2) by 9%. The coefficient of contraction was 0.9, nearly the same as recommended by Sobersky et al. (1971). Figure 5.4 shows how air velocity distribution varies with different heights of 200mm and 100mm.

Analysis of the data demonstrates that the reduction of the outlet height by half from 200mm to 100mm was beneficial in increasing the coefficient of contraction from 0.55 to 0.9, and the average air velocity from 0.17m/s to 0.26m/s (Table 5.3). Further reduction to 80mm increases the average air velocity to 0.33m/s. This was probably due to the fact that the separation at the sharp-edge was reduced. The decrease of the outlet height to 100mm or less was advantageous in terms of the flow efficiency and the outlet average air velocity.

Table 5.3 Difference between flow path and outlet height.

Average air velocity	Outlet height	Actual area	Vena contracta	Height of flow	Coefficient of contraction
m/s	mm	m ²	m	mm	--
0.17	200	0.24	0.132	110	0.55
0.26	100	0.12	0.110	90	0.90
0.30	80	0.10	0.10	80	1.00

Recommended coefficient of contraction (C_c) = 1.00

5.4.2.1.2 The effect of cavity width on the outlet air velocity

To study the effect of the cavity width on the outlet air velocity, the width was varied as follows: 300mm, 200mm, 100mm and 80mm. The outlet height was 100mm. The air velocity at the outlet was measured and average values were determined using the statistical package SAS (Statistical Analysis System). It is able to determine the mean and the standard deviation.

Figure 5.6 shows no outlet air velocity variation with time, regardless of the width. The average air velocity was found to be affected by the width of the cavity. The average air velocity at the outlet was greater when the cavity width was 100mm than those with wider widths. It was 0.27m/s and decreased to 0.20m/s and 0.16m/s when the cavity width increased from 200mm and 300mm respectively (Figure 5.7). In contrast, a large decrease in average outlet air velocity from 0.27m/s to 0.13m/s was observed when the cavity width was decreased from 100mm to 80mm. It was even lower than that observed in the 300mm and 200mm widths. The coefficients of variance associated with the outlet average air velocity in the 100mm and 80mm cavity widths were about 6% and 10% respectively. Analysis shows that the reduction of the cavity width below 100mm caused a drop in the outlet air velocity, and also indicated that cavity widths of 300mm and 200mm were disadvantageous.

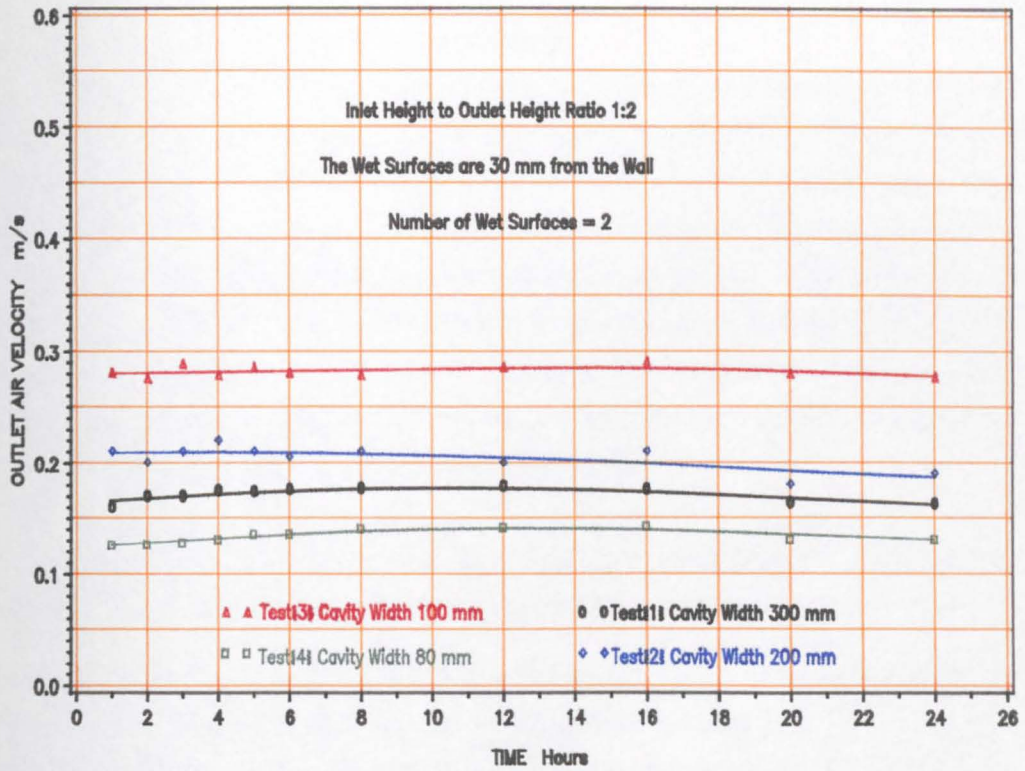


FIG 5.6 The effect of time on outlet air velocity

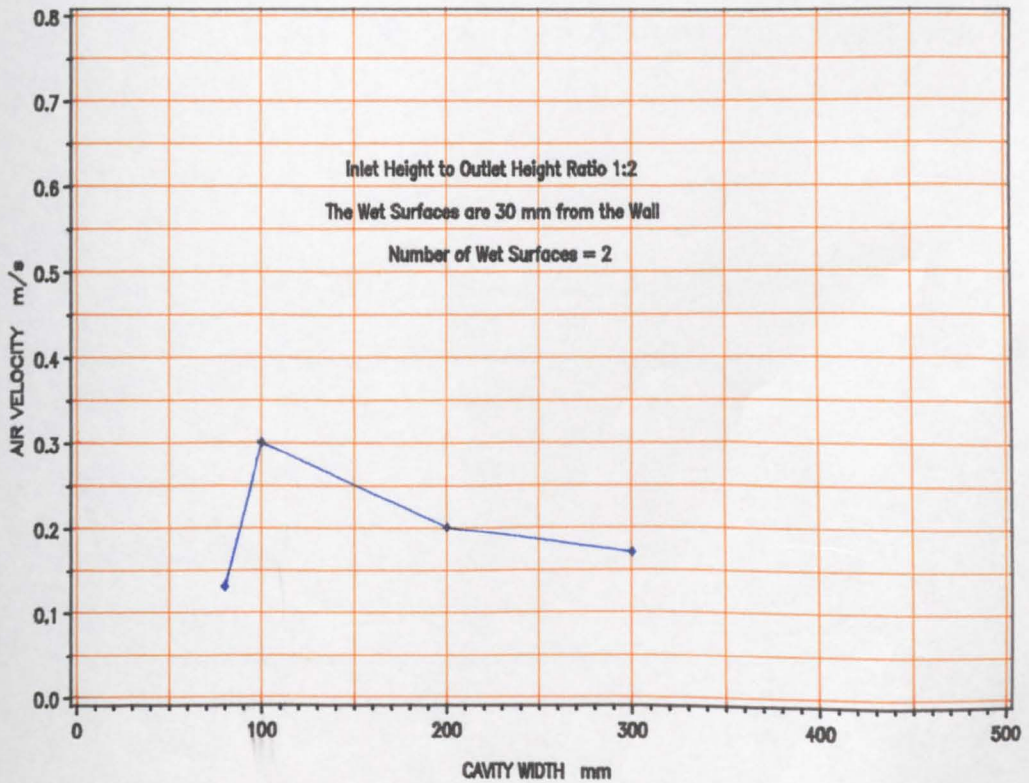


FIG 5.7 The effect of cavity widths on mean outlet air velocity

5.4.2.2 Outlet air relative humidity

The outlet air relative humidity and its temperature were needed to determine the density of the air at the outlet so that the cooling could be established. Air density was obtained from the CIBSE Psychrometric chart (1986). Measured values of air temperature and relative humidity were employed to determine the state point of the air on the chart thus finding its density. Since the variation in the density of the air by buoyancy is small (at air temperature drop of 6K), the determination of the outlet average air relative humidity was of great importance. Measurements were taken at 24 points across the outlet to show the distribution of the relative humidity. Four cavity widths (300mm, 200mm, 100mm and 80mm) were used.

Analysis shows that in all tests of cavity widths 300mm, 200mm, 100mm and 80mm, the coefficient of variance was about 2% at an inlet air temperature and relative humidity of $21\pm 1^\circ\text{C}$ and $70\pm 2\%$. Figure 5.8 shows the air relative humidity distribution over the outlet. It was found that the average outlet air relative humidity was affected by the cavity width. The average outlet air relative humidity for the 300mm cavity was $81\pm 3\%$ (assuming a normal distribution with a mean value of 95% confidence). In the 200mm and 100mm cavity widths, it increased slightly by 4% and 9% respectively (Table 5.4). An increase of 13% in the outlet relative humidity was obtained with the 80mm cavity (Table 5.4). This indicates that the decrease of the cavity width from 300mm to 80mm increases the average outlet air relative humidity to approach saturation ($94\pm 2\%$).

Table 5.4 Measured variations of the outlet air relative humidity.

Cavity width	mm	300	200	100	80
Average outlet R.H.	%	81	85	90	94
Inlet R.H.	%	70	70	69	70
Inlet temperature	$^\circ\text{C}$	19	21	20	22
R.H. increase	%	11	15	21	24

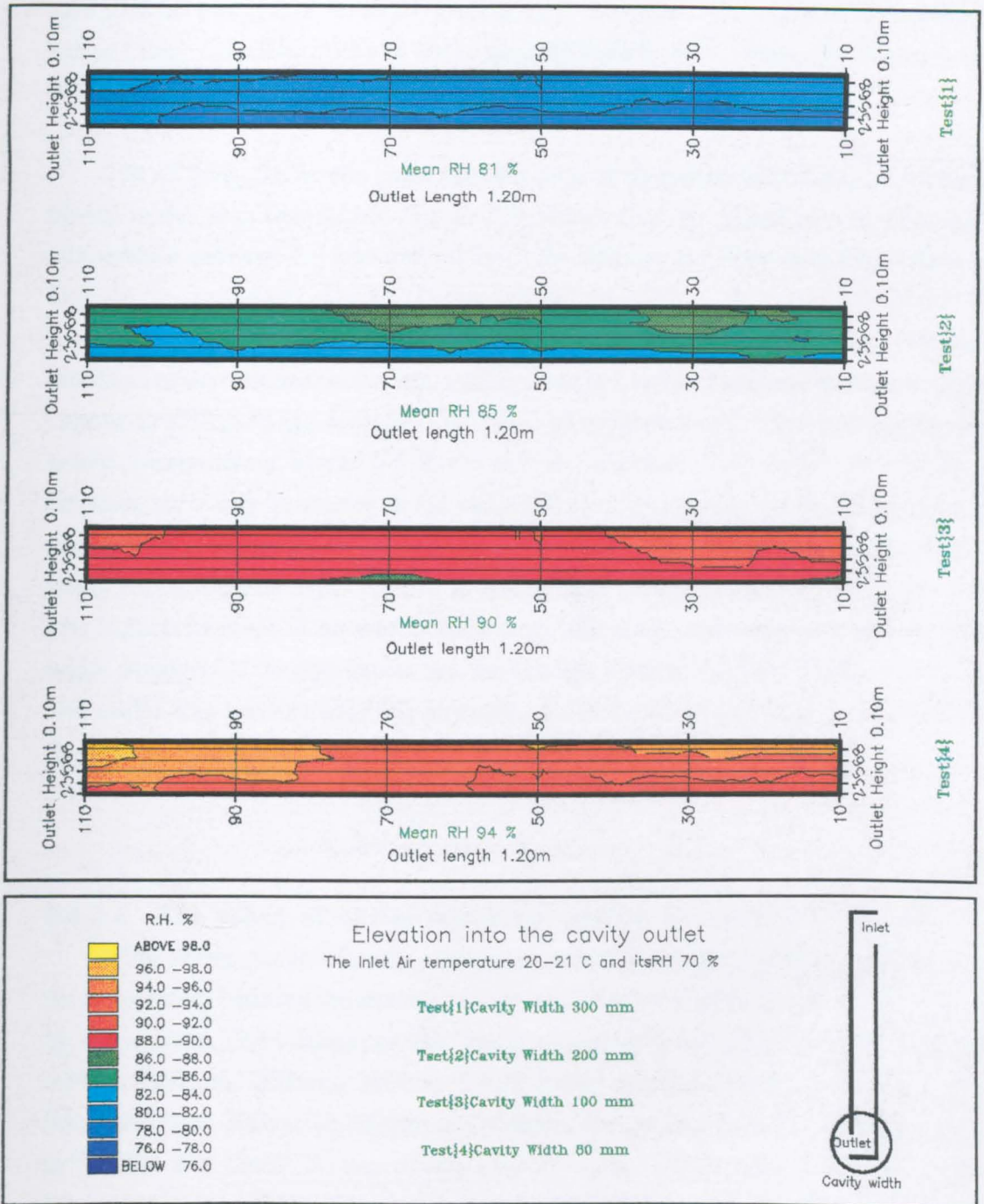


FIG 5.8 The Effect of Cavity Width on Outlet Air Relative Humidity Distribution

The Wet Surfaces are 30 mm from the Dry walls

5.4.2.3 The effect of cavity width on air temperature drop

To study the effect of the cavity width on the drop in air temperature between the inlet and the outlet as a result of cooling by evaporation, the width of the cavity was varied (Table 5.1). The inlet and outlet air temperatures were measured (Figure 4.14) at different cavity widths (300mm, 200mm, 100mm and 80mm).

In all tests, the results show that the drop of air temperature increased when the cavity width was decreased. Figure 5.9 shows that no effect on the drop of air temperature between the inlet and outlet in the 200mm and 300mm cavity widths with time. In the narrower cavity of 100mm and 80mm width, a slight initial decrease of air temperature drop was observed and then no further drop. This was probably because of the effect of dryness within the wet mat layer caused by the increased resistance of water vapour to diffusion (as described in detail in chapter three). This will be discussed below. Nevertheless, Figure 5.6 shows that the variation of the outlet air velocity was constant, so it may be related to the variation of air temperature in the laboratory. The average air temperature drop was increased from 2.6K to 3.6K and 4.5K when the width was decreased from 300mm to 200mm and 100mm respectively (Figure 5.10). The highest increase of air temperature drop (about 6K) was observed with the 80mm width. Analysis of the data shows that the average air temperature drop between the inlet and outlet was increased by 3K as result of cavity width reduction from 300mm to 80mm.

5.4.2.4 The effect of cavity width on cooling by buoyancy air flow

The above results of outlet average air velocity, relative humidity and the drop in air temperature between the inlet and outlet were used to established the average cooling by evaporation. The cooling per unit length of the cavity was determined for four cavity widths (300mm, 200mm, 100mm and 80mm). Analysis shows that as the cavity decreased from 300mm to 200mm and 100mm, the cooling was increased from 66W/m to 93W/m and 136W/m respectively (Figure 5.11). The cooling decreased with the 80mm cavity by 43W/m. This was due to the drop of the outlet air velocity (Figure 5.6).

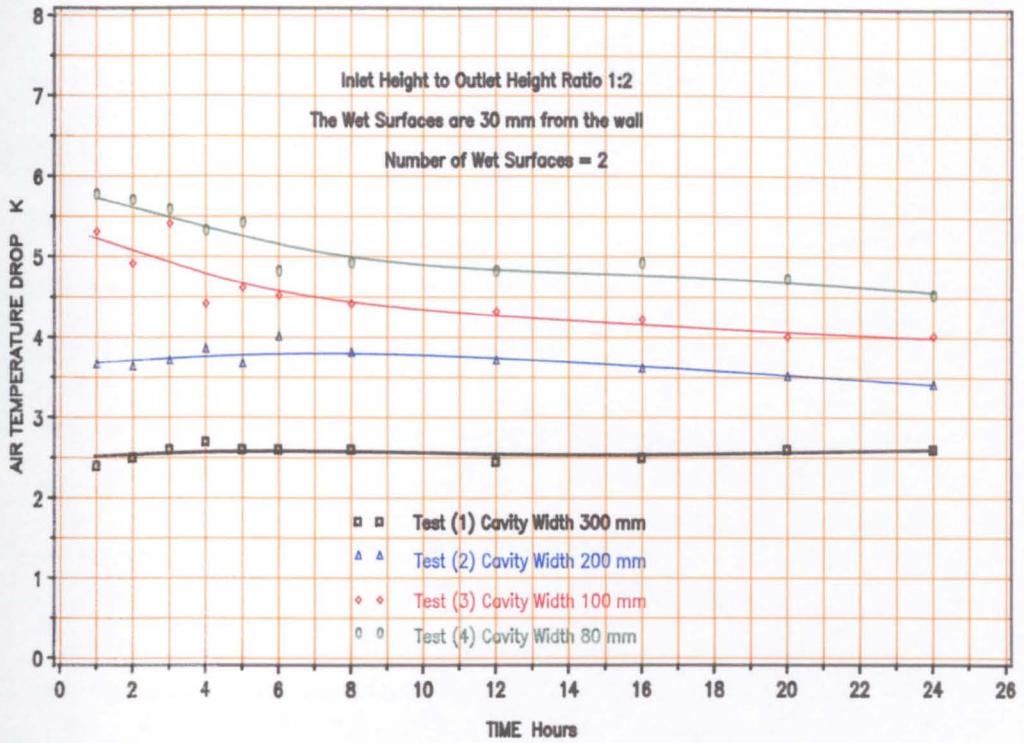


FIG 5.9 The effect of cavity width on air temperature drop between the inlet and outlet

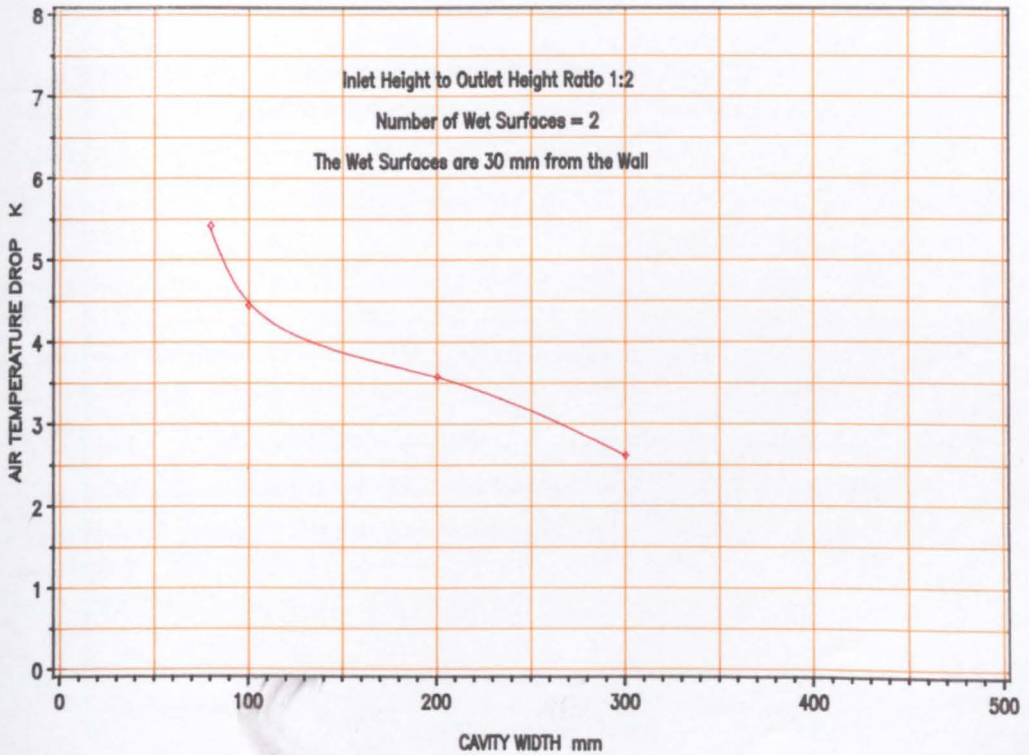


FIG 5.10 The effect of cavity width on mean air temperature drop between the inlet and outlet

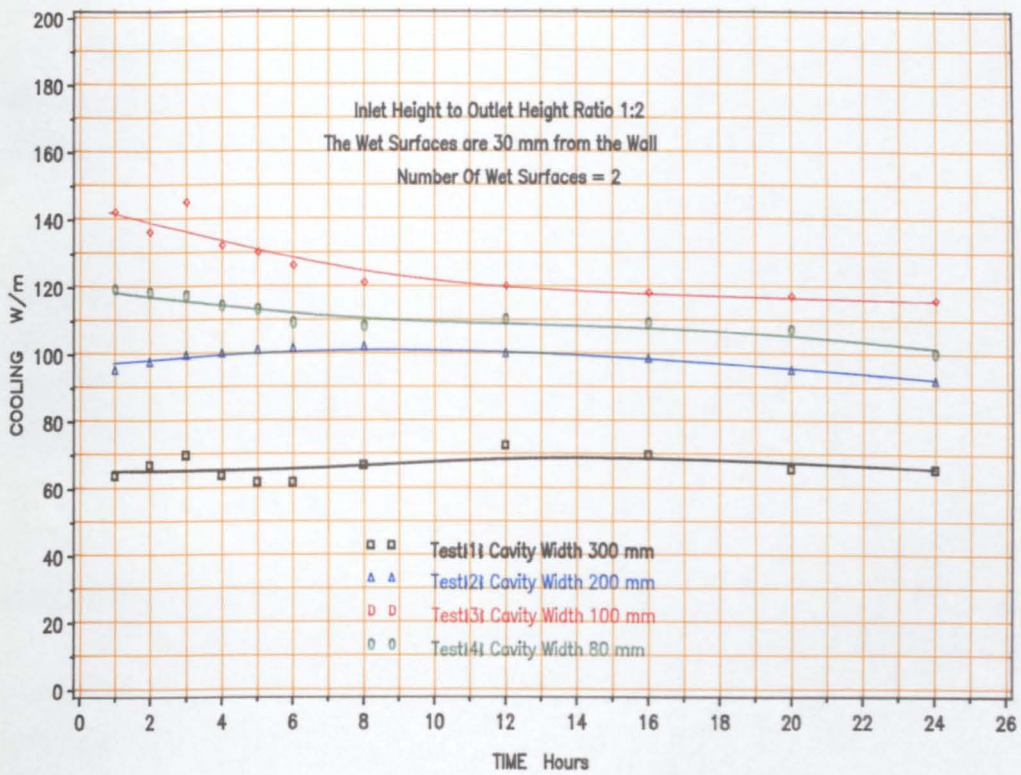


FIG 5.11 The effect of time on cooling

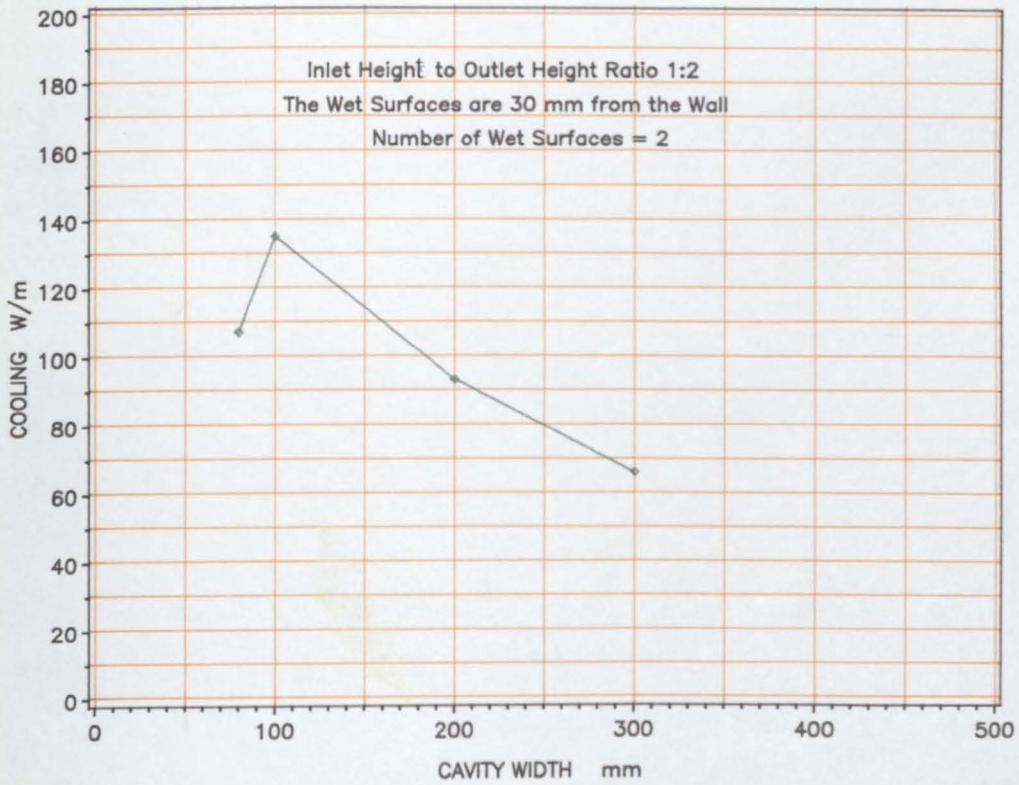


FIG 5.12 The effect of cavity width on cooling Rate

This indicates that the highest average cooling per metre length (136W/m) was found at cavity width of 100mm, and also suggests that cavity width below or above 100mm was disadvantageous in terms of increasing the average cooling by evaporation.

Results of tests so far show that the changes of air temperature drop, the air velocity and the rate of cooling with time were small. However, the 80mm and 100mm cavity widths show some changes (Figure 5.6 and Figure 5.9). Therefore it was necessary to investigate these variations with time to give a value of humidity ratio difference which is one of the main factors affecting evaporation.

5.4.3 Difference in the humidity ratio (Δg)

The humidity ratio is the mass of water vapour carried per unit mass of dry air. Due to the difference in the humidity ratio between the saturated boundary layer and the air adjacent to it, evaporation takes place. It was essential to determine the difference in the amount of water vapour between the incoming air and the saturated boundary layer (known as the difference in the humidity ratio difference, Δg) with time so that the decrease in the cooling could be established. In the text it is called the 'difference in the humidity ratio'.

The changes in the humidity ratio were found by subtracting the humidity ratio of the incoming air from that of the saturated boundary layer. Each humidity ratio was determined at a given measured air temperature and relative humidity. Results of the differences in the humidity ratio with time at different cavity widths are shown in Figure 5.13.

The changes of the difference in humidity ratio with time at the 200mm and 300mm cavity widths was very little (Figure 5.13), but the 80mm and 100mm cavity widths show some variation with time. These variations could be negligible because of their small values compared with those of the temperature error of the incoming air. The maximum changes of the humidity ratio with time (Figure 5.14) are less than those of the temperature error of the incoming air. For example; at $\pm 0.25\text{K}$ error in the temperature of the incoming air at 22°C at a constant relative humidity of 70%, the error

in the humidity ratio was found to be 0.0003kg/kg (Figure 5.14). It could be increased to 0.0004kg/kg if the error in the temperature of the incoming air is $\pm 0.5\text{K}$. An error of +2% in the relative humidity produces an error of 0.0004kg/kg with the humidity ratio.

The error of the humidity ratio was found to increase to 0.0007kg/kg when both air temperature and relative humidity errors are considered. This indicates that the changes in the humidity ratio were negligible.

The measured data of the 80mm and 100mm cavity widths were regressed at a 95% confidence limit and the relationships between the humidity ratio difference with time are shown to be linear. The regression coefficients R_c were 0.96 and 0.92 respectively (Figure 5.14). This indicates that about 95% of the data are correlated and the time could be negligible factor.

The above analysis suggests that very little variation found with the 'difference in the humidity ratio'. The relative decrease of the 'difference in the humidity ratio' per hour was of the order of 4% and the average was about 10%.

5.4.3.1 Water removed by evaporation

The amount of water removed by evaporation for different cavity widths can be calculated from:

$$W_r = \Delta g m \quad \text{kg/s} \quad [5.2]$$

where

Δg = the difference in the humidity ratio kg/kg

m = mass flow rate at the cavity outlet kg/s

Since two wet mats (giving four areas of evaporation) were used in each cavity, the amount of water removed by evaporation was determined per cavity. Results are given in Table 5.5.

Table 5.5 Average amount of water removed by evaporation.

Cavity width mm	Average air velocity m/s	Mass flow rate kg/sm	Av. humidity ratio difference kg/kg	Av. water removed by evaporation kg/hm
80	0.13	0.015	0.0011	0.063
100	0.27	0.032	0.0007	0.080
200	0.20	0.024	0.00014	0.013
300	0.16	0.019	0.00043	0.030

Although the humidity ratio difference of the 100mm cavity was less than that with the 80mm width, the amount of water removed from the wet mats by evaporation was greater with the 100mm cavity than that with 80mm width (Table 5.5). This was due to the increase of mass flow in the 100mm cavity. The amounts of water removed using cavities 200mm and 300mm wide were too small. The lower value of the 200mm cavity may be related to the error associated with the humidity ratio difference as mentioned above since the air velocity with both cavity widths was nearly the same (Table 5.5).

Assuming that the wet mats are behaving like a pool of water, the humidity ratio difference may be taken as a maximum value (Figure 5.15). Thus, the amount of water needed for evaporation, based on maximum values of humidity ratio difference, (Figure 5.15) would increased. It would be 0.4kg/m for the 80mm cavity and 0.6kg/m for the 100mm one, and a negligible increase will take place for the 200mm and 300mm widths (Figure 5.13).

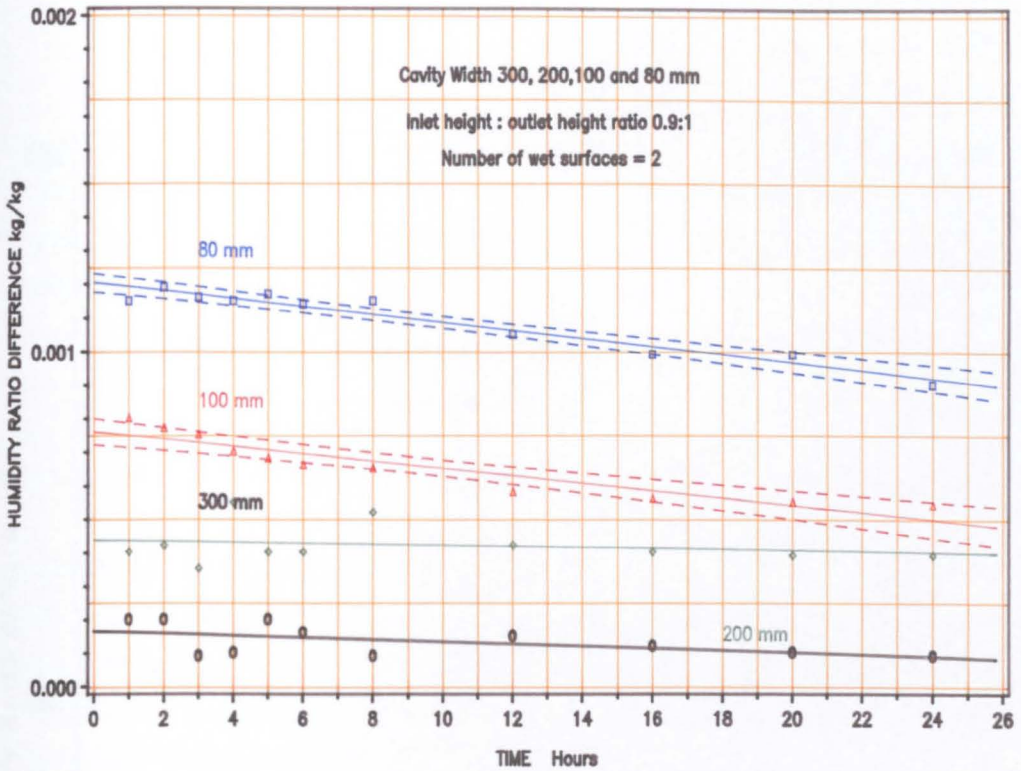


FIG 5.13 The changes of humidity ratio with time at different cavities

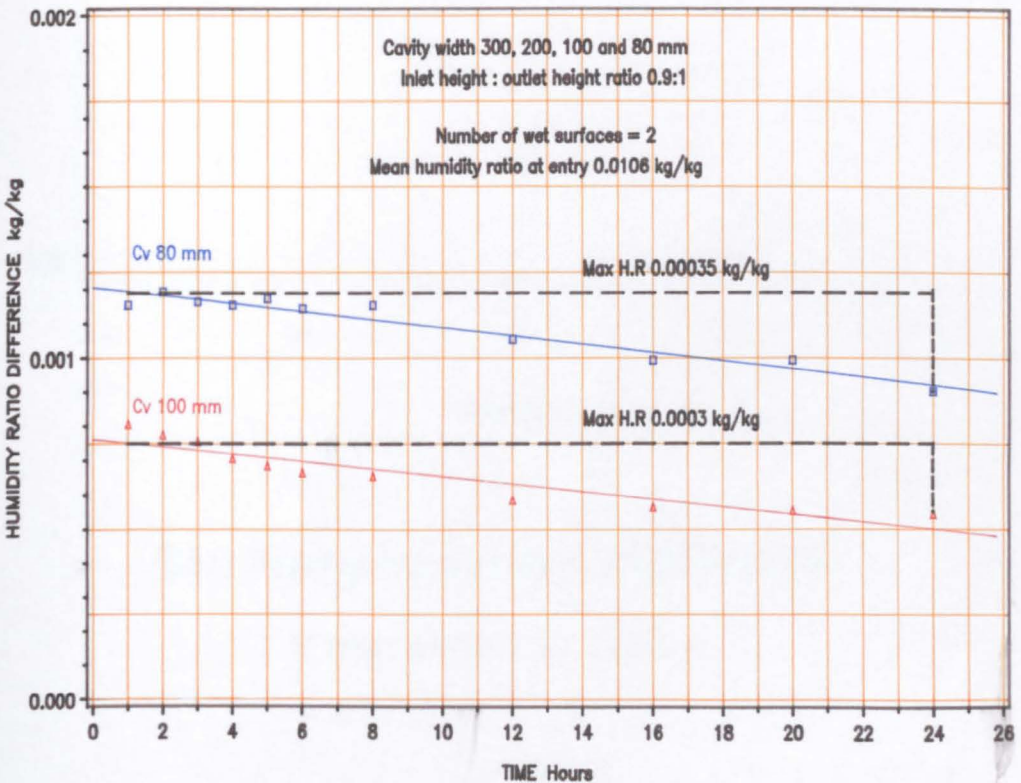


FIG 5.14 The maximum changes of humidity ratio difference with time

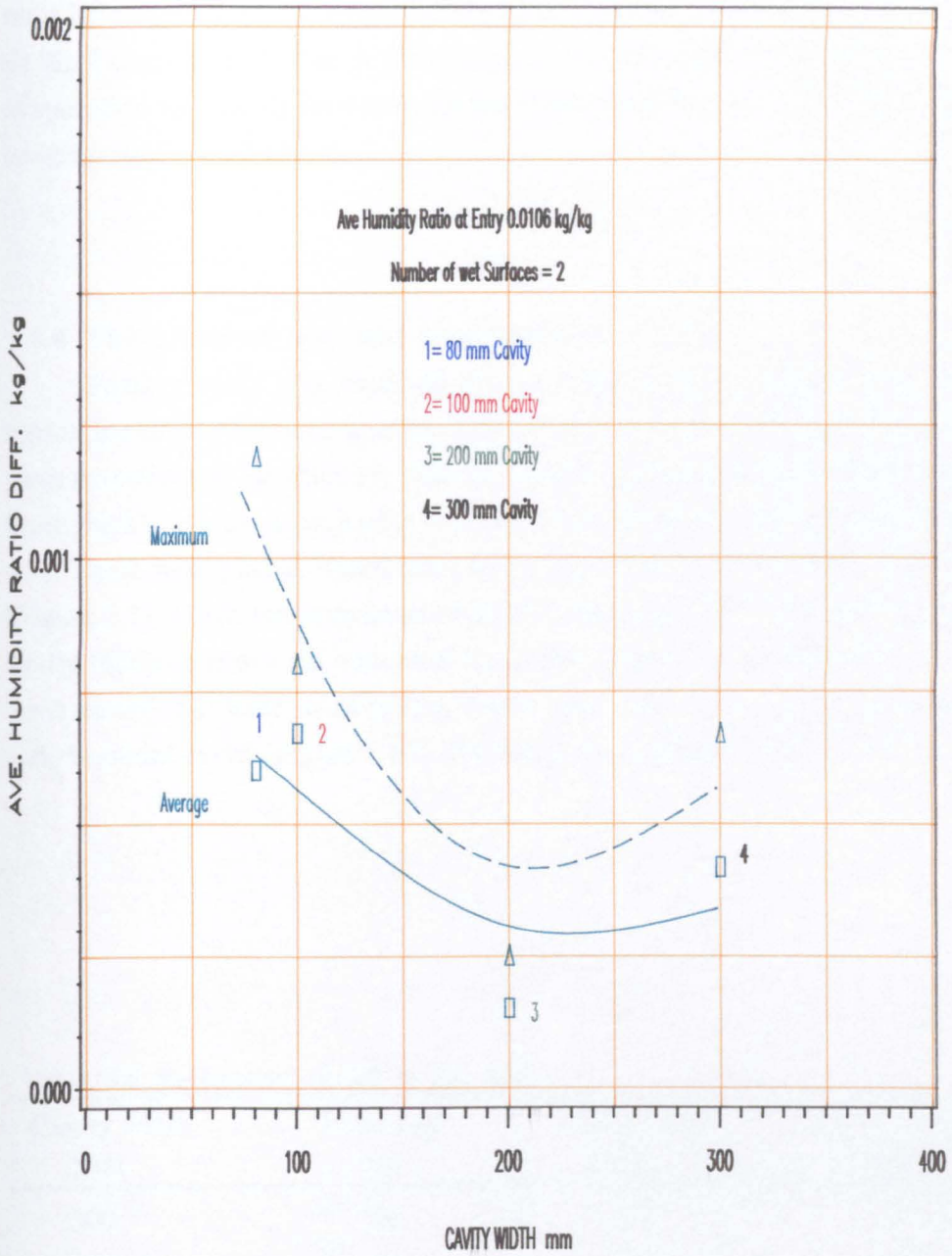


FIG 5.15 The average changes of humidity ratio at different cavities

Wet surfaces separation 20, 30, 130 and 230 mm

The above suggests that the average amount of water removed from the two wet mats by evaporation was small (0.08kg/hm). It could be increased to the maximum (in an ideal case) of 0.1kg/hm. It also suggests that the width of the cavity influences the evaporation and the air flow through the separation between the wet mats. This will be investigated in detail below.

5.4.4 The effect of wet mat separation on cooling

Further study was made to give a better understanding of the effect of the separation of the wet mats in relation to the cavity width on cooling. Three parameters were investigated: air velocity, relative humidity and temperature. Two wet mats (each 5mm thick) were used, each with two wet sides giving four areas of evaporation (Figure 4.7). These were placed 30mm from the cavity walls, thus dividing the cavity into three (Figure 5.1). Micro-measurements of air velocity and relative humidity were made in the cavity [650mm above the bottom of the cavity (Figure 4.9)]. In all tests, measurements were recorded at least at 24 points. These were made in the inlet cavity, central cavity and the outlet cavity (Figure 5.16). The variable parameters are given in Table 5.6.

Table 5.6 Parameters varied in the tests.

Cavity width mm	Inner gap mm	Central gap* mm	Outer gap mm
300	30	230	30
200	30	130	30
100	30	30	30

* Central gap = separation between wet mats

5.4.4.1 The effect of wet mat separation on air velocity

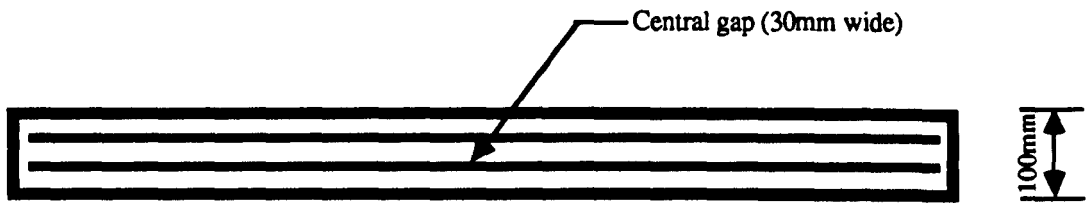
To study the effect of wet mat separation in the cavity on air flow, the width of the cavity was varied. Each cavity was arranged as shown in Figure 5.16.

In the 300mm cavity, it was found that the air velocity distribution in the inner gap was similar to that in the outer. It was much greater than that in the central gap. The average air velocity was 0.25m/s, 0.03m/s and 0.23m/s in the outer, central and inner gap respectively (Table 5.7).

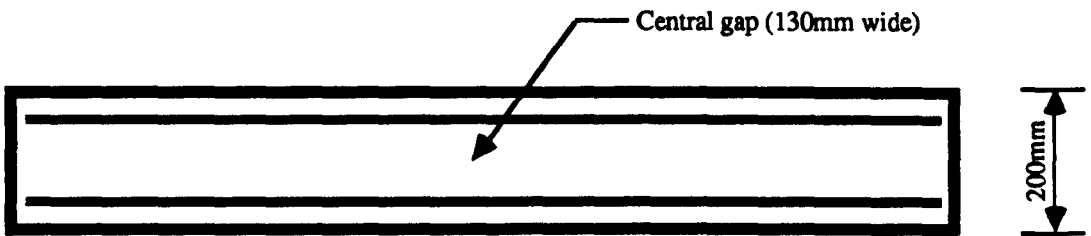
As temperatures of the incoming air and those of the mats at the entry of each gap were nearly the same, evaporation on each wet surface would be expected to be the same. Evaporation may be greater in the central gap because of the greater area of evaporation. Analysis of the data showed a different performance.

Table 5.7 Measured average air velocity at different cavity widths.

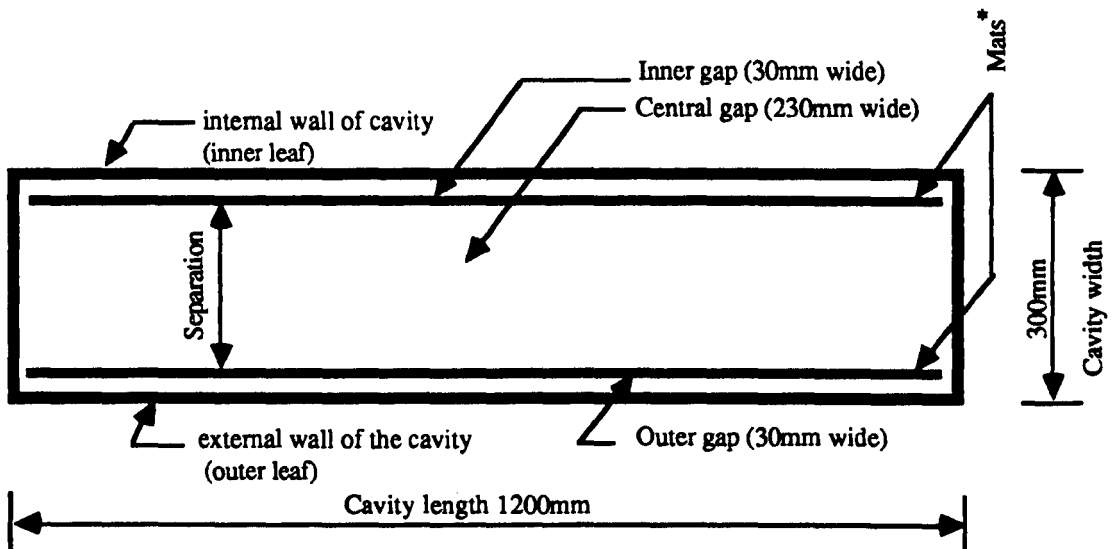
Cavity width	Gap	Width	Average air velocity (v)	Separation
mm	---	mm	m/s	mm
300	Outer	30	0.25	200
	Central	230	0.03	
	Inner	30	0.23	
200	Outer	30	0.25	100
	Central	130	0.02	
	Inner	30	0.23	
100	Outer	30	0.25	---
	Central	30	0.27	
	Inner	30	0.24	



Cross-sectional plan of the 100mm cavity



Cross-sectional plan of the 200mm cavity



Cross-sectional plan of the 300mm cavity

* Mat thickness 5mm.

The outer and the inner gaps in all tests are 30mm wide.

Figure 5.16 Plan of cavity widths with different wet mat separation.

Figure 5.17 a shows the air velocity distribution of the 300mm cavity. It shows a separation (about 200mm) between the evaporative boundary layers in the central gap (very low speed of 0.03m/s). The air velocity was 0.05m/s near the two wet mats in the central gap. This indicates that 30mm width of the inner and the outer gaps were more effective in terms of evaporation and thus cooling, and it also emphasises that the air velocity of the central gap (230mm) was insufficient to promote evaporation (nothing happening away from the wet mats).

In the 200mm cavity (Figure 5.17 b), the trend was nearly the same except that the separation between the wet mats was smaller than that of the 300mm cavity. The reduction of the separation area in the central gap from 200mm to 100mm was ineffective in promoting evaporation.

This suggests that further reduction of the separation between the wet mats in the central gap was needed so that the still air zone (below 0.05 m/s) in the centre could be eliminated (Figure 5.17).

A considerable difference was found in the 100mm cavity. Figure 5.17 c shows that in the central gap of 30mm, air velocity was much greater compared with that of the 130mm and 230mm gaps. Figure 5.17 c indicates that still air zone in the central gap was eliminated. The average air velocities are given in Table 5.7. The maximum variation was 0.03m/s and the coefficient of variance was ± 0.06 .

5.4.4.2 Nature of the flow

The nature of the air flow was determined using the Reynolds number (Re). For flow in pipes, the flow is laminar if $Re < 2000$ and turbulent at $Re > 3000$. When air flows between parallel plates, the Reynolds number is dependent upon the "hydraulic diameter" which for a wide cavity is twice the actual separation (CIBSE guide, 1986). The Reynolds number of each cavity was determined using measured average air velocity (Table 5.7). Results are given in Table 5.8.

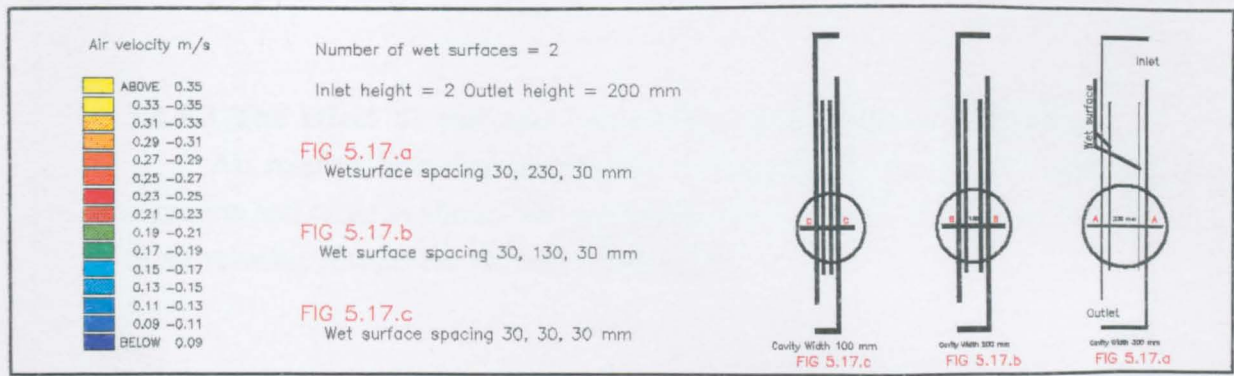
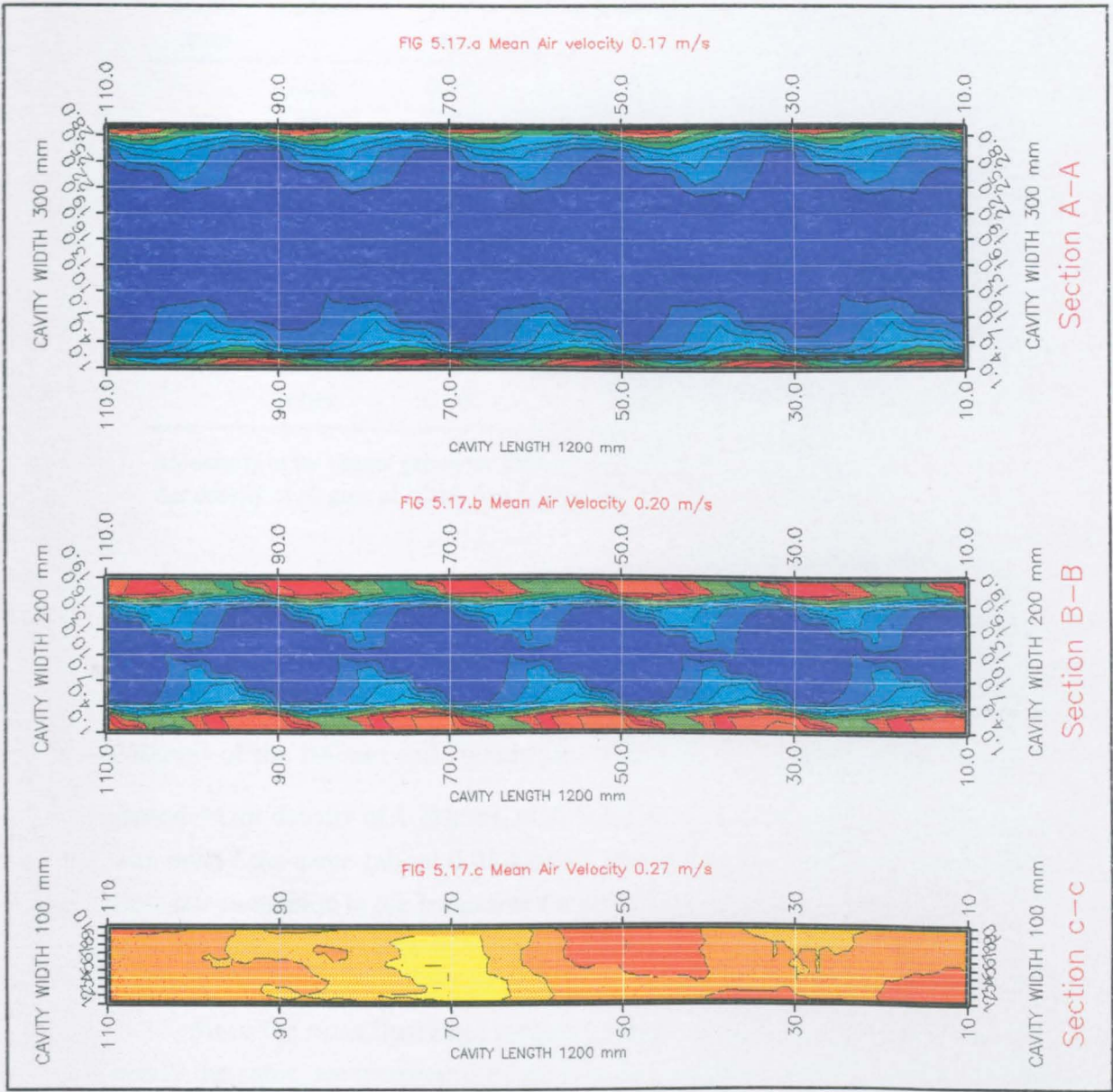


FIG 5.17 The Effect of Cavity Width on Measured Air Velocity Distribution

Table 5.8 Reynolds number for different cavity widths.

Cavity width mm	Gap location ---	Width m	Reynolds number (Re) ---	Mass flow rate (air) kg/sm
300	Outer	0.03	885	0.009
	Central	0.23	772	0.008
	Inner	0.03	814	0.008
200	Outer	0.03	885	0.009
	Central	0.13	728	0.007
	Inner	0.03	814	0.008
100	Outer	0.03	885	0.009
	Central	0.03	956	0.01
	Inner	0.03	850	0.085

Air density in the central gap of the 200mm and 300mm was 1.12 kg/m^3

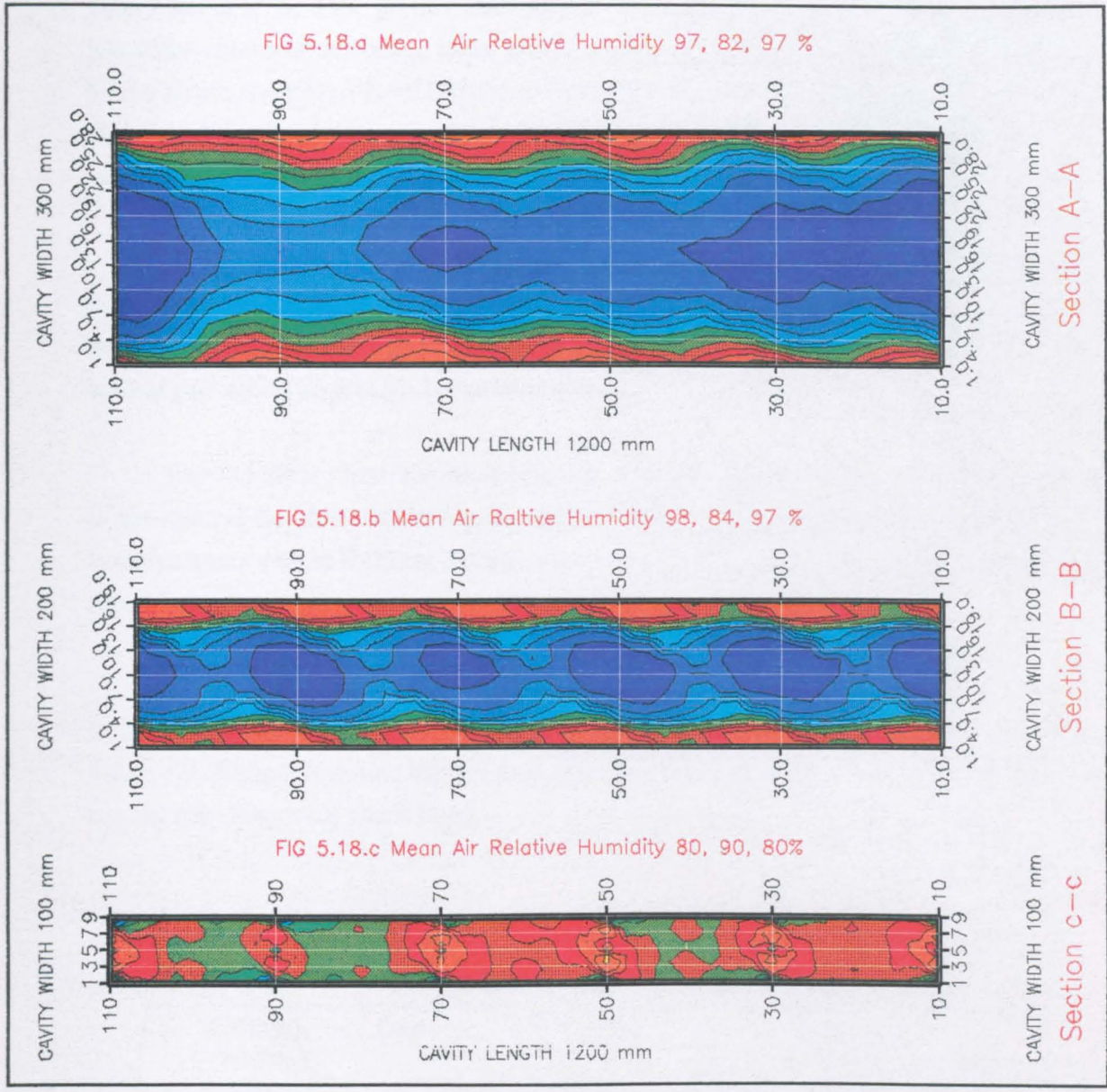
Air density in all gaps of 30mm was 1.18 kg/m^3

The Reynolds numbers in all cavities were much below 2000, and this indicates that the flow was laminar. Despite the velocity of air in both the central gap (30mm and 230mm) of the 100mm and 300mm cavity widths, the mass flow rate per unit length (based on air density of 1.2 kg/m^3 , at 82% relative humidity and air temperature 10°C) was nearly the same (about 0.01 kg/sm). Table 5.8 shows the variations in the mass flow rate in relation to the separation between wet mats inside different cavity widths. It indicates that the mass flow rate decreased little as the separation increased.

Since the mass flow rates resulting from wet mat separation in all cavities were nearly the same, measurements of air relative humidity were important to explain the cause of air velocity variations.

5.4.4.3 The effect of wet mat separation on air relative humidity

Air relative humidity distribution measurements were made under the same condition and order as above. Measurements were recorded simultaneously with those of air velocity. Results are shown in Figure 5.18.



<p>Air Relative Humidity %</p> <ul style="list-style-type: none"> 98.0 - 100.0 96.0 - 98.0 94.0 - 96.0 92.0 - 94.0 90.0 - 92.0 88.0 - 90.0 86.0 - 88.0 84.0 - 86.0 82.0 - 84.0 80.0 - 82.0 BELOW 80.0 	<p>Number of wet surfaces = 2</p> <p>Inlet height = 2 Outlet height = 200 mm</p> <p>FIG 5.18.a Wetsurface spacing 30, 230, 30 mm</p> <p>FIG 5.18.b Wet surface spacing 30, 130, 30 mm</p> <p>FIG 5.18.c Wet surface spacing 30, 30, 30 mm</p>	<p>FIG 5.18.c</p> <p>FIG 5.18.b</p> <p>FIG 5.18.a</p>
--	---	---

FIG 5.18 The Effect of Cavity Width on Measured Air Relative Humidity Distribution

In the 300mm cavity width, air relative humidity in the 30mm gaps (outer and inner) found to be 15% greater than that of the central gap. The average air relative humidity values of the outer, inner and the central gap are given in Table 5.9. Figure 5.18 a shows the lowest level of relative humidity (80%) in the central gap of 230mm. It also shows that little change in relative humidity took place in the separation between the wet surfaces of the central gap.

Analysis of the data shows that the air relative humidity at both sides of mat was different. Air relative humidity at the side facing the inner and outer gaps was 10% greater than that facing the central gap. It was expected that the relative humidity in the central gap would be greater, because evaporation being doubled.

Beyond 30mm from the wet surface the central gap, there were very little changes in the relative humidity of the air (Figure 5.18 a and Figure 5.18 b). This was probably because water vapour diffuses through a layer of air only about 30mm while going from top to bottom.

In the 200mm cavity, the trend was nearly the same in the inner and the outer gap as in the central gap (Figure 5.18 b). Average air relative humidity values are given in Table 5.9. Although some changes took place near the inner side of each wet mat of the central gap, they were small (4%).

Table 5.9 Average air relative humidity at different cavity widths.

Cavity Width mm	Gap --	Gap width mm	Average relative humidity %
300	Inner	30	97
	Central	230	82
	Outer	30	97
200	Inner	30	98
	Central	130	84
	Outer	30	97
100	Inner	30	80
	Central	30	90
	Outer	30	80

The study of the 300mm and 200mm width cavities suggests that separation between two parallel vertical wet mats greater than about 60mm was insufficient to promote evaporation.

In the 100mm cavity (unlike the 300mm and the 200mm cavity), it was found that air relative humidity near the wet mats in the inner and outer gap was less than that of the central gap the difference was up 10% (Figure 5.18 c). Figure 5.18.c shows that the constant air relative humidity zone observed in the previous central gaps no longer existed. This was probably that the saturated boundary layers are too close or may interact. Thus, saturated air became denser and moves downwards much faster. This explains the great increase of average air velocity observed in the 30mm central gap of the 100mm width (Table 5.7). The average air relative humidity distribution in the outer, central and inner gaps of the 100mm, 200mm and 300mm widths are given in Table 5.10.

5.4.4.4 The effect of wet mat separation on humidity ratio difference.

The humidity ratio differences in all tests were affected by the wet mat separation. Figure 5.15 shows that as the wet mat separation decreases the maximum and the average humidity ratio difference increases. At a constant convective heat transfer coefficient, the rate of evaporation may increase due to the reduction of the wet mat separation (increase of the humidity ratio) from 230mm to 20mm. Observation shows that the cooling decreased at a wet surface spacing of 20mm. This was due to the drop in air velocity (Figure 5.7).

To give a quantitative value of the humidity ratio due to the wet mat separation in the central cavity of each width, the humidity ratio (g) of both the saturated boundary layer and the incoming air were determined. The humidity ratio of the incoming air was determined from the CIBSE Psychrometric chart (1986) using measured temperature and relative humidity of the air at entry. For the saturated boundary layer, it was determined using the measured temperature of the wet mats.

Table 5.10 Average air relative humidity distribution in different cavity widths according to Figure 5.18.

Cavity width mm		30mm			30mm			30mm					
		Inner gap			Central gap						Outer gap		
		a	b	c	d	e	f	g	h	i	j	k	l
300		30mm			230mm						30mm		
R.H.		90	94	98	90	84	82	81	85	91	98	93	91
200		30mm			130mm						30mm		
R.H.		90	93	98	94	86	83	84	86	93	97	94	92
		The same as above									The same as above		
					n	m		o					
100		30mm			30mm						30mm		
R.H. %		77	80	90	94	83		95		89	80	78	

- Cavity wall
- Wet mat
- Intervals each 10mm

a to o are the label for each interval

All illustrations are vertical sections into the cavity, where the cross-sectional plans of these distribution are shown in Figure 5.18

Figure 5.19 shows the average humidity ratio of both the incoming air and the saturated boundary layer. The average partial pressure difference between the saturated boundary layer and that of the incoming air are given in Table 5.11. At 30mm separation (100mm cavity), the average humidity ratio difference was greater than those of the 20mm, 130mm and 230mm separation. Although the humidity ratio g (both the incoming air and saturated boundary layer) of the 30mm separation was less compared with other widths (20mm, 130mm and 230mm), it has the largest difference of Δg . The small humidity ratio obtained was due to the small range of measured temperatures of the incoming air in relation to that of the wet mat.

Table 5.11 Average partial pressure difference between the incoming air and the saturated boundary layer

Central gap width	Air temperature	Wet surface temperature	relative humidity at inlet	P.Pressure w.v. of wet surface	P. Pressure w.v. of air	P.P. Difference air+wet surface
mm	°C	°C	%	Pa	Pa	Pa
230	19	15	70	1675	1545	130
130	21	16.5	70	1888	1768	120
30	19	13	64	1510	1360	150
20	22	17	68	1949	1824	125

w.v. = water vapour
 $g (160 \times 1000) = \text{Pa} \cdot \text{D}$

Despite the decrease of the humidity ratio difference of the 80mm cavity (wet mats separation of 20mm), the outlet relative humidity increased (Figure 5.20). This increase was due to the saturated air moving in the 20mm central gap of the 80mm width cavity.

The above suggests that because of the small humidity ratio difference between the incoming air and the saturated boundary layer, the convective heat transfer coefficient of air between the two surfaces may be of great influence on the evaporation, and therefore measurements were used to determine the appropriate convective heat transfer

coefficient to give better insight in view with the observations. This will be carried out in Chapter Seven.

It may be expected that with a cavity divided into three (30mm each), the pressure drop may be greater than that of the central gap of 130mm and 230mm and therefore, have less resistance to air flow. This would result in a greater mass of air flowing along the cavity and therefore more cooling. However, the calculated pressure loss using eqn. [3.28] indicates that the losses in the 30mm gap was greater than that of the 230mm, but both were negligible compared with that of entry and exit. Results are given in Table 5.12.

Table 5.12 The pressure losses in different central cavity widths

Central gap mm	Average air velocity m/s	Hydraulic diameter m	Reynolds number –	Pressure loss Pa
230	0.03	0.374	628	3×10^{-4}
130	0.05	0.23	644	2×10^{-4}
30	0.27	0.058	929	9×10^{-2}

Air density = 1.12 kg/m^3 for the 130mm and 230mm central gap

Air density = 1.18 kg/m^3 for the 30mm central gap

It could be useful to increase the separation from 30mm to 50mm so that more air could flow through the gaps in the cavity and result in more cooling. However, the pressure drop would be more negligible with the 50mm gap. Some tests were carried out to investigate this.

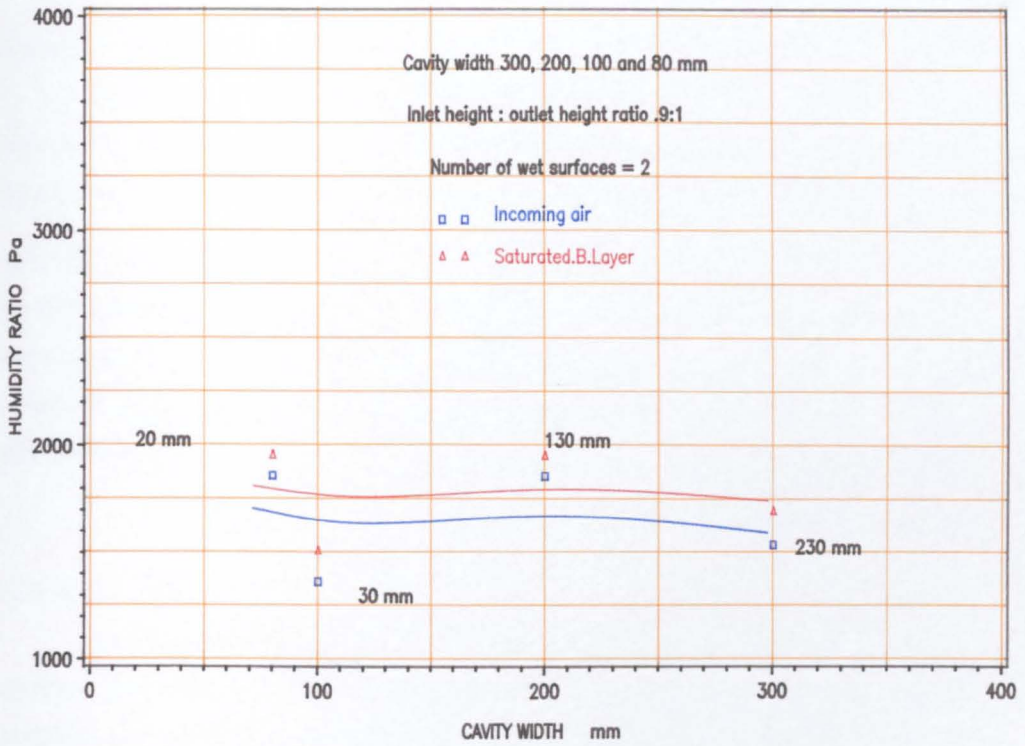


FIG 5.19 The humidity ratio of the incoming air and saturated boundary layer

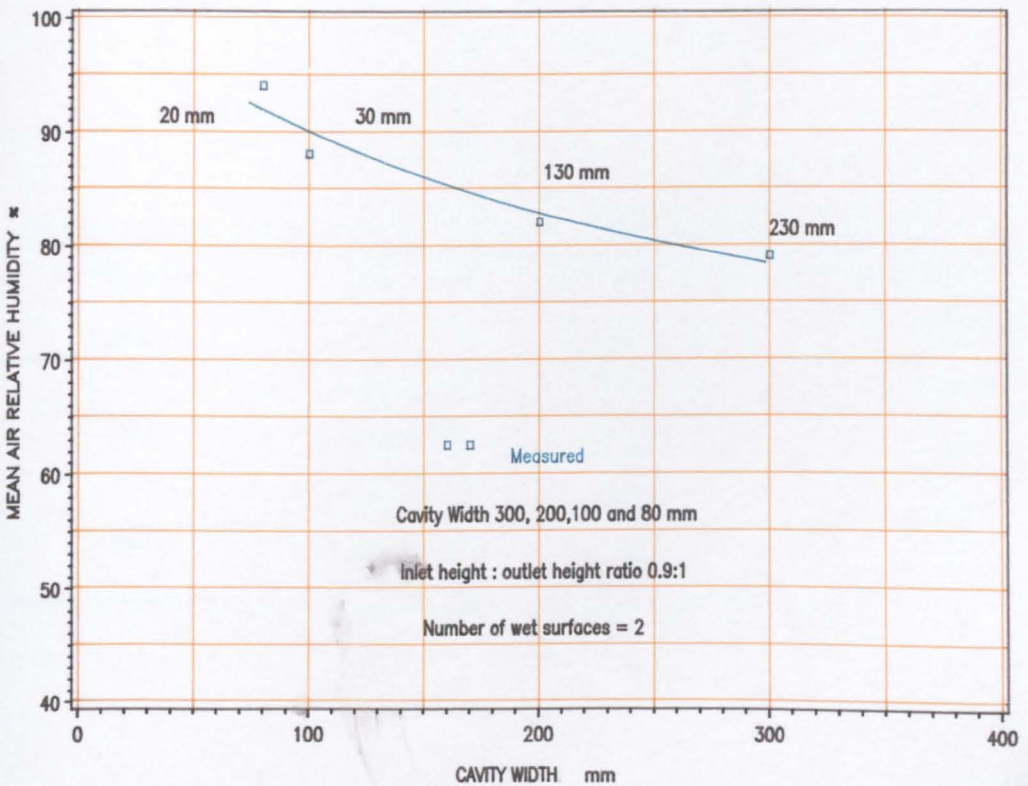


FIG 5.20 The effect of wet mat separation on outlet relative humidity

5.4.4.5 The effect of wet mat separation on the mass flow rate

To study the effect of wet mat separation on the mass flow rate in view of the above results, two tests were carried out at two cavity widths: 100mm and 160mm. Each cavity was divided into three (Figure 5.21). The inlet air temperature and relative humidity were almost the same: 21°C and 60% in the 100mm cavity, and 20°C and 65% in the 160mm one (a maximum variation of 1K and 5%). Calculations of the pressure drop and mass flow rate in each cavity require measured values of air velocity and relative humidity. Measurements were made as above. Results of both tests are presented below.

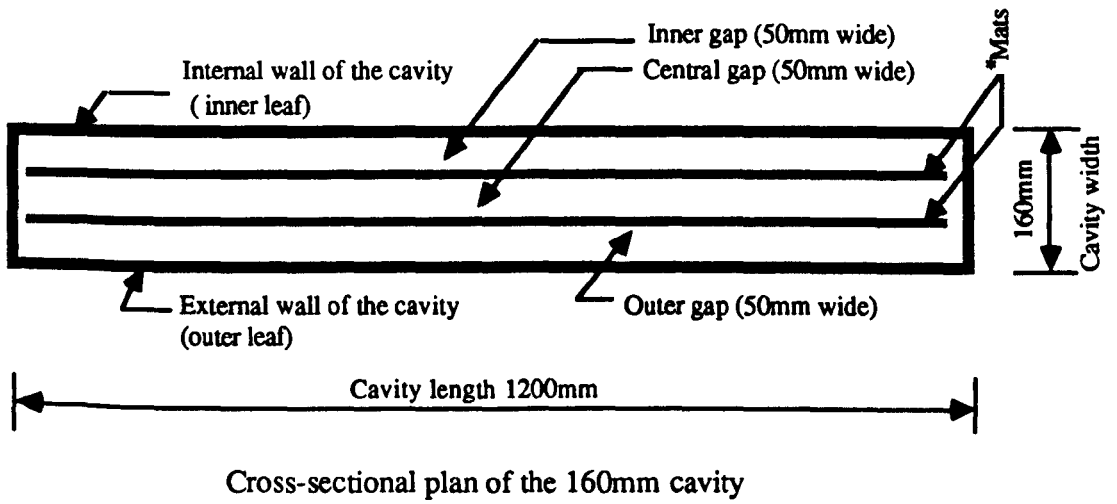
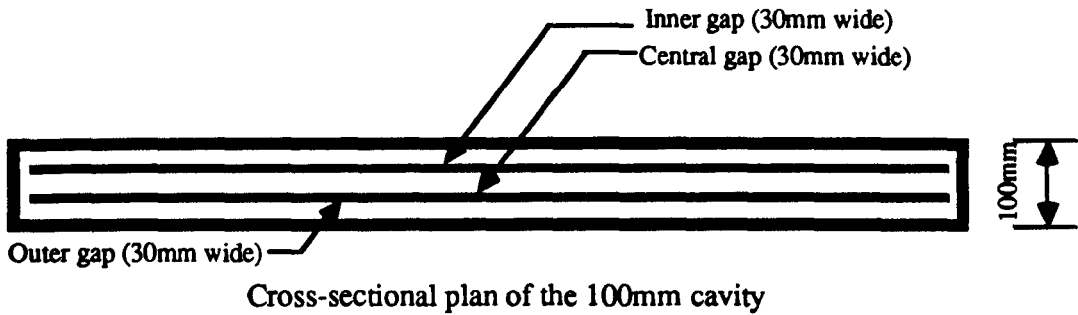
5.4.4.5.1 Air velocity distribution

Analysis of the data shows that in the 160mm cavity, the air velocity in the 50mm central gap was half that measured in the inner and outer gaps (Figure 5.22 a). The average air velocity for the 100mm and 160mm cavity are given in Table 5.13.

The measurements indicate that increasing the separation between the wet mats in the central gap from 30mm to 50mm decreased the air velocity.

Table 5.13 Measured average air velocity at different cavity widths.

cavity width mm	Gap --	width mm	Average air velocity (v) m/s
100	Outer	30	0.25
	Central	30	0.27
	Inner	30	0.23
160	Outer	50	0.15
	Central	50	0.075
	Inner	50	0.13

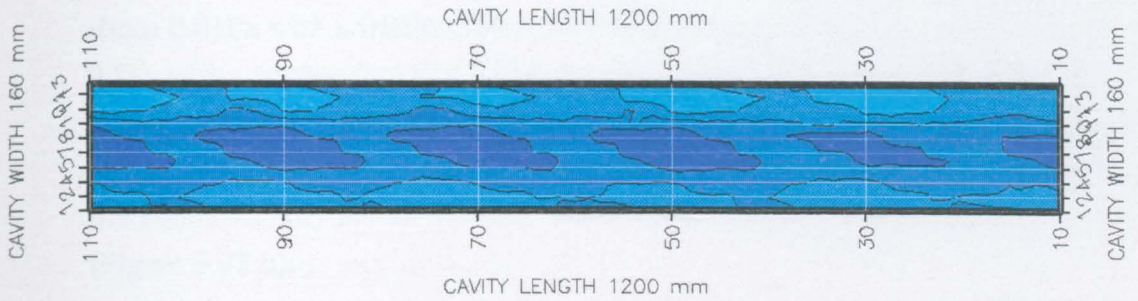


* Mat thickness 5mm.
Evaporation takes place on four surfaces.

Figure 5.21 Plan of the 100mm and 160mm cavity widths with different wet mat separation.

FIG 5.22.a Mean Air Velocity in each Gap 0.15, 0.075, 0.13 m/s

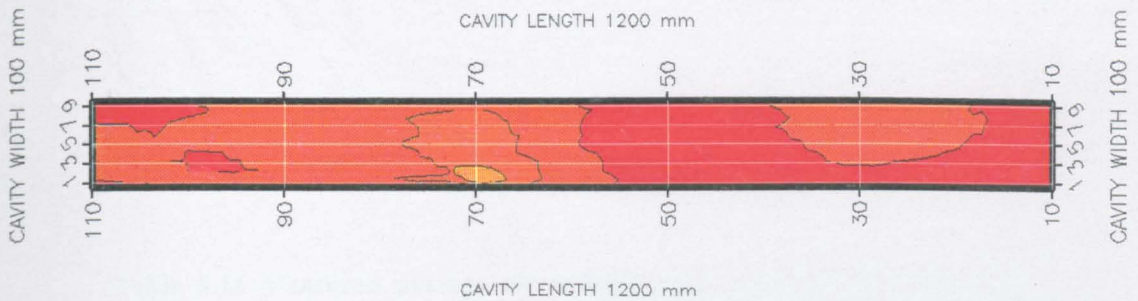
The wet surfaces are 50 mm from the dry walls



Section A-A

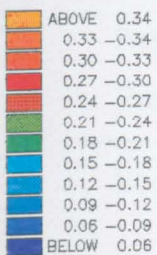
FIG 5.22.b Mean Air Velocity in each Gap 0.25, 0.27, 0.24 m/s

The wet surfaces are 30 mm from the dry walls



Section B-B

Air Velocity m/s



Number of wet surfaces = 2

Inlet height = 2 Outlet height = 200 mm

FIG 5.22.a

Wet surface spacing 50, 50, 50 mm

Air temperature 20 C and its R.H. 67 %

FIG 5.22.b

Wet surface spacing 30, 30, 30 mm

Air temperature 21 C and its R.H. 61 %

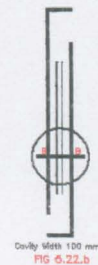


FIG 5.22 Air Velocity Distribution at Different Cavity Widths

With laminar air flow, friction inside rectangular ducts or cavities is negligible, (CIBSE Guide 1986). Assuming that the drop in air velocity in the 50mm central gap of the 160mm width was due to friction, it would be expected that the air velocity would decrease in the central gap of 30mm of the 100mm width as well. Calculated pressure drop in the 50mm central gap obtained from eqns.3.45 and 3.49 (chapter three) was about 0.01Pa with a friction factor of 0.032, whereas in the 30mm central one it was 0.1Pa with a friction factor of 0.014. Analysis shows that the calculated pressure drop in the 30mm gap was considerably greater than that of the 50mm gap. Although the friction coefficient was smaller in the 30mm gap than that of the 50mm gap, results show that in the 100mm cavity the air velocity was 3.6 times greater than that of the 160mm one (Figure 5.22 b).

Air at 17°C, relative humidity 94% has a density of 1.2kg/m³. From eqn. 3.68 (chapter three) air velocity would be of the order of 0.13m/s. But the measured air velocity was double this value (0.27m/s). The calculated and measured values of air velocity and calculated pressure drop of the 100mm and 160mm are given in Table 5.14.

Table 5.14 Measured average air velocity and calculated pressure drop.

Total cavity width	mm	100	160
Central gap	mm	30	50
Measured air velocity	m/s	0.27	0.075
Expected air velocity	m/s	0.13	--
Reynolds number	—	955	430
Pressure drop	Pa/m	0.096	0.0096

Air density is about 1.2 kg/m³ (15°C and R.H. 94%).

The mass flow was computed in each gap, given in Table 5.15. The mass flow rate at the cavity outlet was also computed. The mass flow rate of the inner and outer gaps of both the 100mm and 160mm widths were found to be nearly the same (0.01kg/sm), except that of the central one of the 160mm (0.005kg/sm). A mass balance between the outlet and central gap to conform with what was measured, shows that the mass flow rate was less by about 0.001kg/sm than that of the outlet.

Table 5.15 Calculated mass flow rate of the 100mm and 160mm cavity width.

Cavity width mm	Gap	Average air velocity m/s	Mass flow rate kg/sm	Reynolds number
30	Inner	0.25	0.009	875
30	Central	0.27	0.001	944
30	Outer	0.23	0.008	805
50	Inner	0.15	0.009	843
50	Central	0.075	0.005	429
50	Outer	0.13	0.008	730

The area of the flow of the 30mm gap = 0.03m^2 and the 50mm gap = 0.05m^2

The density of the air = 1.2kg/m^3

Apart from the fact that the mass flow rate was the same as a result of the separation increase, the average cooling decreased as the cavity width increased. In the 160mm cavity, it was 124W/m and increased to 200W/m as the width decreased to 100mm. This increase of cooling was probably due to the increase of the outlet air velocity from 0.18m/s of the 160mm cavity to 0.27m/s of the 100mm one.

In the 160mm cavity, the great drop in the air velocity with the 50mm central gap (half that of the 50mm inner and outer gaps and about quarter that with the 30mm central gap of the 100mm cavity width) shows the importance of visualising the air flow.

5.4.4.5.2 Flow visualisation of the 160mm cavity

- Verification of air velocity measurements.

To study the possibility of error of air velocity measurements, smoke tests were carried out. Smoke was injected into the air at the top of the cavity. A video recorder was used. Measured smoke speeds were compared with those of the hot-wire anemometer. The point where the smoke flow started was marked and at a known distance another point was also marked so that the distance between them could easily be determined. The time in which a smoke curl would take to travel between two points was recorded. The results of both smoke and the hot-wire anemometer measurements are given in Table 5.16. The results in Table 5.16 show that smoke and the hot-wire anemometer reading were nearly agreed.

**Table 5.16 Verification of measured air velocity with smoke
in the 50mm central gap of the 160mm cavity.**

Number of test	Distance between points m	Time recorded s	Velocity (from smoke) m/s	Average air velocity m/s	Hot-wire anemometer m/s
1	0.17	1.97	0.086	0.08±0.01	0.075±0.002
	0.17	2.80	0.061		
	0.17	1.88	0.090		
2	0.17	1.87	0.091	0.09±0.004	
	0.17	1.27	0.096		
	0.17	2.02	0.084		
3	0.090	1.10	0.082	0.085±0.002	
	0.090	1.03	0.087		
	0.090	1.03	0.086		
Overall av.				0.085±0.008	

- Air flow pattern

The smoke in Figure 5.23 shows that when the air passed over a wet mat exposed in the 50mm central gap it was flowing stably. As it passed the top edge of the wet mat, it started to waver. The smoke pattern shows that the flow is neither laminar nor turbulent but 'transitional' (Figure 5.23). Calculated Reynolds number (based on the measured air velocity 0.075m/s) in both central gap (30mm and 50mm) show that air flow was laminar (about 430, Table 5.15); much below 2000. Smoke patterns demonstrate that the flow is transitional. According to Rouse (1946) it could be at a low degree of turbulence. This highlighted the contradiction between the calculated Reynolds number and the nature of the flow shown by smoke. This established the irrelevance of applying Reynolds number to determine the nature of the air flow in the 160mm cavity.

The use of Raleigh number Ra ($G_T P_T$) to resolve the nature of the flow showed that it was 3.4×10^9 . This is slightly greater than the upper transitional limit $Ra > (10^9)$ given by Wong (1977) and that of $Ra > (10^8)$ by ASHRAE (1986). Calculated Raleigh numbers are given in Table 5.17. This confirms that the flow was approaching a low degree of turbulence (Pittes 1987).

Figure 5.24 shows the upward movement of some smoke as it departs from the wet mat are encountered with the other wet mat forming the central gap and encouraged abruptly to leave from the direction of the downward flow.

Stoecker (1982) indicates that the reverse movement of the smoke might produce losses in the kinetic energy and hence lower air velocity. The drop in air velocity of the 50mm central gap was probably related to the decrease of the flow as it converged with the wet surface (1982 and Rouse1946). Such discontinuity produces separation of the flow from the saturated boundaries. The upward movement of some smoke after departing from the wet mat and encountered with the other wet surface of the mat in the central gap may be responsible for the reverse movement from the incoming air flow (1982). This confirms that due to reverse and non-uniform flow, the Reynolds number is irrelevant. The considerable increase in the air velocity in the 30mm central gap with the 100mm cavity compared with that of the 50mm may be because:

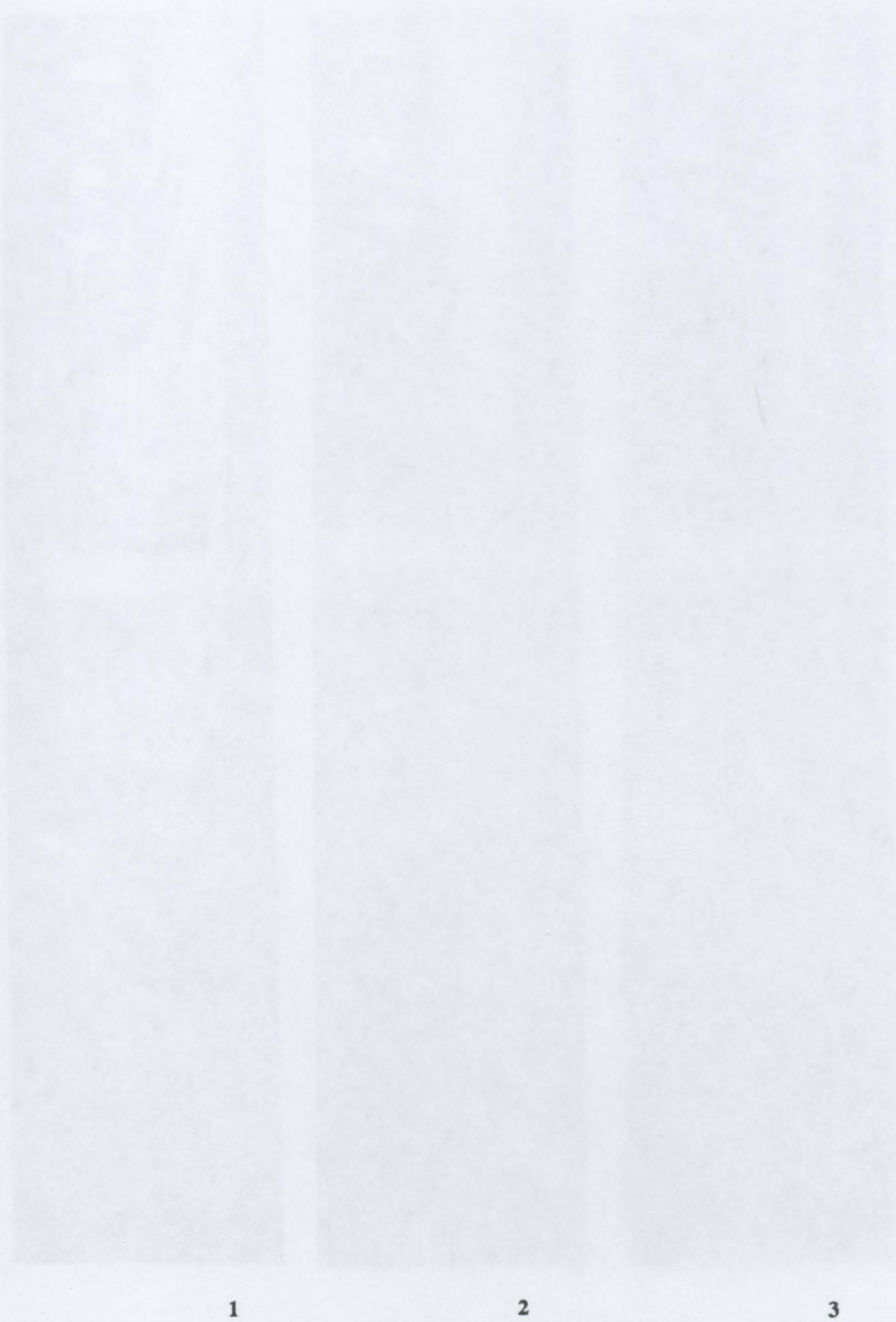
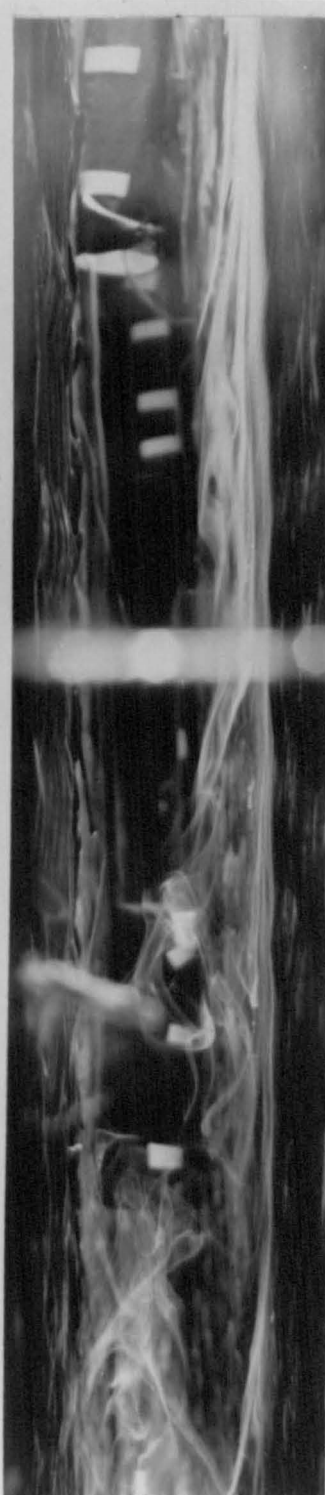
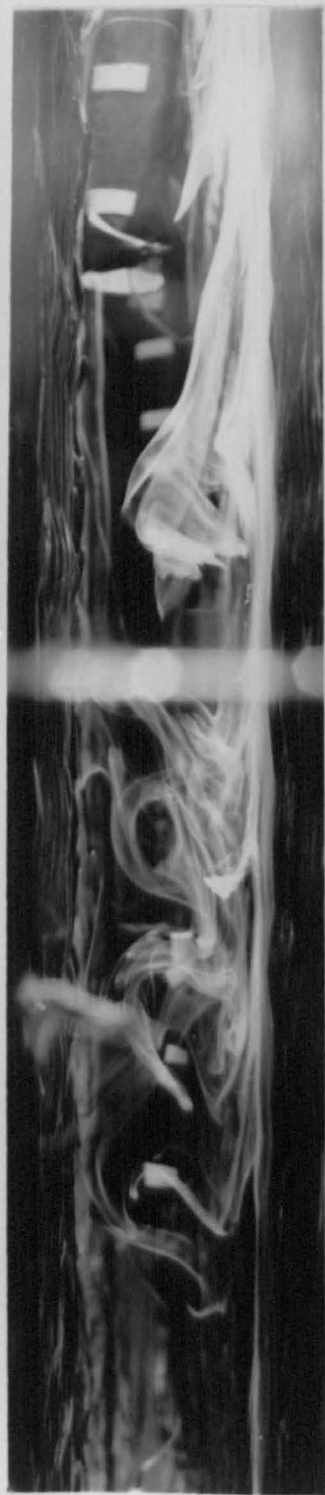


Figure 5.23 Air flow in the 50mm central gap of the 160mm cavity.



Figure 5.23 Air flow in the 50mm central gap of the 160mm cavity.



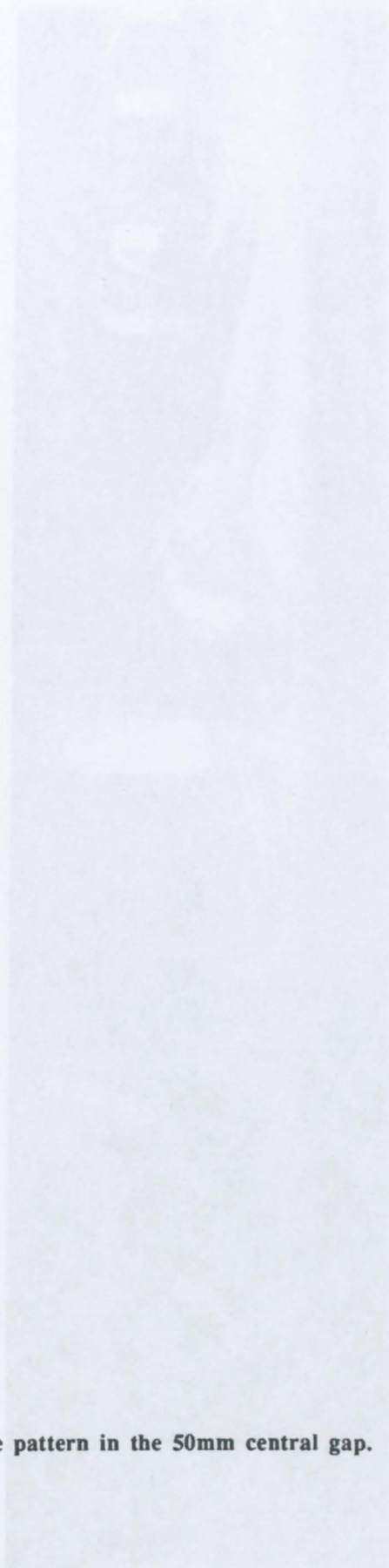


Figure 5.24 Smoke pattern in the 50mm central gap. (mean air velocity 0.085m/s)

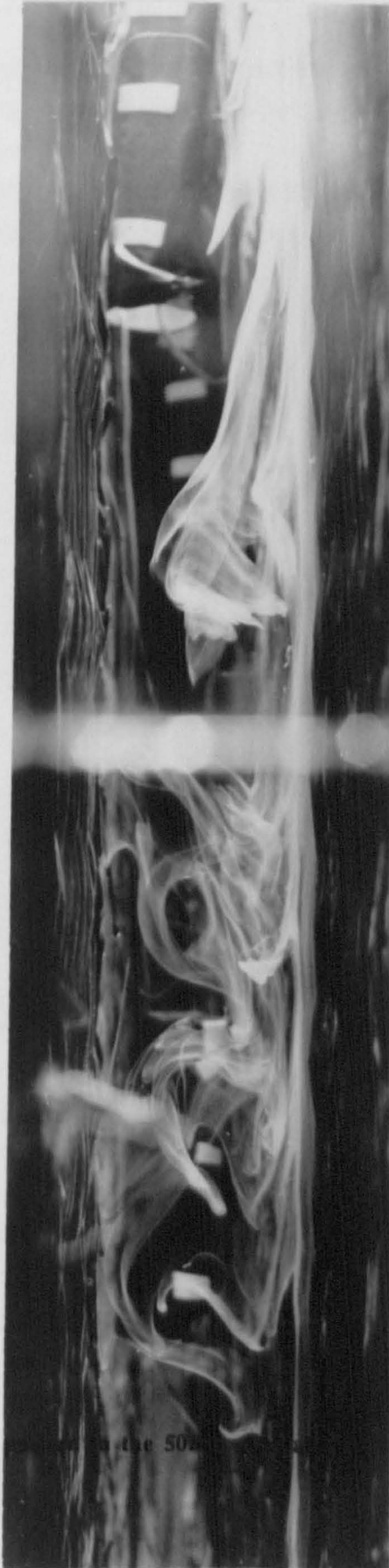
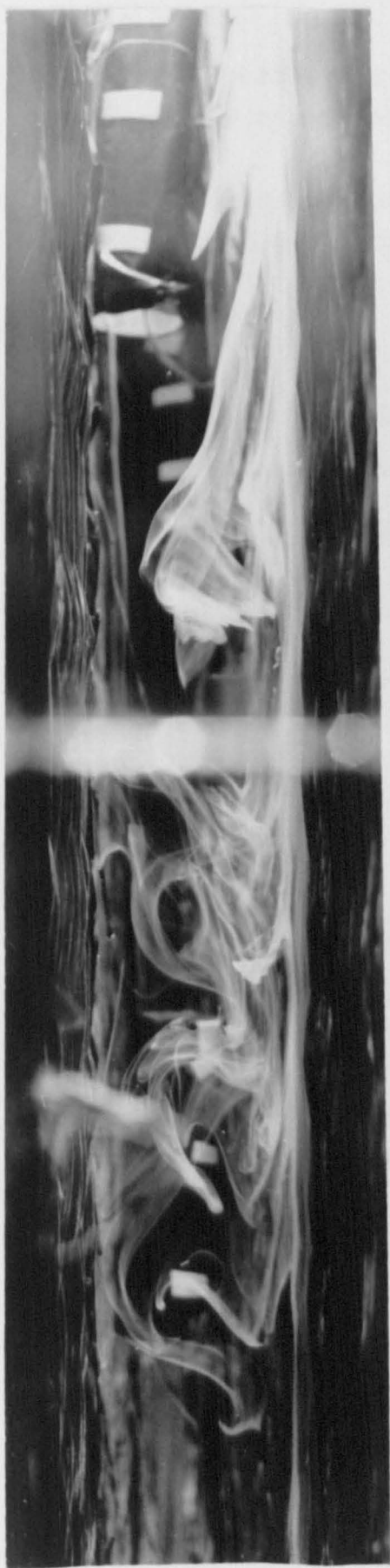


Figure 5.24 Smoke

at the 50cm

(mean air velocity 0.085m/s)

6



- the increased air temperature difference between the wet surface and the surrounding air by 4K increases the convective heat transfer and hence the evaporation eqn. 3.24;
- the decrease of the separation between the wet mats may reduce the separation between the saturated boundaries and diminish the reverse flow.

Table 5.17 Calculated Raleigh number of the 160mm cavity.

Cavity width	cavity location	Ave. inlet air temperature	Ave. surface temperature		Ave. temp. difference	Raleigh number
mm	-	°C	mat °C	wall °C	ΔT K	$R_a = \frac{G}{L} P_r$
50	Outlet	19	14	18	3	2×10^9
50	Central	19	15	-	4	3.4×10^9
50	Inlet	19	14.5	19	2.25	2×10^9

$$R_a = [(\beta g \rho^2 \Delta T L^3) / \mu^2]$$

$$P_r \text{ for air} = 0.72$$

$$L = 2m$$

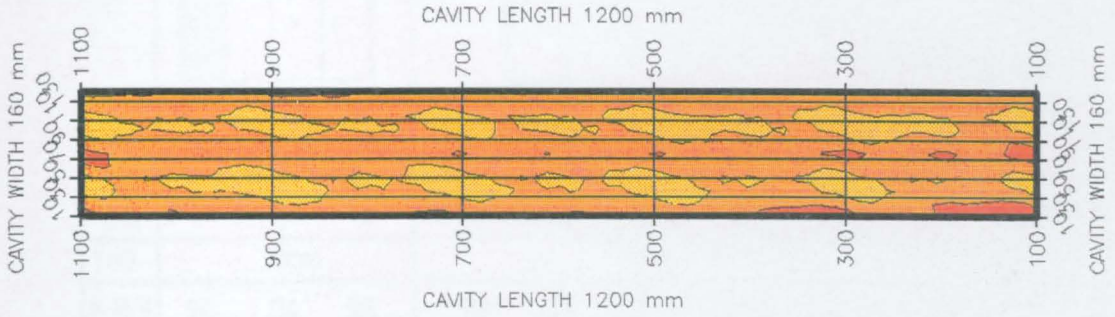
5.4.4.5.3 Air relative humidity distribution

The above results suggest that the relative humidity may give better understanding of the changes in air velocity. Two tests were carried out as above (Figure 5.21). Measurements were made simultaneously with that of the air velocity.

Analysis of the data shows that in the 100mm cavity the relative humidity was 10% less than with the 160mm cavity. Figure 5.25 shows the air relative humidity as function of the wet mats separation. Figure 5.25 a shows that in the 100mm cavity the relative humidity in the central gap is higher than that of the inner and the outer gaps. In the 160mm cavity, air relative humidity was about the same in all gaps of 50mm (Figure 5.25 b). The average relative humidities of both cavity widths are given in Table 5.18.

FIG 5.25.a Mean Air Relative Humidity in each Gap 86, 95, 86 %

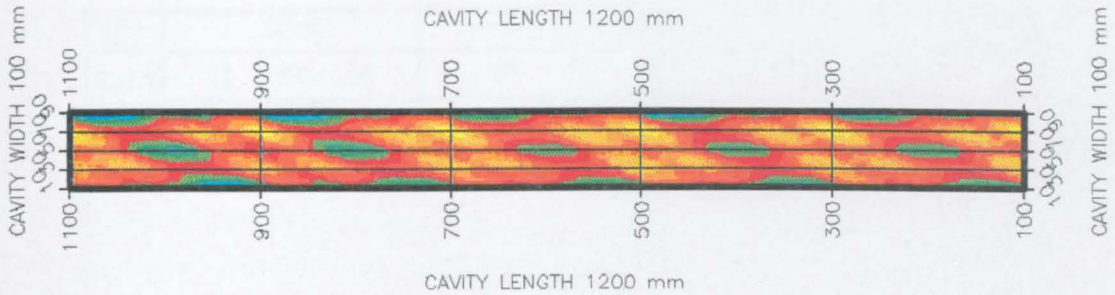
The wet surfaces are 50 mm from the dry walls



Section A-A

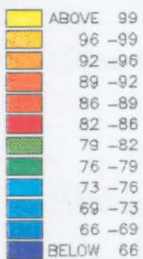
FIG 5.25.b Mean Air Relative Humidity in each Gap 80, 96, 81 %

The wet surfaces are 30 mm from the dry walls



Section B-B

R.H. %



Number of wet surfaces = 2

Inlet height = 2 Outlet height = 200 mm

FIG 5.25.a

Wet surface spacing 50, 50, 50 mm

Air temperature 20 C and its R.H. 67 %

FIG 5.25.b

Wet surface spacing 30, 30, 30 mm

Air temperature 21 C and its R.H. 61 %

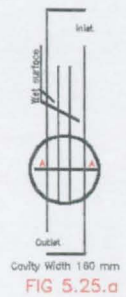
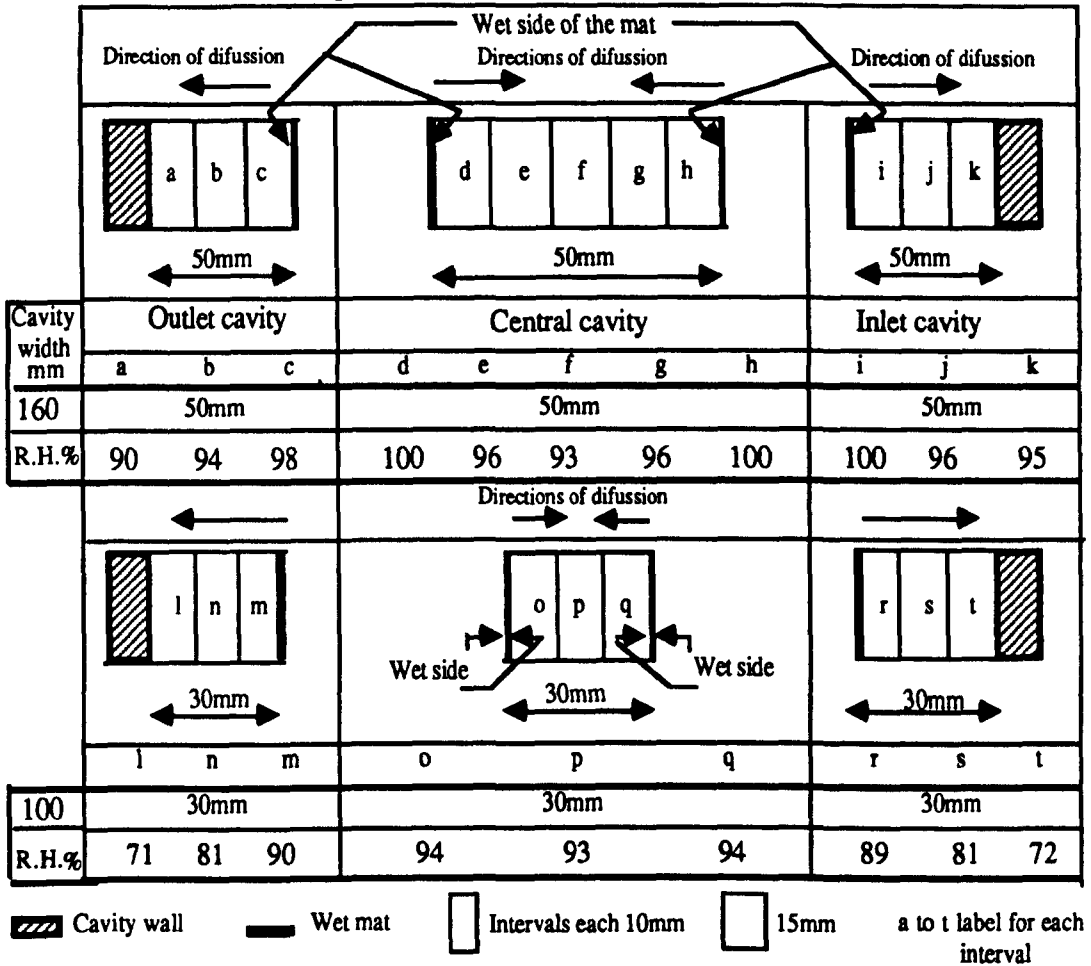


FIG 5.25 Air Relative Humidity Distribution at Different Cavity Widths

Table 5.18 Average air relative humidity distribution.



The tests show that average air relative humidity in the cavity was greater with the 160mm width than with the 100mm width.

The above suggests that the best cavity to provide cooling by evaporation is a 100mm wide divided by two wet mats (giving four areas of evaporation) into three equal gaps of 30mm thus allowing twice 5mm for the thickness of the mats with an outlet height of 100mm and an inlet of 200mm.

5.4.5 Measured cooling as function of time, or 'cavity life'

It is important to estimate the period for which the wet surface remains sufficiently wet for satisfactory cooling. The cavity was divided into three small gaps as above and two tests were carried out. The inlet air temperature and relative humidity were 18°C and 66%. The test was continued for 48 hours.

Observation shows that the drop in cooling was little in the first 24 hours, compared with that of the next 24 hours (Figure 5.26). It was initially 175W/m and decreased to 155W/m after 24 hours. Cooling falls steadily by about 0.08%/h.

A study of the humidity difference was carried out to explain the decrease of cooling with time. The humidity was calculated as mentioned above. The maximum change of the humidity ratio with time at the 100mm cavity was 0.00023kg/kg (nearly equal to that shown in Figure 5.14).

The calculated amount of water removed over 24 hours (time of the test) using eqn.5.2 was about 0.3kg/m, 0.013kg/hm (based on a mass air flow rate in the cavity of 0.011kg/sm). This amount of removed water from the wet mats caused the cooling to decrease by about 20W/m. The decrease of 11% in the rate of cooling is small, but not negligible if the rate of cooling is needed for much longer.

This suggests that the cooling over a period of 24 hours was satisfactory and may be acceptable for a further 24 hours, without re-wetting. It also indicates that the amount of water required for 24 hours cooling is small.

For a longer 'life', the humidity ratio difference (Δg) required to provide satisfactory cooling from evaporation per hour can be found from the linear equation obtained from:

$$10^{-3} \Delta g = a - 0.01 b t \quad \text{kg w.v./kg}_{\text{dry air}} \quad [5.3]$$

where a and b are constants (1.11kg/kg and 5.8 kg/kg respectively) from the fitted line of regression at 95% confidence limit which yields a regression coefficient R_c 0.92, and t is the time required for cooling

5.4.6 The effect of inlet air temperature on cooling

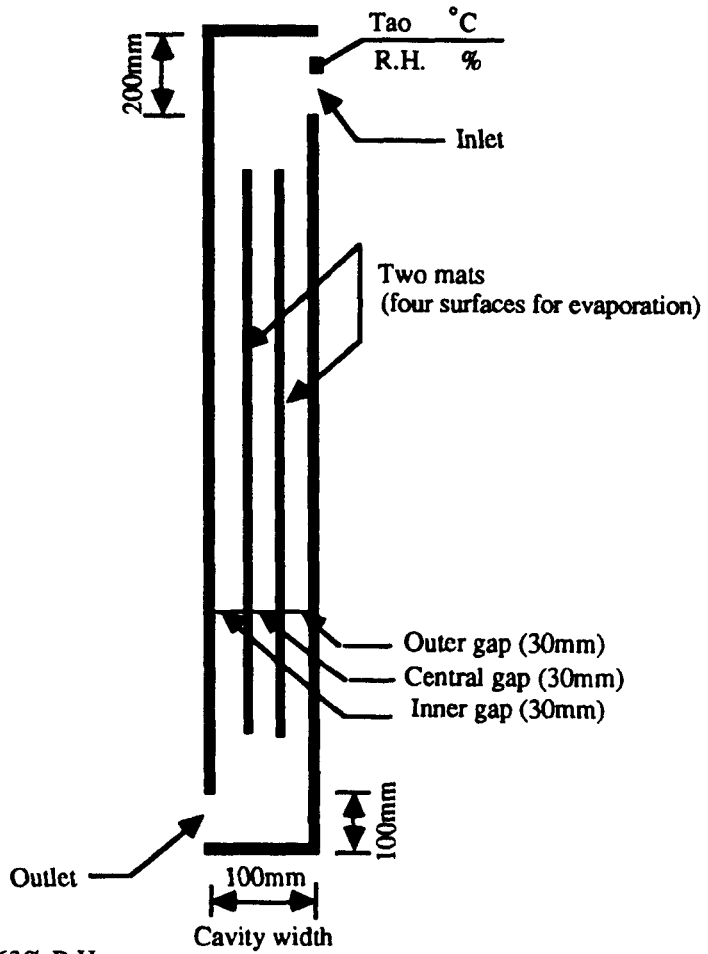
Two tests were carried out to investigate the effect of the inlet air temperature at the cavity on cooling by buoyancy. The environment within the laboratory restricted the range of the air temperature variation so that these tests were carried out with two inlet air temperatures: 19°C and 17°C; air relative humidity 63% and 56%. Arrangements of the tests are shown in Figure 5.27. They were also carried out under two conditions: with small temperature difference between the air at the inlet and that in the room attached to the cavity.

Figure 5.28 shows that with little temperature difference, the cooling increased as the outside air temperature increased. The average cooling was 125W/m (Test [2], Figure 5.27) and increased to 175W/m (Test [1], Figure 5.27). It also shows that the average cooling increased as the difference in air temperature between cavity inlet and the room increased. Although the temperature difference between the air at the inlet and that in the room increased, the cooling was constant at temperature difference of 9K and above.

The convective current between the air in the room and that at the outlet may result in an increase of the temperature of the air at the outlet, and therefore causes the temperature difference of the air between inlet and outlet to be less.

This suggests that cooling from evaporation could be promoted by about 50W/m (40% of test [2]) when the temperature of the air at the inlet increased by 2K. If the difference in temperature between the air in the room and that outside was 4K (Figure 5.28). This could be explained by the increase of the temperature difference between the wet surface and the air outside.

The above suggests that cooling by evaporation could be achieved by using two vertical wet mats inside a cavity (1000mm long, 100mm wide and 2200mm high) separated by 30mm. Evaporation could be promoted when a temperature difference of 5K between the wet surface and the air outside is provided. A mass flow of about 0.033kg/s could be achieved with an average air velocity of the order of 0.30m/s.



Test [1] $T_{ao} = 19^{\circ}\text{C}$ and 63% R.H.

Test [2] $T_{ao} = 17^{\circ}\text{C}$ and 65% R.H.

Figure 5.27 Arrangement of cavity for tests [1] and [2].

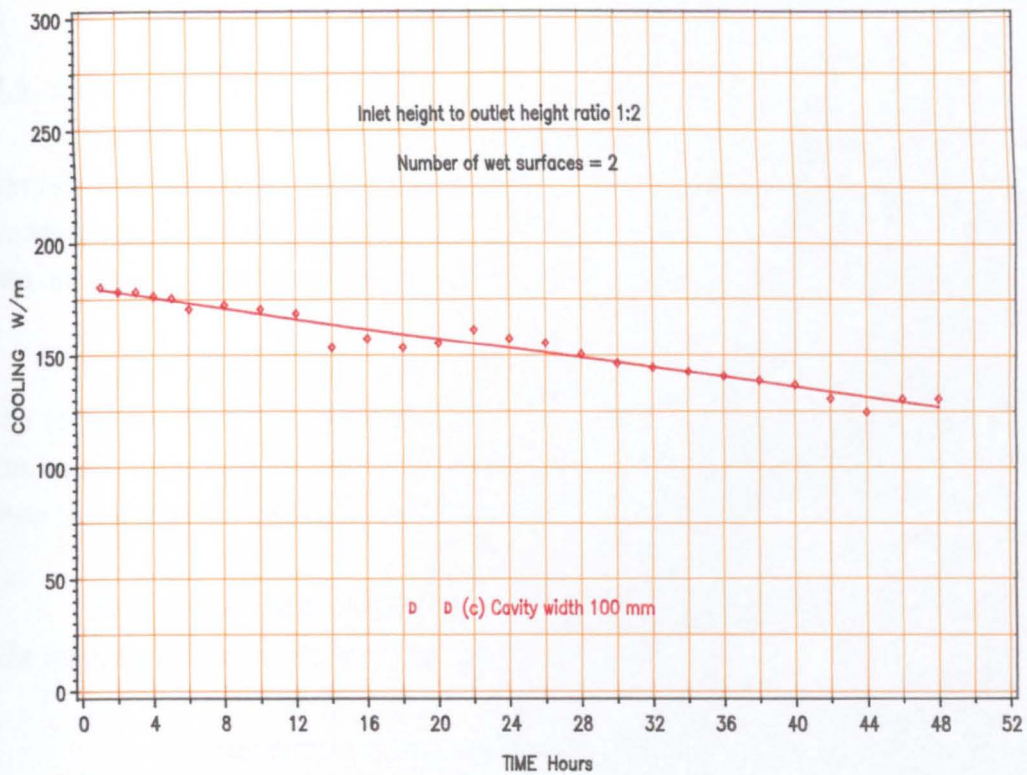


FIG 5.26 The effect of time on cooling

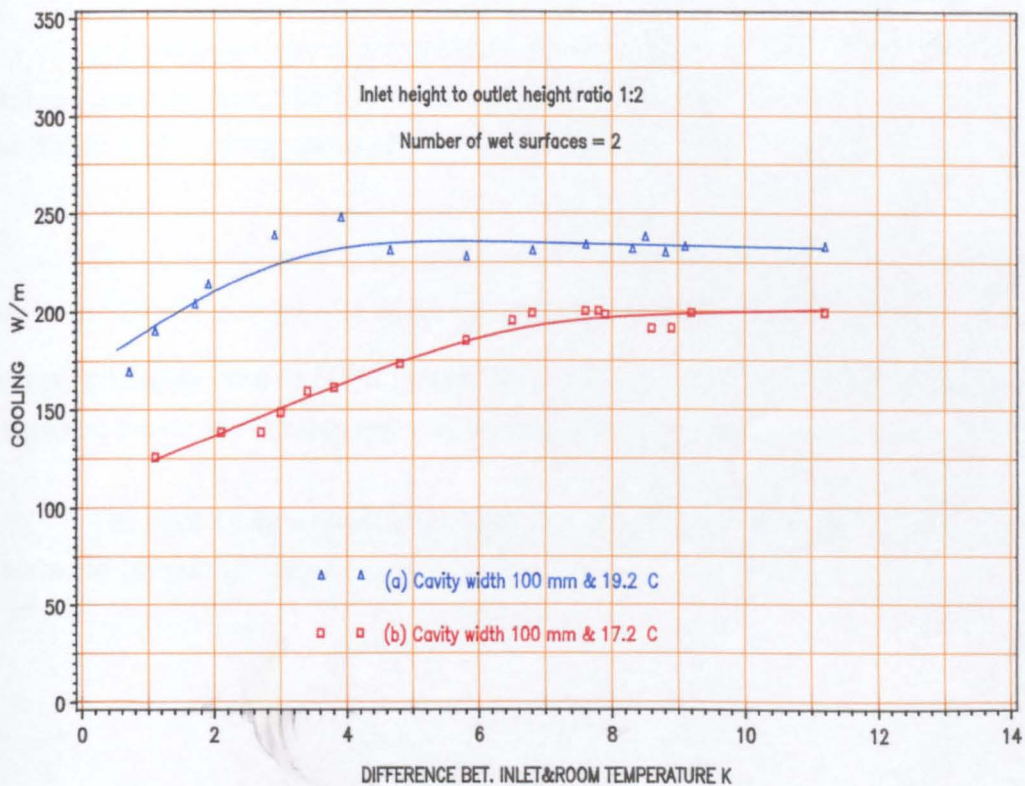


FIG 5.28 The effect of inlet air temperature on cooling

5.5 TESTS OF GROUP TWO

The obtained optimum width of the cavity to promote cooling was chosen for a further investigation. As before, parameters were investigated when there was no temperature difference between the air in the room and that at the cavity inlet. The cavity was studied in relation to a room, 3.6m long 2.1m wide 2300mm high (Figure 5.29).

In practice, the cavity would be usually on the shaded side of a dwelling (where the air temperature is lower than that of the sunlit side). Because of the heat flow from the sunlit walls into the room, the temperature of the air in the room would be higher than that at the inlet (specially in the afternoon).

To study the effect of varying the air temperature in the room in relation to that at the inlet, the following parameters were investigated:

- air temperature drop between the inlet and outlet as a result of evaporation
- air velocity at the outlet
- relative humidity at the outlet
- cooling and ventilation rates.

The optimum size of the cavity (100mm) studied in tests of group one was used for the investigation. The 80mm cavity was also included. The variables used are given in Table 5.19. Arrangements of the tests are shown in Figure 5.30.

The air temperature at the inlet (17°C to 19°C) and relative humidity (60% to 65%) were used most, being those in the laboratory (Figure 5.30). The air temperature in the room gradually rose to 30°C (when the outlet was shut), and temperature difference between the air in the room and that outside was up to 11K.

The cooling as a result of evaporation was calculated as above. Results of these tests are presented below.

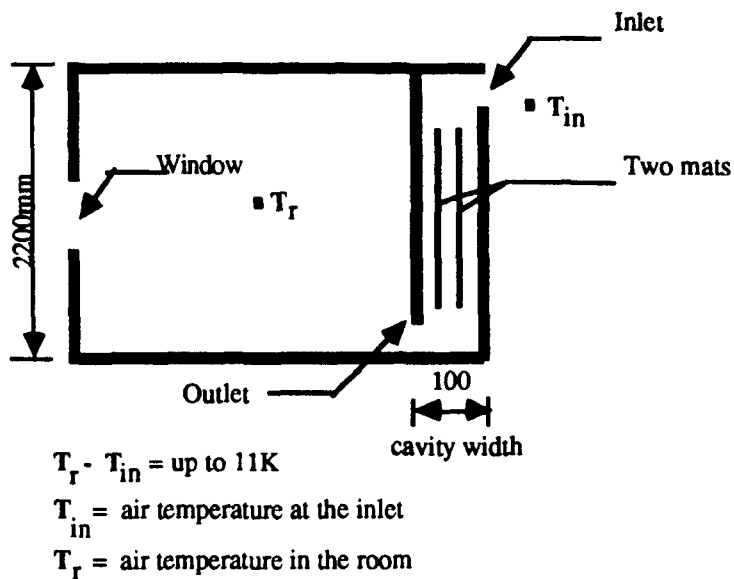


Figure 5.29 Vertical section through the cavity attached to the room.

Table 5.19 Variables input used in the study.

Variable parameters				
Cavity width	Separation between mats	Inlet air temperature	Inlet air relative humidity	Temperature difference between air in room & inlet
mm	mm	°C	%	K
100	30	17	60 to 65	0.2
80	40	19		2.0
	20	21		4.0
				6.0
				8.0
				10.0

Mat temperature in all tests was 15 to 16°C

Outlet height was 100mm

Inlet height was 200mm

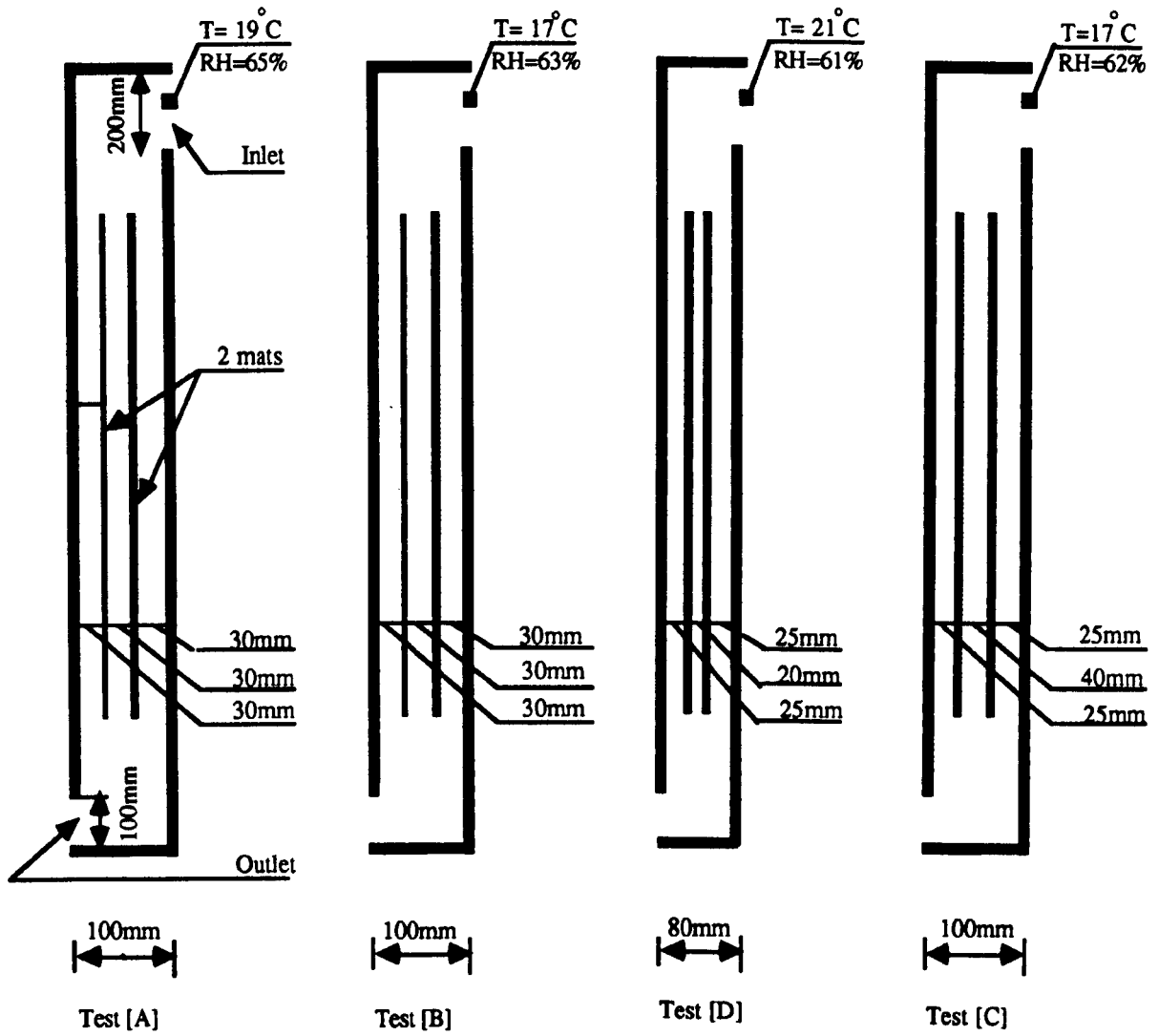


Figure 5.30 Arrangements for cavity of tests A, B, C and D.

5.6 RESULTS

5.6.1 The effect of the temperature difference between the air in room and that at the inlet on air temperature drop from evaporation

Four tests A, B, C and D were carried out to study the effect of the temperature difference between the air in the room and that at the cavity inlet on air temperature drop from evaporation (Figure 5.30).

In all the tests, the temperature drop between air at the inlet and that at the outlet as a result of evaporation decreased as the temperature difference between the air in the room and that at the inlet increased. Test A (Figure 5.31) shows that as the temperature difference between the air in room and that at inlet increased up to 6K, the air temperature drop between the inlet and outlet decreased by about a quarter (4.4K to 3.4K). A further increase of 5K only contributed to an air temperature drop of about 0.5K (Figure 5.31). This was probably due to the small increase of the outlet air temperature despite the large increase of air temperature difference between the room and the inlet. Test A also shows that when the temperature difference increased by about 6K, the outlet air temperature only increased by 0.5K (Figure 5.34). Test B had almost the same result as test A, but with little change. Tests C and D had the same results (Figure 5.31), and therefore suggests that an increase of the temperature difference between the air in room (25°C) and that at the inlet (19°C) beyond 6K was advantageous.

5.6.2 The effect of the temperature difference between the air in the room and that at the inlet on the outlet air velocity

The same group of tests was carried out as above. Figure 5.32 shows how the outlet air velocity varied with the temperature difference between air in the room and that at the inlet. The outlet air velocity increased substantially as the temperature difference between the air in the room and that at the inlet increased.

The outlet air velocity of test A and B was initially 0.27m/s (at a temperature difference between the air in the room and that at the inlet of about 1K) and nearly doubled to 0.5m/s and 0.6m/s respectively, when above temperature difference was raised to 10K (Figure 5.32). The study shows that increases beyond the 6K of test A were ineffective.

The increase of the outlet air velocity of test D was smaller (from 0.25m/s to 0.32m/s) in relation to the temperature difference increase of 6K. The results of tests A and B was better than those of C and D.

This suggests that the temperature difference of 6K between the air in the room and that at the inlet significantly increased outlet air velocity.

5.6.3 The effect of the temperature difference between the air in the room and that at the inlet on the outlet air relative humidity

Figure 5.33 shows the outlet air relative humidity as function of the temperature difference between the air in the room and at the inlet. The outlet air relative humidity in all tests decreased as the temperature difference increased (figure 5.33).

An increase up to 6K decreased the relative humidity from 86% to 79%. A further increase up to 11K only decreased it by about 10% (Figure 5.33, test A). It decreased by 9% (86% to 77%) in test B and remained constant. This was probably due to the small increase in the measured outlet air temperature (Figure 5.34). Test C showed the same except that the outlet air relative humidity was higher than that of tests A and B.

This suggests that the drop in outlet air relative humidity as a result of the increase in the temperature difference between the air in the room and the inlet was disadvantageous if the relative humidity is the most important parameter in assessing thermal comfort.

5.6.4 The effect of the temperature difference between the air in the room and that at the inlet on cooling

Four tests were carried out to investigate the effect of the temperature difference on cooling as above. The cooling was determined as mentioned above.

Cooling increased in all tests when the temperature difference between the air in the room and that at the inlet increased. Cooling increased considerably with an increase of up to 4 K (tests C and D) and up to 8K (tests A and B) then remained constant

(Figure 5.35). The cooling was initially 175W/m in test A (at a difference of 0.5K). As air temperature difference increased up to 4K, the cooling increased by nearly half. Although the temperature difference was then gradually increased, the cooling remained constant (Figure 5.34). The cooling of test A was more than those of tests B, C and D (Figure 5.34). Average cooling of all tests are given in Table 5.20.

Table 5.20 Average cooling at different temperature differences.

	Test	Cavity width mm	Temperature difference between air in the room and at inlet				
			K				
			up to 1	4	6	8	10
Cooling W/m	A	100	175	240	230	225	225
	B	100	140	175	190	200	195
	C	100	110	175	175	175	175
	D	80	120	150	150	150	150

The increase of cooling is related to the large increase of the outlet air velocity which nearly doubled from 0.27m/s to 0.5m/s (Figure 5.32), while the drop in air temperature between the cavity inlet and the outlet decreased only by 1K as shown in Figure 5.31. This indicates that the increase in mass flow was sufficient to compensate for the slight drop in temperature.

Figure 5.34 shows that with a temperature difference between the air in the room and that at the cavity inlet greater than 4K, the increase of outlet air temperature in determining the cooling was more significant than that of the outlet air velocity.

The investigation suggests that an increase of the air temperature difference between the room and the inlet beyond 5K was disadvantageous.

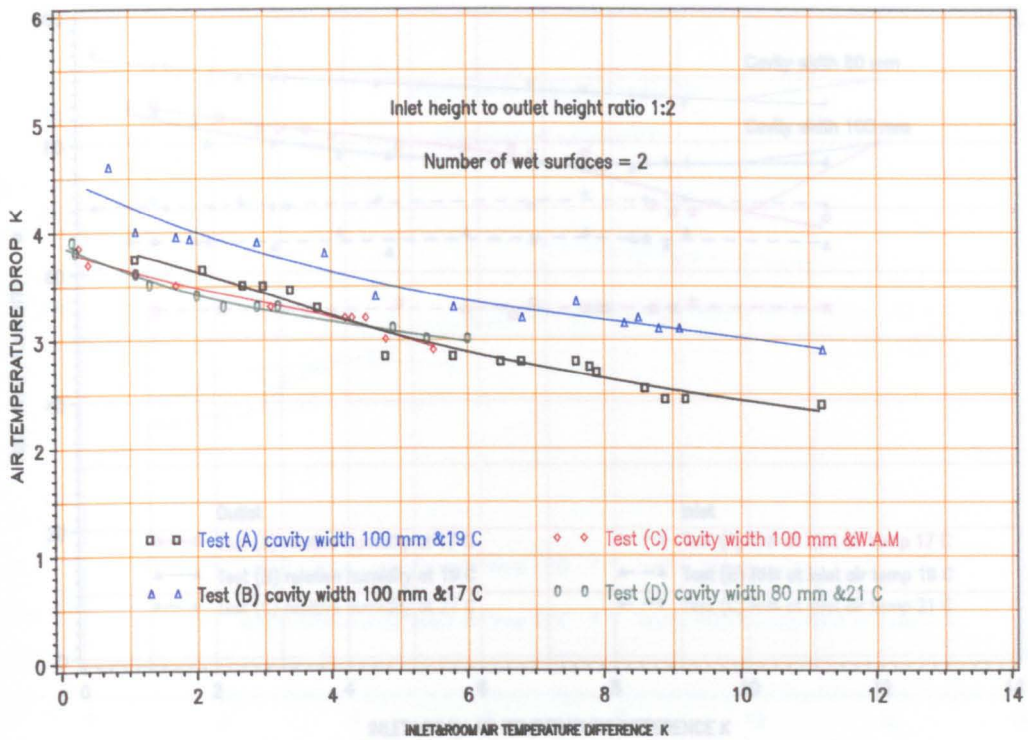


Figure 5.31 The effect of room air temperature on air temperature difference between the cavity inlet and outlet

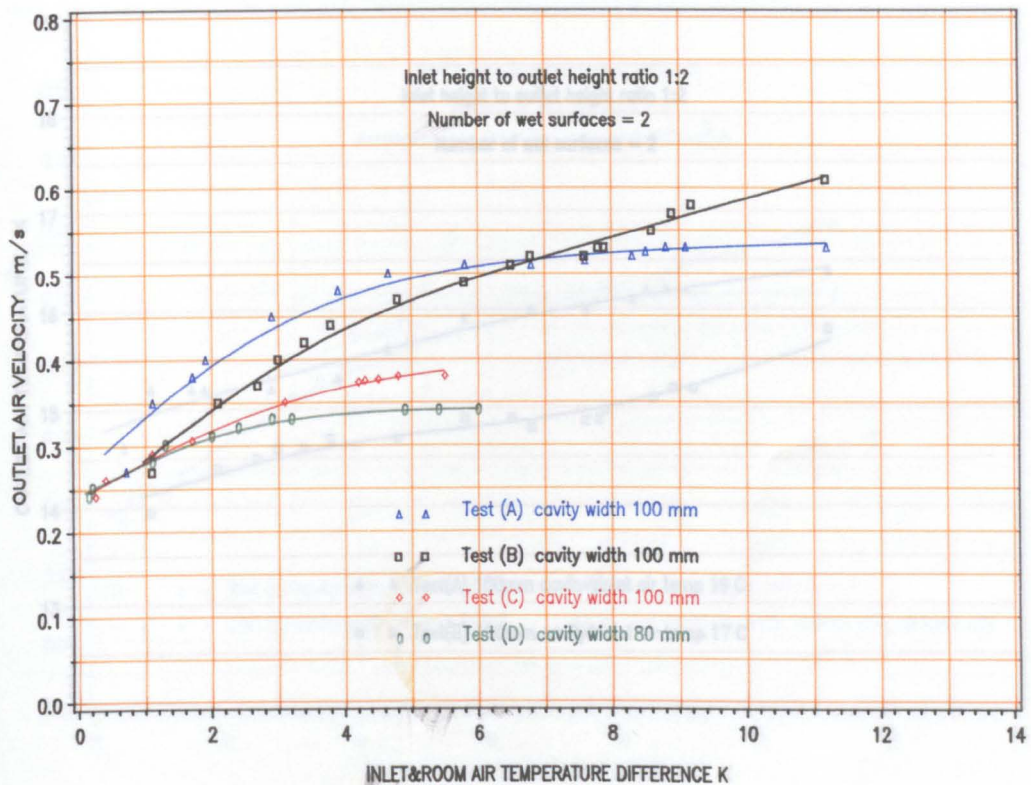


Figure 5.32 The effect of room air temperature on outlet air velocity

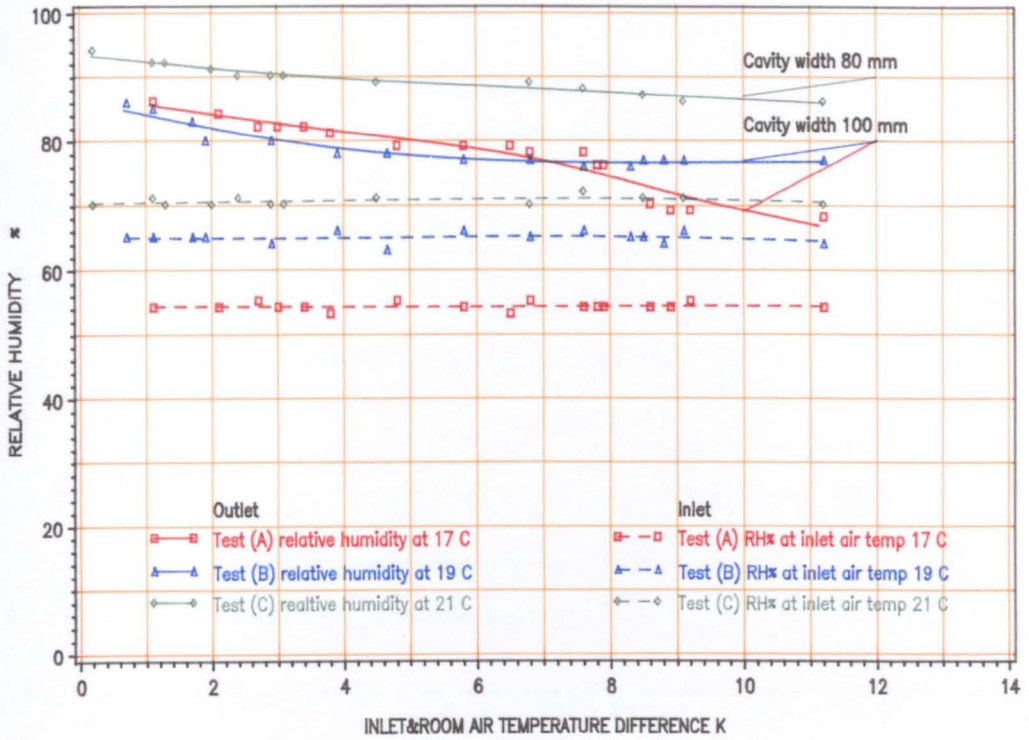


Fig 5.33 The effect of room air temperature on outlet air relative humidity

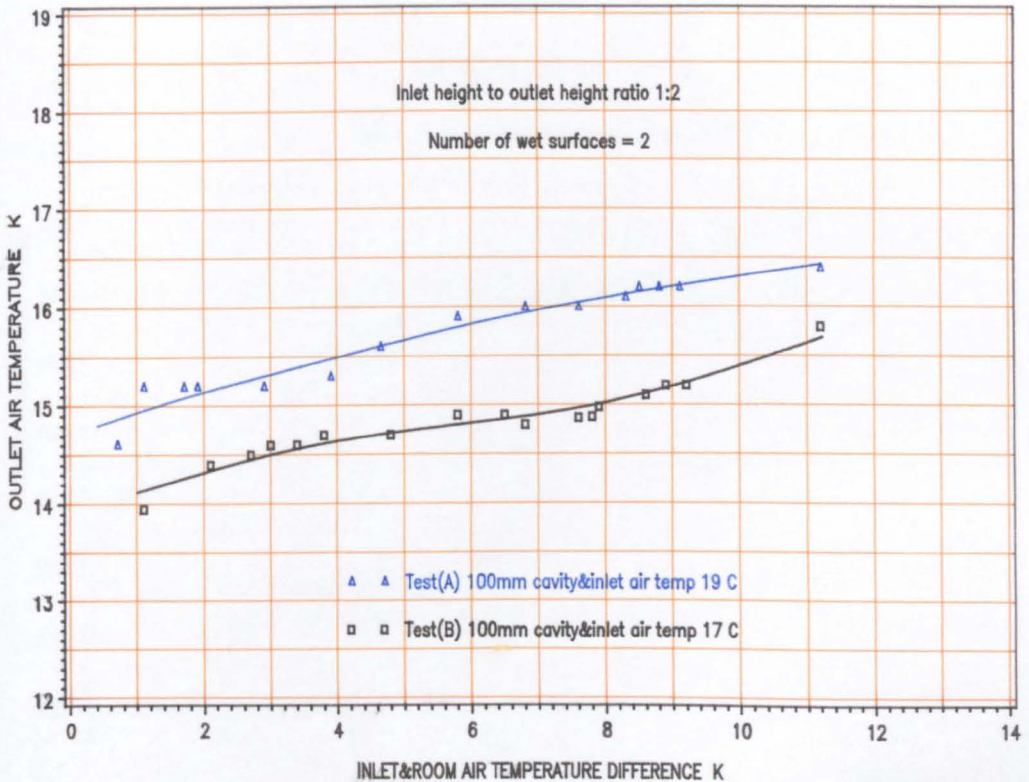


Fig 5.34 The effect of room air temperature on outlet air temperature

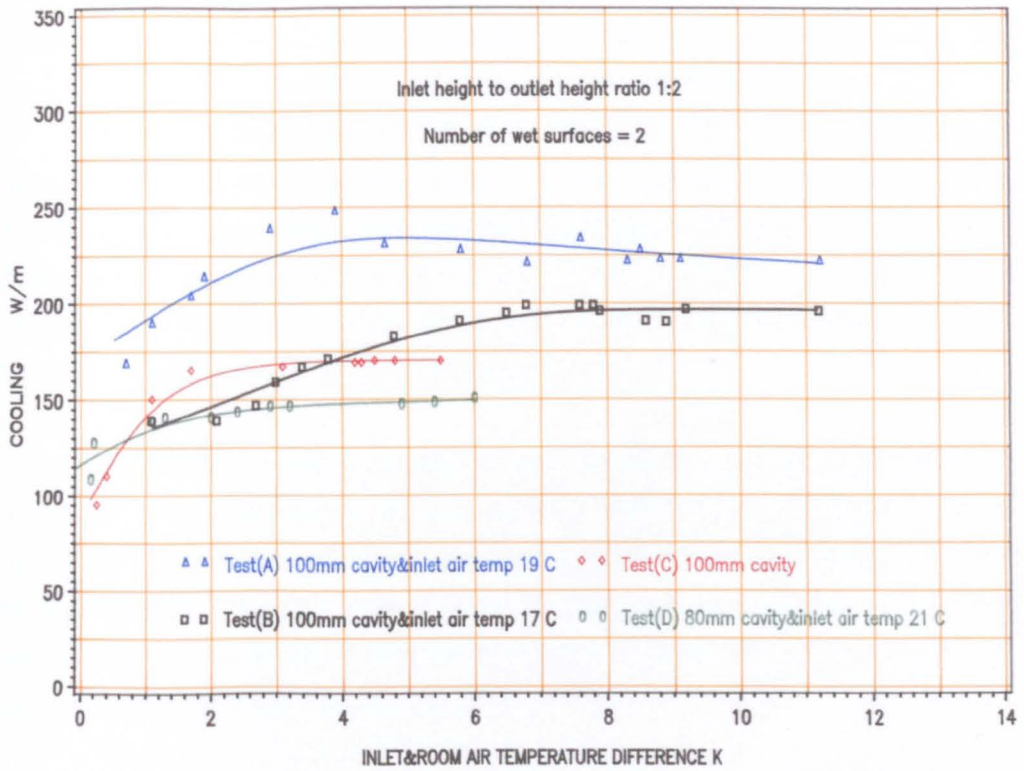


Figure 5.35 The effect of room air temperature on cooling

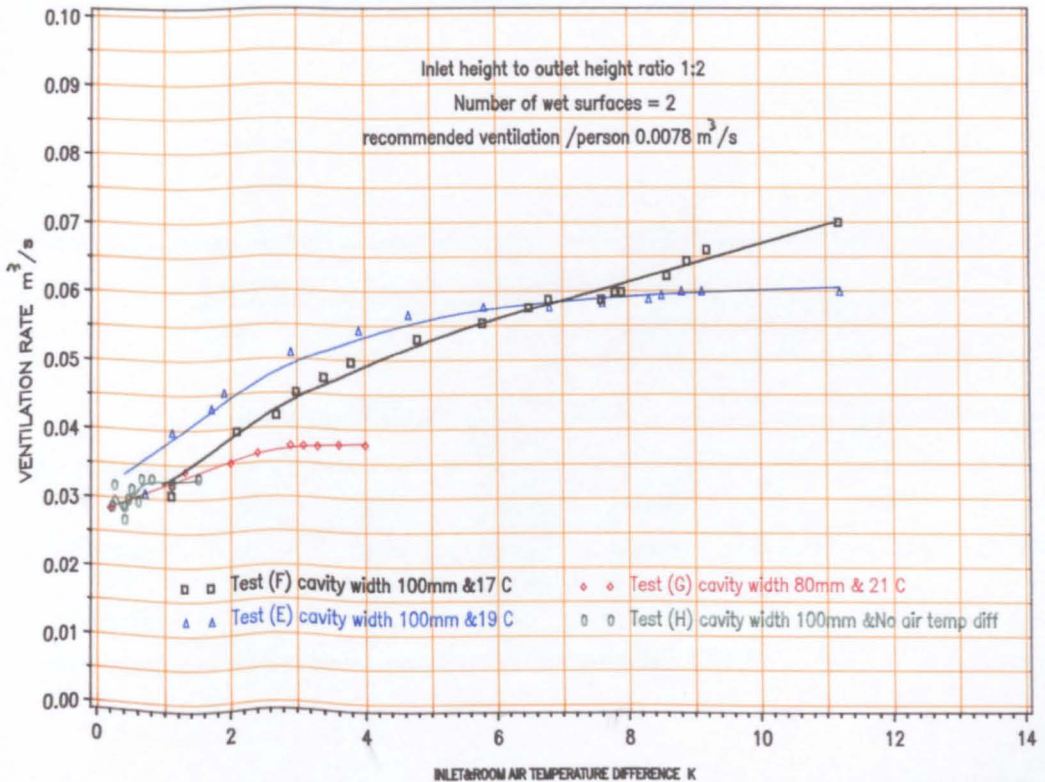


Figure 5.36 The effect of room air temperature on ventilation rate

5.6.5 The effect of the temperature difference between the air in the room and that at the inlet on the ventilation rate

The significance of air temperature difference between the room and the cavity inlet on the ventilation rate was determined by multiplying the outlet air velocity m/s by the flow area at the outlet m². Four tests were carried out (E, F, G, and H) under the same conditions as above, except that in test H there was no air temperature difference between the air in the room and that at the inlet. Ventilation rates are plotted against air temperature difference in Figure 5.36.

The ventilation rate increased as the temperature difference between the air in the room and at the inlet increased. It was nearly doubled in test E (from 31 L/s to 60 L/s) when the temperature difference gradually increased to 7K. Further increase to 11K hardly increased the ventilation at all. This indicated that an increase of air temperature difference beyond 7K was insignificant in promoting the ventilation rate; it is, therefore, of no advantage. Results of other tests are given in Table 5.21

The ventilation obtained from test H was 30 L/s (with no temperature difference between the air in room and that at the inlet) which is acceptable when compared with the recommended rate per person 8 L/s of ASHRAE (1986). This indicates that the performance of test E and F was satisfactory in promoting ventilation. Study of the ventilation effect on a room will be carried out in chapter eight.

Table 5.21 Measured ventilation rates at different temperature differences between the air in the room and that at the inlet.

Test	Cavity width mm	Temperature difference between air in the room and at inlet					
		up to 1	4	6	8	10	
Ventilation rate m ³ /s/m	E	100	0.032	0.050	0.056	0.063	0.070
	F	100	0.034	0.045	0.053	0.057	0.060
	G	100	0.027	0.035	0.035	—	—
	H	80	0.03	—	—	—	—

5.7 DISCUSSION AND CONCLUSION

5.7.1 Tests of group one

The study shows that cooling by buoyancy flow from evaporation could be increased as a result of decreasing the cavity width, which in turn, eliminates the separation between the two saturated boundary layers. Observation shows that air falls downwards by buoyancy as result of the buoyancy pressure caused by the difference in density between the cool air in the cavity and the warmer air outside. It also shows that separation from the wet mats of more than 30mm is ineffective in promoting more evaporation and thus cooling. For two parallel mats inside a cavity, the separation between them is recommended to be of the order of 30mm.

When the height of the outlet was equal to that of the inlet (200mm), air velocity distribution at the outlet was unsatisfactory. The use of an outlet height of 200mm introduced a disparity between air velocity at the top and bottom half of the outlet. The drop in the air velocity over the outlet height shows that the outlet height was important parameter in determining the average air velocity and thus the cooling. The cause is probably the abrupt change in flow direction and the enlargement of the air flow from the 100mm cavity width to the 200mm outlet height.

The decrease of the outlet height to 100mm reduced the differences in air velocity distribution.

The average relative humidity at the cavity outlet increased progressively with the reduction in cavity width. It increased with the 100mm cavity width by about 18% (from 70% to 88%). With the 300mm and 200mm cavities, the small increase of the outlet relative humidity shows the role of the mat separation on lowering the relative humidity. The moderate increase in the outlet relative humidity of the 100mm and 80mm tests was due to the convergence of the saturated boundary layers within the 30mm and 20mm central gaps.

The drop in air temperature between the inlet and the outlet increased as the cavity width was reduced. The reasons for this is that less "transfer" air, which the evaporation cannot reach, is flowing.

The reduction of the cavity widths from 300mm to 100mm shows that the outlet

air velocity is moderately increased to about 0.3m/s. This is related to the elimination of the still air zone between the two mats of central gap. A further small reduction of the cavity width to 80mm shows a drop in the outlet air velocity, and demonstrates that a reduction beyond 100mm is disadvantageous. This is related to the effect of the 20mm central cavity on the heat transfer mechanism which will be investigated in chapter seven.

The air velocity distribution of the 160mm cavity shows behaviour unprecedented in the 50mm central gap. This was first thought to be caused by surface roughness to the air flow. At the 100mm cavity width, the air velocity in the 30mm central gap would be expected to be about 0.13m/s. The measured value was 0.27m/s. It would be also foreseen that the reduction of central gap from 50mm to 30mm may increase pressure losses, causing resistance to the flow. However, the pressure drop in the 50mm central gap of 160mm cavity was less than that with the 30mm gap of the 100mm cavity.

The use of smoke enables us to trace the downward air movement by buoyancy and also to determine the nature of the flow. Calculated Reynolds number in both central gaps shows that the air flow was laminar, but smoke patterns demonstrate that the flow is transitional. The observation shows that the interpretation of the meaning of Reynolds number to determine the nature of the air flow must be done with care.

Although Raleigh number Ra to determine the nature of the flow was slightly greater (3.8×10^{10}) than that of $Ra > 10^9$ given by Wong (1977), and that of $Ra > 10^8$ by ASHRAE (1986), it showed a good agreement.

The drop in air velocity with the 50mm central gap was probably related to the decrease of the flow as it is converged with the wet surface. The upward movement of some smoke after departing from the wet mat is encountered with the parallel wet surface of the mat and encouraged abruptly to leave from the downward direction of the flow (Stoecker 1982). Because of the reverse flow, losses in kinetic energy may occur and therefore decreases velocity of air flow.

The considerable increase in the air velocity in the 30mm central gap of the 100mm cavity compared with that of the 50mm may be for two reasons:

- the increase of the air temperature difference between the wet surface and

the surrounding air increases the convective heat transfer eqn. 3.24.

-the decrease of the separation between the wet mats may reduce the separation between the saturated boundaries and diminish the reverse flow.

The cavity width should be 100mm to provide sufficient air flow, hence cooling. The relation between the cooling rate and the wet mats separation is linear. The small steady decrease of the cooling indicates that the performance of the 100mm cavity is satisfactory up to 24 hours. Continuation for another 24 hours could be acceptable.

The study suggests that best performance in terms of cooling and ventilation is that of the 100mm width be divided by two vertical mats (1550mm high) into three equal cavities (each 30mm). Evaporation could be achieved when the difference between the temperature of the wet mats and that of the air at the inlet is about 5K. If the cavity is 3000mm long and 2200mm high air temperature could be reduced by about 6K with mass flow rate of 0.11kg/s and air velocity of about 0.30m/s. This could result in cooling of about 700W and ventilation rate of about 0.1m³/s (100 L/s).

These values could be increased if the height of the cavity were higher. However, in practice it is limited to that of the dwelling. The measured ratio between the width D and the height of the cavity Z is given by:

$$Z / D = 20 \quad [5.4]$$

The relation between the mat height M_h and that of the cavity is given by:

$$M_h / Z = 0.7 \quad [5.5]$$

For a bigger cavity height of say 4000mm, the width of the cavity will be wider (of the order of 200mm) and the height of the mat will be higher (of the order of 2800mm).

Observation shows that for two parallel vertical wet mats (1550mm high), the relation between the saturated boundary layer and the height of the mat to promote sufficient evaporation for cooling could be found from:

$$b / M_h = 90 \times 10^{-4} \quad [5.6]$$

where

b = the thickness of the saturated layer

Evaporation will increase the relative humidity by about 20% when the relative humidity of the incoming air is about 70%. If the relative humidity at the inlet is like that in the hot dry climates (summer below 30%, Table 1.2), the above increase of the relative humidity will actually be much larger.

As stated above (chapter one), the bioclimatic analysis of Cairo suggests that an average moisture content of about 0.01 is needed in the air flowing through dwellings to bring the outside dry air to be comfortable. Cooling by evaporation with the 100mm cavity suggests that at incoming air temperature of 21°C and 60% relative humidity (0.0096), the increase of the moisture content in the air flow would be of the order of 0.0007 when air temperature fell by about 5K (0.0103). This result approaches the target suggested by the analysis, and considered to be acceptable.

When the mean air temperature in hot arid climates is about 30°C and 30% relative humidity (0.0082), a drop of the air temperature by 4K and an increase of the relative humidity to 80% are needed to reach the target (0.018). This is approximately equal to the result of the 100mm cavity. Nevertheless, the maximum target of moisture content in the air of 0.014 could be reached if the air is cooled by about 2K and relative humidity is increased to about 85%.

As was mentioned above in chapter one, comfort in a dwelling can be improved if air movement over the body is increased. CIBSE (1986) recommended a resultant temperature for thermal comfort in hot dry climates of the order of 28°C without air motion. Nicol (1975) shows that the resultant temperature could be higher at 32°C to 36°C with air movement of the order of 0.25m/s.

Measurements show that cooling by evaporation using a 100mm cavity wide can provide an outlet air velocity of the order of 0.27m/s, slightly higher than that given by Nicol (1975). Using eqn.1.4 as given by Nicol (1975), the resultant temperature T_{res} when air velocity in the room is about 0.1 to 0.15m/s can be found from:

$$T_{res} = 0.45 T_{mr} + 0.55 T_a \quad ^\circ C \quad [5.7]$$

The influence of the mean radiant temperature is reduced as the velocity of the air increased (eqn 5.7). Assuming the mean radiant temperature 37°C and outside air temperature 30°C, the resultant temperature in the room without 'evaporative cooling cavity' will be about 33°C. When an 'evaporative cooling cavity' is attached to the room, outside air temperature (say 32°C) could be reduced by about 6K to be of the order of 26°C. With the mean radiant temperature as above, the resultant temperature in the room will be of the order of 31°C. This is comfortable according to Nicol (1975).

5.7.2 Tests of group two

Observation shows that the performance of the cavity to promote cooling ventilation in dwellings could be improved when the air temperature in the room is higher than that of the inlet by about 6K. The cooling achieved with air temperature difference between the inlet and the room could be as large as 250W/m. This increase shows the importance of the outlet air velocity in relation to the other parameters such as: outlet air temperature and relative humidity as well as the drop in air temperature between the outlet and inlet.

The flow rate provided by the 100mm cavity is increased to 0.072kg/sm, and the relationship is well demonstrated by the quadratic relation between the outlet air velocity and the difference in air temperature between the room and the inlet (Figure 5.32).

Although this non-linearity showed the importance of outlet air temperature and relative humidity, these parameters were only important beyond an air temperature difference of 5K or more despite the continuing increase of the outlet air velocity. The significance of outlet air velocity to increase the cooling is related to a limited increase of air temperature difference of 5K between the room and the cavity inlet.

The constancy of cooling beyond 8K difference is related to the drop in air temperature between the inlet and the outlet which results from the convective current increase between the room and the outlet. This illustrates that an increase in the air temperature difference between the room and the inlet above 8K is insignificant.

The increase of the relative humidity at the outlet could be reduced if the temperature difference between the air in the room and that at the inlet is about 6K. This is because of the increase of the outlet air temperature which results from the convection current between the air at outlet and that in the room.

An increase of the inlet air temperature by 2K is significant in improving cooling. In a typical hot dry climate, this will be factor in increasing evaporation potential, reducing the air temperature in the room then the radiant temperature of the surrounding, hence improving comfort.

CHAPTER SIX

EVAPORATIVE COOLING BY FORCED AIR FLOW: RESULTS

6.1 INTRODUCTION

6.2 PRELIMINARY OBSERVATION

- 6.2.1 Air velocity distribution at the inlet
 6.2.2 Air flow across the cavity
 6.2.2.1 The effect of cavity width on air flow pattern

6.3 Evaporative cooling observations

6.4 RESULTS

- 6.4.1 The effect of wet mat number and their separation
 6.4.1.1 Air temperature drop
 6.4.1.2 Air relative humidity at the outlet
 6.4.1.3 Cooling

- 6.4.2 Outlet air velocity
 6.4.2.1 The effect of the outlet height on air flow
 6.4.2.2 The effect of the cavity width on air flow at the outlet
 6.4.3 Outlet air relative humidity
 6.4.4 Temperature drop
 6.4.4.1 The effect of the cavity width on air temperature drop between inlet and outlet.
 6.4.4.2 The effect of outlet height on air temperature drop
 6.4.5 Relative humidity
 6.4.5.1 The effect of the cavity width on air relative humidity
 6.4.5.2 The effect of the outlet height on air relative humidity
 6.4.6 Cooling
 6.4.6.1 The effect of the cavity width on cooling
 6.4.6.2 The effect of the outlet height on cooling

6.4.7 Further analysis

- 6.4.7.1 The 'humidity ratio difference'
 6.4.7.2 The effect of wet mat separation on the 'humidity ratio difference'
 6.4.7.3 The convective heat transfer coefficient

6.8 DISCUSSION AND CONCLUSION

CHAPTER SIX

EVAPORATIVE COOLING BY FORCED AIR FLOW: RESULTS

6.1 INTRODUCTION

The forced air flow apparatus described in Chapter Four was used to examine an 'evaporative cooling cavity' with downward forced air flow induced by a fan. Cooling resulting from evaporation was investigated using two flow rates and different cavity widths. Tests were carried out at the unsteady state. The air temperature drop between the inlet and outlet, and the increase in outlet air relative humidity were determined. Water removed by evaporation was assessed. Results are reported and discussed.

6.2 PRELIMINARY OBSERVATIONS

6.2.1 Air velocity distribution at the inlet

Preliminary tests were needed to check whether the air flow was distributed uniformly across the inlet and the cavity, and whether it was at the required velocity. Air velocities used in the tests were 0.18m/s and 0.37m/s (see Chapter Four). Air temperature and relative humidity were maintained at 30°C and 40%. The inlet (1140mm long x 250mm high) was divided into 30 equal rectangles (Figure 4.10). The air velocity measurements were carried out as described above (Chapter Four). The emissivity of the aluminium foil of the cavity wall near the inlet was 0.05. Tests were performed at the steady state, each test was run for at least 20 hours to ensure that a steady state was achieved.

Six tests were carried out: four tests with air velocity of 0.37m/s and the remaining with 0.18m/s. Some tests were also carried out at random to take into account the systematic and the random errors. Readings were recorded and averaged. Figure 6.1 and Figure 6.2 show the air velocity distribution across the inlet at 0.37m/s and 0.18m/s respectively. The variation of air velocity among different tests was $\pm 2\%$. The difference found with air velocity measurements ranged between $\pm 0.008\text{m/s}$ (Figures 6.1 and 6.2). As a result, required average air velocities across the inlet were confirmed experimentally, and they were fairly constant.

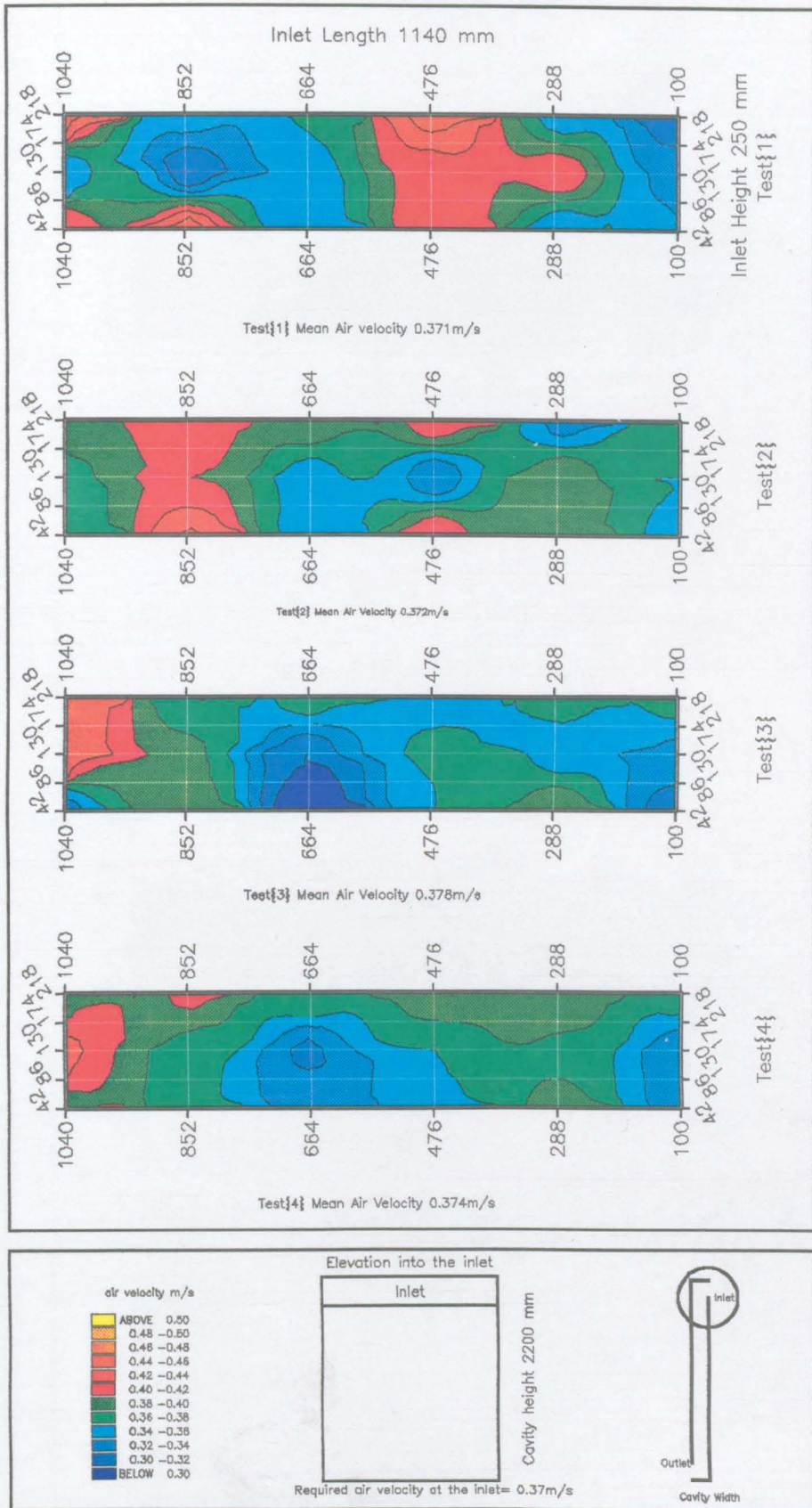


FIG 6.1 Measured air velocity distribution at the cavity inlet

Inlet air temperature 30 C and relative humidity 40%

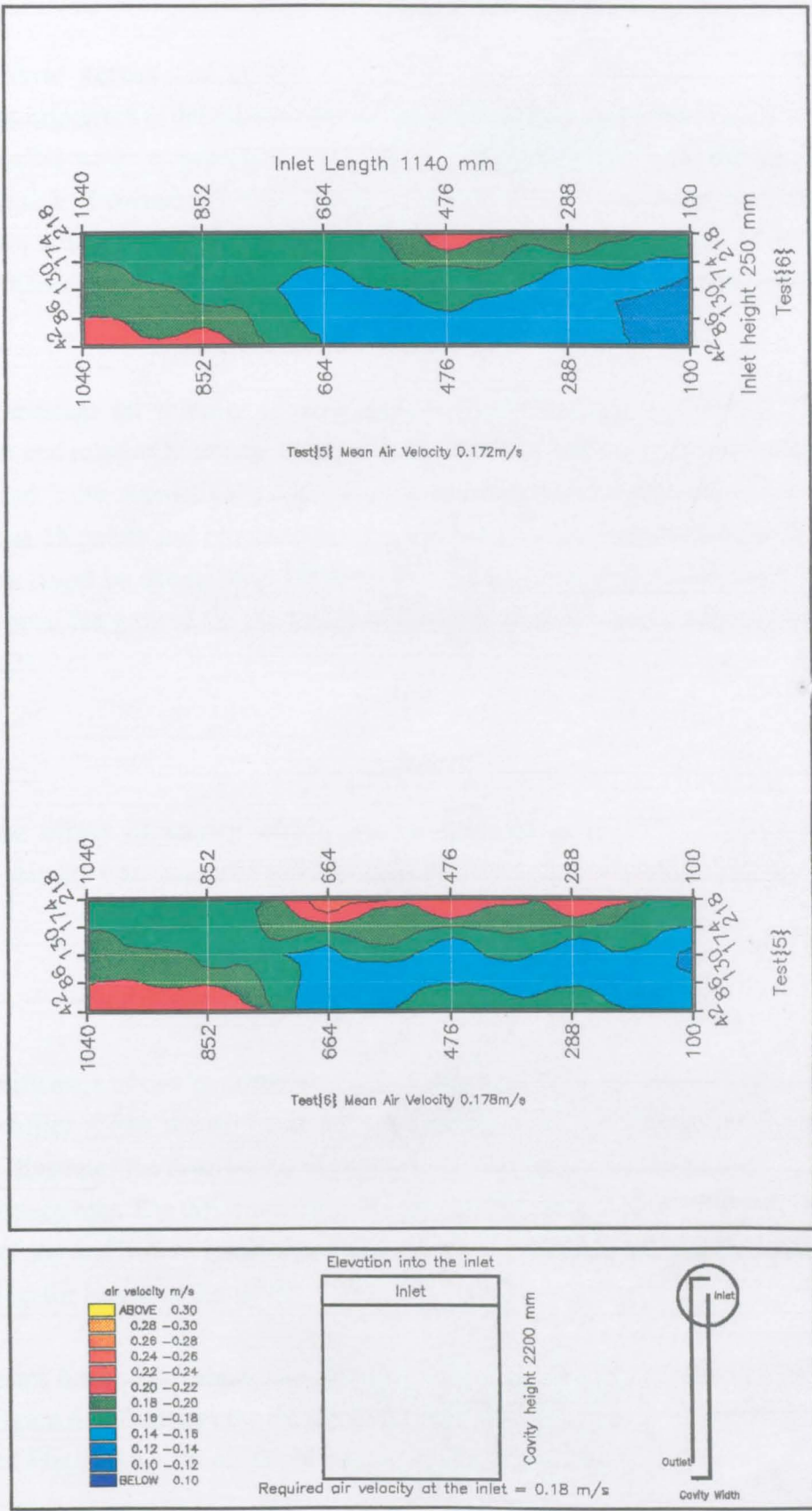


FIG.6.2 Measured air velocity distribution at the cavity inlet
 Inlet air temperature 30 C and relative humidity 40%

6.2.2 Air flow across the cavity

It was important to determine whether the air flow was uniform across the cavity (between walls) when evaporation takes place. The cavity has to be thought of as reducing the size of the room. It was decided to use the 400mm width as a maximum. A set of 6 tests without any wet surfaces was carried out at cavity widths of 400mm, 300mm, 200mm, 160mm, 125mm and 100mm so that air flow pattern could be examined.

The average air velocity at the inlet was fairly constant at 0.37m/s. The air temperature and relative humidity were the same as above with maximum variation of about 1K and 2.0% respectively. The velocity measurements across the cavity were carried out at 18 points and recorded at three different levels (Figure 4.12) so that the flow pattern could be determined. Level A was 100mm below the inlet, level B was 1000mm above the ground (in the middle) and level C was 100mm above the outlet (Figure 4.12).

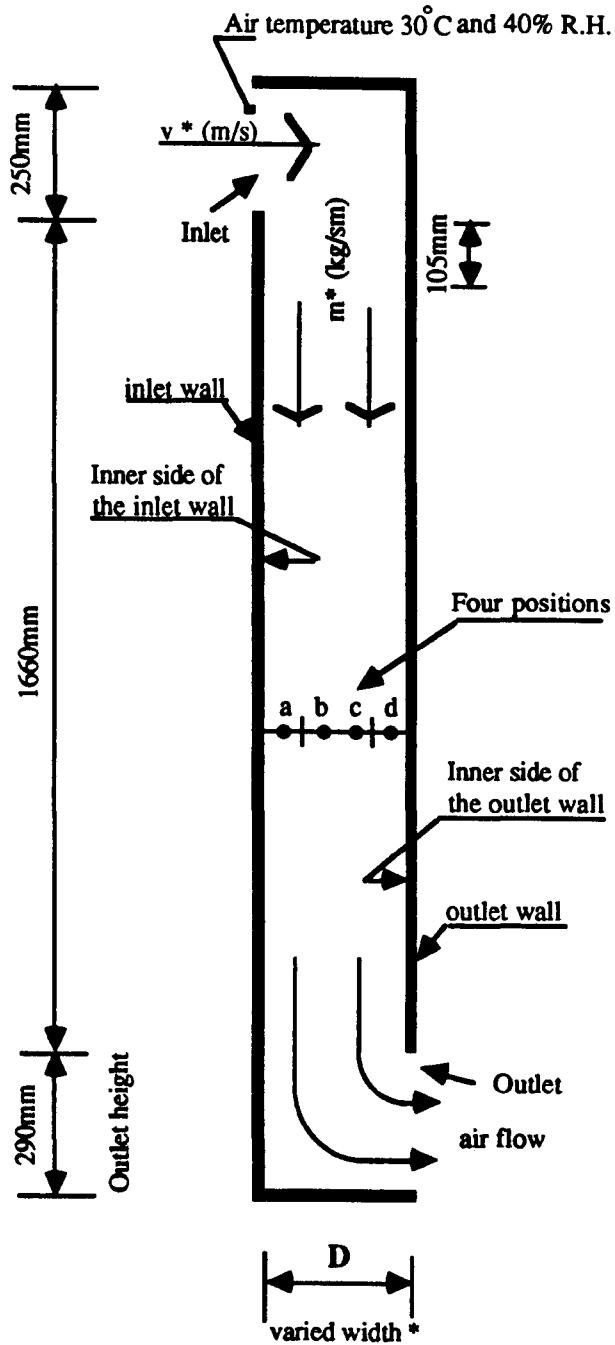
6.2.2.1 The effect of cavity width on air flow pattern

Air velocity was measured at four positions across the cavity (Figure 6.3);

- one near the inner side of inlet wall (a)
- two in the middle of the cavity (b and c)
- and one near inner side of the outlet wall (d).

Significance of cavity width on air flow was evaluated by comparing measured velocity profiles across the cavity at three different levels (the 400mm cavity width). Figure 6.4 illustrates the distribution of air velocity at these levels. It was 0.12, 0.15 and 0.18m/s respectively. The difference between the average air velocity of the middle level and those of top and bottom levels was about 6% which indicates that very little variation took place up the height of the cavity.

Figures 6.5 and 6.6 show how the air velocity distribution varies with different cavities. Figure 6.5 illustrates the distribution of the 400mm, 300mm and 200mm cavity widths, and Figure 6.6 with widths of 160mm, 125mm and 100mm.



v^* air velocity, 0.37m/s

m^* mass flow rate in the cavity 0.12kg/s.

cavity width varied from 400mm to 100mm.

Postions of measured air velocity (a, b, c and d).

Figure 6.3 Description of the cavity used for velocity profile tests.

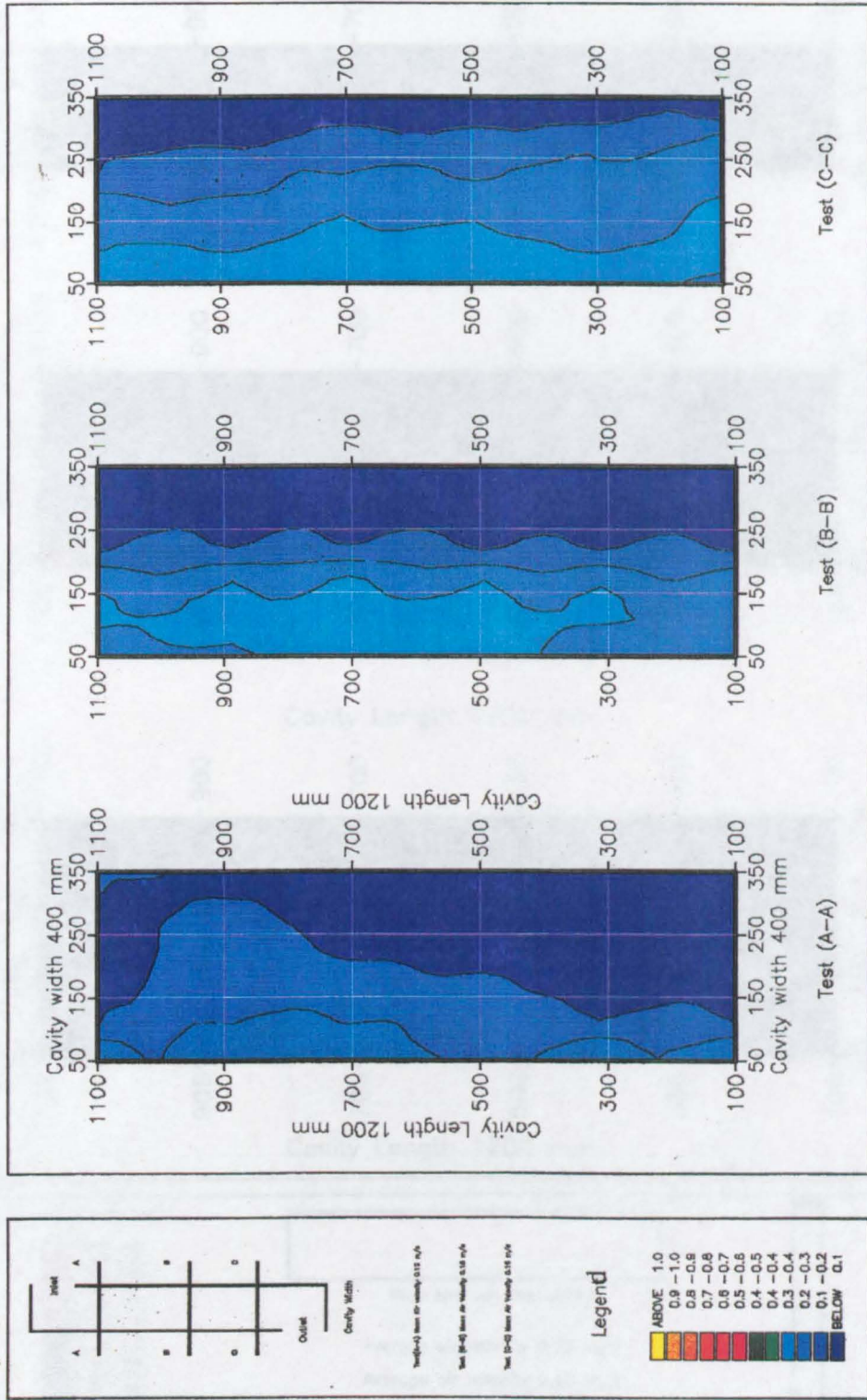


Figure 6.4 - Measured Air Velocity Distribution at the Cavity Cross-section
Inlet Air Temperature 30 C and Relative Humidity 40 %

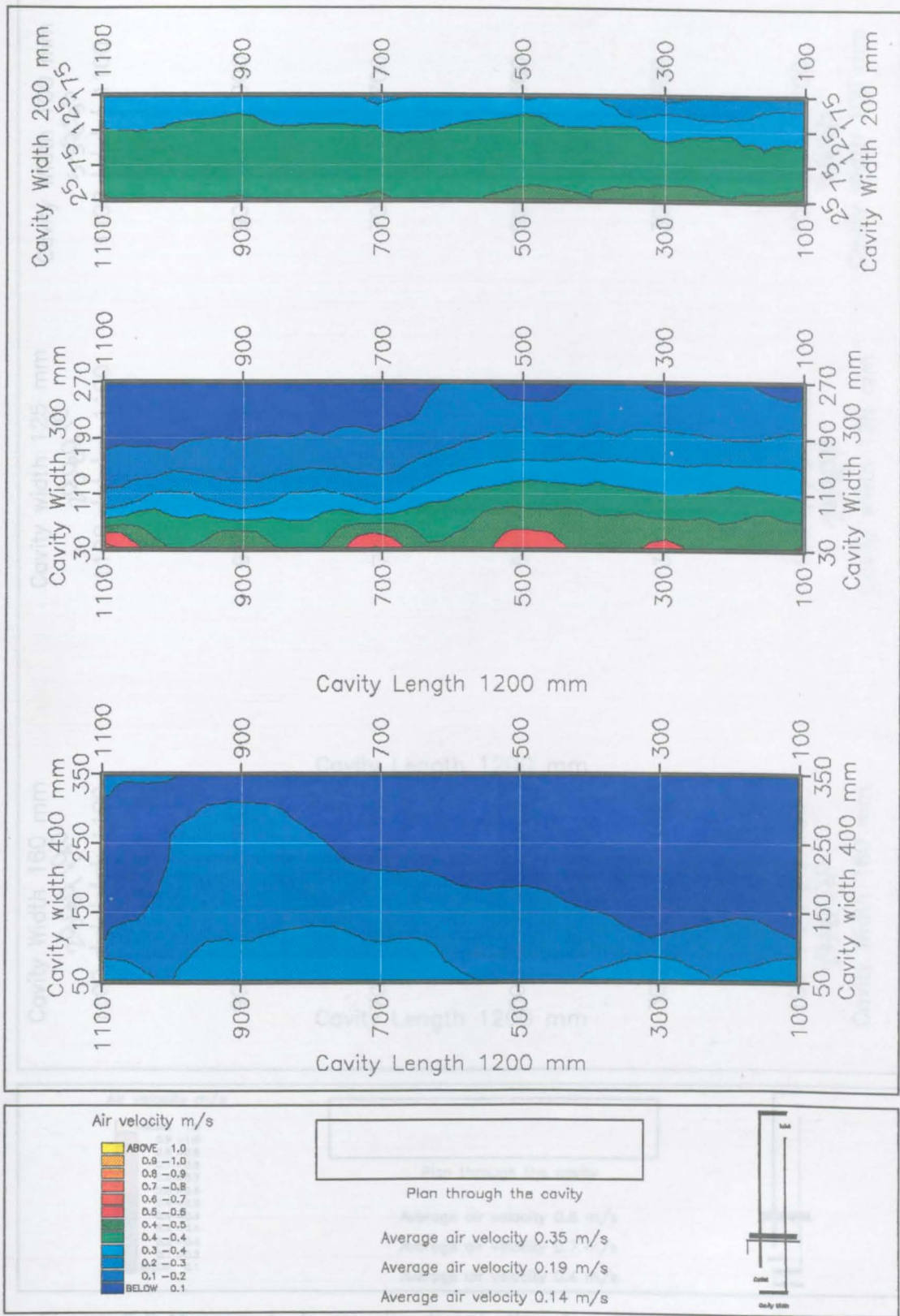


Figure 6.5 Measured air velocity distribution for different cavities

Inlet air temperature 30 C and relative humidity 40%

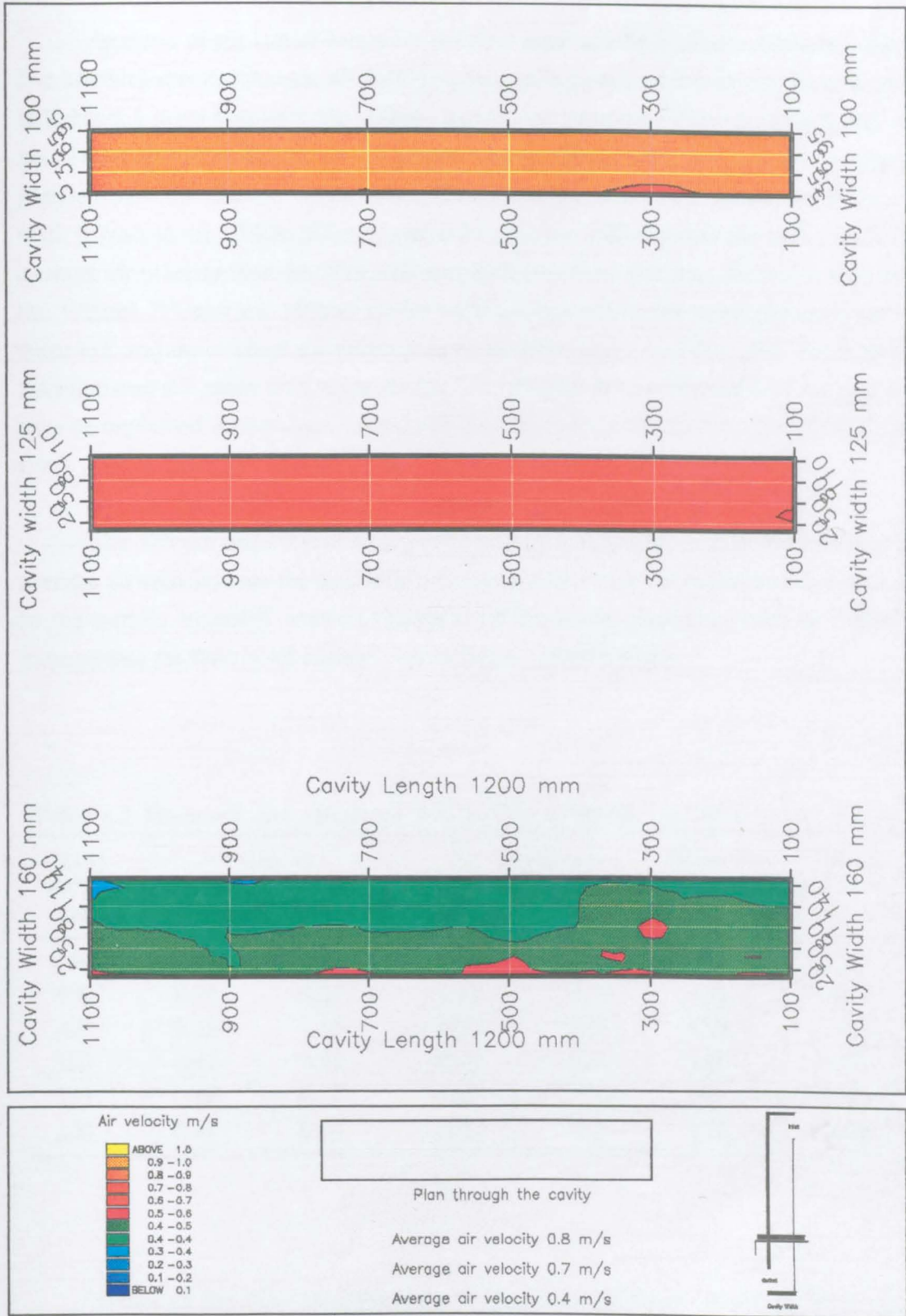


Figure 6.6 Measured air velocity distribution for different cavity widths

Inlet air temperature 30 C and relative humidity 40%

Analysis of the initial data with the first four widths (400mm, 300mm, 200mm and 160mm) showed that the air flow was not uniform across the cavity. Results given in Table 6.1 show that with the 400mm cavity, the measured average air velocity was about 40% less than the calculated. Measurements (Figure 6.5) show that air velocities profile across the 400mm width were 0.04m/s and 0.02m/s in the 100mm near the inlet wall, 0.1m/s in the middle 200mm, and 0.2m/s in the 100mm near the outlet wall. The average air velocity near the inlet wall was 80% less than that near the outlet wall. With the 300mm, 200mm and 160mm cavity widths (Figure 6.5), the same phenomenon was recorded, and the average air velocity near the inlet wall was 72%, 38% and 32% less than that near the outlet wall respectively. This drop in the air velocity near the inlet wall may be explained by the sharp-edged effect of the inlet as described above (see chapter five).

The 125mm and 100mm cavity widths (Figure 6.6) show a uniform air flow. The average air velocity near the inlet wall was equal to that near the outlet wall but increased in the middle by small amount (Table 6.1). Reynolds numbers given in Table 6.1 indicate that the flow in all cavities was turbulent (above 2000).

Table 6.1 Measured and calculated average air velocities related to cavity widths.

Cavity width mm	Air velocity		Av. air velocity		Difference m/s	Reynolds number, Re —
	inlet wall m/s	outlet wall m/s	measured m/s	calculated m/s		
400	0.04	0.20	0.14	0.23	0.09	6335
300	0.08	0.29	0.19	0.30	0.11	6450
200	0.25	0.46	0.35	0.45	0.10	7920
160	0.37	0.57	0.43	0.56	0.13	7780
125	0.66	0.68	0.67	0.73	0.06	9620
100	0.82	0.84	0.83	0.90	0.07	9400

Although the flow length (cavity height) was the same (fixed) in all tests, the velocity distribution varied with cavity width. (Figures 6.5 and 6.6). However, the velocity distribution across cavity widths of 100mm and 125mm (Figure 6.7 a) show

some similarity and tend to approach the 'fully developed' turbulent velocity profile by ASHRAE, 1985 (Figure 6.7 b). This therefore indicates that both boundary layers near the cavity walls have nearly the same average air velocity and the separation from the inlet wall which took place in wider cavities has been eliminated.

The above investigation indicates that the increases of the cavity width may be disadvantageous in terms of air flow pattern and suggests that cavities above 125mm wide may be inadequate to achieve a uniform air flow near the cavity walls. Hence, this observation suggests that if two vertical wet mats are exploited, evaporation then could take place effectively.

On the basis of the above findings a decision has been made to carry out all tests to examine the 'evaporative cooling cavity' with fan-assisted air flow at width of 125mm or less.

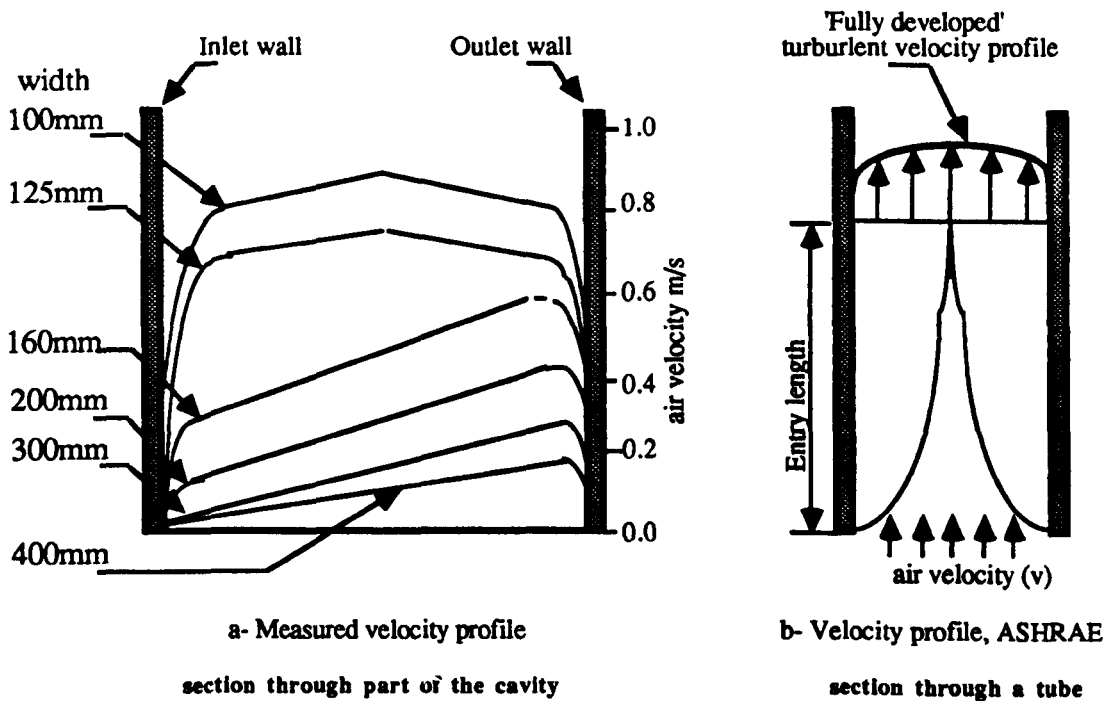


Figure 6.7 Developed flow in ducts according to ASHRAE (1985) and those measured.

6.3 Evaporative cooling observations

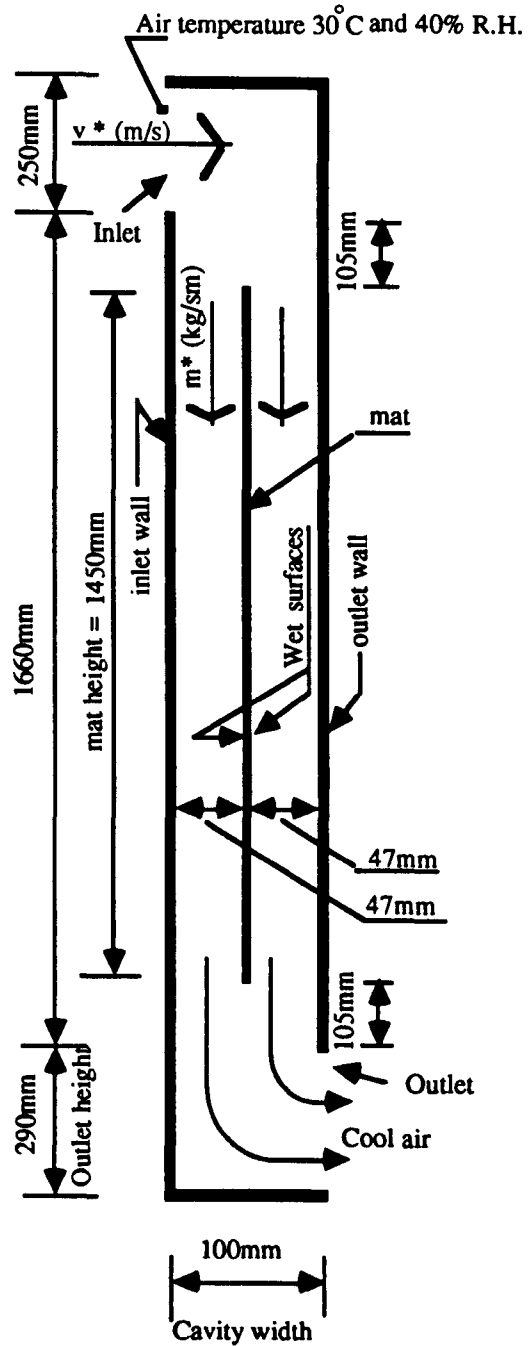
Cooling as a result of evaporation by fan-assisted 'forced air flow' was measured with cavity widths of 125 mm, 100mm, 60mm and 40mm. The flow rate, the number of wet surfaces (mats) and their separation were varied. Arrangements of cavities are shown below (Figure 6.8 to Figure 6.11). Air temperature, relative humidity and velocity at the inlet in all tests were maintained: 30°C, 40%, and 0.18m/s and 0.37m/s, with a maximum variation of 1K, 4% and 0.01m/s respectively. Based on the above velocities, the flow rate was fairly constant at 0.06kg/sm and 0.12kg/sm. One or two mats were employed.

In order to examine cooling from evaporation using one or two wet mats, measurements of the air temperature drop between the inlet and outlet, the velocity and relative humidity at the outlet were needed. Twenty tests were carried out to investigate this. Parameters investigated during observations were:

- separation between wet mat
- air velocity at the outlet
- the drop of air temperature between the inlet and the outlet
- the relative humidity
- cooling
- the 'humidity ratio difference'
- water vapour removed by evaporation
- the convective heat transfer coefficient.

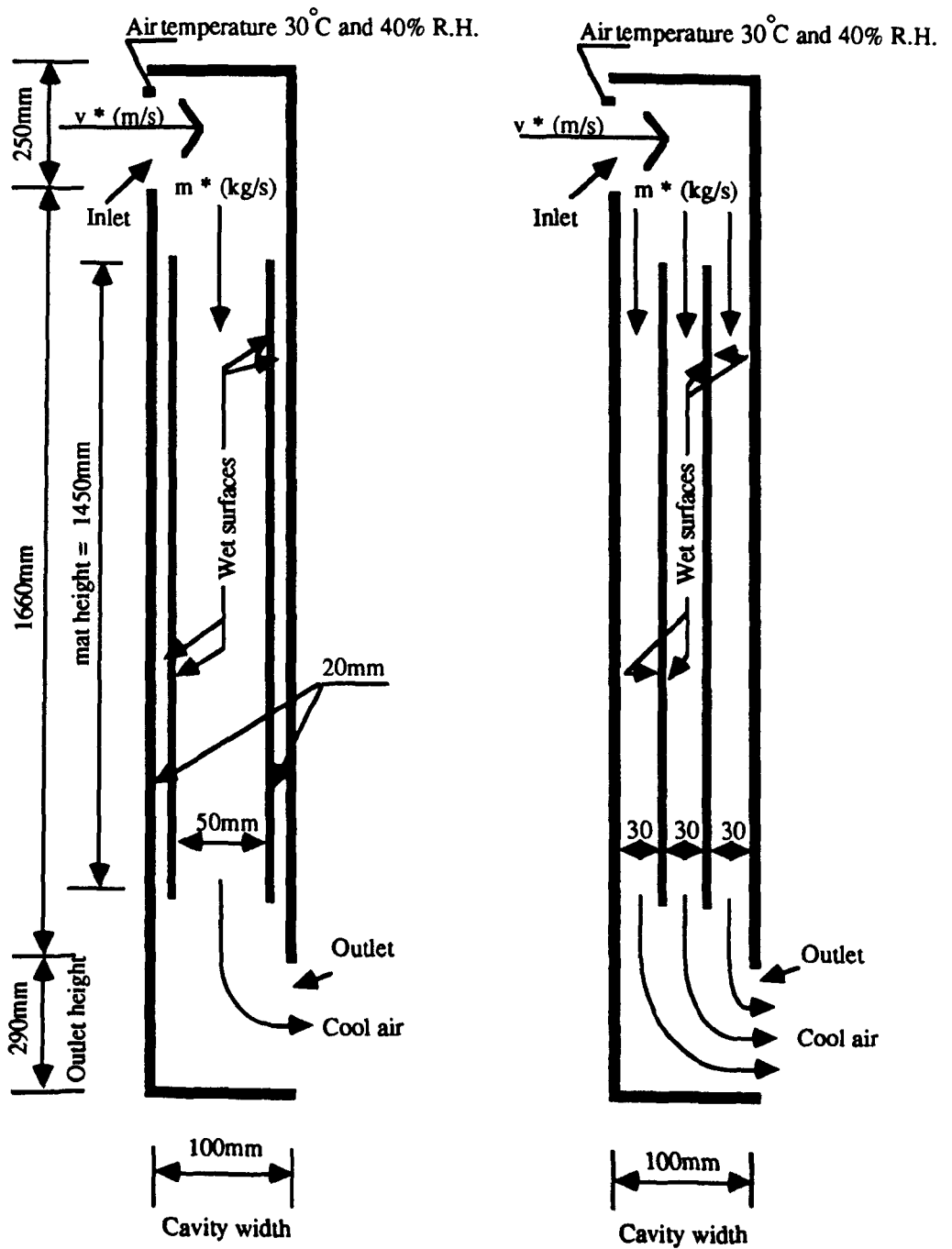
6.4 RESULTS

The significance of the cooling by evaporation could be determined using the enthalpy difference method or the cooling (heat removal eqn.3.44, chapter three). The analysis shows that the error of the enthalpy difference was large. The error associated with the use of the enthalpy difference method and cooling using eqn.3.44 are given in Appendix B. To determine the cooling (W/m), measured air temperature drop between the inlet and outlet (K), and the mass flow rate (kg/sm) - [which includes: the air velocity (v), the area of the flow at the outlet A (m²) and the density of the air at the outlet (kg/m³)] were needed.



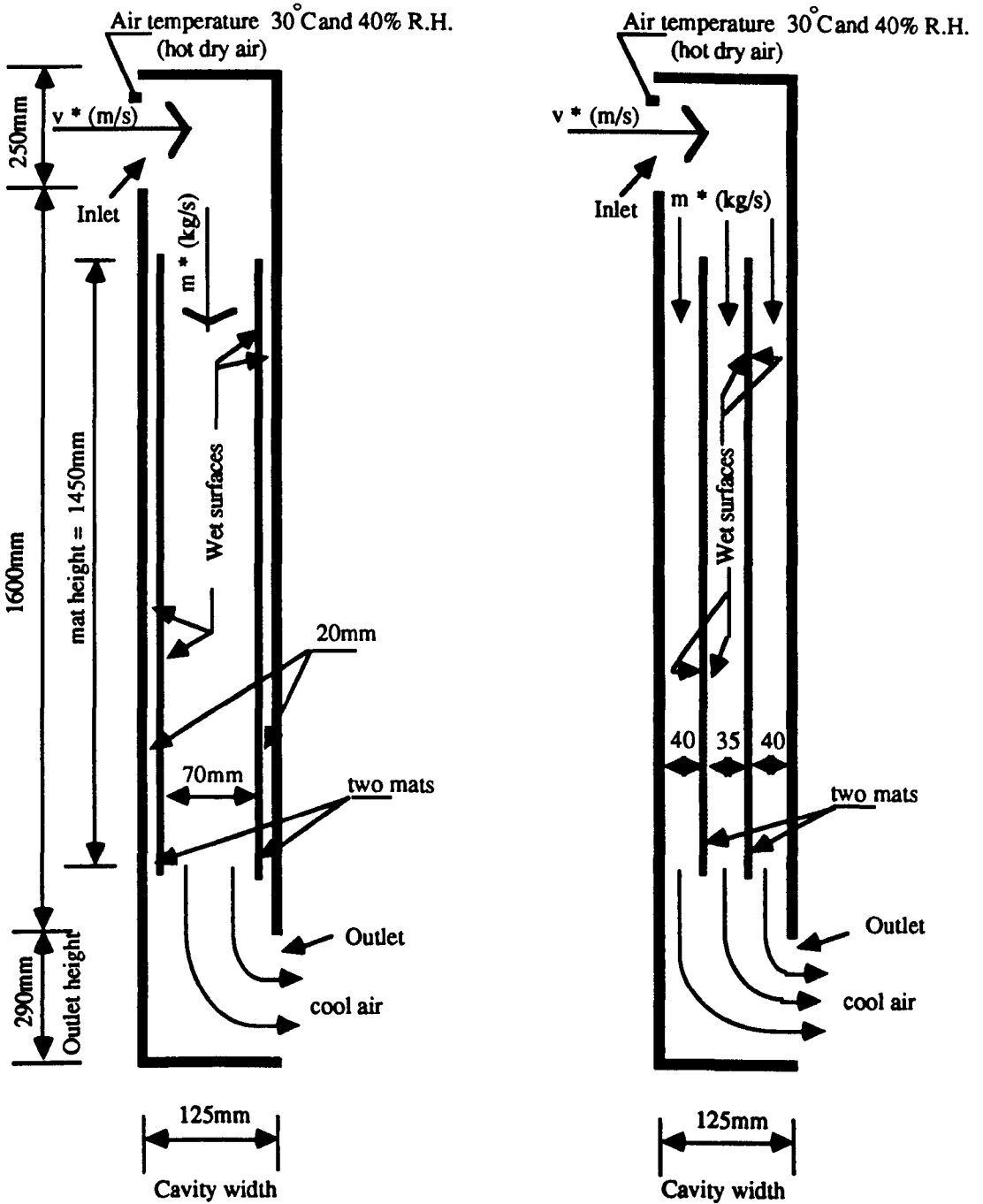
v^* air velocity at the inlet were 0.18m/s and 0.37m/s
 m^* mass flow rate in the cavity were 0.06kg/s and 0.12kg/s.
 mat thickness about 5mm.

Figure 6.8 Shows the arrangements of cavities with one mat, 100mm wide.



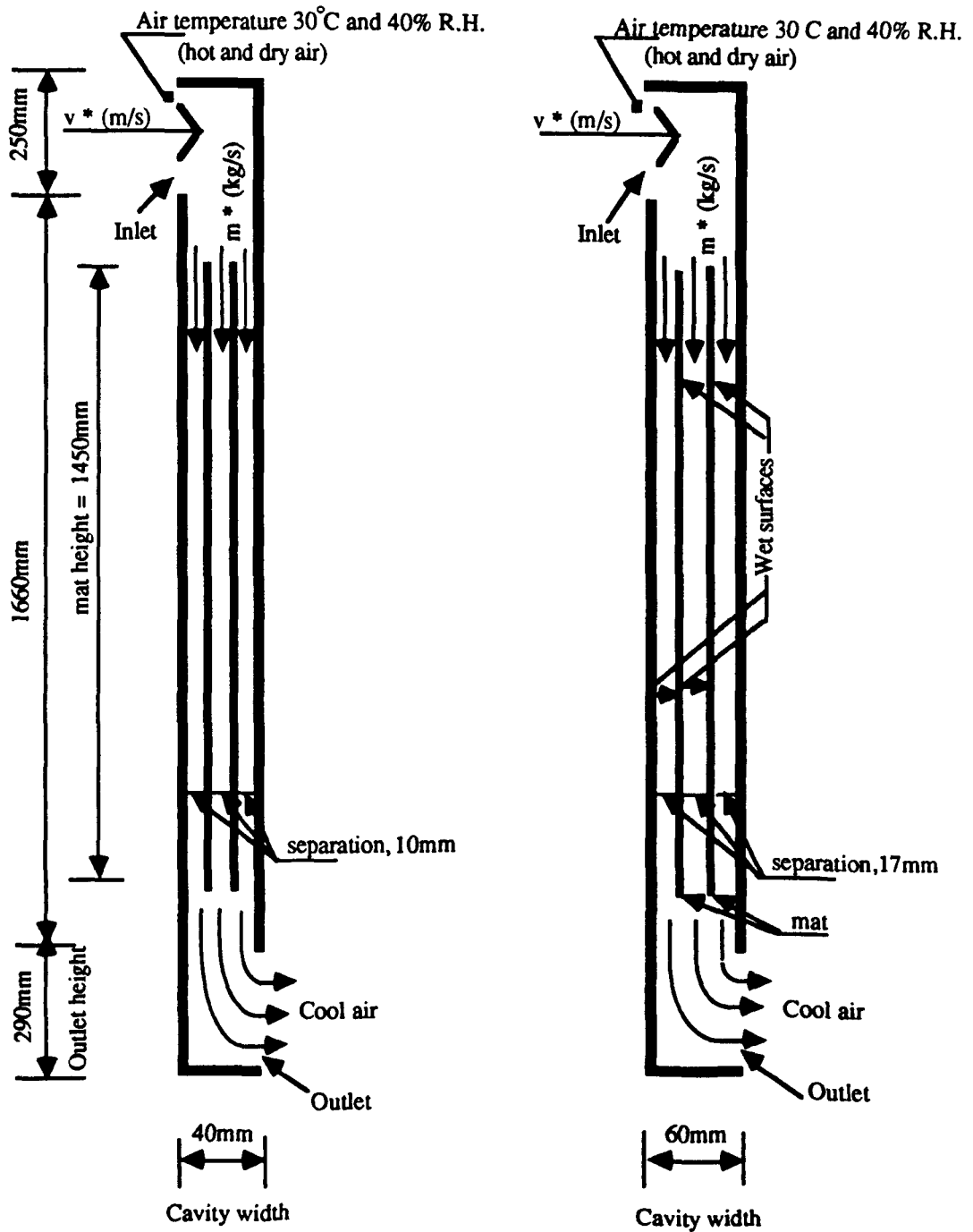
v^* air velocities were 0.18m/s and 0.37m/s.
 m^* mass flow rates were 0.06kg/s and 0.12kg/s.
 mat thickness about 5mm

Figure 6.9 Shows the arrangements of cavities with two mats, 100mm wide.



v^* air velocities were 0.18m/s and 0.37m/s.
 m^* mass flow rates were 0.06kg/s and 0.12kg/s.
 mat thickness was 5mm.
 all dimensions in mm.

Figure 6.10 Shows the arrangements of cavities with two mats, 125mm wide.



v^* air velocities were 0.18m/s and 0.37m/s.
 m^* mass flow rates in the cavity were 0.06kg/s and 0.12kg/s.
 mat thickness about 5mm.

Figure 6.11 Shows the arrangements of cavities with two mats, 40mm and 60mm wide.

6.4.1 The effect of wet mat number and their separation.

It was important to establish an arrangement for the wet mat inside the cavity so that the effect of cavity width on cooling can be investigated. Six tests were carried out to study the effect of the number of wet surfaces and their separation within the cavity on: air temperature drop between the inlet and outlet, the outlet air relative humidity and cooling. The cavity was maintained at 100mm wide. Number of wet mats and their separations within the 100mm cavity width were arranged as shown in Figures 6.8 and 6.9 (three arrangements). Flow rates of 0.06kg/s and 0.12kg/s were used. The inlet air temperature, relative humidity and the velocity were: 30°C, 42%, and 0.18m/s and 0.37m/s, with maximum variation of about 1K, 2% and 0.01m/s respectively. Results are presented below.

6.4.1.1 Air temperature drop

Figure 6.12 shows that the lowest air temperature drop (3K) was of the first arrangement (Figure 6.8, cavity with one wet mat). An increase of 2K and 3K obtained with that of the second and third arrangements (Figures 6.8 and 6.9).

Although the flow and the separation between wet mats, especially in the second and third arrangements, were varied, there was a small change (about 1K) in the air temperature drop between the inlet and outlet (Figure 6.12). This indicates that the reduction of the separation between the wet mats from 50mm to 30mm is insignificant in terms of increasing the air temperature drop, but the number of wet mats is significant because of the increase of the evaporation area.

6.4.1.2 Air relative humidity at the outlet

Figure 6.13 shows the variation in the air relative humidity. It illustrates that the lowest increase of the relative humidity was measured when one wet mat was used with both flow rates. The average air relative humidity at the outlet (with 20 hours test operation) was 46% and 59% with 0.06kg/s and 0.12kg/s respectively.

Small changes of the air relative humidity were measured with the second and third arrangements. An increase of the outlet air relative humidity by 7% was measured due to the increase of the flow from 0.06kg/s to 0.12kg/s. This indicates that the average outlet air relative humidity increases by a small amount of the increase of the flow rate.

The above observation suggests that the reduction of the separation between the wet mats (from 50mm to 30mm) has little significance on increasing the outlet air relative humidity, but the area of evaporation (number of the wet mats) was more important. The evaluation of the outlet air relative humidity increase is important for assessing the thermal comfort which will be discussed in chapter eight.

6.4.1.3 The cooling rate

Figure 6.14 shows the changes in the cooling due to the variation of the number of wet mats and the separation between them. The average cooling with flow of 0.06kg/s (one wet mat) was 180W/m, and increased by 40W/m with the second and third arrangement (Figure 6.9). Cooling increased by 275W/m when the flow rate was increased to 0.12kg/s, especially with the second and third arrangements (Figure 6.14).

This indicates that the increase of the evaporation area (number of wet mats) was significant in increasing the cooling, but the separation between wet mats was less significant. The increase of the flow rate was also significant.

The above observations suggest that cooling can be increased with the second and third arrangements (four areas of evaporation, Figure 6.9). However, the small increase with the second arrangement (Figure 6.14) is negligible, and therefore a decision was made to carry out all tests to examine the parameters mentioned in (Sec. 6.3) on cooling by evaporation with the third arrangement (Figure 6.9).

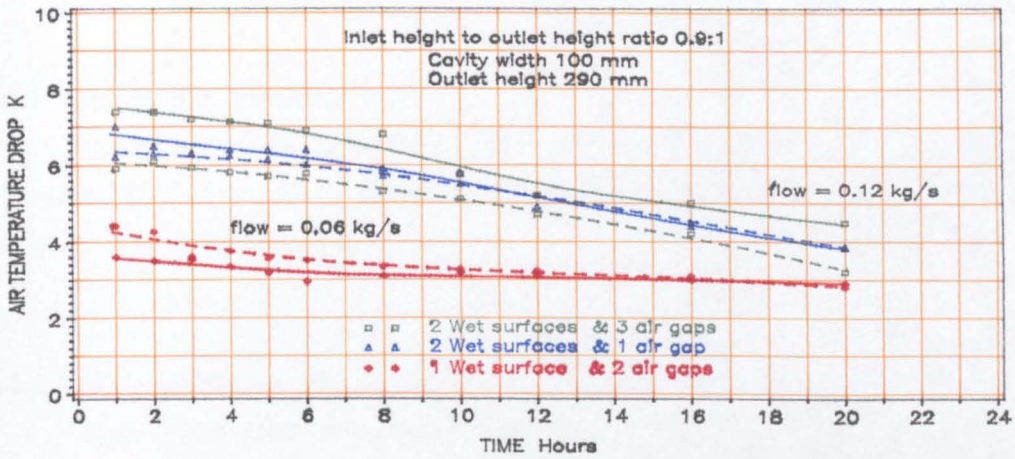


FIG 6.12 The effect of wet surfaces spacing on air temperature drop between the Inlet and outlet

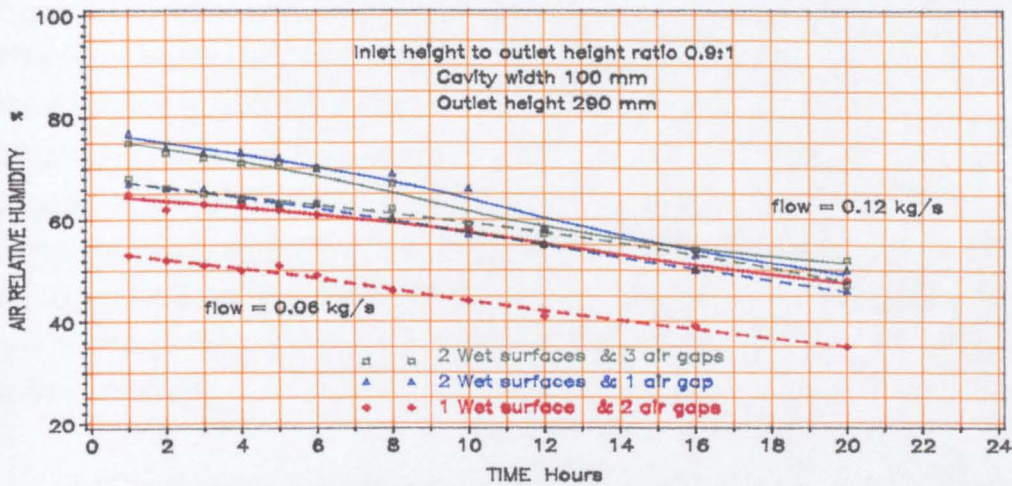


FIG 6.13 The effect of wet surfaces spacing on air relative humidity

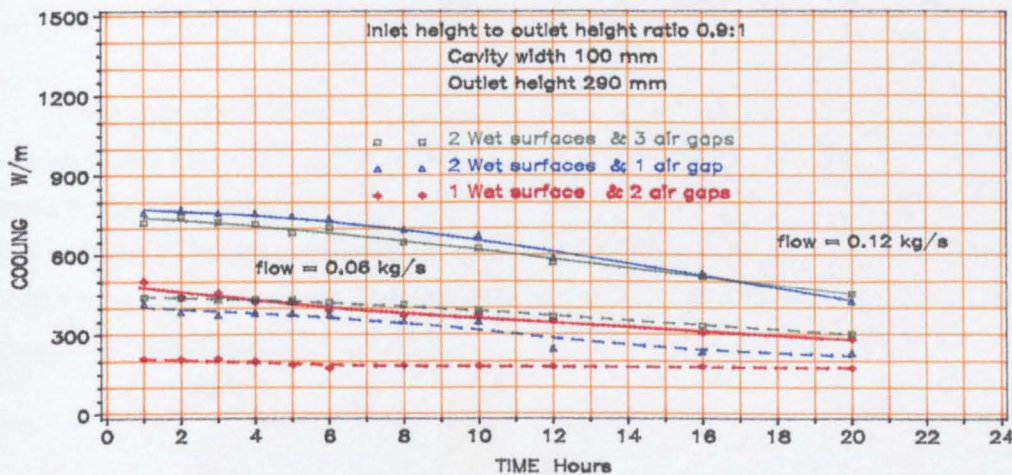


FIG 6.14 The effect of wet surfaces spacing on cooling

6.4.2 Outlet air velocity

The velocity of the air at the outlet was measured at 36 points across the air path, (Figure 4.11, Chapter Four). The effect of the outlet height and the width of the cavity on the air flow were assessed.

6.4.2.1 The effect of the outlet height on air flow

To study the effect of the outlet height on air flow, heights of 290mm and 100mm were tested. The width of the cavity was maintained at 40mm. The data show that the air velocity across the outlet height was not distributed uniformly. The velocity of the air at the top half was far lower than that of the bottom. Very little air flow was on the top 110mm of the 290mm height (Figure 6.15) which is represented by the dark blue zone (Figure 6.15 a). The green and hatched green zones represent the flow at the lower part of the outlet height (34% of the height). The average air velocity decreased from 0.63m/s (at the bottom) to 0.05 m/s (at the middle). These variations were only across the lower 120mm of outlet height. For example: in one vertical set of points of nine measurements across the outlet height, the air velocities were as follow: at the bottom five points, it was 0.64m/s and decreased upwards to 0.48m/s, 0.35, 0.18 and 0.05m/s, and then no flow at all (Figure 6.15 a). The above variation was because of the enlargement of the air flow from 40mm (cavity width) to 290mm (outlet height), and the change in the downward air flow direction.

Analysis shows that the average air velocity along the outlet length has little variation unlike that of the height. The average air velocity is given in Table 6.2. It was found that the velocity variation at the outlet height may lead to a standard error as large as $\pm 40\%$ when the height of 290mm was used in determining the cooling. As a result, the height of the outlet has to be reduced.

When the height was reduced to 100mm, Figure 6.15 b shows that the variation was less than that of the 290mm height despite little air velocities (below 0.05m/s) at some points. The maximum air velocity is represented by the hatched yellow and the orange zones. The average air velocity is given in Table 6.2. The reduction of the outlet height by about two thirds (290mm to 100mm) increases the average air velocity by about three times (0.23m/s to 0.7m/s).

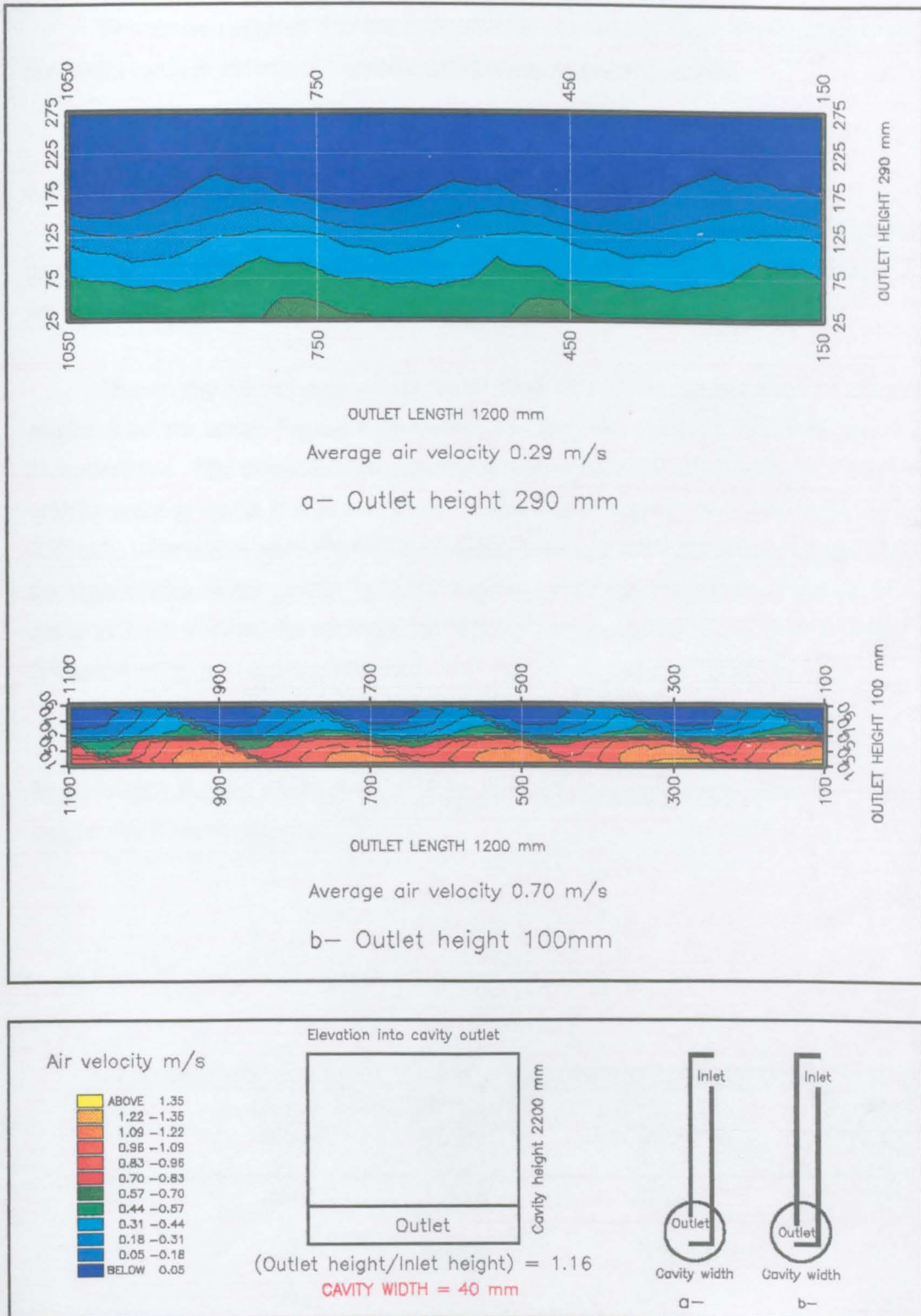


FIG 6.15 The effect of the outlet height on measured air velocity distribution

The above suggests that the reduction in the outlet height significantly increases the outlet average air velocity and its distribution across the outlet.

6.4.2.2 The effect of the cavity width on air flow at the outlet

Two tests were carried out to observe the outlet air velocity variations at two cavity widths (40mm and 60mm). The outlet height was maintained at 290mm. Results are shown (Figure 6.16).

Due to the consistency of the mass flow rate in the tests, the outlet air velocity ought to be the same. Figure 6.16 shows that the measured air velocity was less than that predicted. The measured air velocity at the outlet with the 40mm and 60mm cavity widths were given in Table 6.2. Both values were slightly less than that predicted of 0.31m/s, a little less with 40mm width and much less with the 60mm. This emphasises the significance of the cavity width on the flow. Although the height of the outlet was the same in both widths, the average air velocity at the outlet of the 40mm cavity width (Figure 6.16 b) was greater than that with the 60mm width (Figure 6.16 a).

The above suggests that air flow distribution at the outlet is significantly affected by its height and the width of the cavity. To achieve a uniform air flow at the outlet, its height should maintained at 100mm.

6.2 Average air velocity at different outlet heights and their standard errors				
Cavity width	Outlet height	Mean air velocity	Air velocity standard error	Maximum standard error
mm	mm	m/s	m/s	%
40	290	0.28	0.01	32
60	290	0.13	0.02	50
40	290	0.23	0.04	40
40	100	0.65	0.06	9

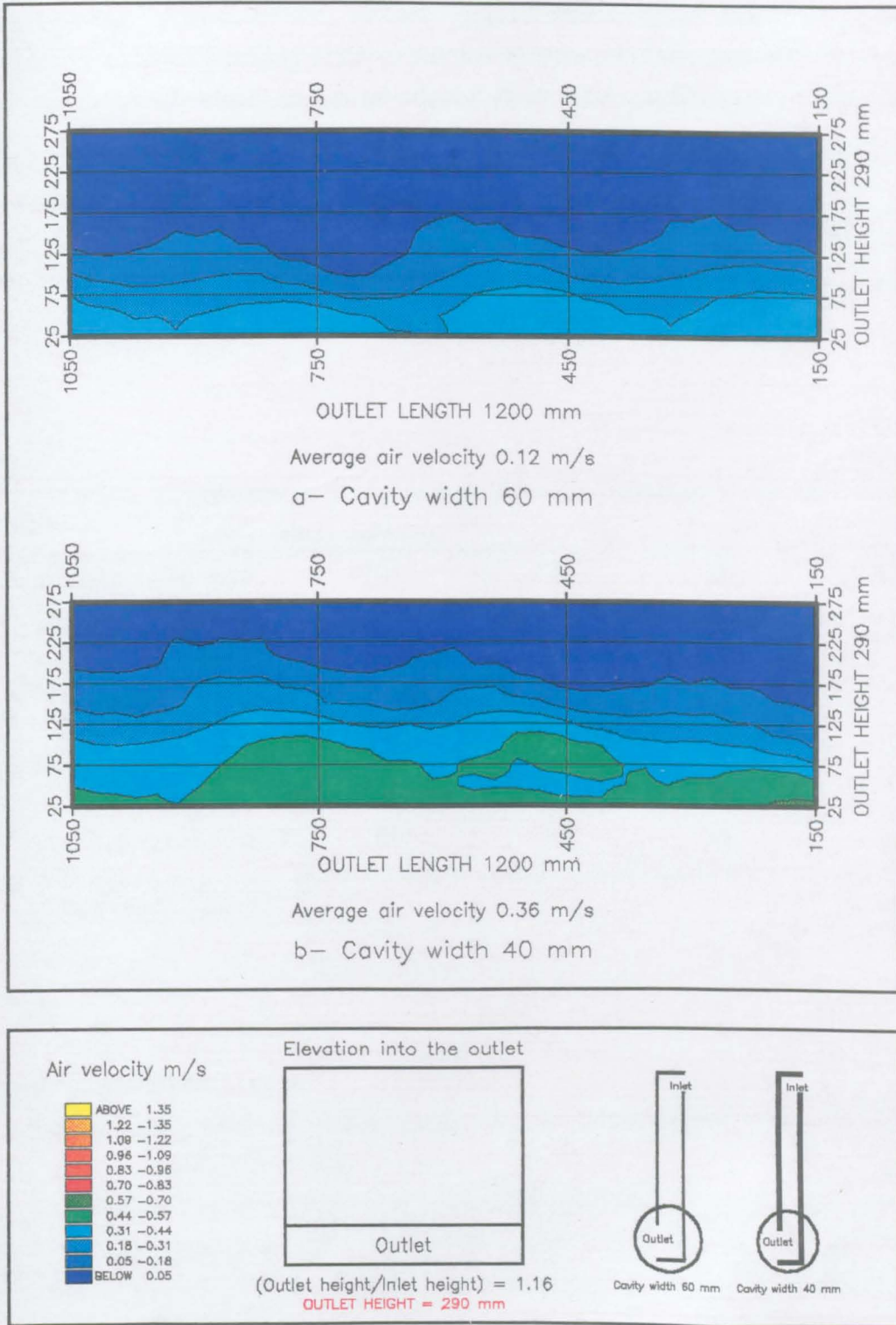


FIG 6.16 The effect of the cavity width on measured outlet air velocity

6.4.3 Outlet air relative humidity

Four tests were carried out to measure the outlet air relative humidity with four cavity widths: 40mm, 60mm, 100mm, and 125mm (Figures 6.9 to 6.11). The average air relative humidity at the outlet was determined from measured values along the outlet cross-sectional area as mentioned above. The coefficient of variance of air relative humidity at the inlet was 3% at a constant air temperature of $30 \pm 0.5^\circ\text{C}$. The variation of the outlet average air relative humidity in all tests was $\pm 3\%$. The average air relative humidity at the outlet as a result of decreasing the width of the cavity are given in Table 6.3. It indicates that with a decrease of cavity width from 125mm to 40mm, the increase of the average relative humidity was only about a quarter.

Table 6.3 Differences of the measured relative humidity at the outlet due to cavity width variation.

Cavity width mm	125	100	60	40
Inlet R.H. %	41	43	44	44
Mean outlet R.H. %	55	61	66	68
Relative increase of R.H. %	100	111	120	124
Difference of R.H. %	14	18	22	24

Inlet air temperature 30°C

6.4.4 Temperature drop

6.4.4.1 The effect of cavity width on air temperature drop between inlet and outlet.

Eight tests were carried out to measure the drop in air temperature between the cavity inlet and outlet as a result of evaporation. Cavity widths used were: 40mm, 60mm, 100mm, and 125mm. The inlet air velocity and the air temperature were nearly constant ($0.37 \pm 0.01\text{m/s}$ and $30^\circ\text{C} \pm 0.5$ respectively) throughout the observation of each

test. Two wet mats were used. Two air flow rates were used (0.06kg/s and 0.12kg/s). Arrangements are shown above (Figures 6.10 and 6.11). Results are shown in Figures 6.17 and 6.18.

The relationship between the average air temperature drop between the inlet and outlet and cavity width with their error bars are shown in Figures 6.19 and 6.20. The average air temperature drop was based on two tests durations (20 hours and 12 hours). Tests with flow of 0.12kg/s (20 hours) show that the drop of the air temperature increased when the cavity width decreased (Figure 6.19). The average air temperature drop with the 125mm width was $4.7 \pm 0.5K$ with a maximum of 5.5K. With the 100mm cavity, it was $5.6 \pm 0.5K$ with a maximum of 6K. This indicates that the average air temperature drop between the inlet and outlet increased by about 1K as the width decreased. In both the 40mm and 60mm cavity width, the average air temperature drop was higher ($7 \pm 0.5K$ and $8 \pm 0.5K$, with a maximum of 8K and 9K respectively). The above suggests that the reduction of the cavity width from 125mm to 60mm and 40mm significantly increases the average air temperature drop between the inlet and outlet by 3K.

Table 6.4 shows that with 20 hours operation, The standard error varies from $\pm 1\%$ with the 125mm cavity to about $\pm 5\%$ with the 40mm, 60mm, and 100mm cavity widths. It was nearly the same with 12hours operation. This indicates that the standard errors of both operation periods were small. An air temperature drop of 1K was obtained when the operation was carried out for only 12 hours.

Figure 6.20 shows that with flow rate of 0.06kg/s, the average air temperature drop was about the same (7K) despite the variations of cavity width.

Table 6.4 showed that despite the differences of the flow rate, the air temperature drop was about the same for the 40mm and 60mm cavity. It also showed that for cavities 100mm and 125mm wide with flow rate of 0.06kg/s, the air temperature drop was 2K greater than with the flow rate of 0.12kg/s. Table 6.5 shows that the difference with flow rate of 0.12kg/s was greater than that of 0.06kg/s. This was due to the effect of air velocity with the first flow (0.12kg/s) on evaporation. The relative increase of air temperature drop due to cavity width variations are given in Table 6.6.

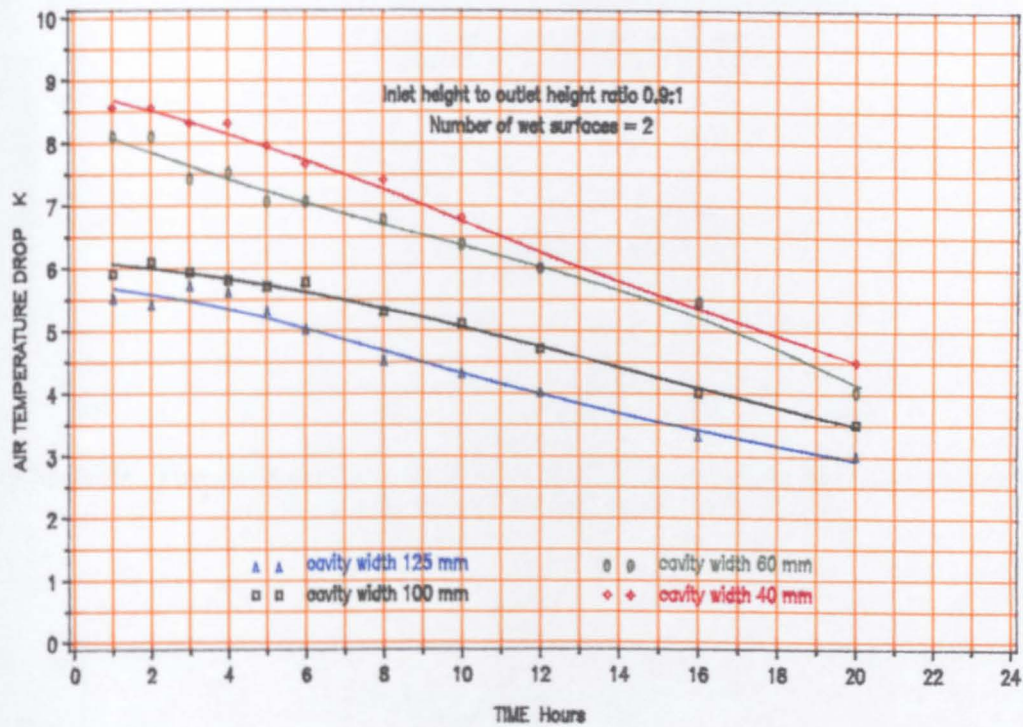


FIG 6.17 The effect of cavity width on air temperature drop between the inlet and outlet (flow 0.12 kg/s)

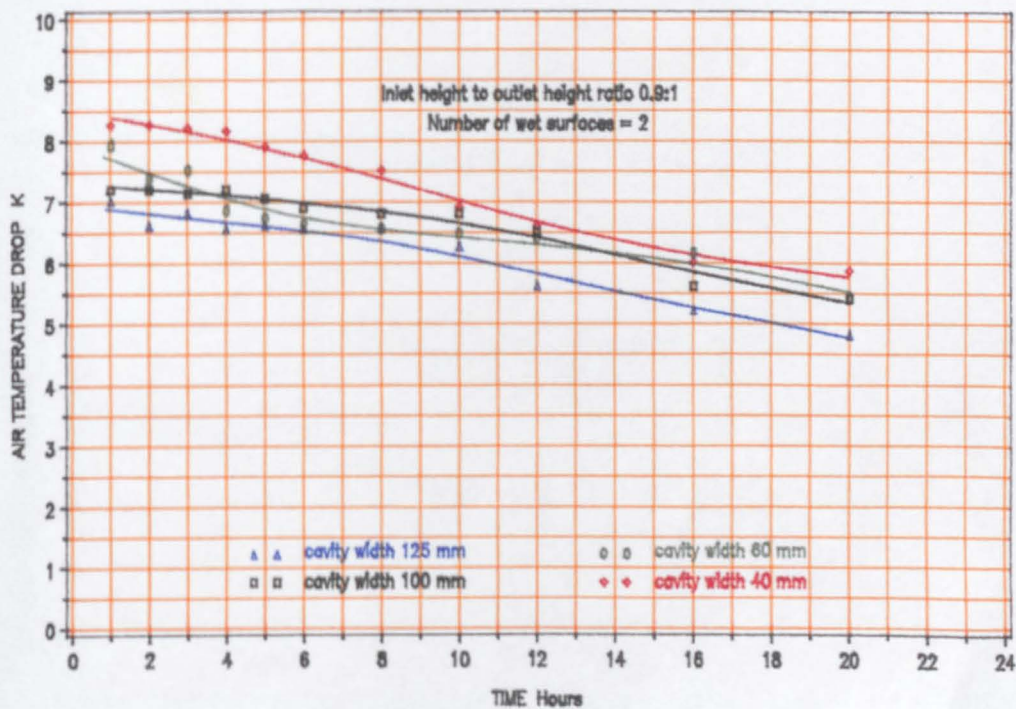


FIG 6.18 The effect of cavity width on air temperature Drop between the inlet and outlet (flow 0.06 kg/s)

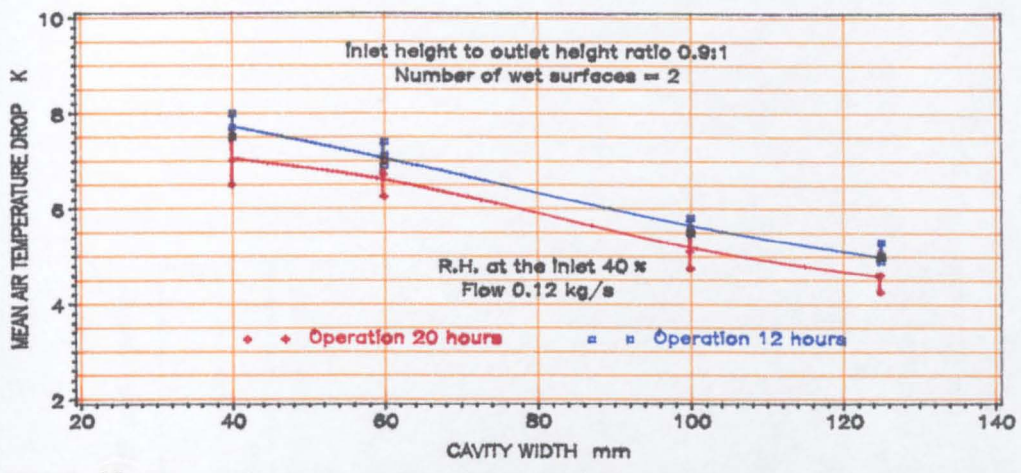


FIG.6.19 The effect of cavity width variation on mean air temperature drop between the Inlet and outlet

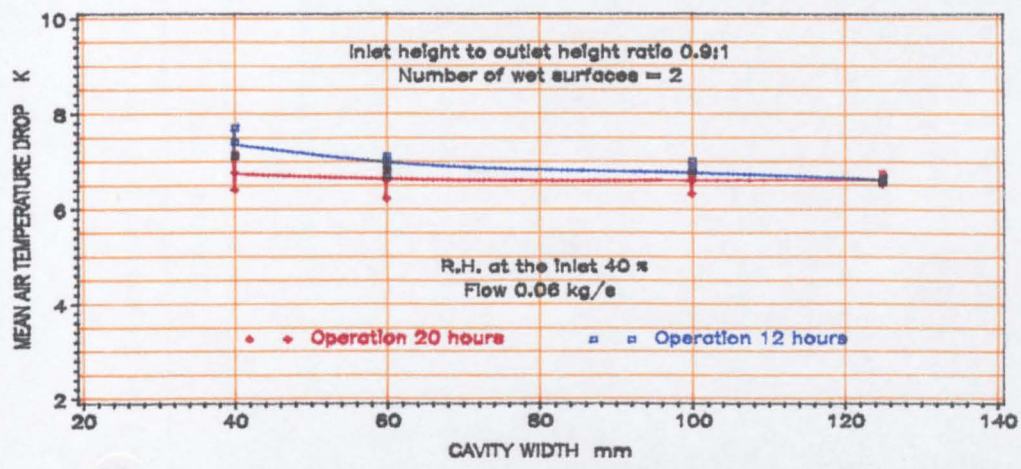


FIG.6.20 The effect of cavity width variation on mean air temperature drop between the Inlet and outlet

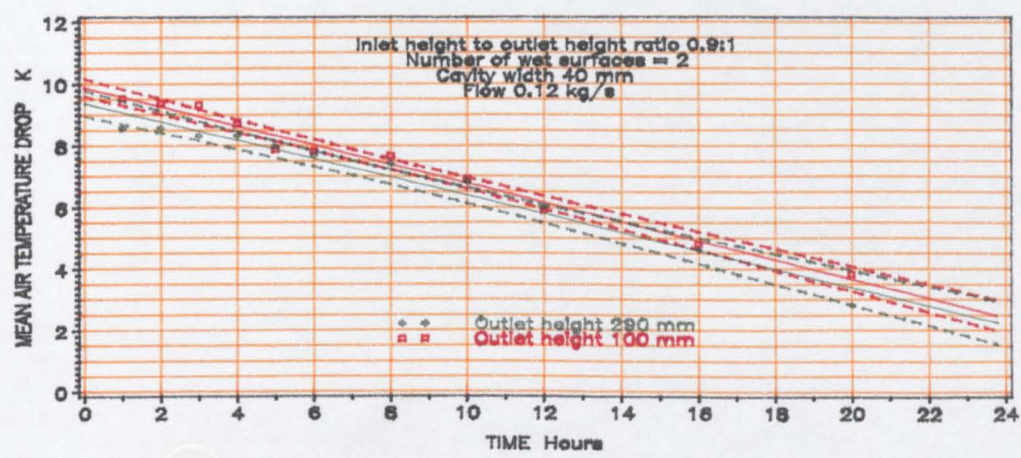


FIG 6.21 The effect of outlet height variation on mean air temperature drop between the Inlet and outlet

Table 6.4. Standard errors of measured air temperature drop, outlet air relative humidity and cooling.

Cavity width		Standard Errors														
		Flow 0.06kg/s						Flow 0.12kg/s								
		20 hours Operation+		12 hours Operation+		12 hours Operation+		20 Hours Operation†		12 hours Operation †		12 hours Operation †				
mm	Mean *	S.E*	%	Mean*	S.E*	%	Mean*	S.E*	%	Mean*	S.E*	%	Mean*	S.E*	%	
R. Humidity %	125	60	2	3	62	1	2	54	2	4	56	2	3			
	100	67	3	4	60	2	3	60	2	3	63	1	2			
	60	73	3	4	77	2	3	65	3	5	69	2	3			
	40	77	3	4	81	2	3	69	3	4	72	2	3			
Temperature Drop K	125	6.7	0.1	1	6.7	0.1	1	4.6	0.3	7	5.0	0.2	4			
	100	6.6	0.3	4	7.0	0.1	1	5.0	0.4	8	5.6	0.2	3			
	60	6.6	0.3	5	7.0	0.2	3	6.7	0.4	6	6.0	0.2	3			
	40	6.8	0.4	4	7.0	0.3	4	7.0	0.6	8	7.7	0.3	4			
Cooling Rate W/m	125	380	10	3	394	4	1	562	40	7	614	25	4			
	100	393	15	4	411	8	2	627	40	6	679	19	3			
	60	393	19	5	414	11	3	820	48	6	877	31	4			
	40	438	19	4	459	15	3	878	59	7	954	36	4			

+ Number of Replicates = 11

† Number of Replicates = 9

* Mean value

** Standard error of the mean

Table 6.5 Air temperature drop between inlet and outlet at different operation periods.

Air temperature drop between the inlet & outlet K								
Cavity width mm	Flow 0.12kg/s				Flow 0.06kg/s			
	Test operation (hours)				Test operation (hours)			
	Initial	10	20	Diff.* K	Initial	10	20	Diff.* K
40	8.6	6.5	3.0	5.6	8.5	7.0	4.7	3.8
60	8.2	6.3	4.0	4.2	7.8	6.5	4.0	3.8
100	6.0	5.2	2.5	3.5	7.5	6.3	4.7	2.8
125	5.3	4.5	2.0	3.3	7.0	6.2	4.5	2.5

Average air temperature and relative humidity at the inlet are 30 ± 1 C & $42\pm 2\%$.

* Difference between the initial and end of operation

Table 6.6 Relative increase* of air temperature drop between inlet and outlet due to cavity width variations.

Cavity width mm	20 hours Operation				12 hours Operation			
	125	100	60	40	125	100	60	40
Flow 0.12kg/s								
Air temp. drop K	4.6	5.0	6.7	7.0	5.0	5.6	7.0	7.7
Relative increase* %	100	109	146	152	100	112	140	154
Flow 0.06kg/s								
Air temp. drop K	6.6	6.7	6.7	7.0	6.7	7.0	7.0	7.5
Relative increase* %	100	102	102	105	100	105	105	112

* Relative increase in relation to cavity width of 125mm.

6.4.4.2 The effect of the outlet height on the air temperature drop between inlet and outlet

The air temperature drop was measured under the same condition as given above except that the outlet height was reduced to 100mm. Results show that an increase of the mean air temperature drop by about 1K is possible when the outlet height was reduced from 290mm to 100mm (Figure 6.21). This variation was probably due to the contraction of the air flow in the lower part of the outlet where the velocity of the air was much greater than that of the upper part of the outlet (Figure 6.6). However, the standard deviation along the regression line of the air temperature drop between the inlet and outlet with the outlet of 290mm overlapped with that of the 100mm. This indicates that the reduction of the outlet height has little importance on increasing the air temperature drop between the inlet and outlet.

6.4.5 Relative humidity

6.4.5.1 The effect of cavity width on air relative humidity at the outlet

Eight tests were carried out under the same condition as above to measure the air relative humidity at the cavity outlet. Analysis shows that the air relative humidity at the outlet increased as the cavity width decreased. Figures 6.22 and 6.23 illustrate the variations of the outlet air relative humidity with time of operation. The trend was that the air relative humidity is initially greater than that at the end of operation period. This was because of the decrease of the surfaces wetness with time which will be discussed below.

The highest increase of the average relative humidity was measured when the cavity width was 40mm (for flow of 0.06kg/s). It was $77\pm 2\%$ and $81\pm 2\%$ at test duration of 20 and 12 hours respectively. It was less for the flow of 0.12kg/s. The increase was 68% and 73% at the same duration. The differences between the inlet and outlet air relative humidity are given in Table 6.7. The outlet air relative humidity at different operation periods and their differences are shown in Table 6.8

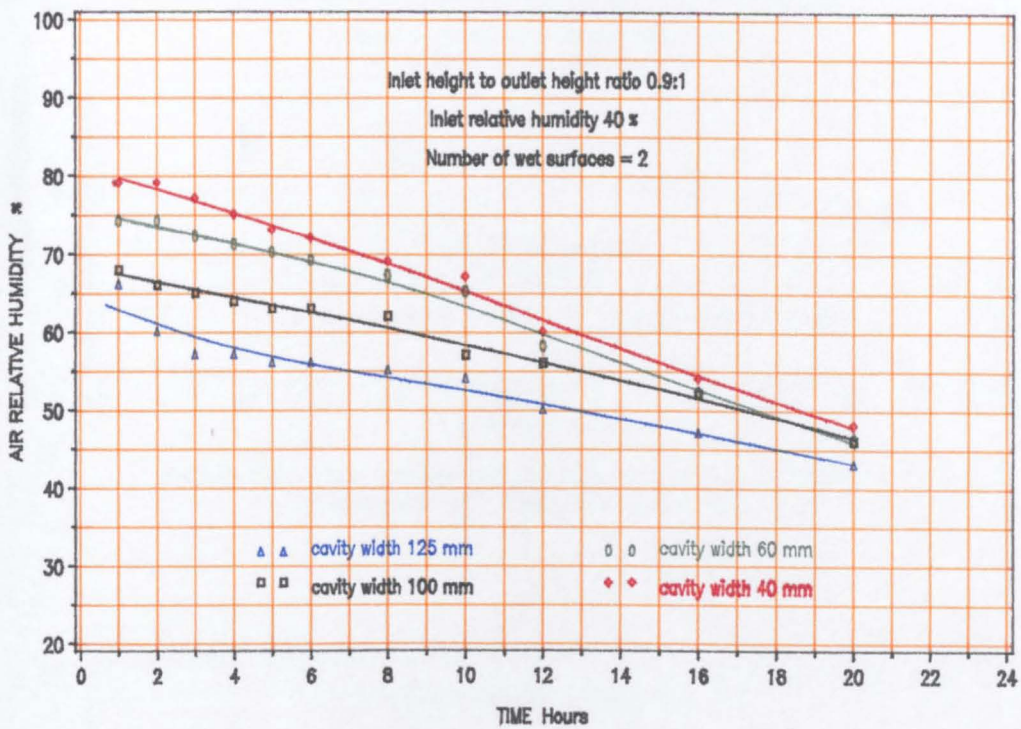


FIG 6.22 The effect of cavity width on air relative humidity at the outlet
(flow 0.12 kg/s)

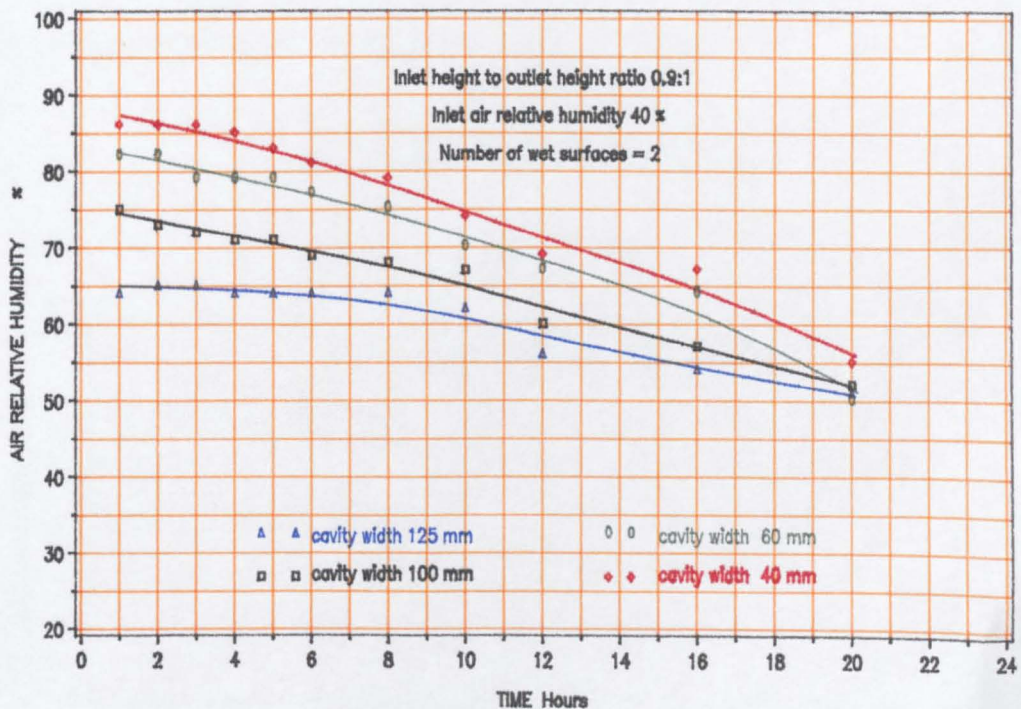


FIG 6.23 The effect of cavity width on air relative humidity at the outlet
(flow 0.06 kg/s)

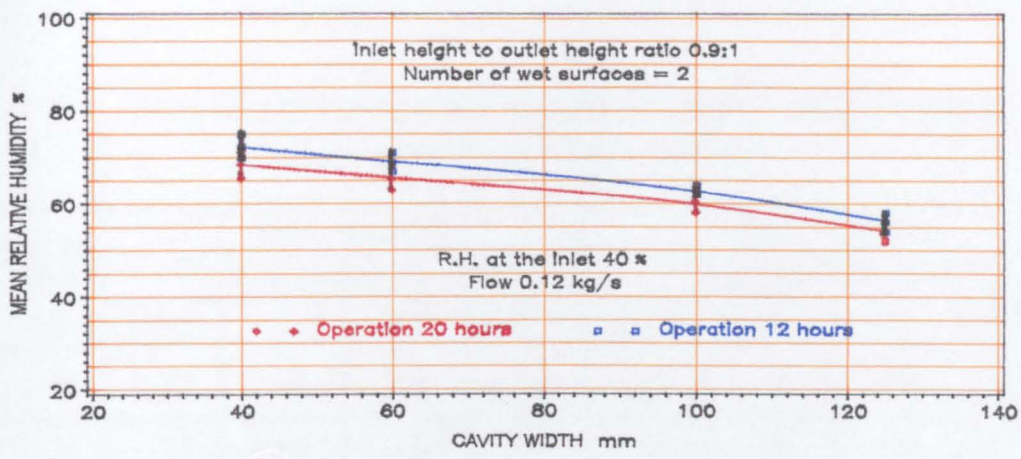


FIG.6.24 The effect of cavity width variation on the outlet air relative humidity

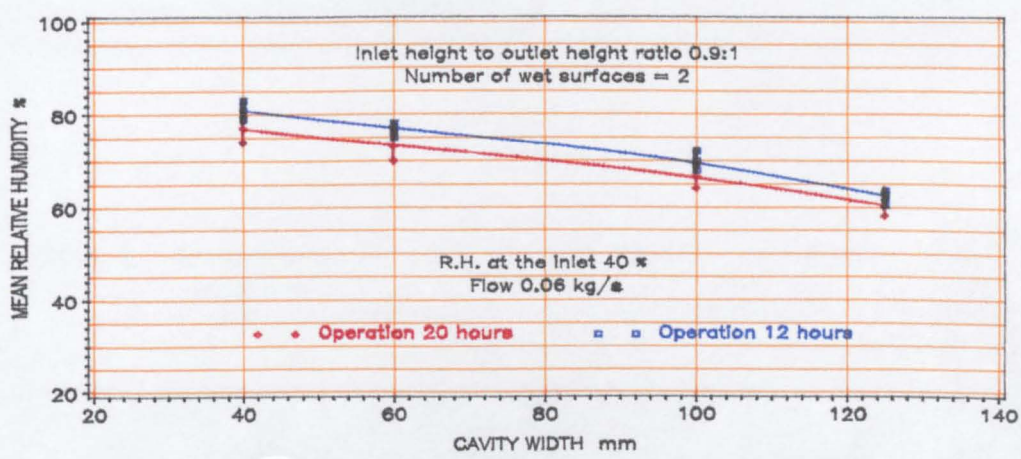


FIG.6.25 The effect of cavity width variation on the outlet air relative humidity

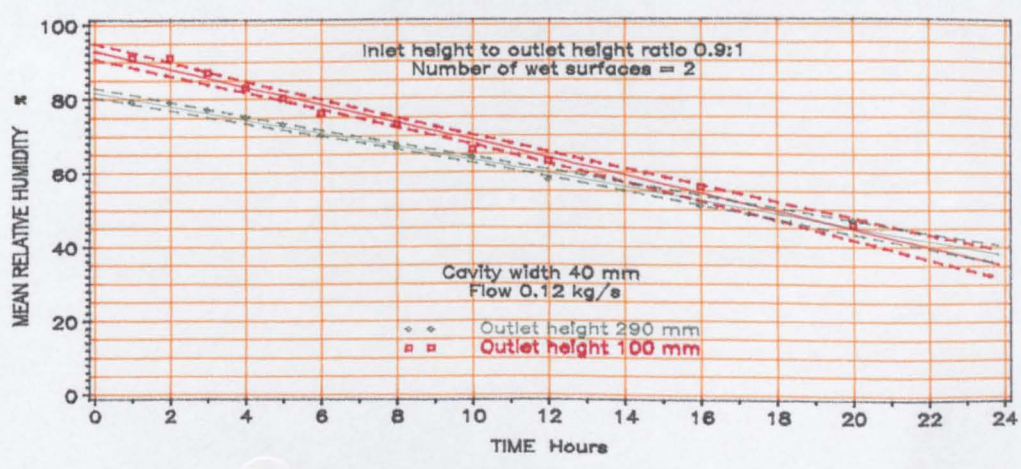


FIG 6.26 The effect of outlet height variation on mean air relative humidity

Table 6.7 Outlet air relative humidity at different operation periods.

Outlet air relative humidity %								
Cavity width mm	Flow 0.12kg/s				Flow 0.06kg/s			
	Test operation (hours)				Test operation (hours)			
	Initial	10	20	Diff.*%	Initial	10	20	Diff.*%
40	79	67	48	39	86	74	53	38
60	75	65	46	39	83	71	52	37
100	66	52	44	33	64	61	50	22
125	66	52	44	33	64	61	50	22

Average inlet air relative humidity $42 \pm 2\%$.

* Difference between initial and end of operation = $100 (1 - \text{R.H. at 20hours}/\text{initial R.H.})$

Table 6.8 Relative increase* of air relative humidity due to cavity width variations.

Cavity width mm	20 hours Operation				12 hours Operation			
	125	100	60	40	125	100	60	40
Flow 0.12kg/s								
Relative humidity %	54	60	65	69	56	63	69	73
Relative increase* %	100	111	120	128	100	113	123	130
Flow 0.06kg/s								
Relative humidity %	60	67	73	77	62	70	77	81
Relative increase* %	100	112	122	128	100	113	124	131

* Relative increase in relation to cavity width of 125mm

The average outlet air relative humidity is plotted against cavity width at different operation periods (Figures 6.24 and 6.25). The changes in outlet air relative humidity due to the cavity width variations was small (Figure 6.24). As cavity width decreased from 125mm to 40mm, the maximum increase of the average outlet air relative humidity was 18% (Figure 6.25). The measured outlet air relative humidity with the associated standard errors are shown in Figures 6.23 and 6.24. Analysis show that the standard errors of the mean were $\pm 3\%$ and $\pm 2\%$ with both flow rates, which were small and acceptable (Figures 6.17, 6.18 and Table 6.4).

6.4.5.2 The effect of the outlet height on relative humidity

Two tests were carried out with flow rate 0.12kg/s to measure the effect of outlet height on relative humidity. Heights of 290mm and 100mm were used. All parameters were maintained as before. Results are shown in Figure 6.26.

The outlet air relative humidity was a little greater when the height was reduced to 100mm. It was initially at 92% and 79% for the 100mm and 290mm respectively.

The average outlet air relative humidity after 20 hours of operation was 74% and 67% with the 100mm and the 290mm heights respectively. For lesser operation (such as of 12 hours), it was 76% and 70%. This indicates that the reduction of the outlet height from 290mm to 100mm increased the air relative humidity by 10%. This was probably because of the flow contraction at the bottom of the outlet and the increase of the velocity of the air (Figure 6.15). However, the effect of outlet height reduction in terms of air temperature drop between the inlet and the outlet is more important than that of the air relative humidity since the temperature error was about 7%.

6.4.6 Cooling

6.4.6.1 The effect of the cavity width on cooling

Results of the air temperature drop and relative humidity were used to determine cooling from evaporation for cavities 40mm, 60mm, 100mm and 125mm wide. Cooling from evaporation was established at two flow rates (0.06kg/s and 0.12kg/s). Analysis showed that the cooling increased as the width of the cavity decreased. The cooling per metre length was plotted against the operation period of tests (Figures 6.27 and 6.28). Both Figures show that cooling became less as the width of cavities

increased, and also with time. Cooling was initially greater than that at the end of each test operation. This was because of drying of the wet surfaces, and the change in the surface resistance to the flow of water vapour through the wet surface (as described above in chapter three). The decline rate of cooling with time is given in Table 6.9. Table 6.10 shows the percentage difference between cooling at the initial and the end of test operation, and Table 6.11 shows the relative increase of the cooling rate in relation to cavity width.

The observed average cooling per metre length and their standard errors with flow of 0.06kg/s and 0.12kg/s are shown in figures 6.29 and 6.30. Analysis showed that the standard errors of cooling with the flow of 0.12kg/s (20 and 12 hours operation) were about $\pm 6\%$ and $\pm 4\%$, and they were about $\pm 4\%$ and $\pm 3\%$ with the flow of 0.06kg/s respectively. The values of the standard errors and the average cooling are given above in Table 6.4.

Figures 6.29 and 6.30 show small changes of cooling when the cavity was reduced from 125mm to 100mm. Based on a 12 hours test operation, the increase was about 20W/m and 60W/m with flow of 0.06kg/s and 0.12kg/s respectively. When the cavity width was reduced from 100mm to 60mm, the average cooling (with flow of 0.12kg/s) increased from about 625W/m to 825W/m (20 hours operation) and from about 700W/m to 900W/m (12 hours operation). Further reduction of the cavity width to 40mm increased cooling by about 80W/m. In contrast, the width of the cavity shows little effect on increasing the average cooling with the flow of 0.06kg/s, except that of the 40mm. It increases cooling by 30W/m (Figure 6.30). This indicates that the reduction of the cavity width to 40mm with both air flows was advantageous in terms of increasing the average cooling, but still small.

6.4.6.2 The effect of outlet height on cooling

Two tests were carried out to measure the effect of outlet height on cooling. The heights were the same as above, and all the parameters were kept the same. Results are shown in Figure 6.31. The average cooling was determined by regressing the data over 20 hours. The relationship is approximated to be linear. The average cooling was 860W/m and 800W/m with outlet height of 100mm and 290mm respectively.

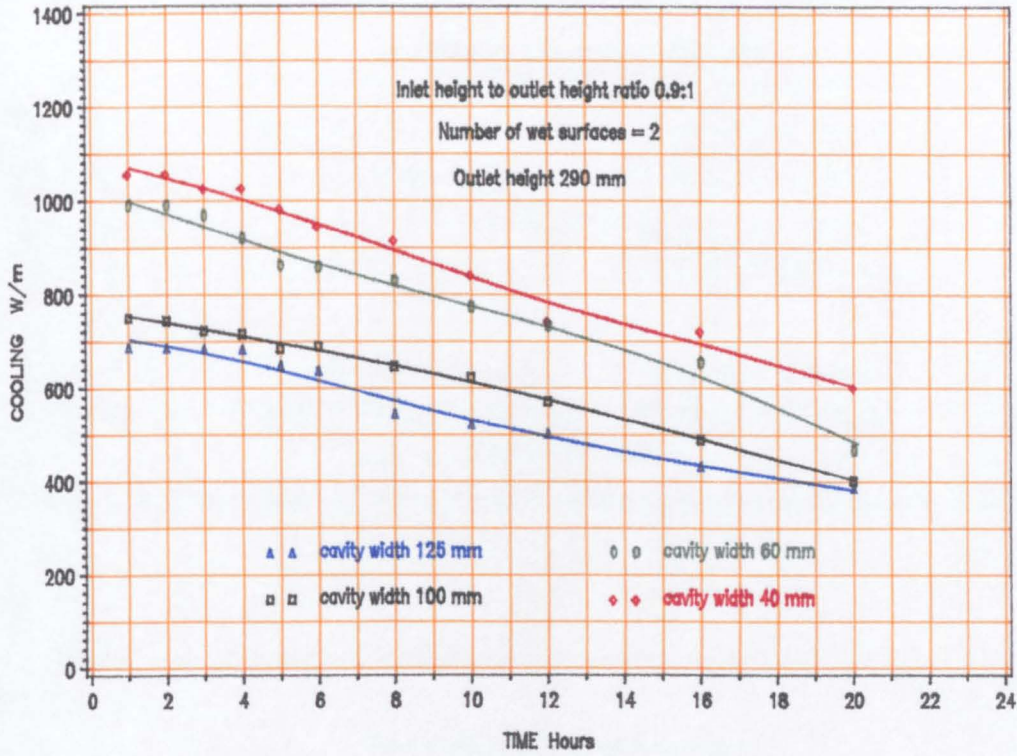


FIG 6.27 The effect of cavity width on cooling
(flow 0.12 kg/s)

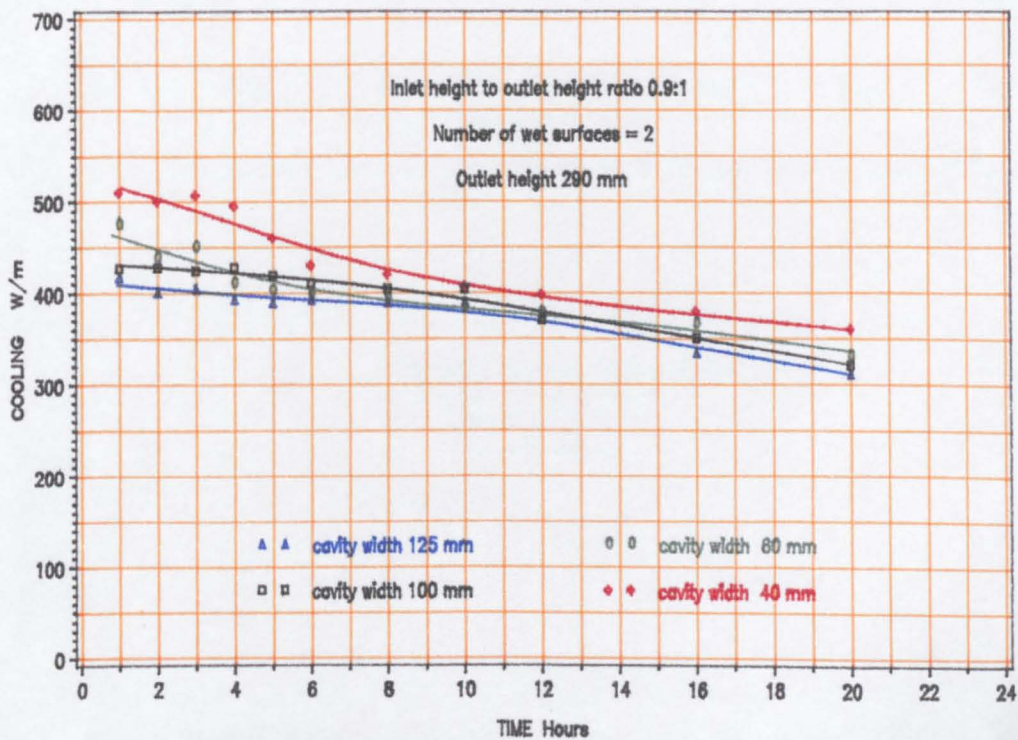


FIG 6.28 The effect of cavity width on cooling
(flow 0.06 kg/s)

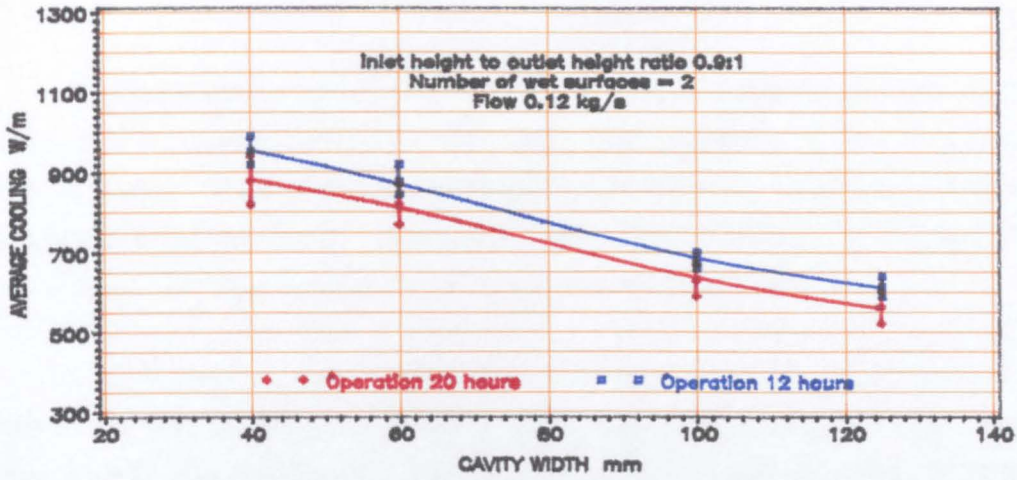


FIG.6.29 The effect of cavity width variation on the average cooling

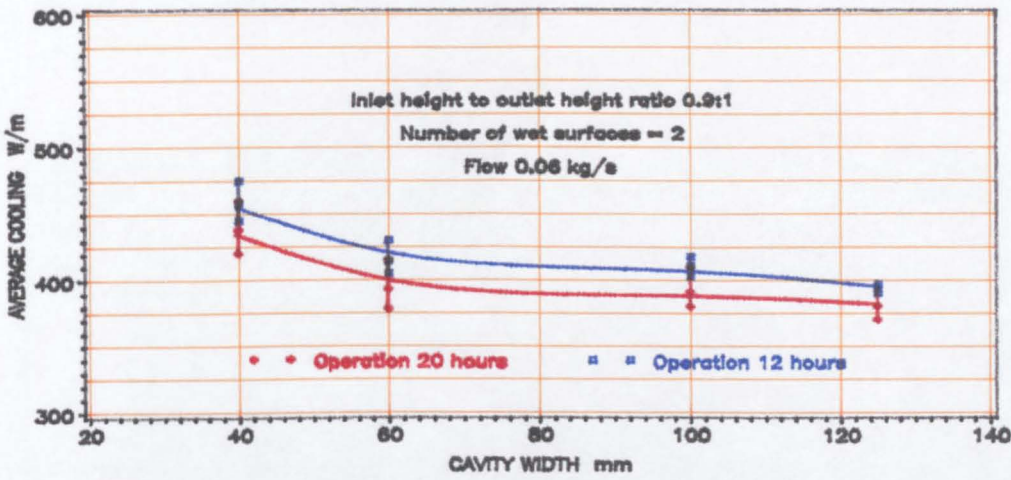


FIG.6.30 The effect of cavity width variation on the average cooling

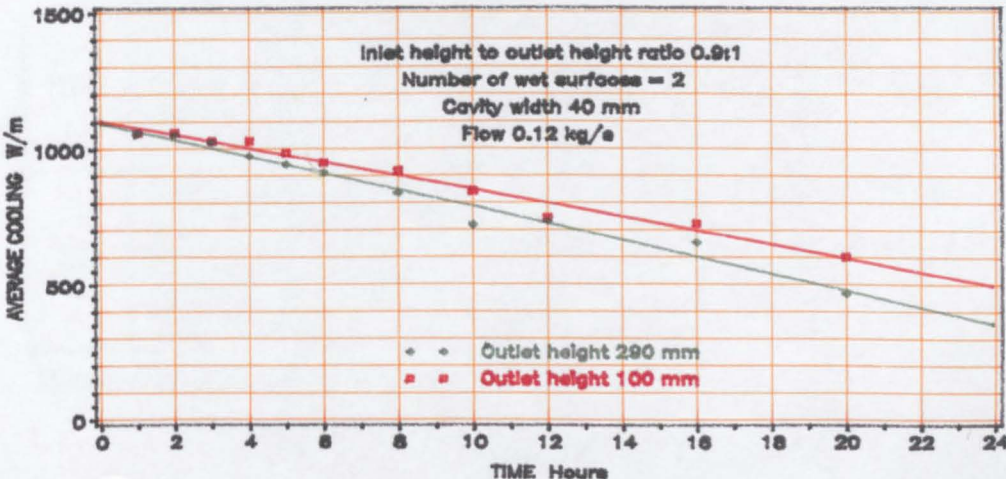


FIG 6.31 The effect of outlet height variation on the average cooling

The cooling decreased a little later during the first four hours with the 290mm outlet. The increase was of a 100W/m (13%). With exception of these data points, the trend in general was that cooling increased when the outlet height was reduced. This indicates that the assessment of the outlet height effect on average cooling could only be justified after four hours where the change in the trend occurred.

With regard to the standard error of $\pm 6\%$ with measured cooling (Table 6.4), the increase of cooling with the 290mm outlet height could be less if the error was encountered. Therefore, the reduction of the outlet height was advantageous in terms of increasing the rate of cooling. The significance of the outlet height reduction on cooling increases was less if compared with that of the air velocity. However, it confirms that of the velocity measurements (Figure 6.15).

Table 6.9 Rate of decline with measured cooling at different cavities.

Cavity width mm	Flow 0.12kg/s			Flow 0.06kg/s			
	Test operation (hours)			Test operation (hours)			
	Initial	10	20	Initial	10	20	
40	Cooling W/m	1050	850	600	520	420	325
	Drop W/m	200	250		100	95	
	Relative decline* %	100	81	57	100	81	62.5
	Decline %/h	1.9	2.4		1.9	1.85	
60	Cooling W/m	1000	780	500	475	390	330
	Drop W/m	220	280		85	60	
	Relative decline* %	100	78	50	100	82	69
	Decline %/h	2.2	2.8		1.8	1.3	
100	Cooling W/m	740	620	420	425	380	320
	Drop W/m	120	200		45	60	
	Relative decline* %	100	84	57	100	89	75
	Decline %/h	1.6	2.7		1.1	1.4	
125	Cooling W/m	690	530	390	415	370	320
	Drop W/m	160	140		45	50	
	Relative decline* %	100	77	56.5	100	89	77
	Decline %/h	2.3	2.1		1.1	1.2	

*Relative decline=[(cooling at 10h x 100)/ intial cooling].

Table 6.10 Cooling rate with different operation periods.

Cavity width mm	Cooling rate W/m							
	Flow 0.12kg/s				Flow 0.06kg/s			
	Test operation (hours)				Test operation (hours)			
	Initial	10	20	Diff.* %	Initial	10	20	Diff.* %
40	1050	850	600	43	520	420	325	38
60	1000	780	500	50	475	390	330	31
100	740	620	420	43	425	380	320	25
125	690	530	390	43	415	370	320	23

* Difference between initial and end of operation = $100 [1 - (\text{cooling at 20hours}/\text{initial cooling})]$

Table 6.11 Relative increase* of cooling due to cavity width variation

Cavity width mm	20 hours Operation				12 hours Operation			
	125	100	60	40	125	100	60	40
	Flow 0.12kg/s							
Cooling rate W/m	563	627	820	878	614	680	877	954
Relative increase* %	100	111	146	156	100	111	143	155
	Flow 0.06kg/s							
Cooling rate W/m	380	392	393	438	394	411	414	459
Relative increase* %	100	103	103	115	100	104	104	118

* Relative increase in relation to cavity width of 125mm.

6.4.7 Further analysis

The above results indicate a decrease with time of the air temperature drop between the inlet and outlet; the increase of the air relative humidity at the outlet; and cooling. Evaporation is the main cause for cooling, and therefore, it is important to study the rate of evaporation. The rate of evaporation depends on: the difference between the water vapour (moisture content) in the saturated boundary layer and that in the incoming air, and the convective heat transfer coefficient. The first is known as 'the difference in humidity ratio' (Δg). The larger the difference in humidity ratio the greater the rate of evaporation when the convective heat transfer coefficient is assumed to be constant.

6.4.7.1 The difference in the humidity ratio

Difference in the humidity ratio between the saturated boundary layer and the incoming air was calculated as described in chapter five. Results are shown in Figures 6.32 and 6.33. The difference in the humidity ratio between the saturated boundary layer and the incoming air decreased with time. This indicates that the variation pattern seems unsteady. However, the rate of decrease was almost constant with time. Figure 6.33 shows the measured average difference in the humidity ratio when the air flow was 0.06kg/s. With 10mm wet mat separation (40mm width), it was greater than with the 17mm, 30mm and 40mm separation. It was less than those with the 30mm and 40mm separation with flow 0.12kg/s (Figure 6.32).

Analysis showed that changes of the difference in the humidity ratio between the saturated boundary layer and the incoming air with time could be negligible since the maximum changes are almost equal to or less than that of the error which may accompany the calculated humidity ratio of the incoming air. For example: due to a $\pm 1\text{K}$ error of the temperature of the incoming air into the cavity at 30°C and 40% air relative humidity, the error with the difference in the humidity ratio was $0.0006\text{kg}_{\text{w.v.}}/\text{kg}_{\text{dryair}}$. It could be higher ($0.001\text{kg}_{\text{w.v.}}/\text{kg}_{\text{dryair}}$) when the error of the air relative humidity was also considered. However, the maximum changes with wet surface separation of the 40mm and 60mm cavity were 0.0011 and $0.0009\text{kg}_{\text{w.v.}}/\text{kg}_{\text{dryair}}$ with air flow of 0.06kg/s, and 0.00097 and $0.005\text{kg}_{\text{w.v.}}/\text{kg}_{\text{dryair}}$ with air flow of 0.12kg/s respectively.

When the changes of the difference in the humidity ratio with air flow of 0.06kg/s were compared with the above errors, they show that the error associated with a $\pm 1\text{K}$ of the temperature of the incoming air and $\pm 2\%$ of the relative humidity were equal to the maximum changes. The regression analysis of the data showed that the relation between the changes of the difference in the humidity ratio with time was linear (Figure 6.34 and Figure 6.35). The regression coefficients were 0.91 and 0.93 ($P > 0.0001$). It was found that the maximum variation from the line of regression yielded a difference in the humidity ratio of the order of $0.0005\text{kg}_{\text{w.v}}/\text{kg}_{\text{dry air}}$, and this could be a result of $\pm 0.5\text{K}$ error with the temperature of the incoming air. This indicates that discrepancy along the regression line is acceptable and the relationship show that the rate of change of the difference in the humidity ratio between the saturated boundary layer and the incoming air with time is almost constant. This suggests that the changes of the difference in the humidity ratio can be assumed as a steady state, and thus a mean value of the difference in the humidity ratio was taken.

6.4.7.2 The effect of wet mat separation on the difference in the humidity ratio

The difference in the humidity ratio was affected by the wet mats separation (Figures 6.34 and 6.35). The average difference in the humidity ratio increased when the separation between wet surfaces was decreased. It was greater with the 10mm separation $0.0018\text{kg}_{\text{w.v}}/\text{kg}_{\text{dry air}}$, and decreased with the 40mm separation to $0.00045\text{kg}_{\text{w.v}}/\text{kg}_{\text{dry air}}$. In contrast, the difference in the humidity ratio with air flow of 0.12kg/s was less with the separation of 10mm and 16mm than that of the 30mm. It was $0.0005\text{kg}_{\text{w.v}}/\text{kg}_{\text{dry air}}$ and $0.00035\text{kg}_{\text{w.v}}/\text{kg}_{\text{dry air}}$ with the 10mm and 16mm, and $0.001\text{kg}_{\text{w.v}}/\text{kg}_{\text{dry air}}$ with the 30mm respectively.

The average partial pressure of both the incoming air and the saturated boundary layer with air flow of 0.06kg/s and 0.12kg/s are shown in Figure 6.36. With air flow of 0.06kg/s, the partial pressure of both the incoming air and the saturated boundary layer adjacent to the wet surface increased as the wet surface separation decreased. Figure 6.36 shows that the difference also increased with the separation reduction.

When the changes of the difference in the humidity ratio with air flow of 0.06kg/s were compared with the above errors, they show that the error associated with a $\pm 1\text{K}$ of the temperature of the incoming air and $\pm 2\%$ of the relative humidity were equal to the maximum changes. The regression analysis of the data showed that the relation between the changes of the difference in the humidity ratio with time was linear (Figure 6.34 and Figure 6.35). The regression coefficients were 0.91 and 0.93 ($P > 0.0001$). It was found that the maximum variation from the line of regression yielded a difference in the humidity ratio of the order of $0.0005\text{kg}_{\text{w.v}}/\text{kg}_{\text{dry air}}$, and this could be a result of $\pm 0.5\text{K}$ error with the temperature of the incoming air. This indicates that discrepancy along the regression line is acceptable and the relationship show that the rate of change of the difference in the humidity ratio between the saturated boundary layer and the incoming air with time is almost constant. This suggests that the changes of the difference in the humidity ratio can be assumed as a steady state, and thus a mean value of the difference in the humidity ratio was taken.

6.4.7.2 The effect of wet mat separation on the difference in the humidity ratio

The difference in the humidity ratio was affected by the wet mats separation (Figures 6.34 and 6.35). The average difference in the humidity ratio increased when the separation between wet surfaces was decreased. It was greater with the 10mm separation $0.0018\text{kg}_{\text{w.v}}/\text{kg}_{\text{dry air}}$, and decreased with the 40mm separation to $0.00045\text{kg}_{\text{w.v}}/\text{kg}_{\text{dry air}}$. In contrast, the difference in the humidity ratio with air flow of 0.12kg/s was less with the separation of 10mm and 16mm than that of the 30mm. It was $0.0005\text{kg}_{\text{w.v}}/\text{kg}_{\text{dry air}}$ and $0.00035\text{kg}_{\text{w.v}}/\text{kg}_{\text{dry air}}$ with the 10mm and 16mm, and $0.001\text{kg}_{\text{w.v}}/\text{kg}_{\text{dry air}}$ with the 30mm respectively.

The average partial pressure of both the incoming air and the saturated boundary layer with air flow of 0.06kg/s and 0.12kg/s are shown in Figure 6.36. With air flow of 0.06kg/s, the partial pressure of both the incoming air and the saturated boundary layer adjacent to the wet surface increased as the wet surface separation decreased. Figure 6.36 shows that the difference also increased with the separation reduction.

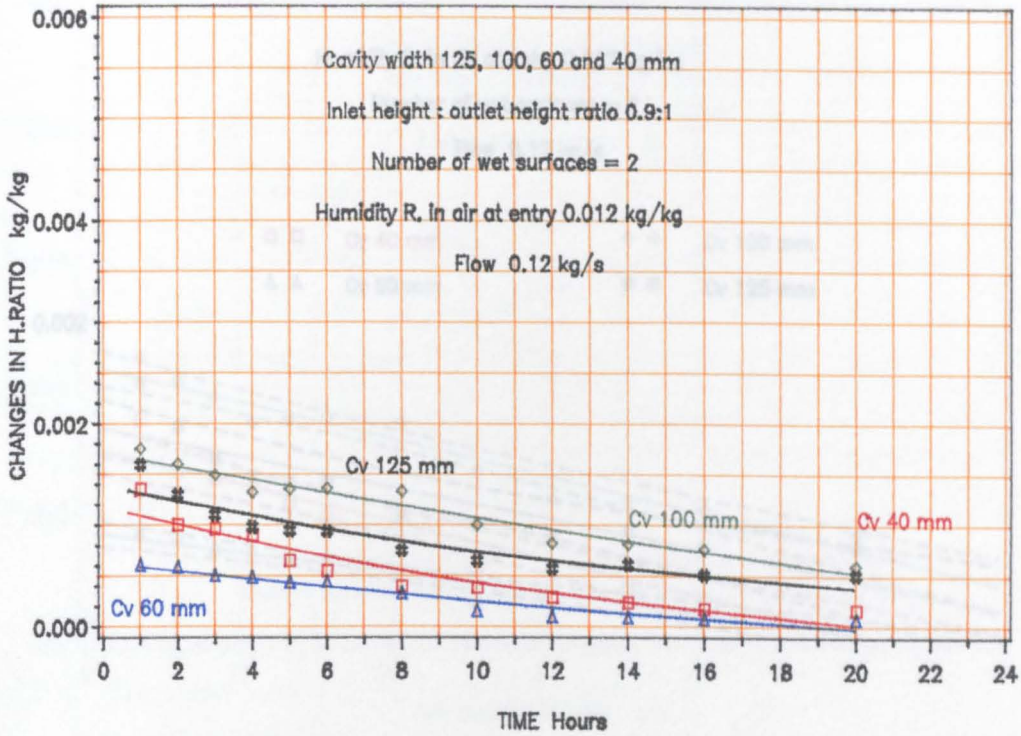


FIG 6.32 The changes of humidity ratio with time for different cavity width
Spacing between wet Surfaces 10, 17, 30 and 40 mm

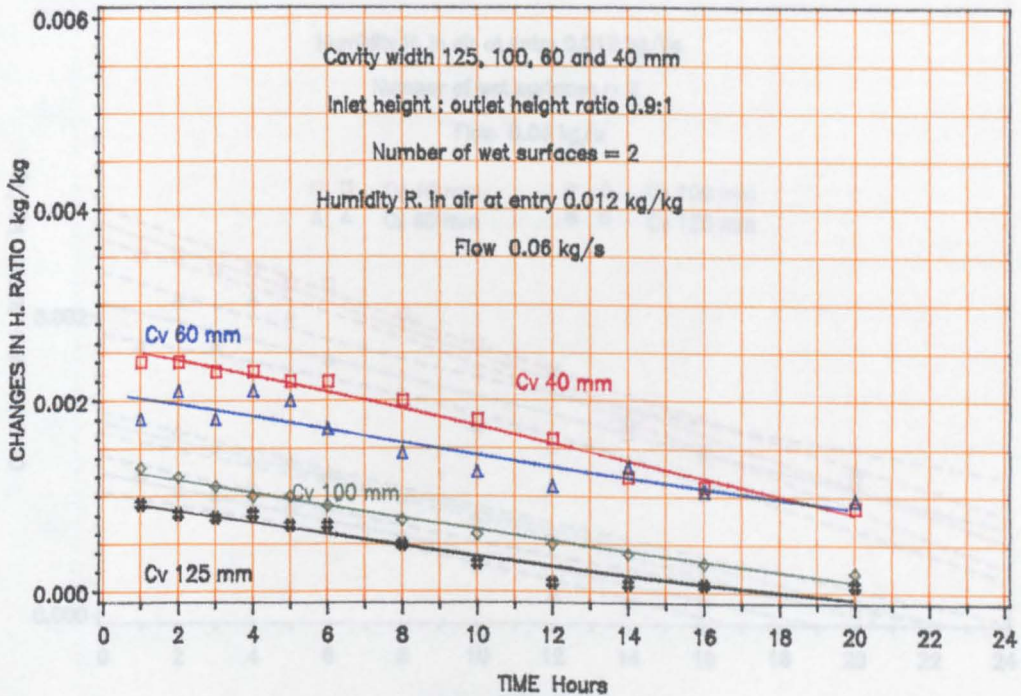


FIG 6.33 The changes of humidity ratio with time for different cavity width
Spacing between wet surfaces 10, 17, 30 and 40 mm

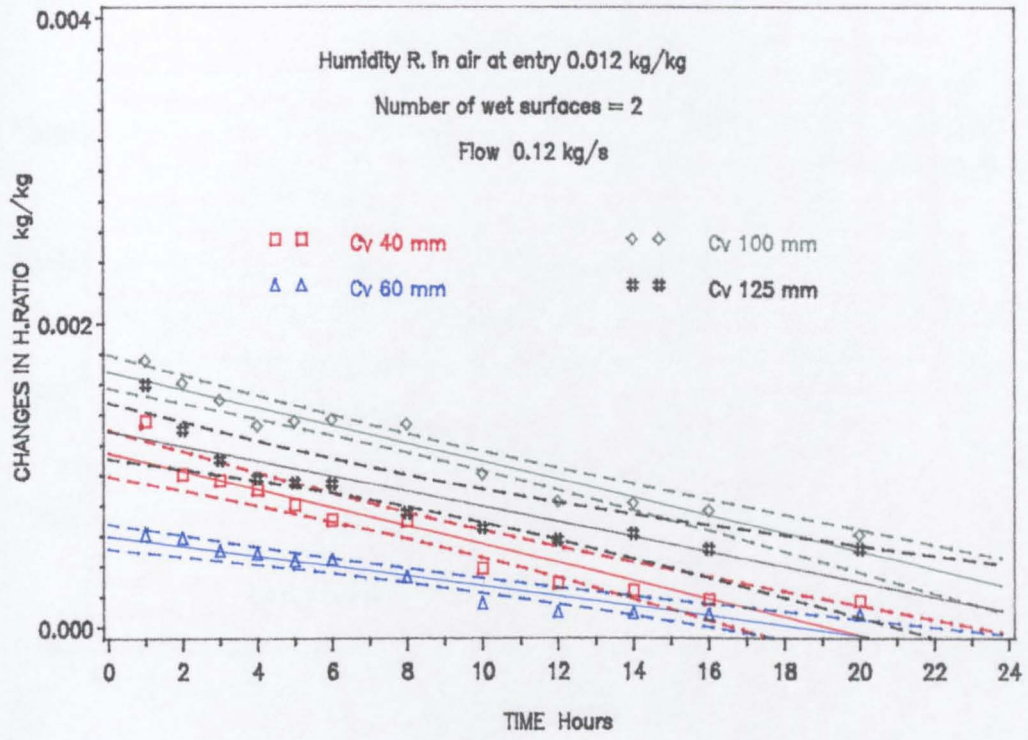


FIG (6.34) The relation between the changes of humidity ratio with time
Spacing between wet Surfaces 10, 17, 30 and 40 mm

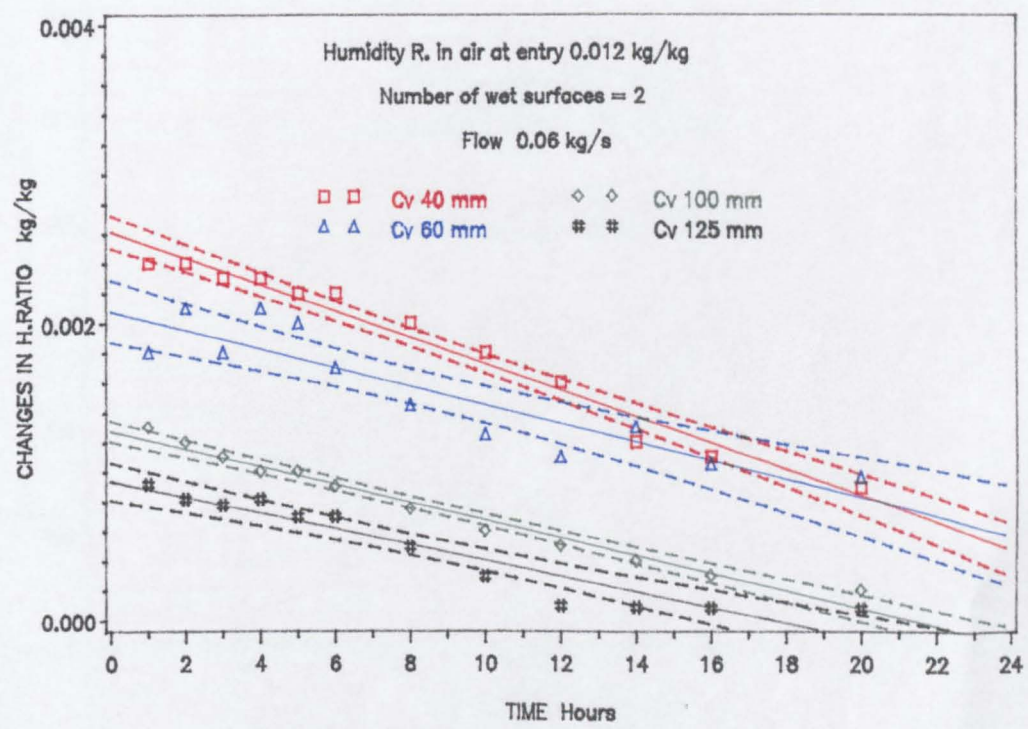


FIG (6.35) The relation between the changes of humidity ratio with time
Spacing between wet Surfaces 10, 17, 30 and 40 mm

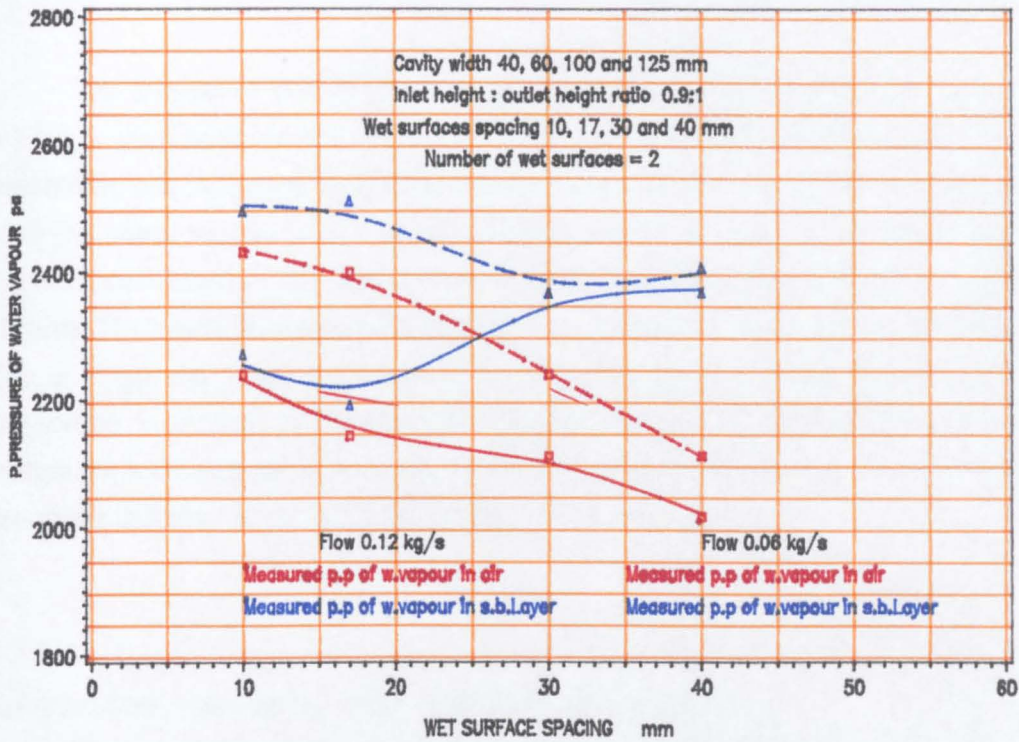


FIG 6.36 The effect of wet surface spacing on the partial pressure of water vapour

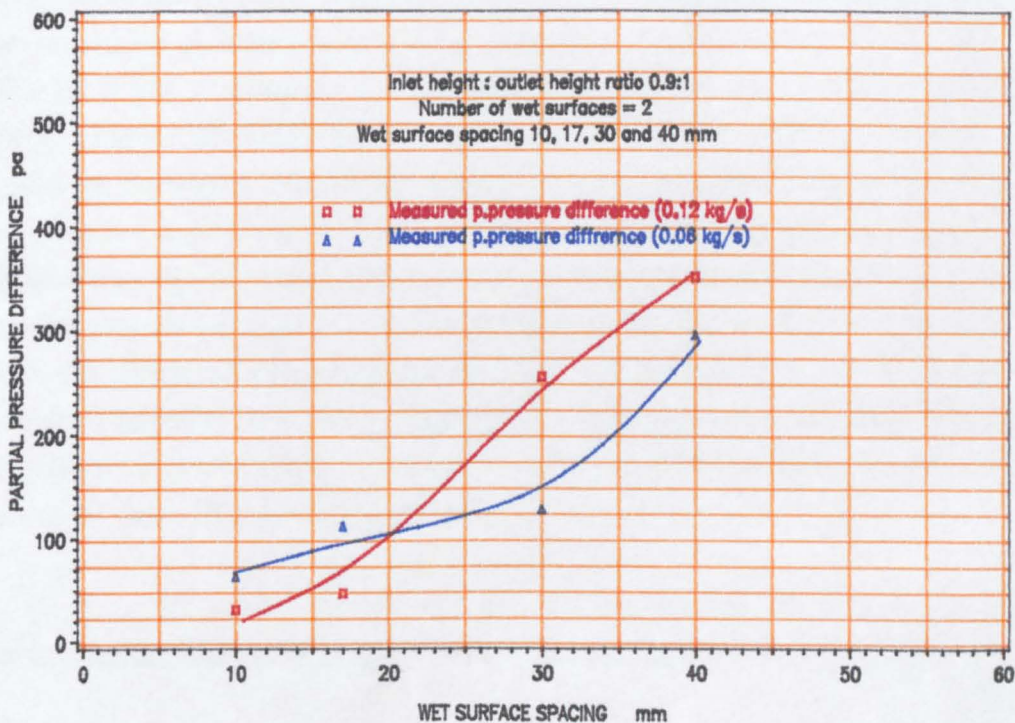


FIG 6.37 The Effect of wet surfaces spacing on partial pressure difference between the air and wet surface

The measured partial pressure in the incoming air at the inlet with flow of 0.12kg/s increased as the separation decreased (about 2000Pa with the 40mm separation, and increased by 200Pa with separation of 10mm). There were little changes with the water vapour of the saturated boundary layer. The difference of the partial pressure decreased as the wet surface spacing decreased (from 40mm to 30, 16, and 10mm). The smallest measured difference was 32Pa with 10mm separation (Figure 36). The average measured difference of the partial pressure difference in relation to separation is plotted in Figure 6.37. The above analysis indicates that the rate of evaporation decreased as a result of the decrease of the partial pressure difference assuming that the convective heat transfer is constant.

6.4.7.3 The convective heat transfer coefficient

The rate of evaporation not only depends on the humidity ratio difference between the saturated boundary layer and incoming air at the inlet, but also on the convective heat transfer coefficient (eqn.3.24 , chapter three). Observations show that with air flow rates of 0.06kg/s and 0.12kg/s, the convective heat transfer coefficient increased as the wet surface separation decreased. For air flow of 0.06kg/s, the increase was small compared with that of the 0.12kg/s. Figure 6.38 shows that it increased from 5.7 to 6.5W/m²K as the separation decreased from 40mm to 10mm, and from 6.8 to 11.8W/m²K (with the flow 0.12kg/s) respectively. The increase of the surface mass transfer coefficient due to the spacing variation is shown in Figure 6.39. This indicates that the rate of evaporation could be increased due to the above increase. However, the calculated rate of evaporation according to eqn.3.19 using the above data showed that the rate of evaporation was decreased. The average rate of evaporation as a result of the reduction of wet surfaces separation is plotted in Figure 6.40. In general, the rate of evaporation with the 10mm separation depends on the difference in the humidity ratio between the saturated boundary layer and the incoming air more than that of the surface mass transfer coefficient since the slope of the rate of evaporation and the humidity difference were about the same (Figures 6.37 and 6.40).

The data were regressed and the relation between the surface mass transfer coefficient and the rate of evaporation was linear (Figures 6.41 and 6.42).

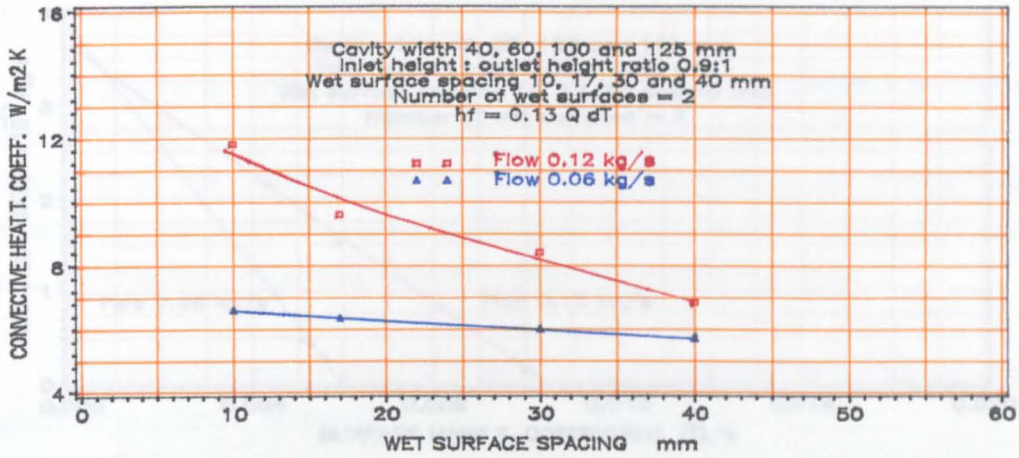


FIG 6.38 The effect of wet surfaces spacing on the convective heat transfer coefficient

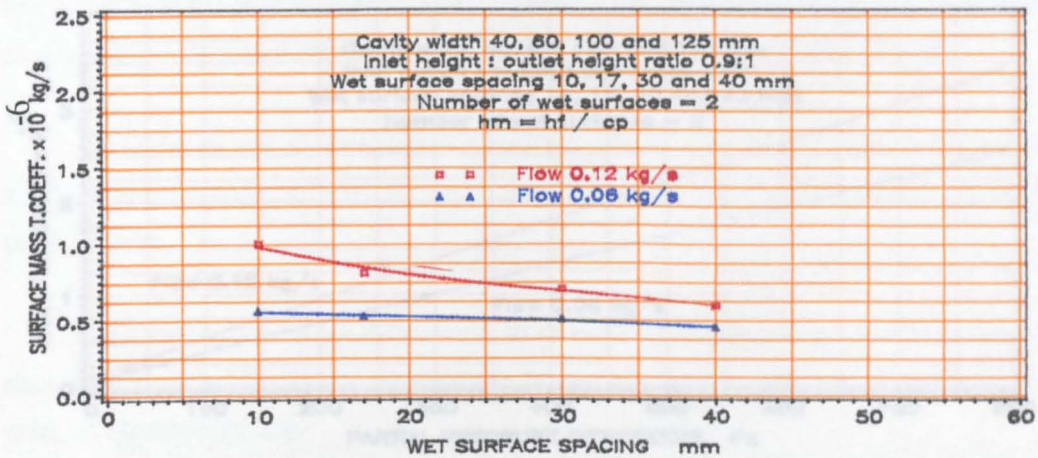


FIG 6.39 The effect of wet surfaces spacing on the surface mass transfer coefficient

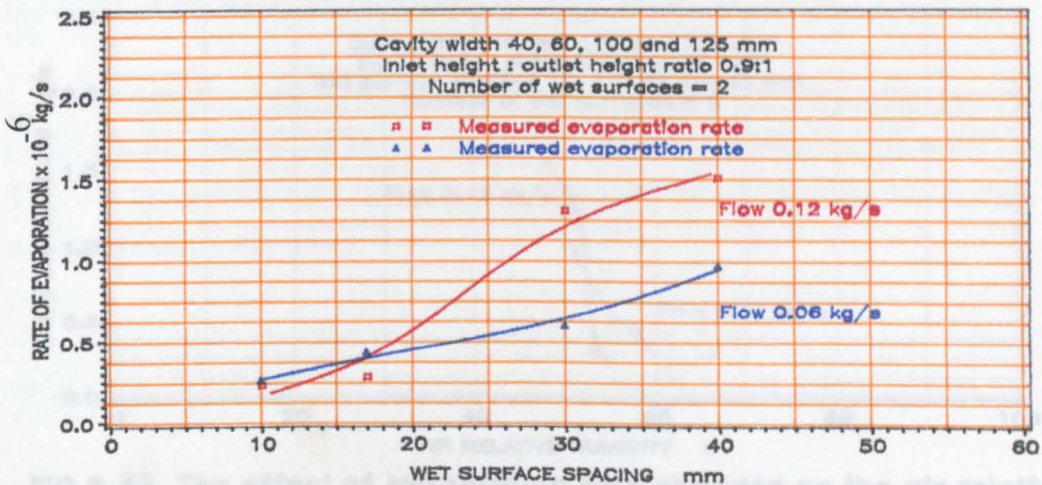


FIG 6.40 The effect of wet surfaces spacing on the evaporation rate

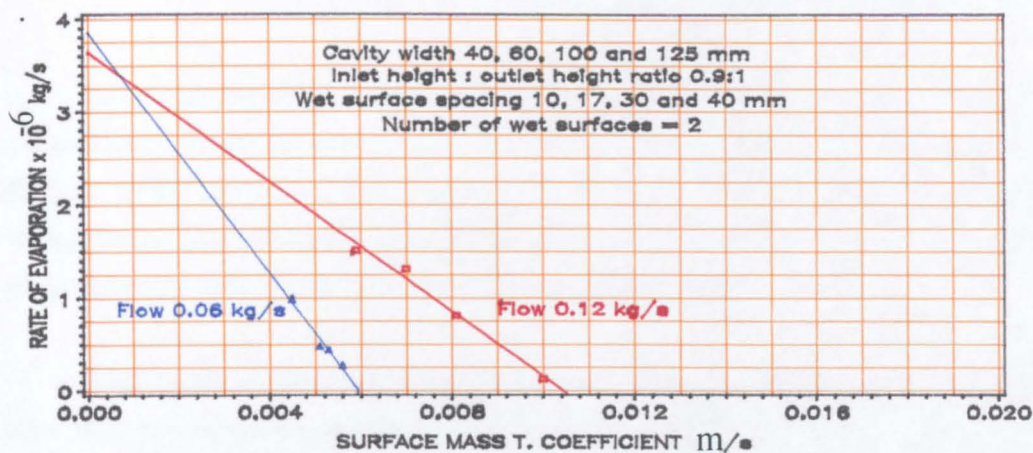


FIG 6.41 The effect of the surface mass transfer coefficient on evaporation rate

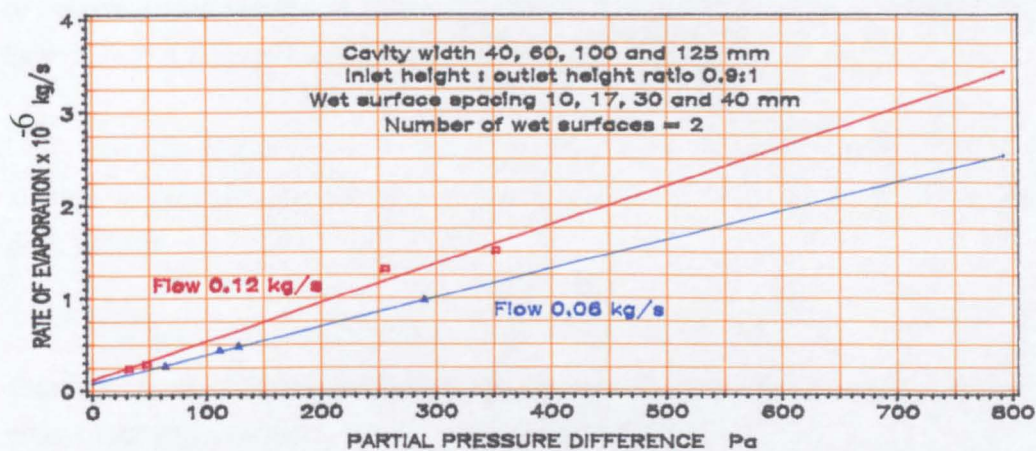


FIG 6.42 The effect of the partial pressure difference on evaporation rate

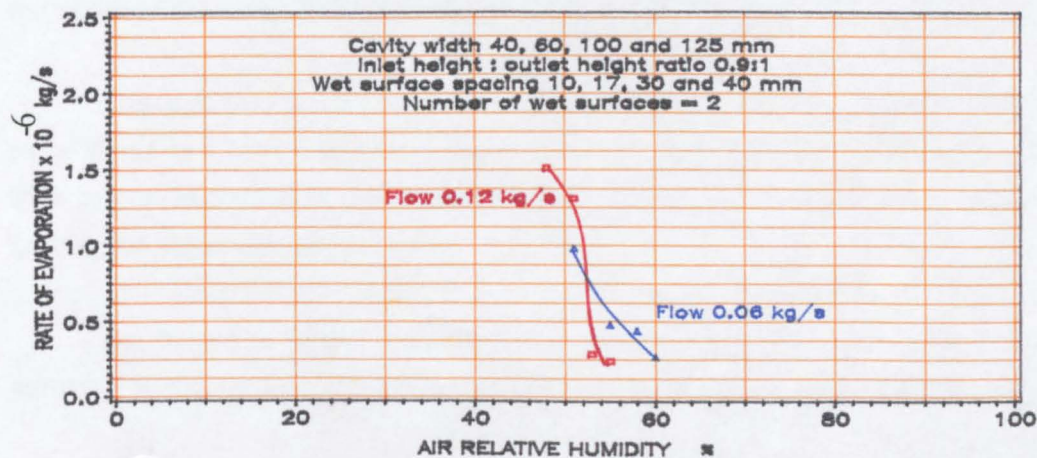


FIG 6.43 The effect of evaporation rate changes on the air relative humidity in the cavity

Although the above analysis shows that the rate of evaporation decreased, the air relative humidity in the cavity increased, but was small (Figure 6.43). It increased from 49% to 55% (air flow of 0.12kg/s), and from 53% to 60% (air flow of 0.06kg/s) respectively. This increase may be explained by the increase of the saturation within the air as the separation decreased, especially with the 10mm and 16mm.

The above suggests that the difference in the humidity ratio was an important parameter to promote evaporation

6.8 DISCUSSION AND CONCLUSION

Preliminary tests used to check the pattern of air flow across the cavity enabled us to determine the width of the cavity in which air flow is uniform. Air flow across the cavity shows a non-uniform profile with cavity widths greater than 125mm.

In order to use an 'evaporative cooling cavity' (about 2m high) with fan-assisted air flow to promote cool ventilation in dwellings, the width of the cavity should be less than 125mm.

The use of enthalpy difference to determine the cooling rate from evaporation should be done with care because of the large error which may occur resulting from the error of air temperature.

The wet mat separation within the 100mm cavity width shows the significance of the area of evaporation on air temperature drop, the increase in the relative humidity of air at the outlet and cooling, and suggests the best arrangement (two wet mats, dividing the width of the cavity into three air gaps, Figures 6.10 and 6.11).

Although the rate of evaporation decreased as the wet surface separation reduced from 30mm to 17mm and 10mm, the relative humidity of the air at the outlet increased. This can be explained by the removal of the saturated air near the wet surface by the moving air inside the cavity.

The height of outlet is an important parameter in determining the average air velocity at the outlet. The reduction of the outlet height from 290mm to 100mm

increased the average air velocity from 0.29m/s to 0.7m/s (Figure 6.15). When the outlet height (290mm) is greater than the cavity width, its width becomes also important. The decrease of the cavity width from 60mm to 40mm increases the velocity of the air at the outlet from 0.12m/s to 0.36m/s (Figure 6.16).

Measurements show that the use of an 'evaporative cooling cavity' with fan-assisted air flow can reduce the temperature of the incoming air by an average of the order of 7K (from 30°C to 23°C), if the air flow in the cavity (40mm or 60mm) is 0.06kg/s or 0.12kg/s, and incorporate two vertical wet mats (Figure 6.11).

The reduction of the cavity width from 125mm to 100mm, 60mm and 40mm (with air flow of 0.06kg/s) shows little changes of the measured mean air temperature drop between the inlet and the outlet. This was probably due to the small changes in the convective and surface mass transfer coefficient (Figures 6.41 and 6.42). In cavities with air flow of 0.12kg/s, the reduction of the cavity width (as above) increases the mean air temperature drop by 2K (if the cavity is operated for a lengthy period of 20 hours). With shorter operation (12 hours), the above temperature drop could be increased to 3K. This increase may be related to the increase of the surface mass transfer coefficient from 0.006 to 0.01 m/s (Figure 6.39).

With air flow rates of 0.06 and 0.12kg/s, the air temperature drop, relative humidity and cooling decreased with time. This could be explained by the constant decrease of the difference in the humidity ratio (Figures 6.32 and 6.33). The decrease of the difference in the humidity ratio is caused by the surface resistance to the flow of water vapour diffusing through the wet surface. However, when a slice (one mm thick) of a wet surface is no longer wet, the diffusion of water vapour through that layer may be reduced hence the difference in the humidity ratio difference between the saturated boundary layer and the incoming air. In practice, it is not always the case.

The changes of the difference in the humidity ratio (Δg) with time showed that the pattern was in fact unsteady state, but the decrease of the difference in humidity ratio (Δg) between the saturated boundary layer and the incoming air into the cavity with time showed a linear relationship (Figure 6.34 and 6.35). These changes with time were too

small, and could be equal to an error of $\pm 0.5\text{K}$ and $\pm 2\%$ with the temperature and relative humidity of the incoming air respectively. This indicates that the changes could be negligible, and therefore, the above changes could be assumed as a steady state.

The reduction of the cavity width from 125mm to 40mm increases the average outlet air relative humidity by 15% (from 52% to 67%) with air flow of flow 0.12kg/s, and 13% (from 61% to 74%) with air flow of 0.06kg/s respectively. The outlet air relative humidity was greater with air flow of 0.06kg/s than of the 0.12kg/s because of the increase of the difference in the humidity ratio by double (from 0.0002 to 0.0004kg_{w.v}/kg_{dry air}).

The reduction of the cavity width shows little significance in increasing the rate of cooling with the air flow of 0.06kg/s. This can be related to the small increase of the convective heat transfer coefficient (Figures 6.38 and 6.39), and the decrease of the rate of evaporation as a direct effect of the reduction of the difference in the humidity ratio (Figure 6.40). Nevertheless, the decrease of the cavity width from 100mm to 60mm shows a constant cooling (Table 6.10), which can be explained by the small changes of the convective heat transfer coefficient (Figure 6.38), and that of the difference in the humidity ratio.

Although the difference of the humidity ratio between saturated boundary layer and the incoming air was greater with the 125mm cavity than that with the 40mm, the relative increase of cooling is slightly small. This may be related to the small change with the convective heat transfer coefficient.

The air temperature drop and the relative humidity increase resulting from evaporation using cavity widths of 40mm and 60mm, indicate that comfort can be achieved (Figure 6.44). Fitzgerald and Houghton-Evans (1987) indicate that with air relative humidity approaching saturation using ASHRAE 'Comfort' chart (1985) comfort could be achieved, and therefore, the above values are far from saturation.

The optimum width of the 'evaporative cooling cavity' to maximize cooling from evaporation is that of the 40mm wide with fan-assisted air flow of 0.12kg/s. It provides cooling of the order of 1kW/m resulting from a temperature drop of the incoming air of

the order of 8K (from 30°C to 23°C), and a maximum outlet air relative humidity increase of 40% to enter the dwelling at 80%, and moving air at velocity of 0.7m/sm through an outlet 100mm high, if water within the wet surfaces is maintained. However, a cavity 60mm wide can be used with less satisfaction, but remains acceptable.

As evaporation continued water vapour within the wet mats becomes less, and therefore cooling can be reduced to an average of about 850W/m (after 10 hours operation). To ensure that the cooling will remain at 1kW/m, water vapour should be maintained within the wet surfaces.

The above arrangement using eqn.3.14 given by Abrams (1985) yielded a "Saturation Efficiency" SE of 80% which agrees well with that recommended by Sodha et al. (1986).

The difference in the humidity ratio suggests that water vapour removed by evaporation is about $16 \times 10^{-4} \text{kg}_{w,v}/\text{kg}_{\text{dryair}}$ (Figure 6.34). With air flow rate 0.12kg/s, the amount of water vapour becomes $8 \times 10^{-5} \text{kg}_{w,v}/\text{s}$. This indicates that the water vapour required to maintain cooling near 1kW/m is of the order of $3.5 \times 10^{-2} \text{kg}_{w,v}/\text{h}$.

The results obtained compare well with that given by Givoni (1984). As mentioned above (chapter one), Givoni (1984) suggested an acceptable air velocity up to 1.0m/s into dwellings to provide comfort in hot arid climates. The air velocity at the outlet of 0.7m/sm with fan-assisted air flow is near the above.

The resultant temperature T_{res} of eqn.1.4 according to Nicol (1975) at air velocity of 0.25 m/s becomes:

$$T_{\text{res}} = 0.39 T_{\text{mr}} + 0.61 T_{\text{ai}}$$

The influence of the mean radiant temperature is reduced as the velocity increased. Assuming that the mean radiant temperature 40°C and outside air temperature 35°C, without air motion, the resultant temperature in the room will be about 37°C which is above the comfort limit (32°C to 36°C) given by Nicol (1975). When an 'evaporative

cooling cavity' is attached to the room, the outside air can be cooled and drop to 27°C. With the above mean radiant temperature, the resultant temperature in the room will be lowered to 32°C (below Nicol's limits). As air in the room is cooled, the mean radiant temperature of the surroundings may drop to 35°C, and therefore the resultant temperature becomes 30°C which is comfortable in hot arid climates.

The 'evaporative cooling cavity' 40mm wide suggests that if the incoming air in hot arid climates is about 40% and 30°C, the amount of water vapour which will be added to the air flowing into a room in a dwelling can be of the order of 0.0022kg_{w.v}/s (Table 6.11), about half the suggested by the 'bioclimatic' analysis of Cairo (chapter one). If the incoming air is at low relative humidity (30%), water vapour in the air can be higher (0.005kg_{w.v}/s), enough to bring the outside dry air to be moist according to the target suggested above by the bioclimatic analysis of Cairo without causing thermal discomfort for the occupants inside dwellings. When outside air during summer is below 30% (Table 1.2), evaporation potential could be higher. Assuming the same increase of the outlet air relative humidity and the drop of air temperature, the above value will be increased to 0.008kg_{w.v}/s which satisfied both zone 2 and 3 (Table 1.6), but less than that of zone 4.

Table 6.11 Suggested water vapour 'moisture content' added to the air flowing into dwelling from an 'evaporative cooling cavity'.

cavity width	Flow of 0.06 kg/sm					Flow of 0.12kg/sm			
	g (inlet)	ΔT	R.H. (outlet)	g (outlet)	Δg	ΔT	R.H. (outlet)	g (outlet)	Δg
mm	kg/kg	K	%	kg/kg	kgw.v/s	K	%	kg/kg	kgw.v/s
40	0.0108	8.4	86	0.014	0.0032	8.6	80	0.013	0.0022
60	0.0108	8.0	83	0.0139	0.0031	8.0	75	0.0126	0.0018

Inlet air temperature 30°C and relative humidity 40%
 g the humidity ratio
 Δg the humidity ratio difference

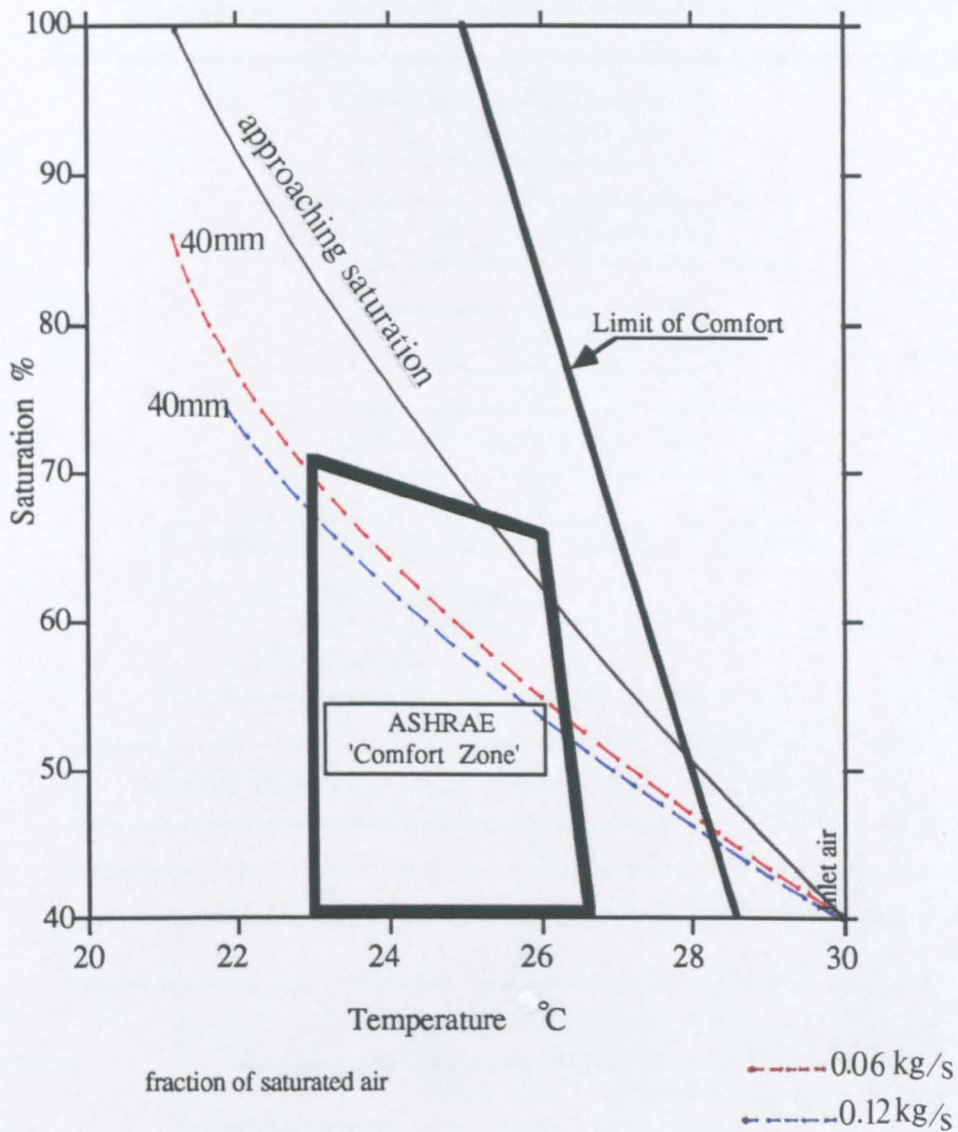


Figure 6.44 Comfort according to measured air temperature drop and relative humidity by 'evaporative cooling cavity' with forced air flow.

CHAPTER SEVEN**PREDICTED AND OBSERVED CONVECTIVE HEAT TRANSFER COEFFICIENT: GENERAL DISCUSSION****7.1 INTRODUCTION****7.2 THE UNCERTAINTIES****7.3 RESULTS****7.3.1 Buoyancy air flow**

Preliminary comparison of "observed" and "predicted"
7.3.1.1 Outlet air velocity
7.3.1.2 Air temperature drop between inlet and outlet
7.3.1.3 Cooling

7.4 THE SURFACE MASS TRANSFER COEFFICIENT h_m **7.5 MEASURED CONVECTIVE HEAT TRANSFER COEFFICIENT h_c** **7.5.1 Convective heat transfer coefficient h_c
for a 'free' vertical surfaces****7.6 DISCUSSION AND CONCLUSION**

CHAPTER SEVEN**PREDICTED AND MEASURED CONVECTIVE HEAT TRANSFER
COEFFICIENTS: GENERAL DISCUSSION****7.1 INTRODUCTION**

In order to predict the behaviour of the cavity in conditions different from that of Leeds (air temperature and relative humidity 17°C to 23°C and 50% to 70% respectively), the behaviour of the cavity was analysed as described in chapter three. Theory and observation were first compared assuming a convective heat transfer coefficient ($3\text{W/m}^2\text{K}$) similar to that given by the CIBSE Guide (1986) for a vertical surface since appropriate convective heat transfer coefficients were not found in the literature. Temperature and relative humidity of the incoming air and of the saturated boundary layer were also considered to determine the rate of evaporation. The pressure drop at entry was assumed to vary from one to three velocity heads. These parameters are given in Table 7.1. For each observation, the analysis predicts the outlet air velocity, the rate of evaporation, the drop in air temperature and the rate of cooling.

Since a convective heat transfer coefficient for air flowing between parallel plates was not found in the literature, measurements of the buoyancy air flow model were used to obtain the appropriate convective heat transfer coefficient. A heat balance on the cavity, equating the sensible heat entering and leaving, taking account of the latent heat of evaporation, and of heat gain of the air from the walls, were used to obtain the measured convective heat transfer coefficients for air flowing between parallel surfaces. Cooling by convection 'sensible' was compared with that by evaporation 'latent'. Different values of h_c for air flowing over 'free' vertical plates were discussed. A correlation of measured convective heat transfer coefficient was developed in relation to the wet surface separation.

7.2 THE UNCERTAINTIES

In order to compare the measured and the predicted values, their uncertainties need to be considered. The uncertainty of the measured rate of cooling was determined as $\pm 5\%$. An error analysis was carried out to give an order of magnitude to the uncertainties of the theoretical analysis. Parameters are given in Table 7.2.

Table 7.1 Input data to the analysis.

Inlet air temperature °C	Relative humidity %	moisture content in the air kg/kg	moisture content in the saturated b. layer kg/kg
17.0	60	0.0073	0.0122
18.0	60	0.0078	0.0130
19.0	60	0.0083	0.0138
20.0	60	0.0089	0.0148
21.0	60	0.0094	0.0157
22.0	60	0.0100	0.0167
23.0	60	0.0107	0.0178

The height of the wet surface is 1550mm, (70% of the cavity height).

Table 7.2 Standard error of the input parameters.

Parameters in the Analysis		Uncertainty δ
Air velocity	m/s	$\pm 3\%$
Cavity width	m	$\pm 2\text{mm}$
Wet surface height	m	$\pm 2\text{mm}$
Air relative humidity	%	$\pm 2\%$
Temperature difference	K	± 0.5
Rate of evaporation	kg/m ² s	$\pm 9\%$
Velocity heads assumed	Pa	$\pm 5\%$
Vapour pressure in air	Pa	$\pm 3\%$
V.P.in saturated b. layer	Pa	$\pm 3\%$

The uncertainty of the predicted parameters (outlet air velocity, drop in air temperature and rate of evaporation and cooling) were determined according to Taylor (1982). If q be a function of several variables x, \dots, z , assuming that each variable is random and independent, the uncertainty of q is given by :

$$\delta q = \{[(\partial q/\partial x)^2 \cdot \delta x] + [\dots] + [\dots] + [(\partial q/\partial z)^2 \cdot \delta z]\}^{1/2} \quad [7.1]$$

The uncertainty associated with the outlet air velocity v (m/s) depends upon the uncertainty of the constant α , the rate of evaporation W , the width and the height of the cavity D and Z respectively, and the pressure difference which described as a function of the velocity heads n , these variables of eqn.7.2 were derived from the theoretical analysis carried out in chapter three as:

$$v = \alpha [WZ^2 / n.D]^{1/3} \quad [7.2]$$

where

α = constant	--
W = the rate of evaporation	kg/m ² s
Z = height of the cavity	m
n = number of velocity heads	--
D = cavity width	m

As described by Taylor (1982), eqn.7.2 can be written as:

$$\delta v = \{[(\partial v / \partial \alpha)^2 \cdot \delta \alpha] + [(\partial v / \partial W)^2 \cdot \delta W] + [(\partial v / \partial Z)^2 \cdot \delta Z] + [(\partial v / \partial n)^2 \cdot \delta n] + [(\partial v / \partial D)^2 \cdot \delta D]\}^{1/2} \quad [7.2.a]$$

The predicted outlet air velocity uncertainties from eqn.7.2.a. are given in Table 7.3 a.

Table 7.3 a The standard error of the predicted air velocity at the outlet.

Variables	Cavity width mm	Mean air velocity m/s	Standard error m/s	% error of the mean %
Air velocity m/s	80	0.32	±0.014	4
	100	0.29	±0.012	4
	200	0.23	±0.016	7
	300	0.20	±0.017	8

The uncertainty associated with the rate of evaporation W ($\text{kg}/\text{m}^2\text{s}$) depends on the parameters given in eqn. 7.3:

$$W = \dot{O} (P_s - P_a) / RT \quad [7.3]$$

where

\dot{O}	= surface mass transfer coefficient	m/s
P_s	= vapour pressure of saturated boundary layer	Pa
P_a	= vapour pressure of in the incoming air	Pa
R	= gas constant	J/kgK
T	= absolute temperature	°K

Using eqn.7.3 in principle, the standard error can be determined as:

$$\delta W = \{[(\partial W/\partial \dot{O})^2 \cdot \delta \dot{O}] + [(\partial W/\partial P_s)^2 \cdot \delta P_s] + [(\partial W/\partial P_a)^2 \cdot \delta P_a] + [(\partial W/\partial \Delta T)^2 \cdot \delta \Delta T]\}^{1/2} \quad [7.3.a]$$

The values of uncertainties associated with the predicted rate of evaporation are also given in Table 7.3.b.

Table 7.3 b The standard error of the predicted rate of evaporation.

Variable	Mean rate of evaporation $\text{kg}/\text{m}^2\text{s}$	standard error $\text{kg}/\text{m}^2\text{s}$	% error of the mean %
Rate of evaporation $\text{kg}/\text{m}^2\text{s}$	11×10^{-6}	1×10^{-6}	10

The uncertainties of the constants α and β in eqns.7.2 and 7.3 depend on Ψ which is given by:

$$\Psi = Z (T_{in} - T_{out}) / n v^2 \quad [7.4]$$

It is seen from eqn 7.4 that the uncertainty of Ψ depends on the drop of air temperature between inlet and outlet ΔT , the height of the cavity Z , the velocity of the air v and the pressure difference in terms of velocity heads n . Analysis showed that the uncertainties in Ψ were $\pm 10\%$ and $\pm 11\%$ for cavities of 80mm and 100mm widths, whereas they were $\pm 17\%$ and $\pm 23\%$ for the 200mm and 300mm cavities respectively (Table 7.4). Accordingly, the uncertainties of both α and β were found as $\pm 3\%$, $\pm 3\%$, $\pm 6\%$ and $\pm 8\%$ for the 80mm, 100mm, 200mm and 300mm cavities respectively (Table 7.4).

Table 7.4 The uncertainties of the constants ψ , α and β as functions of the cavity widths.

	Cavity widths mm			
	80	100	200	300
constant	ψ			
Mean	30±3	30±3	30±5	30±7
% S. Error	±10%	±11%	±17%	±23%
constant	α			
% S. Error	±3%	±3%	±6%	±8%
constant	β			
% S. Error	±3%	±3%	±6%	±8%

The temperature of incoming air is 21°C

The uncertainty of the air temperature drop $\delta\Delta T$ from evaporation depends on the rate of evaporation W , the height and the width of the cavity Z and D respectively, and the pressure difference which described in terms of velocity heads n :

$$\Delta T = \beta [(WZn) / D^2]^{1/3} \quad \text{K} \quad [7.5]$$

from which:

$$\delta\Delta T = \{[(\partial\Delta T/\partial\beta)^2 \delta\beta] + [(\partial\Delta T/\partial W)^2 \delta W] + [(\partial\Delta T/\partial Z)^2 \delta Z] + [(\partial\Delta T/\partial n)^2 \delta n] + [(\partial\Delta T/\partial D)^2 \delta D]\}^{1/2} \quad [7.5.a]$$

The uncertainties of the predicted drop in air temperature based on eqn.7.5.a are given in Table 7.5.

Table 7.5 The uncertainty of the predicted air temperature drop between the inlet and outlet

Cavity width mm	Air temperature drop K	S.E. of β \pm	S.E. of ΔT $\pm K$	% of S.E %
80	5.5	0.03	0.44	± 8
100	4.7	0.02	0.38	± 8
200	3.0	0.03	0.31	± 10
300	2.3	0.03	0.025	± 11

Analysis shows that the uncertainty of the predicted air velocity was about $\pm 4\%$ for the 80mm and 100mm cavities, and increased to $\pm 7\%$ and $\pm 8\%$ for the 200mm and 300mm cavities respectively. This increase is due to the rise in the uncertainty of the constants Ψ and α as shown in Table 7.5. The uncertainties associated with the predicted air temperature drop between the inlet and the outlet $\delta\Delta T$ were even higher, about $\pm 8\%$ for the cavities of 80mm and 100mm widths, and increased to $\pm 10\%$ and $\pm 11\%$ with cavities of 200mm and 300mm widths respectively. This increase was caused by the uncertainties of $\pm 3\%$ to $\pm 8\%$ of the constant α which was originally caused by the error of $\pm 10\%$ to $\pm 23\%$ with the constant Ψ . The highest uncertainties of the predicted analysis were found with cavity widths of the 200mm and 300mm. The uncertainty of the predicted cooling was about $\pm 4\%$ for cavities of 80mm and 100mm, and increased to $9\pm\%$ and $\pm 11\%$ with the 200mm and 300mm cavities.

7.3 RESULTS

7.3.1 Buoyancy air flow

In order to give insight into the behaviour of the cavity, measurements were first compared with analysis. Since an appropriate convective heat transfer coefficient was not found in the literature, the unknown convective heat transfer coefficient of eqn.3.21 (theoretical analysis of the buoyancy air flow) was assumed to be $3\text{W/m}^2\text{K}$, similar to that given by the CIBSE Guide (1986), Table A10-3. The predicted values of the outlet air velocity, the drop in air temperature between the inlet and outlet, cooling and the rate of evaporation as a function of the cavity widths are given in Table 7.6. For each predicted parameter, the rate of evaporation was assumed to be at two rates: that of the entry (first assumption); the average evaporation rate between the inlet and outlet (second assumption: see chapter three). The incoming air temperature and its relative humidity at the cavity inlet were 20°C and 60%.

7.3.1.1 Outlet air velocity

The percentage differences between the measured outlet air velocity and that predicted are shown in Table 7.7. It shows an overestimation of air velocity with the 80mm cavity width with the evaporation rate in the cavity assumed to be equal to that at entry, and the number of velocity heads equal to unity. An overestimation of the outlet air velocity was also found when the above assumption was taken as the average between the inlet and outlet rate (half the rate above). In general, Table 7.7 and Figure 7.1 indicate that the analysis highly overestimates the outlet air velocity with the 80mm cavity width. This was due to the simplified assumption that the flow may be uniform in the 20mm central gap of the 80mm cavity width. Observation showed that the air velocity dropped to 62% of that predicted (from 0.27m/s to 0.08m/s , chapter five). With the 200mm and 300mm cavity widths, the difference with the first assumption was greater than that with the second.

The decrease of the difference between measured and predicted values indicates in general the importance of the assumption that the rate of evaporation in the cavity is the average between those of the inlet and outlet (eqn.3.61, chapter three). As shown in Table 7.7, the decrease in the difference in percentage (%) between measured and predicted values was 8%, 67% and 75% with the 100mm, 200mm and 300mm cavity widths respectively. This confirms that the rate of evaporation is reduced as the air moves down the cavity. This means that it may be half the rate at entry.

Table 7.6 Predicted outlet air velocity, air temperature drop and cooling at different cavities.

		Evaporation rate at entry kg/m ² s			Mean rate of evaporation between entry and cavity			
		Width mm	Number of velocity heads n					
			3	2	1	3	2	1
Outlet air velocity m/s	80	0.4	0.46	0.57	0.32	0.36	0.46	
	100	0.37	0.42	0.53	0.29	0.34	0.42	
	200	0.29	0.34	0.42	0.23	0.27	0.34	
	300	0.26	0.29	0.37	0.20	0.23	0.29	
	400	0.23	0.27	0.34	0.19	0.21	0.27	
	500	0.22	0.25	0.31	0.17	0.20	0.25	
	600	0.20	0.23	0.29	0.16	0.19	0.23	
Air temperature drop K	80	8.7	7.6	6.0	5.5	4.8	3.8	
	100	7.5	6.5	5.2	4.7	4.0	3.3	
	200	4.7	4.0	3.3	3.0	2.6	2.0	
	300	3.6	3.1	2.5	2.3	2.0	1.6	
	400	3.0	2.6	2.0	1.9	1.6	1.3	
	500	2.6	2.3	1.8	1.6	1.4	1.0	
	600	2.3	2.0	1.6	1.4	1.3	0.99	
The rate of cooling W/m	80	499	501	493	251	247	250	
	100	398	394	395	196	201	197	
	200	196	201	197	98	101	100	
	300	134	131	133	65	65	66	
	400	98	101	100	51	49	50	
	500	81	80	79	39	40	40	
	600	65	65	66	33	34	33	

Wet surface = 1550mm (70%) of the cavity height.

Air density = 1.20 kg/m³

Table 7.7 Differences between measured outlet air velocity, air temperature drop, cooling rate and analysis (%)

	Width mm	Evaporation rate at entry kg/m ³ s			Mean rate of evaporation between entry and cavity		
		Number of velocity heads n					
		3	2	1	3	2	1
Outlet air velocity m/s	80	208%	254%	338%	146%	177%	254%
	100	37	56	96	7	26	56
	200	45	70	110	15	35	70
	300	44	61	106	11	28	61
	400	--	--	--	--	--	--
	500	--	--	--	--	--	--
	600	--	--	--	--	--	--
Air temperature drop K	80	74	52	20	10	4	24
	100	69	46	17	7	10	25
	200	31	11	8	17	28	44
	300	39	20	4	12	23	39
	400	--	--	--	--	--	--
	500	--	--	--	--	--	--
	600	--	--	--	--	--	--
The rate of cooling W/m	80	375	377	369	139	135	138
	100	98	96	97	2.5	0.0	2
	200	106	112	107	3	6	5
	300	100	96	99	3	3	1.5
	400	--	--	--	--	--	--
	500	--	--	--	--	--	--
	600	--	--	--	--	--	--

Wet surface = 1550mm (70%) of the cavity height

Air density = 1.20 kg/m³

The reduction of the difference between measured and predicted values (with the assumption that the rate of evaporation in the cavity is half that at entry) pointed out the significance of the velocity heads. Table 7.7 shows that the difference was reduced by an average of 83% with widths of 100mm, 200mm and 300mm. This decrease emphasises the importance of increasing the number velocity heads to three in the model rather than using one (see eqn.7.2, 7.4 and 7.5).

Figure 7.1 compares the measured outlet air velocity with that predicted for different cavity widths. The agreement between observations and analysis when the rate of evaporation was assumed as half that at entry was good. The ratios between measurement and analysis are given in Table 7.8, and were in general close to unity. The ratio of 0.41 with the 80mm cavity width may be because of the simplification in the analysis (see chapter three).

Tables 7.7 and 7.8 and Figure 7.1 showed an agreement between the measured and predicted outlet air velocity of the 100mm cavity width under Leeds conditions (the difference was only 7%). Consequently, this agreement using the Leeds coefficients supports further analysis to predict the outlet air velocity with the Cairo coefficients (see chapter three) since the errors associated with the measured and predicted values were only about $\pm 2\%$ and $\pm 4\%$ respectively. The outlet air velocity is a non-linear function of the cavity width (Figure 7.7).

Table 7.8 Measured and predicted outlet air velocity.

Cavity width mm	Air velocity		[$\frac{\text{Measured}}{\text{Predicted}}$]
	Measured m/s	Predicted m/s	
80	0.13	0.32	0.41
100	0.27	0.29	0.93
200	0.20	0.23	0.87
300	0.18	0.20	0.90

Number of velocity heads 3

Mean rate of evaporation 11×10^6 kg/ms

Wet surface height 1550mm.

Incoming air 21°C and 60% R.H.

7.3.1.2 Air temperature drop between the inlet and outlet

A good agreement was obtained when the measured air temperature drop between the cavity inlet and the outlet were first compared with predictions (Table 7.9). The difference was about $\pm 0.5\text{K}$. The difference between measured air temperature drop between the inlet and outlet and those predicted as a function of cavity widths are given in Table 7.7. Figure 7.2 shows an overestimation of the predicted air temperature drop when the rate of evaporation in the cavity was assumed equal to that at entry. The maximum overestimation was 74% and 69% with the 80mm and 100mm cavity widths respectively (Figure 7.2). An underestimation of 8% and 4% between prediction and measurements with the 200mm and 300mm cavity widths was found when the velocity head was assumed as unity according to the CIBSE Guide (1986).

Table 7.9 Measured and predicted air temperature drop between the inlet and outlet.

Cavity width mm	Air temperature drop		[$\frac{\text{Measured}}{\text{Predicted}}$]
	Measured K	Predicted K	
80	5.0	5.5	0.91
100	4.4	4.7	0.94
200	3.6	3.0	1.18
300	2.6	2.3	1.10

Number of velocity heads 3

Mean rate of evaporation 11×10^6 kg/ms

Wet surface height 1550mm.

Incoming air 21°C and 60% R.H.

An underestimation of 44% was found with the 200mm cavity width when one velocity head was assumed. Observation agreed with prediction when velocity heads was taken as three (Table 7.7). The decrease by 34% and 32% with the 80mm and 100mm cavity widths respectively pointed out the significance of increasing the number of velocity heads to three rather than unity. The decreases by 61% and 69% with the 200mm and 300mm cavity widths support that the velocity heads to be of the order of three which is greater than that given by the CIBSE Guide (1986).

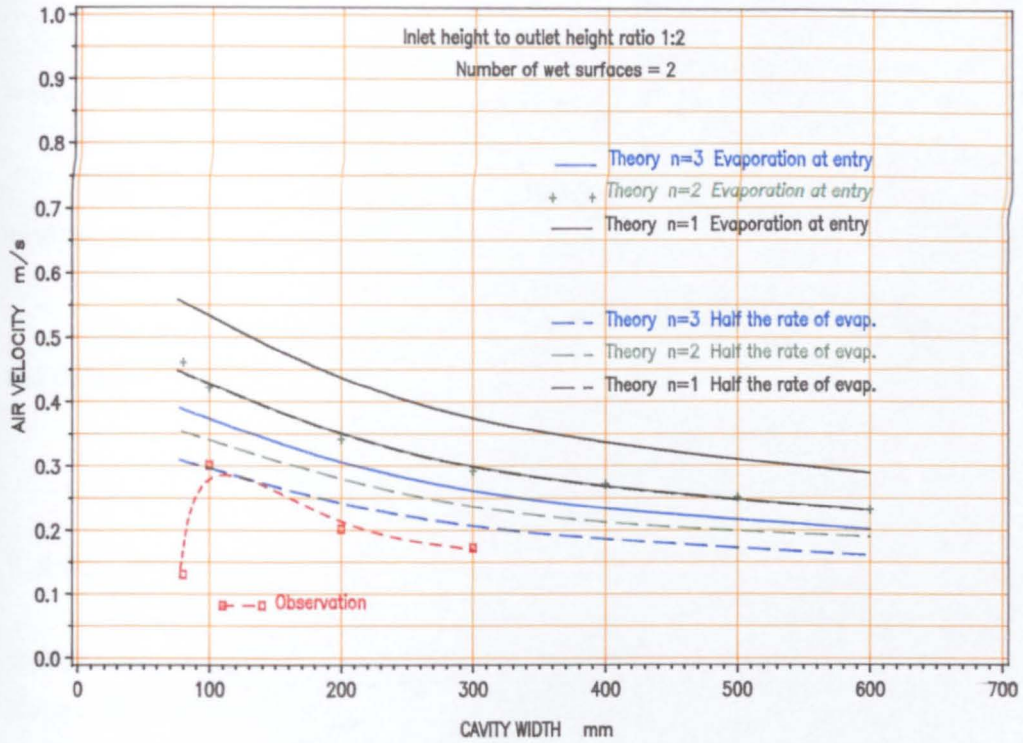


FIG 7.1 Comparison between measured and predicted outlet air velocity
The wet surfaces are 30 mm from the walls

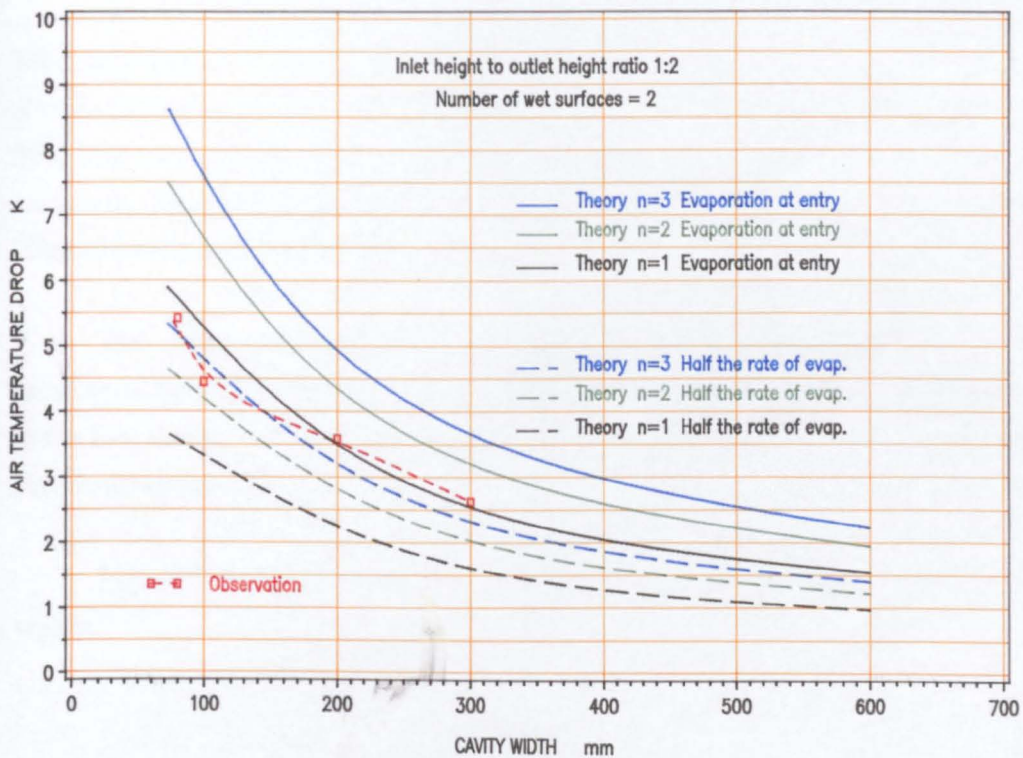


FIG 7.2 Comparison between measured and predicted air temperature drop
The wet surfaces are 30mm from the walls

A good agreement between observation and prediction with the 100mm cavity width was found (Figure 7.2).

Although the analysis underestimated prediction for the 200mm and 300mm cavities, the results are acceptable.

The study yields the best prediction of the number of velocity heads (n) to be of the order of 2.6.

7.3.1.3 Cooling

The measured cooling with different cavity widths based on eqn.3.21 (chapter three) was compared with those predicted with the same assumptions. Table 7.11 shows the predicted cooling per metre length with their standard errors. The difference between the measured and predicted cooling with the 80mm cavity width shows an overestimation of nearly four times when evaporation in the cavity was assumed equal to that at entry (Table 7.7). This was about halved with the 100mm, 200mm and 300mm cavity widths respectively.

The difference of an average of only 3% with cavities of 100mm, 200mm and 300mm indicates that the measured cooling rate agreed well with those predicted. The elimination of error by the second assumption shows that it was far better than that of the first. The best agreement was that of the 100mm cavity (Figure 7.3). The ratio between measured and predicted cooling rate is given in Table 7.10. With the 100mm and 300mm cavity widths, the ratio was virtually 1.

The overestimation in the cooling rate with the 80mm cavity was probably because of the effect of the 20mm central gap which may behave as a stagnant layer due to the low thermal conductivity of the "still air" (below 0.1m/s) [Sodha et al. (1986) and van Straatan (1967)].

Figure 7.3 indicates that the rate of cooling was a non-linear function of cavity width.

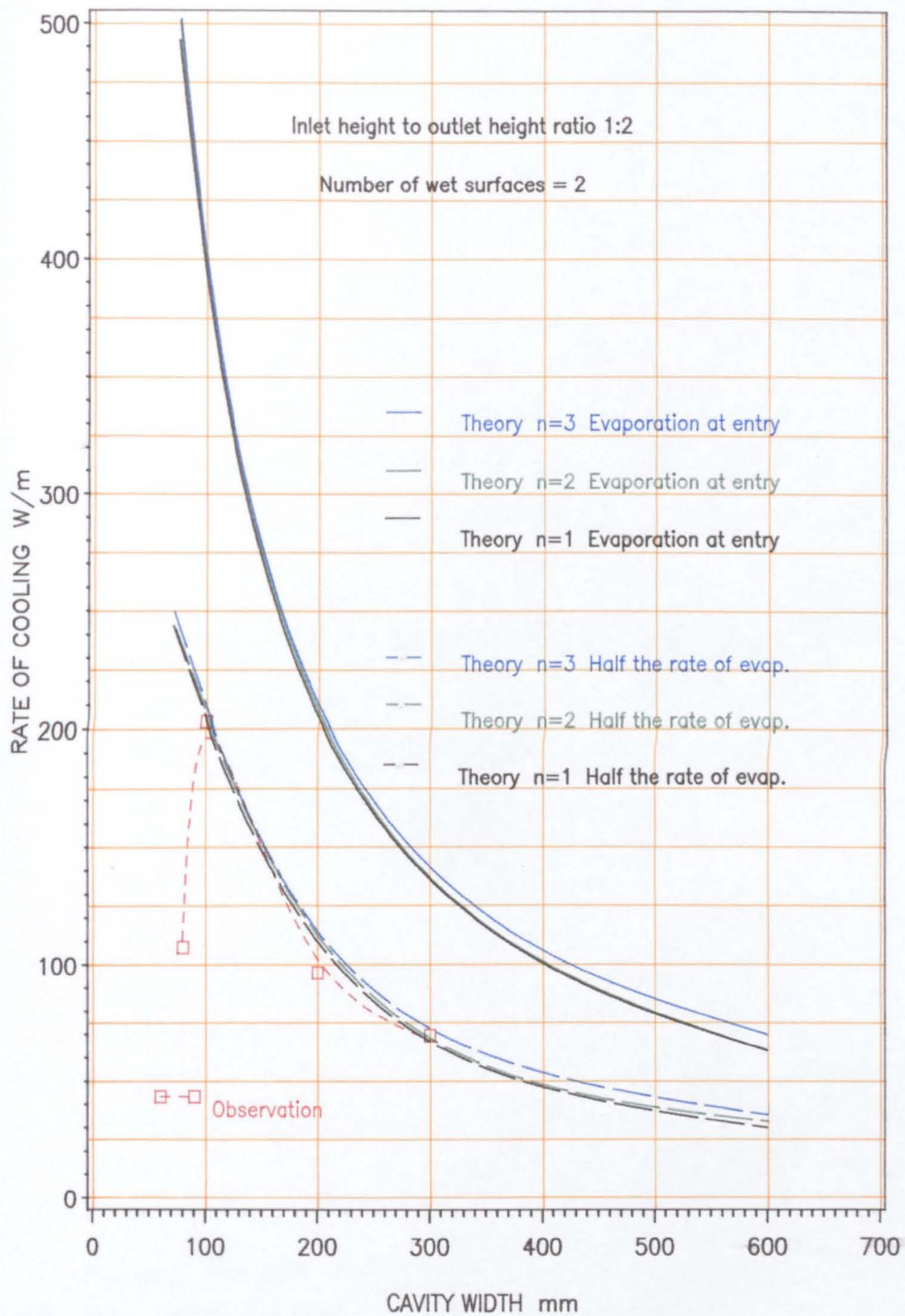


Figure 7.3 Comparison between Measured and predicted cooling rate
The wet surfaces are 30mm from the walls

Table 7.10 Measured and predicted cooling.

Cavity width mm	Rate of cooling		[$\frac{\text{Measured}}{\text{Predicted}}$]
	Measured W/m	Predicted W/m	
80	105	251	0.42
100	201	196	1.03
200	95	98	0.97
300	67	65	1.03

Number of velocity heads 3

Mean rate of evaporation 11×10^6 kg/m²

Wet surface height 1550mm

Incoming air 21°C and 60% R.H.

Table 7.11 The standard errors of measured and predicted cooling.

Cavity width mm	Rate of cooling		Standard error	
	Measured W/m	Predicted W/m	Measured ±W/m	Predicted ±W/m
80	105	251	5	15
100	210	196	6	10
200	95	98	5	10
300	67	65	3	11

Number of velocity heads 3

Mean rate of evaporation 11×10^6 kg/m²

Wet surface height 1550mm

Incoming air 21°C and 60% R.H.

Although the first comparison shows agreement between observation and prediction of cooling, it was not conclusive since an appropriate convective heat transfer coefficient was not found in the literature. The $h_c=3\text{W/m}^2\text{K}$ given by the CIBSE Guide, (Table A10-3, 1986), may be used when the sensible heat by convection is negligible. However this may not be justified since the given convective heat transfer h_c is for a free vertical plate. The cavity of 100mm width with an average measured air temperature and

surface temperature of 20°C and 14.5°C respectively, using eqn.3.16 (chapter three) when $h_c = 3\text{W/m}^2\text{K}$, has yielded a sensible heat transfer by convection of the order of 24W/m (about 11% of the measured total cooling, Table 7.12). This suggests that convection is a small fraction of the cooling (latent and sensible), but not negligible. The sensible heat by convection with the 80mm, 200mm and the 300mm cavity widths was of the order of 20W/m (Table 7.12).

**Table 7.12 Cooling by convection in relation to the total cooling
(latent and sensible)**

Cavity width mm	Inlet temp. °C	Outlet temp. °C	Mean air temp. °C	Surface temp. °C	ΔT K	Sensible cooling W/m	Total cooling W/m	$\frac{\text{Sensible}}{\text{Total}}$ %
80	22.5	18.0	20.25	16.7	3.55	21	110	19
100	20.5	16.5	18.5	14.5	4.0	24	210	11
200	21.5	18.75	20.0	16.75	3.25	20	95	21
300	19.0	16.5	17.75	14.5	3.25	20	70	28

$x = 2\text{m}$ and $h_c = 3\text{W/m}^2\text{K}$

When the heat removed by convection was compared with the cooling, values of heat transfer by convection were about 25% of the cooling (the 130mm and 230mm separation, Table 7.12). This indicates that the convective heat transfer coefficient for a vertical plate given by the CIBSE Guide (1986) can only be applied if the sensible heat by convection is negligible and the diffusion between the two wet parallel surfaces is considered as from free surfaces, and consequently suggests that eqn.3.24, in chapter three, must be modified to include the appropriate heat transfer coefficient h_{cm} .

In order to determine the appropriate heat transfer coefficient h_{cm} , the measured cooling 'sensible and latent heat' were used.

7.4 THE SURFACE MASS TRANSFER COEFFICIENT h_m

The surface mass transfer can be determined using the 'Lewis correlation' (CIBSE Guide 1986, eqn. A10-1) if the convective heat transfer coefficient is known. For water vapour in air, the surface coefficient of mass transfer h_m is related to the convective heat transfer coefficient h_c . The calculation of h_m is mainly dependent on the convective heat transfer coefficient since ρ and c_p are 1.2kg/m^3 and 1000J/kg/K respectively, at 20°C (similar to the Leeds conditions). Thus, the surface mass transfer coefficient is given by:

$$h_m = h_c / \rho c_p = h_c / 1200 \quad \text{m/s} \quad [7.7]$$

7.5 MEASURED CONVECTIVE HEAT TRANSFER COEFFICIENT h_c

The heat transfer coefficient h_c for convection for air flowing between a pair of vertical parallel plates, and the plates was not found in the literature, but may be found from a heat balance on the cavity, equating the sensible heat entering and leaving, taking account of the latent heat of evaporation taking place, and of heat gain of the air from the walls. This heat gain is small compared with the latent heat, but it is not negligible. It was important to consider the heat content of the evaporated water into the air, but it is negligible.

The heat balance is:

$$\text{heat gained by water (EW) + } m c_p (\theta_{in} - \theta_{out}) = \text{latent heat loss (LHL) - convective heat gain (CHG)} \quad [7.8]$$

where

$$\text{LHL} = \{(h_c / \rho c_p) (A L_e / RT)\} \{P_{wall} - (P_{in} + P_{out}) / 2\} W \quad [7.8.a]$$

and

$$\text{CHG} = h_c A \{ (T_{wall} - (\theta_{in} + \theta_{out}) / 2) \} W \quad [7.8.b]$$

and

$$\text{EW} = W_e c_{p \text{ water}} \{ (T_{wall} - (\theta_{in} + \theta_{out}) / 2) \} W \quad [7.8.c]$$

here P_{wall} is the saturated partial pressure of water vapour in the air of the boundary layer, for the temperature of the wall, T_{wall} , and P_{in} and P_{out} are the partial pressure of

water vapour of the air entering and leaving the system, taking account of the temperatures and the appropriate relative humidities. In eqn 7.8.c, the W_e is the mean water evaporated into the air, and $c_{p\text{water}}$ is the specific heat capacity of the water 4200J/kgK.

In the determination of WE, a mean value of water vapour of both the inlet and the outlet were considered. For air entering at 20°C and 65% relative humidity, and leaving at 15°C and 88% relative humidity, the mean water vapour W_e into the air is found to be 1.1×10^{-6} kg/s.

In the determination of CHG, a somewhat different value would be obtained if, instead of using the arithmetic temperature difference, the logarithmic mean temperature difference were used, but as the convective heat transfer is small compared with that due to evaporation, the effect on the value of heat transfer coefficient obtained is negligible. The same approach to the pressure difference term in the evaluation of LHL, makes a difference of much less than one percent.

In the consideration of the error in the heat transfer coefficient, CHG may be ignored, as it is small compared with LHL, so that then:

$$h_c = \rho c_p^2 R T m (\theta_{in} - \theta_{out}) / AL_e \{P_{wall} - (P_{in} + P_{out})/2\} \quad [7.9]$$

where the uncertainty in $(\theta_{in} - \theta_{out})$ is very much greater than the uncertainties in the other parameters, so that the proportional errors in h_c and the temperature difference are the same, at about 0.4 (at best) divided by 6 (observed value of air temperature difference between the inlet and the outlet), giving 0.07, it could be 0.06 and 0.08 if divided by 7 and 5 respectively. One may allow for other uncertainties empirically by stating that the uncertainty in the observed heat transfer coefficient is not more than 10%.

In the comparison of WE with that of CHG, a fraction of one W/m was found (1/1000 of the value of CHG). This heat gained by water vapour is negligible.

If the convective heat transfer for a 'free' vertical surface were well established, and the convective heat transfer coefficient for the cavities used in the present observations were known more accurately, it would be possible to determine the extent to which the present cavities differ from being 'free' vertical surfaces, if there be any difference. This is not possible, because the literature gives varying values for the convective heat transfer coefficient at a 'free' surface.

7.5.1 The convective heat transfer coefficient h_c for a 'free' surface

Wong (1977) indicates that for laminar air flow and single vertical plate, h_c is given by:

$$(h_c x) / k = 0.8 (Gr.Pr)^{1/4} \quad 0.64 \quad W/m^2 K \quad [7.10]$$

where $(Gr.Pr) = [(g\beta\rho^2\Delta T x^3 Pr) / \mu^2]$, k is the thermal conductivity of the air 0.0262 W/mK, Prandtl number for air $Pr = 0.72$, and x is the height of the surface. At air temperature $27^\circ C$, eqn.7.10 becomes:

$$h_c = 1.27 (\Delta T / x)^{1/4} \quad W/m^2 K \quad [7.11]$$

where ΔT = temperature difference between the surface and that of the air and x is the height of the plate. When the air at about $21^\circ C$ eqn. 7.11 becomes:

$$h_c = 1.32 (\Delta T / x)^{1/4} \quad W/m^2 K \quad [7.12]$$

If the temperature difference $\Delta T=5K$ and $x=2m$: $h_c = 1.66W/m^2K$. When the temperature difference is double or halved, we get: $h_c=1.97W/m^2K$ and $1.40W/m^2K$ respectively. The values of h_c according to Wong (1977) are given in Table 7.13. It is clearly shown that the values of h_c (Table 7.13) are about half that given by the CIBSE Guide, Table A10-3 (1986).

Almadri and Hammond (1983) as mentioned above (eqn.3.41, chapter three), developed a relation valid for laminar and turbulent flows. The convective heat transfer coefficient over a vertical surface, where heat flow is horizontal, is given by:

$$h_c = \{ [1.5 (\Delta T/L)^{0.25}]^6 + [1.23 (\Delta T)^{0.33}]^6 \}^{1/6} \quad W/m^2 K \quad [7.13]$$

According to Almadri and Hammond (1983), the convective heat transfer coefficient h_c resulting from the temperature difference between the wet surface and the air of the cavity widths (80mm, 100mm, 200mm and 300mm) are about $2.00W/m^2K$ (Table 7.13). This is about two thirds of that given by the CIBSE Guide (1986).

Observations showed that the two wet surfaces were separated by approximately 130mm and 230mm in the 200 and 300mm cavities respectively (Figures 5.12 and

5.13). Eckert (1961) indicates that for separation more than 100mm between two surfaces, each surface may behave as a 'free' vertical plate, but his surfaces were too small. Wong (1977) gives the correlation for a 'free' vertical plate as:

$$(h_c x)/k = 0.246\{(Gr Pr)^{2/5}\} [(Pr)^{1/6} / (1+0.494 (Pr)^{2/3})]^{2/5} \quad [7.14]$$

with same temperature difference, eqn.7.14 becomes:

$$h_c = 1.1 (\Delta T)^{2/5} \quad W/m^2K \quad [7.14 a]$$

Eqn.7.14 a with the temperature difference between the surface and average air temperature (Table 7.12) yielded a convective heat transfer coefficients h_c about 2.00W/m²K with all separations, similar to those yielded by Almadri and Hammond (1983), and two thirds that given by the CIBSE Guide (1986).

Table 7.13 The calculated convective heat transfer coefficients h_c according to the literature.

separatiom mm	Temperature difference £ K	Wong* eqn. [7.12 a]	Wong** eqn. [7.14]	Almadri et al.+ eqn. [3.41]	CIBSE ++ Table A10-3
20	3.60	1.47	2.0	2.04	3.0
30	4.00	1.60	2.0	2.00	3.0
130	3.40	1.50	2.0	2.00	3.0
230	3.25	1.13	2.0	1.98	3.0

£ difference between the surface and the average air temperautre.

* Wong (1977) eqn.7.12.a, a 'free' vertical plate and laminar air flow.

** Wong (1977) eqn.7.14, a 'free' surface with separtion > 100mm.

+ Almadri et al. (1983) eqn.3.41, a 'free' vertical plate and horizontal heat flow (laminar air flow).

++ CIBSE Guide (1986) for a 'free' vertical plate and air speed below 0.1m/s "still air".

The above indicates that calculated convective heat transfer coefficients using the above correlations for a laminar air flow were lower than that suggested by the CIBSE Guide (1986) which indicates that values obtained according to those given by the literature were inappropriate for the present cavity, and therefore an appropriate h_c has to be found.

In order to determine the measured convective heat transfer coefficient equations 7.8 was used. The *measured convective heat transfer coefficient* h_c is found from eqn 7.15 which obtained from eqns 7.8, whence:

$$h_c = \frac{m c_p (\theta_{in} - \theta_{out}) / A}{\frac{L_e}{RT \rho c_p} \{ P_{wall} - (P_{in} + P_{out}) / 2 \} - \{ T_{wall} - (\theta_{in} + \theta_{out}) / 2 \}} \quad [7.15]$$

Measured temperature, partial pressure of the wall and air entering and leaving were used in the above eqn. and results are plotted in Figure 7.4.

The values of the *measured* convective heat transfer coefficient were found to vary from 0.6 W/m²K to 2.0W/m²K. It was 0.6 W/m²K with separation of 20mm, and increased slightly to 2.0W/m²K when the separation was 30mm and remains at about 1W/m²K with both the 130mm and 230mm separation. The regression of the data yielded a linear relationship (Figure 7.4), and suggests that the convective heat transfer found to independent of the surfaces separation. However, the values of the measured convective heat transfer coefficient h_c with separation from 30mm to 230mm showed a value about half that given by the CIBSE Guide (1986), and near those of Table 7.13.

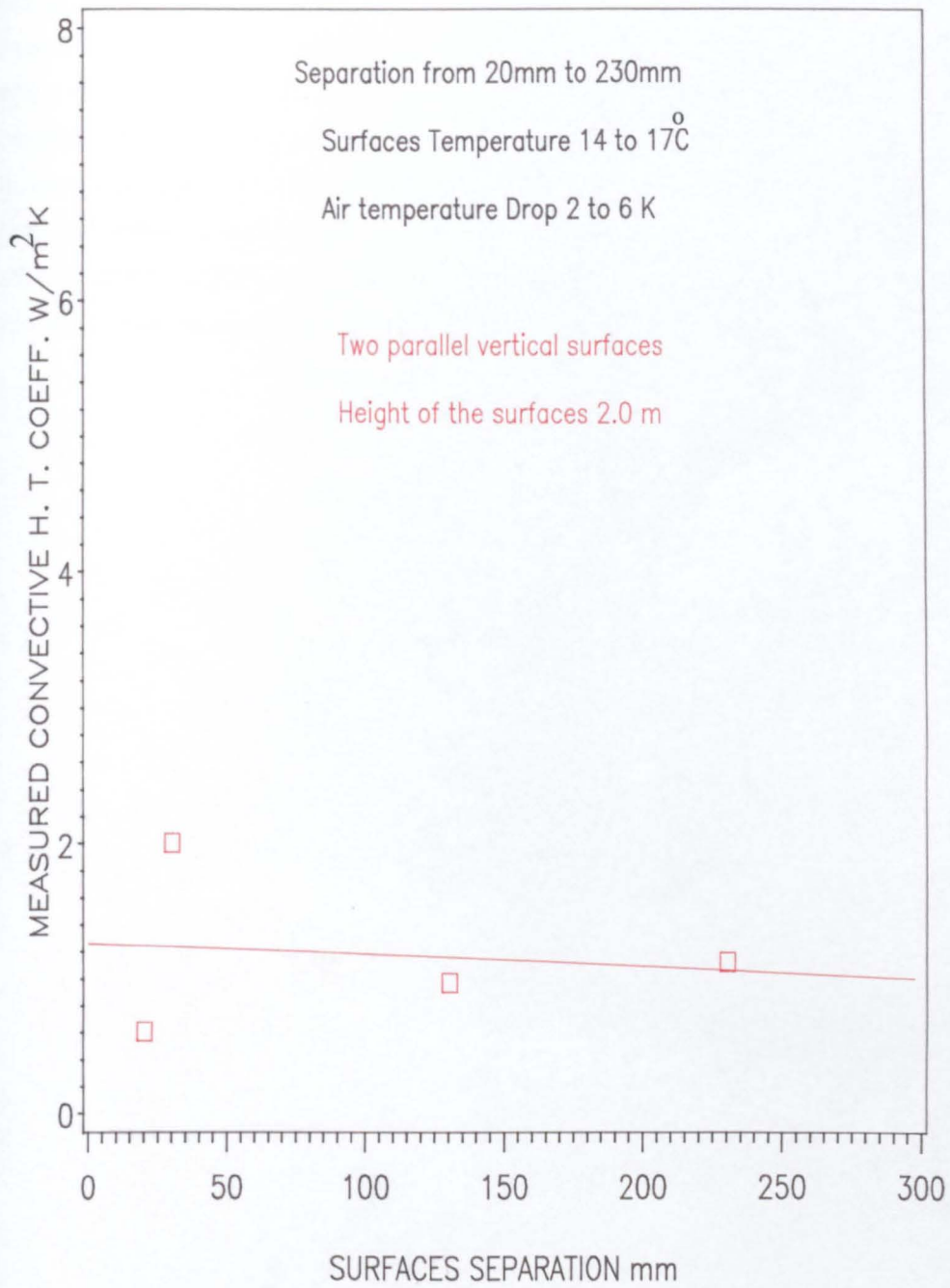
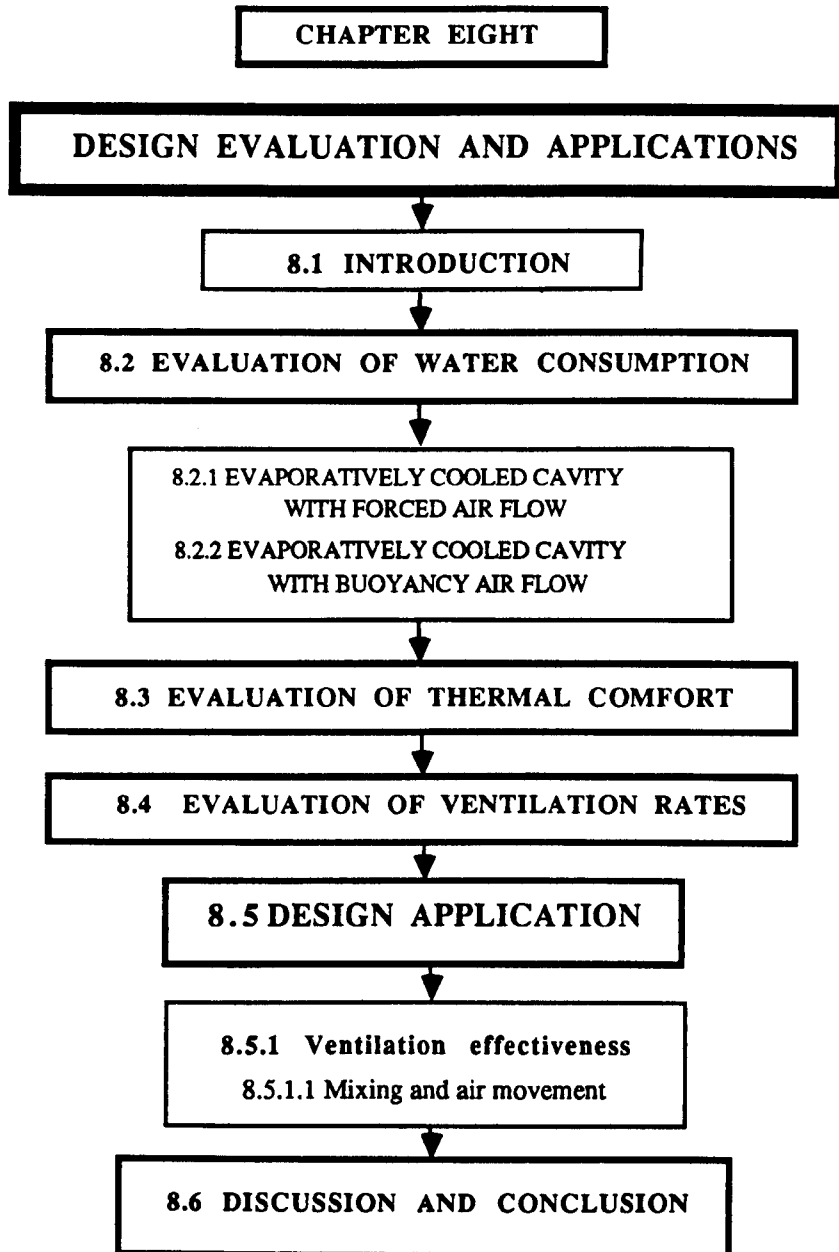


FIG 7.4 Measured Convective Heat Transfer Coefficients

7.6 DISCUSSION AND CONCLUSION

The uncertainty of the values of the h_c , as measured, is up to $\pm 10\%$, as shown using eqn.7.9, so that there is little point in comparing these values with convective heat transfer, given in the literature for a 'free' vertical surface, given in Table 7.13, quite apart from the fact that different observers report very different values. These conclusions are unpleasing, but it can be said that one of the results of the present work is that measured values of the convective heat transfer coefficient for air flowing between vertical parallel plates, and the plates, have been obtained, without making the assumption that the plates are 'free'. The measured values are of limited accuracy, but measurements are preferable to uncertain assumptions.



CHAPTER EIGHT

DESIGN EVALUATION AND APPLICATION

8.1 INTRODUCTION

The analysis of moisture content changes, in the previous chapters (five and six) highlights the importance of water consumption as a major parameter in the design application. This chapter deals with the evaluation of the relative importance of each of these parameters in order to assess their significance in the design application of the cavity attached to a typical a dwelling. The evaluation covers evaporative cooling cavities with buoyancy and fan-assisted air flow. The best widths of the cavity obtained from measurements were used in the analysis, they were: 80mm and 100mm cavity width with buoyancy air flow, and 40mm and 60mm with forced air flow respectively.

The criteria of the evaluation are: the water evaporated, cooling and ventilation rate and the effect on the thermal comfort in a room of these cavities. The question of whether to use the 40mm or the 60mm cavity is also discussed, and results are presented.

8.2 EVALUATION OF WATER CONSUMPTION

8.2.1 Evaporatively cooled cavity with forced air flow

In this evaluation, it was essential to know how much water is required for the cavity to perform acceptably over a period of time. The amount of water needed or 'consumed' w_c for the evaporation over a period of time is calculated from :

$$w_c = [(P_{wall} - P_{air}) m t] / A_{ev} \quad \text{kg/ m}^2 \quad [8.1]$$

where

$(P_{wall} - P_{air})$ = the difference in the partial pressure between the saturated boundary layer and the incoming air. Pa.

m = the flow rate of the moving air kg/s.

t = time of operation s.

A_{ev} = the area of evaporation m^2

The area of evaporation used in the observation was about 6.20 m², thus eqn.8.1 becomes:

$$w_c = 0.162 (P_{\text{wall}} - P_{\text{air}}) m t \quad [8.2]$$

The performance of both cavities with regard to the difference in the humidity ratio with air flow rates of 0.06kg/s and 0.12kg/s are plotted against time (Figures 8.1 and 8.2). It is apparent that the difference in the humidity ratio with the 60mm cavity width is less than that with the 40mm. It is shown that the humidity ratio was lower with the 60mm cavity. The differences between the humidity ratio at the starting time and the end of observation were 0.00097kgw.v/kgdry air and 0.0005kgw.v /kg dry air with the 40mm and 60mm cavity width and air flow of 0.12kg/s. Water consumption is given in table 8.1. It shows the average (daily and hourly), and the maximum amount of water needed for evaporation. The average amount of water required per square metre to operate the 40mm and 60mm cavity over 24 hours were 1.63 litres (0.068 litre/m²/h) and 0.91litres (0.038 litre/m²/h).

This indicates that the exploitation of the 60mm cavity was better than the 40mm in terms of water conservation. However, it is apparent from Figures 8.1 and 8.2 that the variation of humidity ratio changes with time can be approximated to a linear relationship with a regression coefficient of 0.9 and 0.92 (p>0.0001). Hence, the changes of the humidity ratio can be found from :

For the 40 mm:

$$\Delta w = 1.07 \times 10^{-3} - 5.8 \times 10^{-5} t \quad [8.3]$$

For the 60 mm:

$$\Delta w = 5.95 \times 10^{-4} - 3.3 \times 10^{-5} t \quad [8.4]$$

where

Δw = the change in the humidity ratio kg/kg.

t = time s

Table 8.1. The average (daily and hourly) and the maximum water used per square metre of wet surfaces at different flow rates.

Flow rate	Cavity width	Quantity of water per square metre				cooling rate
		Mean /h	Maximum /h	*Mean /Day	Maximum /Day	
kg/s	mm	litre	litre	litre	litre	W/m
0.06	40	0.10	0.185	2.40	4.44	520
	60	0.075	0.135	1.80	3.24	475
Difference %		25	27	25	27	10
0.12	40	0.068	0.142	1.63	3.41	1050
	60	0.038	0.078	0.91	1.87	1000
Difference %		44	45	44	45	5

Assuming that the water within the wet surface is maintained, the amount of water required for the evaporation is 0.14 litre/m²/h for moving air at a rate of 0.12kg/s. However, this could be reduced to 0.078 litre/m²/h, if the 60mm cavity is used. This suggests that the 40mm cavity requires about twice the amount of water consumed by the 60mm cavity. For air moving at 0.06kg/s the same trend is maintained. Figure 8.3 shows the amount of water per square metre per day at different cavity widths and flow rates, and Figure 8.4 shows the amount per hour.

8.2.2 Evaporatively cooled cavity with buoyancy air flow

Water consumption of the buoyancy air flow was evaluated using the 80mm and 100mm cavity widths. As observed, Figure 5.14 (chapter five) shows that the average difference in the humidity ratio was higher with the 80mm cavity width than that of the 100mm. The maximum difference was about 0.00035kg/kg in both cavities. Although the difference in the humidity ratio was high in the 80mm cavity than that of the 100mm, the amount of water required for evaporation was less than that of the 100mm cavity. This is because of the low motion of air "still" at 0.08m/s through the 20mm separation between the two wet surfaces in the central gap of the 80mm cavity width (Figure 5. 7).

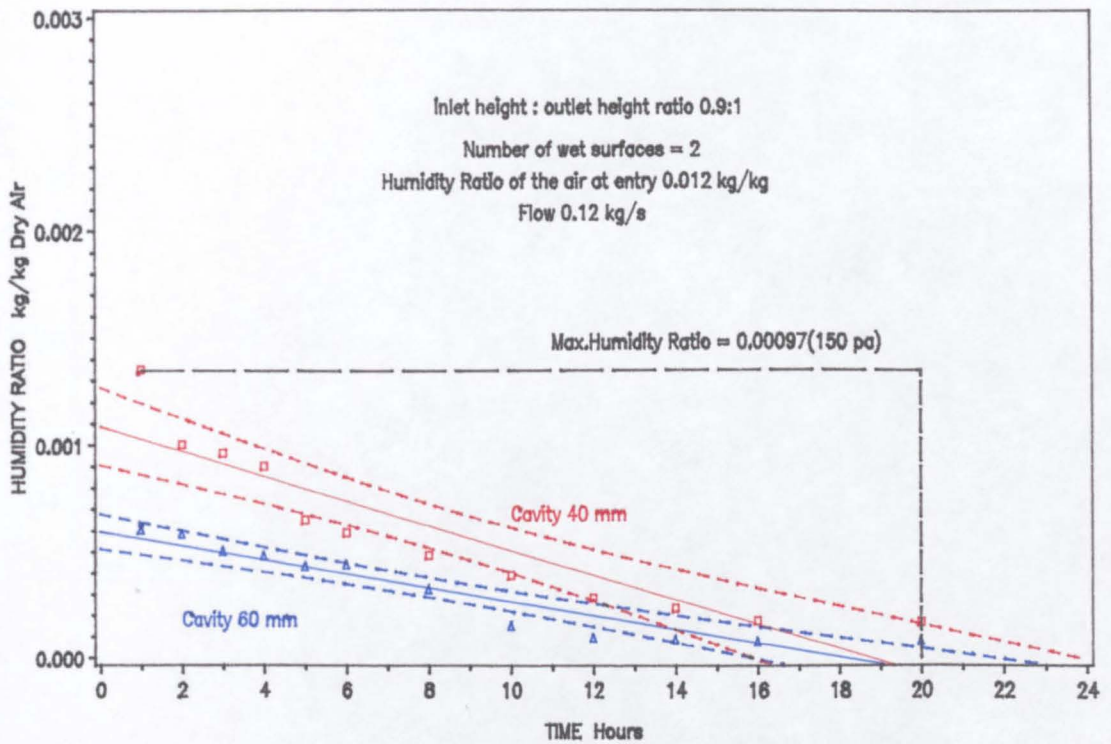


FIG 8.1 The maximum changes of humidity ratio with time
 Wet surface spacing 10 and 16 mm

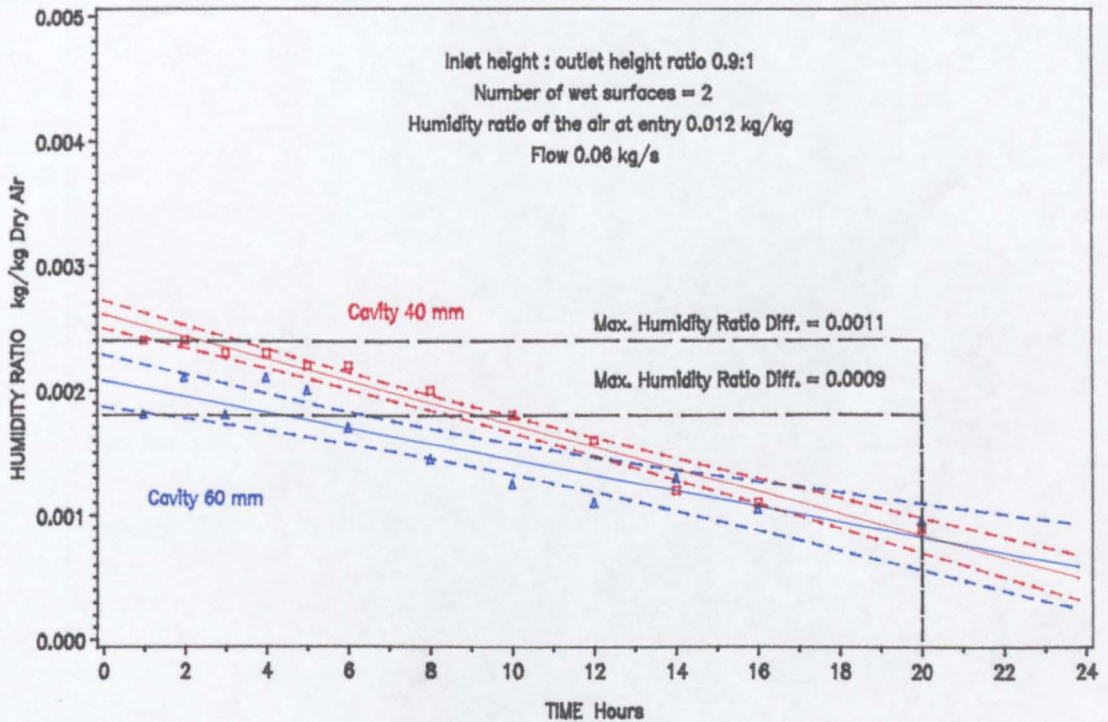


FIG 8.2 The maximum change of the humidity ratio with time
 Wet surface spacing 10 and 16 mm

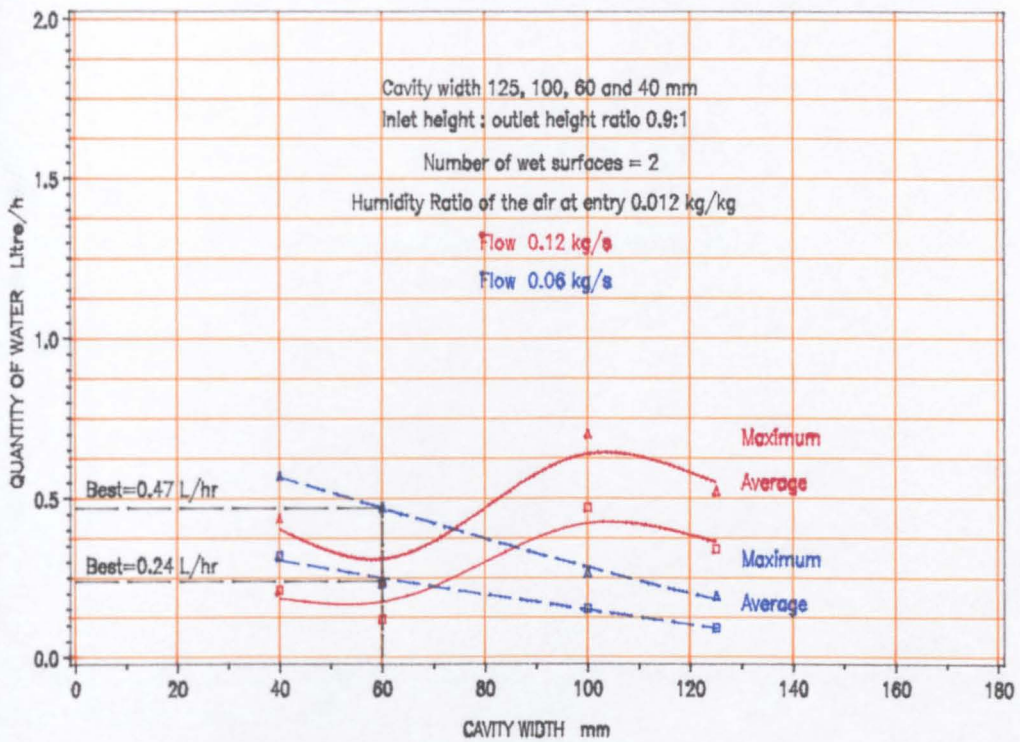


FIG 8.3 The variations in the water consumption by evaporation
 Wet surfaces spacing 10, 16, 30 and 40 mm

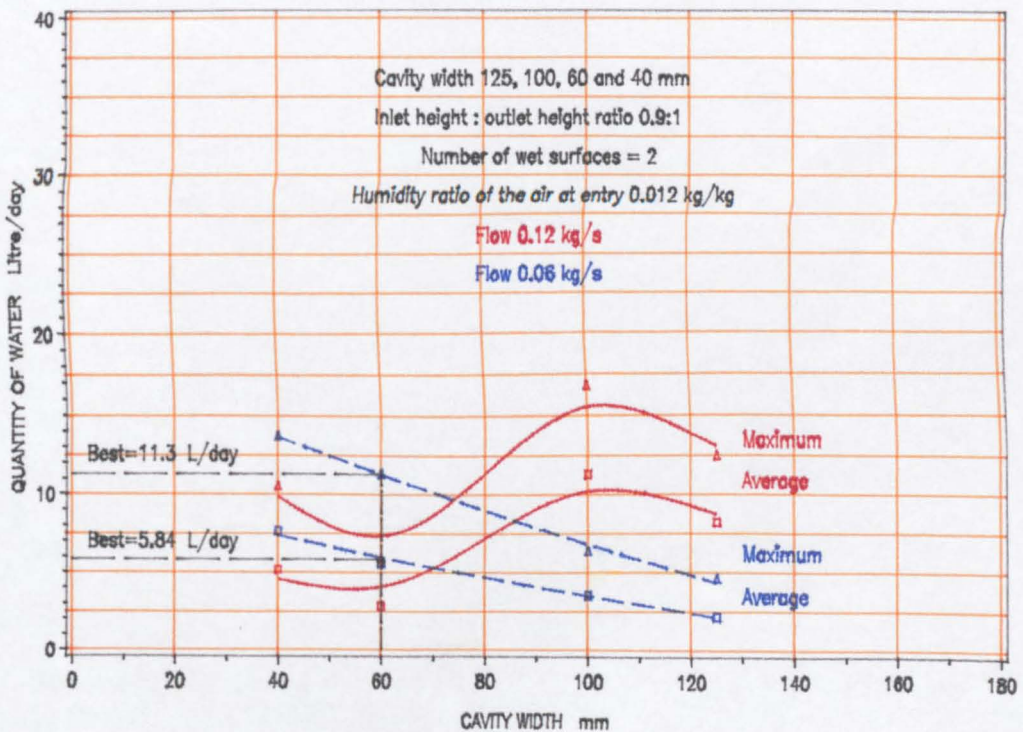


FIG 8.4 The variations in water consumption by evaporation
 Wet surfaces spacing 10, 16, 30 and 40 mm

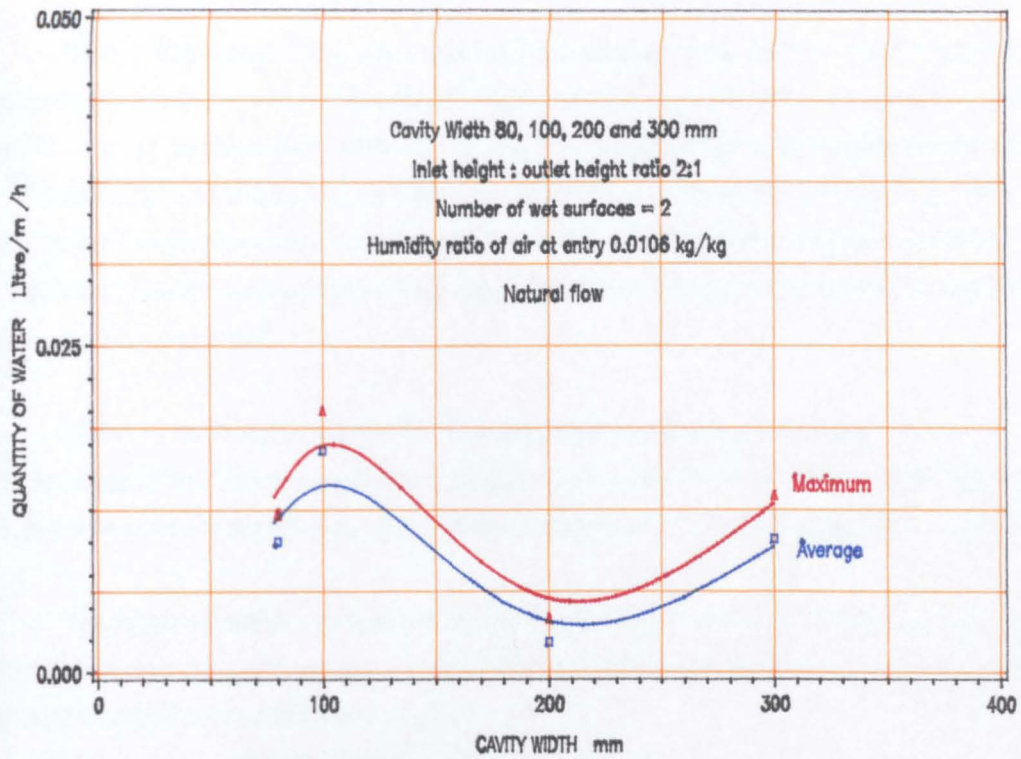


FIG.8.5 The water consumed by evaporation at different cavities
 Wet surfaces spacing 20, 30, 130 and 230 mm

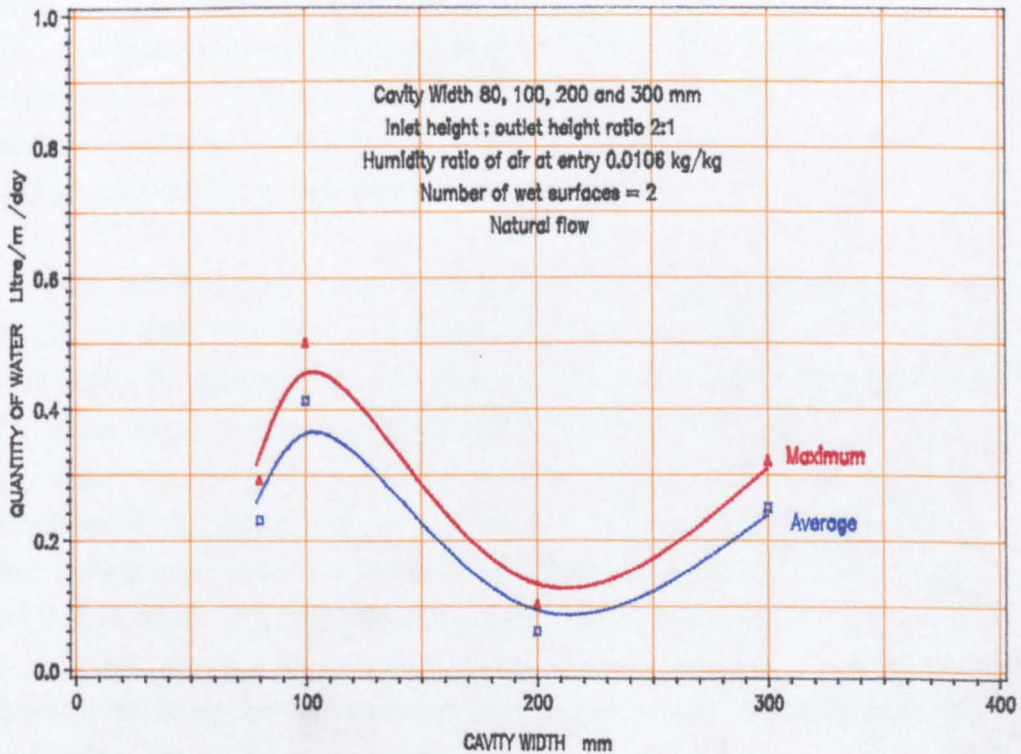


FIG.8.6 The water consumed by evaporation at different cavities
 Wet surfaces spacing 20, 30, 130 and 230 mm

Figure 8.5 shows the average and maximum amount of water required for evaporation per hour. A maximum of 0.02litre/m²/h and 0.012litre/m²/h was needed to cool the air by evaporation with cavity 100mm and 80mm wide respectively. (Figure 8.5). The daily maximum amount of water needed is shown in Figure 8.6. It shows that the required water for evaporation per day was 0.5litre/m² and 0.3litre/m² in the 100mm and 80mm cavity respectively. This indicates that the amount of water required for evaporation is too small.

In the consideration of the 21% increase of the average cooling rate as the width was increased from 80mm to 100mm (Figure 5.11) the cavity of 100mm width is certain to be the best width regardless of the maximum amount of water needed over 24 hours.

The issue of water consumption in the evaluation process may be more important with regard to other parameters, but the influence of these parameters may determine the concept of application; they are:

- the area where the cavity be built
- the thermal comfort
- the thermal performance in conjunction with a room
- the cooling rate
- the rate of ventilation

In hot arid climates where water is often short, the distinction between different cavities such as the 40mm and 60mm width in terms of water conservation may be of more priority. Meigs (1953) has stated that : "Arid areas are those in which the rain on a given place of land is not adequate for crop production".

Dry climates cover most of the world's land; according to Koppen (1968), and they occupy 26%, 14% is semi-arid and 12% is arid according to Alawa (1980). In view of the above, the 60mm cavity may be preferable in hot arid climates. However, Fanger (1979) and Nicol (1975) showed the significance of air temperature and mean radiant temperature on thermal comfort. Fanger (1979) indicates that comfort requires a 1.5K reduction in the mean radiant temperature when air temperature rises by 1K. Observations show that the mean outlet air temperature with air flow 0.12kg/s has risen by 1K as a result of increasing the cavity width from 40mm to 60mm (Table 6.5). Accordingly, the best width of the cavity remains uncertain. To assess whether the 40mm or the 60mm cavity should be applied, an evaluation of these parameters was conducted.

The first assessment of the cavity with air flow rate 0.12 kg/s (Table 8.1) shows that the increase of the average cooling rate was about 5% to 10% as a result of decreasing the width of the cavity from 60mm to 40mm, in contrast, the water required for evaporation increased by 44%. This indicates that it is preferable to use the 60mm cavity. However, the parameters which affect the thermal comfort may be more significant in this assessment, specially with regard to Fanger's remarks.

8.3. THE EVALUATION OF THERMAL COMFORT

Yaglou (1937) indicates that for men and women at rest and dressed according to season, the acceptable range of air temperature usually is between 18°C and 24°C in cold climate. In hot climates, it is between 24°C and 28°C. ASHRAE (1986) gives values for summer comfort of 23°C to 26.5°C. Recent tests by ASHRAE (1989) have shown that the summer comfort zone can be expanded even further if air movement could reach 0.8m/s with air temperature of 28°C. Saini (1980) mentioned that Campbell has arrived at an average air temperature over the range of 29°C as the upper limit of comfort which may be considered for minimum standard of design. This upper limit is based on experiments in hot regions where the relative humidity is high. In hot arid zones, where the relative humidity is always between 20% and 50% (Table 1.2) these values could be even higher. However, observation shows that the outlet relative humidity was found to vary from 65% to 70% in both cavities, and therefore, Campbell's value was used in the evaluation. Thermal comfort can also be assessed according to the CIBSE Guide (1986) as mentioned in chapter one using eqn.1.4 to obtain the dry resultant temperature in a room.

It is reasonable to use the DRT to evaluate both cavities in terms of comfort. In order to determine the DRT, both radiant and air temperature are needed for calculation. As the room in reality is exposed to sun during the day and dynamic heat flows in cycles, the calculation of the mean radiant and air temperatures in the room requires the development of an unsteady state model. This could be a complicated task. However, The Admittance Method (Milbank 1974) predicts the the environmental temperature under this situation to a good approximation. A computer program developed by the BRE (1979) is used to determine the DRT and the environmental temperature on hourly basis. In the consideration of the cavity (Figure 8.7) some difficulties emerged in using the computer program. The difficulty lies in the internal wall of the cavity (Figure 8.7). Assuming that the wall in question is an external wall and is not receiving direct, diffuse radiation or reflected radiation from the ground, and the cavity is usually in the shaded

side of the building, the radiation exchange with the internal walls of the cavity is negligible. The size of the room used in the calculation is 4.0m x 3.0m x 2.7m (Figure 8.7). The room selected for the analysis is of the first floor of a typical three-storey building with rooms 2.7m high, standard for rooms in dwellings in Egypt.

In the thermal comfort evaluation, two cavity widths were used: 40mm and 60mm. The cavity used first is one metre long and faces North. The mean air temperature on the sunlit side is taken as 37°C and that on the shaded side is 30°C. This comes from field measurements in summer for a group of dwellings in Egypt (Younes 1983, Table 1.9). This room had the following specifications:

- roof: 150mm flat slab concrete with a solar absorptivity of 0.3, White
- external walls: 250mm brickwork , 20mm rendering
- internal walls: 20mm plaster, 120mm brickwork, 20mm rendering
- window: single glazing facing South, 15% of the wall area.
- orientation: North-South.

The appropriate thermal properties for these materials were taken from the CIBSE Guide (1986) and are given in (Table 8.2). The solar gain factor of the window was taken as 0.76 and the alternating solar gain factor 0.42 (Markus 1980). The ventilation rates considered in the calculation are observed values: 0.08 and 0.06m³/s/m of the 40mm and 60mm cavity.

Table 8.2 The thermal properties of the material used in the analysis.

	Thermal conductivity	Specific heat capacity	Density
	W/mK	J/kg K	kg/m ³
Plaster 106 mm	0.6	1000	1300
Brickwork 250 mm	0.84	800	1700
Brickwork 160 mm	0.84	800	1200
Concrete 150 mm	1.40	1400	2100

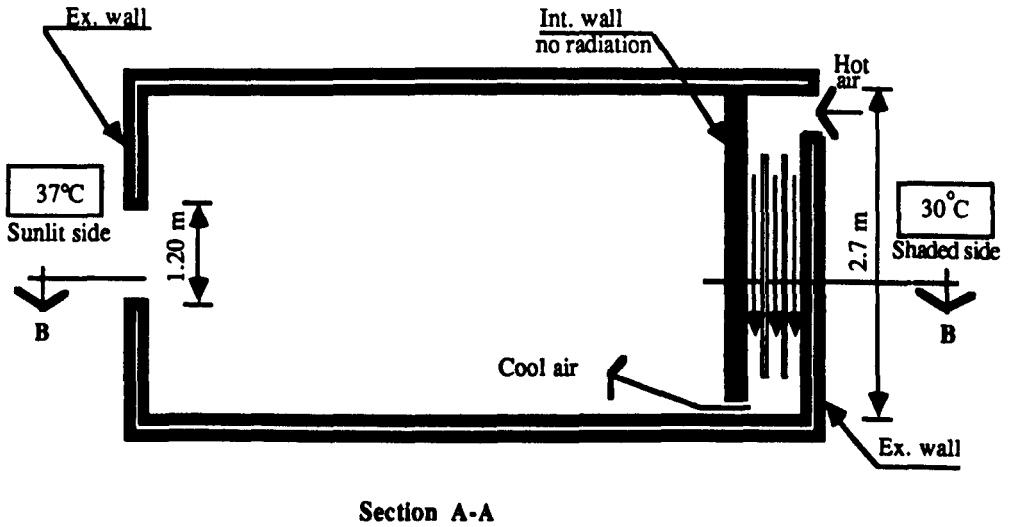
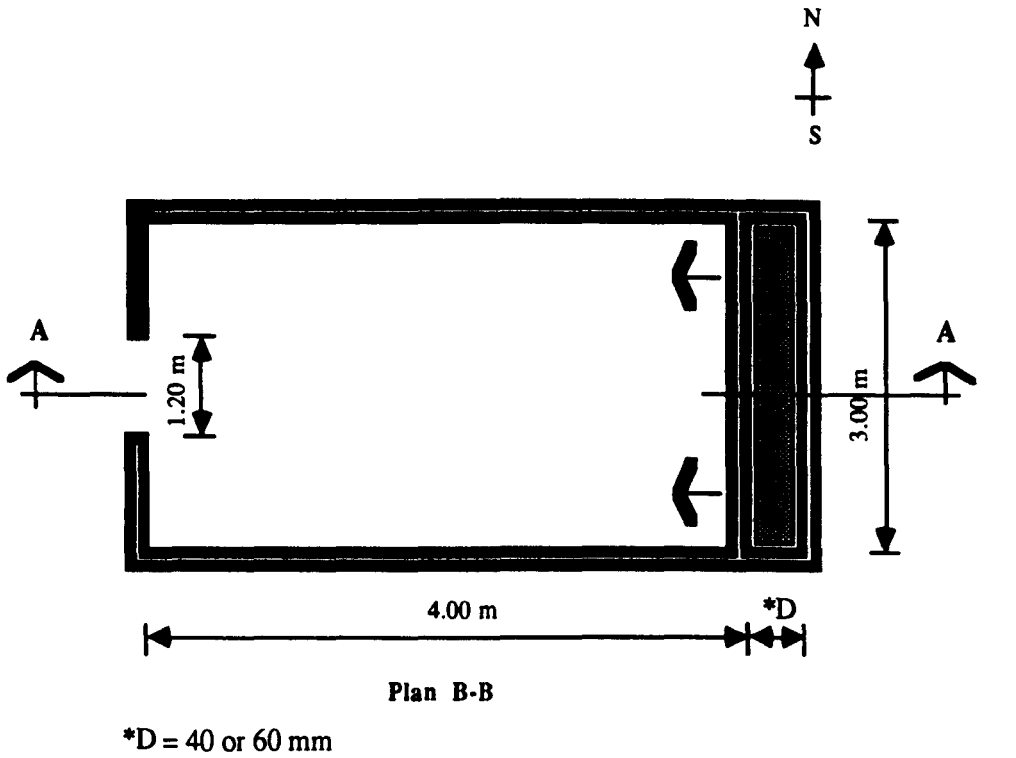


Figure 8.7. Plan and section of the cavity attached to a room facing East-West.

Accordingly the ventilation rate is considered as "number of air changes per hour". The values of air changes rate are those observed for the 40mm and 60mm cavities. These were 7.4 and 10 air changes per hour. The computer program was run to give the values of the DRT and air temperature in the room without the cavity, assuming that the ventilation was minimum at "one air change per hour". These temperatures were then computed when a cavity is introduced. Since the air speed in the room was less than 0.1 m/s, the MRT was then calculated from eqn.1.4.

Figure 8.8 shows the DRT in the room with and without the cavity over 24 hours. The mean DRT as a result of exploiting the 40mm cavity width was 1.4K less than that of the 60mm. It also illustrates that both temperatures are below the upper limits of comfort in hot arid climates. However, the DRT was 1K below the lower limits of the thermal comfort in Summer. Table 8.3 compares the effect of the 40mm and 60mm cavity upon the parameters involved in the thermal comfort evaluation; the outlet air temperature, relative humidity and velocity.

It was essential to consider some known indices as mentioned in chapter 1 to assess the thermal comfort in order to ensure a better judgment on the evaluation. These evaluations involved the Dry Resultant index developed by Missenard (1933), the Effective Temperature index ASHRAE (1986), the Olgay Bioclimatic chart (1967) and the developed Psychrometric Format by Arens et.al (1984) as well as Fanger Comfort lines (1979).

The relation between the measured values and the other thermal indices shows that the environment in the room as a result of attaching the 40mm and 60mm cavity lies within the comfort zone. This indicates that the effect of exploiting both cavities in conjunction with a room induces acceptable dry resultant temperatures, and consequently a satisfactory comfortable environment. This indicates that the significance of small variation of the cavity width on thermal comfort is small. Thus far the evaluation covers four parameters; the next parameter is the ventilation rate.

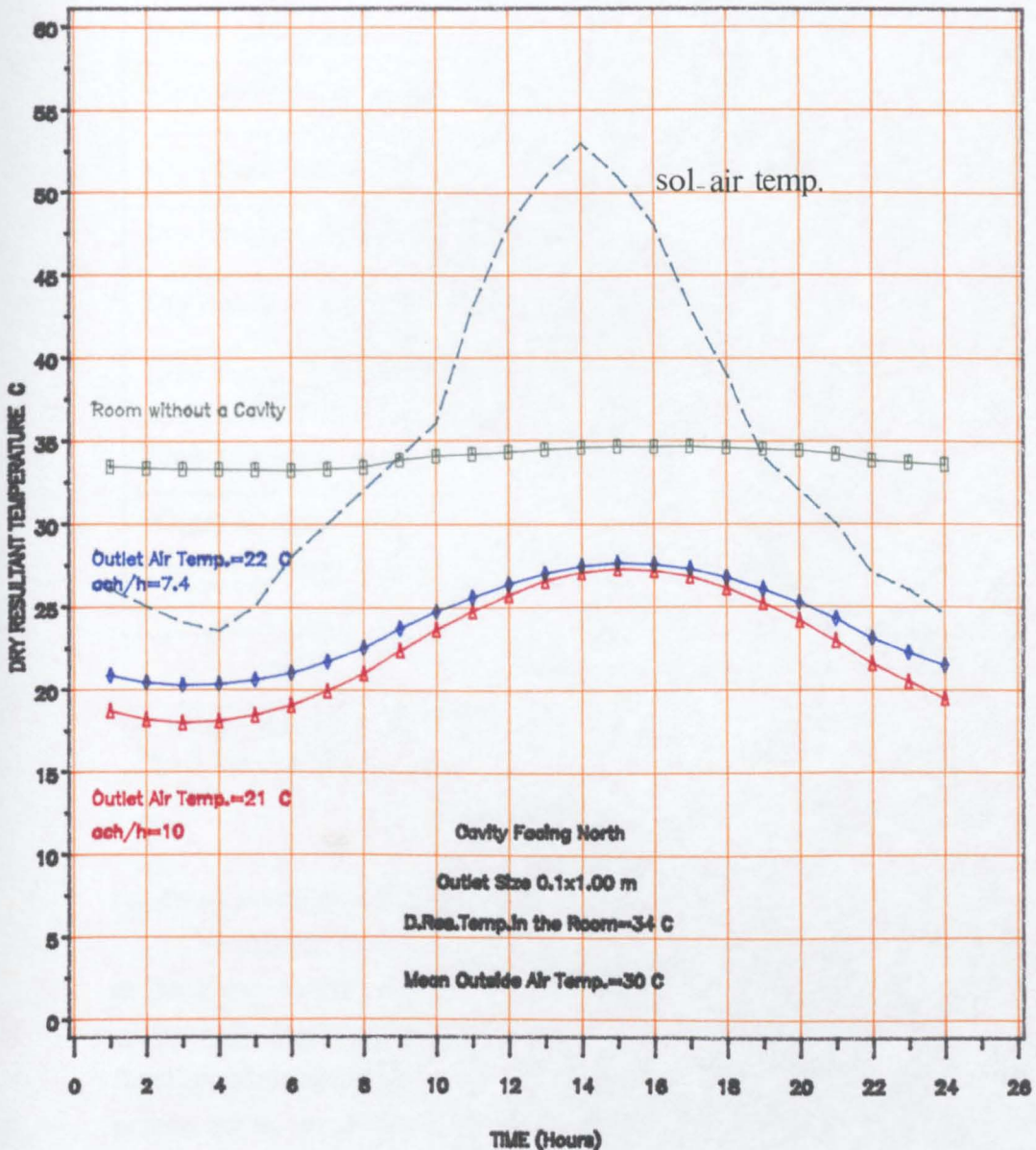


FIG 8.8 The effect of the Cavity on the Thermal Comfort within a Room

Cv 40 mm - Dry Resultant Temp.=22.6 C

Cv 60 mm - Dry Resultant Temp.=24.0 C

Table 8.3 Comparison between the effect of the use of the 40 mm and 60 mm cavity on comfort

	Cavity width mm		Recommended values
	40	60	
Outlet air temperature °C	21.0	22.0	--
Relative humidity %	69.0	65.0	70.0
Indoor air temperature °C	22.3	23.5	24.0 - 28.0
Mean radiant temperature °C	23.0	24.6	24.0
Wet - Bulb Temperature °C	18.3	19.0	12.0- 19.0
Dry Resultant Temperature °C 0.1 m/s	22.6	24.0	fig.8.6.a
Dry Resultant Index by Missenard	20.5	22.0	fig.8.6.b
Effective T. Index ETI by ASHARE	20.0	21.0	fig.8.6.c
Fanger Comfort Lines	Below B Line Comfortable	Above B Line Comfortable	ABC Lines B Best
*Olgay Bioclimatic Chart	Upper Limit Comfort	Upper Limit Comfort	23.5°C & 65% 20.0°C & 79%
**Arens et.al Psychrometric Format	Below U.Limit Comfort	Upper Limit Comfort	26.0°C & 20% 20.0°C & 80%
*****	Low Summer Comfort	Comfort	27.0°C & 20% 22.0°C & 70%

* 1.3 Mat. 0.8 clo

** 1.3 Mat. 0.8 clo.

8.4 EVALUATION OF THE VENTILATION RATE

Ventilation may be an effective parameter in the judgement on whether the 40mm or the 60mm cavity should be used from two points of view: ventilation for health and summer comfort. Van Straatan (1967) recommended the ventilation rate for health as a function of air space per person (Table 1.6). The minimum desirable rate required per person for an unconditioned building is 0.015m³/s, for as little as 3m³/per person. It could be reduced to 0.004m³/s, if the space per person is 15m³. For a typical room about 25m³, occupied by three persons, the ventilation rate required in the room for health is 0.024 m³/s or "3.5 air change/h".

Comparison between the ventilation rate of the 40 and 60 mm cavity indicates that in both cases the ventilation rate entering the room is well above those recommended values by van Straatan (1967). Table 8.4 shows these values with those recommended for health.

Table 8.4 Measured ventilation rates induced by assisted flow and those recommended

Flow kg/s	Ventilation for Health m ³ /s			differences
	Forced flow		Recommended per person	
	40 mm	60 mm		
0.12	0.08	0.06	0.015/3 persons	5 times greater
0.06	0.057	0.053	0.03/4 persons	3 times greater
	Ventilation for Summer comfort m/s			
0.12	0.80	0.60	*0.6 - 1.0	reasonable
0.06	0.57	0.50	**up to 1.0	acceptable

* Evans [1980]

** Givoni [1988]

The purpose of Summer ventilation is to provide indoor comfort. Givoni [1988], indicates that ventilation for thermal comfort is not dependent on the temperature of air and the vapour pressure within the building. Also, Evans [1980], illustrates that ventilation must result in air movement at a sufficiently fast speed to be felt. The above author also points out that the cooling effect is not only due to the coolness of the air, but also to the cooling effect of the velocity of the moving air as it increases the evaporation heat.

Evans shows air speeds which are effective for body cooling. However, Givoni indicates that to achieve better thermal comfort in buildings in hot arid climates, the maximum indoor air velocity induced by cooled air should not exceed 1m/s (1984).

Table 8.4 shows the ventilation rates for thermal comfort as a result of using either the 40mm or the 60mm cavity. It shows that with air flow rate 0.102m³/s both cavities induce acceptable ventilation rates when compared with the recommended

values. The flow of $0.05\text{m}^3/\text{s}$ produces slightly less ventilation. The measured ventilation rates induced by the buoyancy air flow with those recommended are given in Table 8.5. It shows that the measured ventilation rates meet the demands for health, whereas Summer ventilation for comfort requirements were only met when the cavity is 2 or 3 m long.

Table 8.5 Measured ventilation rates induced by natural flow and those recommended

Flow kg/s	Ventilation for Health. m^3/s		differences
	Natural flow 100 mm	Recommended per person	
0.043	0.036	0.015/3 persons	2.3 times greater
0.078	0.065	0.03/4 persons	2.1 times greater
	Ventilation for Summer comfort m/s		
0.043	0.30	* 0.6 - 1.0 ** up to 1.0	low
0.078	0.55	* 0.6 - 1.0 ** up to 1.0	reasnable
0.086	0.60	* 0.6 - 1.0 ** up to 1.0	acceptable

* Evans 1980

** Givoni 1988.

The criteria for evaluating satisfactory ventilation depends on the type of occupancy and on the climate. The desired pattern of air flow and distribution of velocities in the room vary with the function of the room. In a living room where most of the space is occupied by the people sitting, the best distribution would be when the velocities are about the same various points of the room and the main air flow is at the height of about a metre above the floor level. Thus the best criterion for evaluation of ventilation is the average velocity at height of 1.0 m. However, this criterion demands a study of air flow pattern across the room at that height in order to determine the average air velocity. Exact values of this analysis may require measurements. Since the ventilation evaluation is concerned with the implementation of one of the two cavities to

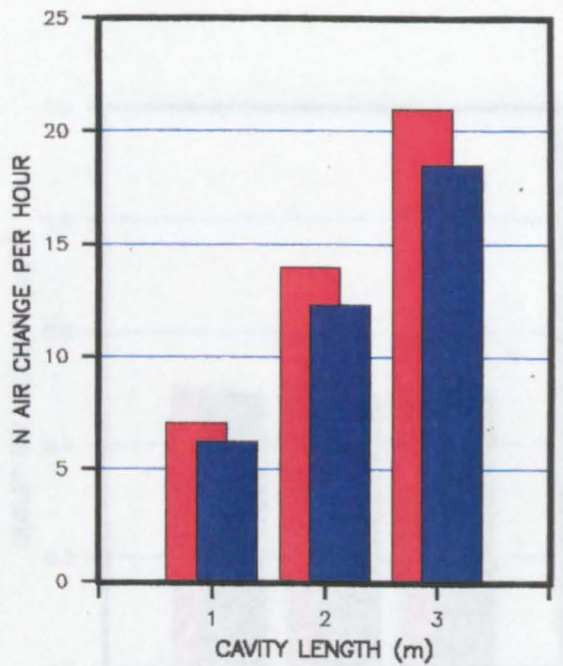
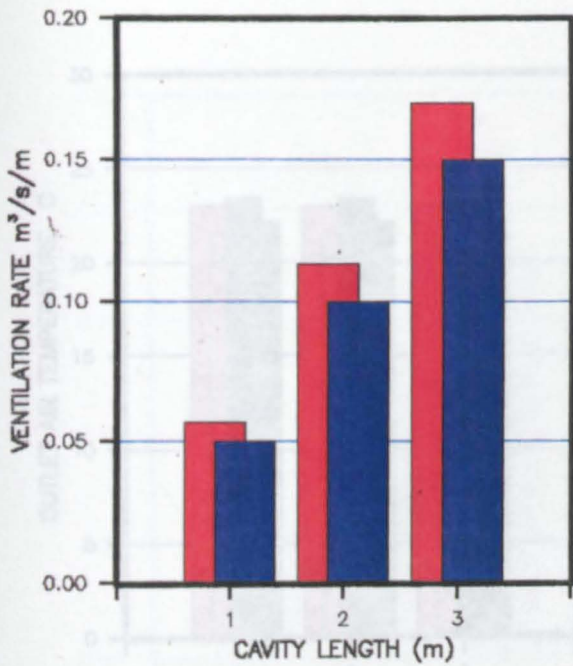
the room, the study of air flow pattern inside the room is a separate issue. Our concern at this stage is the ventilation in terms of air speed, and therefore, it is clear that both of the 40mm and the 60mm cavity could achieve the thermal comfort required.

For 40mm and 60mm cavities having the same length, the previous evaluative analysis shows that both the 40mm and 60mm produce good agreement with the recommended values specially of that of health requirements. The variation of 1K of the outlet air temperature on the degree of thermal comfort is of little significance and both cavities demonstrate satisfactory results.

Despite the results being acceptable the importance of thermal comfort on the evaluation is minor. In addition, the increase of the cooling rate as a result of decreasing the cavity from 60mm to 40mm was very small (5%) (Table 8.1). In contrast, the consumption of water for the evaporation increased by 44% as the cavity was decreased from 60mm to 40mm. It seems that the water consumption is a dominant factor in the judgment whether the 40mm or the 60mm cavity is preferable. It is thus preferable to exploit the 60mm wide cavity in a room in hot arid climates if water conservation is of great importance. Nevertheless, the 40mm cavity may be applied with a slightly better performance if water conservation is unimportant.

8.5 DESIGN APPLICATION

The length of the cavity with view to the above results may be important. It also raises the question of how the induced cooling as a result of evaporation with regard to the water issue is acceptable. As shown from Figures 8.11 and 8.13, the outlet air relative humidity, temperature and velocity were independent of the cavity length. Therefore, the main parameters in this analysis were the cooling rate, ventilation and water consumption. With the number of people more than three and large spaces the length of the cavity becomes significant. In the following evaluation the ventilation rate is interpreted as air changes per hour, the cooling rate as Watts per metre length of cavity and the amount of water needed for evaporation as litres per square metre per hour. The values used in the analysis are shown in a form of monograms in Figures 8.10, 8.12 and 8.14. These were based on laboratory observations. Figures 8.10 and 8.12 are concerned with the cavity with assisted flow 0.12kg/s and 0.06kg/s. Other values are illustrated for design purposes in Figure 8.11 and 8.13. The ventilation effectiveness in terms of 'air mixing' is reviewed to give a better insight into the evaluation of the cavity length on design application.



■	M=maximum	cavity 60mm
■	A=average	cavity 60mm
■	M=maximum	cavity 40mm
■	A=average	cavity 40mm

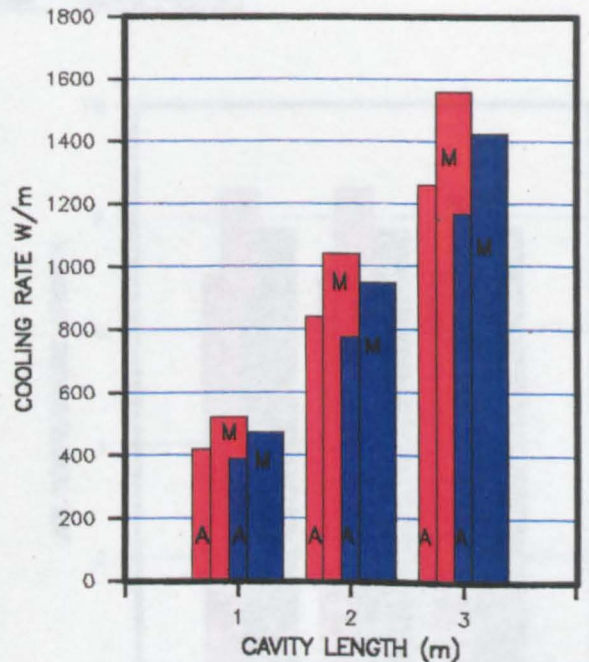
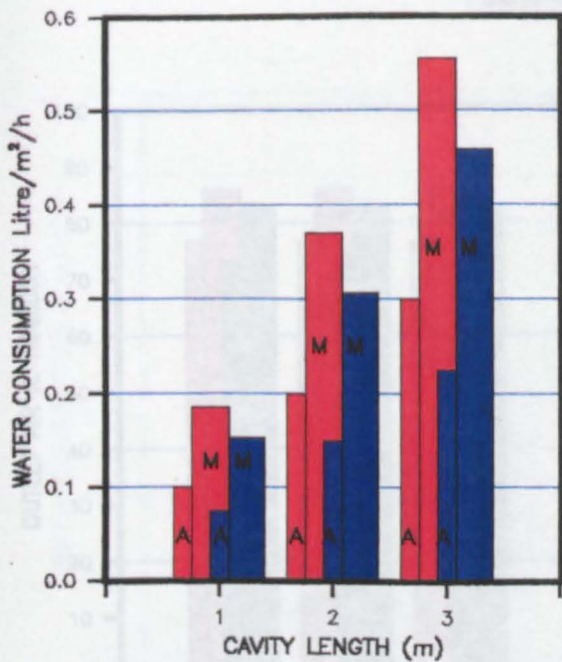
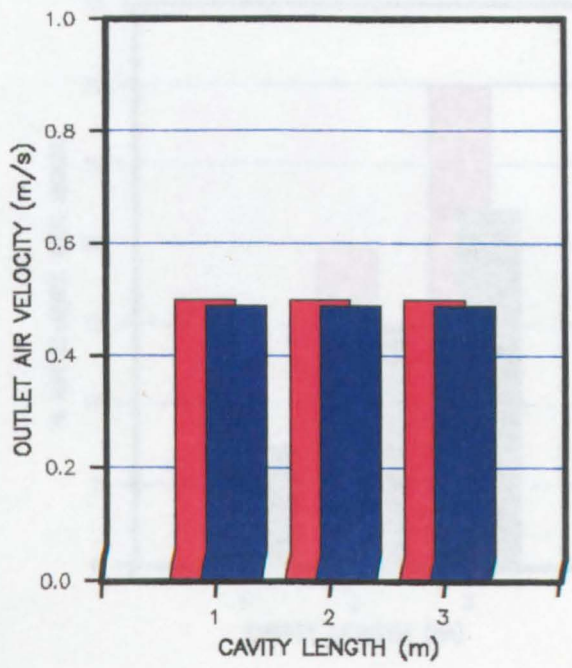
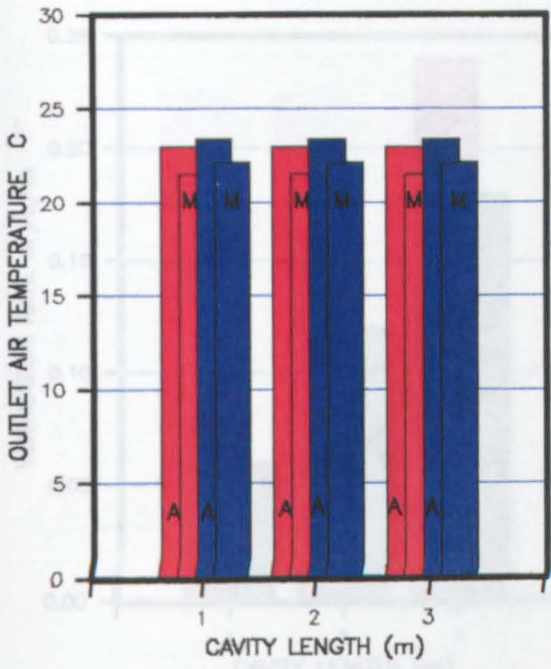


Fig.8.10 Parametric evaluation of cavity width for design applications.

Inlet air temperature and R.H. 30 C & 40%

Flow 0.06 kg/s



■ M=maximum cavity 60mm
■ A=average cavity 60mm
■ M=maximum cavity 40mm
■ A=average cavity 40mm

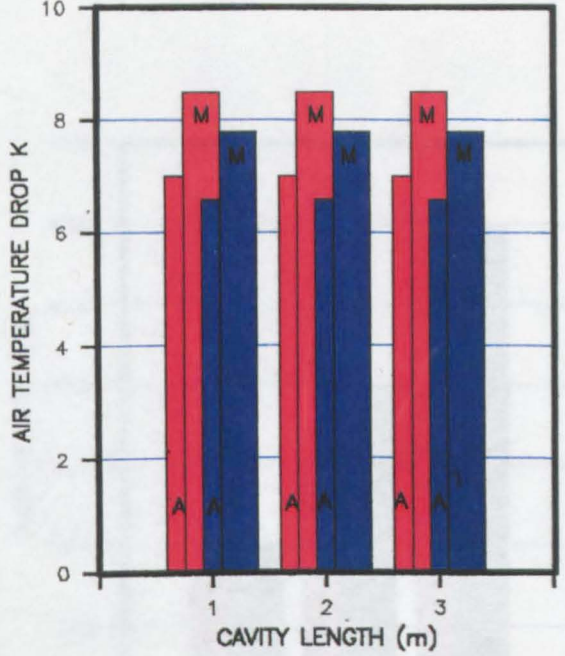
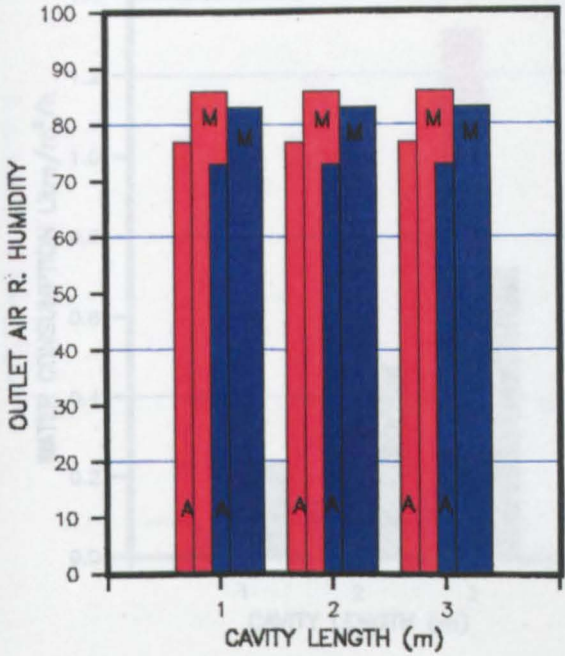
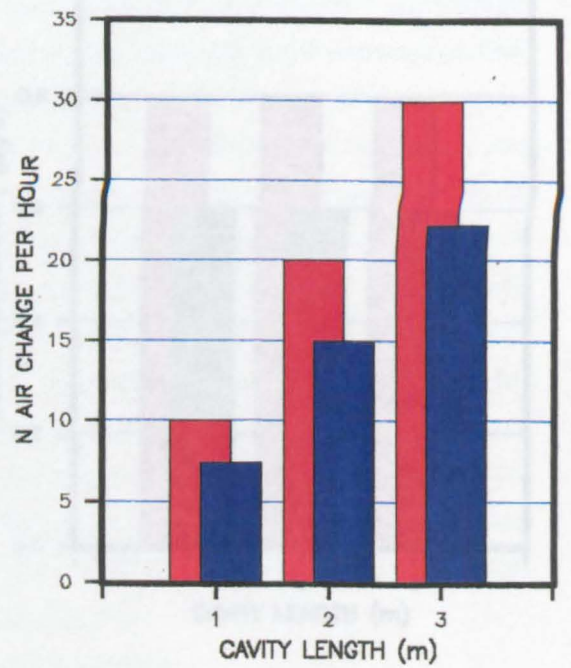
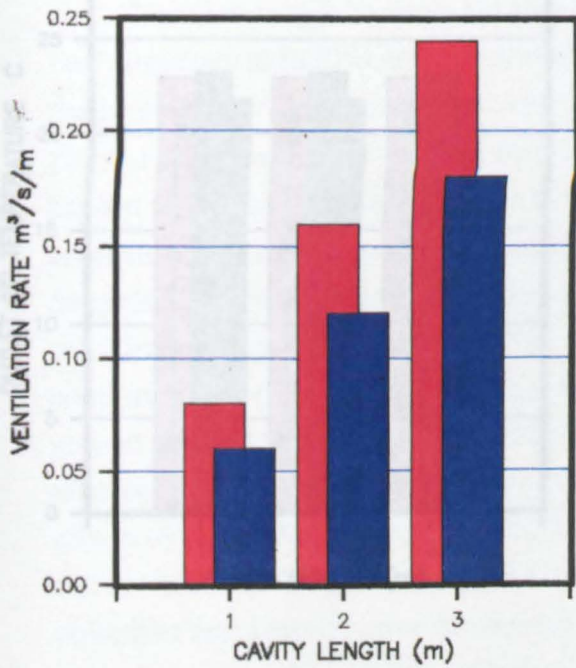


Fig.8.11 Parametric evaluation of cavity width for design applications.
 Inlet air temperature and R.H. 30 C & 40%
 Flow 0.06 kg/s



■ M=maximum cavity 60mm
■ A=average cavity 60mm
■ M=maximum cavity 40mm
■ A=average cavity 40mm

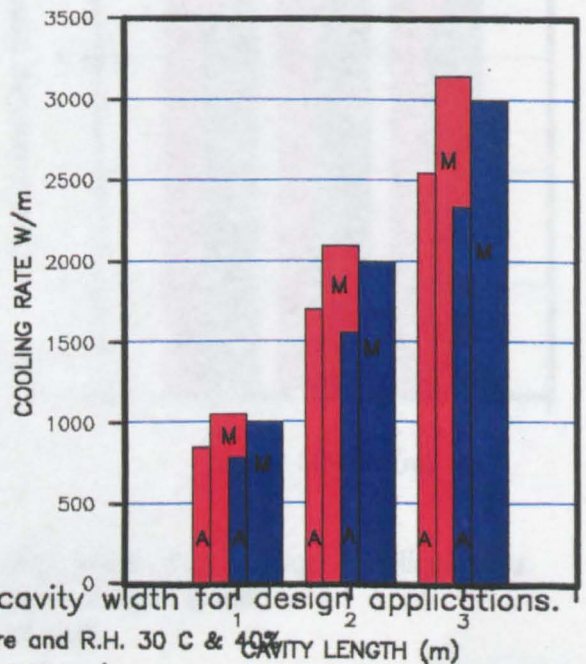
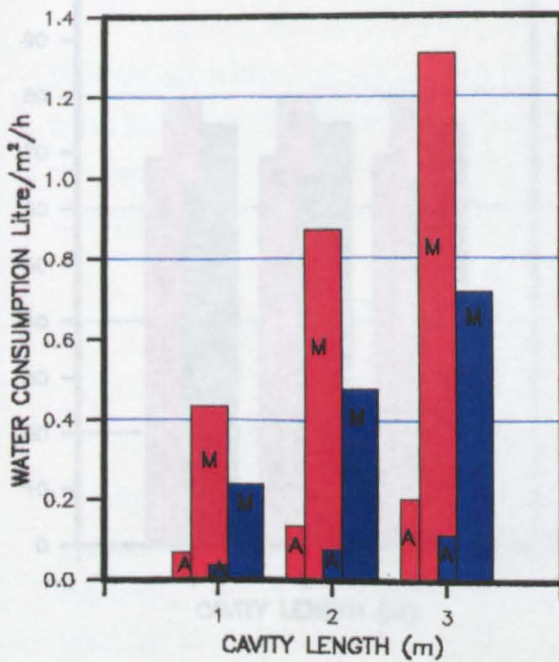
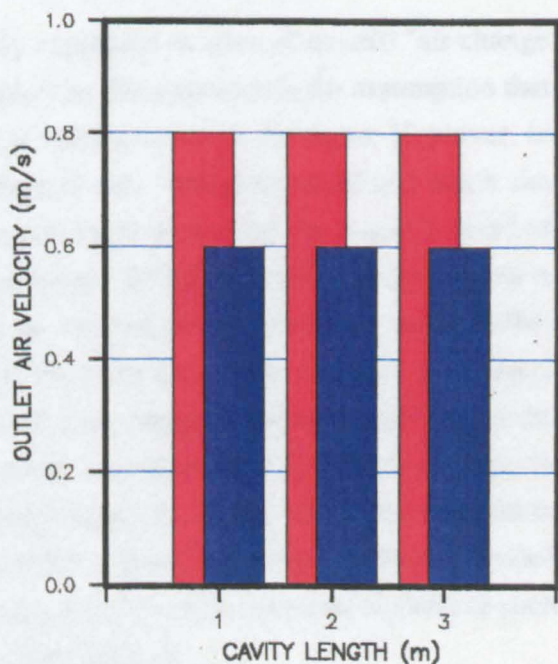
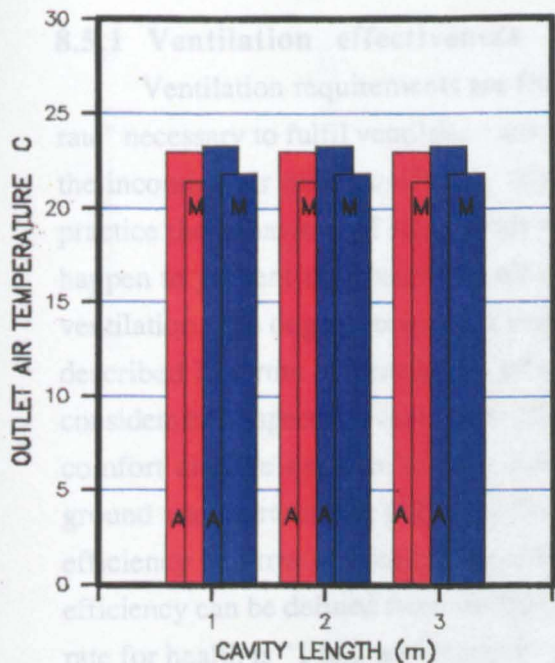


Fig.8.12 Parametric evaluation of cavity width for design applications.

Inlet air temperature and R.H. 30 C & 40%

Flow 0.12 kg/s



■ M=maximum cavity 60mm
■ A=average cavity 60mm
■ M=maximum cavity 40mm
■ A=average cavity 40mm

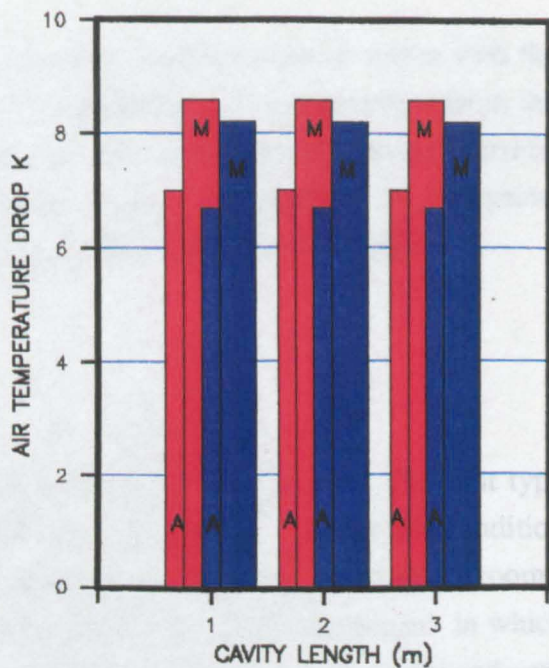
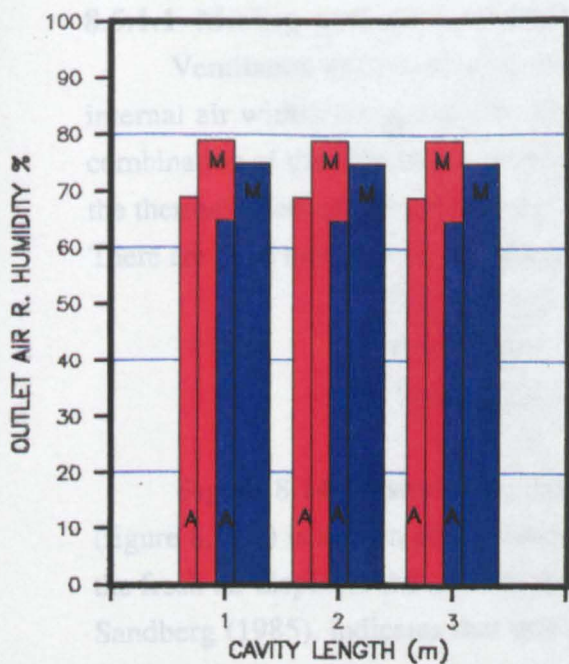


Fig.8.13 Parametric evaluation of cavity width for design applications.
 Inlet air temperature and R.H. 30 C & 40%
 Flow 0.12 kg/s

8.5.1 Ventilation effectiveness

Ventilation requirements are frequently expressed in term of overall "air change rate" necessary to fulfil ventilation needs. Implicit in this approach is the assumption that the incoming air mixes uniformly with that already present in the room. However, in practice the behaviour of internal air movement is not straightforward and much can happen to prevent the prescribed air change rate from providing the required level of ventilation. The degree to which a ventilation system fulfils ventilation requirements is described in terms of ventilation efficiency or ventilation performance. Laret (1984) considers two aspects of ventilation efficiency: these are the need to maintain the thermal comfort and the need to achieve low level of contaminants (odour, radon from the ground and surrounding pollution from plastics). Sandberg (1985) defines ventilation efficiency in terms of controlling contaminants. However, in hot arid zones ventilation efficiency can be defined from the thermal comfort point of view since the recommended rate for health is "1 to 2 air change/h". Liddament (1987) indicates that to achieve such objectives many aspects must be considered, these include:

- an understanding of room air movement
- regard for thermal comfort
- knowledge of the strength and location of pollution sources
- occupancy details and definition of zone of occupancy
- climatic data.

8.5.1.1 Mixing and air movement

Ventilation effectiveness is related to the way in which fresh air mixes with the internal air within the space. The pattern of the room air movement comes from the combination of the momentum of the incoming air and the convective current created by the thermal effect of the surfaces surrounding the air space, heat emitters and occupants. There are three extremes of air mixing conditions given by Liddament (1987):

- I - Displacement flow
- II - Perfect flow
- III- Short circuiting.

Figure 8.14 illustrates the differences between these extremes. The first type (figure 8.14 .a) is known as the most efficient form of ventilation. Under this condition the fresh air displaces the air with the room without mixing. However, in single rooms, Sandberg (1985), indicates that this type relies on the thermal displacement in which fresh air is slightly below room air temperature and distributes at a low level and very low speed (typically below 0.1 m/s).

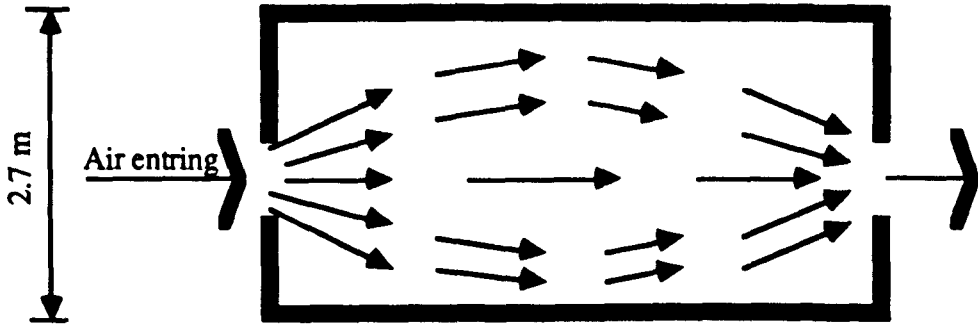


Figure 8.14 a. Displacement flow

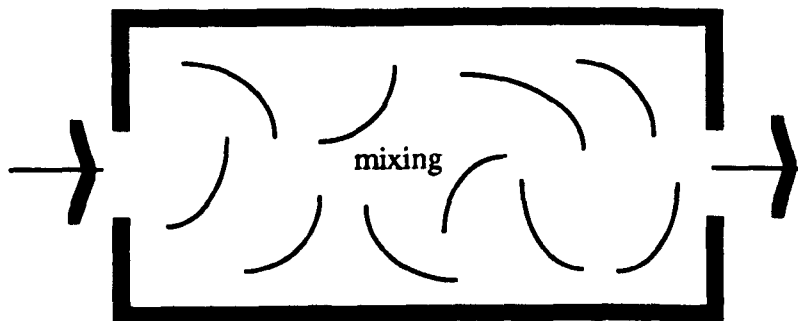


Figure 8.14 b. Perfect flow

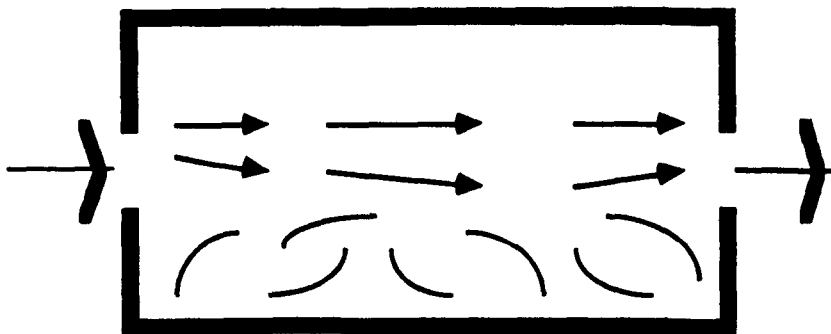


Figure 8.14c. Short circuiting

Figure 8.14 Extreme condition of air mixing in rooms

The second type (figure 8.14.b) is the most common design in building. This happens when incoming air continuously and uniformly mixes with interior air. The poorest ventilation takes place when fresh air leaves by the window without reaching where it is required (figure 8.14.c).

With regard to the cavity application, it is shown from the observations that air entering the room is always cooler than the air within the interior. In addition, the cavity outlet location is at the bottom of the room. So that it may contribute towards achieving the first example. In the following analysis ventilation is expressed in term of air changes h^{-1} with the assumption that air is perfectly mixed.

Considering a typical size of a room ABC with a length A, breadth B and height C and a 60 mm cavity is attached along the room breadth B, with air entering the room at a known air change rate h^{-1} at the bottom as shown in Figure 8.16. Assuming that air is mixing uniformly, the velocity of the air inside the room v_r can be calculated from :

$$v_r = N C / 3600 \quad [8.5]$$

where

v_r = the velocity of air inside the room m/s
 N = air change rate h^{-1}
 C = length of the room parallel to air movement direction m

With a room of 3.0 x 3.0 x 2.7 m the above equation.becomes:

$$v_r = 833 \times 10^{-6} N \quad [8.6]$$

In this part of the evaluation, the cavity was considered at three lengths 1, 2 and 3m. In the buoyant air flow the cavity width was 100mm, and for the forced flow it was 40mm and 60mm. The height of the outlet was 100mm. The results of the natural flow were divided into two sets: the first one was that of the ventilation induced by evaporation when there was little air temperature difference between the cavity inlet and the room. The second set was of the ventilation rate when the temperature difference between the inlet and the room was significant. The length of the cavity was varied at 1m intervals. The corresponding air change rate, the velocity of air inside the room, and the cooling rate are given. Tables 8.6 and 8.7 show the results of the buoyant air flow and Table 8.8 shows the forced air flow.

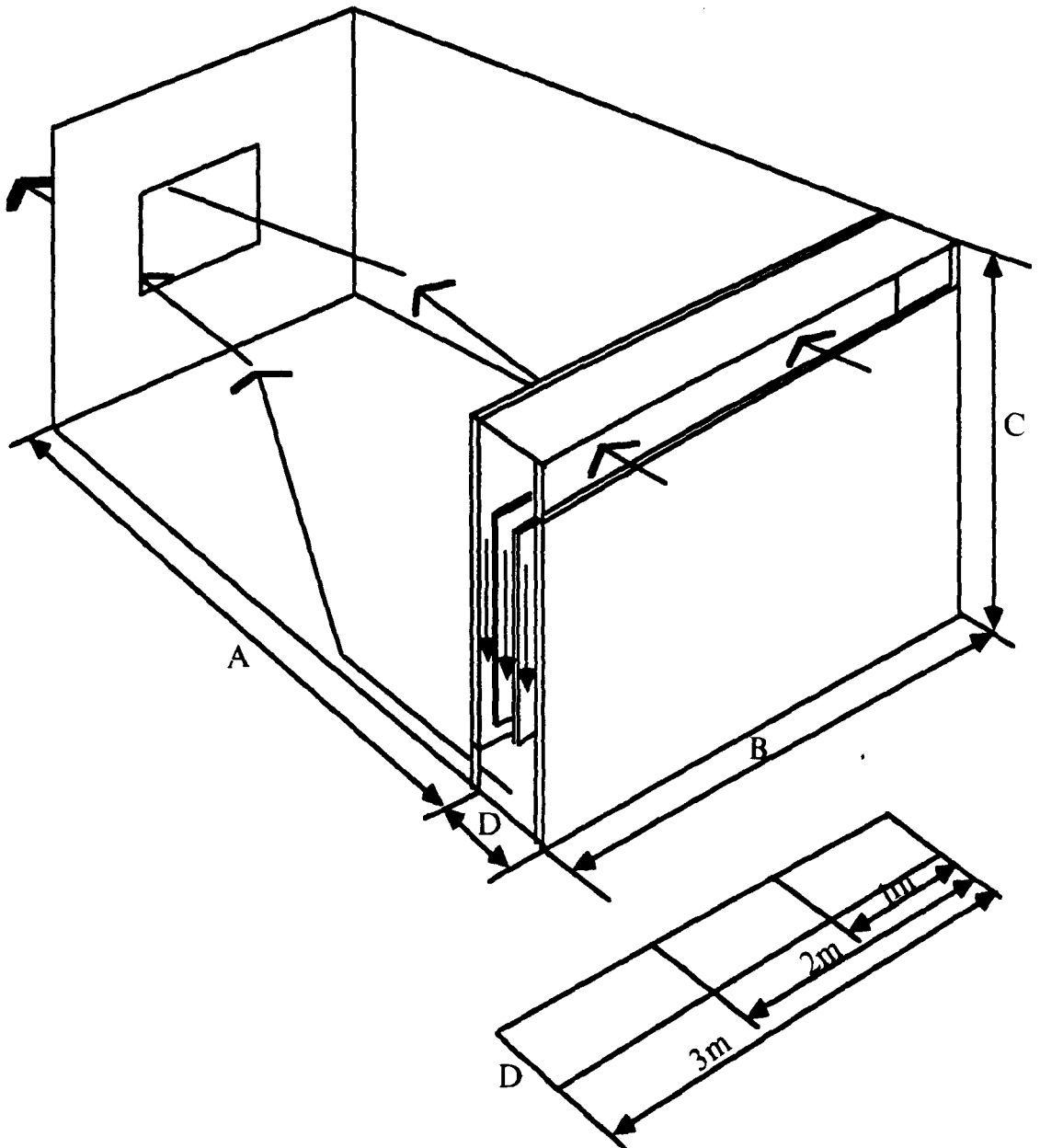


Figure 8.16. The cavity of 60mm attached ^{to} a room ABC

Table 8.6 The effect of the cavity length variations on air change rate, velocity of the air in the room and cooling

Length m	Ventilation rate $\text{m}^3/\text{s}/\text{m}$	Air change rate h^{-1}	Air velocity $\text{m}/\text{s}/\text{m}$	Cooling W/m
1.0	0.03	4.44	0.004	135
2.0	0.06	8.90	0.0075	270
3.0	0.09	13.30	0.01	405

Cavity with buoy. flow.

Table 8.7 The effect of the cavity length variations on air change rate, velocity of the air in the room and cooling

Length m	Ventilation rate m^3/s	Air change rate h^{-1}	Air velocity m/s	Cooling W/m
	Air temperature difference between the inlet and the room 2 K			
1.0	0.045	6.7	0.006	210
2.0	0.09	13.3	0.011	420
3.0	0.135	20.0	0.02	630
	4 K			
1.0	0.035	8.0	0.007	240
2.0	0.106	16.0	0.013	480
3.0	0.16	24.0	0.02	720
	6 K			
1.0	0.06	9.0	0.008	240
2.0	0.12	18.0	0.015	480
3.0	0.18	27.0	0.023	720

* Cavity with BUOY. flow

Table 8.8 The effect of the cavity length variations on air change rate, velocity of the air in the room and cooling

Cavity width mm	Ventilation rate m ³ /s/m	Air change rate h ⁻¹	Air velocity m/s	Cooling W/m
* Cavity length 1 m				
40	0.08	12.0	0.01	1050
60	0.06	9.00	0.0075	1000
* Cavity length 2 m				
40	0.16	24.0	0.02	2100
60	0.12	18.0	0.015	2000
* Cavity length 3 m				
40	0.24	36.0	0.03	3150
60	0.18	27.0	0.033	3000

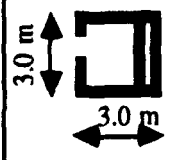
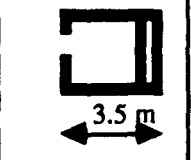
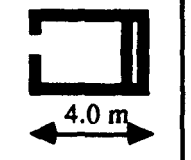
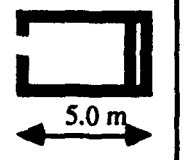
* Cavity with assisted flow 0.12 kg/s

Results of the first set indicate that for air moving in the cavity at a rate of 0.12kg/s, entering a room of a volume of 24.3m³. The air change was 4.44 h⁻¹, and increased to 9 and 13 h⁻¹ with a corresponding air velocity inside the room of 0.004, 0.0075 and 0.01m/s when the length is 1, 2 and 3m. In addition, the cooling rate was 135W/m and increased to about 400W/m. These values were considerably increased when air temperature difference between the room and the inlet exists, specially the cooling rates.

It is shown in table 8.7 that, the cooling rate induced by evaporation could be as high as 630 W/m and 720 W/m if 2K and 4K can maintained between the cavity inlet and the room attached. The corresponding air change rate and velocity of the air inside the room are 24 h⁻¹ and 0.020m/s.

The analysis also considers the variation of the size of the room in the flow direction (length m) up to a maximum of 5 m. The variations and their results are presented in Table 8.9.

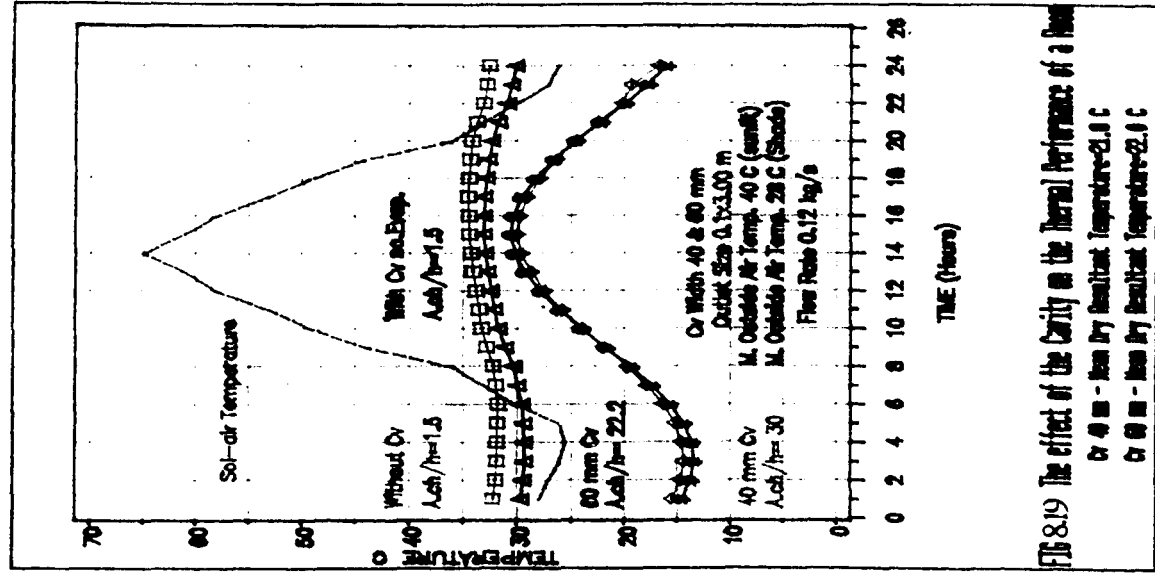
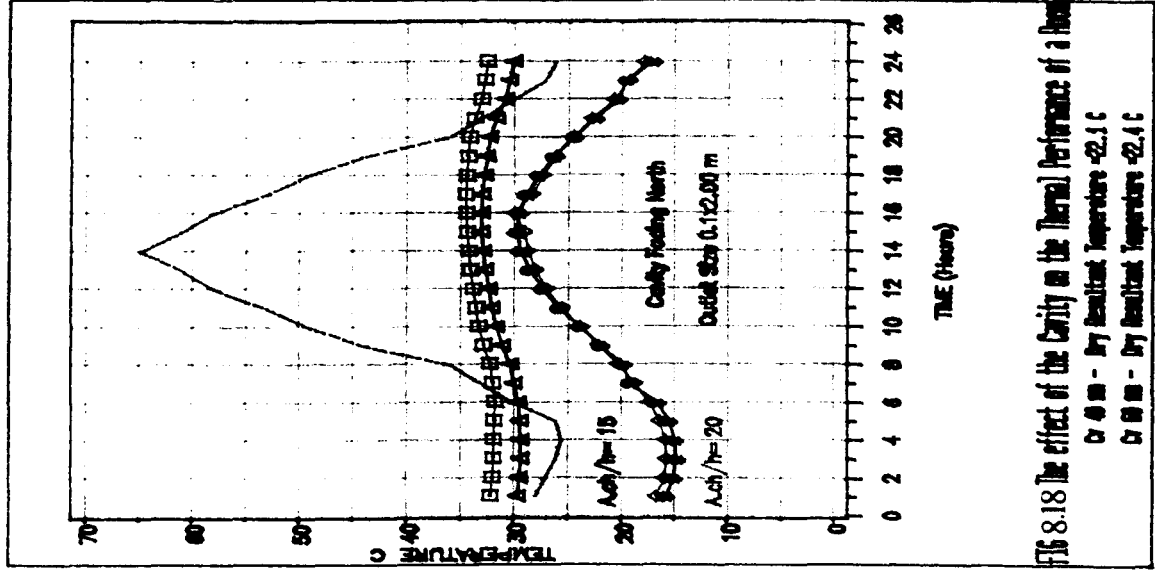
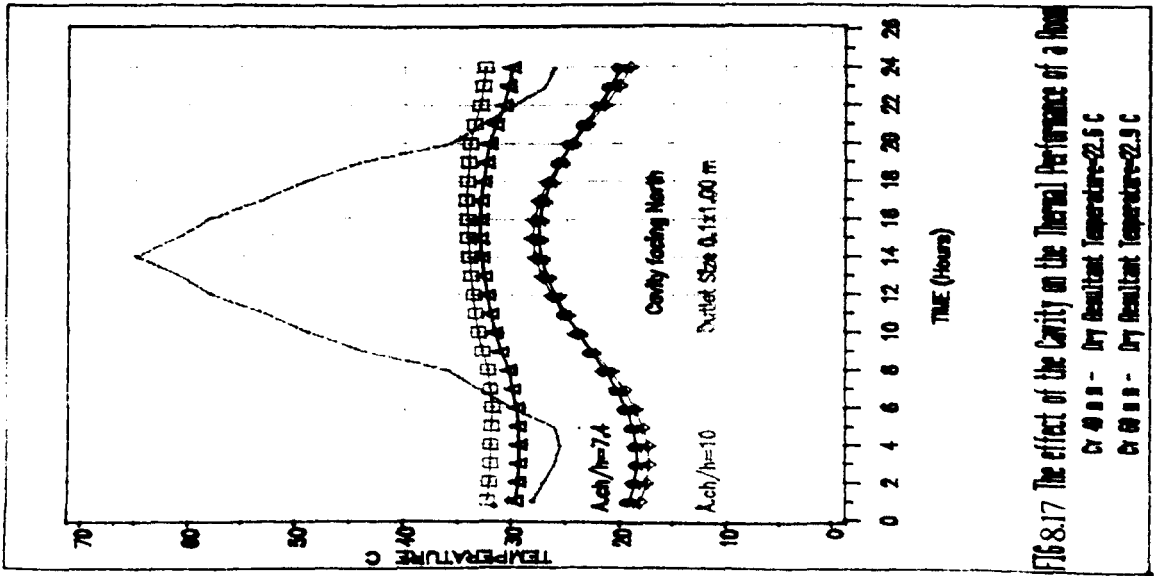
Table 8.9. Air change rate induced by the natural flow cavity in different rooms

Length m	Volume of the room m ³			
	24.30	28.35	32.40	40.50
Air change rate h ⁻¹				
1.0	4.44	3.81	3.33	2.70
2.0	8.90	7.60	6.70	5.30
3.0	13.30	11.4	10.00	8.00
	Room [1]	Room [2]	Room [3]	Room [4]
				

Cavity with buoy. flow.

The variation of the room size illustrates that the application of the cavity with buoyancy air flow should be limited to rooms of a maximum volume about 28.0m³ (Room [2]), where the height is 2.7m and the length of the cavity is 1 m if ventilation for summer comfort is an objective. This could be expanded to volumes of 40.0m³ (Room [4]) if the cavity length is 2 and 3m. In addition, for the 60mm cavity with forced air flow, the cooling rate 1 kW/m with "9 air change per hour" and could reach 3kW/m if the cavity is 3m long with "27 air change per hour". Nevertheless, this could be applied to rooms of bigger sizes if the height is less than 2.7m.

The final step in the evaluation is concerned the performance of the cavity with different lengths to determine to what extent the above results are acceptable. The parameters used in this analysis are the same as mentioned in section 8.3, except that,

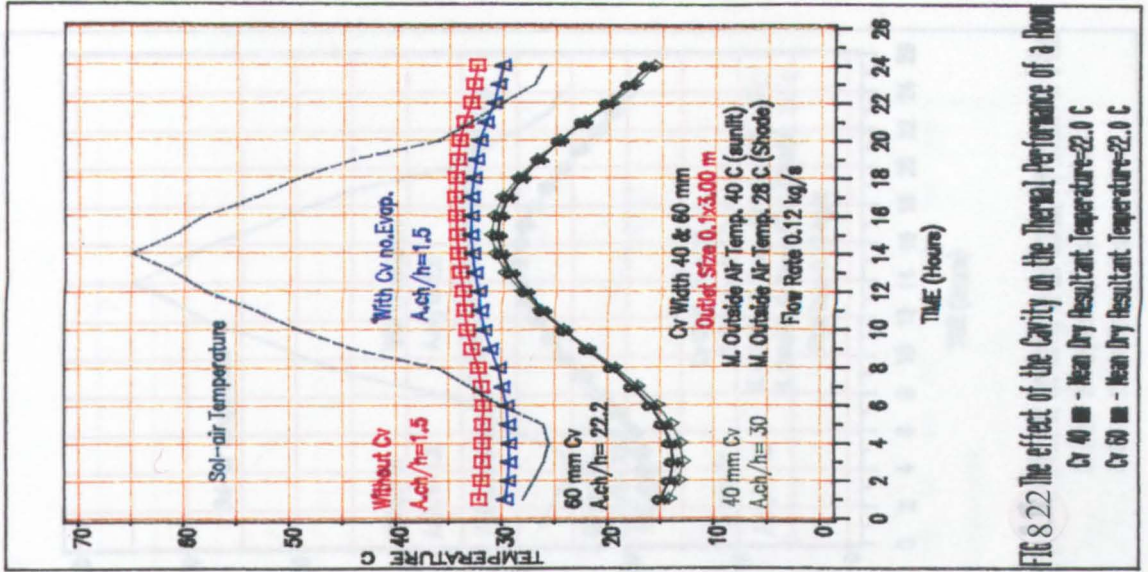
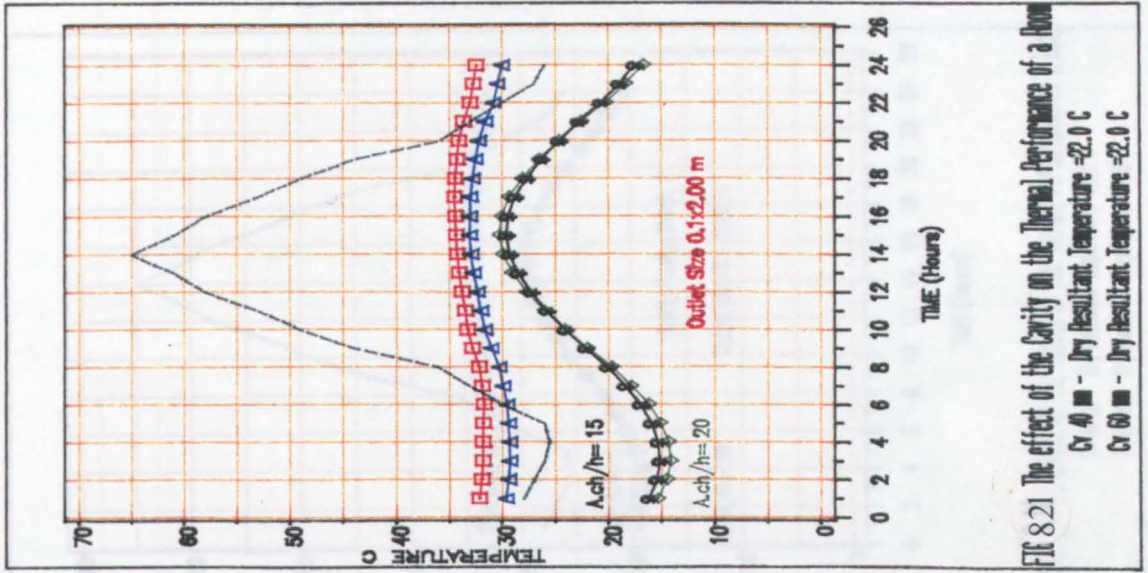
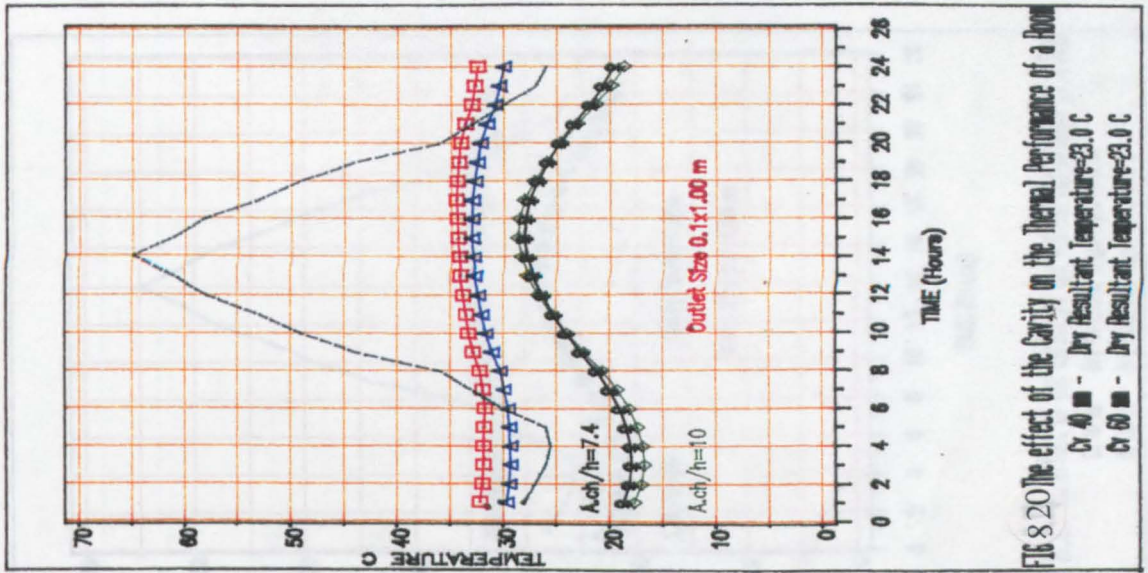


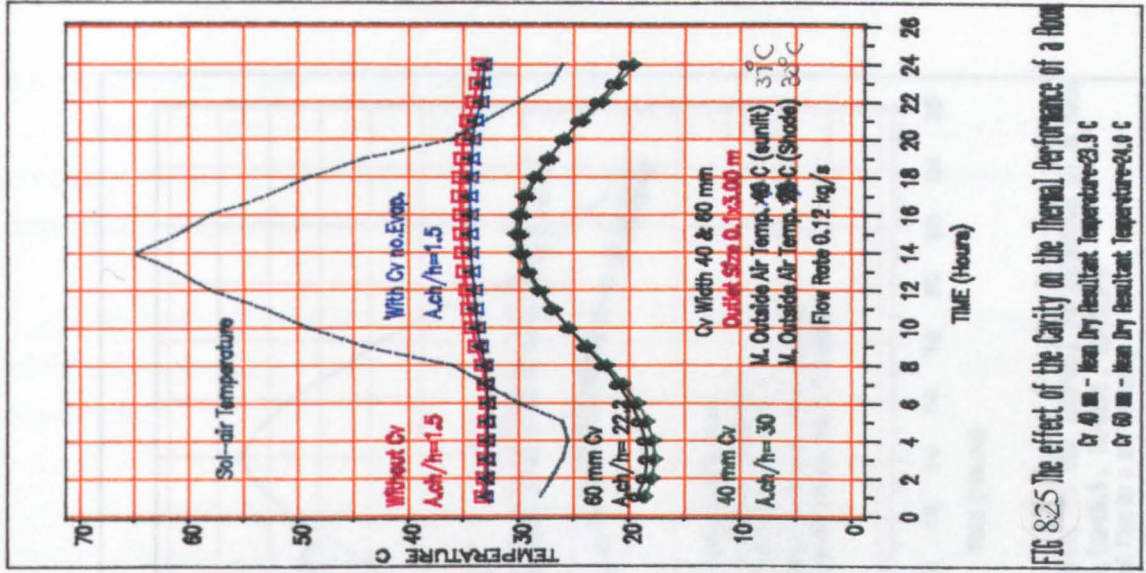
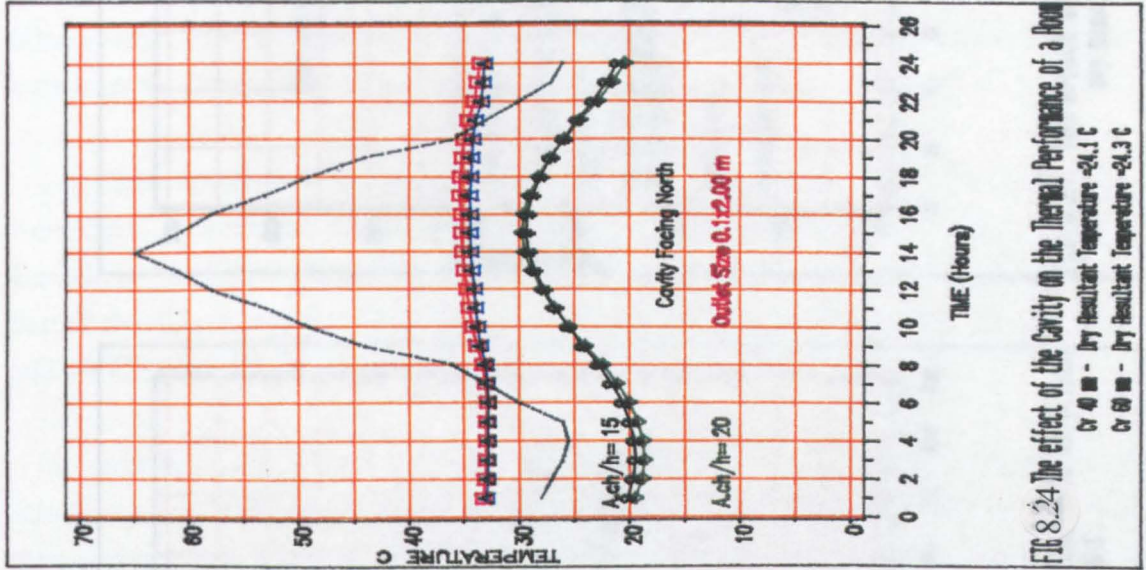
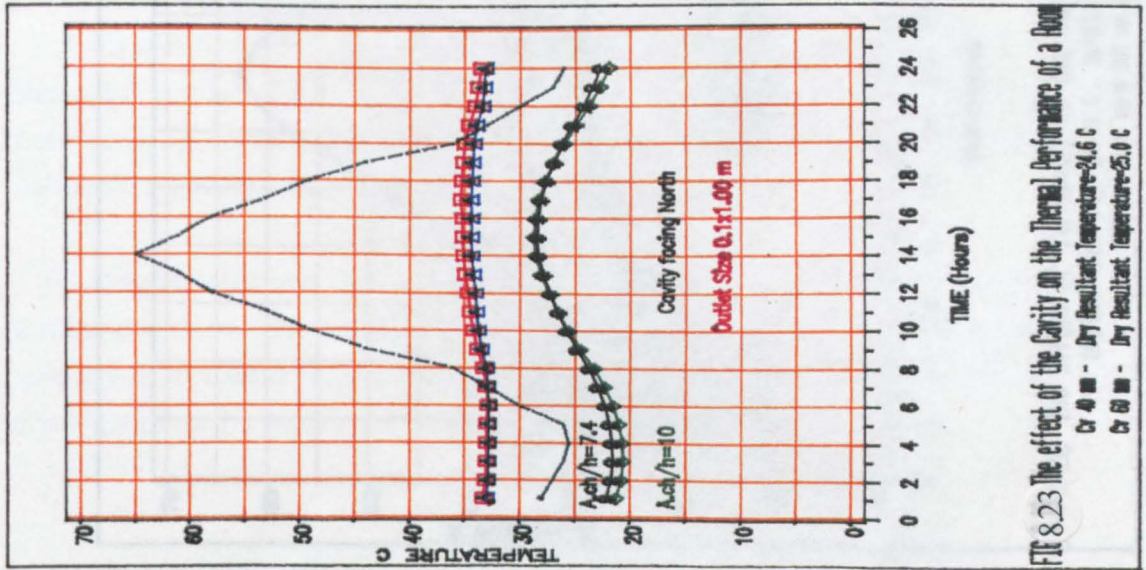
the East-West orientation of the room is also considered and the area of the glazing are 10% and 15% of the wall. In the calculation, day ventilation was operated at 10.00 and night ventilation at 20.00. Two ranges of outside air temperature were used; 40°C and 37°C. The performance of the room with and without the cavity with regard to these variables are shown in Figures 8.17 to 8.25 for the forced flow cavity and, Figure 8.26 to 8.27 for the buoyancy flow one.

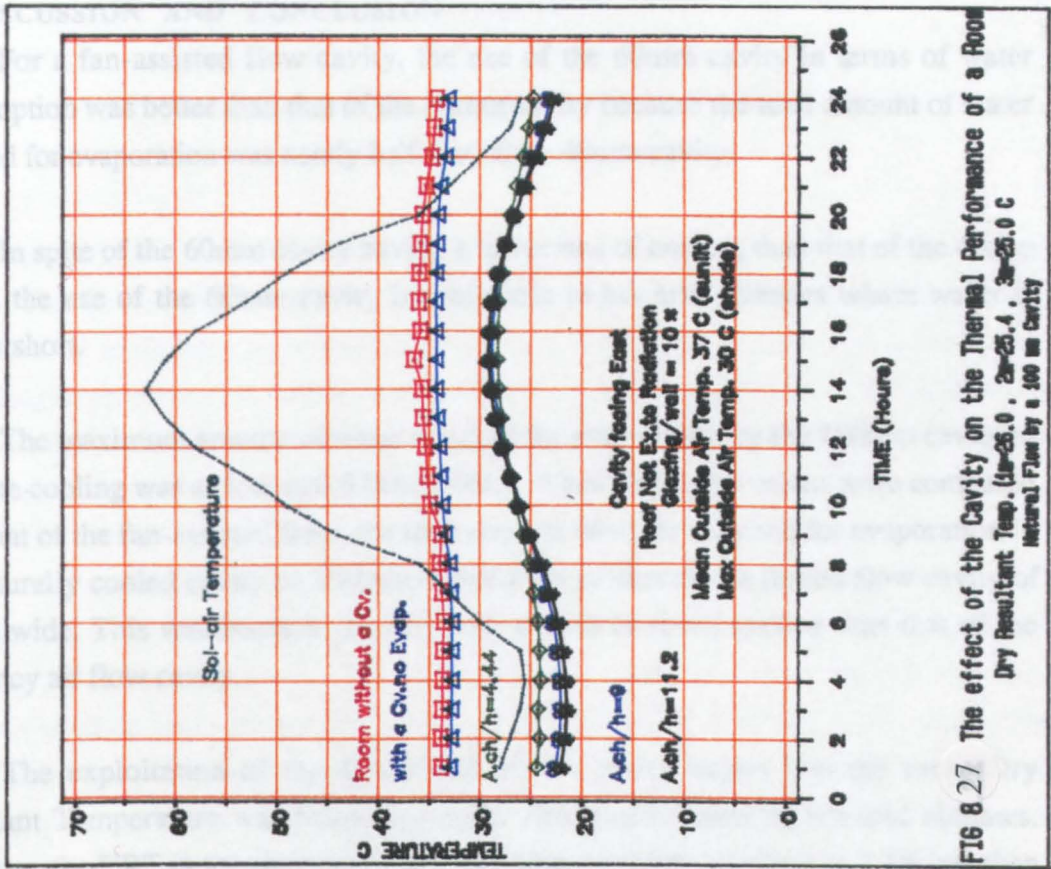
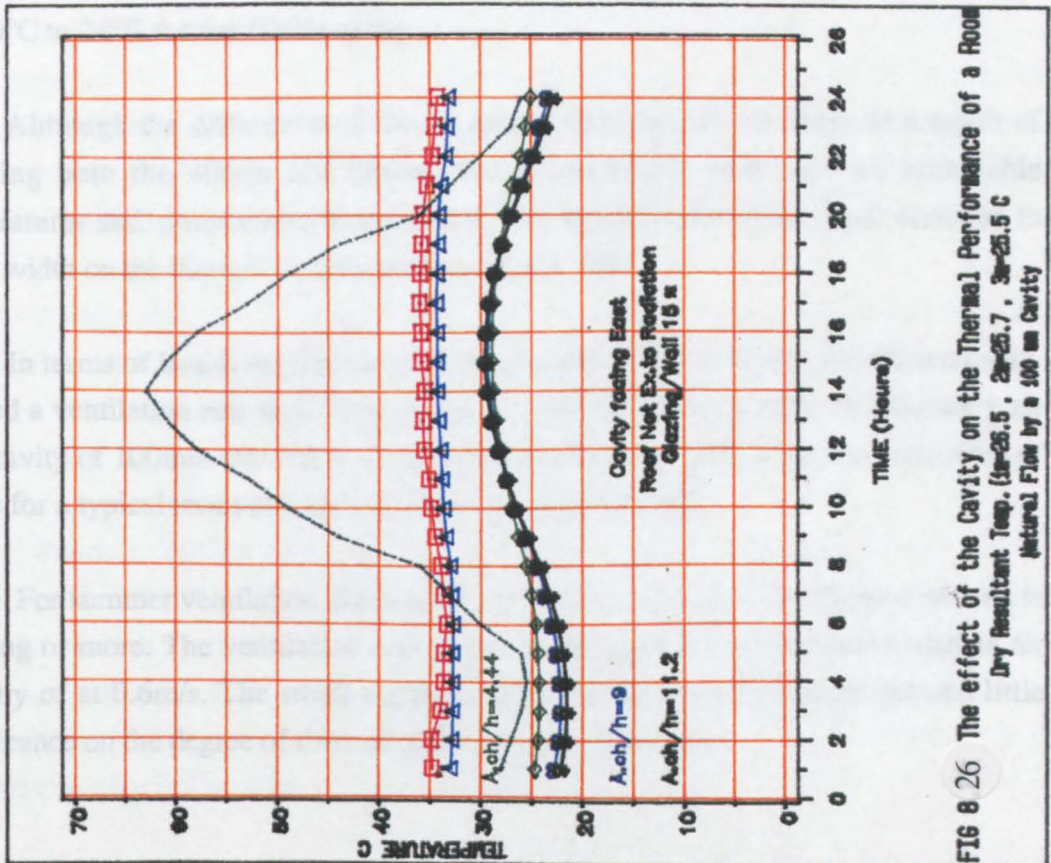
Figures 8.17, 8.18 and 8.19 show the thermal behaviour of a room size 32m³ with 40mm and 60 mm cavity facing North, at lengths of 1, 2 and 3m and outlet height of 0.1m. The thermal behaviour without the cavity and with the cavity with no evaporation are also shown. It is apparent that little changes in the mean Dry Resultant Temperature with reference to the ambient air temperature of 37°C in the sunlit side, and 30°C in the shaded side. The mean DRT in the middle of the room without a cavity was 34°C. The application of the cavity with no evaporation at ventilation rate 1.5 Ac/h reduced the mean DRT in the room by 1K. This was probably due to the ventilation resulting from convective cooling induced by the height difference of 2.7m. Figure 8.18 also shows that, the mean DRT was reduced substantially by about 8 K from 33°C to 25°C when cooled air at a ventilation rate of about 10 Ac/h was introduced from the 40mm and 60mm cavity. This indicates that the cooled ventilation as a result of evaporation by the 0.12kg/s forced flow of the 60mm cavity was significant to modify the internal environment inside a typical room of 32m³. The use of the 40 mm and 60mm cavity provides a minute drop in the mean DRT. In contrast, it shows a drop about 2 K when the length was varied from 1 to 3m (Figures 8.18 and 8.19). This was due to the increase of the ventilation rate by 20 Ac/h from 10 Ac/h at the 1m length to 30 Ac/h at the 3m which in fact increases the movement of the air current across the room and thus produces good mixing between the warm air at the top part of the room and the cooled air coming from the bottom upwards. Figure 8.18 shows the thermal behaviour of the with cavity of 40mm and 60mm facing east with the same condition as mentioned above. It is seen that the mean DRT was less by about 2K than that of facing north.

The thermal behaviour of the room in conjunction with the buoyancy flow cavity of 100mm at different lengths facing East in the middle of a three-storey building having a wall facing west in which 15% is glazing are shown in figure 8.26 and 8.27. It is shown that the mean DRT in the middle of the room attached to 1m long cavity was reduced by 6K from 33°C to 27°C due to induced cool ventilation at rate of 4.44 Ac/h.

It also shows that further reduction of about 2K and may take place when the length of the cavity is extended from 1 m to 3 m due to the increase of the ventilation rate from 4.44 to about 11 Ac/h. The mean DRT in the room was about 27, 26 and 25.5K when the length was 1, 2 and 3 m respectively. In addition, a drop of 1K of the mean DRT was found as the glazing was reduced from 15% to 10% of the wall facing west. This indicates that the smaller the glazing area in the wall facing west the lower the mean DRT in the middle of the room, this is due to the minimising of the solar gain through the fabric which added to the heat building up inside the room.







8.6 DISCUSSION AND CONCLUSION

For a fan-assisted flow cavity, the use of the 60mm cavity in terms of water consumption was better than that of the 40mm cavity because the total amount of water required for evaporation was nearly half that of the 40mm cavity.

In spite of the 60mm cavity having a lower rate of cooling than that of the 40mm cavity, the use of the 60mm cavity is preferable in hot arid climates where water is always short.

The maximum amount of water required for evaporation by the 100mm cavity to promote cooling was as low as 0.5 litre/m²/day. When the above values were compared with that of the fan-assisted flow, the total amount of water required for evaporation in the naturally cooled cavity of 100mm is one sixth of that of the forced flow cavity of 60mm wide. This was because the flow rate was three times greater than that of the buoyancy air flow cavity.

The exploitation of the 40mm and 60mm cavity shows that the mean Dry Resultant Temperature was below the upper limits of comfort in hot arid climates. However, the DRT in the room as a result of using the 40mm cavity was 1.4K less than that of the 60mm cavity. They were reduced from 30°C to 22.5°C for the 40mm cavity and 30°C to 24°C for the 60mm cavity.

Although the difference of the air temperature within the room as a result of attaching both the 40mm and 60mm cavity was small, both induced acceptable temperatures and comfortable environment. The significance of the small variation in cavity width on the thermal comfort evaluation was little.

In terms of health requirements of ventilation, both the 40mm and 60mm cavity showed a ventilation rate well above the recommended figures. Also the buoyancy air flow cavity of 100mm showed a ventilation rate 50% higher than the recommended of 2.4L/s for a typical room of 25m³ occupied by three persons.

For summer ventilation, the buoyancy air flow cavity is only effective when it is 2m long or more. The ventilation rate of the 2m long cavity was 0.11m³/s with an air velocity of at 0.6m/s. The small variation of the outlet air temperature showed little significance on the degree of thermal comfort within the room.

CHAPTER NINE

CONCLUSIONS AND SUGGESTIONS FOR FUTURE WORK

9.1 CONCLUSION

This investigation suggests that thermal comfort can be improved in hot arid climates by exploiting an evaporative cooling cavity built on the shaded side of a dwelling to promote cool ventilation during the day and at night. The study emphasises that comfort can be provided cheaply for the poor. The feasibility of 'natural' ventilation in places without electricity is attainable.

The experimental work played an important role in determining the rate of ventilation, cooling and evaporation provided by an evaporatively cooled cavity, and for finding the best optimum dimension for the cavity. It was shown that diffusion of water vapour reached up to 30mm from the wet surfaces over the height of the cavity, and separation between the wet surfaces greater than 30mm introduced a zone of still air (velocity below 0.1m/s) not offered by the evaporation. This zone became as wide as 170mm when the separation was 230mm.

Appropriate convective heat transfer for air flowing between two parallel vertical wet surfaces was not found in the literature. The measurements of the full scale model contributed successfully towards finding the convective heat transfer coefficient for air flowing between the two surfaces in cavity. The overall heat and mass balance enabled us to derive the appropriate coefficient.

Results showed that heat transfer by convection was small, but not negligible, especially with the separation of 30mm or below. However, as the separation increases to more than 100mm between the two wet surfaces convection becomes significant in determining the amount of heat transferred.

The values of the appropriate convective heat transfer coefficient were near to that given by the CIBSE Guide for 'free' vertical surfaces until the separation become less than 30mm, but more cannot be said because of large uncertainty in the measured heat transfer coefficient. The convective heat transfer coefficient found to be independent of the separation between the two wet surfaces above 30mm. It was affected by the separation only below 30mm.

Comparing the measured convective heat transfer coefficient with those given by the literature means little, owing to the uncertainty of the measured coefficient.

The investigation showed that the rate of evaporation required to induce ventilation cooling of 200W/m was of the order of 50×10^{-6} kg/sm generated by surface mass transfer of the order of 0.01kg/sm and water vapour pressure difference between the incoming air and the saturated boundary layer of the order of 700 Pa.

For a cavity 2m high with a top inlet of 0.2m high and a bottom outlet 0.1m high, the optimum width for cool ventilation was about 0.1m, divided by two wet partitions 5mm thick and 1.55m high, separated by 30mm in which four wet surfaces were provided. With a cavity of greater height, the optimum width would be greater.

Results showed that the use of outlet height greater than 0.1m lead to separation of the air flow about 0.09m from the top height of the outlet, and statistically showed that a lower average air velocity would be obtained as a result of this separation. Separation was eliminated when the outlet height was decreased.

The use of smoke to trace the downward air flow in the cavity enables us to determine the nature of the air flow. According to its Reynolds number the flow was laminar, but observation showed that the air flow was "transitional".

The smoke showed that air flow was mainly downward in the cavity and there was no reverse flow, except for a 50mm separation between the two parallel wet surfaces of the 0.16m cavity width. The reverse flow may be responsible for drop in the air velocity to of 0.075m/s where the average air velocity in 50mm separation ought to be 0.16m/s.

Observation showed that for an air temperature difference of about 6K between the incoming air and the wet surfaces, an air flow of about 0.04 kg/s per meter length can be achieved by an evaporatively cooled cavity. This could be thus increased by three times if the cavity were made 3m long. The outlet air velocity achieved with an outlet height of 0.1m is in the order of 0.3m/s.

A temperature drop of the incoming air of the order of 5 to 6K can be achieved by evaporation in a cooled cavity, and air enters the dwelling from the bottom of the cavity with sufficient air velocity to bring the air temperature in the dwelling to a comfortable

region. For example, with a mean radiant temperature of the surroundings of 37°C and incoming air into the dwelling without an evaporative cooling cavity the resultant temperature will be 33°C. When an evaporative cooling cavity is attached to the shaded side of a dwelling, the air coming into the dwelling will be cooled by 5K and enters at 25°C, reducing the resultant temperature by 3K to about 30°C.

In a very hot arid climate, the use of an evaporative cooling cavity can improve comfort if a temperature difference of 4K is maintained between the incoming air and that in the dwelling. When this temperature difference can be maintained, an outlet air velocity of 0.6m/s can be achieved. For example: as the outside air at 35°C enters the cavity, it will be cooled by 5K, and flows into the dwelling at 30°C. If the mean radiant temperature of the surrounding is about 37°C, the resultant temperature in the dwelling will be about 33°C, still in the comfort region. As the mean radiant temperature becomes lower, the resultant temperature may be decreased.

Observation showed that an evaporatively cooled cavity can increase the humidity of the incoming air by 20%, and this is a good indicator for a hot arid climate since the bioclimatic analysis of Cairo suggests that to bring the hot and dry outside air into dwellings, the moisture content in the air should approach an average of the order of 0.01. Cooling by evaporation with a cavity 0.1m wide showed that the incoming outside air at 21°C and 60% relative humidity (moisture content of 0.0096) can increase the moisture content in the air flowing into the dwelling by about 0.0007 as the temperature of the air fell by about 5K (0.0103)

The results suggest that in a hot arid climate, when the mean air temperature of the outside air is 30°C and 30% relative humidity (moisture content 0.0082), a drop of the temperature by 4K and an increase of its relative humidity to 80% are needed to reach the target suggested by the bioclimatic analysis of Cairo. The maximum target of a moisture content of 0.014 could be attained if the air is cooled by 2K and relative increased to 85%. This increase of the relative humidity is still in the upper region of comfort according to Arens et al. (1983).

The results showed that water removed by evaporation from the wet surface for cooling is in the order of 0.08kg/hm, with a cavity 2m high and 0.1m wide. The observed 'cavity life' to promote cooling was about 24 hours provided that a water content of about 2kg/m is maintained within the wet surfaces.

The study suggests that in places with cheap electricity, an evaporative cooling cavity with a fan can be used to promote cooling. The results showed that with a uniform air flow in the cavity, evaporation could take place effectively if the width of the cavity be below 0.125m.

For a cavity 2m high, with a top inlet of 0.25m and bottom outlet 0.1m high, the optimum width was about 40mm divided by two wet partitions (mats) each 5mm thick and 1.55m high, separated by 10mm, providing four wet surfaces for evaporation. A ventilation rate of 0.07m³/sm can be promoted which provides an outlet average air velocity of about 0.7m/s as air enters the inlet at an average velocity 0.37m/s. A temperature drop of the incoming air of about 8K could result from evaporation by which an average cooling of the order of 700W/m can be achieved. If the cavity is long enough (3m), this could increase the rate of ventilation to 0.21m³/s, hence cooling to about 2kW.

Observation showed that cavity width of 60mm can be used with satisfactory results.

The study indicates that water vapour within the wet surface became less with time, resulting of a cooling decreased from 1kW/m to 850W/m at a rate of 25W/hm. The rate of cooling decline was 2%/h for the first 10 hours and rising to 2.5%/h for another 10 hours, and that suggests that water should be maintained at a rate of 0.024kg/hm within the wet surfaces to ensure that cooling of 1kW/m is prolonged.

If electricity is expensive, an air velocity at the inlet of the order of 0.2m/s can induce cooling of about 500W/m provided by a temperature drop of the incoming air of 7K and an outlet air velocity about 0.5m/s with an evaporative cooling cavity.

Comfort can be improved with fan assisted air flow in an evaporative cooled cavity, but the fan is not essential. As the air temperature in hot arid climate could be 35°C, with a mean radiant temperature of 40°C, if the cavity is not working, the

resultant temperature in the dwelling will be 38°C which is above the comfort limit (32°C to 36°C). When the cavity is working, the air will be cooled by 8K, and enter the dwelling at 27°C. The resultant temperature can be reduced to 32°C. The resultant temperature could be lowered to 29°C when the mean radiant temperature is reduced from 40°C to 33°C.

For hot arid climates, the study suggests that the humidity of the dry air flowing into dwellings can be increased to comfort with a fan assisted evaporative cooling cavity 0.04m wide. For example: if the incoming air is about 30°C and 40% relative humidity, the amount of water vapour added to the air flowing into the dwelling as a result of evaporation can be about $0.0022\text{kg}_{\text{w.v.}}/\text{kg}_{\text{dry air}}$ (about half that suggested by the bioclimatic analysis of Cairo, Table 1.6). If the incoming air has a relative humidity of about 10% less relative humidity, $0.005\text{kg}_{\text{w.v.}}/\text{kg}_{\text{dry air}}$ can be added to the air, enough to make the outside air moist. When the relative humidity is below 30% (at noon in a hot arid climate), the evaporation potential can be higher. Assuming the same drop in the temperature of the incoming air and increase in its relative humidity, the above value could be $0.008\text{kg}_{\text{w.v.}}/\text{kg}_{\text{dry air}}$ which satisfies the recommended value for summer.

9.1.1 Design application

In order to built an evaporative cooling cavity to promote cool ventilation, the following advice is offered:

- the measured ratio between the height of the cavity Z and its width D to promote cool ventilation ought to be:

$$Z / D = 20 \quad [9.1]$$

- the height of the wet surface M_h should be proportional to the cavity height Z so that:

$$M_h / Z = 0.7 \quad [9.2]$$

If for example the cavity is required to be 4m high, the width of the cavity would be 0.2m and the height of the wet surfaces inside should be about 2.8m.

- the measured ratio between the outlet height O_h and cavity height Z to achieve sufficient rate of ventilation for cooling ought to be:

$$O_h / Z = 20 \quad [9.3]$$

- the separation between the wet surface M_s and the cavity height Z should be related by:

$$Z / M_s = 66 \quad [9.4]$$

- to provide enough air through the cavity, the inlet height I_h should be related to the cavity height Z by:

$$I_h / Z = 0.1 \quad [9.5]$$

- the cavity should be as long as possible to reach the air flow and its cooling as large as possible.
- the north or eastwardsides of the dwelling are recommended for building the cavity so that air for most of the day comes from the shade.
- the inlet and the outlet of the cavity could be extended along the whole length of the cavity to maximise air flow in the cavity and into the dwelling.
- the use of the two mats in the cavity to promote cool ventilation are recommended to last in good condition for at least a year.

However, with extended inlet and shorter outlet the air velocity into the dwelling may be increased provided that the rate of ventilation achieved by a longer cavity is more than enough for ventilation. The increase of air velocity which may result from reducing the outlet length could reduce the resultant temperature in the dwelling even further. We believe that if the outlet size is reduced to be at height of 0.08m and 0.7m long, with a

cavity 3m long, the outlet air velocity would be 0.6m/s enough to reduce the resultant temperature in the dwelling to 28°C, if the incoming outside air is 38°C and the mean radiant temperature is 37°C.

The investigation of an evaporative cooling cavity showed that it can be a useful way of achieving comfort in dwellings. Nevertheless, there are several disadvantages:

- in a tall building, the temperature of the outside air flowing into the cavity of the top dwellings may be higher than those at the lower levels of the building due to the density difference between air along its height, and this may affect the performance of the cavity to promote the suggested rate of cool ventilation. However, it is an advantage for the dwelling at the lower levels in which outside air may remain cooler.

- the effect of short-wave radiation, especially at noon when the solar intensity is maximum, at the top of the evaporative cooling cavity may contribute toward reducing the cooling, however, this may be considered to be small since the width of the cavity is small (0.1m). Meanwhile, achieving comfort may be affected by the increase of the mean radiant temperature of the ceiling of a top storey dwelling of the building.

- insects and birds may enter the cavity since it is cooler than the outside, however, to eliminate this a mesh with little resistance to the air flow can be built at the inlet since the total pressure difference created by density difference in the cavity is mainly consumed at the inlet.

- additional cost may result from building the cavity because of the construction of the internal wall. However, it may be acceptable in view of the benefit resulting from achieving comfort in hot arid climates.

Ventilation can be maximised if a sun-warmed cavity 2m high and 0.2m wide (a 'solar chimney') is built on the sunny side of the dwelling (Bouchair 1989). For example: for a room volume of 40m³ (3.2m x 5.0m x 2.5m). With both cavities, ventilation will be enhanced since the evaporative cooling cavity will provide ventilation for a volume of 20m³, and the sun-warmed cavity will remove the air from the second 20m³ at nearly the same rate of ventilation. As a result "20 air changes per hour" may be provided. Such a rate will cool the dwelling effectively, and the quality of the air will be

improved for a better healthy environment.

The concept of attaching a solar chimney to a dwelling having an evaporative cooling cavity (Figure 9.1) may be a good application in terms of providing ventilation during the day and at night. For example: cool ventilation during the day may be achieved by an evaporative cooling cavity since the outside air is hot and dry, meanwhile the solar chimney is storing heat within its walls. At night, the inside air temperature is low, the stored heat within the dwelling's fabric starts to dissipate the heat inwards by radiation. To achieve comfort, the solar chimney can be used.

Where the air is too hot at night, ventilation may be improved by operating both cavities.

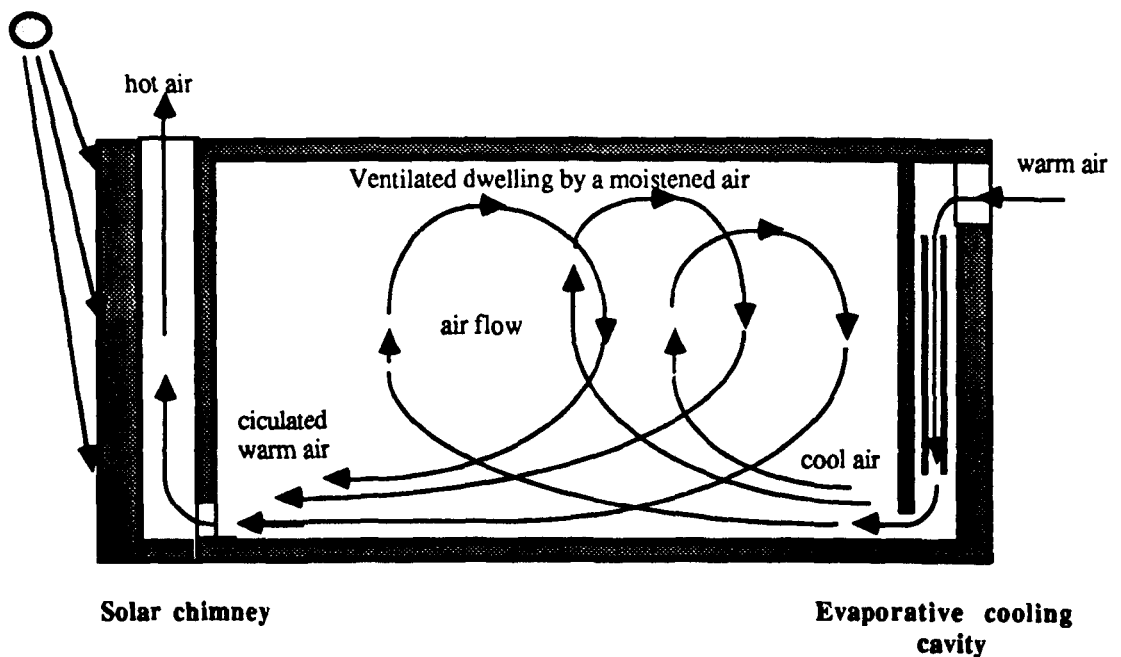


Figure 9.1 A suggestion for a combined 'evaporative cooling cavity' with a 'solar chimney' to a dwelling in hot arid climate.

9.2 SUGGESTIONS FOR FURTHER WORK

During the investigation, it became clear that further work might be desirable and it is outlined below :

- the actual values of convective heat transfer coefficients are needed when the cavity is built as high as 4m with wider separation and a temperature difference between the incoming air and the wet surfaces greater than 6K.

- observation of the convective heat transfer coefficient are needed when a solar chimney is attached to the dwelling.

- more studies are needed for the separation of 20mm between the two wet surfaces.

- it is useful to obtain field measurements of a full scale evaporative cooling cavity built on a shaded side of an occupied dwelling in hot arid climate in which the actual performance can be determined. The effect of actual climate, wind interference and other effects may influence the performance of the cavity.

- observations on both the evaporative cooling cavity and the solar chimney working together are required to assess the actual rate of ventilation and cooling on achieving comfort.

- observations on the effect of the ceiling of the top storey dwelling in a multi-storey building are required to assess the efficiency of ventilation and cooling promoted by an evaporatively cooled cavity.

- observations on the effect of the temperature of the soil at ground level to assess the performance of the evaporative cooling cavity in terms of ventilation cooling, especially when the surface temperature of the soil reaches 65 °C.

- more analysis is required on the air flow pattern inside a dwelling with an evaporative cooling cavity.

- observations are required to assess the performance of a full scale cavity when its built as high as 4m to provide comfort in public buildings.

REFERENCES

Abrams, D. W. (1985). "Low-Energy Cooling" A Guide to the practical Application of Passive Cooling and Cooling Energy Conservation Measures, VAN NOSTRAND REINHOLD COMPANY, N.Y., U.S.A, 1985.

Adolph, E. F. (1974). "Physiology of man in desert," New York, p.p. 1S, 1974.

Aitchison, G. A. (1962). "A consideration of vegetation landscaping and microclimate conditions for building comfort, *M. Arch.Thesis (unpublished)*- University of Melbourne, 1962.

Akbarzadeh, A., Charters, W. W. S. and Lesslie, D.A. (1982). "Thermo-circulation characteristics of Trombe wall passive test cell". *Solar energy*, vol. 28, No.6, pp.461-468, 1982.

Alamdari, F. and Hammond, G. P. (1983). "Improved data correlations for buoyancy-driven convection in room". *BSE & T*, vol. 4, no. 3, pp. 106-12, 1983.

Alawa, S. (1981). "Housing design in extreme hot and arid zones with Special reference to thermal comfort." *Dept. of building Science*, Lth. University of Lund, Lund, Sweden, 1981.

Arens, E. (1981). Cities in World Literature Review and Annotated Bibliography, "Passive Cooling by Natural Ventilation" *FSEC-CR 81-21(TT)*, Florida Solar Energy Centre, 300 State Road, Cape Canaveral, Florida, 1981.

Arens et al . (1984). " A new bioclimatic chart environmental design" 1984.

ASHRAE, (1985). "Handbook of Fundamentals". *American Society of Heating Refrigerating and Air-conditioning Engineers*. Atlanta, GA, U.S.A.

Bahadori, M. N. (1978). "Passive cooling systems in Iranian architecture" *Scientific American*, vol. 238, pp. 144-154.

- Bahadori, M. N. (1979).** "Natural cooling in hot arid regions" *Solar Energy in Buildings*, A.A.Sayigh, editor, Academic Press, New York, pp. 198-225, 1979.
- Bahadori, M. N. (1981).** "Pressure coefficients to evaluate air flow patterns in wind towers" *Proc. Int. Passive and Hybrid Cooling Conf., vol. I, Miami beach, Fla. International Solar Energy Society*, pp. 206-210, 1981.
- Bahadori M. (1985).** "An Improved Design of wind towers for Natural Ventilation and Passive Cooling", *Solar Energy*, Vol. 135, No. 2, pp.119-129, Pergamon Press Ltd., London, 1985.
- Balcomb, J. D. (1978).** " State of the Art in Passive Solar Heating and Cooling", *2ND National Passive Solar Conf. held Philadelphia, US*, pp. 5-12, Mar 1978.
- Barry and Chorley R. J. (1971).** "Atmosphere, weather and Climate.", PP. 345-360, London, 1971.
- Batchelor, G. K. (1954).** " Heat transfer by free convection across a closed cavity between vertical boundaries at different temperatures" *Quarterly of applied mathematics*, vol.12, No.3 pp.209-233. 1954.
- Bedford, T. (1936).** "The warmth factor in comfort at work" *Medical Research Council, Industrial Health Reseach Board*, Report No. 76, 1963.
- Bezett J. D. (1949).** "The regulation of body temperature" Newburgh : Phsiology of heat regulation and science clothing, New York, Sawnders, pp. 109- 192, 1949.
- Blant, S. M. (1958).** "Report on Spray roof cooling System", Ind. Exp. Prog. Facts for industry Ser., Bull, No. 9, North Carolina State College, N. Carrollina, USA, 1958.
- Boguslawa Prucnal-Ogunsido and Olusimiloo. O. Ogunsote, 1988.** "CLODHOT: A Design Aid for Multi-Index Design Stress Analysis." *Architectural Science Review*, vol. 31. No. 3, pp. 99-106, 1988.
- B.R.E. (1973).** "British Research Establishment" *Digest No. 60*, 2nd Series, pp. 1-7.

B.R.E. (1978). "British Research Establishment" *Digest No. 210*, pp.1-7

B.M.A. (1988). "The British Medical Association", London, 1988.

Broughton, H. E. (1955). "The Thermal Insulation of Building", *HMSO*, London , 1955.

CIBSE 1986. "CIBSE Guide" Volume A. *Chartered Institution of Building Services Engineer*, London.

CIBSE 1986. "CIBSE Guide" Volume C. *Chartered Institution of Building Services Engineer*, London.

Count, R.1890. "D'hulst, The Arab Houses of Egypt.", Royal Institute of British Architects Transactions, Vol. 1, pp. 221 - 243, 1890.

Creswell, K. A. C. (1959) "A.D. Ekistics" Vol. 744, pp. 451-453, 1959.

Creswell, K. A. C. (1959). "Studies in Islamic Art of Architecture ", pp 95-105, Cairo, 1965.

Danby, M. (1973). "The design of building in hot-dry climates and the internal environment" (*Build International*). Vol.6, pp. 55-73, England. 1973.

Denies, (1959) in Givoni 1984.

Dunham, D. (1960). "The Courtyard House as a Temperature Regulator.", *The new Scientist*, pp. 663, 3rd Sep. 1960.

Dunkle, V. (1966). "Regenerative Evaporative Cooling Systems *CSIRO, AIRAH TRANSACTION*, Australia Refrigeration, Air Conditioning and Heating, January, 1966.

Eckert, E. R. G. and Carlson, W. O. (1961)."Int. J. Heat Mass Transfer" vol. 2, p. 10, 1961.

Eckert, E. R. G. and Jackson, T. W. (1950). *NACA Tech. Note*, 2207.

Elenbaas, W. (1948). "Dissipation of heat by free convection" *Part I and II, Philips Research Report 3*, N. V. Philips' Gloeilampen Fabrieken, Eindhoven, Netherland, pp. 338-360 and 450-465, 1948.

Emery, E., and Chu, N. C. (1965). "Heat transfers across vertical layers." *Trans. Am. Soc. Mech. Press* division John Wiley and Sons, New York, 1965.

Etheridge, D. W. and J. A. Nolan (1979). "Ventilation Measurements at Model Scale in a Turbulent Flow", *Building and Environment*, Vol. 14 pp. 53-64, Pergamon Press Ltd , 1979.

Evans, M. (1980). "Housing Climate and comfort" The Architectural Press, London Halsted press division John Wiley and Sons, New York.

Fanger, P. O. (1970). "Thermal Comfort, an analysis and application in Environmental Engineering." McGraw Hill, London, 1979.

Fanger, P. O. (1979). "Thermal comfort". 1979.

Fathy, H. (1986). "National Energy and Vernacular Architecture", Principles and Examples with Reference to hot and climates, edited by Water Shower, the published for United Nation University, by the University of Chicago, USA , 1986.

Fitzgerald, D. and Houghton-Evans, W. (1987). "The Sun and Ventilation" *International Solar Energy SOLAR WORLD CONGRESS*, Humburg, September 1987, pp.4.

Fuchs R. and McClelland J. F. (1979). "Passive Solar Heating Using Transwall Structure" *Solar Energy*, 23,123-128, 1979.

Fathy, H. (1973). " The Arab house" Exeter University, England, 1973.

Ettouny, S. (1974). "An Investigation of Acoustic and Winds Environments of Courtyard Housing.", Ph.D Thesis, The university of Sheffield, England, 1974.

- Giles, R. V. (1977).** "Fluid Mechanics and Hydraulics", 2/nd. Schum's outline series, McGraw-Hill book company, London, 1977.
- Givoni, B. (1979).** "Passive Cooling of Building by Natural Energies." *Energy and Buildings*, 2 Elsevier Sequoia S.A, Lausanne, pp. 279-285.
- Givoni, B. (1981).** "Cooling Building by Passive Systems", *Proceeding to International Conference on Passive Cooling*, Maimi Beach, Florida, PP. 988-996, 1981.
- Givoni, B. (1984).** "Man Climate and Architecture" Applied Science Publication, London, pp 278, 1981.
- Golany, G. (1980).** "Housing in Arid Lands, Design and Planning" The Architectural Press Ltd, London, 1980.
- Holder, L. H. (1957)** "Automatic roof cooling", Aril Showers Company, Washington DC, 2. 1957.
- Houghton et al. (1940).** " Sumer Cooling loads as affected by heat Gain through dry, Sprinkled and water covered Roof", *ASHVE TRANS.*, 64.pp231-1940.
- Incropero F. P. & Dewit D. P. (1985).** "Introduction to Heat Transfer" John Willey & Sons, New York, 1985.
- ITO, N., K. Kimura and J. OKA. (1972).** "A Field Experimental Study on The Convective Heat Transfer Coefficient on Exterior Surface of a Building", *Building Research Institute*, Japanese Ministry of Construction, Tokyo, Japan, 1972.
- Jakob, M. (1946).** "Free Heat Convection through Eclosed Plane Gas Layers", *Trans. ASME*, vol. 68, p. 180, 1946.
- Jakob, M. (1949).** "Heat Transfer" Jhon Wiley & Sons, Inc., New York, 1949.
- Klauss, A. K., Tull R. H., Roots, L. M. and Pfafflin, J. R. (1970).** "History of Changing Concepts in Ventilation Requirements" *ASHRAE Journal*, vol. 12, No. 6, pp. 51-55, 1970.

- Konya, A. (1980).** "Desert Primer for Hot Climate", The Architectural Press, London, 1980.
- Koenigsberger, O. H., Ingersoll, T. G., Mayhew, A., and Szokolay, S. V. (1974).** "Manual of tropical housing and building." *Climatic design* . Longman group Ltd, London, 1974.
- Kreith, F. (1973).** "Principles of Heat transfer." Intext Educational Publishers, New-York, 1973.
- Lane, E. W.(1938).** "An account of manners and customs of modern Egyptians", Vol.1, pp 21-48, London, 1938.
- Lee, J. B. G., (1979).** "Development and optimization of thrombe's solar wall", Ph. D. Thesis, Dept. of Civil Eng., The University of Leeds.
- Lezine, A. (1972).** "Toris Palais d'epoque Ottomane au Caire", pp 140, le Caire 1972.
- Liddament, M. W. (1986).** "Air infiltration calculation techniques-An application guide." *Air Infiltration and Ventilation Centre*, Bracknell, U.K.
- McAdams, W. H. (1954).** "Heat transmission" McGraw-Hill Publishing Co. Ltd. New York, 1954.
- MacGegor, R. K. and Emery, A. F. (1969).** "Free Convection through Vertical Plane Layer-Moderate and High Prandtl number Fluids." *Journal of heat Transfer*, vol. 91 pp. 391-403, 1969.
- Maloney, T. (1978).** "Four Generation of water wall Design", Conference 2, 489-492, 1978.
- Martin, M. (1981).** "State of art in Passive Cooling", Sunworld, Vol. S. No. 6, pp. 177-183, 1981

Markus, T. A. and Morris, E. N. (1980). "Building, Climate and Energy." Pitman Publishing Ltd, London, 1980.

Mignon, G. V., W. A. Cunningham and T. L. Thompson. (1985). "Passive Cooling with solar Updraft and Evaporative Downdraft Chimneys", Interim report for work performed 6/15/84 to 3/1/185 under U.S. *Departement of Energy* , Contract No, 1985.

Milbank J. & Harrington-Lynn J. (1974)."Thermal response and admittance procedure", 1974.

Mohsen, M. A. (1979) "Solar Radiation and Court-Yard House Farms, I.A. Mathematical model", Pergaman Press Ltd London.*Building Service Engineers*, vol.42 pp. 38-51., *Building and Environment*, Vol. 14, pp 89-106. Peraman Press Ltd. G. Bratin, London 1979.

Missenard, A. (1933). "Etude physiologique et technique de la ventilation" *Librairie de l'Enseignement Technique*, Paris, 1933.

Moody, C.D., T. L. Thompson and J. F. Peck. (1978). "The Downdraft Chimney: Passive Evaporative Cooling for the southwest, *Report to the Arizona Solar Energy Commission*, 1978.

Nicol, J. F. (1975). "An analysis of some observations of thermal comfort in Roorkee India andBaghdad, Iraq." *Building Research Establishment*, Garston Watford U.K, 1970 .

Oakley, D. J. (1961). "Tropical houses" pp.90-133, London, 1961.

O'Callaghan (1980). "Building for energy conservation", Pergman press Oxford, 1980.

Olgay, V. (1963). "Design with climate-Bioclimatic approach to architectural regionalism." Princeton University Press, Princeton, New Jersey 1963.

Page, J. K. (1964). "Environmental Research Using Models", *The Architects Journal Information Libaray*, March, 1964.

Parry Jr , J. E. (1977) " Mathematical modelling of the performance of passive solar heating system" , *Los Alamos Scientific laboratory*, University of California, Los Alamos New Mexico 875-945, Report No. LA.UR-7Z 2345, PP37, 1977.

Pathorn, H. (1983). "A Guide to Architectural Style" , Phaidon, Oxford, U.K, 1983.

Pratts, A. w. (1981). "Heat transmission in buildings", John Wiley and Sons, New York, 1985.

Pittes, A. C. (1987). "Assessing Ventilation System in Hot Buildings Environments", *Building and Environment*, vol. 21, No. 3/4 pp. 145-148, 1987.

Revoult, J. and Maury, B., (1975). "Palais et maisons de Caire.", I 1975, II 1975, III 1979, 480 P.

Rshmi, V., Bansal N. K. and Grag, H. P. (1986). "The comparative Performance of Different Approaches to Passive Cooling", *Building and Environment*, Vol. 21, No. 2, pp. 65-69, Pergamon, (1986)

Sabady, P. R. (1978). "The Solar House", A guide to solar energy utilisation in domestic, industrial and commercial building, London. Boston, 1978.

Saini, B. S. (1980). "Building in hot day climates", Dept. of Architecture, University of Qeenland, Shan Wiley and Sons, Chichester, 1980.

Sharples, S. (1984). "Full-Scale Measurements of Convective Energy Losses from Exterior Building Surfaces", *Building and Environment*, Vol. 19, No. 1, pp. 31-39, 1984.

Sobersky, R. H. and et al. (1971). " Fluid flow", 2nd, london, 1971.

Sodha, M. S., Ashutorm S., Kumar A. , Sharma A. K.(1986). "Thermal Performance of an Evaporatively Cooled Multi-Storey Building", *Building and Environmental*, Vol. 21, No. 2, pp 71-79. Pergaman Jauranl, 1986.

Sodha, M. S. Bansal N. K. & Kumar A. (1986.a). "Solar passive buildings",

Pergamon Books Ltd. Loondon, 1986.

Sodha, M. S., Seth, S. P. Bansal N. K. and Seth A. K. (1981.a)
 "Optimum distributions of Concrete in double hollow concrete slab," *International J. Energy Research*, 5, 289-295, 1981.

Sodha, M., S., Seth, S. P., Bansal N. K. and Seth A. (1982).
 "Conservation and Management", 22, 143, 1982.

Sodha, M. S., Singh, U., Srivastought, and Tiwari G. N. (1981).
 "Experimental Validation of Thermal Model of open roof pont," *Building and Environmental*, 16, 93, 1981.

Sadha, M. S., Seth, S.P., Bansal N. K. and Seth A. K. (1981.a)
 "Comparison of the thermal performance of single and double hollow concrete slabs." *Applied Energy* ,9, 201-209, 1981.

Stoecker, W. F., and Jones, J. W. (1982). "Refrigeration and Air Conditioning", Second Edition, McGraw-Hill book Company, London, 1982.

Sutton , G. C. (1950). "Roof Spray for reduction in Transmitted Solar radiation", *ASHVE, TRANS.* , 131, Sept. 1950.

Trombe F. (1972). "US Patent 3 832-992, 1972.

Trombe F. (1974). "Marisons Solaires, Technique Deinginiea , 3, CTM, 1974.

Thapper, W. C. (1943). "Excessive Temperature in Flat-top building, Refrigerating Engineering, 163, 1943.

Tiwari, G. N. et al. (1982). "A review-cooling water Evaporation over roof", *Energy* , 1982.

Tredgold, T. (1836). "The principle of warming and ventilation public buildings." M. Taylor. London 1836.

Taylor, J. R. (1982). "An introduction to error analysis." U.S.A., Oxford

University Press, 1982.

United Nation Publications (1981 to 1986). "Energy Statistics Yearbook", *United Nation*, New York., 1981 to 1986.

van Straaten, J. F. (1967). " Thermal performance of buildings, " Elsevier, 1967.

Watts, J. R. (1963). "Evaporative-Air Conducting", The Industrial Press, New York, 13.Mars 1963.

Webb, C. G. (1964). "Thermal discomfort in a tropical environment." *Nature*, 202, 1193-1194, 1964.

Winslow, C. E. A., Gagge, A.P. and Herrington, L. P. (1939). "The influence of air movement upon heat losses from the clothed human body." *J. Physiol*, 127: 505-518, 1939.

Wong, H. Y. (1977) ."Handbook of essential formulae and data on Heat transfer for engineers." Longman Group Ltd. London,1977.

Yaglou, C. P. and Whitheridge, W. N. (1937). "Ventilation requirements." *ASHRAE Transactions*, Part 2, vol. 43, pp. 423-436, 1937.

Yagoubi, M. A. and Golneshan, A. A. (1986). "Passive cooling of an underground room (Sardab)." *Iranian Journal of Science & Technology*, vol. 10, No. 1&2, Shiraz, Iran, 1986.

Yellot, J. I. (1969). "Roof cooling with Intermittance Water Sprays, *ASHAE 73rd Annual Meeting in Toronto*, Ontario, Canada, June 27-29, 1969.

Yellot, J. I. (1969)."Natural air conditioning with roof pands or movable insulation", *ASHRE.*, 75 (part 1), 1969.

Younes A. EL.S. (1983). "The Islamic Architecture as a mean for the Passive design system."*General Organisation for housing building and Planning Research*, Cairo, Dokki, P.O.Box 1770. Egypt, 1983.

Appendices

Appendix A : Climatic data of the city of Cairo (1976 - 1985)

Latitude 30 08' N, Longitude 31 44 E, Altitude 111.5 m

Months	Jan.	Feb.	Mar.	Apr.	May	June	July	Aug.	Sept.	Oct.	Nov.	Dec.
<i>Dry Temperature</i>												
Extreme max.	30.2	33.6	37.9	43.2	45.4	44.7	42.6	42.0	43.7	39.2	35.7	27.9
Mean monthly max.	24.6	27.3	33.4	38.9	41.5	41.5	38.6	37.9	37.9	35.5	30.4	25.1
Mean daily max.	19.0	20.8	24.0	28.4	32.4	34.7	34.8	34.5	34.9	29.9	25.0	20.4
Mean	14.7	15.6	18.3	22.1	25.6	30.2	31.7	29.6	25.9	24.5	20.2	16.1
Mean daily min	8.8	9.6	11.6	14.4	17.5	20.2	21.9	21.8	20.1	17.9	13.9	10.3
Mean monthly min	5.4	6.3	7.0	10.8	14.0	17.6	19.5	19.9	17.6	14.8	10.3	7.0
Extreme Min	1.2	0.8	4.4	7.6	11.5	15.5	18.2	17.5	14.5	12.0	5.0	3.0
Mean diurnal range	10.2	11.2	12.4	14.0	14.9	14.5	12.9	12.5	12.4	12.0	11.1	10.1
<i>Relative Humidity</i>												
Mean daily max.	60	59	57	57	59	64	71	72	70	68	69	64
Mean daily Mini	37	32	29	26	23	21	25	29	29	29	31	39
Mean humidity	44	42	40	35	37	37	40	41	40	42	45	46
Mean vapour press.	6.7	6.8	7.3	8.2	9.8	12.4	14.9	15.7	14.2	12.0	10.1	7.6
No. of days of fog (mean)	1.5	1.0	1.0	1.1	0.8	1.2	2.4	3.7	1.9	2.0	2.1	1.9
<i>Precipitation</i>												
Mean monthly mm	4.9	3.7	2.4	1.1	0.5	0.2	0.0	Tr	Tr	1.0	3.5	6.5
Max. in 24 hrs	9.6	10.4	10.0	4.6	6.0	3.6	0.0	Tr	0.1	13.8	18.5	50.0
Mean days with 0.1mm/ more	3.4	2.2	1.6	0.9	0.4	0.1	0.0	0.0	0.0	0.5	1.3	3.0
<i>Sky</i>												
Hours of sunshine	7.5	7.8	8.7	9.6	10.8	11.6	11.7	11.2	10.2	9.5	8.5	7.4
Mean Cloud cover Oktas	2.5	2.4	2.5	2.3	1.8	0.9	1.1	1.2	1.3	1.7	2.3	2.7
<i>Wind</i>												
Max velocity m/s	25	29	30	24	22	20	16	19	17	22	23	25
Mean velocity m/s	3.9	4.1	4.4	4.5	4.5	4.1	3.4	3.3	3.4	3.7	3.2	3.8
Prevailing direction	SSW	SW	NE	NNW	NNW	NW	NW	NW	NNE	NE	NE	SSW
			/NW	/NE	/NE	/NE	/NE	/NE	/NE			

Source : The Egyptian Meteorological Authority

Appendix B. Error analysis of using different methods to determine the rate of cooling as a result of evaporation caused by a forced air flow.

Inlet	TEMP.	R.H	Enthalpy	Enthalpy Error	T	RH	Enth.	ΔE	Mean E	% Error	Cooling		Diff.
	°C	%	at Entry	kJ/kg							°C	kJ/kg	
	30	40	57		25.5	52	52.6	+1.80					
			at Outlet	3.50	25.5	48	51.6	-0.80					
	25	50	53.5		24.5	52	50.0	-0.80	50.8	51	619	481	29
					24.5	48	49.0	-1.80					
Error	±0.5	±2							±1.80				

* Air Density at Entry 1.14 kgm⁻³
 Air Density at exit 1.16 kgm⁻³

E = Enthalpy

= Error

Appendix C

Measured data of the buoyancy air flow at different surface separation

Table A.3.a. Measured data used to obtain the convective heat transfer coefficient at wet surfaces separation of 20, 80 mm cavity and average air velocity 0.08 m/s

Air temp.		Temp. diff.	Surf. temp.	Moisture content		Δg	Absolute temp.
T_{in}	T_{out}	ΔT	T_s	P_a	P_s	Pa	$^{\circ} K$
$^{\circ} C$	$^{\circ} C$	K	$^{\circ} C$	kg/kg	kg/kg		
22.5	17.2	5.3	16.5	0.01140	0.01195	88	292.8
22.6	17.3	5.3	16.7	0.01139	0.01200	98	292.9
22.8	18.0	4.8	16.7	0.01155	0.01200	80	293.0
22.5	18.0	4.5	16.7	0.01136	0.01200	102	293.3
22.7	18.2	4.5	16.7	0.01140	0.01200	96	293.4
22.5	18.0	4.5	16.7	0.01137	0.01200	101	293.3
22.6	18.1	4.5	16.7	0.01139	0.01200	98	293.4
21.9	17.3	4.6	16.8	0.01114	0.01220	124	292.6
22.3	17.7	4.6	16.8	0.01140	0.01200	96	292.0
22.5	17.9	4.6	16.7	0.01136	0.01200	102	293.2

- air density = 1.205 kg/m³- absolute temperature = (273+ T_{av})

- separation between surfaces=20mm

Table A.3.b. Measured data used to obtain the convective heat transfer coefficient at wet surfaces separation of 30, 100 mm cavity and average air velocity 0.27 m/s

Air temp.		Temp. diff.	Surf. temp.	Moisture content		Δg	Absolute temp.
T_{in}	T_{out}	ΔT	T_s	P_a	P_s	Pa	$^{\circ} K$
$^{\circ} C$	$^{\circ} C$	K	$^{\circ} C$	kg/kg	kg/kg		
20.7	16.5	4.2	15.3	0.01050	0.01095	72	291.6
20.6	16.4	4.3	15.0	0.01045	0.01085	64	291.5
20.8	16.4	4.5	14.8	0.01055	0.01077	63	291.6
20.5	16.0	4.5	14.5	0.01040	0.01079	63	291.3
20.4	15.8	4.6	14.4	0.01039	0.01080	68	291.1
19.7	15.1	4.6	14.4	0.00980	0.01020	64	290.4
20.3	15.7	4.6	14.5	0.01020	0.01060	66	291.0
19.6	15.0	4.6	14.0	0.00970	0.01020	68	290.3
20.2	15.2	5.0	14.3	0.01020	0.01060	66	291.7
20.5	15.6	4.9	14.4	0.01025	0.01068	69	291.1

- air density = 1.205 kg/m³- absolute temperature = (273+ T_{av})

- separation between surfaces=30mm

Table A.3.c. Measured data used to obtain the convective heat transfer coefficient at wet surfaces separation of 130, 200 mm cavity and average air velocity 0.05 m/s

Air temp.		Temp. diff.	Surf. temp.	Moisture coefficient		Δg	Absolute temp.
T_{in}	T_{out}	ΔT	T_s	P_a	P_s	Pa	$^{\circ}K$
$^{\circ}C$	$^{\circ}C$	K	$^{\circ}C$	kg/kg	kg/kg		
21.1	18.3	2.8	16.5	0.01101	0.01180	126	292.7
21.3	18.3	3.0	16.7	0.01120	0.01840	115	292.8
21.4	18.3	3.1	16.7	0.01120	0.01195	120	292.8
21.8	18.5	3.3	16.7	0.01134	0.01200	106	293.2
22.0	18.9	3.1	16.7	0.01150	0.01220	80	293.4
22.0	18.9	3.1	16.7	0.01150	0.01220	80	293.4
21.9	18.7	3.2	16.7	0.01140	0.01200	96	293.3
22.0	19.0	3.0	16.8	0.01150	0.01200	96	293.5
21.8	18.4	3.4	16.8	0.01140	0.01200	96	293.2
21.9	18.6	3.3	16.7	0.01140	0.01200	96	293.3

- air density = 1.18 kg/m^3

- absolute temperature = $(273+T_{av})$

- separation between surfaces=130mm

Table A.3.d. Measured data used to obtain the convective heat transfer coefficient at wet surfaces separation of 230, 300 mm cavity and average air velocity 0.04 m/s

Air temp.		Temp. diff.	Surf. temp.	Moisture content		Δg	Absolute temp.
T_{in}	T_{out}	ΔT	T_s	P_a	P_s	Pa	$^{\circ}K$
$^{\circ}C$	$^{\circ}C$	K	$^{\circ}C$	kg/kg	kg/kg		
18.9	16.5	2.4	14.5	0.00960	0.01038	125	290.7
19.0	16.5	2.5	14.5	0.00962	0.01038	122	290.8
19.1	16.5	2.6	14.5	0.00963	0.01038	121	290.8
19.3	16.5	2.7	14.6	0.00975	0.01040	104	291.0
19.2	16.6	2.6	14.6	0.00963	0.01040	124	290.9
19.2	16.6	2.6	14.7	0.00963	0.01044	130	290.9
19.3	16.5	2.8	14.7	0.00975	0.01044	110	290.9
19.0	16.5	2.5	14.5	0.00962	0.01038	121	290.7
18.7	16.0	2.7	14.4	0.00980	0.01039	98	290.4
19.2	16.4	2.8	14.8	0.00984	0.01050	100	290.8

- air density = 1.19 kg/m^3

- absolute temperature = $(273+T_v)$

- separation between surfaces=230mm